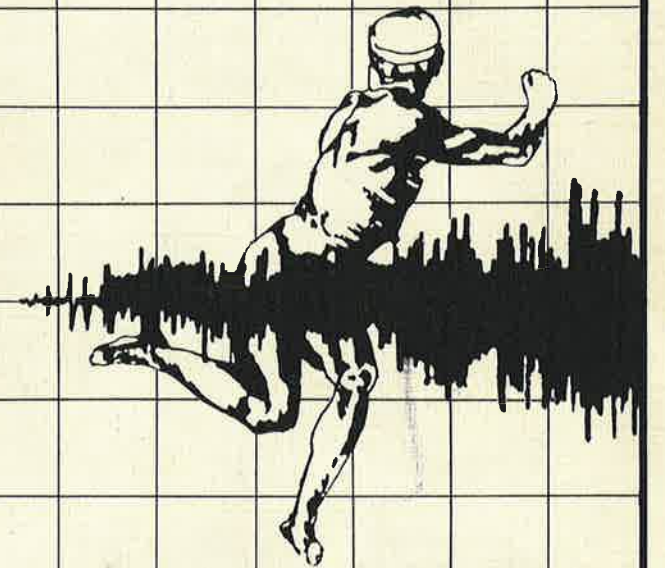


electro- physiological kinesiology

editors:
w. wallinga, h.b.k. boom
j. de vries



excerpta medica

international congress series 804

wallinga, boom
de vries
editors

**electrophysiological
kinesiology**

ICS 804



ISBN 0 444 81032 3

electrophysiological kinesiology

proceedings of the 7th congress of the
international society of electrophysiological
kinesiology, held in enschede,
the netherlands, 20–23 june 1988.

editors:

willemien wallinga,

associate professor of biomedical engineering,
school of electrical engineering,
university of twente, enschede, the netherlands

herman b.k. boom,

professor of biomedical engineering,
chairman of the biomedical engineering department,
school of electrical engineering,
university of twente, enschede, the netherlands

jaap de vries

rehabilitation physician, senior research scientist,
rehabilitation center het roessingh,
enschede, the netherlands



1988

excerpta medica

amsterdam – new york – oxford

© 1988 Elsevier Science Publishers B.V. (Biomedical Division)

All rights reserved. No part of this publication may be reproduced, stored in a retrieval system or transmitted in any form or by any means, electronic, mechanical, photocopying, recording or otherwise without the prior written permission of the publisher, Elsevier Science Publishers B.V., Biomedical Division, P.O. Box 1527, 1000 BM Amsterdam, The Netherlands.

No responsibility is assumed by the Publisher for any injury and/or damage to persons or property as a matter of products liability, negligence or otherwise, or from any use or operation of any methods, products, instructions or ideas contained in the material herein. Because of rapid advances in the medical sciences, the Publisher recommends that independent verification of diagnoses and drug dosages should be made.

Special regulations for readers in the USA – This publication has been registered with the Copyright Clearance Center Inc. (CCC), 27 Congress Street, Salem, MA 01970, USA. Information can be obtained from the CCC about conditions under which photocopies of parts of this publication may be made in the USA. All other copyright questions, including photocopying outside the USA, should be referred to the copyright owner, Elsevier Science Publishers B.V., unless otherwise specified.

International Congress Series No. 804
ISBN 0 444 81032 3

Published by:
Elsevier Science Publishers B.V.
(Biomedical Division)
P.O. Box 211
1000 AE Amsterdam
The Netherlands

Sole distributors for the USA and Canada:
Elsevier Science Publishing Company Inc.
52 Vanderbilt Avenue
New York, NY 10017
USA

Printed in The Netherlands

PREFACE

The study of the neuromuscular system is the general topic bringing together scientists and clinicians at Congresses of the International Society of Electrophysiological Kinesiology (ISEK).

The society aims the advancement in research and teaching in the broad field of the Electrophysiological Kinesiology. At the seventh congress, ISEK-88, many papers have been presented. In these proceedings a selection of them is published.

The organisers are affiliated to institutes with research experience especially in the fields of Electromyography, Functional Electrical Stimulation (FES) and Rehabilitation. Besides the mondial achievements in these research fields, the progress in many other aspects of the Electrophysiological Kinesiology is presented.

This book may contribute to the dissemination of the knowledge about the neuromuscular system in normal and diseased states. The progress of research linked to fundamental and clinical rehabilitation in the last decennia is intriguing and faces new possibilities.

The status quo is changing fast. The authors of this volume are greatly honoured for their papers with current information. We look forward to the further developments in the field of the Electrophysiological Kinesiology!

Willemien Wallinga
Herman B.K. Boom
Jaap de Vries

ACKNOWLEDGEMENTS

The papers of this book were presented at the 7th Congress of the International Society of Electrophysiological Kinesiology, held from 20–23 June in Enschede, The Netherlands.

The congress and this proceedings volume were ultimately made possible by the (financial) support of the Rabo Bank, Nicolet Instruments Benelux, Medelec Limited, Norwich Eaton, Sandoz, Basko/Camp, Tracor, Toornend Orthopaedie Service B.V., Otto Bock Orthopädische Industrie, Infotronic Medical Engineering, St. Joris Foundation, Huka Developments, KLM, Twente Technology Transfer, Toennies Orthopaedische Instrument Makerij Het Roessingh, and last but not least the University of Twente and the Rehabilitation Center Het Roessingh.

Many people have given essential support to arrange a kind and stimulating atmosphere during the congress. They are too numerous in number to mention. The continuous coordination by Frans Sniijders of the Congres Buro Twente, is acknowledged gratefully. With him, and especially Kasper L. Boon, Gerald Zilvold and Dirk Rotman, the organisation was succesful and grew to a good experience.

We thank especially the members of the program committee for their contribution in refereeing the abstracts submitted for the congress:

Andersson, G.B.J., *Rush-Presbyterian-St. Luke's Medical Center, Chicago, USA*
 Baumgartner, R., *Dept. Techn. Orthopaedics and Rehabilitation, Münster, FRG*
 De Luca, C.J., *Neuromuscular Research Center, Boston, USA*
 Denier van der Gon, J.J., *Dept. of Med. and Physiol. Physics, Utrecht, The Netherlands*
 de Weerd, J.P.C.M., *Nicolet Biomedical Instruments, Madison, USA*
 Dimitrijević, M.R., *Baylor College of Medicine, Houston, USA*
 Dubowitz, V., *Royal Postgraduate Medical School, London, UK*
 Hermens, H.J., *Rehabilitation Center Het Roessingh, Enschede, The Netherlands*
 Kernell, D., *University of Amsterdam, Amsterdam, The Netherlands*
 Mano, Y., *Nara Medical University, Nara, Japan*
 Notermans, S.L.H., *Catholic University of Nijmegen, Nijmegen, The Netherlands*
 Rabischong, P., *INSERM, Montpellier, France*
 Rozendal, R.H., *Free University of Amsterdam, Amsterdam, The Netherlands*
 Rutten, W.L.C., *University of Twente, Enschede, The Netherlands*
 Schaars, A.H., *Rehabilitation Center Het Roessingh, Enschede, The Netherlands*
 Sniijders, C.J., *Erasmus University, Rotterdam, The Netherlands*
 Solomonow, M., *Louisiana State University, New Orleans, USA*
 Stålberg, E., *University Hospital, Uppsala, Sweden*

van Alsté, J.A., *University of Twente, Enschede, The Netherlands*
 Visser, S.L., *Academic Hospital Free University, Amsterdam, The Netherlands*
 Zilvold, G., *Rehabilitation Center Het Roessingh, Enschede, The Netherlands*

Ultimately it is the assembly of authors that determines the value of this book.
 We thank them for their contributions.

CONTENTS

KEY REVIEW

- The use of science in rehabilitation
J.P. Paul 3

MOTOR CONTROL

Control of voluntary movement

- Motor control: Aspects of its organisation, control signals and properties
J.J. Denier van der Gon 9
- Muscular coactivation and its relevance to the control of movement
M. Solomonow, R. Baratta and R. D'Ambrosia 19
- Mechanisms underlying accuracy in fast goal-directed arm movements in man
J.H.P. van der Meulen, J.J. Denier van der Gon and C.C.A.M. Gielen 25
- Acceleration curve analysis during fast forward arm elevation upon
 different conditions
P.G. Gatev, N.T. Tankov and G.N. Gantchev 29

Activation patterns of motor units

- The common drive of motor units
C.J. De Luca 35
- Remarkable differences in motor-unit activation during slow isotonic
 movements and isometric contractions
A.A.M. Tax, J.J. Denier van der Gon and C.C.A.M. Gielen 39
- Firing frequency during maximal voluntary contraction
P. Pinelli, G. Miscio and P. Pisano 43

Spinal reflexes

- Stretch reflexes regulate stiffness in restoration of hand position
T. Sinkjaer and R. Hayashi 51
- Spatial averaging of the bioelectric double hit short latency spinal reflex
J.S. Ekiel and M.J. Zieniewicz 55

ARTIFICIAL STIMULATION**Fundamental research**

Effects of patterned electrical stimulation (PES) in the rehabilitation of the upper limb in chronic quadriplegic patients <i>J.P. Boucher and A. Pépin</i>	61
Fatigue of quadriceps muscle continuously activated by functional electrical stimulation in paraplegics <i>M. Levy, J. Mizrahi, Z. Susak and P. Solzi</i>	65
The skeletal muscle in ischemia and in reperfusion during efferent motor nerve stimulation <i>H.M. Scheja and P. Eckert</i>	69
Histological examination after epineural electrode application <i>W. Happak, R. Koller, W. Girsch, H. Gruber, J. Holle, U. Losert, W. Mayr and H. Thoma</i>	75
A study of peripheral nerve regeneration in comparison with utilizing a silicone tube and a bioresorbable collagen membrane <i>K. Hosokawa, T. Satou, M. Takahashi, S. Hashimoto, F. Akai and M. Ioku</i>	79
Modelling of volume conduction	
Electrical nerve stimulation: Experiments and simulations <i>P.H. Veltink, J. Holsheimer and J.A. van Alsté</i>	85
Modelling considerations for the stimulation of the motor cortex with transcranial electrodes <i>F. Grandori and P. Ravazzani</i>	89
Analysis of spinal cord stimulation I. Field potentials calculated for a homogeneous medium <i>J. Holsheimer and J.J. Struijk</i>	95
Analysis of spinal cord stimulation II. Simulation of field potentials in an inhomogeneous medium <i>J.J. Struijk, J. Holsheimer, B.K. van Veen, F.P.H. van Beckum and P.H. Veltink</i>	99
Feedback and control strategies	
Accelerometers and functional electrostimulation <i>A.T.M. Willemsen, J.A. van Alsté and H.B.K. Boom</i>	105

An improved strategy to minimize muscle fatigue during FES-induced standing <i>A.J. Mulder, H.J. Hermens, J.A. van Alsté and G. Zilvoid</i>	109
Practical closed loop stand/sit and walking systems for mid thoracic paraplegics <i>D.J. Ewins, P.N. Taylor, T.L. Whitlock, B.A. Fox, R.T. Lipczynski and I.D. Swain</i>	113
On the multi-joint control of lower extremity using functional electrical stimulation <i>Y. Iguchi, K. Kubo, K. Fujita, N. Itakura and H. Minamitani</i>	117
Spectral analysis of stimulated muscle EMGs to provide feedback in closed loop FES systems <i>T.L. Whitlock, D.J. Ewins, P.N. Taylor, I.D. Swain and R.T. Lipczynski</i>	121
Implantable stimulators	
Dual channel implantable stimulator <i>B. Kelih, J. Rozman, U. Stanič and M. Kljajić</i>	127
Implantable stimulator for functional electrical stimulation of the peroneal nerve <i>J. Rozman, B. Kelih, U. Stanič and M. Kljajić</i>	131
Sensitivity, selectivity and bioacceptance of an intraneural multi electrode stimulation device in silicon technology <i>W.L.C. Rutten, H.J. van Wier, J.H.M. Put, R. Rutgers and R.A.I. de Vos</i>	135
Implantable systems for restoration of function	
Implantable neurostimulators: The phrenic pacemaker - Technology and rehabilitation strategies <i>H. Thoma, H. Gerner, W. Girsch, J. Holle, W. Mayr and H. Stöhr</i>	143
Functional electrical stimulation of the posticus muscle in bilateral recurrent nerve paralysis <i>M. Zrunek, W. Streinzer, W. Mayr, H. Gruber and H. Thoma</i>	153
Functional electrostimulation in the treatment of traumatic injuries of cervical spinal cord <i>J. Kiwerski and R. Paśniczek</i>	157
Urinary incontinence in elderly women - Treatment with functional electrical stimulation <i>B. Kralj and A. Lukanovič</i>	161

Evaluation of functional electrical stimulation in standing up and walking

The Calis project <i>P. Rabischong and J. Woloszko</i>	537
Longitudinal study of gait pattern of hemiparetic patients using subcutaneous peroneal electrical stimulation <i>M. Kljajić, R. Aćimović, J. Krajnik, E. Vavken, M. Maležić, A. Ahlin and M. Gregorič</i>	167
Paraplegic locomotion using a hybrid orthosis: mechanical and functional electrical stimulation of gluteal muscles with implanted electrodes <i>S.J. Jennings, A.V. Nene and J.H. Patrick</i>	171

Evoked potentials

Cerebral evoked potentials <i>M.R. Dimitrijević</i>	177
Clinical evaluation of pulsed magnetic stimulation in degenerative diseases of the central nervous system <i>K. Ikoma, Y. Mano, T. Nakamuro and T. Takayanagi</i>	187
The safety of magnetic stimulation <i>Y. Mano, I. Funakawa, T. Nakamuro, K. Ikoma, T. Takayanagi and K. Matsui</i>	191
Evaluation of acetaminophen (setamol) analgesia by argon laser induced pain related cortical responses <i>L. Arendt-Nielsen and P. Bjerring</i>	195

ELECTROMYOGRAPHY**Electrical activity of motor units and single muscle fibres**

Motor unit topography viewed by different EMG techniques <i>E. Stålberg</i>	201
Power spectra of muscle fiber extracellular potentials <i>G.V. Dimitrov, Z.C. Lateva and N.A. Dimitrova</i>	211
Possible mechanisms of bioelectric phenomena associated with disorders of neuromuscular transmission <i>N.A. Dimitrova and G.V. Dimitrov</i>	217
Activity of single muscle fibres recorded at known distances <i>W. Wallinga, B.A. Albers, J.H.M. Put, W.L.C. Rutten and P. Wirtz</i>	221

Surface EMG: Modelling and effect of electrode – configurations

Volume conductor modelling of motor unit action potentials in the surface electromyogram <i>T.H.J.M. Gootzen, H.M. Vingerhoets and D.F. Stegeman</i>	227
A stochastic model for simulation of surface EMG patterns <i>H.J. Hermens, T.A.M. van Bruggen, W.L.C. Rutten, G. Wilts, K.L. Boon, W. Wallinga-de Jonge and G. Zilvold</i>	231
Surface EMG: The effect of electrode-configuration parameters <i>J.A. de Kreek, J. Harlaar and H. Bakker</i>	235

Endplate position, conduction velocity and fibre type proportion

Innervation zone and delay density estimates <i>S.W. Davies and P.A. Parker</i>	243
Noninvasive investigation of the excitation of single motor units by means of multi-lead electrode arrays <i>G. Rau, J. Schneider and J. Silny</i>	247
Noninvasive measurement of conduction velocity in motor units influenced by temperature and excitation pattern <i>J. Schneider, J. Silny and G. Rau</i>	251
A close relationship between mean power frequency and fibre type proportion <i>K. Henriksson-Larsén, B. Gerdle and M-L. Wretling</i>	255

Cross talk in surface EMG

Crosstalk assessment in human thigh muscles <i>M. Knaflitz, R. Merletti and F. Catani</i>	261
Crosstalk of the intrinsic lumbar back muscles <i>H.A.M. Daanen and P. Vink</i>	265

Spectral parameters during muscle fatigue

Muscle fiber conduction velocity and EMG spectral parameters in voluntary and stimulated contractions <i>R. Merletti, M. Knaflitz and C.J. De Luca</i>	271
Stationarity of voluntary and electrically elicited surface myoelectric signals <i>G. Balestra, M. Knaflitz and R. Merletti</i>	275

- Recovery from severe isometric, concentric or eccentric contractions in the human biceps muscle
G.W. Kroon and M. Naeije 279
- The influence of force and circulation on the average muscle fiber conduction velocity during local muscle fatigue
M.J. Zwarts and L. Arendt-Nielsen 283
- Electromyography in walking of patients with intermittent claudication
A.L. Hof, G.J.J. Bonga, W.D. Kuipers, A.A. Wouda, and L. de Pater 287
- An all-poles model for the study of the muscular sound
M. Maranzana-Figini, A. Pizzino and B. Diemont 291
- A study of fatigue by the cross spectrum of muscular sound and surface EMG
B. Diemont, M. Marazana-Figini, C. Orizio, R. Perini and A. Veicsteinas 295

Surface EMG in occupational health studies

- Surface electromyography in work-physiological field studies for the analysis of muscular strain and fatigue
A. Luttmann, M. Jäger and W. Laurig 301
- Quantitative and qualitative electromyography in the evaluation of ergonomic measures
B. Jonsson 305
- Influence of whole body vibration on neck and shoulder muscle activity
E. Machida, B. Jonsson, U. Landström and L. Brundin 309
- The effects on EMG load levels of different kinds of pauses in VDT work
G. Sundelin, M. Hagberg and U. Hammarström 313
- EMG and mechanical performance during shoulder forward flexions at different angular velocities
B. Gerdle, J. Elert and K. Henriksson-Larsén 317
- Relations between electromyographic signs of fatigue during work and occupational myalgia in the shoulder region
G. Hägg and J. Suurküla 321

REHABILITATION

Training and evaluation in rehabilitation

- Evaluation in rehabilitation
G. Zilvold and R. Baumgartner 327
- Belgrade active A/K prosthesis
D. Popovic and L. Schwirtlich 337

- An electropneumatic platform for a cognitive approach in rehabilitation of hemiplegic patients
A. Pepino, M. Bracale, M. Iocco and N. Misasi 343
- Quantified myofeedback in muscle (re)education by computerized video games
R. Soerjanto and R. Phillips 347
- Effects of specific muscle power increase in case of flat-foot
M. Crivellini, G. Dacquino, L. Divieti, G.C. Santambrogio and M. Stucchi 351

Hemiplegia and spasticity

- Assessment of muscle function in hemiplegic and healthy subjects by kinesiologic EMG-registration during repetitive movements
J. Becher, J. Harlaar, T.W. Vogelaar and H. Bakker 357
- The cumulative vibratory index of the soleus H-reflex: A new quantitative measure for spasticity
L.J. Bour and B.W. Ongerboer de Visser 361
- Measurement of biomechanical and myoelectrical properties of elbow muscles with pendulum test
D. Miklavčič, S. Reberšek and N. Gros 367
- Quantitative assessment of patellar tendon reflex using an angular accelerometer
M.K. Yoshida, L.W. Lamoreux, M.E. Johanson, R. St. Helen, S.R. Skinner and R.K. Ashley 371
- Comparison between phenolisation of the motor points of the gastrocnemius muscle and phenolisation of the tibial nerve
D. Wever, M. Schlecht and H.J. Hermens 377

NEUROMUSCULAR DISEASES

Therapeutic methods and fundamental research

- Effects of electrical stimulation on muscles of patients with progressive muscular dystrophy
M. Gregorič, V. Valenčič, A. Zupan and A. Klemen 385
- The value of light-weight orthoses in the prevention of scoliosis in Duchenne muscular dystrophy
E.B. Rodillo, E. Fernandez-Bermejo, J.Z. Heckmatt and V. Dubowitz 389
- Force of dystrophic mouse hindleg muscles and the effect of early immobilization
L. Brocks, H. Janssen, W. Wallinga-de Jonge and P. Wirtz 393

- Glycogen depletion of fast glycolytic motor units in mouse skeletal muscle
A.F. Evenhuis, W. Wallinga-de Jonge, P. Wirtz and H.M.Th. Loermans 399

Evaluation of muscular dystrophies

- Comparison of clinical evaluation methods and surface EMG in a follow-up study of patients with Duchenne dystrophy
A.H. Schaars, H.J. Hermens, M.C. Schlecht and G. Zilvold 407
- Automatic analysis of EMG interference pattern in patients with progressive muscular dystrophy (PMD)
N. Marcello, F. Ortaggio, A. Lanfranchi and D. Guidetti 411
- EMG quantitative analysis of muscle fatigue in myotonic dystrophy
B. Rossi, G. Siciliano, M. Angelotti and R. Risaliti 417

Evaluation of other neuromuscular diseases

- Isokinetic strength evaluation and strength exercise in spinal muscular atrophy
C. Granata, L. Merlini, M. Colombari, S. della Villa and F. Bombardi 423
- Abnormal fatigue in myotonia congenita
M.J. Zwarts and T.W. van Weerden 427
- Analysis of the surface electromyogram in pathologic fatigue
J.P. Braakhekke, D.F. Stegeman, E.M.G. Joosten and S.L.H. Notermans 431

BIOMECHANICS

Biomechanics of the spine and shoulder

- Dynamic analysis of lifting
G.B.J. Andersson, O.D. Schipplein, J.H. Trafimow and T.P. Andriacchi 437
- A spatial dynamic biomechanical model for the analysis and assessment of lumbar stress during whole body movements
M. Jäger and A. Luttmann 441
- Displacement of the spine during lifting
I. Gilad 445

Activity of trunk and back muscles

- EMG assessment of muscular deficits associated with chronic low back pain
S.H. Roy, C.J. De Luca, D.A. Casavant and M.S. Emley 451
- Sensory nerve endings in the posterior ligaments of the lumbar spine
H. Yahia, M. St. Georges and N. Newman 455

- Different EMG - Force relationships of the low-back muscles during standing and sitting
L.J. Mouton, S. Besseling, A. Hidding and J. van der Bij 459
- Electromyography investigation of trunk control in the sitting position
M.E. Johanson 463
- Sitting posture: Balans chair vs. conventional chair
P. Anderson, D. Belk, A. Connors, C. Levitan, E. Maguire, K. McNamara, T. Shapiro and C. Shelton 467

Biomechanics of locomotion

- The prediction of human walking patterns
H.F.J.M. Koopman, H.J. Grootenboer and H.J. de Jongh 473
- Modelling and simulation of human gait in three dimensions using multibond graphs and implicit integration routines
P.C. Matthijsse and P.C. Breedveld 477
- Biomechanical model of quadruped with flexible spine
E.V. Birjukova, M. Dufosse, A.A. Frolov, M.E. Ioffe and J. Massion 481
- Muscle coordination in elite and trained speed skaters
J.J. de Koning, G. de Groot and G.J. van Ingen Schenau 485
- EMG and movement pattern in manual wheelchair propulsion
H.E.J. Veeger, L.H.V. van der Woude, R.H. Rozendal, H.J. Bieleman and J.A. Paul 489
- Dynamic changes of the medial arch of the foot in childhood during walking
H. Fujii, N. Matsusaka, M. Fujita, T. Norimatsu and R. Suzuki 493
- The dynamic changes of the medial arch of the foot during slope walking
S. Takesako 497

KINESIOLOGY

Analysis of standing up, squatting and walking

- Kinesiological analysis of standing-up movement
Y. Mano, T. Sakakibara and T. Takayanagi 503
- Dynamic analysis of squat postural sways
H. Iwakura, S. Tanaka and S. Kashiwabara 513
- Hip abductor action during level walking
R.F.M. Kleissen, M.C. Schlecht and G. Zilvold 517

Activity at muscle level in the leg

Data reduction by preprocessing of EMG during dynamic isometric contraction <i>R.F.M. Kleissen, J. Harlaar and J.A. de Kreek</i>	523
Statistical electromyography of cyclic muscle action <i>F. Bodem, K. Alt, A. Wackerhagen, H. Wagner, F. Brussatis and V. Walther</i>	527
Influence of contraction-history on EMG and torque during isokinetic knee extension <i>J. Harlaar, M. Bobbert, B.J. Hanhart and H. Bakker</i>	531
Author index	549
Keyword index	553

KEY REVIEW

THE USE OF SCIENCE IN REHABILITATION

J P PAUL

Bioengineering Unit
University of Strathclyde
Glasgow, Scotland

Modern science and technology covers many disciplines and end products. To some the development of materials for special purposes is the forefront of current work. Lasers are an application of technology in their own right although their control may utilise computer or micro processor facilities. The development of digital computers and associated micro processors has made a particularly large impact on many fields including that of rehabilitation and obviously in a review such as this they will receive considerable attention. For the seriously disabled patient complete mobilisation may depend on the availability of a lightweight power source in association with appropriate control systems. Additionally, the effective delivery of rehabilitation can only be assessed by appropriate instrumentation and measurement systems whether they be based on methods of imaging or on the acquisition of physical quantities relating to patient performance. Finally, mention will be made to some of the areas in which power sources and micro processors can be utilised for the more effective provision of functional electrical stimulation.

Materials development may be viewed as being in the field of metals, polymers and composites. In metals, the availability of titanium and its alloys has been recognised in the provision of orthopaedic implants-joint replacements and fracture plates - and also in the components of some artificial leg systems. The combination of high strength with low mass in association with minimum tissue reaction give it a place beside the classical cobalt chrome alloys for these purposes. New generations of polymers have widespread uses. Improvements in biocompatibility allow implants for slow release of appropriate drugs as well as the avoidance of problems of thrombus formation in extracorporeal blood treatment. Plastics have been utilised for a long time in protheses and orthoses and it is interesting to see the application of composites to provide strength and lightness to artificial limb components.

Lasers in medical practice are usually thought of as means of sectioning tissues and coagulating bleeding points. Their use in fusion of the retina in ophthalmology is however revolutionising this kind of surgery and there is the possibility of their effective use through fibre optic delivery systems to break up atheromatous plaques in major arteries and blood vessels and possibly even in coronary arteries. At the University of Strathclyde we have been involved in development and assessment of the use of appropriate lasers to assist in the joining of vessels as is required in coronary artery surgery and this procedure seems to have considerable promise due to the avoidance of leakage and foreign body reaction associated on occasion with the use of sutures. Their major contribution however may be the reduction in the time of surgery and a measure of "de-skilling". Two other aspects of laser contribution to rehabilitation are less well known but have also been developed at the University of Strathclyde. One relates to the use of a pulsed ruby laser for the removal of tattoo marks. This is now an established technique being regularly used in a plastic surgery clinic. The other is the use of a tuned dye laser for the removal of port wine stain birthmarks or haemangiomas. In both of these techniques selection of the appropriate laser wave length is important so that they can penetrate the skin without giving up an amount of energy which would cause burning and consequent scarring and yet interact effectively with the target material. In the case of the tattoo mark the target is the blue or black pigment and delivery of the appropriate energy causes disruption of the pigment material resulting in its disappearance after three or four treatments. For the port

wine stain birthmark the ideal target material would be the collagen material of the superfluous blood vessels from which the red colouration of blood is seen through the skin. This however is not practical since the constitution of the blood vessels and of the external skin of the body is practically identical. The target in this case therefore is the blood itself and delivery of appropriate amounts of energy does not burn the skin but being absorbed preferentially by the blood cells gives rise to rapid local heating with disruption of the blood vessels and denaturation of their material. Normal body repair processes replace these with normal tissue without the excessive microvasculature structure.

A laser light source has been used by Fernie and others in Toronto to obtain the 3-D data relating to the size of an amputated stump; thus allowing the use of CAD-CAM techniques for socket construction. This of course involves very considerable computer facilities in association with the shape definition system. In civil and structural engineering as well as in large engine manufacture the laser is often used as an aid to correct alignment of machines and buildings under construction. Since the function of a lower limb amputee depends critically on the alignment of his prosthesis it may be that lasers should be used to assist the determination and measurement of the alignment parameters so that replacement limbs can be rapidly and reliably constructed with exactly the same characteristics as the original.

One aspect of the use of computers in rehabilitation which is not always recognised is the use of its memory for patient data recording so that quantitative assessments of patient performance can be rapidly recalled for review and prospective studies more easily organised. Another aspect of its utilisation is that of its prime purpose of mathematical calculation allowing finite element stress analysis of complicated components, the solution of the equations corresponding to poroviscoelastic deformation as associated with the lumbar spinal discs or predictions of flow and shear stress variation with time at bifurcations in the arterial system.

Associated with the computer's facility for mathematical calculation is the rapid development in imaging of all kinds. The enhancement of X-ray pictures has now been overshadowed by the clarity, detail and three dimensional imaging characteristics of the CAT scan and nuclear magnetic imaging (NMI). Unfortunately, because of the high basic cost of these types of instrumentation the results are not always available to assist in clinical decision making.

More obviously relevant to rehabilitation of the disabled are the data acquisition systems for gait analysis such as those based on television computer systems, light emitting diodes and polarised light goniometers. Similarly the output from other equipment related to gait analysis is frequently sampled, stored and manipulated by computer. One thinks of the interaction of ground to foot force measurement with displacement data or that from force transducers incorporated in prostheses or even simple centreless goniometers. While the computer can acquire the information from such devices the output is best presented in a form easily assimilated by the user in the clinic if most advantage is to be obtained. In this connection presentation of the ground to foot force vector relative to a video image of the leg is a useful technique. Unfortunately, 3-D visualisation of the situation requires double images and in neither case can even a trained eye readily detect the consequences of rotation of the limb about its own axis or a vertical axis. This is most important because it can change a flexion/extension moment into a moment tending to adduct or abduct! For those interested in foot problems the pedobarograph now offers direct dynamic data acquisition of the pressures between ground and foot during a walking cycle and this should be of particular use in the diabetic clinic as well as in the orthopaedic foot specialist's premises.

One might imagine that modern science and technology could be utilised in the development of artificial arms and hands in the same way as robotic techniques are largely used in mass production manufacture. Work is certainly underway in several centres using modern miniature electric motors and modern concepts in control systems to develop improved artificial hands and arms. The major problems remain, however, in giving rapid, precisely controlled movement to the extremity in association with the

appropriate 3-D orientation of the hand. A complete functioning shoulder, elbow, wrist and a primitive grip may involve the control of seven functions on a continuous controlled basis from what may be a minimum of four control sites. While hierarchical control systems may be appropriate for locomotion, utilisation in the upper extremity may cause great frustration.

Modern technology in electrical storage batteries appears to have solved the energy problem for upper extremity prostheses of the present generation. Consideration has often been given to the possibility of utilising the same energy supply systems for the lower limb and here the electrical battery proves to be insufficient. The major problems are the simultaneous requirements of rapid controlled movement in swing phase associated with the development of substantial moments at the joint axes in the stance phase. It would be ideal if appropriate power systems could be developed to assist both amputees and orthosis users but this solution seems distant.

Functional electrical stimulation has however the capacity for utilising the body's metabolic energy in locomotion of patients with deficits in their neuromuscular control system. FES has been in existence for several decades, but has yet to bring about a real benefit in the rehabilitation of significant numbers of people. Current research is primarily directed towards spinal cord injured quadriplegics and paraplegics. Patients with stroke and other neurological conditions may ultimately also obtain some benefit.

In Europe, most applications in the lower limbs have used surface electrodes, while in the USA there has been more development of percutaneous and implanted electrodes. In the future, implanted systems will offer the best function and convenience to the patient. Surface systems will remain useful for training and diagnostic uses, as well as for backup and shorter term use.

The technology involved in portable surface stimulators is comparatively simple. The major technological opportunity is now offered by low power single chip microcomputers. With these, it is possible to design sophisticated control systems for the generation of useful functions such as manipulating objects by quadriplegics, and standing and walking by paraplegics. The two major directions in FES research at present are control (in which we aim to improve function) and assessment (in which we examine what improvements we may have achieved). These aspects can be illustrated in the lower limb functions of standing and walking.

Standing is useful to paraplegic subjects for both therapeutic and functional purposes, as well as contributing to some improvement in self-image. The processes of raising and lowering the body between the standing and sitting positions are most easily controlled by the subject taking part of his body weight through the upper limbs on a standing frame or walking aid. The problem in control is in prolonging the upright position, since the quadriceps muscles tend to fatigue rapidly. It is necessary to maintain stability while minimising muscular action. Posture switching and muscle cycling have been shown to be of benefit here.

Closed loop control of knee angle has been implemented using a knee goniometer and a proportional controller implemented on a portable microcomputer. A more dramatic reduction in muscle action can be obtained with hybrid orthoses. The feedback signal indicates the knee extension moment being applied by the mechanical component of the brace and FES is used to supplement that moment in order to maintain stability.

It is possible that further improvements in stability, and hence in the muscle action required, will be obtained by incorporating some measure of sensory feedback for the user of the orthosis. Sensory feedback can be used by patients to help maintain a mechanically stable range of postures.

Walking presents a tougher challenge to the designer of controllers than does standing. It is possible to synthesize a functional gait using only two channels of stimulation per limb (one for extension of the knee and the other for the flexion withdrawal reflex), with hand switches to change over the stimulation channel; but this form of gait is

barely functional, being slow to progress and quick to fatigue. Improved controllers have tended to pursue one of two main approaches.

The first may be described as open loop cyclical sequencing. Patterns of muscle actions are designed which mimic those of natural gait derived from EMG recordings. Natural looking gait can be achieved by this method, but it is inherently unstable, and unable to compensate for disturbances.

The second is the finite state model. Here, gait is divided into an arbitrary number of states (such as double-support, push-off, swing). Each state is associated with one or more actions, which may include local closed loop controllers. The transitions from one state to another are governed by a set of rules describing a number of discrete events.

The finite state model may be hierarchical, in that certain levels of decision making are abstracted from other levels. Decisions about the subject's intentions (such as standing, walking, transferring) govern the next lower level of the decision hierarchy (stance phase, swing phase etc). These decisions in turn govern lower levels (which muscles should be activated at what levels), which in turn call on the programme which drives the stimulator.

The finite state approach offers the possibility of designing complex controllers from simple building blocks. Further improvements in gait synthesis will require better sensors than we have now, as well as better knowledge of the appropriate control strategies.

Standing function has traditionally been measured in terms of postural stability, estimated as the sway in the centre of gravity or centre of pressure. More important is the time period during which a person can remain standing. This of course is closely related to the reduction in muscle activity or duty cycle which can be achieved by a controller. While therapeutic standing may benefit from increased muscle activity, functional standing should aim to minimise activity and consequent fatigue.

In the assessment of walking function, kinematic and kinetic gait analysis has a useful role to play. Data from force plates, from instrumented walking aids, and from position and angle sensors present useful diagnostic tools for the designer of FES controllers. From the user's point of view, the important parameters are function and efficiency. How far or how fast can he go before he is drained by exhaustion? Can he manage stairs or rough ground? Does FES help in transferring or in the activities of daily living? The technology of FES has much potential to offer. How much of this is realised will depend on our understanding of the action of the stimulator and the nerves and muscles and human skeleton all acting together as a unified system.

The scientific input to all of these aspects of rehabilitation is obvious. Equally the application of the science is dependent on appropriate technology. It is the essential that the two go hand in hand for optimum progress in rehabilitation.

MOTOR CONTROL

Control of voluntary movement

MOTOR CONTROL : ASPECTS OF ITS ORGANISATION , CONTROL SIGNALS AND PROPERTIES

J.J. DENIER VAN DER GON

Department of Medical and Physiological Physics, Rijksuniversiteit Utrecht,
Princetonplein 5, P.O. Box 80.000, 3508 TA Utrecht, The Netherlands

INTRODUCTION

Current studies on motor control deal with a large variety of topics. These include the overall organisation of the motor system, the functional role of reflexes, the coordination of muscles, gradation mechanisms of muscle force, stiffness control and motor programmes. Fig. 1 shows a flow diagram of the motor control system as part of a larger system.

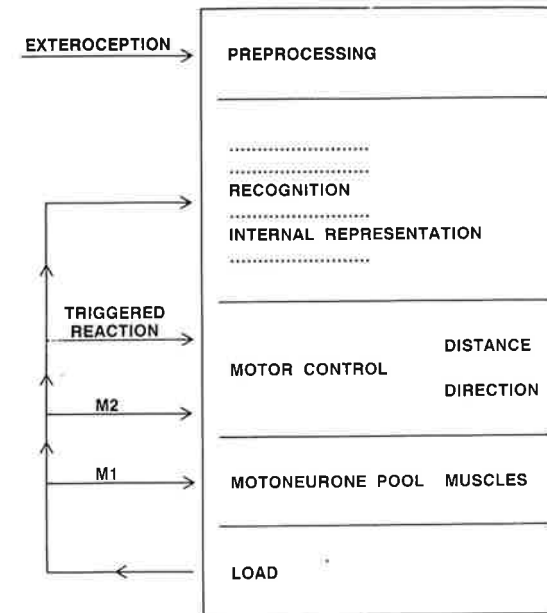


Fig. 1 . Perception, cognition and muscle properties play a role in motor control. Proprioceptive information is fed back to different levels in the control system : short latency (M1) loops to the motoneuron pool, medium or long latency (M2) loops involving muscle coordination centres, loops with still longer latencies (triggered reactions?) involving movement pattern generators and finally a loop that involves kinesthesia and the internal representation.

It stresses the fact that motor functions should not be studied separately from perceptive and cognitive functions and muscle properties. Proprioception interacts with the motor system at different levels giving rise to reflexes of different latencies. The functional role of short latency stretch reflexes (M1) is probably to stiffen muscles that are stretched unexpectedly (1). Medium (or long) latency reflexes (M2; \approx 50-80 ms) are sometimes called functional stretch reflexes. These reflexes may give rise to appreciable forces which counteract mechanical disturbances (2). Recently it has been found that it is not only the muscles that are stretched by the disturbance which are activated. Other muscles may be involved in this medium latency response as well. As illustrated in Fig. 2, coordinated muscle activity in medium latency reflex contractions develops in a way similar to the coordinated muscle activity in voluntary contractions (3).

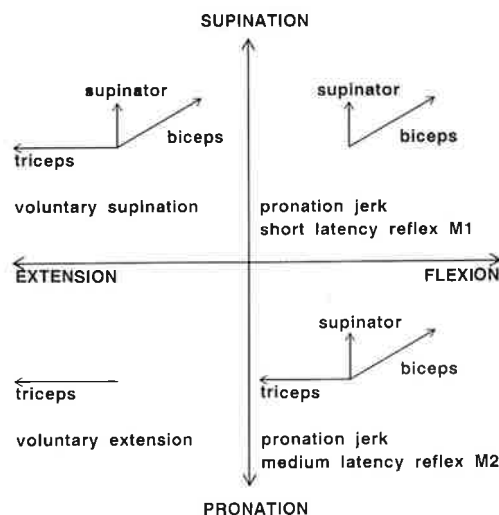


Fig. 2 . When a supination force is exerted voluntarily, the m. supinator, m.biceps and m.triceps are activated, the latter muscle compensating for the flexion force component of the m.biceps (upper left panel). In voluntary extension, only the m.triceps is activated (lower left panel). Applying a pronation jerk to the forearm stretches the m.supinator and the m.biceps (upper right panel). A short latency reflex is then elicited in these two muscles. Following a pronation jerk the medium latency reflex also shows activity in the triceps muscle. It appears that in this medium latency reflex the muscles are activated in a similar way as when a preload in pronation direction is voluntarily counteracted.

This suggests that in both processes the same nerve centre is stimulated which is responsible for muscle coordination in relation to movement direction. Muscle spindles are sense organs which probably play a role in this reflex, but there may be other sources too. For a further analysis of muscle coordination we refer to (4,5).

Simple models may help us to analyse the motor control system in a more quantitative way. In the following sections we shall take a closer look at the motor programme generator or muscle activation pattern generator and consider some of the problems concerning the coding of relevant variables in nerve activities.

An activation pattern generator for goal directed movements

Fast goal directed movements are elicited by a burst of activity of agonist muscles, followed by a burst of braking activity of antagonist muscles. This pattern is for the most part generated without the use of feedback signals from the moving limb (6,7). Since distance of movement depends on the amount or intensity I of agonist muscle activity as well as on the duration T of this activity it follows that the activation pattern generator is able to compute I and T with respect to each other in such a way that a correct movement is carried out.

The initial velocity of a movement is directly related to I . It is likely that in goal directed movements a subject chooses I as the independent variable, i.e. he chooses to move slowly or quickly. He then computes T such that the correct distance is covered. For instance in handwriting I is kept more or less constant whereas T depends on the size of the letter strokes (8). The same holds for the movements of a violinists left hand along the finger board of his instrument. The tempo of the tune determines I and T is adapted such that the hand moves over the correct distance (7). Apparently the subject has at his disposal an internal model of the muscle-load system.

If a goal directed movement is not carried out very fast, the muscle activation patterns can be modulated by afferent feedback. Presumably this modulation occurs by means of feedback signals that carry velocity information of the moving limb (9). These feedback signals adjust T in such a way that this part of the system can be regarded as a powerful mechanism for correcting for wrong estimates or misjudgements of the load!

A simplified scheme of the activation pattern generator is presented in Fig. 3. Reset mechanisms and the internal model of the muscle-load system are

omitted from this scheme. The "subject" chooses a velocity or intensity I

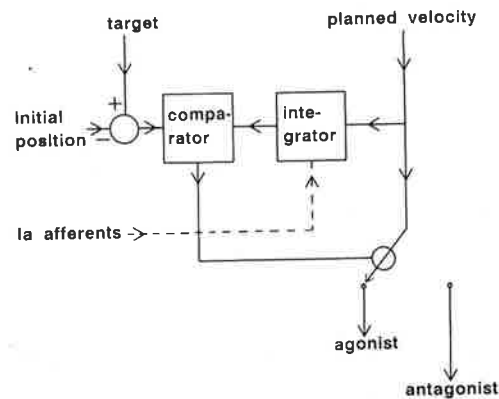


Fig. 3 . The diagram depicts a simplified version of a movement pattern generator. A muscle activation level, related to planned movement velocity is chosen. The pattern generator estimates the distance covered and compares it to the distance to be moved. Movement time is computed in this way. As soon as proprioceptive velocity signals (Ia afferents) become available, the planned velocity is replaced by the actual velocity for computing movement time.

which is then fed into the muscle system and determines the activation levels. As soon as velocity signals from the moving limb reach the activation pattern generator they can be used to correct for discrepancies between the actual and the planned velocity. The velocity signals are fed into an integrating system that computes the distance covered. As soon as this distance matches about half the distance to be covered, the activation of the agonist muscles stops and that of the antagonist muscles begins. In (9) it is shown that if a muscle that is stretched during a goal directed movement is vibrated mechanically, the movement falls short in that it stops too early. The activation level of the agonist muscle is not affected. This finding fits in with the model. One can test the model further by changing the movement velocity, i.e. by choosing different I values. In the case of very fast movements, movement time is too short for the pattern generator to take advantage of feedback signals. One therefore expects that in that case the movement will not be disturbed by vibration. We estimate the effective feedback delay to be about 180 ms: it was found (7) that a mechanical position-disturbance may elicit EMG activity after some 110 ms with characteristic features of a goal directed correction

movement. Then it is another 70 ms until a movement actually starts after the muscles are activated (10). The slower the movement, the more one can rely upon feedback signals and the larger will be the effect of a disturbed feedback, resulting for instance from mechanical vibration.

Fig. 4 shows experimental data concerning goal directed movements, derived from (11). The subject carried out goal directed movements while his arm was hidden from his sight. The muscle that was stretched during the movement was vibrated; it is seen that the slower movements do indeed fall short. We estimate the vibration-induced velocity sensation to be about 50 deg/s (12).

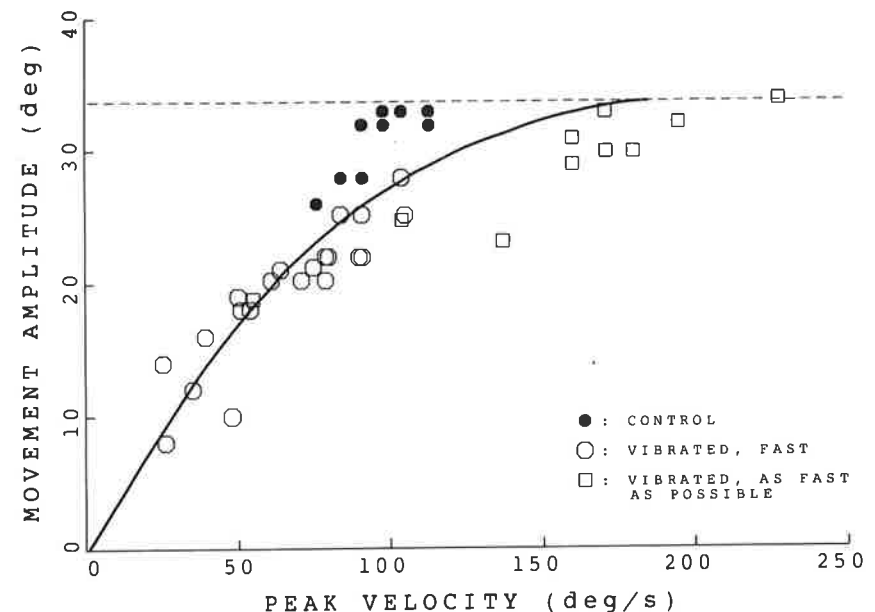


Fig. 4 . Results of an experiment (data derived from (11)) are shown in which a subject had to make goal directed extension movements over a distance of 33 cm. In these experiments the subject could not see his own arm. During the movements the biceps tendon was vibrated mechanically (1.2 mm; 77 pulses/s, open symbols). Movement amplitude is plotted as a function of peak velocity of the movement. The target was attained if the movement was very fast. Slower vibrated movements showed an undershoot which increased with decreasing velocity. The drawn line was computed according to the model described in the text.

If we assume that the activation pattern generator switches over to the use of this velocity after 180 ms following the start of the movement, we can compute the distance that will be covered. In Fig. 4 it is shown that this model describes the experimental data quite nicely.

Linear processing of information in the Central Nervous System by groups of neurons

In the model discussed above and many other models it is assumed that the central nervous system has knowledge of variables like position of limbs and movement velocity. It is not really possible for these variables to be represented by activities of single cells; these variables are represented by activities of groups of cells. A likely candidate for the representation of a variable is a weighted sum of nerve activities of a group of cells. In the models it is therefore implicitly assumed that activities of groups of cells are processed. The central nervous system is able to carry out linear operations for which the superposition principle holds. Muscle activation shows such linear addition properties (13,14). Movements and stiffness can be superimposed (15) and in motor learning different motor patterns can be learned separately and combined later on. In any case, the superposition principle appears to hold at the motoneuronal level since muscles may contribute in an additive way to different tasks and combinations of these tasks.

The linear transfer properties of motoneuron pools may be understood for subpopulations of motoneurons that are activated homogeneously, i.e. a neuron that projects on to the motoneuron pool innervates each motoneuron with the same relative strength. We consider a pool with sets of input fibres ($i \in I$), ($k \in N$),, and a set of output fibres ($j \in M$) see Fig. 5. e, f and g

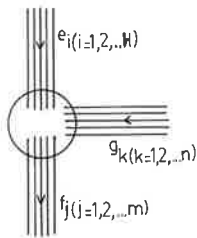


Fig. 5 . A neuron pool with output fibres (axons) j and two sets of input fibres i and k . e , f and g denote firing frequencies.

represent firing rates along the fibres. We define signals

$$E = \sum_1^h u_i e_i ; G = \sum_1^n w_k g_k ; F = \sum_1^m v_j f_j$$

u , v and w are weights.

f_j will generally be a non linear function of the input of motoneuron j :

$$f_j = f \left(\frac{UE + WG + \dots}{\rho_j} \right)$$

ρ_j being a threshold or scaling factor related to cell size or input impedance of motoneuron j , U and W overall weights of the signals E and G .

Now it can be shown that

$$F = \sum_1^m v_j f \left(\frac{UE + WG + \dots}{\rho_j} \right) \approx \text{const.} (UE + WG + \dots)$$

if three conditions are fulfilled:

First of all, the non linear function f should show saturation properties, i.e. the firing frequency of a motoneuron should become a constant at high inputs, see e.g. Fig. 6. Secondly the threshold ρ_j should be distributed

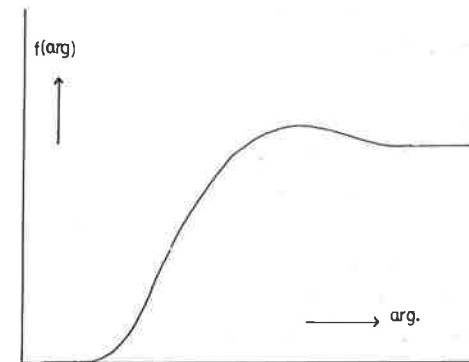


Fig. 6 . Example of a non linear function showing threshold and "saturation" properties.

inversely, i.e. the larger units (higher threshold) are found less frequently. Thirdly, muscle unit force should be proportional to threshold. The latter two conditions are known to be fulfilled in a statistical sense (16).

If we interpret v_j as muscle unit force, F equals total force and

$$F \sim U E + W G + \dots$$

Fig. 7 shows this approximately linear relationship in the special case that f equals a step function, i.e. force is only graded by recruitment.

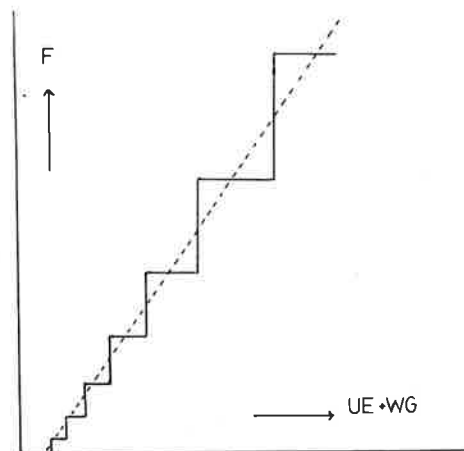


Fig. 7 . The force F exerted by a muscle as a function of the input to the motor neuron pool in case of recruitment force grading.

The foregoing considerations help us interpreting records of single unit activities in relation to motor tasks. For isometric contraction tasks it is known that subpopulations of motor units are activated homogeneously and so the theory developed is likely to hold for such tasks. In short latency reflexes motoneuron pools are partly homogeneously activated. Also, preliminary results on slow movement tasks bring about a homogeneous activation, be it with other overall weights of the activation of the muscles involved (A.A.M. Tax et al., these proceedings). Promising further subjects of investigation along these lines are medium and long latency reflexes, common drive of motor units and the organisation of task groups.

REFERENCES

1. Allum JHJ, Mauritz KH (1984) *J Neurophysiol* 52 : 797-818
2. Melvill Jones G, Watt DGD (1971) *J Physiol Lond* 219 : 709-727
3. Zuylen EJ van (1988) Thesis University of Utrecht
4. Jongen HAH, Denier van der Gon JJ, Gielen CCAM, Zuylen EJ van (1986) *Neuroscience Letters Suppl* 26 : 215
5. Gielen CCAM, Zuylen EJ van (1986) *Neuroscience* 17 : 527-539
6. Sanes JN, Jennings VA (1984) *Exp Brain Res* 54 : 23-32
7. Wadman WJ, Denier van der Gon JJ, Geuze RH, Mol CR (1979) *J Human Movement Studies* 5 : 3-17
8. Denier van der Gon JJ, Thuring JPh (1965) *Kybernetik* 2,4 : 145-148
9. Sittig AC, Denier van der Gon JJ, Gielen CCAM (1987) *Exp Brain Res* 67 : 33-40
10. Gielen CCAM, Oosten K van den, Pull ter Gunne F (1985) *J Motor Behavior* 17 : 421-442
11. Sittig AC (1986) Thesis University of Utrecht
12. Sittig AC, Denier van der Gon JJ, Gielen CCAM (1985) *Exp Brain Res* 60 : 445-453
13. Haar Romeny BM ter, Denier van der Gon JJ, Gielen CCAM (1984) *Exp Neurology* 85 : 631-650
14. Vincken MH, Gielen CCAM, Denier van der Gon JJ (1984) *Human Movement Science* 3 : 269-280
15. Vincken MH, Denier van der Gon JJ (1985) *Human Movement Science* 4 : 307-319
16. Milner-Brown HS, Stein RB, Yemm R (1973) *J Physiol Lond* 230 : 359-370

**MUSCULAR COACTIVATION AND ITS RELEVANCE TO
THE CONTROL OF MOVEMENT**

M. SOLOMONOW, R. BARATTA AND R. D'AMBROSIA

**BIOENGINEERING LABORATORY
DEPARTMENT OF ORTHOPAEDIC SURGERY
LOUISIANA STATE UNIVERSITY MEDICAL CENTER
NEW ORLEANS, LOUISIANA 70112**

INTRODUCTION

A series of studies in which the simultaneous EMG activity of the agonist and antagonist muscles of the human elbow and knee joints in isometric, isokinetic and free movement were performed. The analysis of the data obtained strongly suggest that the antagonist muscle assumes the role of a "joint regulator", compensating for various internal and external disturbances, such as variations in joint speed, changes in the muscles moment arm, orientation of the gravity vector, skill acquisition, strength training, level of activity of the agonist and ligament deficiencies. The new information has significant implications in the design of FES systems for defunct joints due to spinal cord injury and for the development of new therapeutic modalities for ligament deficient joints.

METHODS

SUBJECTS: Several subject groups were used, including normals, high performance volleyball and basketball players who do not engage in additional exercise and others who routinely exercise their hamstrings. A group of patients with anterior cruciate ligament tears were also tested.

PREPARATION: Subjects were instrumented with silver-silver chloride, prepasted electrodes, which were applied over the midline

of the elbow and knee flexor and extensor muscle groups, on either side of the estimated motor point. The raw EMG was recorded with a gain of up to 100,000, and at CMRR of 110 db. The signal was then low pass filtered at 120 msec. time constant to yield its mean absolute value (MAV). Subjects were trained to generate their maximal voluntary effort contraction.

PROTOCOL: Isometric flexion and extensions were performed on the Cybex II system set at 0 deg./sec. speed at 45 degrees, 90 degrees and 135 degrees flexion. Each trial was performed with 10% increasing force increments from 10% to 100% (MVC) force in flexion and extension.

Isokinetic maximal effort flexion and extension were performed at a speed of 15 deg./sec. Four trials recorded from each subject. Additional MVC flexion and extension were performed at 30, 60, 120 and 240 deg./sec., to assess the effect of joint velocity on the coactivation EMG recorded from the antagonist.

ANALYSIS: The MAV of the EMG recorded from the antagonist was normalized with respect to its maximal effort MAV at the same joint angle, and plotted as normalized MAV vs. joint angle. The data from all subjects, including the four trials from each subject, was pooled, and the mean and SD were calculated and plotted.

RESULTS

The results of the isometric elbow tests show that as the agonist force increases, the antagonist coactivation is also increasing. Furthermore, while the slope of the MAV vs. force of the agonist does not change, the antagonist slope changes with joint angle for contractions made along the gravity vector. Figure 1 shows the variations of the MAV vs. angle slopes of the flexors and extensors when acting as antagonist. It is evident that the effect of gravity on the limb mass influences the activity

of the antagonist. To further emphasize the effect of gravity, EMG recordings from the flexors and extensors during elbow flexion-extension, with 10 lb. weight on the arm, are shown in Figure 2. The shoulder angle was changed in the three trials from 0 degrees to 90 degrees and 180 degrees forward extension, such that the gravity vectors effect on the forearm mass was fully reversed. It is evident that, although the elbow performed flexion, the triceps substantially increased their activity such that flexion was performed by triceps relaxation, rather than by biceps/brachialis contraction.

During isokinetic contractions at 15 deg./sec., the normalized antagonist coactivation MAV was inversely related to the variation of the muscle moment arm as a function of joint angle, when the flexion-extension was performed parallel to the ground to eliminate the effect of gravity. As the speed was increased, the antagonist EMG tended to decrease upon the initiation of the movement to allow limb acceleration and to increase towards the end of the movement to allow dynamic braking.

Data from athletes with highly skilled performance demonstrated inhibited antagonist coactivation, which gradually increased to normal level at the end of three weeks of daily exercise of the muscle, as shown in Figure 3.

ACL deficient patients demonstrated reflex activation of the hamstrings upon joint subluxation during extension, further demonstrating the antagonists ability to compensate for disturbances.

CONCLUSIONS

The results of this study suggest that substantial and diverse regulatory functions are provided to the joint by the antagonist muscle during various types of movement. This regulatory action

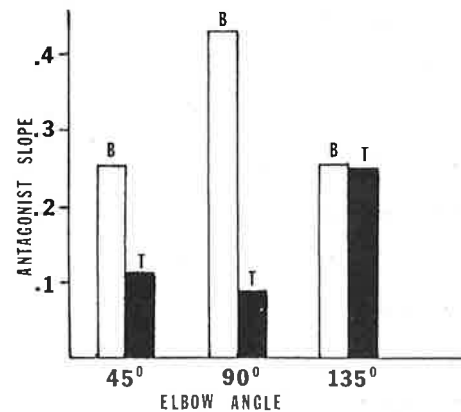


FIGURE 1 THE SLOPES OF THE EMG vs FORCE CURVES OF THE ELBOW FLEXORS AND EXTENSORS WHEN ACTING AS ANTAGONIST AT DIFFERENT JOINT ANGLES.

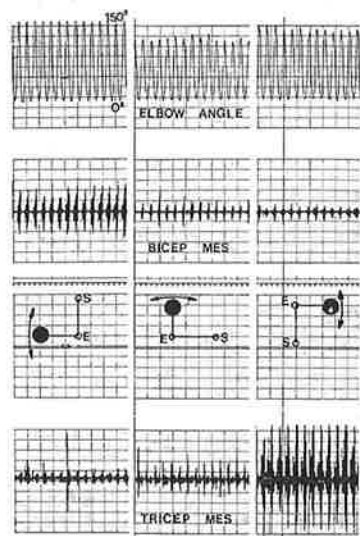


FIGURE 2 SHOWS ELBOW ANGLE (TOP), FLEXORS EMG (SECOND ROW), SHOULDER POSITION (THIRD ROW) AND TRICEPS EMG (BOTTOM) E-ELBOW, S-SHOULDER, BLACK DOT-10 lbs WEIGHT.

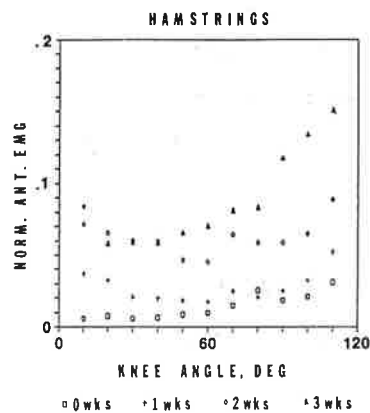


FIGURE 3 THE HAMSTRINGS ANTAGONIST EMG vs KNEE ANGLE TAKEN BEFORE AND AT THE END OF EACH WEEK OF DAILY RESISTIVE EXERCISE.

was provided for disturbances of internal and external origin, with the objective of allowing safe, accurate and well controlled motion. Such information has substantial implication in the design of high performance FES systems, as well as in the development of therapeutic modalities for various musculoskeletal deficiencies.

REFERENCES

1. M. Solomonow, A. Guzzi, R. Baratta, H. Shoji and R. D'Ambrosia. "EMG-Force Model of the Elbows Antagonistic Muscle Pair". *Am. J. Physical Medicine*, 65:223-244, 1986.
2. M. Solomonow, R. Baratta, B. Zhou, H. Shoji, W. Bose, C. Beck and R. D'Ambrosia. "The Synergistic Action of the ACL and Thigh Muscles in Maintaining Joint Stability". *Am. J. Sports Medicine*, 15:207-213, 1987.
3. R. Baratta, M. Solomonow, B. Zhou, D. Letson, R. Chuinard and R. D'Ambrosia. "Muscular Coactivation", *Am. J. Sports Medicine* 16(2):110-122, 1988.
4. M. Solomonow, R. Baratta, B. Zhou and R. D'Ambrosia. "EMG Coactivation Patterns of the Elbow Antagonist Muscles During Slow Isokinetic Movement", *Exp. Neurology* (In Press).

MECHANISMS UNDERLYING ACCURACY IN FAST GOAL-DIRECTED ARM MOVEMENTS IN MAN

J.H.P. VAN DER MEULEN**, J.J. DENIER VAN DER GON*, C.C.A.M. GIELEN*

Depts. of Child Neurology** and Medical Physics*, University of Utrecht,
Princetonplein 5, 3584 CC Utrecht (The Netherlands)

INTRODUCTION

The aim of this study was to investigate to what extent open-loop controlled motor commands on the one side and adjustments based on feedback of efferent and/or afferent information on the other side contribute to accuracy of fast goal-directed arm-movements. It is well-known that motor performance deteriorates if visual or proprioceptive information about the ongoing movement is withdrawn (e.g. 1-2). Furthermore, there is growing experimental evidence supporting the notion that a feedback loop of efferent information plays a role in the control of voluntary movements (3-4).

We reasoned that the variability in the initial acceleration of the arm provides a measure of the variance of the open-loop controlled level of activation of the agonist muscles. Compensatory adjustments based on feedback of efferent or afferent information will be apparent as a reduction of the effect of the variability in the initial acceleration on the distance travelled in certain phases of a movement.

A task was developed in which subjects had to make aiming movements as fast as possible within an accuracy demand. The role of visual feedback was explicitly investigated by comparing movements made with and without vision of the moving arm.

MATERIALS AND METHODS

The apparatus consists of a horizontal rail along which a handle can be moved (5). Movements are restricted to a straight line. The subject's hand is strapped to the handle and the wrist is immobilized. Two arrays of light-emitting-diodes (LEDs) placed over the movement trajectory are used to indicate respectively the start position and target area and the position of the handle. Visual feedback during the movement could be eliminated except for an area of 1cm around the prescribed start position.

Twelve healthy subjects (age 24-35 years) had to make 6 series of 24 movements. In these series three different distances (i.e. 8, 16 and 24cm) were presented in random order with target width varying proportionally with distance (1, 2 and 3cm respectively). The series of 24 movements were alternately performed with and without visual feedback.

The subjects were instructed to move the handle as fast as possible to the target and to stop it within the target area. There were no constraints with

regard to reaction time. The target exposition time (i.e. the period of time the LEDs spanning the target area stayed visible) was at the beginning of each session individually adjusted by gradually decreasing the target exposition time until approximately 50% of the movements were executed incorrectly (i.e. handle did not come to a standstill within the target area during the target exposition time).

The position data were filtered and differentiated to obtain velocity and acceleration trajectories. The 24 movements performed under equal conditions with respect to target and feedback condition were averaged and used for the calculation of average movement parameters.

RESULTS

Movements with visual feedback

Table I shows (row SE and VE) that the spatial accuracy decreased with target distance. There is a large effect of target distance on the systematic error (SE) -i.e. the difference between the mean distance moved and the distance between the start position and the middle of the target area- indicating that the tendency to undershoot the target increased with target distance. Also, the variable error (VE) -i.e. the within-subject standard deviation of the total distance moved- was clearly smaller in movements over 8 than in movements over 16 and 24cm. There was no significant effect of target distance on movement time (MT). So, differences

TABLE I

MOVEMENT TIME (MT), SYSTEMATIC ERROR (SE) AND VARIABLE ERROR (VE)

Group means and standard deviations of the individual means between brackets

	visual feedback	Distance			Friedman
		8 cm	16	24	
MT (ms)	p*	429 (.66)	447 (.72)	447 (.64)	n.s.
	a**	428 (.65)	436 (.67)	454 (.61)	<0.05
	Wilcoxon	n.s.	n.s.	n.s.	
SE (cm)	p*	.02 (.23)	-.33 (.24)	-1.15 (.33)	<0.01
	a**	.25 (.68)	-.45 (1.13)	-1.11 (1.40)	<0.01
	Wilcoxon	n.s.	n.s.	n.s.	
VE (cm)	p*	.70 (.17)	.94 (.19)	.95 (.19)	<0.01
	a**	1.01 (.27)	1.30 (.29)	1.40 (.30)	<0.01
	Wilcoxon	<0.01	<0.01	<0.01	

* visual feedback present

** visual feedback absent

TABLE II

VARIATION COEFFICIENTS OF MOVEMENT PARAMETERS

Group means and standard deviation of the individual means between brackets; see text for explanation of the symbols

VC	visual feedback	Distance			Friedman
		8 cm	16	24	
A70	p*	.39 (.09)	.38 (.15)	.33 (.10)	n.s.
	a**	.45 (.13)	.38 (.15)	.38 (.14)	n.s.
	Wilcoxon	<0.05	n.s.	n.s.	
Dacc	p*	.14 (.03)	.11 (.02)	.09 (.02)	<0.01
	a**	.15 (.03)	.13 (.03)	.09 (.02)	<0.01
	Wilcoxon	n.s.	n.s.	n.s.	
D	p*	.09 (.02)	.06 (.01)	.04 (.01)	<0.01
	a**	.12 (.03)	.08 (.02)	.06 (.01)	<0.01
	Wilcoxon	<0.01	<0.01	<0.01	

* visual feedback present

** visual feedback absent

in movement time can not explain the differences in accuracy.

The initial acceleration (A70) showed a large variability. The coefficient of variation (VC) of A70 -i.e. the within-subject standard deviation divided by the mean value- is presented in table II. It is obvious that the VC of the distance moved during the acceleration phase (Dacc) should be at least equal to the VC of A70 in case of an independent variation of the duration of the acceleration phase (Tacc). We found, however, a strong negative correlation between A70 and Tacc (median values of r; -0.83, -0.84 and -0.83 for the three different target distances. This resulted in a considerable reduction of the VC of Dacc with respect to the VC of A70 (see table II).

The VC of the total distance moved (D) appeared to be smaller than the VC of Dacc for all three distances (table II). These results are contrary to the notion (e.g. 6) that there is symmetry between the acceleration and deceleration phases of the movements. In case of such a symmetry the VC of Dacc and the VC of D should be equal. To investigate the relation between the acceleration and deceleration phases further we computed the correlation coefficient between Dacc and Ddec -the distance moved during the deceleration phase- (median values for r: -0.19, -0.33 and -0.56 for the three target distances in ascending order).

Movements without visual feedback

Withdrawal of visual feedback had a significant effect on movement accuracy.

The variable error increased, but differences in the group mean of the systematic error could not be shown (see table I). There was no significant effect on MF.

We could not demonstrate difference in parameters of the acceleration phase between the two feedback conditions (see table II). It appeared however that the coefficient of the correlation between D_{acc} and D_{dec} was significantly larger in the absence of visual feedback for all three target distances (median values for r : 0.47, -0.11 and -0.08).

DISCUSSION

The results of this study show a powerful variability compensating mechanism within the acceleration phase. The large variability in the initial acceleration is at least partly compensated for by adjustments of the duration of the acceleration phase. This implies that the duration of the agonist activity and the onset of antagonist activity are highly dependent on the initial open-loop controlled level of agonist activity. Withdrawal of visual feedback does not seem to affect this mechanism. This suggests that feedback of efferent information (efference copy) or proprioceptive information to the motor programme generator is responsible for the timing of these agonist and antagonist activity.

Our results indicate an asymmetry between the acceleration phase and deceleration phase. This asymmetry contributes to a reduction in the relative variability. So, the control of the size of antagonist activity is adjusted to the size and duration of agonist activity. The effect of withdrawal of visual feedback on movement accuracy (i.e. an increase of the variable error) and on the correlation between D_{acc} and D_{dec} implies that during the deceleration phase visual feedback contributes to movement accuracy in the adjustment of antagonist activity.

Research is in progress on the role of these mechanisms in the development of motor control and in movement disorders.

ACKNOWLEDGEMENTS

This research is financially supported by Ciba-Geigy and the Dutch Foundation for the Technical Sciences.

REFERENCES

1. Woodworth RS (1899) *Psychol Rev* 3: 1-114
2. Sittig AC, Denier van der Gon JJ, Gielen CCAM (1987) *Exp Brain Res* 67: 33-40
3. Angel W (1976) *Neurology* 26: 1164-1168
4. Cooke JD, Diggles VA (1984) *J of Mot Behav* 16: 348-363
5. Van den Berg R, Mooi B, Denier van der Gon JJ, CCAM Gielen, Van der Meulen JHP (1987) *Med Biol Eng Comput* 25:311-316
6. Flament D, Hore J, Vilis T (1984) *J Physiol* 349: 195-203

ACCELERATION CURVE ANALYSIS DURING FAST FORWARD ARM ELEVATION UPON DIFFERENT CONDITIONS

P. G. GATEV, N. T. TANKOV and G. N. GANTCHEV
Institute of Physiology, Department of Motor Control, Bulgarian Academy of Sciences, 1113 Sofia, Bulgaria

INTRODUCTION

Acceleration curve analysis was widely involved in the study of programmed movements^{1,2}. It was confined however within the limits of the early part of the acceleration curve of the fast movement performed during sitting position in a horizontal plane with arm and forearm supported. In the present study we have also used this kind of analysis to reveal which of amplitude and temporal parameters of an acceleration curve remain invariant and which of them change with task conditions, namely different start position, movement amplitude and load. The experimental design was arranged to make an attempt to study the movement in a frontal plane during standing. In that case the task was complicated by postural requirements and dynamic changes in the load manipulation due to different musculo-skeletal geometry with different arm position in the workspace. Another attempt was made to take into account the later part of the acceleration curve which reflected bracking the movement and arm positions corections superimposed on the whole history of movement resulting in the kinetic and stored elastic energy³.

METHOD

Seven males were studied, aged from 20 to 55 years without problems of joint or muscular origin. The subjects were easy standing and were instructed to keep the elbow straight and the forearm semi-pronated during as fast as possible forward arm elevation. The linear accelerometric transducer was in the hand, strictly oriented in the direction of the movement. The frequency response of the whole accelerometric system was linear from 2Hz to 16kHz. Four series were performed: a/ from start position of 0° to 5°, 45° and 90° forward arm flexion; b/ from start position of 45° to 90° forward arm flexion; c/ and d/ as above but the arm was loaded with a load of 2 kg before the movement. The following parameters were measured: i/ amplitudes of early acceleration (A+); and deceleration (A-); ii/ time parameters of the early part of the curve: time to peak acceleration

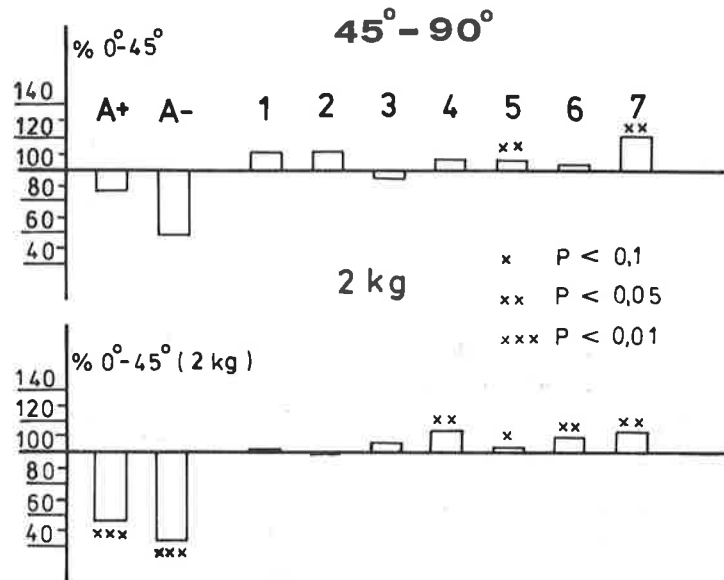


Fig. 1. Changes in the amplitude and time parameters of acceleration curve with different start positions. Top- arm unloaded. Bottom -arm loaded.

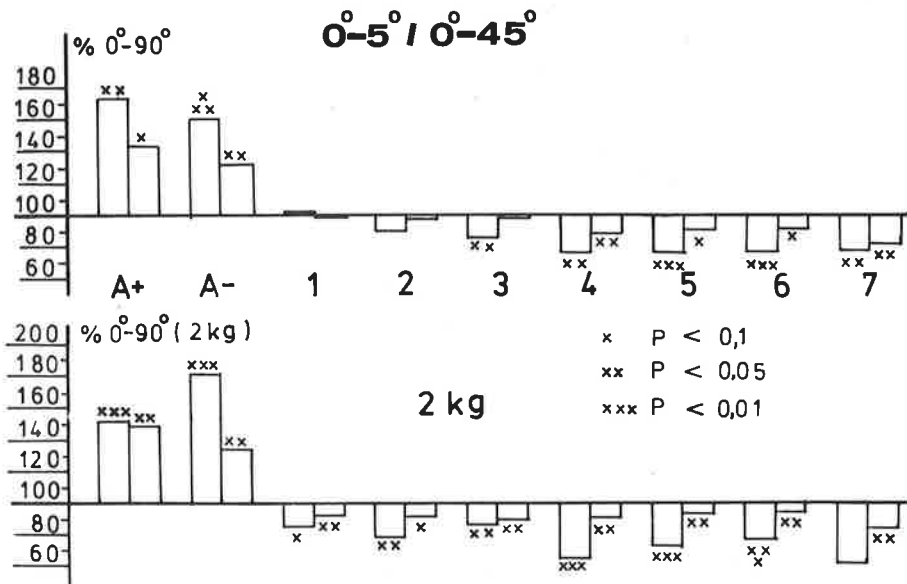


Fig. 2. Changes in the amplitude and time parameters of the acceleration curve with the change of the amplitude of the movement. Top- arm unloaded. Bottom arm-loaded.

(parameter 1), time to its end (parameter 2), time to peak of deceleration (parameter 3); iii/ time to the beginning of braking the movement (parameter 7); iv/ time parameters of the later part of the curve: times from the movement onset to the first zero crossings after the braking (parameters 4, 5 and 6). All parameters were calculated as a mean of 15 trials. The statistical significance was evaluated by means of Student's two tailed pair test.

RESULTS AND DISCUSSION

The main finding was that the number of invariants were not constant, but task dependent and diminished with the increase of task difficulty. The change of start position with arm unloaded lead to an increase in a few parameters of the later part of the curve only in the case of start position of 45° (Fig. 1 top). This change might be due to the changes of the musculoskeletal geometry when the start and target points were shifted by a 45° forward arm flexion. When the arm was loaded, a significant decrease of the acceleration and deceleration amplitudes was added to the above changes (Fig. 1 bottom). When the start position was 45° forward arm flexion many of the motor units which would have been involved in the movement had been already active at the start. This lead to the diminution of capacity of mechanisms for compensation of nonlinear properties of the muscle and for position corrections during braking. It was reflected also in the increase of time to braking of the movement (parameter 7). When the start position was one and the same, but the movement amplitude decreased and the arm was unloaded (Fig. 2 top) the time parameters of the later part of the curve decreased and the amplitude parameters increased. Time to the braking of the movement decreased also. From the early time parameters only the time to peak of deceleration showed a significant decrease with amplitude of 5° compared with 90°. When the arm was loaded (Fig. 2 bottom) a significant decrease of the early time parameters with the decrease of movement amplitude was found in addition to all previous changes. All these changes were inproportional to the movement amplitude.

Another interesting finding was that amplitude of deceleration was found to be significantly higher than amplitude of acceleration (p < 0,05) in all series except the movement from 45° to 90° with arm unloaded and probably the movements from 0° to 45° with arm unloaded and from 45° to 90° with arm loaded (p < 0,1).

Our results suggested that the programming of the fast aimed movements depends on the task conditions. Probably different compensatory mechanisms were consecutively involved. Loading, for example led to the extension of the time for the movement beyond 190 ms. and more time was allowed for visually guided corrections⁴. Second mechanism was the reflex gain programming varying with the preexisting level of motor discharge⁵, the programming itself was closely connected with the stiffness regulation⁶. Next possible mechanism was the modulation of triphasic pattern programming and especially programming of the size and duration of the first agonists burst as well as phase relationships between the three bursts^{7,8}. Nevertheless all these mechanisms have their limitations due to the neural constraints⁹. In summary, we believe that two main conclusions might be drawn. First, the change of the movement amplitude lead to a more restricted number of invariants than the change in the start position in our case. Second, the diminution of number of invariants with increase of task difficulty followed a sequential order. The time parameters of the later part of the curve were affected first, followed by the amplitudes of initial acceleration and deceleration and the time parameters of early part of the curve at the end.

REFERENCES

1. Bouisset s, Lestienne F (1974) Brain Res 71:451-457
2. Schmidt RA, Zelaznik HN, Howkins B, Frank JS, Quinn JF (1979) Psychological Review 85:415-441
3. Partridge LD (1965) American J of Physiol 20:150-156
4. Keele SW, Posner MI (1968) J Exp Psychol 77:353-363
5. Matthews PBC (1986) J of Physiol 374:73-90
6. Crago PF, Houk J, Hasan Z (1976) J Neurophysiol 39:925-935
7. Cooke JD, Brown S, Forget R, Lamarre Y (1985) Exp Brain Res 60:184-187
8. Brown SH, Cooke JD (1986) J Human Mot Stud 12:297:312
9. Benecke R, Meinck H-M, Conrad B, (1985) Exp Brain Res 59: 470-477

Activation patterns of motor units

THE COMMON DRIVE OF MOTOR UNITS

CARLO J. DE LUCA

NeuroMuscular Research Center, Boston University, Boston, MA 02215

INTRODUCTION

To understand the strategy (or strategies) which the nervous system uses to control motor units for the purpose of generating and modulating the force of a muscle, three central questions arise: (1) Is there a strategy or are there rules which govern the process of motor unit recruitment? (2) Is there a strategy or are there rules which govern the behavior of firing rates of active motor units? (3) Is there any interaction between recruitment threshold and firing rate? The first question has received considerable attention. Notable contributions have been made by Henneman and his colleagues. The other two questions have not engaged a comparable level of excitement, possibly due to the technical complexity of the experiments necessary to address it.

BASIC ASPECTS

To address properly the question concerning the behavior of the firing rate it is necessary to observe it as a function of time and force of contraction. Several reports (Tanji and Kato, 1973; Monster and Chan, 1977; and others) have all demonstrated that the firing rates of active motor units increase proportionally with increasing force output. This implies that increased excitation to the muscle motoneuron pool increases the firing rates of all the active motor units.

This commonality in the behavior of the firing rates was studied in detail by De Luca, *et al.* (1982b). We observed the behavior of the firing rates of up to eight concurrently active motor units in the first dorsal interosseous and deltoid muscles during various types of isometric contractions: attempted constant force, linear force increasing and force reversals. Since that study, we have performed similar investigations on the flexor pollicis longus, extensor pollicis longus, tibialis anterior, extensor carpi ulnaris and extensor carpi radialis longus. Also, the firing rates of 11 consecutively active motor units have been studied in more recent works.

The studies of De Luca *et al.* (1982 a,b) described a unison behavior of the firing rates of motor units, both as a function of time and force. This property has been termed the *common drive*. Its existence indicates that the nervous system does not control the firing rates of motor units individually. Instead, it acts on the pool of the motoneurons in a uniform fashion. Thus, a demand for modulation of the force output of a muscle may be represented as a modulation of the excitation and/or inhibition on the motoneuron pool. This is the same concept which comfortably explains the recruitment of motor units according to the size principle. Since our initial report, other independent reports of the common drive have been published (Nordstrom *et al.*, 1986; Stashuk and deBruin, 1988).

Figure 1a provides an example of the behavior of the firing rates of four motor units during an attempted constant-force contraction of the deltoid muscle. The firing rates have been filtered with a 400 ms Hanning window. Note the common behavior of the fluctuations of all the firing rates. This commonality becomes more apparent in Figure 1b which presents the cross-correlations of the firing rates. The high correlation-values and the lack of any appreciable time shift with respect to each correlation function indicates that the modulations in the firing rates occur essentially simultaneously and in similar amounts in each motor unit. If the firing rates of the motor units are cross-correlated with the force output of the muscle, an appreciably high cross-correlation is also evident (Figure 1c). The peaks of the cross-correlation functions occur at a time corresponding to the time delays of the force built-up after excitation in the muscle fibers. This testifies to the fact that the fluctuations in the force output are causally related to the fluctuations in the firing rates.

Similar behavior is seen during force-increasing and force-decreasing contractions (Fig. 2). In this case, the firing rate fluctuations are superimposed on a "bias" firing rate value. This bias value displays the common and proportional association with force output which has been documented by several investigators. That is, as an increase in the force output of a muscle is required, all the active motor units increase their firing rates proportionally. Given that the initial (or minimal) firing rates of motor units at recruitment are quite similar, it follows that the higher force-threshold, faster-twitch motor

units will always have lower firing rates than the lower force-threshold, slower-twitch counterparts. Recently this behavior has also been observed in the human massator muscle by Miles and Turker (1987). This arrangement indicates a peculiarity of motor unit control during voluntary contractions. That is, the firing rate behavior is not complimentary to the mechanical properties of the motor units. Higher threshold motor units tend to have shorter contraction times and twitch durations, and thus require higher firing rates to produce fused contractions. De Luca *et al.* (1982a) calculated that in some cases, the faster-twitch motor units never achieved a fused contraction during voluntary effort. This behavior provides a basis for the concept that in man, the full force generation potential of the muscle fibers may not normally be utilized during voluntary contractions. Conceivably, it may be held in abeyance for occasional dramatic displays of force. The relatively lower firing rates of the fast fatiguing motor units provide for the precautionary employment of these motor units, making them able to sustain their force generating ability longer.

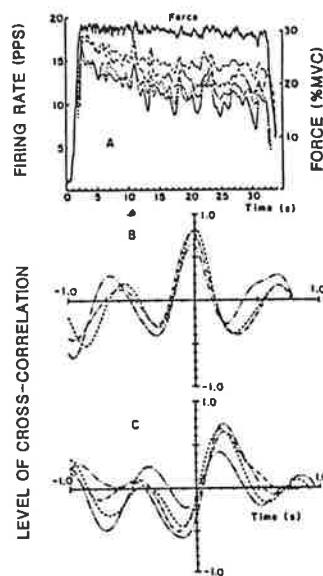


Figure 1

Common Drive Across Muscles: The *common drive* has also been observed to exist in an agonist-antagonist set of muscles simultaneously. In a recent study involving the flexor pollicis longus and the extensor pollicis longus, the sole controllers of the inter-phalangeal joint of the thumb, De Luca and Mambrito (1987) have noted the *common drive* in both muscles. During voluntary stiffening of the inter-phalangeal joint, with near zero net torque, the firing rates of motor units in the two muscles were highly correlated with essentially no time shift. Although the force or torque output was approximately zero, the *common drive* was evident even among motor units of the two muscles. This particular example points to the necessity of associating the behavior of the motor unit control to the effect on the motoneuron pool rather than on the output of the joint. (See De Luca and Mambrito, (1987)).

Common Origin of Nerve Fibers? There remains the concern that the cross-correlation observed in the flexor pollicis longus and the extensor pollicis longus may be partially due to the common origin of the major portion of their efferent nerve fibers, the C_8 root. The anatomical proximity of the two motoneuron pools might facilitate the interaction of the firing rates. To dispel this concern, Kamen

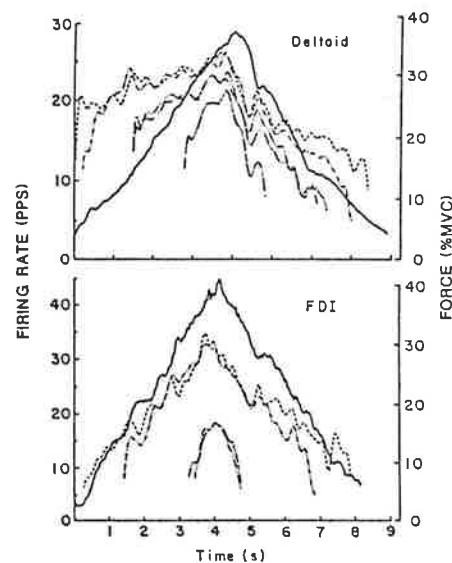


Figure 2

and De Luca studied the right and left tibialis anterior muscles which were simultaneously coactivated isometrically at 30% maximal voluntary level (MVC). In this case, the motoneuron pools do not share physical proximity. Similar experiments by Kamen, Solar and De Luca involving the ipsilateral first dorsal interosseous and tibialis anterior muscles showed no evidence of cross-correlation of the motor unit firing rates in four subjects.

Stretch Reflex? Within one muscle, existence of *common drive* could be partially explained by the wide-spread homogeneous influence of the stretch reflex mechanism, especially the arborization of the Ia fibers. However, the reciprocal arrangement of the Ia and Ib fibers with the alpha motoneuron fibers of antagonist muscles does not favor formation of zero-time shift firing rate fluctuations between the motoneuron pools of the two muscles. This concept is supported by the finding which show that during coactivation, the average value of the maximal cross-correlation of the firing rates of motor units among antagonist muscles is significantly ($P < 0.0001$) lower, approximately 60% that of the motor units in the individual muscles.

Functional Association or Mechanical Linkage of Muscles? The existence of the *common drive* among the antagonist muscle set during co-activation may be used to argue for a functional association or mechanical linkage between the muscles. Their cross muscle behavior was investigated further by cross-correlating the firing rates of motor units in the right and left first dorsal interosseous muscle when they were contracting in a mechanically coupled fashion (the two index fingers abducting against each other) and when they were not in contact. The *common drive* was seen only when the index fingers were in contact. This latter observation argues for the need for a mechanical linkage between two muscles for the *common drive* to exist. However, another set of experiments performed on simultaneously dorsiflexing but not touching tibialis anterior right and left muscles did show *common drive*. In this case, the *common drive* cannot be attributed to mechanical coupling, and is most likely due to tightly-coupled spinal connectives which are more prevalent in lower limbs than in upper limbs.

Central or Suprasegmental Origin? The notion that the *common drive* may be at least in part, of central origin is supported by the observations of Fetz and Cheney (1980) and Cheney and Mewes (1986). They reported the existence of corticomotoneuronal cells in the pre-motor cortex and rubromotoneuronal cells whose activity was noted to be correlated to motor unit action potentials in groups of simultaneously active muscles in the forearm of primates executing coordinated volitional contractions. Their results suggest that individual cortical cells have a connection to motor units in separate muscles. Such an arrangement could be exploited as a mechanism for imparting the *common drive*. However, more direct proof is required for a convincing argument.

The role of suprasegmental versus segmental sources for the *common drive* remains to be clarified.

Synchronization of Discharges? The presence of the high level of cross-correlation in the firing rate cannot be interpreted as evidence of motor unit discharge synchronization. It simply means that the average pulses per epoch of time discharged by one motor unit behave similarly to those of all the other active motor units in the same epoch of time. It is, therefore, an indication of the control of motor units over a larger time scale than that which effects the properties of synchronization that relate to individual discharges of motor units.

If synchronization of motor unit discharges were studied by cross-correlating the interpulse intervals directly, synchronization may or may not be seen. A study currently in progress in our Center is beginning to show that synchronization of discharges occurs sporadically during a substantial contraction. The fact that the firing rates of motor units calculated over a window of 400 ms, or approximately 6-8 pulses, are cross-correlated; while the pulse-to-pulse discharge does not necessarily show any evidence of synchronization implies that the nervous system transmits information through groupings of discharge rather than by individual discharges. In fact, studies involving only the analysis of individual discharges may reveal more about the connections of the neurons rather than the information transmitted through them.

Low-Pass Filtering at the Anterior Horn These observations suggest that the anterior horn in the spinal cord behaves as a low-pass filter which demodulates the low-frequency from the discrete discharges of the numerous neural inputs that converge upon it. It is this low-frequency (1-2 Hz) information in the firing rates which modulates the force output of the muscle. The muscle fibers cannot respond mechanically to the individual discharges. Thus, it follows that the low-pass operation performed to calculate the firing rates reveals behavioral information, such as the *common drive*, of the motoneuron discharges.

Properties of the Common Drive In general, during isometric contraction, the concept of the *common drive* embodies the following behavioral properties:

1. The average firing rates of all motor units are modulated simultaneously, or with a relative delay of a few milliseconds.
2. The noisy modulation of the average firing rates of the motor units causes a modulation in the force output of a muscle; consequently, the force cannot be strictly isometric.
3. The average firing rates of motor units vary in proportion to the net excitation present in the motoneuron pool; with the earlier recruited motor units having greater average firing rates than the latter recruited motor units.
4. During force diminution, the earlier-recruited faster-firing motor units decrease their average firing rate before the later-recruited slower-firing motor units. This behavior complements the mechanical properties and provides a control strategy which enables all the motor units to provide their force contribution effectively.

Acknowledgement

This work was accomplished with the combined contributions of many of my associates and students. Financial support for this work was provided by Liberty Mutual Ins. Co.

REFERENCES

- Cheney, P.D. and Mewes, K.N. Properties of rubromotoneuronal cells studied in the awake monkey. *Abst. of Symposium on Neural Control of Limb Movement*, 1986.
- De Luca, C.J., LeFever, R.S., McCue, M.P., and Xenakis, A.P. Behaviour of human motor units in different muscles during linearly varying contractions. *J. Physiol.*, 1982a, 329: 113-128.
- De Luca, C.J., LeFever, R.S., McCue, M.P. and Xenakis, A.P. Controls scheme governing concurrently active human motor units during voluntary contractions. *J. Physiol.*, 1982b, 329: 129-142.
- De Luca, C.J. and Mambrito, B. Voluntary control of motor units in human antagonist muscles: Coactivation and reciprocal activation. *J. Neurophysiol.*, 1987, 58: 525-542.
- Fetz, E.E. and Cheney, P.D. Postspike facilitation of forelimb muscle activity by primate corticomotoneuronal cells. *J. Neurophysiol.*, 1980, 44:751-772.
- Miles, T.S. and Turker, K.S. Decomposition of human electromyogramme in of an inhibitory reflex. *Exp. Brain Res.*, 1987, 65: 337-342.
- Monster, A.W. and Chan, H. Isometric force production by motor units of extensor digitorum communis muscle in man. *J. Neurophysiol.*, 1977, 40: 1432-1443.
- Nordstrom M.A., Miles, T.S. and Turker, R.S. Evidence of common drive in human masseter. *Proc. of the 30th Int. Congress of Physiological Sciences*, 1986, 111.01.
- Stashuk, D. and de Bruin, H. Automatic decomposition of selective needle detected myoelectric signals. *IEEE Trans. Biomed. Eng.*, 1988, 35: 1-10.
- Tanji, J. and Kato, M. Firing rate of individual motor units in voluntary contraction of abductor digiti minimi muscle in man. *Exper. Neurol.*, 1973b, 40: 771-783.

REMARKABLE DIFFERENCES IN MOTOR-UNIT ACTIVATION DURING SLOW ISOTONIC MOVEMENTS AND ISOMETRIC CONTRACTIONS

A.A.M. TAX, J.J. DENIER VAN DER GON, C.C.A.M. GIELEN

Dept. of medical and physiological physics, University of Utrecht, P.O. Box 80.000, 3508 TA Utrecht (The Netherlands)

INTRODUCTION

We have compared muscle activation in the control of slow isotonic movements and of slow isometric contractions. Specific attention has been given to the contribution that the two force-grading mechanisms, the recruitment of motor units and the modulation of the firing frequency of motor units already recruited, make to movement tasks¹.

By using intramuscular fine-wire electrodes, we have recorded motor-unit activity in the m. biceps brachii both during isometric contractions and during slow isotonic flexion and extension movements with a constant angular velocity in the elbow joint.

METHODS

During the experiments the right arm of the subject was 80 deg abducted and supported under the elbow joint. The wrist was tightly fixed in a wrist holder. Two types of trial can be distinguished: 'isometric' and 'isotonic'.

Isometric. In this condition the wrist holder was fastened in such a way that no movement was possible in any direction. The angle between upper arm and forearm was 100 deg (full extension corresponds to 180 deg). The subject was asked to slowly increase the isometric flexion torque up to typically 20% of the maximum

¹A paper, in which these experiments are discussed in more detail, is submitted for publication to *Experimental Brain Research*.

voluntary contraction.

Isotonic. The forearm was free to move in flexion/extension direction. Before each trial the experimenter increased the preload in extension direction up to a certain torque level. To counteract the preload the subject had to exert a constant flexion torque. Then the subject was asked to move the forearm from 90 deg to 110 deg (extension movement) or from 110 deg to 90 deg (flexion movement) with a constant velocity.

RESULTS

Recruitment behaviour. During isometric trials the recruitment threshold was determined for each motor unit under study of m. biceps. Then it was investigated whether the same motor unit was active or not for different combinations of torque and movement velocity. In this way it was possible to determine, for each movement velocity, the recruitment threshold for each motor unit. Compared to the recruitment threshold for 'isometric' contractions the recruitment threshold for 'isotonic' movements is considerably decreased, not only for active shortening (flexion movement) but also for active lengthening (extension movement) of the m. biceps brachii. This decrease was already found for angular velocities as low as 2 deg/s. At increasing velocities the recruitment threshold remains approximately constant. The order of recruitment during successive 'isotonic' trials remains constant and is in fact the same as found in 'isometric' trials.

Firing frequency behaviour. At an elbow angle of 100 deg the motor-unit firing frequency (i.e. the number of action potentials per second) was determined for each 'isometric' trial both at recruitment and at higher torques. Also, for each 'isotonic' trial with a prescribed angular velocity of 3 deg/s the motor-unit firing frequency of the same unit was determined near an

elbow angle of 100 deg. At a particular flexion torque above the recruitment threshold for 'isometric' contractions, the motor-unit firing frequency is significantly higher for isotonic flexion movements and tends to be lower for isotonic extension movements than for 'isometric' contractions.

The minimum initial firing frequency at which the motor unit starts firing regularly is higher for 'isotonic' flexion movements and lower for 'isotonic' extension movements than for 'isometric' contractions. It can be concluded that the initial firing frequency of a motor unit of m. biceps is certainly not the same for different tasks ('isometric', 'isotonic' flexion movement and 'isotonic' extension movement).

CONCLUSIONS AND DISCUSSION

It can be concluded from these results that the concept of one single activation parameter (e.g. the total synaptic drive) cannot account for the motor-unit behaviour observed during our experiments. Firing frequency at recruitment is not the same during different movement tasks. The motoneurone starts firing at recruitment with a higher firing frequency during flexion movements than during isometric contractions. The motoneurone starts firing with a lower firing frequency during extension movements than during isometric contractions. So, at least two activation parameters are needed to describe the activation of a motoneurone during movement tasks. In other words, the relative contribution of both force-grading mechanisms, recruitment and modulation of firing frequency, is different for different tasks.

The recruitment threshold of all motor units of m. biceps brachii is considerably lower during slow isotonic movements than during slow isometric contractions. So, during an identical exerted flexion torque many more motor units of m. biceps are

active during slow movements than during isometric contractions. In the case of flexion movements the firing frequency is also increased compared to the firing frequency during isometric contractions. We conclude that the motor units of m. biceps clearly contribute relatively stronger to the total exerted flexion torque during an isotonic flexion movement than during an isometric contraction.

It was checked whether co-contraction occurred during our experiments. It can definitely be excluded. Apparently the distribution of activity among flexor motoneurone pools is different for isotonic movement tasks and isometric tasks. In fact, preliminary results indicate that a redistribution of activity has taken place between the motoneurone pools of m. biceps and m. brachialis which might partly explain our findings: during movement tasks the summing units of the m. biceps are more activated and the population of motor units of the m. brachialis under study is less activated than during isometric tasks.

FIRING FREQUENCY DURING MAXIMAL VOLUNTARY CONTRACTION

PAOLO PINELLI*, GIACINTA MISCIO, FABRIZIO PISANO

*1st Neurological Clinic, University of Milan. St Paolo Teaching Hospital. Via Rudini 8. 20142 Milan. Tel. 02/818441
Dept. of Neurology. Medical Center of Rehabilitation. Clinica del Lavoro Foundation. Institute of Care and Research. 28010 Veruno (NO). Tel. 0322-800101.

INTRODUCTION

As it's known since 1929 (1), the recording of a volley of discharges from single Motor Units (MUs) in the muscle during voluntary contraction, allows to know the frequency of discharges conducted along the peripheral MN: this parameter depends on the intrinsic properties of the correspondent MU (2).

However taking into account the fact that this experiment involves a "voluntary" activation we reasonably could so draw out some information also about the function of the correspondig upper MNs.

The task of the present work concerns the modalities of investigation which are more appropriate to get this double information in normal subject as a basic knowledge for an evaluation of possible changes occuring in motor neuron disease.

METHODOLOGY

The MU activity was systematically investigated from the first dorsal interosseous muscle of the hand and from the tibialis anterior of two normal subjects.

Some research has been carried out also in the biceps brachii and soleus.

The same research was conducted in 35 patients with motorneuron disease (MND).

Preliminary tests according to Marsden's methodology (3) were carried out with a 60 seconds maximal voluntary contraction (MVC). Audio-visual feedback (AVF) was associated to facilitate a maximal psychological engagement. The MVC test was repeated thrice in the same basal conditions.

Moreover graduated voluntary contractions were requested in order to add more specific information about the central control of MU recruitment and firing (4-5). The force elicited was measured with trasducers (load cell) and expressed as percentage of the force output during MVC.

Very selective recording electrodes (single fibre electrodes) were used to investigate the discharges of single MUs in normal subject.

In paretic muscles less selective needle electrodes (monopolar concentric

Adrian electrode, Basmajan electrode) and/or surface electrodes could be used, sometime in simultaneous double recording.

The investigation was directed to measure:

- 1) The firing frequency during the whole MVC test. The frequency of onset (F_o), the maximal frequency (F_{mx}) and the decline in frequency (F_x): $(F_o - F_x / F_o) \times 100$ could be extracted.
- 2) The frequency reached by the first MU when a second MU is recruited (F_r).
- 3) Double discharges, that is discharges appearing with an interval shorter than 50% of the previous interval.
- 4) Histograms of the interspike intervals (ISI) for the whole test or for some periods.

RESULTS

A) All MUs investigated showed a decline of F_{mx} during the 60" test of MVC in spite of a constant effort of contraction. Volleys with an interval longer than 300msec were excluded from the evaluation, since longer intervals may be due to an interruption of the effort. In fact the decline in frequency corresponds to a neuronal fatigue that is probably modulated by a feed-back from the muscle: the so-called MU wisdom (3).

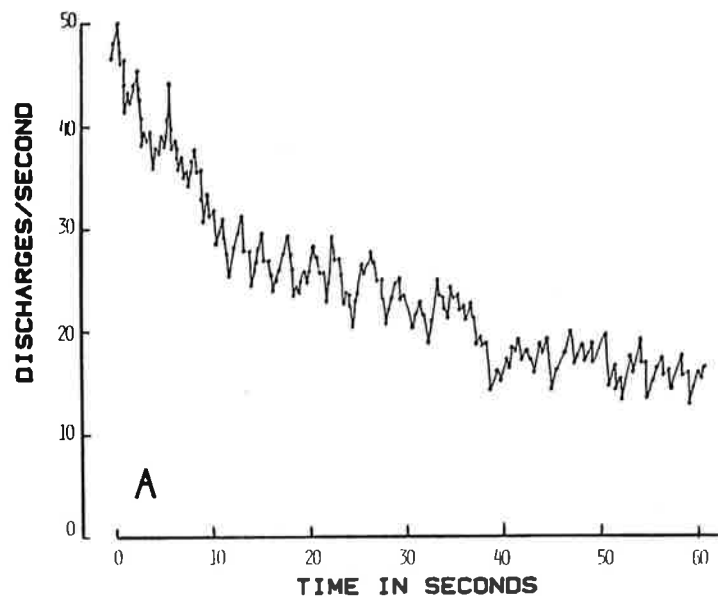


Fig. 1. Discharge frequency of single MUs during MVC for 60 seconds. Normal subject (male, 64 y.o.).

One of the three main patterns of firing of different MUs is reported in Fig.1.

In paretic muscles much lower values of endurance (few seconds) and a more marked decline of frequency were found.

B) Variations in the value of ISI is evident in the firing frequency curves reported for the whole period of 60 seconds of MVC. The changes of mean values for each ten successive intervals are rather small even in the last period of the test. More detailed evidence is given in the histogram of ISI for the first two seconds of MVC from biceps brachii.

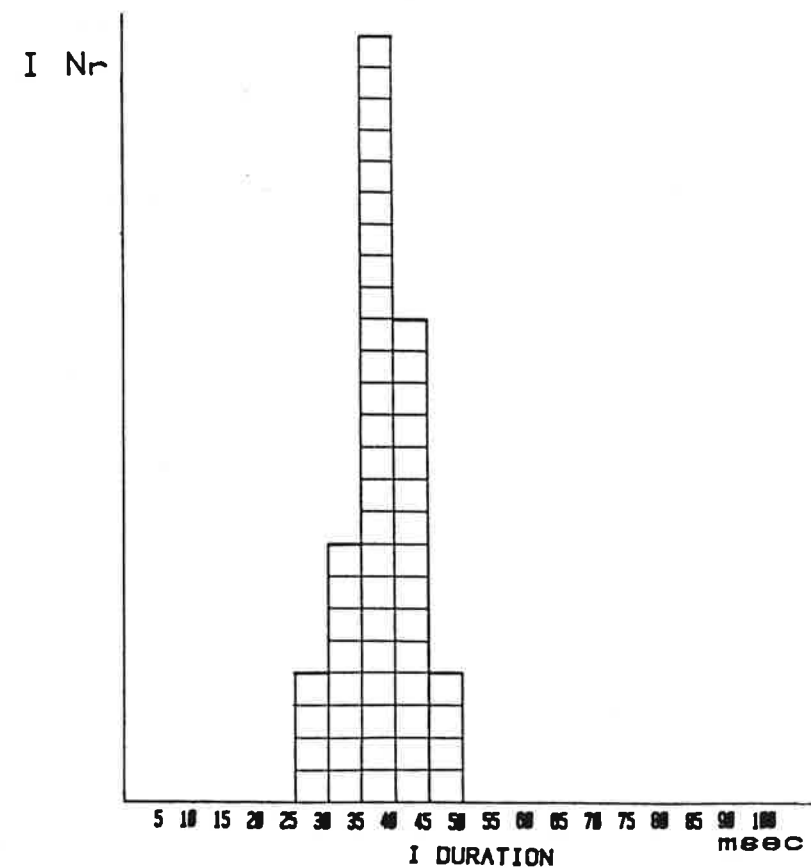


Fig. 2. G.R. Normal Biceps brachii. ISI of a single MU recorded with single fibre needle electrode at MVC during the first 2 seconds.

However in some muscle, like soleus, a much higher irregularity of the ISI has been found: the histogram for the first 6 seconds is reported in Fig. 3.

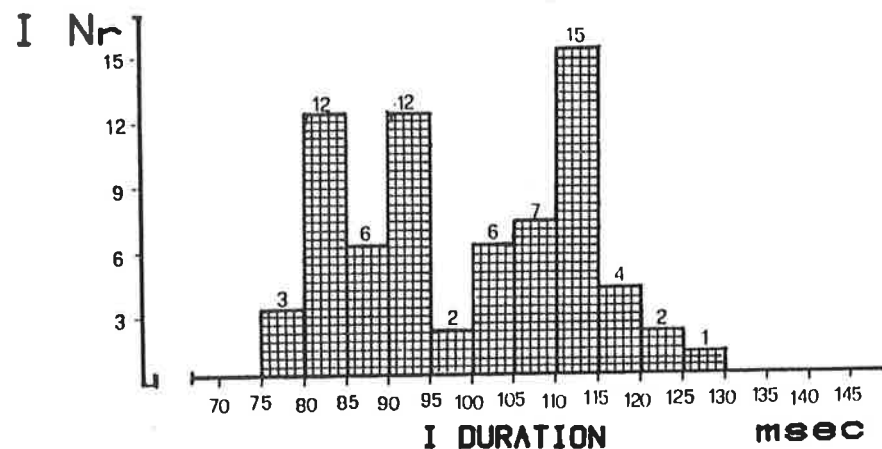


Fig. 3. P.P. Normal Soleus M. ISI of a single MU recorded with single fibre needle electrode at MVC during the first 6 seconds.

C) Double discharges without a compensatory increase in the following interval represented a rather frequent event during the first second of activation at MVC. During graduate contraction they appeared frequently also at the end of the contraction.

D) The values of Fr were very low in most MUs (about 5 Hz). Higher values corresponding to 8-12 Hz were calculated when single fibre electrodes were used and the second recorded MU belonged probably to a later order of recruitment.

DISCUSSION

The aim of our research was essentially the search for the range of variations in recruitment and firing in normal subject for the assessment of abnormalities occurring in "sick" MUs of patients affected by MND.

A preliminary condition for a reliable comparison of the MVC test concerns the constancy of the voluntary effort for 60 seconds. By performing three trials under AVF a reasonably constant motivation of the subject is maintained while the possible learning effects are cancelled. In fact we evaluated the third performance that was requested after a period of 5 minutes rest. With this

procedure fatigue after effects were also eliminated.

The fair constancy of the MU activation is well documented by the discharge frequency curves of the first dorsal interosseous and tibialis anterior and by ISI histograms of the biceps brachii. This is not the case for the soleus muscle. In agreement with the prominent tonic and automatic function of this muscle, a MU recruitment can only inefficiently be induced by voluntary effort. The voluntary activation of these kind of muscles deserves further investigation; an automatic or reflex modality of activation seems the most appropriate way to test the function of MUs in these conditions.

The elicitation of double discharges at the beginning of quick, strong contraction is in agreement with the interpretation of Burke et al. (6) who have experimentally shown that this pattern allows an optimal output force. However the occurrence of double discharges without compensatory pause in slight contraction could rather depend upon the after hyperpolarization processes of alpha motorneurons activated by the previous cortico-spinal impulses.

A correct measurement of Fr in normal conditions is quite important for evaluating neurophysiological changes of recruitment of the alpha motorneurons occurring at a constant pattern of the descending cortico-spinal impulses.

REFERENCES

1. Adrian ED, Bronk DV (1929) Discharge of impulses in motor nerve fibers. *J Physiol* 67: 119-51
2. Henneman E (1981) Recruitment of motorneurons: the size principle. In: Desmedt JE (ed) *Progress in Clinical Neurophysiology, Vol 9 Motor Unit Types, Recruitment and Plasticity in Health and Disease*, Karger, Basel, pp 16-20
3. Marsden CD, Meadows JC, Merton PA (1969) Muscular wisdom. *J Physiol, London* 200: 15.
4. Grimby L, Hannerz J (1981) Flexibility of recruitment order of continuously and intermittently discharging motor units in voluntary contraction. In: Desmedt JE (ed) *Progress in Clinical Neurophysiology, Vol 9 Motor Unit Types, Recruitment and Plasticity in Health and Disease*. Karger, Basel, pp 201-211.
5. Petajan JH (1981) Motor unit frequency control in normal man. In: Desmedt JE (ed) *Progress in Clinical Neurophysiology, Vol 9 Motor Unit Types, Recruitment and Plasticity in Health and Disease*. Karger, Basel, pp 184-200.
6. Burke RE (1981) Motor Units: anatomy, physiology and functional organization. In: Brookhart J and Mountcastle VB (eds) *Nervous System II, 1. Am Physiol Soc Bethesda, Maryland*, pp 345-422.

Spinal reflexes

STRETCH REFLEXES REGULATE STIFFNESS IN RESTORATION OF HAND POSITION

THOMAS SINKJÆR AND RYOICHI HAYASHI

Department of Medical Informatics and Image Analysis, Aalborg University, Badehusvej 23, DK-9000 Aalborg (Denmark), and Department of Medicine (Neurology), Shinshu University School of Medicine, Matsumoto (Japan).

INTRODUCTION

The objectives of the experiments were to examine how the stretch reflexes affect the inertia, viscosity and elasticity of the wrist, and thereby the dynamic relation between the force and length responses during a perturbation of the wrist palmarflexors. From the dynamic compliance function with intact and abolished reflexes the transfer function describing the reflex arc was found.

METHODS

Experimental set-up. A computer controlled torque motor was used to generate randomly timed angular displacements at the wrist joint in four normal subjects. Subjects were seated in a chair with the forearm immobilized to restrict movement to the wrist joint¹.

Data collection. Wrist position and torque were recorded together with EMG activity over the flexor carpi radialis and extensor carpi radialis muscles. At random times, step perturbations of 1.8 Nm lasting for 50 ms were introduced. These resulted in an extension of the palmarflexors at the wrist joint. The subjects were instructed neither to assist nor to resist the perturbation.

Data analysis. The compliance transfer function, relating position $P(t)$ and torque of the wrist $T(t)$, was analysed from a non-parametric model² and a parametric model. A second order parametric model $COM(s)$ described the inertia (I), viscosity (D) and elasticity (K) of the wrist:

$$COM(s) = P(s)/T(s) = [Is^2 + Ds + K]^{-1} \quad (1)$$

Agarwal and Gottlieb³ used a similar transfer function to describe the dynamic ankle compliance and Hunter and Kearney⁴ the inverse of the transfer function to describe the dynamic ankle stiffness. The dynamic compliance $COM(s)$ was calculated around an operating point, where the background values of the measured torque and position before a perturbation were subtracted.

The reflex arc transfer function RFX(s). If we consider the torque around the wrist $T(s)$ as input to a feedback system, and the position of the wrist as the output $P(s)$, we can define two transfer functions. One function describes the properties of the feed forward system, $COM_a(s)$, relating the input signal $T(s)$ minus a feedback signal $R(s)$ to the output $P(s)$. One relates the output signal $P(s)$ to the feedback signal $R(s)$, called the reflex arc transfer function $RFX(s)$. $COM(s)$ in equation 1 can here after be written as:

$$COM(s) = \frac{COM_a(s)}{1 + COM_a(s)RFX(s)} \quad (2)$$

Knowing $COM(s)$ and $COM_a(s)$ we can calculate $RFX(s)$ from equation 2:

$$RFX(s) = \frac{1}{COM(s)} - \frac{1}{COM_a(s)} \quad (3)$$

RESULTS

Subjects maintained the wrist in a target zone at the neutral position against an extension torque produced by a torque motor. After control trials a blood pressure cuff was inflated to 200 mmHg pressure around the upper arm for 20 minutes and the experiments were repeated. The reflex EMG levels were then decreased to less than 15% of control levels.

In the intact limb, the original wrist position was quickly restored after the extension perturbation. This restoration was accompanied by a reflex burst of EMG activity in wrist flexors occurring between 30 and 90 ms after the perturbation onset. During ischemia, the wrist was displaced further from the initial starting position by the perturbation even though the applied torque by the motor was the same (1.8 Nm in 50 ms). During ischemia, the original wrist position was eventually achieved after approximately 500 ms⁴.

Figure 1 shows the position of the wrist and the torque around the wrist before and after stretch reflexes were abolished from 500 ms prior to torque input to 500 ms after.

Changes in inertia, viscosity and elasticity after abolishing the stretch reflexes.

To estimate the changes in the restoration of the movement after abolishing the reflexes, the inertia, viscosity and elasticity were predicted from a second order parametric model (equation 1). The variation in these parameters is shown below.

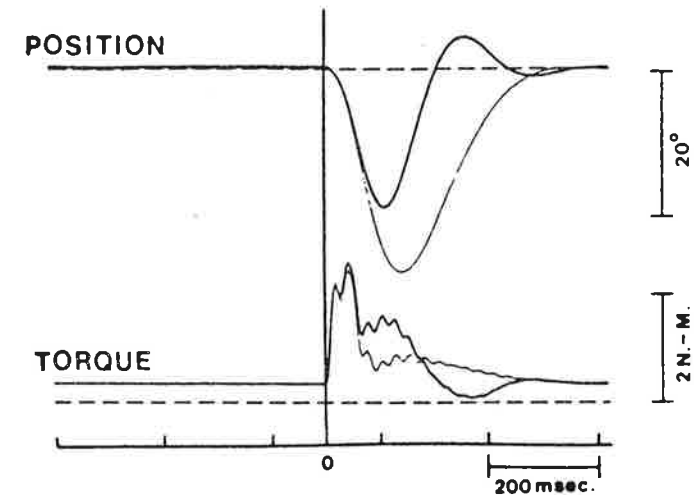


Figure 1. The position and the torque around the wrist before and after abolishing the stretch reflexes (responses with abolished reflexes are marked with dotted curves). The torque input was applied at time zero and all conditions were matched prior to a stretch of the flexor muscles. The data shown was averaged over 10 trials.

	<u>Inertia</u> [Nm/degree*s ²]	<u>Viscosity</u> [Nm/degree*s]	<u>Elasticity</u> [Nm/degree]
With intact reflexes	0,00148	0,01074	0,45
With abolished reflexes	0,00142	0,01238	0,21
Per cent changes	5	-13	114

Table 1 The mean values before and after abolishing the reflexes and per cent changes of the predicted inertia, viscosity and elasticity from four subjects.

Characteristics of the reflex arc.

Figure 2 shows the gain of the reflex arc and the phase of the open loop system $COM_a(s)*RFX(s)$ estimated by a nonparametric and a 5th order parametric system identification technique. The gain of the reflex arc was flat from 0 to 5 Hz with an amplitude of -25 dB Nm/degree. It then increased and crossed 0 dB at 12 Hz. The phase of the open loop system was turned 180 degrees at 6 Hz, which resulted in a stable system at frequencies where the gain was larger than 1. Similar results were obtained in all subjects.

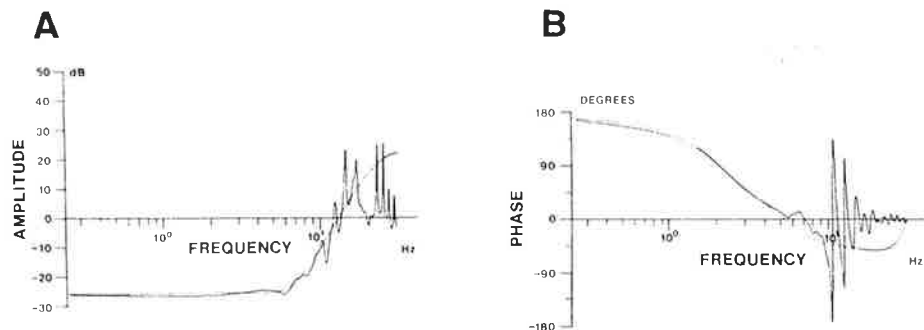


Figure 2. An estimate of the transfer function describing the reflex arc. A) The gain of the reflex arc in dB Nm/degree predicted from the frequency responses in the non parametric identification and a 5th order parametric model. (The parametric model is shown with dotted lines). B) The phase of the open loop system $RFX(s) \cdot COM_a(s)$. Same subject as in figure 1.

DISCUSSION

The data in table 1 suggest that the stretch reflexes only modifies the stiffness of the wrist, while inertia and viscosity is locked to the intrinsic properties of the wrist. It was calculated that the reflex arc increased the natural frequency of the wrist by 50% and fasten the response by decreasing the damping ratio by 42% in mean. These observations are in agreement with the "equilibrium point" hypothesis of Feldman⁵ as applied to intact and deafferented muscle, and to findings in the flexors around the ankle joint⁶.

REFERENCES

1. Hayashi R, Becker WJ, White DG, Lee RG (1987) Brain Res. 403:341-344.
2. Hunter I, Kearney RE (1983) Medical. Biological Eng. & Comp. 21:203-209.
3. Agarwal GC, Gottlieb GL (1977) Trans. Am. Soc. mech. Engrs 99:166-170.
4. Hunter IW, Kearney RE (1982). J. Biomech. 15:747-752.
4. Becker WJ, Hayashi R, Sinkjær T, White D, Morrice BL and Lee R.G. (1986), Soc Neurosci Abstr.
5. Feldman, A.G (1974) Biofizika 19: No. 4, 749-753.
6. Sinkjær T, Toft E, Andreassen S, Hornemann BC (1988) J. Neurophysiol. In press.

SPATIAL AVERAGING OF THE BIOELECTRIC DOUBLE HIT SHORT LATENCY SPINAL REFLEX

Juliusz S. Ekiel, Małgorzata J. Zieniewicz

Institute of Biocybernetics and Biomedical Engineering, KRN 55, 00-818 Warsaw, Poland

INTRODUCTION

It is known that voluntary movements are under continuous reflex control by sensory receptors. Thus investigation of reflexes provides information about the mechanisms underlying the motor control in man.

There are various methods of evoking muscle reflexes in man. One of the most popular is the electrical stimulation of a nerve or a muscle /2,5/. Another method is the investigation of muscle responses to vibrations /8/. Forced sinusoidal oscillations /3/ are also used as a forcing. Some researchers use various kinds of rapid displacements which cause the stretch of the muscles /1,6,7,10/. Mechanical forcings are not very commonly used because they are not easy to control and thus responses to stimuli are uncomparable /9,11/.

We have developed a new method of investigation of reflex bioelectric muscle activity. As the forcings evoking the reflexes we have chosen mechanical stimuli comparable with the disturbances occurring in normal everyday life.

METHOD

The experiments were performed on a healthy standing subject. The subject hold his forearm flexed /90°/ pointing forward and the thumb uppermost. The experimental arrangement with which the subject's forearm was connected near the wrist had the following parameters: moment of inertia $I_a = 0.05 \text{ kgm}^2$, angular stiffness $K_a = 38.8 \text{ Nm/rad}$. The forearm was loaded with constant mass $m = 0.5 \text{ kg}$ on a radius $r = 0.3 \text{ m}$.

The subject's task was to maintain an approximately steady position with as little muscle effort as possible and to avoid responding voluntarily to applied stimulus. The position of the subject's hand was monitored during the experiments on an oscilloscope /visual biofeedback/.

The reflexes in subject's biceps brachii were evoked by mecha-

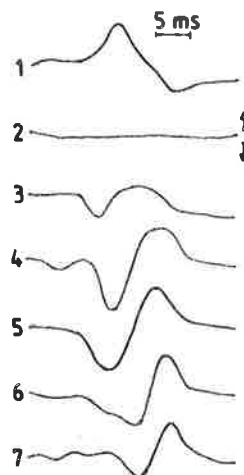


Fig. 1. Local reflex EMGs. Arrows indicate directions of the propagation of excitation wave.

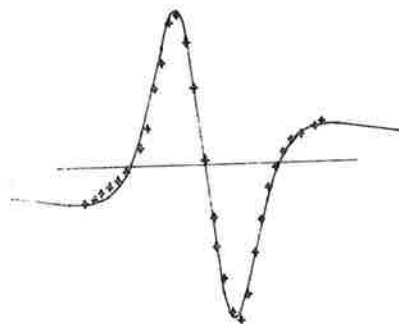


Fig. 2. Comparison of experimental data /dotted line/ with theoretical model /solid line/.

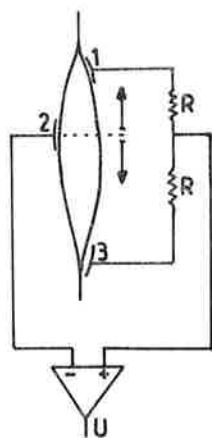


Fig. 3. Neutral zone electrodes /NZE/, where: 1,2,3 - electrodes, U - signal from NZE.

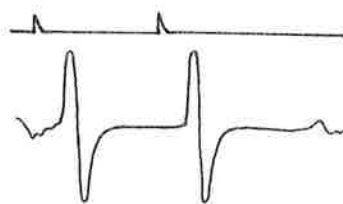


Fig. 4. Double hit reflex EMG from NZE. Upper trace - mechanical stimulus, lower trace - EMG.

nical stimulus acting on processus styloideus radii and through the bones and tendons on the muscle /4/. The electrically controlled stimulus consisted of one or two mechanical forcings of impulse type with changeable interfering delay /5-100 ms/.

For investigating the bioelectric muscle activity we used several surface electrodes placed along the biceps brachii, parallel to the arm axis. The distances between the centres of the electrodes were 1 cm. The signals from the electrodes were amplified, recorded and processed.

RESULTS

Fig. 1 shows the simultaneous registrations obtained from several surface electrodes, representing the local reflex EMGs in response to a single mechanical stimulus. This experiment enabled us to find a neutral line /Line 2/ from which the excitation wave begins to propagate in two opposite directions, ie. the directions from Line 2 to each of muscle tendon.

We analysed one local reflex EMG /Line 5/ from Fig. 1. The experimental registration was compared /Fig. 2/ with the model of electromagnetic field caused by higher order multipoles /12/. The experimental data were consistent with this model.

A new method of investigating the muscle surface EMG was developed. This method was based on the analysis of the local reflex EMGs /Fig. 1/. A new system of neutral zone electrodes /NZE/ consists of three surface electrodes /Fig. 3/ placed along the muscle in a special way: first electrode on the higher part of the biceps, as high as possible, second electrode near the neutral line, third electrode in the lower part of the biceps, as low as possible. The excitation wave begins to flow from the neutral line in opposite directions, thus the EMG signal obtained as a voltage between the first and the third electrodes can be very small or even zero. This kind of lead causes the cancelation /neutralization/ of the voltages, partly or even totally. In NZE a linear operator of spatial averaging was used. The signal U obtained from NZE is:

$$U = 0.5 / U_{21} + U_{23} /$$

where:

U_{21} - the voltage between the second and the first electrodes,
 U_{23} - the voltage between the second and the third electrodes.

Fig. 4 shows the double hit reflex EMG obtained with the help of NZE lead. The second multiphasic reflex response occurs at the

end of the silence period of the first one.

DISCUSSION

In our experiments we found a place with zero EMG signal - neutral line, so we localized the "primum movens" of the biceps brachii excitation wave, using several small electrodes placed along the muscle. The "primum movens" is near the Line 2 on Fig. 1, that is the place from which the excitation wave begins to propagate in opposite directions. Our experimental results suggest that this place is not only the "primum movens" for the bioelectric reflex activity but also for the normal voluntary activity.

Our method enabled us to investigate local /several surface electrodes/ and global /NZE/ bioelectric muscle activity. The global bioelectric muscle activity is a result of the spatial and time averaging of the local bioelectric activity of the various parts of the muscle.

The comparison of the experimental results with the theoretical model /Fig. 2/ allows for the hypothesis that the reflex excitation wave can be described by the moving multipoles of higher order.

Proposed method and our experimental results may show some new perspectives in the investigation and interpretation of the surface bioelectric field of the muscle.

REFERENCES

1. Allum JHJ, Mauritz KH /1984/ J Neurophysiol 52: 797-818
2. Brooke JD, McIlroy WE /1985/ EEG clin Neurophysiol 60: 39-45
3. Cannon SC, Zahalak GI /1981/ Proc ASME Biomech Symp AMD 43: 117-120
4. Ekiel JS, Lebedowska MK, Zieniewicz MJ /1987/ Proc Mechano-receptors Symp, Prague, Aug /in press/
5. Frank JS /1986/ EEG clin Neurophysiol 63: 361-370
6. Ma SP, Zahalak GI /1985/ J Biomech 18: 585-598
7. Matthews PBC /1984/ J Physiol London 348: 545-558
8. Matthews PBC /1986/ J Physiol London 374: 73-90
9. Ongerboer de Visser BW /1985/ In: Struppler A, Weindl A /eds/ Electromyography and evoked potentials, Springer, Berlin - Heidelberg, pp 146-153
10. Soechting JF, Dufresne JR /1980/ Biol Cybern 36: 63-71
11. Tarkka IM /1986/ Eur J Appl Physiol 55: 401-404
12. Thirring W /1978/ Klassische Feldtheorie, Springer, Berlin

ARTIFICIAL STIMULATION

Fundamental research

EFFECTS OF PATTERNED ELECTRICAL STIMULATION (PES) IN THE REHABILITATION OF THE UPPER LIMB IN CHRONIC QUADRIPLEGIC PATIENTS.

JEAN P. BOUCHER AND ANDRÉ PÉPIN

Département de kinanthropologie, Université du Québec à Montréal, Box 8888, Stat. "A", Montréal, Canada, H3C 3P8.

INTRODUCTION

The purpose of the study was to assess the effects of PES upon upper limb muscles in C4-C6 quadriplegic patients. The PES technique utilized in this study consists in stimulating two muscles (biceps and triceps brachii), according to a very specific movement pattern (i.e., elbow flexion). The electrical stimulation pattern utilized reproduces the muscle activation temporal parameters measured during an elbow flexion, that is, the duration of the biceps and triceps bursts, and the latency between the onset of these two bursts.

MATERIAL AND METHODS

Subjects

All patients were selected from the Spinal Cord Society Data and Referral system through the Spinal Cord Center. After selection, all patients were diagnosed functionally complete C4-C6 quadriplegic using standard indwelling EMG techniques, following the ASIA² guidelines. They were then allocated randomly into two groups (PES-1, PES-2) which received different stimulation patterns.

Experimental procedures

Tests. Patients were tested before and after an 8-week treatment period, and every two weeks within this period, for a total of five tests. During these tests, surface EMG recordings of the biceps (BB) and triceps (TB) brachii were carried out (using standard Beckman Ag-AgCl electrodes) during two maximal voluntary isometric flexions and extensions of the elbow joint on both sides. EMG signals were amplified (Grass P511) and for each contraction one second of EMG was digitized online (1 kHz, ISAAC 91A and Apple IIe). Then, the one second bouts of EMG signal were rectified, numerically integrated, and finally reported as a percent of the initial value.

Treatments. Patients were stimulated four times/week for eight weeks where patterns were repeated every five seconds for thirty minutes. Grass stimulators (model S88 with the train delay modification #50779) and isolation units (SIU8T), with Medtronic carbon-rubber electrodes were used for the PES treatments. Patients in the PES-1 group were stimulated according to a slow or ramp elbow flexion movement (140°/s, BB=236 ms, TB=218 ms and latency=278 ms), whereas patients in the PES-2 group received a ballistic elbow flexion pattern (600°/s, BB=150 ms, TB=74 ms and latency=150 ms). Within each

train of stimulation, the pulse duration was set at 0,2 ms and given at a rate of 45 Hz. Before each treatment, the threshold for contraction (i.e., minimum intensity to obtain a visible contraction when one train of pulses is delivered) was determined for every patient, and then the stimulation intensity was set as to obtained an efficient contraction (≈ 20 V over threshold).

RESULTS

Figure 1 presents the mean IEMG values for the right and left BB and TB muscles for the five tests.

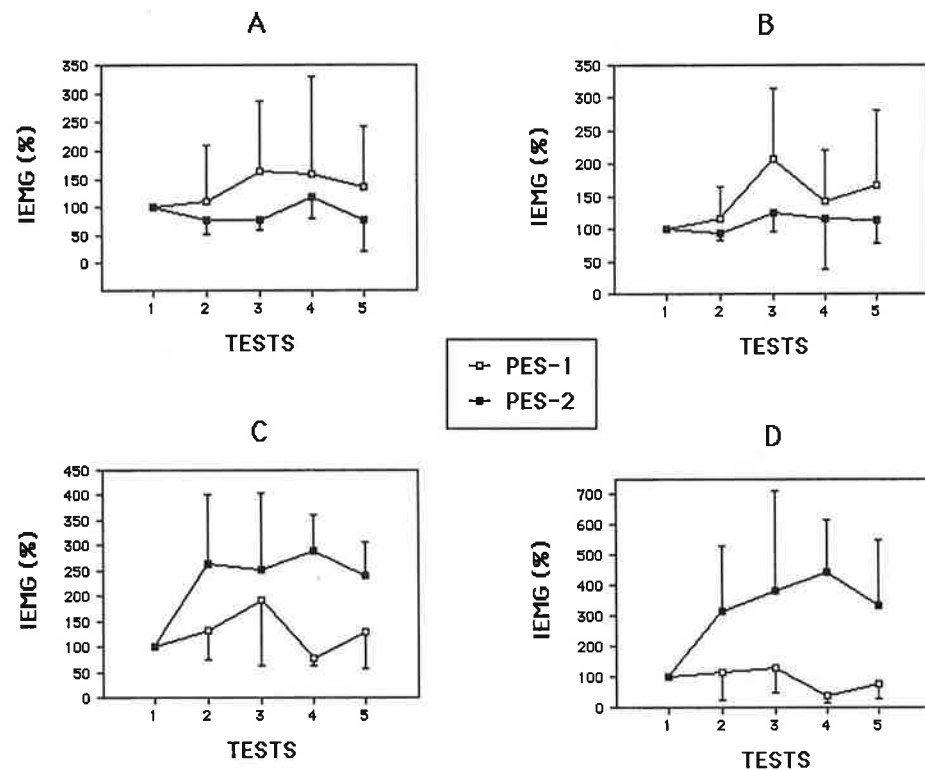


Fig. 1. Mean IEMG results for all groups, tests and conditions reported as a percent of the initial value (IEMG%). (A) Left biceps. (B) Right biceps. (C) Left triceps. (D) Right triceps.

In both groups, very little variation in IEMG values are observed for the BB muscles. Or the other hand, a difference between groups can be observed for the TB muscles. In the PES-1 group, little or no change in IEMG values is observed (variation around 100% on both the left and right TB). However, in this group one subject did show significant recuperation of voluntary EMG in both TB muscles, whereas, all other patients in the same group showed no or very little changes across tests. A significant increase in IEMG, from the first to the last test, is measured in the PES-2 group (increasing up to 300% for the left TB and 450% for the right TB). Finally, the increase in IEMG was accompanied by visible but non-functional contractions (ASIA grade 1 and 1+).

DISCUSSION AND CONCLUSIONS

The results presented above suggest that PES can elicit the recovery of voluntary contractions in paralyzed muscles. Those contractions, though not functional, are visible and can be documented through surface EMG. These results strongly suggest that PES significantly influences control mechanisms regulating muscle contractions, while it has little effect on the muscle structures and mechanisms responsible for the generation of force. These results corroborate those obtained by Boucher³ when a similar technique was utilized in intact individuals. In the latter study learning effects were obtained using PES, but no significant differences were found in muscle strength. Finally, because of stimulator limitation, the type of electrical stimuli known to induce significant modifications in the muscle physiology are different from the one used in PES⁷.

The comparison between PES patterns (PES-1 vs PES-2) shows that the ballistic movement pattern was more efficient than the ramp pattern in inducing recovery of voluntary muscle activity. The nature of the pattern used in PES thus seems to be a crucial element in the success of PES in the rehabilitation of quadriplegic patients. It has now been accepted that the mechanistic events underlying ballistic or fast movements are different from those underlying slower ramp movements¹. However, the lack of data pertaining to the rehabilitation and control of movements limits severely the ability to further discuss such an observation. Future research should then be design to investigate this very question of pattern specificity.

Finally, the following documented mechanisms support the positive effects of PES reported in this study. The unmasking of still intact but undiagnosed fibers^{4,6}, or redundant and dormant pathways⁵ could explain the recovery of voluntary contractions with PES. Indeed, PES could be deemed responsible for reprogramming or unmasking such tracts. Genesis of collateral fibers filling the synaptic void after a denervation or the loss of a given tract has been well documented⁸. In such cases, PES could then claim those newly generated collaterals through a relearning process made possible by the specific afferences that occur during PES induced contractions. As suggested by Massion⁸, tracts could acquire new functions if those conditions prevail. Peripheral roots or alpha motorneurons could furthermore generate collaterals in certain cases of denervation. In this case, PES could

render those collaterals functional and, doing so, increase the output of given motor units. This would explain giant motor unit action potentials monitored in several patients. The last mechanism considered herein, involves the modulation of the motoneuron pool threshold as suggested by Vodovnik⁹. Hence, PES could lower the threshold of a given pool and thus, could allow suprasegmental signal already present in the damaged cord to recruit motoneuron which, in turn, would recruit muscle fibres and generate a contraction.

At the present time, however, much more investigations need to be conducted in order to shed more understanding on the phenomena proposed above. Furthermore, because of the non-functional level of contraction obtained with PES alone, future projects should concentrate on using PES in conjunction with other electrical stimulation techniques in order to first recover control and then increase strength of the recovered or unmasked fibers.

ACKNOWLEDGEMENTS

The authors acknowledge the support of the Spinal Cord Society Canada and the Spinal Cord Center in Minneapolis.

REFERENCES

1. Angel, R.W. Electromyography patterns during ballistic movements in normals and in hemiplegic patients. In J.E. Desmedt (Ed), Motor unit types, recruitment and plasticity in health and disease. Karger: Basel, 347-357, 1981.
2. American Spinal Injury Association. Standards for neurological classification of spinal injury patients. Chicago: ASIA, 1982.
3. Boucher, J.P. Patterned electrical stimulation induced neuromuscular plasticity: I- Effects of averaged patterns in intact individuals. Archives of Physical Medicine and Rehabilitation, accepted for publication, 1988.
4. Gianutsos, J., Eberstein, A., Ma, D., Holland, T., and Goodgold, J. A Noninvasive technique to assess completeness of spinal cord lesions in humans. Experimental Neurology, 98 34-40, 1987.
5. Goshgarian, H.G. A possible anatomical basis for patterned electrical stimulation. Spinal Cord Society Convention, Seattle WA, July 1987.
6. Kakulas, B.A. The clinical neuropathology of spinal cord injury: a guide to the future Paraplegia, 25: 212-216, 1987.
7. Kernell, D. Physiological effects of different patterns of long-term muscle activation Neuromuscular use and disuse: Basic concepts and clinical implications. London, 1988 (In press)
8. Massion, J. The pyramidal system: recent data. In H. Hecaen and M. Jeannerod (Eds.) Du controle moteur à l'organisation du geste. Paris: Masson, 31-51, 1978.
9. Vodovnik, L. Indirect spinal cord stimulation - some engineering viewpoints. Applied Neurophysiology, 44: 1981.

FATIGUE OF QUADRICEPS MUSCLES CONTINUOUSLY ACTIVATED BY FUNCTIONAL ELECTRICAL STIMULATION IN PARAPLEGICS

M. LEVY^{*}, J. MIZRAHI^{*}, Z. SUSAK^{**}, P. SOLZI^{**}.

^{*}Dept. of Biomedical Engineering, Technion, Haifa, Israel; ^{**}Loewenstein Rehabilitation Hospital, Raanana, Israel.

INTRODUCTION

The nature of fatigue of paralyzed muscles activated by functional electrical stimulation (FES) is essentially peripheral. Of the two aspects which characterize normal muscle fatigue, the peripheral and the central (1), the latter is absent in the muscles of the lower limbs of paraplegic patients. A major expression of muscle fatigue under FES is a gradual decay in the force produced. Measurements made in the past of the external output of muscles under FES, included torque of the knee joint (2,3) of paraplegic patients or, more directly, the forces in the stimulated muscles, of experimental animals (4). These previous investigations did not study of the time-dependence of the muscle output as a result of fatigue.

If the leg of a paraplegic patient is treated as a dynamic system, having forces in the activated muscles only, it may be treated as a determinate system, allowing to non-invasively calculate the internal muscle and joint forces developed. In this study, we have developed a method for the in-vivo continuous evaluation of the Quadriceps muscle and knee joint forces of paraplegics, under FES.

MATERIALS AND METHODS

Stimulation

In this study, the Quadriceps muscles of paraplegic patients (with spinal cord injury level between D5-D11) were stimulated externally by monophasic rectangular pulse trains, with parameters ranging as follows: frequency between 18 and 30 Hz, pulse width between 0.1 and 0.3 ms and intensity up to 200 mA (corresponding to 110 V approximately). During the course of stimulation, the frequency and pulse width were usually kept constant at 20 Hz and 0.3 ms respectively. Intensity, however, if also kept constant became increasingly insufficient due to muscle fatigue, resulting in a gradual decay in muscle force.

Apparatus

The measurements were made while the paraplegic patient was in the supine lying position, with each foot hinged at the level of the ankle joint to a horizontal platform, smoothly sliding on guiding rods (Fig. 1). Hence, flexion of the knee resulted in free movement of the platform, on which the foot was supported. Load on the foot was applied by means of a horizontal force transmitted through the hinge of the ankle joint and directed towards the upper part of the body. This load could be either made constant, by means of a dead weight, or

linearly variable by means of a spring.

The platform was instrumented to enable continuous measurement of the reaction forces acting on the foot. During the tests, variations of the length l_3 , therefore also of the knee flexion angle were continuously monitored. All measurements were on-line digitized at 20 Hz into an IBM-XT computer.

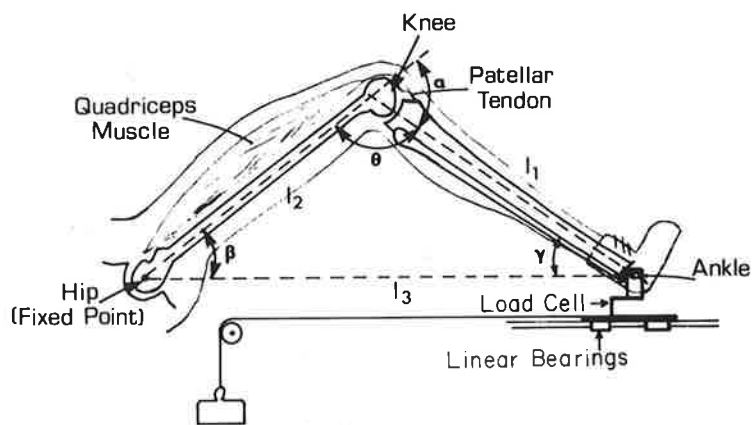


Fig. 1. Schematic description of apparatus used for loading the stimulated leg in the lying supine position, and for measuring kinematic and dynamic data.

Model

With both the measured external loads acting on the leg and its kinematics, a mechanical model was introduced to enable calculation of the force generated in the stimulated Quadriceps muscles in the process of fatigue.

The model's assumptions are as follows:

- During stimulation, all non-stimulated muscles remain passive. Hence any force developed in these muscles due to indirect stimulation, or due to spasticity is neglected. This assumption was confirmed by surface EMG measurements made in our laboratory.
- Motion of the leg in the apparatus used is essentially two dimensional. Frictional forces within the joints and ligaments forces are neglected.
- Gliding motion of the knee is neglected; the contact area in the tibio-femoral joint, represented by a point, is assumed to lie on the shank axis.
- Forces in tendons are assumed to act along their longitudinal directions.
- Hip flexion due to the high insertion of the Rectus Femoris is neglected.

The model relates together both measured (F_1 , l_3 , γ , all time dependent) and anatomical (l_1 , l_2 , W , lever arms) data, the latter obtained either directly, or from data in the literature (Figs. 1,2). The following dynamic moment equation is written about the tibio-femoral contact point k for the shank

$$\Sigma M_k(t) = I_s \ddot{\theta}(t) + m_s \bar{a}_s(t) d(t) \quad [1]$$

where, I_s is the moment of inertia of the lower leg up to the knee joint about its centroid; m_s is the mass of this segment; \bar{a}_s is the linear acceleration of the center of mass of the segment and d is the distance between the center of mass to point k .

Writing explicitly the left hand side of equation [1], see Fig. 2, enables to determine the patellar tendon force F_3 and the tibio femoral joint force F_2 . Further, by using data published for the patello femoral joint (7,8), the Quadriceps tendon force F_5 and the patello femoral joint force F_4 are calculated.

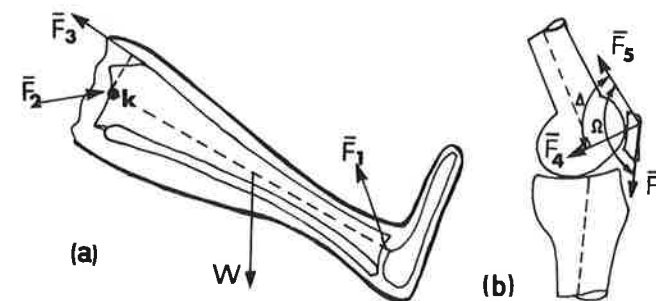


Fig. 2. Free body diagrams of the system treated: (a) Shank, (b) the knee joint and lever arms of patellar and Quadriceps tendons.

RESULTS AND DISCUSSION

The variation of the Quadriceps tendon force with knee flexion angle for various values of loading dead weights (see Fig. 1) for negligibly small accelerations of the leg, is shown in Fig. 3a. It should be stressed that the values obtained for the Quadriceps tendon force are largely sensitive to the lever arm values used for the tendons attached to the patella. For instance, the data taken from Grood et al (6) give Quadriceps force 6 times higher as that obtained from data taken from Nisell (5). The data found in the literature for the angles of these tendons as a function of knee flexion angle are indeed diverse and should therefore be properly selected. The values reported by Ahmed et al (7) are in good agreement with those of Van Eijden (8). The Quadriceps and knee joint forces at different flexion angles were described by Van Eijden et al (9), in maximum voluntary isometric contraction of normal subjects. The values obtained were higher by one order of magnitude than those seen in Fig. 3a; the differences being attributed to the fact that our experiments were 'isotonic' in nature, with relatively low loading on the leg.

Preliminary results corresponding to the variation of the knee flexion angle with time as a result of fatigue are shown in Fig. 3b. The onset of increase of

the flexion angle was almost instantaneous, whenever the stimulus intensity was just sufficient to maintain flexion at the initial state. The increase was thereafter continuous and it was curve fitted by a hyperbolic tangent curve, until full flexion was completed; the whole process lasting altogether less than 2 min. These curves should be used in the next stage of this study in order to evaluate the time dependent forces in the Quadriceps muscles and the knee joint.

Finally, it should be mentioned that surface EMG of the Quadriceps is also being recorded by our group. The repetitive pattern of the signals obtained seems to enable to define signal parameters, by which the mechanical force and corresponding EMG in the stimulated Quadriceps can be correlated.

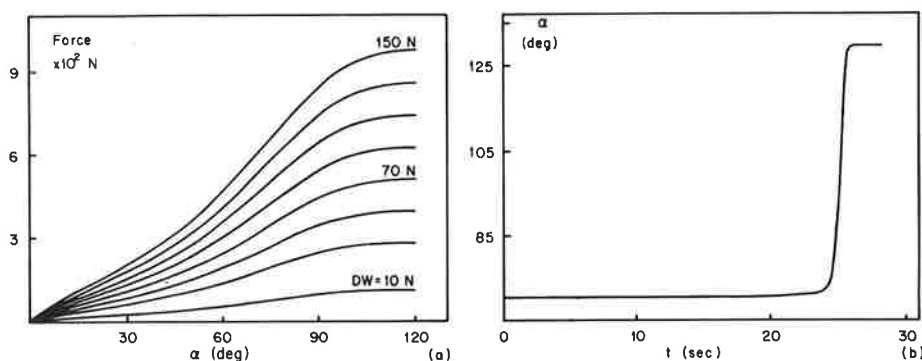


Fig. 3. (a) Variation of the Quadriceps tendon force with knee flexion angle for various values of loading (DW) of the leg, using moment arm data from (5). (b) Variation of knee flexion angle with time as a result of fatigue.

ACKNOWLEDGEMENT

This study was supported by the Technion V.P.R. Fund, the Montreal Bio-Medical Research Fund.

REFERENCES

1. Asmussen E (1979) *Med Sci Sport* 11:313-321
2. Marsolais EB, Kobertic R (1987) *J Bone Joint Surg* 69A:728-733
3. Kralj A, Bajd T, Turk R (1980) *Med Prog Technol* 7:3-9
4. Veltink PH, van Dijk JE, van Alste JA (1986) *Proc 2nd Vienna Intntnl Workshop in Functional Electrostimulation, Vienna*, pp 231-234
5. Nisell R (1985) *Acta Orthop Scand Suppl* No 216, vol 56
6. Grood ES, Suntay WJ, Noyes FR, Butler DL (1984) *J Bone Joint Surg* 66A:725-734
7. Ahmed AM, Burke DL (1987) *J Orthop Res* 5:69-85
8. Van Eijden TMGJ, de Boer W, Weijs WA (1985) *J Biomech* 18:803-809
9. Van Eijden, Weijs WA, Kouwenhoven E, Verburg J (1987) *Acta Anat* 129:310-314

THE SKELETAL MUSCLE IN ISCHEMIA AND IN REPERFUSION DURING EFFERENT MOTOR NERVE STIMULATION

SCHEJA, H. M., ECKERT, P.

Surgical University Clinic Würzburg (Director: Prof. Dr. med. E. Kern)
 Josef-Schneider-Straße 2, D-8700 Würzburg, F R G

PREAMBLE

More and more references are being made in literature to the fact that specific and non-specific damage to the skeletal muscle does not take place until the reperfusion phase. Previously it was assumed that muscle damage originated as a result of deteriorated blood circulation or during total ischemia. However, both these situations appear to have relatively little influence on the damage at least in respect of duration (1,6,9).

The direct influences caused by hypoxemia are seen as the specific damage to the skeletal muscle. The pH drops, the accumulative redox potential increases and lactacidosis forms in the muscles. On the other hand the occurring inflammation symptoms during the reperfusion through ischemia is listed as indirect damage. There is an increase in the free oxygen radicals and interference in the vessel permeability with edema formation. The electrolytes (in the effluat) such as potassium increase and calcium declines.

The main question accompanying this study is: Is it possible through the activation of the ischemia skeletal muscle by means of indirect efferent electrostimulation to influence the blood circulation or the energetic situation in the reperfusion phase?

METHOD

The study was carried out on the musculus gracilis of ten bastard dogs (18+/-3 kg body weight) whereby the muscle was perfused with hydroxemia ethylene starch (HES sterile^(R) 10%) on one collective during the ischemia, at the same time electrostimulation (0.1 ms; 20 Hz; 20 V) was applied and compared with a similar collective without electrostimulation. The ischemia phase followed the reperfusion of the musculus gracilis through the femoral vessel with the blood of the test animal. The following physical and electro-chemical parameters were determined directly in the muscle tissue by an on-line system: pH (insert micro-electrode, Type No. 83334, Ingold, Frankfurt/M; reference electrode - filled with 20% NaCl - Type No. 126387, Ingold, Frankfurt/M; pH meter, Type 742, Knick, Berlin), redox accumulative potential (single rod measuring chain, Type PT 4804 M 6, Ingold, Frankfurt/M) and temperature (digital temperature probe,

Type Tastoherm D 700, impac). The oxygen radicals were determined from the venous effluante of the *M. gracilis*, one measurement being taken preischemically and four measurements postischemically - i. e. during the reperfusion phase of the muscle - by means of chemical luminescence (counter for chemical luminescence: Berthold Biolumat LB 9500 I, graphic registration of the emission on the Servogor recorder using a calculator: Hewlett-Packard 97 S I/O Calculator). Over and above this control measurements of the sodium, potassium and calcium ions and lactate, LDH and other significant clinical and chemical parameters were taken.

Finally the partial oxygen pressure was analysed (multi-wire service electrode according to Kessler and Lübbers with on-line registration on display screen and histogram printout as required).

Used for the efferent motoric electrostimulation of the skeleton muscle was a two-channel anapulse stimulator (Type 302-T, WPI Instruments, Hamden, Connecticut, U S A) with a stimulation modulator and trigger (Type T 912, Tektronix) with the application of a 10 MHz memory oscilloscope. The nerve electrode resistance could be controlled visually and continuously as stimulation voltage on the oscilloscope and be maintained at a constant level by changing the strength of stimulation.

FINDINGS

The direct electro-chemical and physical parameters in the skeleton muscle in the ischemia show a clear change when compared with the initial phase (steady state). The muscle temperature dropped in the reduced blood circulation phase; the partial oxygen pressure was reduced in proportion to the reduction in the blood circulation. Individual of the extra-cellular oxygen radicals produced very widespread values and for this reason no determination was made in the ischemia phase.

The extra-cellular electrolyte concentrations in the postischemic phase showed a significant increase in both cases with just potassium. On the other hand the values for calcium only dropped slightly (cf. table).

The pH fell back to a level of 6.6 without stimulation, the redox potential - as parameter for the integrated redox process, particularly the mitochondrial respiration chain - dropped spontaneously from -40 mV to approx. -90 mV (Figs. 1 and 2, left). The mentioned measuring parameters were compared in the ischemia phase under efferent stimulation with the listed ischemic values without muscle activation. This showed that the pH dropped clearly to values around 6.2 and the redox potential likewise changed quickly to values of around -130 mV (Figs. 1 and 2, right).

During the reperfusion phase there was satisfactory restitution in the case of both the non-stimulated and stimulated muscle expressed by an almost levelling off of values to their initial levels (see Figures on the right).

The temperature was normalized, the pO_2 partial pressure in the superficial muscle tissue showed normal values again. On the other hand the free oxygen radicals as early inflammation indicators in the early reperfusion phase were significantly increased (fig. 3, right) compared with the non-stimulated muscle (fig. 3, left).

DISCUSSION

In the ischemic skeleton muscle there is redistributive capillary perfusion (2) in the hypoxemia. The vessel permeability is increased and shows a pronounced tendency to perform edema as well as intramitochondrial damage (7). The lactate as metabolic product of a forced anaerobe glycolysis increases (7,10) and both potassium and myoglobin are released to an increasing degree (3,8).

The findings allow the conclusion that energy rich phosphate is consumed to an increasing extent in the electrostimulated skeleton muscle due to ischemia. This loss allows hypoxanthine to occur and with the simultaneous Ca^{++} ion inflow there is a protease-dependent transformation of xanthine-dehydrogenase in xanthine-oxydase. This step cannot be completed in the reperfusion with increased oxygen and catalyses so that the released oxygen radicals are converted into uric acid during the reconstruction of the xanthine. The increased occurrence of oxygen radicals must be in turn responsible for the postischemic increased vessel permeability with edema formation and the occurring early inflammation processes on the whole (4,5,6).

	M. gracilis - without stimulation				M. gracilis - with stimulation			
	Na ⁺	K ⁺	Ca ⁺⁺	Cl ⁻	Na ⁺	K ⁺	Ca ⁺⁺	Cl ⁻
I	148	4.50	2.23	117	152	4.35	2.48	120
II	147	4.60	2.18	118	153	5.05	2.41	122
III	148	4.55	2.14	118	153	4.35	2.45	121
IV	147	5.35	2.07	121	153	4.75	2.39	123
V	149	5.05	2.09	125	152	6.10	2.38	125
I	steady state							
II	postischemic effluante							
III	reperfusion (5 min.)							
IV	reperfusion (30 min.)							
V	reperfusion (60 min.)							
	all references in mmol/l							

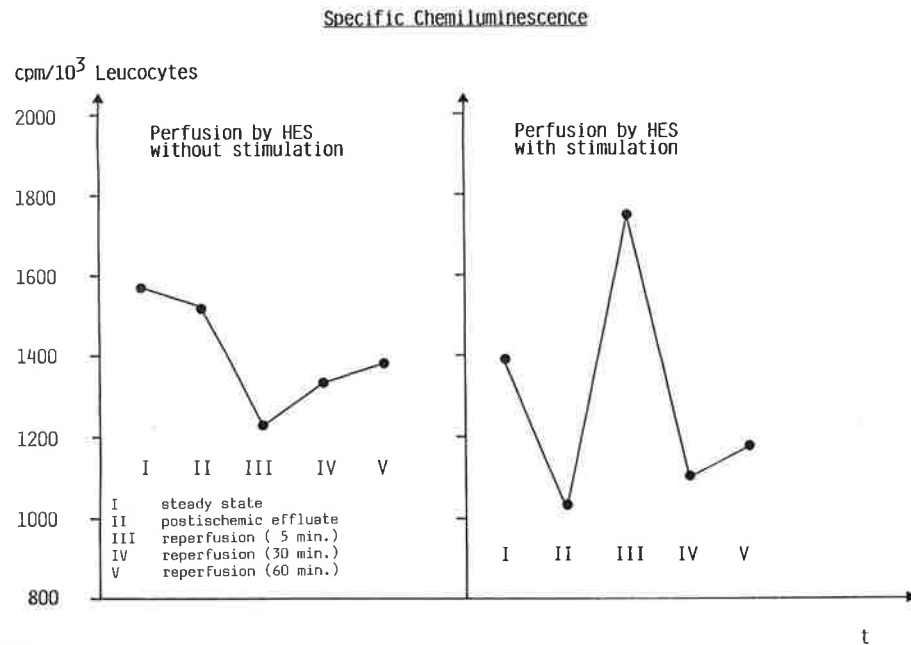


Fig. 1

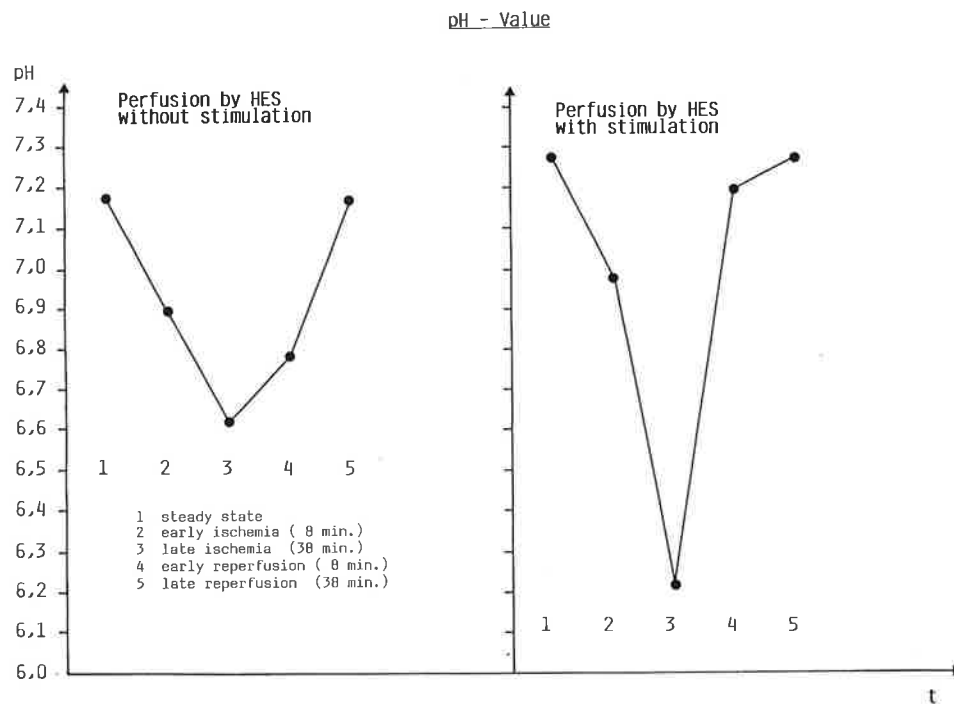


Fig. 2

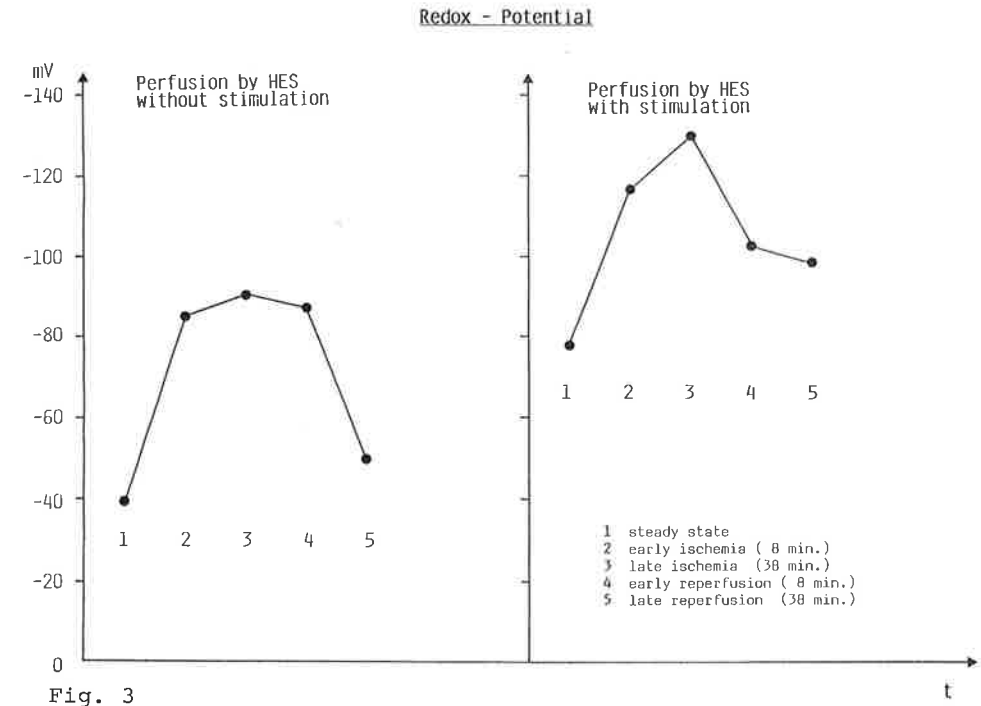


Fig. 3

REFERENCES

- Eckert, P., Henrich, H. A., Kreisköther, E., Scheja, H. M., Electrochemical Parameters and Clinical Significance of Muscle Ischemia, Vienna 1986
- Henrich, H. A., Böhme, M., Kapilläre Durchströmungsmuster im Skelettmuskel, in: Grothe, J., Witzleb, E. (Editors), Durchblutungsregulation und Organstoffwechsel, Wiesbaden 1981
- Hörl, M., Hörl, W. H., Heidland, A., Proteinkatabolismus und Tourniquet-Schock, Rolle proteolytischer Enzyme, Chir. 53, 1982
- Lewis, D. H., del Maestro, R. (Editors), Free Radicals in Medicine and Biology, in: Acta Phys. Scand., Uppsala 1980
- del Maestro, R., The Influence of Oxygen Derived Free Radicals on In Vitro and In Vivo Model Systems, Uppsala 1979
- McCord, J., Oxygen Derived Free Radicals in Postischemic Tissue Injury, New Engl. J. Med., 1985
- Renschop, J., Sauerstoffextraktion, Laktatumsatz und Kontraktionskraft des Musculus gracilis des Hundes unter adäquaten und ischämischen Bedingungen, eine tierexperimentelle Untersuchung, (Diss.) Mannheim 1978
- Scheja, H. M., Eckert, P., Henrich, H. A., Elektrochemische Sensoren zur Beurteilung der Dynamik von ischämischen Muskelerkrankungen, Biomed. Tech. vol. 30, supplement, 1985
- Scheja, H. M., Eckert, P., Henrich, H. A., The Influence of Isoxsuprine on the Postischemic Recovery of Free Muscle Flaps, Vienna 1986
- Schuster, R., Stoffwechseluntersuchungen in der ischämischen Skelettmuskulatur des Hundes, (Diss.) Dresden 1983

HISTOLOGICAL EXAMINATION AFTER EPINEURAL ELECTRODE APPLICATION

W. HAPPAK, R. KOLLER, *W. GIRSCH, H. GRUBER,
*J. HOLLE, *U. LOSERT, *W. MAYR, *H. THOMA

3rd Institut of Anatomie, *2nd. Surgical University Clinic,
Waehringstr. 13, 1090 Vienna, Austria

INTRODUCTION

During the last years in several paretic human patients epineural electrodes have been implanted for functional electrical stimulation^{1,2}. The electrodes were sutured to femoral, gluteal and phrenic nerves in order to stimulate the corresponding muscles indirectly. The effects of this surgical technique concerning the morphological changes in the nerves have not been evaluated numerically until today. In the present study, therefore, electrodes of the same type were implanted in sheep for quantitative analysis of the electrode effects.

MATERIALS AND METHODS

In two anaesthetised adult sheep the femoral nerves were exposed bilaterally and 5 ring shaped stainless steel wire electrodes with a diameter of 1 mm were sutured to the epineurium of each nerve with 6.0 prolene. No stimulation was applied to the nerves. Changes of impedance of every electrode were tested by short trains of stimuli once a day. The data were recorded and evaluated daily. 8 months (sheep 1) and 6 months (sheep 2) after implantation the animals were killed and the electrodes and the nerves were excised. From each nerve pieces situated 2 cm proximal (immediately below the inguinal ligament), at the site of the electrodes and 2 cm distal to the electrodes were used for histological examination. If the femoral nerve was already ramified at the inguinal level, only the electrode carrying branches were used for histology. The nerves were fixed in 3% glutaraldehyde, postfixed in 2% buffered osmium tetroxide and embedded in Epon. For quantitative evaluation 2 µm thick sections of the pieces proximal and distal to the electrodes were cut on an ultramicrotome and transmitted via TV-camera from the microscope (ZEISS-Axiomat) to a personal computer (IBM AT3) for image analysis. The cross-sectional area of the myelinated nerve fibers was determined and expressed by the calculated diameter of a circle of the same area. In nerve fascicles showing patho-

logical changes all myelinated fibers were evaluated. In undamaged fascicles about 40% of the myelinated fibers were analyzed and calculated for the whole fascicle. In addition in all specimen the fascicles were counted and classified under the microscope into normal and pathologically changed fascicles.

RESULTS

The median fiber diameters of the femoral nerves proximal to the electrodes were in sheep 1 12,5 μm (right) and 14,5 μm (left), in sheep 2 6,5 μm (left) and 7,5 μm (right) (Tab. 1). Only in one femoral nerve the distal part (sheep 1, right) showed a significant decrease in median diameter from 12,5 to 8,5 μm . In other nerves the diameters showed no changes (sheep 1 left, sheep 2 right) or even became larger (sheep 2 left).

In all nerves, except sheep 1 right, the total number of myelinated fibers decreased from proximal to distal (Tab. 1). This fact may be explained by branching off of few cutaneous branches and the branch to the sartorius muscle, which usually leaves the nerve at the level of the electrode application. The difference between sheep 1 and sheep 2 concerning the number and diameter of fibers is caused by the fact, that in sheep 1 the electrodes were sutured only to the motor branches of the femoral nerve thus making the examination of the sensory branches unnecessary.

Table 1: Quantitative analysis of sheep femoral nerves after surgical electrode application.

SHEEP NO.	N. SIDE	FEM.	MYELINATED FIBRES		NERVE FASCICLES			
			COUNTS	MEDIAN (μm)	TOTAL	NORMAL	PATHOLOGICAL CHANGES	
							MILD	SEVERE
1	LEFT	PROX.	11.165	14.5	23	23	0	0
		DIST.	10.635	14.5	46	46	0	0
	RIGHT	PROX.	10.657	12.5	30	29	1	0
		DIST.	15.815	8.5	56	33	23	0
2	LEFT	PROX.	21.700	6.5	42	36	5	1
		DIST.	20.099	7.5	77	56	17	4
	RIGHT	PROX.	26.203	7.5	50	46	3	1
		DIST.	22.892	7.5	72	65	6	0

The histograms of the diameters of myelinated fibers in the femoral nerves distal to the electrodes in sheep 1 left and sheep 2 left and right side show a bimodal distribution like in normal motor or mixed peripheral nerves (Fig. 1a). Only one cross section of the femoral nerve distal to the electrode application (sheep 1 right) contained many fibers with diameters between 2 and 4 μm (Fig 1b). To our own experience and according

to other authors^{3,4} these small fibers are regenerating fibers. Therefore the proximo-distal increase in the number of fibers in this nerve (from 10.657 to 15.815) easily can be explained by axonal sprouting after nerve fiber degeneration.

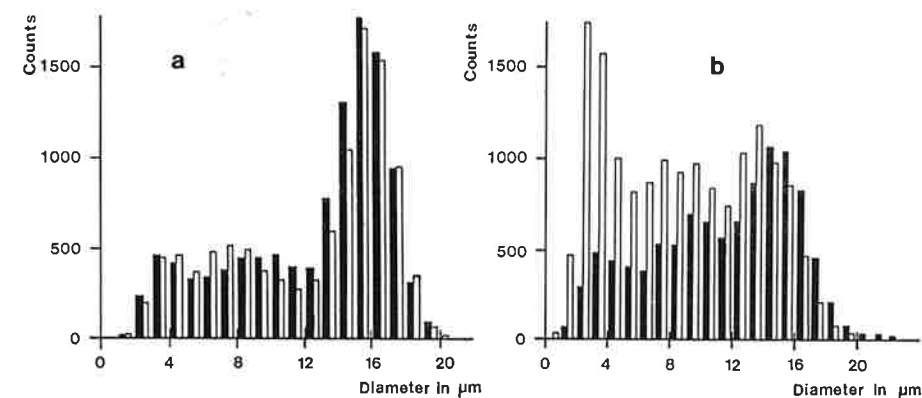


Fig. 1: Number and diameters of myelinated fibers and their changes from proximal (filled bars) to distal (empty bars). Sheep 1 left side (a), and sheep 1 right side (b), which contains a lot of small fibers in the distal specimen.

In sheep 1 the right distal piece of the femoral nerve contained many partly damaged fascicles (Tab. 1). These pathological changes also find expression in the histogram and in the absolute number of fibers. The relation of pathological to normal fascicles is relatively high: The area of altered fascicles comprises 43.5% of the total fascicular area in this specimen. In sheep 2 the distal part of the left femoral nerve contained 17 slightly and 4 severely altered fascicles. The histogram is not obviously changed since the affected fascicles were relatively small compared to the 56 normal ones: These 21 pathologically changed fascicles contribute only 18.9% to the total area of all fascicles. It is remarkable that, with the exception of one specimen, each femoral nerve proximal to the electrodes contained pathologically altered fascicles, too. There is substantial reason to suppose that these defects are not caused by the electrodes themselves, but by the surgical exposure of the nerves before suturing the electrodes. Fascicles in immediate vicinity of the sutured ring electrodes as shown in Fig. 2 appeared completely intact. Therefore we suggest that other factors than electrode application are responsible for fascicular damage⁵.

In summary we found 56 mildly (14 %) and 7 severely (2 %) altered fascicles, in comparison with 333 normal ones, forming 84 % of the total number of fascicles in both sheep.

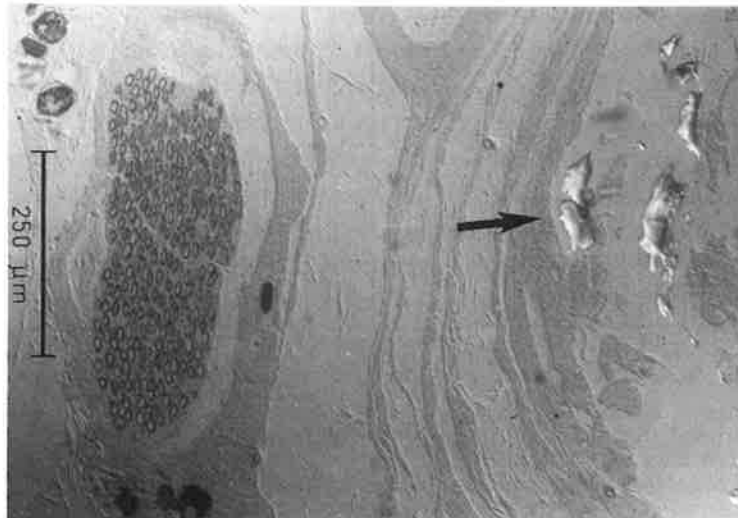


Fig. 2: Sheep 1; Fascicle of the right femoral nerve adjoining the thread. No signs of nerve fiber degeneration. The remains of the 6.0 prolene are marked by an arrow.

REFERENCES

- Holle J, Moritz E, Thoma H, Lischka A (1974) Die Karussellstimulation, eine neue Methode zur elektrophrenischen Langzeitstimulation. *Wien klin Wschr* 86,1:23-27
- Holle J, Frey M, Gruber H, Kern H, Stöhr H, Thoma H (1984) Functional electrostimulation of paraplegics (Experimental investigations and first clinical experiences with an implantable stimulation device). *Orthopedics* 7,7:1145-1155
- Mumenthaler M, Schliack H (1982) *Läsionen peripherer Nerven*. Georg Thieme Verlag, Stuttgart New York, pp 14-25
- Sunderland S (1978) *Nerves and Nerve Injuries*. Churchill Livingstone, Edinburgh London New York, pp 69-218
- Rosenkranz D, Fenzl G, Holle J, Lack W, Losert U, Thoma H (1986) Influence of long-term direct current on rat ischiadic nerves. *Appl Neurophysiol* 49:42-52

A STUDY OF PERIPHERAL NERVE REGENERATION IN COMPARSION WITH UTILIZING A SILICONE TUBE AND A BIORESORBABLE COLLAGEN MEMBRANE

KOUICHI HOSOKAWA, TAKAO SATOU, MANABU TAKAHASHI, SHIGEO HASHIMOTO
 FUMIHARU AKAI*, MASAHIKO IOKU*

Second Department of Pathology and Neurosurgery*
 Kinki University School of Medicine
 377-2 Ohno-Higashi 589 Osakasayama-city, Osaka Japan.

INTRODUCTION

This study aims at determining whether a bioresorbable collagen membrane could be applied to bridging a gap of regenerating and mature peripheral nerve, in comparsion with the application of a silicone tube.(1)

MATERIALS AND METHODS

Forty adult male Wistar rats(250-300g) were anesthetized with sodium pentobarbital(50mg/Kg,i.p.). A small segment of rat sciatic nerves were resected at midthigh, leaving a 10mm gap which was bridged by using a nerve conduit. In the left thigh, both stumps were inserted into a silicone tube and in right thigh both stumps were wrapped by collagen membrane. In addition to the tubing and wrapping, a small amount of collagen gel matrix was injected into the nerve gap space.(2)

a) Electrophysiological examination;

EMG studies were carried out 1,2,3,4,6,9,12 and 15 months after the operation. Fig. 1. The rats were anesthetized with sodium pentobarbital. Stimulating electrodes were positioned alongside the sciatic nerve at the proximal and distal parts and were stimulated with a square wave pulse of 0.1msec duration at a supramaximal intensity. Recording electrodes were inserted into the gastrocnemius muscle. The recording were photographed on the storage oscilloscope screen. The distance between the proximal and distal stimulating electrodes was measured. Latency, duration and amplification of compound muscle action potentials (CMAP) were measured and motor nerve conduction velocity(MCV) was calculated and thereafter compared with normal ranges (mean MCV;60.3m/sec. in our laboratory).

b) Histological measurement

For hitological measurement semithin sections of Epon-embedded were stained with toluidine blue and photographed with the light microscope. The analysis was performed from non-overlapping photographs covering a total nerve area at a final magnification of x2000. The data was computerized for the calculation of regenerative myelinated axon diameter and number, and then histograms were made.

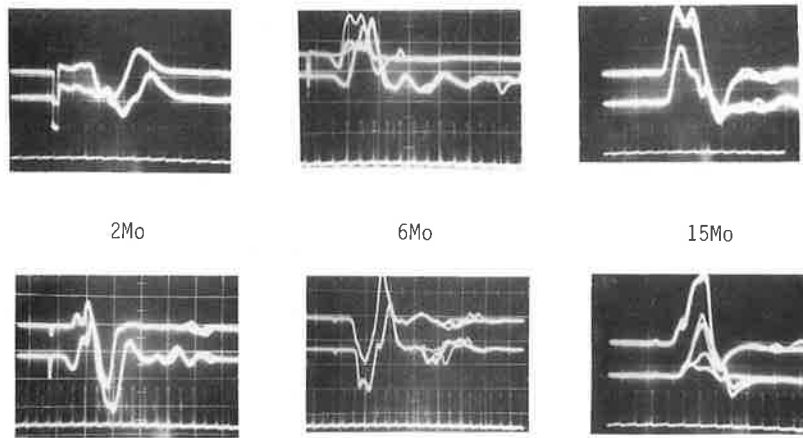


Fig. 1. Examples of EMG in silicone tube graft side and collagen membrane wrapped side were showed at 2,6 and 15 months after the operation. Upper;silicone tube graft side, lower;collagen membrane wrapped side



Fig. 2. At 12 months after the operation it is regenerated in silicone tube (upper) and by utilizing collagen membrane (lower).

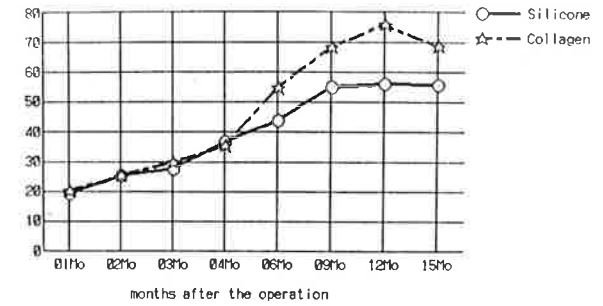


Fig. 3. At 12 months it recovered up to about 70% in collagen membrane and about 50% in silicone tube side.

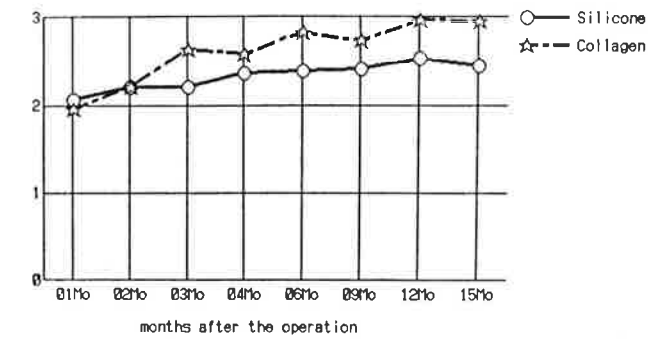


Fig. 4. Since 3 months axon diameter in the collagen membrane side was always larger than silicone tube graft side.

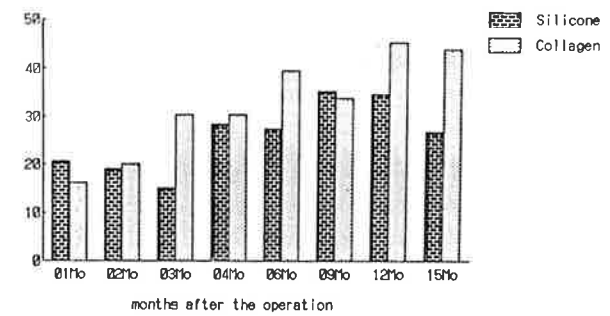


Fig. 5. Histogram showed that the percentage of large diameter (more than 4 micrometer) in the collagen membrane wrapped side was higher than the one in the silicone tube side.

RESULTS

Gross appearance was showed in Fig. 2. Sciatic nerve conductive failures were restored in 36 out of 40 rats after the operation. Onset of innervation potential was at 1 month after the operation in both sides. From 1 to 4 months there was no remarkable difference between both sides in MCV. However after 6 months there was a more remarkable restoration of MCV in the collagen wrapped side than the silicone tube graft side. Finally MCV recovered to about 70% in comparison with the normal rat group at 12 months in the collagen wrapped side, and to about 50% in the silicone tube graft side. Fig. 3. The mean regenerated myelinated axon diameter has almost the same value in both sides 1 and 2 months after the operation. However after 3 months, the myelinated axon diameter in the collagen wrapped side has been always larger than the silicone tube graft side. Fig. 4. The histogram showed that the percentage of large diameter (more than 4 micrometer) in all myelinated axon number in the collagen membrane wrapped side was higher than the one in the silicone tube graft side. Fig. 5.

DISCUSSION

In MCV and myelinated axon diameter, the collagen membrane makes regenerate more effectively than the silicone tube graft, especially for a longer period after the severance of the sciatic nerve. We consider the silicone tube might be a good nerve conduct at an early period in regeneration, but it disturbed segmental blood supply and both sides of suture points might be a kind of entrapment. However these impediments were avoided by utilizing a non-toxic bioresorbable collagen membrane.

CONCLUSIONS

- 1) It was demonstrated that a severed nerve was effectively regenerated by utilizing collagen membrane.
- 2) Electrophysiological and histological studies showed regenerative nerves mature well for a longer period after the operation.
- 3) It was suggested that the collagen membrane wrapping method may avoid a kind of entrapment affect on regenerating nerve trunks.

REFERENCES

- 1) T. SATOU, M. TAKAHASHI, F. AKAI, S. HASHIMOTO, etc.; A MORPHOLOGICAL STUDY ON THE EFFECTS OF COLLAGEN GEL MATRIX ON REGENERATION OF SEVERED RAT SCIATIC NERVE IN SILICONE TUBES: *Acta Pathol. Jpn.* 36(2);199-208,1986.
- 2) G. LUNDBORG, etc.; In Vivo Regeneration of Cut Nerves Encased in Silicone Tubes, Growth across a Six-millimeter Gap; *Journal of Neuropathology and Experimental Neurology*; Vol.41, NO,4 July, 412-422, 1982

Modelling of volume conduction

ELECTRICAL NERVE STIMULATION: EXPERIMENTS AND SIMULATIONS

PETER H. VELTINK, JAN HOLSHEIMER, JAN A. VAN ALSTÉ
University of Twente, P.O. Box 217, 7500 AE Enschede, (The Netherlands)

INTRODUCTION

Artificial nerve stimulation is a promising method in Functional Neuromuscular Stimulation, the aim of which is function restoration of paralyzed extremities. This method may be improved by selective stimulation of non-overlapping groups of motoneurons in a nerve by multi-electrode configurations (1-2), and by a physiological recruitment order with respect to nerve fiber diameter (3). We investigated nerve stimulation both experimentally in rat, and by mathematical modeling.

METHODS

Experimental methods

The Common Peroneal nerve of anaesthetized rats was stimulated (4) and the forces of Tibialis Anterior and Extensor Digitorum Longus muscles were measured isometrically. Multi-electrode intrafascicular and extraneural electrode configurations were used. The intrafascicular configuration consisted of four 25 μm diameter stainless steel wires isolated upto the tip and placed 100 μm apart. The extraneural configuration consisted of four 200 μm diameter wires isolated upto the tip and placed on four sides of a cross-section of the nerve. In each experiment the nerve was stimulated monopolarly, using cathodic monophasic current pulses of 60 μs duration.

Two types of stimulation experiments were performed: (i) *Recruitment curve measurements*. Single twitches were generated at 0.3 or 0.7 Hz stimulation and twitch amplitudes were measured at various stimulation pulse amplitudes. Twitch amplitudes were measured. (ii) *Force addition experiments*. Near tetanic forces were generated by 70 Hz stimulation with a single electrode and with two electrodes. In the latter case alternating stimulation sequences on both electrodes were used. Force addition can provide information about overlap of recruited motoneuron groups.

Mathematical modeling

Two cylinder model with probability description of nerve fiber recruitment. Nerve fiber excitation was modeled in a two-cylinder volume conduction model. A fascicle is represented by the medium within the inner cylinder, the medium between both cylinders represents the connective tissue sheath surrounding the fascicle, and the extraneural tissue is located outside the outer cylinder (5). Two electrodes with a cylindrical symmetry were modeled: an intrafascicular point electrode and an extraneural ring electrode. Nerve fiber excitation was modeled by the McNeal network model (6) using the Frankenhaeuser-Huxley equations. The internodal length L of myelinated nerve fibers was assumed to be proportional to nerve fiber

diameter D . The distance L_0 between the plane of stimulation and the nearest node was assumed to vary between $-L(D)/2$ and $L(D)/2$.

A probabilistic description of nerve fiber recruitment was obtained by considering nerve fiber diameter D , its radial position r and excitation threshold amplitude A as random variables. The probability distribution function $F_{A|D}(A|D)$ can be interpreted as a recruitment curve for nerve fibers with diameter D (5). The relationship between the radial position r of a nerve fiber and its excitation probability is given by the density function $g_{A|D}(r)$:

$$F_{A|D} = \int_0^{r_i} g_{A|D}(r) \cdot dr \quad [1]$$

$$g_{A|D}(r) = f_{r|D}(r|D) \cdot \int_{-L(D)/2}^{L(D)/2} f_{L_0|D,r}(L_0|D,r) \cdot F_{A|D,r,L_0}(A|D,r,L_0) \cdot dL_0 \quad [2]$$

When nerve fibers are assumed to be distributed uniformly over the fascicle $f_{r|D}(r|D)$ is proportional to r . Furthermore, L_0 was assumed to be distributed uniformly between $-L(D)/2$ and $L(D)/2$.

Nerve stimulation model including realistic nerve geometry. Nerve fiber excitation was also simulated with a realistic geometrical model of the small rat Common Peroneal nerve and the multi-fascicular human Deep Peroneal nerve (geometry obtained from Sunderland (7)). Potential distributions were computed numerically using the variational method (8). Nerve fiber excitation was modeled as described above. Recruitment contours were determined which include nerve fibers of diameter D recruited at two node positions: $L_0 = 0$ and $L_0 = L(D)/2$.

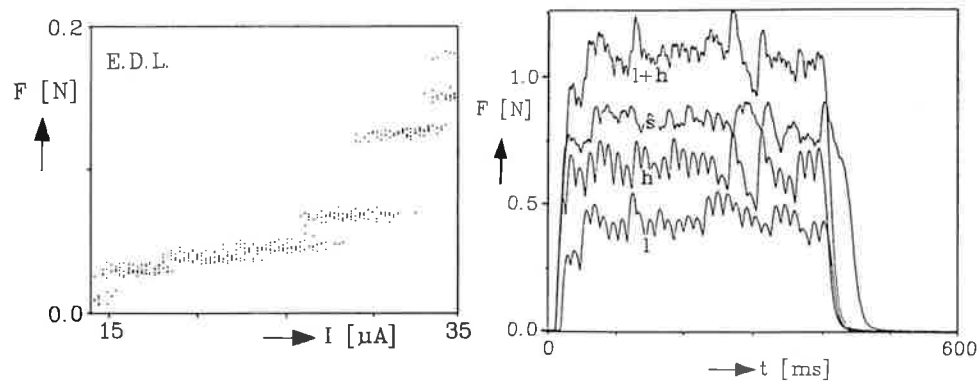


Fig. 1. Typical result of twitch force amplitudes of Extensor Digitorum Longus muscle during intrafascicular stimulation of Common Peroneal nerve of rat. The twitch amplitudes were determined several times at each stimulation pulse amplitude.

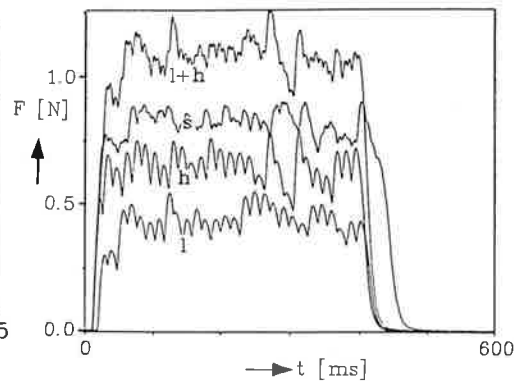


Fig. 2. Typical result of force addition experiments. Force registrations of Tibialis Anterior muscle are shown for extraneural stimulation at 70 Hz with two electrodes. Force responses: l: stimulation with first electrode; h: stimulation with second electrode; s: alternating stimulation with both electrodes; l+h: summation of responses l and h.

RESULTS

Experimental results. An example of a recruitment curve with intrafascicular stimulation is shown in fig. 1. In the case of intrafascicular stimulation a mixed recruitment order instead of a strictly inverse order with respect to nerve fiber diameter was concluded from the distance between discrete force levels. Figure 2 shows a force addition registration. Usually, force addition was only partly obtained (appr. 30% on the average) with both electrode configurations, indicating an extensive overlap of motoneuron groups recruited by different electrodes.

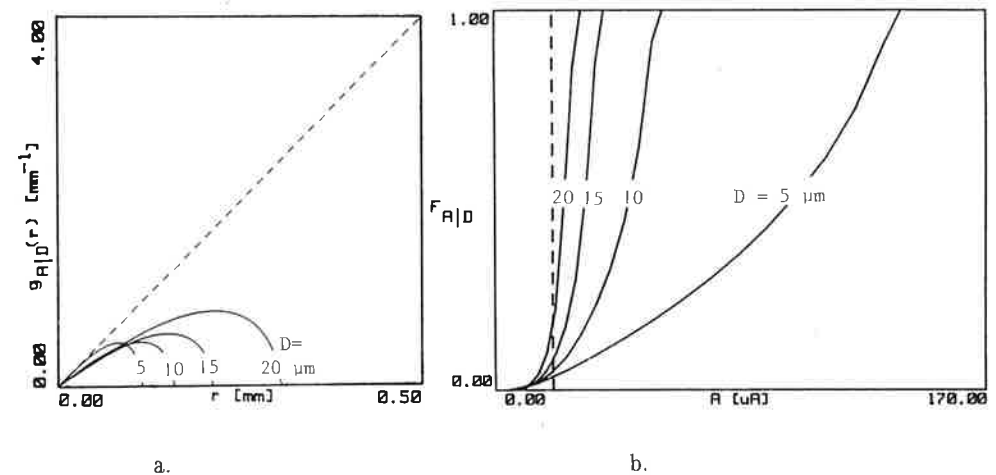


Fig. 3. Example of excitation probability density function $g_{A|D}(r)$ (a) and excitation probability distribution function $F_{A|D}(A|D)$ with intrafascicular stimulation (5). The diagonal line in (a) is $f_{r|D}(r|D)$ and represents excitation of all nerve fibers with diameter D .

Simulations with two-cylinder nerve model. An example of $g_{A|D}(r)$ and $F_{A|D}(A|D)$ for intrafascicular stimulation is shown in figure 3. Volume conduction parameters of the two-cylinder nerve model were varied. Inverse recruitment in a probability sense (increasing recruitment probability with increasing nerve fiber diameter) was found in all simulated cases with minor exceptions. With intrafascicular stimulation mixed recruitment of motoneurons was predicted. With extraneural stimulation inversion of recruitment order was more pronounced at larger distances between electrode and fascicle and at lower extraneural conductivity.

Simulation of nerve stimulation in a realistic nerve model. Figure 4a shows recruitment contours for the rat Common Peroneal Nerve, which was used in our experiments. It was found that variation in node positions induces a wide spread recruitment of nerve fibers in the fascicle. This can result in a considerable overlap of motoneuron groups recruited by different electrodes, as we found experimentally. Fig. 4b shows recruitment contours for a

multi-fascicular human Deep Peroneal nerve, stimulated by an electrode in the epineurium just outside a fascicle. An electrode placed just outside the nerve was predicted to be able to stimulate a number of superficial fascicles at the side of the nerve where the electrode was positioned, like others found experimentally (1-2). The model also predicts that for selective stimulation of a deeper lying fascicle an intraneural electrode in or just outside the fascicle has to be used.

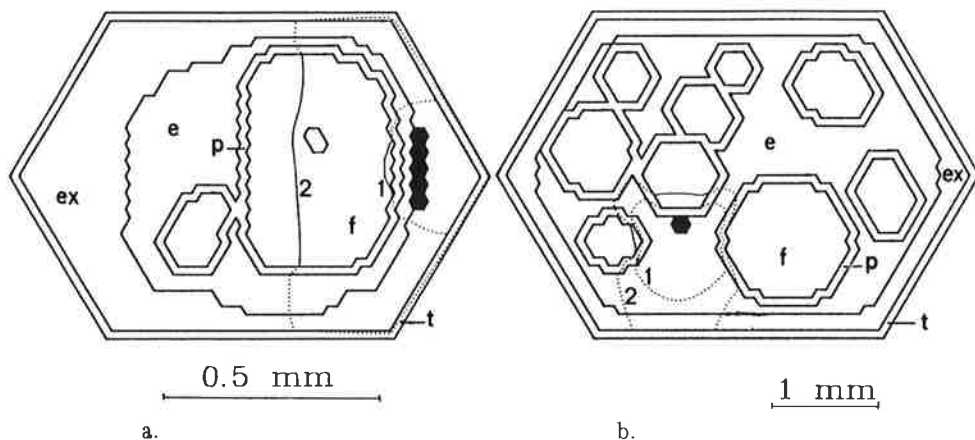


Fig. 4. Examples of simulated recruitment contours in a cross section of rat Common Peroneal nerve (a) and human Deep Peroneal nerve (b). Nerve fiber diameter D is $10 \mu\text{m}$. All nerve fibers will be excited inside the inner contour 1 and none will be excited outside the outer contour 2. Between both contours excitation depends on node position. The model consists of several compartments. The inner compartments (f) represent the fascicles, which are surrounded by a low conducting perineural sheath (p). Fascicles are embedded in the epineural connective tissue (e). The outer compartments are the extraneural medium (ex) and a terminating compartment of the model (t) with low conductivity. The electrode is indicated in black.

REFERENCES

1. McNeal DR, Bowman BR (1985) *Med. & Biol. Eng. & Comput* 23: 249-253
2. Holle J, Moritz E, Thoma H (1974) *Wiener klinische Wochenschrift* 86:23-27
3. Solomonow M (1984) *IEEE Trans. Biomed. Eng.*, 31:752-763
4. Veltink PH, Hermens HJ, Van Alsté JA (1986) *Proc. 8th Ann. Conf. of the IEEE Eng. in Med. & Biol. Soc.*, Dallas, 690-693
5. Veltink PH, Van Alsté JA, Boom HBK (1988) *IEEE Trans. Biomed. Eng.*, 35:69-75
6. McNeal DR (1976) *IEEE Trans. Biomed. Eng.*, 23:329-337
7. Sunderland S (1968), *Nerves and Nerve Injuries*, E&S Livingstone
8. Veltink PH, Van Veen BK, Struijk JJ, Holsheimer J, Boom HBK, *IEEE Trans. Biomed. Eng.*, submitted

MODELLING CONSIDERATIONS FOR THE STIMULATION OF THE MOTOR CORTEX WITH TRANSCRANIAL ELECTRODES

FERDINANDO GRANDORI, PAOLO RAVAZZANI

Centro di Teoria dei Sistemi (C.N.R.), Dipartimento di Elettronica,
 Politecnico di Milano, Milano, 20133, Italy

INTRODUCTION

It has been recently shown that motor pathways can be activated by direct stimulation of the unexposed motor cortex with electrodes arranged on the scalp with various montages (1-4). This paper presents some additional results of a theoretical analysis of the intracranial potential fields produced by surface stimulation (5, 6); since the determinants of the activation of the excitable tissues are the current densities, data on the intracranial current fields are presented here.

THE MODEL

Model Equations.

The model used in the present paper is constituted by three concentric spherical regions of different conductivities, representing the brain, the skull and the scalp tissues, respectively. Solutions of the electric potential fields are determined analytically, following the basic treatment proposed by Rush and Driscoll (1969); current density vectors have been computed from potential data. More details about the methods of computation and the influence on the final results of the basic modelling assumptions have been described elsewhere (5, 6).

Model parameters.

All the results presented in this paper have been obtained with radii for the three spheres of 8, 8.5 and 9.2 cm, respectively; according to Rush and Driscoll (7), resistivity was $220 \text{ Ohm}\cdot\text{cm}$ for the brain and the scalp tissues and 80 times greater for the skull. Values within the same range have been used for these parameters in all published studies on the localization of the intracranial generators of evoked potentials, in terms of dipolar sources (see, e.g., 8).

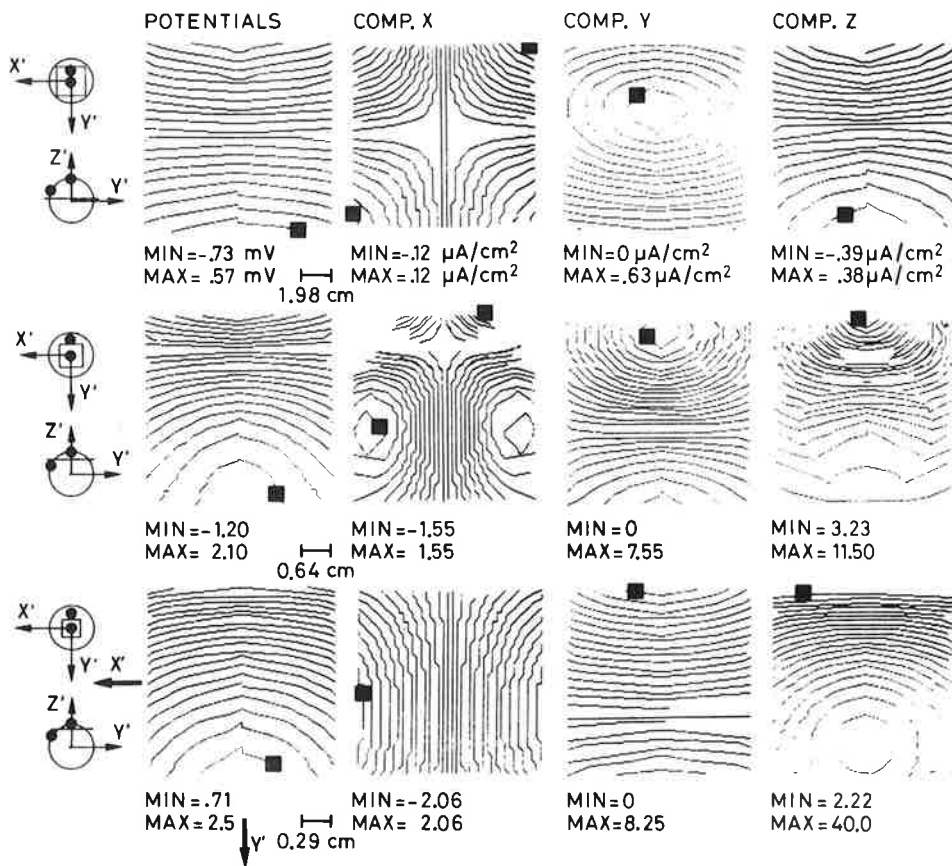


Fig. 1 - Isocontour plots of intracranial potentials and currents (orthogonal components) produced by an anode at CZ and a cathode located on the surface of the outer sphere at a position corresponding to the right hand motor area. Left: schematic representation of the electrodes locations with respect to the axes after rotation. From top to bottom, the maps show the fields computed at various depth, 7.9, 0.5 and 0.1 cm from the surface of the innermost sphere (brain tissues), respectively. Geometric scales for the maps are indicated. Maxima and minima for potentials and current density are given below each map; in most cases, 25 isocontour lines are plotted. Positive maxima are indicated with a filled square in each map.

Electrodes coordinates are estimated on an orthogonal coordinate system with the origin at the center of the sphere that best approximates the head. In the principal coordinate system, the positive x axis extends approximately through the nasion, the positive y axis passes above the left ear, the positive z axis passes through the vertex. Only results for the "bipolar montage" are presented here; coordinates for the two electrodes are $x=0$, $y=0$, $z=0$ for the anode and $x=5.4$, $y=-0.9$, $z=7.39$ cm, for the cathode (for the hand motor area).

RESULTS

In all the present data, the isocontour plots (potentials and currents) are computed on to planes orthogonal to an axis z' passing through the cathode (orientations of axes x' and y' are obtained by simple rotations). Each plane is displayed as viewed from an observer with his feet on top of the plane.

Fig. 1 shows the isocontour plots of the potential fields and of the orthogonal components of the current density obtained on planes at various distances from the center. It is seen from Fig. 1 that the fields are quite regularly distributed in space. For planes located very near to the center of the head, both potentials and currents are very low, as expected. Near to the electrodes (plots in the middle and in the uppermost row), potentials and currents increase. In regions close to the motor cortex area, the components along the z' axis are the greatest, compared to the x' and y' components. For the positive maxima, for example on the plane at 7.9 cm from center, the z' component is around some $40 \mu\text{A}/\text{cm}^2$, versus 2 and $8.25 \mu\text{A}/\text{cm}^2$, for the x' and y' component, respectively. The same happens to planes at 7.5 cm from center, with $11.5 \mu\text{A}/\text{cm}^2$ for the z' component, versus 1.55 and 7.55 for x' and y' .

What should be observed is that a small change in plane location (from 7.5 to 7.9 cm from center, as in Fig. 1) produces a relatively high change in the current density, in particular for the greatest component, and not only for the maximum values as noted previously, but also for the shape of the isocontour plots (compare the plots at the bottom and at middle on the rightmost column of Fig. 1). This high sensitivity of the z' component to the relative location of

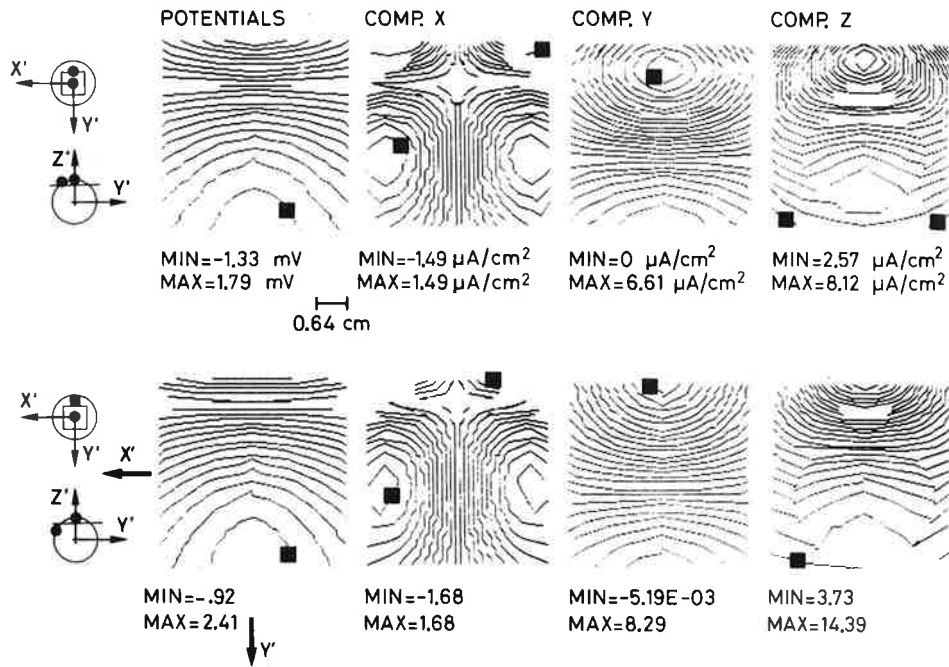


Fig. 2 - Isocontour lines for anode and cathode at separations of 2.5 (top) and 3.5 cm (bottom). Data are displayed as in previous Fig. 1. Plane depth was 0.5 cm from the outer surface of the innermost sphere in all cases.

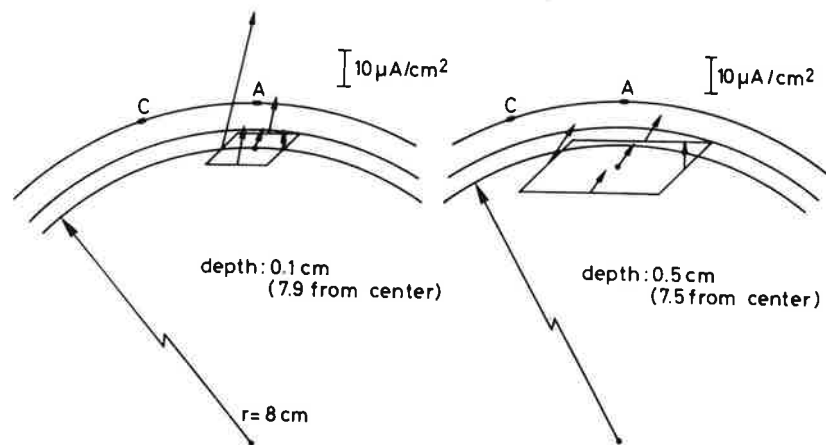


Fig. 3 - Current density vectors at some key positions, on to planes at different depth.

the stimulating electrodes is confirmed by the data of Fig. 2. Consider the plots in the rightmost column illustrating the iso-intensity contours for the z' component when the interelectrode distance between anode and cathode is varied from 2.5 to 3.5 cm; in the region of interest, maxima changes from 8.12 to 14.39 $\mu\text{A}/\text{cm}^2$. By contrast, x' and y' components go through a much lower change. To analyse in more details the behaviour of the current density in the region of interest, the orthogonal components have been combined to obtain, in strength and orientation, the current density vector at same key locations (see Fig. 3). What can be noted in Fig. 3 confirms above observations about the abrupt changes in space of the current density vectors. The greatest changes, as noted earlier, are those of the z component.

DISCUSSION

Examination of the intracranial fields, in terms of potentials and current densities, in regions close to the motor cortex, in a model mimicking a "bifocal montage", reveals that the component of the current density along the z axis is predominant, as expected from simple considerations about the relative locations of the stimulating electrodes. The situation is therefore critical as to the control of the intracranial excitation, in that even small changes of the relative location between the two electrodes produces great modifications in strength and orientation of the current density. This was not evident under any respect in the isocontour plots of the potential fields (see the leftmost columns of Fig. 1 and 2). It is therefore concluded that any theoretical analysis of the intracranial effects produced by surface stimulation must consider the current densities and not only because they are the determinants of the excitation.

REFERENCES

1. Merton PA, Morton HB (1980) *Nature* 285:227
2. Merton PA, Morton HB, Hill DK, Marsden CD (1982) *Lancet* 11:597-600

3. Rossini PM, Di Stefano E, Stanzione P (1985) EEG clin Neurophysiol 60:320-334
4. Rossini PM, Marciani MG, Caramia M, Zarola F (1985) EEG clin Neurophysiol 61:272-284
5. Grandori F, Rossini PM (1988) (submitted)
6. Grandori F (1988) In PM Rossini and CD Marsden (eds.), A.R. Liss, N.Y.
7. Rush S, Driscoll DA (1969) IEEE Trans Biomed Eng 16:15-22
8. Grandori F (1986) HEARING RES 21:51-58.

ANALYSIS OF SPINAL CORD STIMULATION.

I. FIELD POTENTIALS CALCULATED FOR A HOMOGENEOUS MEDIUM

J. HOLSHEIMER AND J.J. STRUIJK

Biomedical Engineering Division, Dept. of Electrical Engineering,
 Twente University, P.O.Box 217, 7500 AE Enschede, The Netherlands

SUMMARY

The effect of different electrode combinations on the recruitment of nerve fibres in spinal cord stimulation was investigated by modelling the spinal cord and surrounding tissues as a homogeneous, resistive medium. It was concluded that longitudinal fibres in the dorsal columns can be recruited best with a single or a double cathode medio-dorsally in the epidural space (and a distant anode). The model also predicts that close to a cathode propagation of action potentials by collaterals towards the dorsal and ventral horn may be blocked. Therefore cathodes should not be placed at segmental levels where these collaterals have to modulate neuronal activity.

INTRODUCTION

Although spinal cord stimulation (SCS) has been applied in the rehabilitation of patients with various neurological disorders since two decades, little progress has been made on the improvement of this method. In our opinion the choice of position and combination of electrodes is essential for the effect of SCS. Because reliable clinical criteria for this selection are not available, we investigated theoretically the effect of stimulation with the usual 4-electrode array [1,2] on nerve fibres with different orientations in the dorsal columns of the spinal cord.

The change in membrane potential of a nerve fibre, resulting from an external stimulus, depends on the partial second derivative of the imposed field potential along the fibre, the *activating function S* [3,4].

VOLUME CONDUCTOR MODEL

In order to calculate the activating function *S* for nerve fibres with different orientations, the spinal cord and surrounding tissues were modelled as a *homogeneous, isotropic, infinite, resistive medium*. The electrodes were represented by equidistant point sources, located at the L-axis of a cartesian coordinate system at intervals *z* (Fig.1), and the potential $V(t,r,l)$ was calculated analytically.

Because $V(t,r,l)$ has a cylindrical symmetry with respect to the L-axis, its second derivative was calculated at positions $P=(0,r,l)$ for three orthogonal

directions: longitudinally (S_l), radially (S_r) and tangentially (S_t) (Fig.1). These activating functions were calculated for several electrode combinations. A positive value of S corresponds with membrane depolarization which can lead to excitation and propagation of an action potential both ortho- and antidromically, while a negative value results in hyperpolarization which can block propagation.

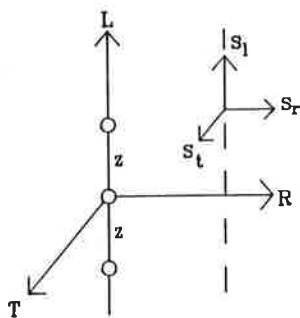


Fig. 1. Three orthogonal activating functions S in a homogeneous volume conductor; the electrodes at intervals z are at the L-axis.

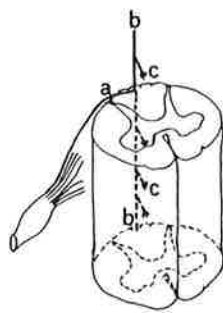


Fig. 2. Spinal cord with dorsal root primary afferent (a), ascending and descending dorsal column fibres (b) and collateral branches (c).

RESULTS

It was shown that S_l , S_r and S_t decrease with at least the 3rd power of r . Because the usual position of the SCS electrode array is medio-dorsally in the epidural space, nerve fibres will be recruited primarily in the dorsal columns (cf. [5]). In this area we can distinguish dorsal root primary afferents with a tangential direction (a), ascending and descending branches with a longitudinal orientation (b) and their collaterals in a radial direction (c) [6]. See Fig.2.

Curves of S_l , S_r and S_t at positions $P=(0.33z,1)$, calculated for a *single cathode* with current $-I$ (and a distant anode), are presented in Fig.3a. S_l and S_t have a positive peak at C (position of the cathode). The peak of S_r is negative and has twice the peak value of S_l and S_t . The S_l curve has negative side lobes and the S_r curve has small positive ones. Except for the inverse sign, the S curves of a single anode and cathode are identical. Therefore it is shown that: (i) *longitudinal* nerve fibres will be depolarized by cathodal and hyperpolarized by anodal stimulation; excitation by an anode will occur by the side lobes of the S_l curve at ≈ 5 times the current needed with a cathode; similarly propagation of an action potential generated by a high cathodal stimulus can be blocked by the side lobes (cf. [4] and [7]); (ii) *radial* fibres will be depolarized by anodal and hyperpolarized by cathodal stimulation. (iii) *tangential* nerve fibres will be depolarized by a cathode and hyperpolarized by an anode.

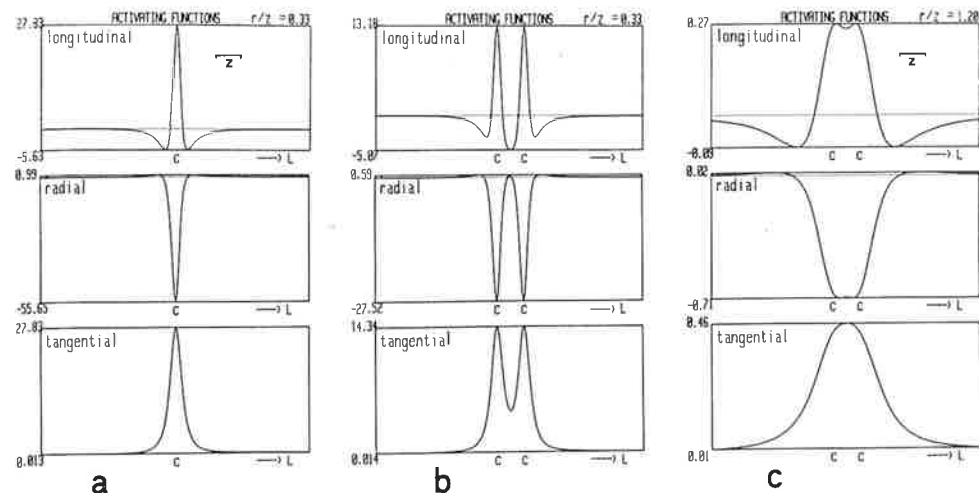


Fig. 3. Activating functions resulting from stimulation with a single cathode at $r=0.33z$ (a) and with a double cathode at $r=0.33z$ (b) and $r=1.2z$ (c).

When using more than one electrode S results from superposition of activating functions due to single electrodes. For a *double cathode* (current at each one $-0.5I$) the S curves have two peaks at a small distance ($r=0.33z$ in Fig.3b), but at larger distance a single maximum in between the cathodes appears ($r=1.2z$ in Fig.3c). With an *anode-cathode-anode* combination (currents $0.5I, -I, 0.5I$) the (negative) side lobes of the S_l curve resulting from the cathode (Fig.3) are superimposed on the (negative) peaks due to the anodal electrodes and hyperpolarization of primary afferent sections a and b (Fig.2) at the anodal levels is increased.

CONCLUSIONS

Several criteria can be used for selection of an electrode combination to recruit the longitudinal dorsal column fibres. (i) Low probability of blocking propagation of evoked action potentials, which means a high ratio $S_l(\max)/S_l(\min)$ (ii) Minimal energy, which means a high ratio $S_l(\max)/I$. (iii) Recruitment of myelinated fibres with different longitudinal positions of their nodes of Ranvier, which requires an S_l peak 1-2mm wide.

A *single or a double cathode* meets these criteria best. Not only ascending and descending fibres but also dorsal root fibres can be recruited in the dorsal columns. Action potentials in the longitudinal fibres will propagate both rostrally and caudally, while in the dorsal root fibres antidromic propagation will occur (Fig.4a). However, collateral branches can be blocked. Therefore it is

concluded that stimulating cathodes should not be placed at those spinal levels where segmental neuronal activity should be modulated by evoked collateral input. The model also predicts that anodal stimulation should be used for selective recruitment of collaterals (Fig.4b).

In this investigation we have considered the volume conductor as a simple homogeneous medium. For a more precise quantitative approach we have to take into account the geometry and electrical conductivity of the anatomical structures in and around the spinal cord [8].

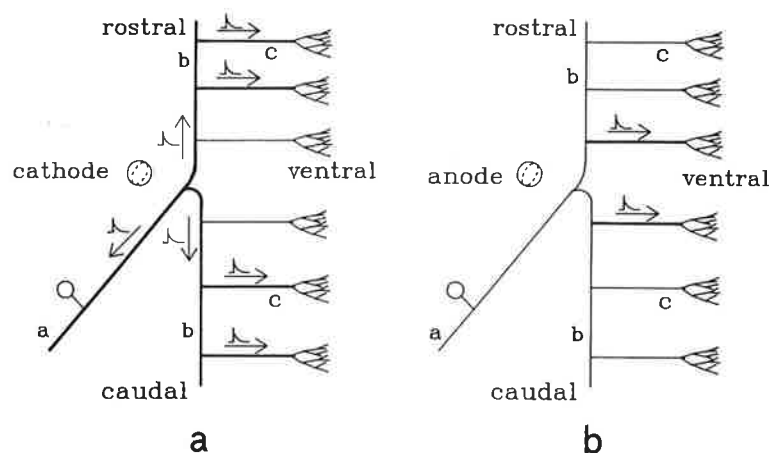


Fig. 4. Dorsal column fibres with different orientations (a,b,c) stimulated by an epidural cathode (Fig.a) and anode (Fig.b); recruited sections are indicated.

REFERENCES

1. Medtronic, Inc., Minneapolis, Minnesota (SE4 quad electrode).
2. Neuromed, Inc., Ft. Lauderdale, Florida.
3. McNeal DR (1976) IEEE Trans Biomed Eng 23:329-337.
4. Rattay F (1986) IEEE Trans Biomed Eng 33:974-977.
5. Dimitrijevic MR, Faganel J, Young RR (1981) Appl Neurophysiol 44:133-140.
6. Davidoff RA (ed.) (1984) Handbook of the Spinal Cord, Vol.2: Anatomy. Dekker, New York, Basel.
7. Ranck JB Jr (1975) Brain Res 98:417-440.
8. Struijk JJ, Holsheimer J, Van Veen BK, Van Beckum FPH, Veltink PH. This volume.

ANALYSIS OF SPINAL CORD STIMULATION.

II. SIMULATION OF FIELD POTENTIALS IN AN INHOMOGENEOUS MEDIUM

J.J. STRUIJK, J. HOLSHEIMER, B.K. VAN VEEN, F.P.H. VAN BECKUM, P.H. VELTINK.

Biomedical Engineering Division, Dept. of Electrical Engineering,
University of Twente, P.O.Box 217, 7500AE Enschede, The Netherlands.

SUMMARY

Field potentials and activating functions were computed in an inhomogeneous, anisotropic volume conductor model of the cervical spinal cord and its surrounding tissues. The electrode position was chosen to be medio-dorsally in the epidural space. It was shown that the activating functions (to which the initial change of the membrane potential is proportional) are different for dorsal column fibers with different orientations. To obtain stable stimulation, epidural spinal cord stimulation should not be applied at a cervical level, due to the sensitivity to variations in the thickness of the subarachnoid space.

INTRODUCTION

Because it is not precisely known which elements in the spinal cord are activated, spinal cord stimulation (SCS) provided little information about the underlying neurophysiological mechanisms. This is one of the main reasons that little progress in SCS has been made during the last decade.

To assess the influence of the electrode configuration on the membrane potential of nerve fibers in the dorsal columns with different orientations [1], the cervical spinal cord and surrounding tissues of the neck were modelled as an inhomogeneous, anisotropic volume conductor. Field potentials and activating functions were calculated in this model.

DESCRIPTION OF THE VOLUME CONDUCTOR MODEL

Longitudinally, the model was composed of 40 layers, each consisting of 3000 wedge shaped volume elements, orderly arranged in 40 rows of 61 to 99 triangles. Each volume element was given an (an)isotropic specific conductivity.

As shown in fig. 1a, the model comprises white matter (wm) (specific conductivity: $0.0060 (\Omega\text{cm})^{-1}$ transversally and $0.00083 (\Omega\text{cm})^{-1}$ longitudinally), grey matter (gm) ($0.0023 (\Omega\text{cm})^{-1}$), epidural fat (ef) ($0.00040 (\Omega\text{cm})^{-1}$) and cerebro spinal fluid (csf) ($0.017 (\Omega\text{cm})^{-1}$). The specific conductivity of the csf was measured in three subjects while conductivities of the other compartments were taken from literature [2]. Vertebral bone, muscle, fat and other tissues of

the neck were represented by a layer with low conductivity, surrounding the epidural space ($0.02 \cdot 10^{-3} (\Omega\text{cm})^{-1}$). Dura mater and arachnoid were not taken into account [3].

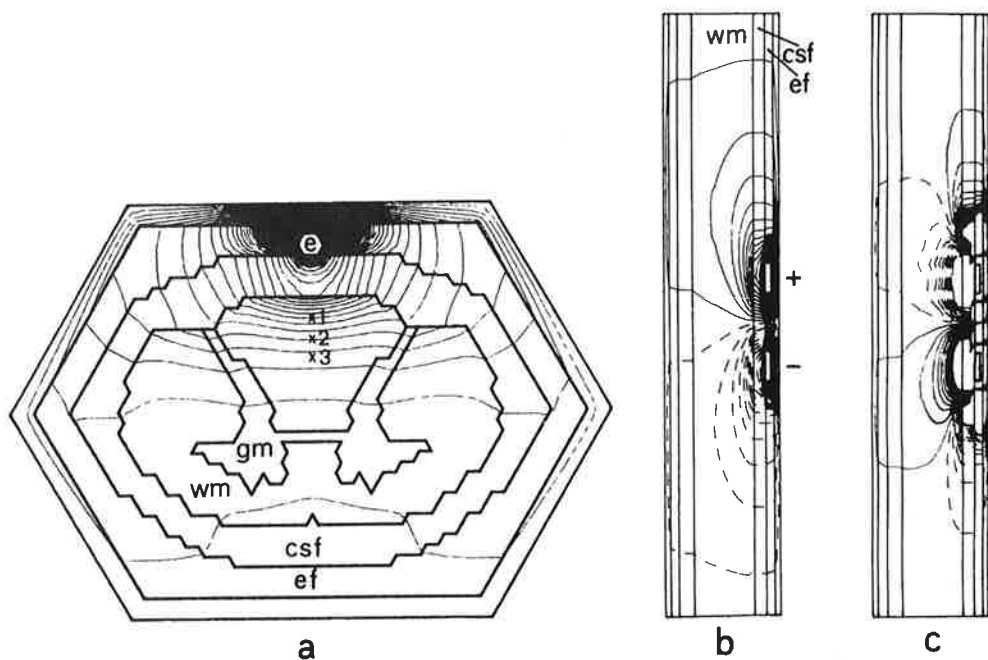


Figure 1. Transverse section (a) of the model with isopotential lines at intervals of 1% of the electrode potential. White matter (wm), grey matter (gm), cerebrospinal fluid (csf), epidural fat (ef), electrode (e) and a surrounding layer. Mid-sagittal section with isopotential lines (b) and isolines of the longitudinal activating function (c).

The width of the subarachnoid space is variable and depends a great deal on the set of the head. Data in literature on the average diameters of the spinal cord and the subarachnoid space are inconsistent: the average saggital diameter of the spinal cord ranges from 6.2 mm [4] to 9.46 mm [5] in normal subjects at level C5. We used a value of 7.5 mm.

COMPUTATIONAL METHOD

Field potential in the volume conductor model was computed by minimizing its power functional (variational principle [8]) which is given by:

$$P(\phi) = \frac{1}{2} \iiint_V (\nabla\phi \cdot \sigma \nabla\phi) dV \quad (1)$$

with ϕ the potential, P the power of the potential field in volume V, $\nabla\phi$ the gradient of ϕ and σ the conductivity tensor. Boundary conditions are: fixed potentials at the electrodes and zero potential at the surface of the model.

From the solution ϕ the activating function S was computed. The activating function can be defined as the second order difference of the external potential along the axon [1,6,7]. The gradient of the initial change of the membrane potential resulting from an external stimulus is proportional to S.

RESULTS

The sensitivity of the field potential in the dorsal columns to several model parameters was determined, both at monopolar and bipolar stimulation. Electrode length was 3 mm and separation 6 mm. Sensitivity was defined as $\Delta\phi/\Delta\sigma$ for small $\Delta\sigma$ (5%), with $\Delta\sigma$ the relative conductivity change in one compartment of the model. Sensitivity to the conductivity of the surrounding layer was small as compared to other conductivities. With mono- and bipolar stimulation the epidural fat was of major importance (sensitivity 0.4 and 0.5 respectively). Using monopolar potentials in the dorsal columns are about twice as high as with bipolar stimulation. So the sensitivity to the conductivities of white and grey matter was larger in the monopolar case.

When the width of the subarachnoid space was increased from 0.7 mm to 1.4 mm field potentials in the dorsal columns decreased by 30%.

For small $\Delta\sigma$ sensitivity of the activating functions to the model parameters was nearly the same as the sensitivity of the field potential.

Figure 1b shows isopotential lines in the mid-sagittal section at bipolar stimulation. Model length is 61.5 mm. In figure 1c isolines of the longitudinal activating function are shown (lines close to the electrode were not plotted). Solid lines represent positive values, dashed lines negative ones.

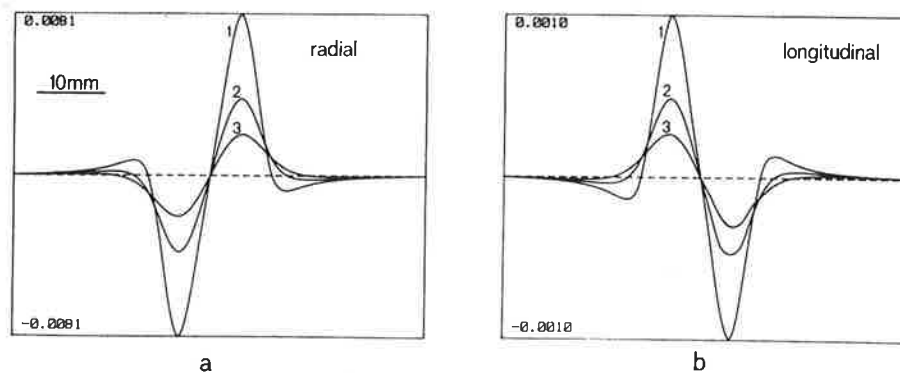


Figure 2. Dorso-ventral (radial) (a) and longitudinal (b) activating functions at three rostro-caudal lines in the dorsal columns (bipolar stimulation).

In figure 2 plots of the (bipolar) radial (a) and longitudinal (b) activating functions, at longitudinal lines in the dorsal columns, are shown. The digits 1,

2 and 3 in the plots correspond with those in figure 1a, where the positions of the longitudinal lines are indicated (x) at 0.7, 1.4 and 2.1 mm from the boundary between the dorsal columns and the csf. The values of the radial activating functions are about 8 times higher than the longitudinal ones, while in a homogeneous medium this is only a factor 2 [1]. The longitudinal activating function is positive at cathodal level, indicating depolarization of longitudinal fibers, and negative near to the anode. In contrast, the radial activating function is negative at the cathode and positive at the anode.

CONCLUSIONS

Orientation of nerve fibers is an important factor. The model predicts that, while longitudinal fibers are activated, dorso-ventral collaterals will be blocked at cathodal level. At anodal level these collaterals can be activated but longitudinal fibers may be blocked.

Due to the relatively high sensitivity of the effect on nerve fibers to the conductivity in the epidural space, the potential distribution can be disturbed by inhomogeneities near the electrode.

Potential distribution also varies a great deal with the width of the subarachnoid space. Because significant changes of this width will result from movements of the head, cervical spinal cord stimulation will be unstable.

REFERENCES

1. Holsheimer J, Struijk JJ This proceedings.
2. Geddes LA, Baker LE (1967) Med & Biol Engng 5:271-293.
3. Sin WK, Coburn B (1983) Med & Biol Eng & Comp 21:264-269.
4. Thijssen HOM, Keyser A, Horstink MWM, Meijer E (1979) Neuroradiology 18:57-62.
5. Nordquist L (1964) Acta Radiologica Suppl 227:1-96.
6. McNeal DR (1976) IEEE Trans Biomed Eng 32:329-337.
7. Rattay F (1986) IEEE Trans Biomed Eng 33:974-977.
8. Pilkington TC, Morrow MN, Stanley PC (1985) IEEE Trans Biomed Eng 32:166-173.

ACCELEROMETERS AND FUNCTIONAL ELECTROSTIMULATION.

A.T.M. WILLEMSSEN, J.A. van ALSTÉ & H.B.K. BOOM.

University of Twente, Biomedical Engineering Department, Faculty of Electrical Engineering,
 P.O. Box 217, 7500 AE Enschede, (The Netherlands)

INTRODUCTION.

Electrical stimulation of paralyzed muscles to restore functional movements (FES) can benefit from feedback control strategies [1,2]. Parameters that can be used for a feedback controller are, in the case of lower extremities, angle, angular velocity and angular acceleration of the different leg segments. We investigate the use of accelerometers for the assessment of these parameters.

The use of accelerometers for the assessment of angular velocity and angular acceleration is well established [3,4,5,6]. However the calculation of the angle is hampered by integration drift. We will show that, under certain circumstances, the angle of the leg segments can be calculated from accelerometer data without integration.

THEORY

The lower extremities can be modelled as a multi-segment rigid-body. Both the orientation of the segments relative to each other and the orientation relative to an inertial reference system (e.g. the ground) are to be determined. Each segment has its own body-fixed reference frame. A seismic accelerometer with DC response (i.e. an accelerometer measuring the component of gravity also) is placed on a segment at a distance r from the body-fixed frames origin. It has been shown [7] that the equivalent acceleration measured at this point is given by

$$\vec{a}(r) = \vec{g} - \ddot{\vec{R}} - r \vec{\omega} \times (\vec{\omega} \times \vec{e}) - r \dot{\vec{\omega}} \times \vec{e} \quad (1)$$

$\vec{a}(r)$: equivalent acceleration vector.

\vec{g} : gravitational acceleration vector.

\vec{R} : vector from the inertial-reference origin to the body-fixed origin.

r : distance from the accelerometer to the body-fixed frames origin.

$\vec{\omega}$: rotation vector.

\vec{e} : unity direction vector from the body-fixed origin to the accelerometer.

We divide the right part of equation (1) in two. The first, $\vec{g} - \ddot{\vec{R}}$, is independent of the distance r , whereas the second part isn't. Usually the first part is divided out by placing accelerometers at two points on one line.

$$\vec{\omega} \times (\vec{\omega} \times \vec{e}) + \dot{\vec{\omega}} \times \vec{e} = \frac{\vec{a}(r_1) - \vec{a}(r_2)}{r_2 - r_1} \quad (2)$$

The components of the equivalent acceleration can be measured in body-fixed coordinates. So by numerical integration, equation (2) could be solved for the components of $\vec{\omega}$ in body-fixed coordinates. Integrating twice we would find the rotational angles themselves. This method is hampered by integration drift, and can only be used for short intervals. We took an alternative approach by eliminating the rotational part of equation (1). This results in :

$$\vec{g} - \ddot{\mathbf{R}} = \frac{r_2 \vec{a}(r_1) - r_1 \vec{a}(r_2)}{r_2 - r_1} \quad (3)$$

Suppose $\ddot{\mathbf{R}} = \vec{0}$. Then the left part of (3) is known in inertial reference coordinates whereas the right part can only be measured in body-fixed coordinates. To solve (3) we translate the left part to body-fixed coordinates by multiplying it with a rotation matrix. This leads to three equations (one for each direction) which can be solved for the three rotational angles. The big advantage of this method is that an integration is no longer necessary. Also we see that the relation is given between the equivalent acceleration and the direction of the gravitational acceleration (absolute measurement).

This method can be extended to angle measurements between two connected segments (e.g. knee angle). We can calculate, without integration, the angle between these segments using accelerometers placed on them, independent of their movements (relative measurement).

Equation (3) is tested using a one-degree of freedom pendulum. Under these conditions (3) reduces to :

$$-g \sin(\theta) = \frac{r_2 a_{1t} - r_1 a_{2t}}{r_2 - r_1} \quad (4a)$$

$$-g \cos(\theta) = \frac{r_2 a_{1r} - r_1 a_{2r}}{r_2 - r_1} \quad (4b)$$

With a_{1t} , a_{1r} : the tangential and radial components of $\vec{a}(r_1)$ respectively.

METHODS and RESULTS.

Preliminary pendulum and lower leg measurements [7,8] have shown the potential of our method. Here we will discuss into greater detail the systematic errors, their compensation and the maximum accuracy obtainable. Four accelerometers (Kyowa AS-5GA) were placed on an 1-degree of freedom pendulum at different distances r from the axle so the effect of different r_1 and r_2 could be studied. Sensitive axes were in the tangential direction (Equation 4a). The accelerometer signals were amplified and low-pass filtered (100 Hz) by a second order Butterworth filter. The signals were sampled for 4 sec. at 1 kHz with a 12 bit ADC on a LSI 11-23 computer. A resolver (Muirhead 11RSF4) was placed on the axle for reference. The signal of this resolver was digitized using a resolver to digital converter (AD 2S80, 14 bit).

Figure 1a shows the difference between the angle calculated from accelerometer data and the angle according to the resolver ($\Delta\theta$) as a function of the angle itself (θ). The systematic part of the error is mainly made up by a linear component and a hysteresis component. The first component is attributed to gain and offset errors in the accelerometer signals and can be compensated for using a linear least square optimisation. The hysteresis is attributed to time delay in the accelerometer signals caused by the pre-sampling filter and the sequential AD-conversion. This is compensated for by digital filtering with a second order Butterworth filter (100Hz) of the resolver signal whereas the accelerometer signals are synchronized using a linear interpolation between consecutive points. The effect of these compensations is illustrated in figure 1b.

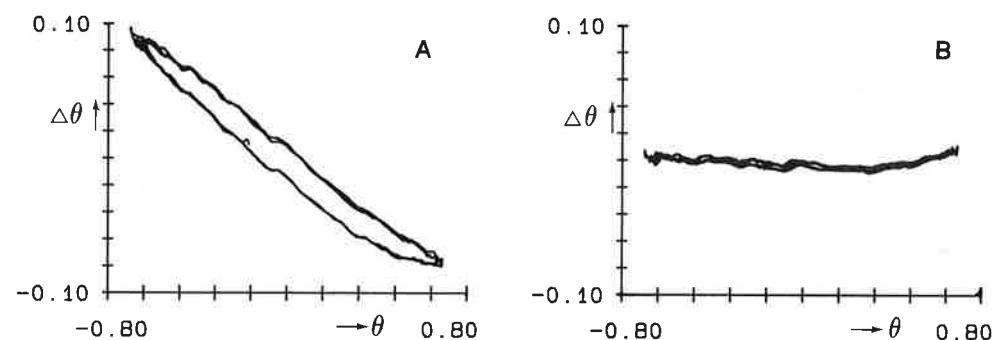


Figure 1. Error in the angle calculated from accelerometer data as function of the resolver angle
a. Before compensation.
b. After compensation for systematic errors.

During 30 min. about 15 measurements were made. The same gain and offset correction factors were used for all measurements. The differences between the angle calculated from the accelerometer data and the angle as given by the resolver is characterized by :

Standard deviation	: $\sigma \leq 0.002 - 0.005$ rad.
Maximum difference	: $\Delta \leq 0.010 - 0.025$ rad.
Average difference	: $\mu \leq \pm 0.004$ rad. (Maximum angles ≤ 0.7 rad.)

Differences were smaller than $\mu \pm 2\sigma$ for at least 95% of the time. We found it to be advantageous if one of the accelerometers was close to the axle and the second at maximum distance (0.65 m). For maximum angles greater than 45° measurements should be made in both the tangential and radial direction [8].

As mentioned in the theory relative angle measurements can also be made. This is being tested on an 2 segment pendulum. Due to a malfunction of one of the sensors only preliminary measurement with a potentiometer instead of the resolver can be presented. Given the limited

accuracy of the potentiometer and the small number of measurements the following results are given as an indication only.

Standard deviation	$\sigma \approx 0.01$ rad
Maximum difference	$\Delta \approx 0.03$ rad.

DISCUSSION.

Most sensors available for the assessment of the feedback parameters (angle, angular velocity and angular acceleration of the lower extremities) have severe limitations for their use with FES. Therefore research into the use of accelerometers was started. Theoretically we showed that accelerometers can be used for the assessment of angle, angular velocity and angular acceleration of the different segments of a ideal multi-segment body. We found that during stance the angle of the lower leg can be calculated without an integration, thus avoiding integration drift. The knee angle can be calculated both during stance and swing phase without an integration.

Analysis of the error in the calculated angle for pendulum measurements show that the error is mainly made up by a linear and a hysteresis component. We found that these errors can be explained for in terms of gain and offset errors in the accelerometer signals and a time delay between the different signals.

Preliminary data [9] indicates that the accuracy obtained with accelerometers after compensation for the systematic errors is high enough for a feedback controller .

REFERENCES.

1. McNeal DR & Bekey GA (1984). Closed-Loop Control of the Human Leg using Electrical Stimulation. Proc. 8th Int. Symp. on External Control of Human Extremities. Dubrovnik 113-126.
2. Wilhere GF Crago PE & Chizeck HJ (1985) Design and Evaluation of a Digital Closed-Loop Controller for the Regulation of Muscle Force by Recruitment Modulation. IEEE Trans Biomed Eng 32, 668-676.
3. Padgaonkar AJ Krieger KW & King AI (1975) Measurement of Angular Acceleration of a Rigid Body Using Linear Accelerometers. ASME J. of App. Mech., 42, 552-556. 2.
4. Smidt GL Deusinger RH Arora J & Albright JD (1977). An Automated Accelerometry System for Gait Analysis. J. of Biomech., 10, 367-375.
5. Mital NK & King AI (1979). Computation of Rigid-Body Rotation in Three Dimensional Space from Body-Fixed Linear Acceleration Measurements. ASME J. of Appl. Mech., 46, 925-930.
6. Gilbert JA Maxwell GM McElhaney JH & Clippinger FW (1984) A System to Measure the Forces and Moments at the Knee and Hip During Level Walking. J Orthop Res 2:281-288.
7. Willemsen ATM & van Alste JA. (1987) Accelerometry: A Method for Angle Assessment of the Lower Extremities with the Potential of Implantation. IX Symp External Control of Human Extremities. Dubrovnik 283-289
8. Willemsen ATM van Alste JA & Boom HBK (1986) Measuring FES Feedback Parameters with Accelerometers. Proc 8th Conf.IEEE Eng Med & Bio Dallas. 671-674
9. Crago PE, Chizeck HJ, Neumann MR & Hambrecht FT (1986). Sensors for use with Functional Neuromuscular Stimulation. IEEE Trans Biom Eng 33:256-268.

AN IMPROVED STRATEGY TO MINIMIZE MUSCLE FATIGUE DURING FES-INDUCED STANDING

A.J. MULDER, H.J. HERMENS, J.A. van ALSTE, G. ZILVOLD
Rehabilitation Centre 'Het Roessingh',
P.O. Box 310, 7500 AH Enschede (The Netherlands)

INTRODUCTION

An important aspect in the clinical application of functional electrical stimulation (FES) is to enable safe standing. This involves to guarantee a reliable locking of the knee, without inducing a fast onset of muscle fatigue. In most institutes, open-loop stimulation is used to let paraplegic patients stand [1]. This easily leads to over-stimulation, limits the standtime, and over-stresses the knee-joint. To solve these problems we study strategies for closed loop control of knee-angle during standing. The main objective is to develop a robust non-fatigueing method to stabilize the knee-joint, using transcutaneous stimulation of the quadriceps.

Problems in the control of stable standing deal with a biomechanical system which is instable due to gravitation, and highly nonlinear and nonstationary muscle characteristics. To overcome part of these problems, adaptive control techniques are used more and more [2]. However problems occur in surface stimulation were parameters are changing fast. As a second problem full state-feedback can not be applied because one of the parameters, the muscle force, can not be measured directly. Only knee-angle (velocity) data can be used for feedback. This will cause the control of muscle force to fail when the knee is in the locked position.

Our solution is to use state-feedback and differentiate between the knee-lock and the knee-unlock state: open-loop ramp-down of the stimulation when the knee is locked and artificial reflex when the knee is unlocked. During state transition we use the mechanical properties of the knee-joint to get an overall stable system. In this way controller adjustment is less critical compared to linear feedback.

MATERIAL AND METHODS

The control strategy

Knee-unlock state. In 1987 we started a model study and computer simulations, to determine a suitable controller to stabilize the unlocked knee-joint [3]. The model we used consists of a three segmental skeleton (trunk, femur and tibia) and a muscle delivering the knee-torque.

The system is open-loop unstable. Nonlinear and nonstationary muscle characteristics were modelled as a varying muscle gain K . From state equations and root-locus plots it was shown that at least a derivative control action is needed to stabilize the system. Further simulations on the PD-controlled system have shown that the system is highly sensitive to variations in muscle gain (figure 1). Decreasing the muscle gain with 5% resulted in a 100% increase of settling-time; increasing the muscle gain with 35% resulted in 20% overshoot.

From experiments in paraplegic patients we found that even under static and isometric conditions the muscle gain varies at least over more than 50%. These variations may be very abrupt. Therefore, for clinical use, we did not consider adaptive control. Instead, we prefer fixed parameter control. To adjust such controller worst-case, PD gain must be high to compensate for decreasing muscle gain. Alternatively we can also simply switch the stimulation to a high level, to return the knee to the locked position. The clinical tests described in this paper are on the latter method, called artificial reflex.

Knee-lock state. When the knee-joint is in the locked position we can not control muscle force using linear feedback of knee-angle. Therefore we apply open-loop ramp-down of the stimulation amplitude to minimize muscle force and muscle fatigue. This will result in another unlock situation ('breakdown'), and the process of stabilization restarts. Ramp-down always starts at a defined level above the last breakdown amplitude. In this way an integrating action is provided, to compensate for static errors.

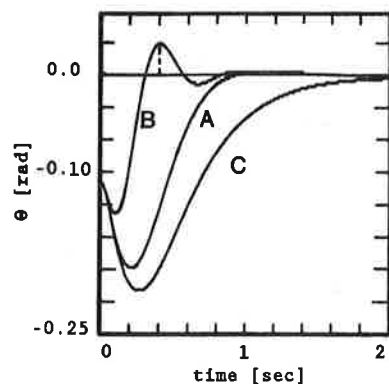


Fig. 1: Step response of PD-controlled knee-joint during standing. Simulation-results for varying muscle gain:
 $K=1.00$, critical damped (curve A)
 $K=1.35$, overshoot 20% (curve B)
 $K=0.95$, settling-time 2 s. (curve C)

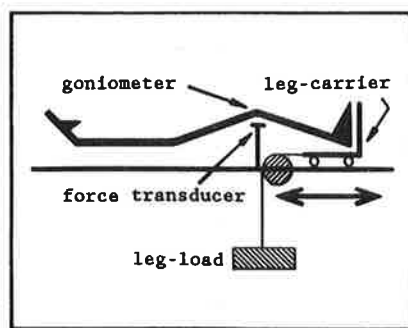


Fig. 2: The stand-simulator. The horizontal moving leg-carrier simulates leg-load and knee-bending during standing.

State transitions. An accurate detection of transitions from lock to unlock and vice versa is important for good controller performance. To determine locking of the knee we use angular velocity data. This makes us independent from goniometer drift, and enables automatic calibration of the locked position after each unlock. Also the natural damping of the knee-joint is used to get an overall stable system. To signal the unlock situation, we use knee-angle information. Disturbance above a threshold of 2 degrees will start the stabilization procedure.

Experimental setup

To test the control strategy in paraplegic patients, we constructed a special stand-simulator (figure 2). The patient is laying on a bench with his feet on a carrier, which can move in a horizontal direction. A mass under the bench provides an artificial leg-load. In this way, the leg-load and movements are reproducible. A force transducer under the knee-joint serves as an artificial kneelock and measures the locking force for evaluation.

To control the stimulation we use an IBM-XT computer with AD-facilities, an electro-goniometer to measure knee-angle, and a current regulated stimulator in which the essential pulse parameters can be controlled by the computer. During the experiments amplitude control was used. To determine knee-angle, the goniometer signal was low-pass filtered (1st order, 15 Hz). To find the angular velocity, the derivative was taken and low-pass filtered (4th order Butterworth, 15 Hz).

RESULTS

Using the outlined set-up, several experiments were carried out on two spinal cord injured patients, both with a complete lesion at level T5-T6. The right-leg quadriceps was stimulated using surface electrodes. To evaluate the controller, the response to a step-change in the leg-load was determined for different controller adjustments. A typical result of a stimulation experiment is shown figure 3. The knee is locked at 30° flexion and the leg-load was 20 kg for one leg. The essential parameters are: sample-rate 100 Hz, puls-rate 20 Hz, pulsduration 0.3 ms, ramp-down 5 mA/sec, integration step 10 mA, knee-angle threshold 2°. Figure 3 shows both the knee-angle response and the stimulation amplitude. It can be seen how after each unlock the stimulation is just switched on. After 11 sec. the leg-load was increased with 5 kg. The extra load was removed after 24 sec. It can be seen how the stimulation level is adapted. The first breakdown at 4 sec. is due to goniometer disturbances. However, the locked position is re-calibrated and the system remains stable.

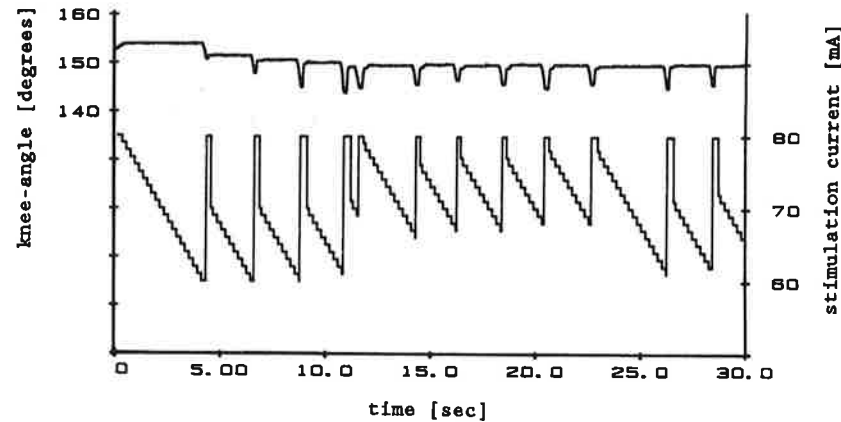


Fig.3: Typical result of a stimulation experiment. Shown are the knee-angle response (*upper curve*) and the corresponding stimulation amplitude (*lower curve*). Refer to the text for details.

DISCUSSION

At this moment the control strategy looks promising. It may result in a patient independent stimulation method for the stabilization of the kneejoint during standing, minimizing the muscle force and providing a dynamic muscle activation. Use of the artificial reflex works satisfying, and the locking velocity is acceptable. Locking of the knee-joint can be adequately detected from knee-angle velocity data. This enables automatic calibration of the locked position and the use of relative angle measurements. Finally, measuring the locking force of the knee, has shown to be a good method for the evaluation of various controller adjustments.

ACKNOWLEDGEMENTS

Our work on FES is supported by the Dutch foundations: 'Stichting Technische Wetenschappen' and 'St. Joris Stichting'.

REFERENCES

1. Peckham PH (1987) Functional electrical stimulation: Current status and future prospects of applications to the neuromuscular system in spinal cord injury. *Paraplegia* 25:279-288
2. Bernotas LA, Crago PE, Chizeck HJ (1987) Adaptive control of electrically stimulated muscle. *IEEE Trans on Biomed Eng* 34:140-147
3. Mulder AJ, Verheijen JME, Hermens HJ, Alsté JA van (1987) Control of standing using functional electrical stimulation. Proceedings of the XI Int Congress of Biomechanics, Amsterdam, ISBN 90.6256.549.2 (in press)

PRACTICAL CLOSED LOOP STAND/SIT AND WALKING SYSTEMS FOR MID THORACIC PARAPLEGICS

EWINS, D.J., TAYLOR, P.N., WHITLOCK, T.L., FOX, B.A., LIPCZYNSKI, R.T., and SWAIN, I.D.

Medical Physics and Duke of Cornwall Spinal Unit (1) Odstock Hospital, Salisbury and Dept. Electrical Eng Bath University (2) U.K.

Introduction

All spinal cord injured patients are encouraged to stand passively on a regular basis, both during rehabilitation following their injury and once they have been discharged from hospital (1,2). Methods commonly used to stand spinally injured patients include; the Tilt Table, Oswestry Standing Frame and lower limb orthoses e.g. plaster of paris backslabs or calipers. Recently the Hip Guidance Orthosis, HGO, and the Reciprocal Gait Orthosis, RGO, have been developed which have the added benefit of providing low energy ambulation.

Over the past ten years functional electrical stimulation (FES) has increasingly been investigated as a means of providing both standing and ambulatory function for paraplegics. This has several advantages over conventional standing, in that the equipment used is small and cosmetically acceptable, not involving a large 'exoskeleton' and that it utilises the patients musculature to achieve function. By stimulating electrically, muscle bulk can return to levels approaching those before injury, producing a corresponding improvement in blood flow.

Open loop standing of mid-thoracic paraplegics is a relatively safe operation to perform in the laboratory (3-5). In recent years much work has been undertaken on the application of closed loop control techniques to the electrical stimulation of muscle. These usually involve the automatic control of one or more stimulation parameters; pulse width, pulse repetition frequency and amplitude. (6-9) Although this work is of fundamental importance, as yet there are not any closed loop systems available for patients to use routinely in the community. The purpose of this research has been to design a simple low cost system to enable paraplegics to stand safely and rapidly in any location and to remain standing for up to ten minutes. Then, equally importantly, enable the user

to sit in a safe, controlled manner. Electrodes and feedback transducers have been kept to a minimum to enable the system to be simply applied while retaining a good cosmetic appearance.

Equipment

The complete system consists of a two channel stimulator which uses knee position and a processor running a modified digital PID controller to control the stimulation amplitude (10). The pulse width and repetition rate are fixed at 350uS and 20pps. 3M Myocare electrodes are used with the positive electrode being placed just proximal to the upper border of the patella. The negative electrode is placed mid way between the patella and the great trochanter, laterally of the mid line to minimise the involvement of rectus femoris which can cause unwanted hip flexion, making functional standing impossible.

This is then used in conjunction with a folding standing frame which replaces the arm rests on a standard National Health Service wheelchair. When not in use this folds away neatly, not increasing the size of the wheelchair in any dimension. It opens out or folds away in a single action, taking less than three seconds for both sides. It is stable and can support up to 100Kg. The 'stand' and 'sit' buttons are located in the ends of the standing frame handles. At present work is proceeding to develop this product further so that it can be used in conjunction with lightweight wheelchairs.

Knee angle is measured by a servo potentiometer attached to a lightweight support pivoted at the knee. This is made from 'Orthoplast' with a 'Plasterzote' backing to ensure a secure fit and minimise slippage. This is worn underneath the clothing.

STANDING

When the user decides to stand they apply the wheelchair brakes, fold away the footrests so that they can position their feet firmly on the floor and fold out the standing frame. They then position themselves on the edge of their chair so that their feet, hands and centre of gravity are all in one plane. The user then turns on the unit and the processor checks a number of system functions, i.e. switches, feedback, calipers, battery condition and EPROM and if any fault is detected the buzzer sounds continually. Given the system is functional the user pushes the 'stand' button for one

second. A PID controller linearly increases the knee angle from 90 to 180 over a period of ten seconds. The leg is then assumed to be straight and the knee angle stored and taken as the calibration position. The PID controller is then replaced with a different control algorithm which maintains the knee in this position within a defined deadband. The gain varies depending in which direction the knee is moving. If the knee moves forward, i.e. out of lock, the stimulation level increases rapidly to prevent further knee flexion. However, if the knee goes into slight hyperextension the stimulation level is decreased very gradually. The processor checks the knee angle every 100mS. Hence the stimulation amplitude can be minimised while maintaining the knee in a stable position. There is a predetermined minimum value to which the stimulation amplitude can fall so that at no time does the control need to be 'bang bang' which has been found to cause problems. This minimum value is increased with time to allow for muscle fatigue.

The user is then able to stand for as long as is required. If they have been standing for so long that the stimulator output is at 95% of its maximum a buzzer sounds to warn them that they should sit down. To sit down the patient holds the sit button for one second and the stimulation level ramps down very gradually. He then sits down keeping his chin tucked in, taking great care not to lean back.

DISCUSSION

In order for a standing system to be used routinely in the community it is essential that the system is safe, reliable and that the user can stand in a wide variety of locations. The system should also be quick and simple to fit and require the minimum of pre-calibration before use. The stimulation level must be controlled automatically so that when the user wants to stand they know they are going to be able to, without any adjustment. These criteria can only be met by a closed loop control system.

The same is true of walking. Our experience with incomplete spinal cord injured patients has shown that variation of response with electrode placement, muscle fatigue and patient condition are too great to enable routine use of open loop devices in the community. At present we have three complete standing systems being used on a regular basis, both in the home and in the

Work is now proceeding to provide similar systems for up to twenty further paraplegics to enable further evaluation. We are also extending this control philosophy to include functional walking for people with incomplete spinal cord injuries and to provide limited walking function for complete mid-thoracic paraplegics. In order to increase understanding and reduction of muscle fatigue we are investigating the use of EMG feedback as an additional control channel.

ACKNOWLEDGEMENTS

The Authors would like to thank the SERC, the DHSS and the Bath Institute of Medical Engineering for helping to fund this work. Dr.R.Orpwood and Mr.R.Nash for the design of the wheelchair standing frame and the staff and patients of the Duke of Cornwall Spinal Treatment Centre.

REFERENCES

- 1 Bromley, I., (1985) Tetraplegia and Paraplegia - A Guide for Physiotherapists Churchill Livingstone ISBN 0-443-03233-5
- 2 Grundy, D., Russell, J., Swain, A., (1986) ABC of Spinal Cord Injuries BMJ Publication ISBN 07279-0108-7
- 3 Bajd T, Krajl A, Turk R, Benko H, Sega J. (1981) Phys Ther 61: 526-7
- 4 Bajd T, Krajl A, Sega A, Turk R, Benko H, Stronjnik P. (1983) Phys Ther 63: 1116-20
- 5 Petrofsky JS, Phillips CA, Heaton III HH (1984) Comput Biol Med 14: 135-49
- 6 Crago PE, Mortimer JT, Peckham PH. (1980) IEEE Trans Biomed Eng BME-27: 306-12
- 7 Crago PE, Wilhere GF, Chizeck HJ, Saito DM. (1982) Soc Neurosci Abstr 8:956
- 8 Crago PE (1983) Eng Med Biol Mag September: 32-6
- 9 Bertonas LA et al (1987) IEEE Trans Biomed Eng BME-34: 140-47
- 10 Ewins, D., et. al. (1988) J.Biomed Eng Vol 10: April 184-8

ON THE MULTI-JOINT CONTROL OF LOWER EXTREMITY USING FUNCTIONAL ELECTRICAL STIMULATION

Y.IGUCHI, K.KUBO, K.FUJITA, N.ITAKURA, and H.MINAMITANI

Department of Electrical Engineering, Faculty of Science and Technology, Keio University, 14-1, Hiyoshi, 3 Chome, Kohoku-ku, Yokohama 223, Japan

INTRODUCTION

Many studies on functional electrical stimulation for human limbs have been carried out in recent years. Basic gait function was attained on hemiplegic patient with an open-loop control system by Kralj *et.al.*. On the other hand, using a closed-loop control system, an adaptive control of joint angle was attempted by Bernotas *et.al.*.

In order to obtain the orthothetic biped gait, multi-joint control with closed-loop system would be suitable. We have carried out the control of ankle and knee joint angles by using PID controller, but these controls are independently done on each joint. For practical action, multi joints should be simultaneously controlled. Two methods for the multi-joint control are considered; one is autonomic decentralized control and the other is coordinate control. When the conventional PID control system is used, autonomic decentralized control is desirable.

During the autonomic decentralized control, however, one of the joint motions interacted with the other joint respectively and the influence is not small. The interaction between joints on realizing the gait control have not yet been discussed enough. From this point of view, this study investigates it and proposes a multi-joint control method with a closed-loop system, then discusses about the incidental problems.

CONTROL SYSTEM

Experiments were carried out with the system shown in Fig.1. Four pairs of rubber electrodes were used to stimulate motor points of both joints. The stimulus waveform was biphasic and their pulse parameter were as follows; 50Hz pulse frequency, 0.3msec pulse width and maximum pulse amplitude of 50mA. Pulse amplitude were determined by 8086 micro processor. The ankle joint angle was measured and controlled with 10msec sample rate.

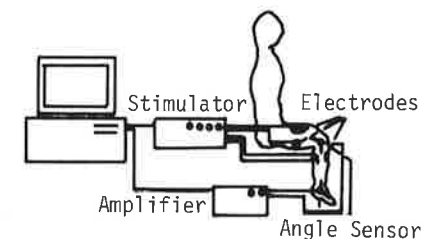


Fig.1 Control system

The angle controller for one joint is shown in Fig.2. It included two PID controllers which were selected in response to the moving direction. The characteristic of control subject was approximated to be linear by subtraction of the threshold amplitude measured in advance from the stimulus amplitude.

Since an oscillatory behavior or a large overshoot was observed in the step response as the result of some trials, a command filter consisted of 3rd-order butterworth LPF with unit gain was appended to the control system in order to obtain less overshoot and good stability.

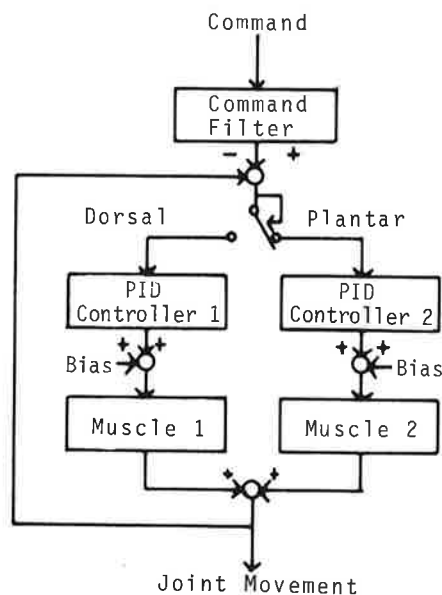


Fig.2 Block diagram of single joint controller

METHOD

The experimental objects are knee and ankle joint angles of normal subject.

Three experiments were carried out for investigation of the influence between knee and ankle joints:

- 1) On condition that knee joint was free while ankle joint was controlled.
- 2) On condition that ankle joint was free while knee joint was controlled.
- 3) Ankle and knee joints were simultaneously controlled.

At the experiment, a leg was mounted on a thin steal pipe and could behave only the rotational movement.

RESULTS AND DISCUSSION

1) Joint movement under the influence that another joint was controlled

Fig.3 (a) shows the motional response when knee joint was controlled on 20° of the angle for extension. Offset angle was 0.6° and it was controlled well. A broken line shows the ankle joint angle on free condition. In this result, the ankle joint moved to the plantar direction. In case of flexion, dorsal movement occurred but was slight. It was thought that the interaction was influenced by the construction of muscle and frame system and the force of gravity. Because the response of extension was sharper than that of flexion, influence of the force of gravity to ankle might be larger than that to knee

The response of ankle joint controlled on 5° of plantar direction is shown in Fig.3 (b). A broken line shows the response of knee joint angle. The influence

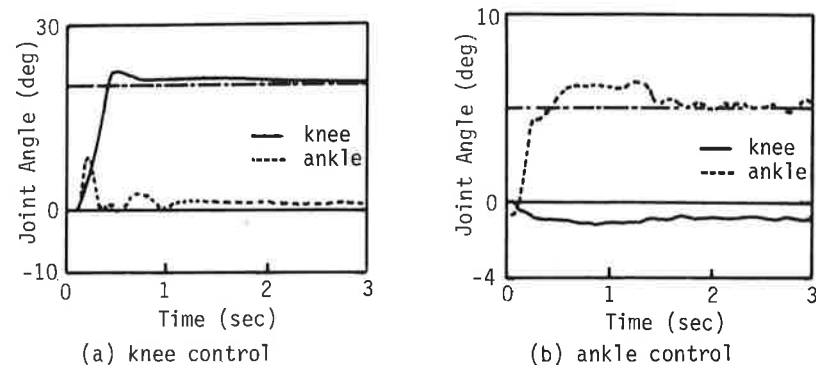


Fig.3 Interaction between two joint angles with step command

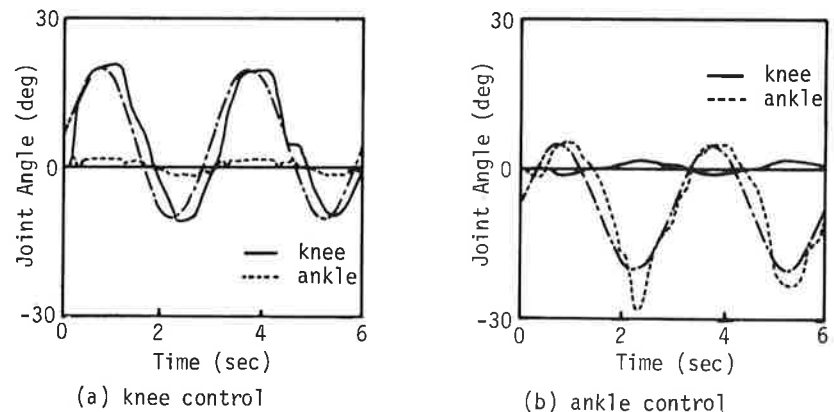


Fig.4 Interaction between two joint angles with sinusoidal command

of ankle movement on knee was slight. The point that we should pay attention to is that the knee joint acted flexional movement when the ankle joint was controlled to plantar direction. It may depend on the construction of the muscle and frame system.

The response to sinusoidal command was also investigated and the result is shown in Fig.4 (a) and (b). (a) is for that the knee joint was controlled and (b) is for the control of ankle joint. Similar tendency to the step response is recognized.

2) Decentralized control of two joints

The response of simultaneous control of two joints is shown in Fig.5. Knee

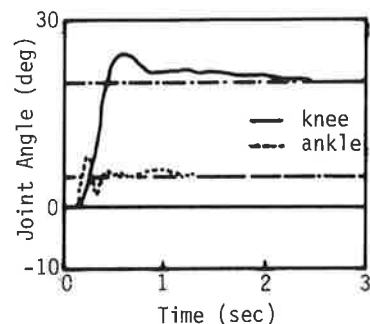


Fig. 5 Step response of knee and ankle joint with PID controller

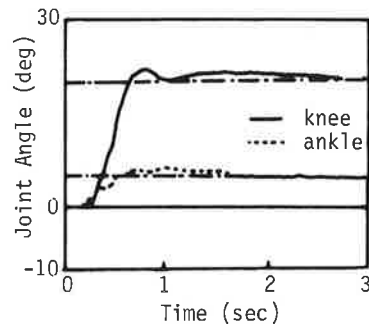


Fig. 6 Step response of knee and ankle joint with PID controller and command filter

joint was controlled on 20° of extension direction while ankle joint was controlled on 5° of dorsal direction. The offset of two joints were within 1° respectively. However, their overshoot were slightly large, and the ankle joint moved oscillatorily.

In order to improve the response, the extension movement of knee joint should be carried out more slowly, and we tried to append a command filter in the knee controller. Fig. 6 shows the response to the application of command filter. Compared with Fig. 5, it was obvious that the response was improved but dead time increased.

CONCLUSION

In this study, the interaction between ankle and knee joint movements was clarified on the application of FES to lower extremity. A method to overcome it was discussed, and the two joints were controlled well by means of the proposed method and closed-loop control system.

REFERENCES

1. A. KRALJ, T. BAJD, R. TURK, J. KRAJNIK, H. BENKO, "Gait Restoration in Paraplegic Patients: A Feasibility Demonstration using Multichannel Surface Electrode FES", *J. Rehabilitation R&D*, Vol. 20, No. 1, 3/20, 1983
2. L. BERNOTAS, P. CRAGO, H. CHIZECK, "Adaptive Control of Electrically Stimulated Muscle", *IEEE Trans. BME*, Vol. 34, No. 2, 140/147, 1987
3. K. FUJITA, N. ITAKURA, K. KUBO, H. MINAMITANI, "Joint Angle Controller with Command Filter for Human Ankle Movement using Functional Electrical Stimulation", *Trans. Jap. IEICE*, Vol. J70-D, No. 8, 1651/1658, 1987

SPECTRAL ANALYSIS OF STIMULATED MUSCLE EMGS TO PROVIDE FEEDBACK IN CLOSED LOOP FES SYSTEMS

T.L. WHITLOCK*, D.J. EWINS*, P.N. TAYLOR**, I.D. SWAIN**, R.T. LIPCZYNSKI*

*School of Electrical Engineering, University of Bath, Bath, England

**Medical Physics Department Odstock Hospital, Salisbury, England

Well documented features of Electromyograms (EMGs) from voluntary muscle contractions are the spectral shift with fatigue and the change in power being a measure of force exerted. This paper discusses the techniques being developed to identify these features quantitatively from surface EMGs to provide feedback for a computer controlled stimulator. This stimulator is being designed to provide practical standing and walking functions for paraplegics. The EMGs arising from the stimulating signal show marked periodicity due to the synchronisation inherent in the Motor Unit Action Potential Trains (MUAPT). This permits the consideration of the EMG as much more of a deterministic process than is possible with voluntary muscle contractions. The work involves the design of a number of differing EMG amplifiers which have been designed to reduce the saturation caused by the stimulating voltage while still providing a large gain to amplify the actual EMG signal. The EMGs are analyzed by Fast Hartley Transforms in 'real-time' using a 68000 microprocessor system which is being replaced by a fast microcontroller. In the frequency domain the signals are filtered to remove effects due to mains interference and stimulating artifacts.

INTRODUCTION

Muscle fatigue is probably the greatest problem limiting the use of FES systems for prolonged function because fatigue occurs faster than during voluntary contractions. This occurs because the same muscle fibres are constantly activated whereas in voluntary muscle the contraction is maintained by the activation of differing groups of fibres. Knowledge of the state of fatigue of a given muscle or group of muscles would be of use as a feedback parameter for computer controlled FES systems². The state of fatigue could provide early warning of the point of failure ensuring the user does not collapse. Many researchers have identified changes that may be observed in the EMG from a voluntary muscle contraction as fatigue occurs¹. One of the most quoted is the spectral shift that occurs in the EMG as the muscle fatigues³. A number of methods have been suggested for monitoring this shift of which the Median frequency is one of the most reliable¹. Other associated features that have been observed are a peaking in the overall power of the EMG and synchronization between individual MUAPTs. Only qualitative use of these features for measuring fatigue has been found. The most often used quantitative feature is the power (amplitude) of the EMG signal^{1,4,5}. This is related to the force being exerted by the muscles from whom the signal was picked up. The relationship of this power to force depends on the investigator^{4,5} but the law may simply be stated as the greater the signal the greater the force. This signal is most often used to control prostheses. In stimulated muscle the use of the Compound Action Potential (CAP) to identify fatigue and force parameters does not appear to have been quantified. The system described here is an attempt to do this by taking the parameters most often described in the literature for voluntary muscle contractions and monitoring them for the stimulated case. The surface EMG is typically less than 2mV whilst the stimulus voltage (constant voltage) is greater than 80V - the majority of this voltage is dropped across the electrode skin interface though. The affect of this stimulus on a normal EMG amplifier leads to artifacts appearing in the recorded signal which not only reduce the signal integrity but may hide it altogether⁹. For the work being carried out here the pickups have to work in conjunction with the stimulator systems already developed, of the constant voltage type. The pickups need to be close to the stimulating site to ensure only the muscles of interest are recorded since future systems may require more channels being active on the limb at once. This paper covers the problems of detecting the CAP with minimized artifact contamination, and sampling and processing of the signal produced from the stimulation to try and identify fatigue and force.

ARTIFACT SOURCES

The main source is the voltage difference between the recording electrodes which is seen as a saturating pulse on the output of the amplifier when the stimulus is present. This pulse is followed by a fast tail due to the subsequent discharge

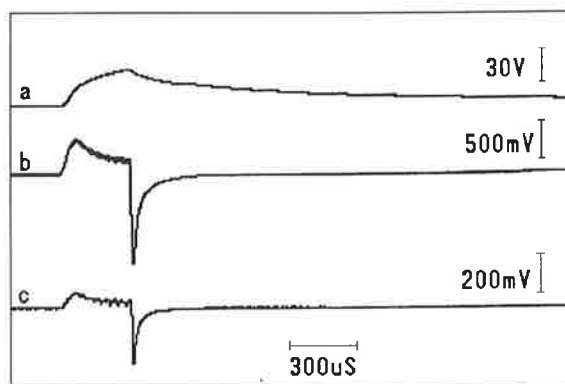


Figure 1. Stimulating Pulse (a) and associated voltage difference seen at the EMG Electrodes; (b) Electrodes not on an equipotential line, (c) Electrodes on an equipotential line.

of the electrodes through the limb (Fig. 1b). This tail is particularly noticeable when using a low output impedance stimulator - after a stimulus pulse from a high output impedance stimulator the skin capacitance discharges through the skin resistance and no current flows through the limb but with a low output impedance stimulator the skin capacitance discharges through the stimulator^{8,9}. A second source of artifact is the effect of the stimulus spike passing through the amplifiers high-pass filter, which causes a slow exponential tail. If the signal is large enough to cause saturation in the amplifier the tail becomes more severe. If this occurs in one of the early stages of amplification the recovery from saturation could take several milliseconds. The size of the tail also be decreased by lowering the cutoff of the high-pass filter⁶. Other sources of artifacts are: any common mode voltage at the recording site, capacitive coupling between the recording and stimulating leads and indeterminant motion artifacts. In these cases if there is an electrode imbalance the common mode signals - assuming equal coupling into each lead- would produce artifacts proportional to the imbalance.

Methods of Artifact Reduction

Some of the artifacts can be reduced to insignificant levels by proper placement of the electrodes. Placing the electrodes on an equipotential line reduces the voltage differences⁹ at the recording electrodes (Fig. 1c). Moving the pickup electrodes so that they are further from the stimulus will reduce the affect of the stimulus and increase the CAP latency time. This will reduce the amplitude of the CAP and information may be lost by the filtering that occurs due to the skin (Figs. 2a, 2b). The use of a constant voltage stimulator means that there is a large artifact due to the discharge current that flows when the stimulator switches off. The design of this particular stimulator means that it has quite a high output impedance. Despite this the best option would seem to be to reduce the electrode charge quickly after the stimulus by clamping the output (Figs. 3a,3b). This generates a large voltage spike on the falling edge which can be removed by one of the modifications described for the EMG amplifiers. The large spike is over in 600µs whilst in the non-clamped case the voltage is still 22mV off the rest potential 5mS after the stimulus. Isolation of the amplifier during the stimulating pulse prevents the amplifier from saturating^{7,8}. This can be achieved in a number of ways:

A sample and hold on the input to the differential amplifier isolates the amplifier and keeps the amplifier close to the voltage that is present when the switch reconnects. To do this a differential sample and hold is necessary as in fig 4.

Switching off the differential amplifier stage when the stimulus is present prevent the stimulus passing through but will not necessarily cause another artifact when it is switched back on because the chip capacitances will not have discharged in the time the amplifier is off.

Computer Artifact Reduction

Any use of the computer system to remove the artifacts will inevitably reduce the rate at which it can update the results. Two obvious options are available, Time Domain or Frequency Domain 'filtering'. Most time domain methods rely on

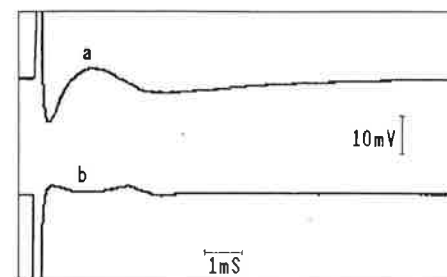


Figure 2. (a) Stimulating Artifact and CAP between Stimulating electrodes. (b) Stimulating artifact and reduced CAP when pickup is remote from Stimulation.

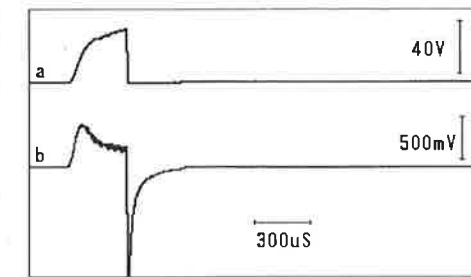


Figure 3 (a) Clamped Stimulating Pulse (b) Resulting voltage seen at EMG Electrodes.

a test being done to get an artifact only signal and then subtracting a scaled version of this from the contaminated CAP. In the frequency domain the effects of the stimulus appear as spectral lines at the stimulus frequency and its harmonics. Mains interference appears at 50Hz (60Hz). Tests on the spectrum of a subthreshold signal indicate that major components are limited to these frequencies. These effects can be removed by deconvolution or by just ignoring the frequency components at the stimulus frequency and its harmonics.

THE SAMPLING AND PROCESSING SYSTEM

The sampling of EMGs assumes that the wave form may be considered stationary. It has been found that EMGs can be considered quasi-stationary over periods of 0.5 to 1.0s⁴ these figures of course apply to voluntary muscle EMGs. In this case the wave form is periodic which therefore means that the sampling must be synchronized to the stimulus pulse it does not necessarily imply that the statistics of the signal itself has changed¹¹. The sampling is synchronized by means of a pulse train from the stimulator that is fed into an input port of the computer and the sampling routine waits for this pulse before starting a set of samples. The processing system is a 68000 based computer running at 8MHz. The A/D is a simple 8 bit converter which is continuously converting at 50kHz. The actual sample rate is set by the rate at which the data is read. For surface EMGs the bandwidth of the signal is about 500Hz^{1,6} so theoretical minimum sample rate of 1kHz is required. The rates chosen are 1024 Hz and 2048 Hz. Analysis of the data is carried out by Fast Hartley Transform (FHT)¹⁰ which is faster in calculating the Power Spectrum than the equivalent FFT routine. For the sample rates mentioned and using a 1024 point FHT gives a frequency resolution of 1 and 2 Hz respectively. The routines use 16 bit signed integer arithmetic returning a spectrum every 600 mS.

DISCUSSION

At the time of writing full quantitative results are not available. However the tests so far carried out do provide some information. Tests carried out on the muscles of people with full voluntary control seem to differ from those carried out on paraplegics. This may be explained by the differing fibre compositions, skin condition, etc. The clamping amplifiers described above have not been available for the initial tests so the removal of the major artifacts is done in the frequency domain by ignoring the stimulus frequency and its harmonics. The tests have been carried out on a number of paraplegics all of whom are part of a standing program. The tests have been carried out at two distinct stages either during stands or once the user is too fatigued to maintain long stands. Two example curves are shown in Figure 4 where it can be seen that the spectral shift downwards occurs in one just at the point at which the stimulus is increased (Fig. 4a). In Figure 4b the spectral shift is in the opposite direction though for each of the stands the force drops more rapidly. As yet there is insufficient evidence to support the validity of these curves however it has been observed on a number of patients that the curve initially follows that suggested for voluntary muscle contraction i.e. spectral shifts downwards

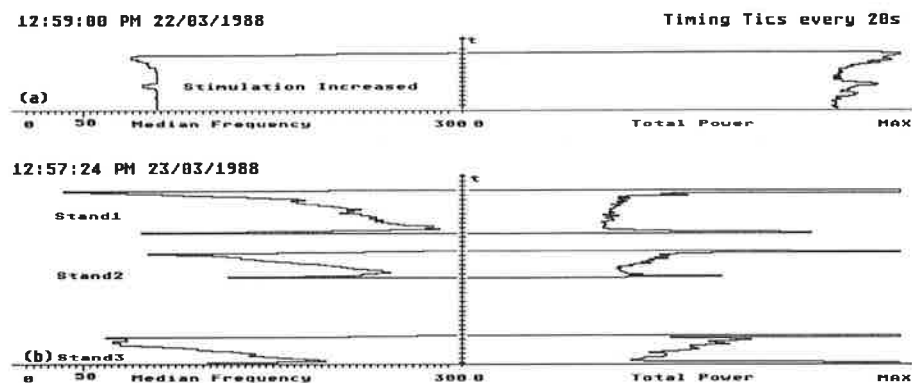


Figure 4. Plots of the Smoothed Median Frequency and Power from Stimulated Muscle EMGs (a) Showing slight frequency drops just before the stimulus is increased to maintain stand (b) Showing median frequency rising during each stand whilst the overall power drops more rapidly

power drops. As the patient does more stands the curve appears to reverse as in Fig. 4b. The power starting level increases but falls faster with the later stands. This would be expected since an increased stimulus and therefore some extra muscle fibres are recruited to maintain the stand, whilst the muscle fibres involved in the earlier contractions would fatigue faster.

REFERENCES

1. J.V. Basmajian and C.J. De Luca "Muscles Alive Their Functions Revealed By Electromyography" Fifth Edition Williams and Wilkins 1985 ISBN 0-683-00414-X.
2. D.J. Ewins, P.N. Taylor, S.E. Crook, R.T. Lipczynski and I.D. Swain "Practical Low Cost Stand/Sit System for Midthoracic Paraplegics" *J. Biomed Eng.*, Vol. 10, pp. 184-188, April 1988.
3. C.J. De Luca "Myoelectrical Manifestations of Localized Muscular Fatigue in Humans" *CRC Critical Reviews in Biomed. Eng.*, Vol. 11 No 4, pp. 251-279, 1984.
4. G.F. Inbar and A.E. Noujaim "On Surface EMG Spectral Characterisation and its application to diagnostic Classification" *IEEE Trans. Biomed. Eng.*, BME-31 No. 9, pp. 760-604, Sept. 1984.
5. J.J. Woods and B. Bigland-Ritchie "Linear and Non-Linear Surface EMG/Force Relationships in Human Muscles" *Amer. J. of Phys. Med.*, Vol. 62 No. 6, pp. 287-299, 1983.
6. V.O. Andersen and F. Buchthal "Low Noise Alternating Current Amplifier and Compensator to Reduce Stimulus Artefact" *Med. & Biol. Engng.*, Vol 8, pp. 501-508, 1970.
7. R.J. Roby and E. Lettich "A Simplified Circuit for Stimulus Artifact Suppression" *Electroenceph. and Clin. Neurophysiol.*, Vol 39, pp. 85-87, 1975.
8. T.L. Babb, E. Mariani, G.M. Strain, J.P. Lieb, H.V. Soper and P.H. Crandall "Sample and Hold Amplifier System for Stimulus Artifact Suppression" *Electroenceph. and Clin. Neurophysiol.*, Vol 44 pp. 528-531, 1978.
9. K.C. McGill, K.L. Cummins, L.J. Dorfman, B.B. Berlizot, K. Luetkemeyer, D.G. Nishimura and B. Widrow "On Nature and Elimination of Stimulus Artifact in Nerve Signals Evoked and Recorded Using Surface Electrodes" *IEEE Trans.*, BME-29 No 2, pp. 129-137, Feb. 1982.
10. R.N. Bracewell "The Hartley transform" Oxford Science Publications 1986 ISBN 0-19-503969-6.
11. D.E. Newland "An Introduction to Random Vibrations and Spectral Analysis" Second Edition Longman Group Ltd 1984 ISBN 0-582-30530-6.

DUAL CHANNEL IMPLANTABLE STIMULATOR

BORUT KELIH, JANEZ ROZMAN, UROŠ STANIČ, MIROLJUB KLJAJIĆ
J. Stefan Institute, E. Kardelj Univ., Ljubljana, Yugoslavia

INTRODUCTION

One channel implantable peroneal nerve stimulators for ankle movement have limitations in as much as it is difficult to correct unwanted inversion or eversion of the ankle. A new dual channel implantable stimulator was developed in order to control two degree of freedom of foot movement, i. e. dorsiflexion and eversion, which enables lifting of the foot, flexion response during swing, stabilization of the knee and hip during stance, and generation of selective patterns of muscle contraction in complex muscle groups. It was hypothesized that a wider range of patients, who were previously not suitable for one channel implantable stimulators, would become eligible for functional electrical stimulation (FES) with a dual channel stimulator (1-3).

SYSTEM DESIGN

Fig. 1 shows a block diagram of the complete system, which comprises of three sections: a programmer, an external transmitter with stimulus control and power unit and an implantable receiver with epineural or epimysial stimulating electrodes.

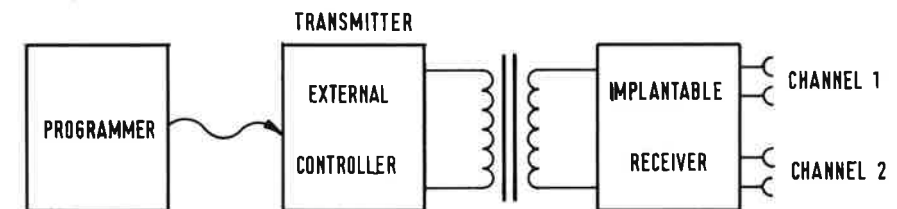


Fig. 1. Block diagram of the complete system

Programmer

The programmer is used for programming the stimulus parameters and stimulation sequences for both channels and for transferring the stimulation data to the external controller by a removable hardwire link. It consists of a keyboard and an alphanumeric display which are controlled by a single chip microcontroller.

External controller

The external controller is also based on a single chip microcontroller which contains the RF output stage, four switches for the amplitude correction and two LED bars for the amplitude indication for both channels respectively.

Implantable stimulator

Hardware of the implant consists of the two separate output stages with bi-phasic current pulses, controlled and powered through a RF antenna. The amplitude and pulse width can be selected for each channel respectively, while the stimulating frequency is common for both channels. These parameters are controlled by an external microprocessor unit. The electronics of the implantable stimulator is assembled with standard 4000-B series CMOS components. The main parts of the electronics are the RF receiver, power supply network, decade counter-decoder, ramp generator, sample/hold, voltage to current converter and two biphasic output stages.

Fig. 2 shows the block diagram of the implantable receiver. The receiving coil is tuned to 2 MHz with a capacitor and is connected to a pulse demodulator and capacitor which stores the energy for powering the stimulator circuits.

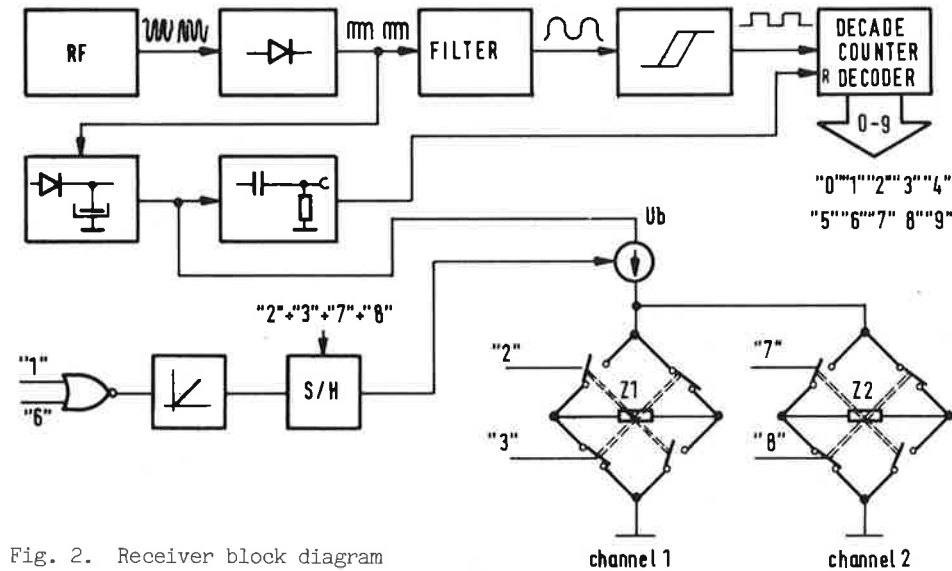


Fig. 2. Receiver block diagram

Signals from the pulse demodulator clock the decade counter-decoder whose outputs control the ramp generator with the sample/hold and output stages.

The timing diagram for the implantable receiver is shown in Fig. 3. Line 1 shows a typical demodulated set of pulses. The first package of five pulses controls the first output stage and the second package of five pulses the second one. At the beginning of stimulation sequences the decade counter-decoder is reset by increasing the power supply and the first output "0" is activated. The second output "1" activates the ramp generator whose output determines the stimulation amplitude. The amplitude linearly depends on the duration of the second

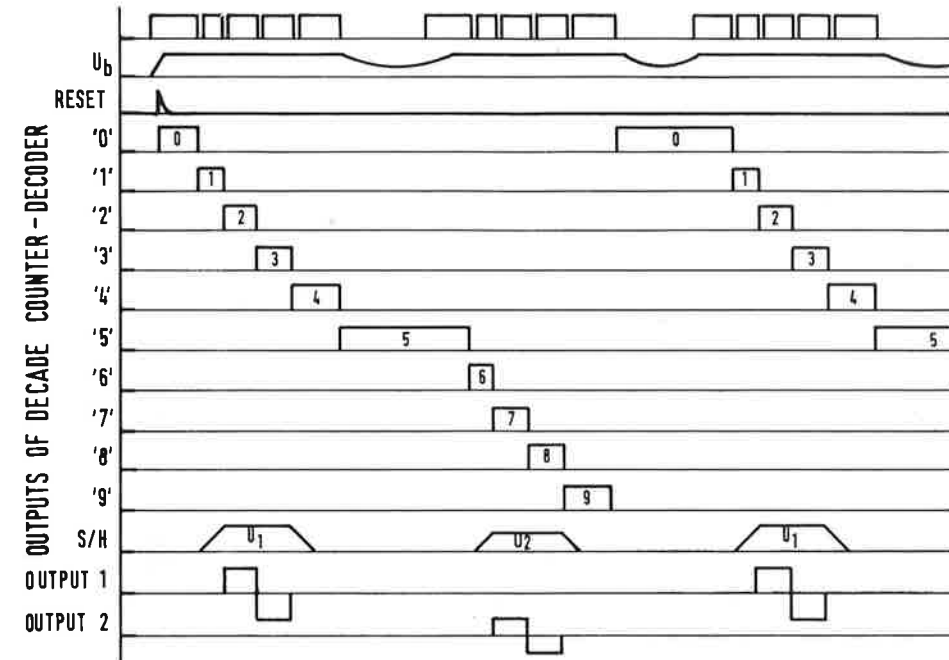


Fig. 3. Timing diagram for the implantable receiver

output "1". The third output "2" is activated by the next pulse on the clock input of the decade counter-decoder which holds the amplitude of the ramp generator and closes the first two electronic switches of the first output stage (Fig. 2). At that moment, the stimulating current flows through the electrodes and the amplitude and pulse duration are determined by the sample/hold voltage and activation of the output "2" respectively. When the fourth output "3" is activated, the current, through electrodes, changes the direction by switching the second two switches of the first output stage. The amplitude of negative pulse is the same as the positive one and pulse width depends on the activation of output "3". The fifth output "4" resets the ramp generator and opens the electronic switches of the first output stage.

The second package of five control pulses clock the output "5" to "9", which control the second output stage.

Fig. 4 shows the thick film multilayer hybrid circuit of the dual channel implant. The new electronic circuit provides the following stimulating parameters: amplitude from 0 to 10 mA, pulse width from 0 to 0.5 ms and frequency from 0 to 100 Hz.

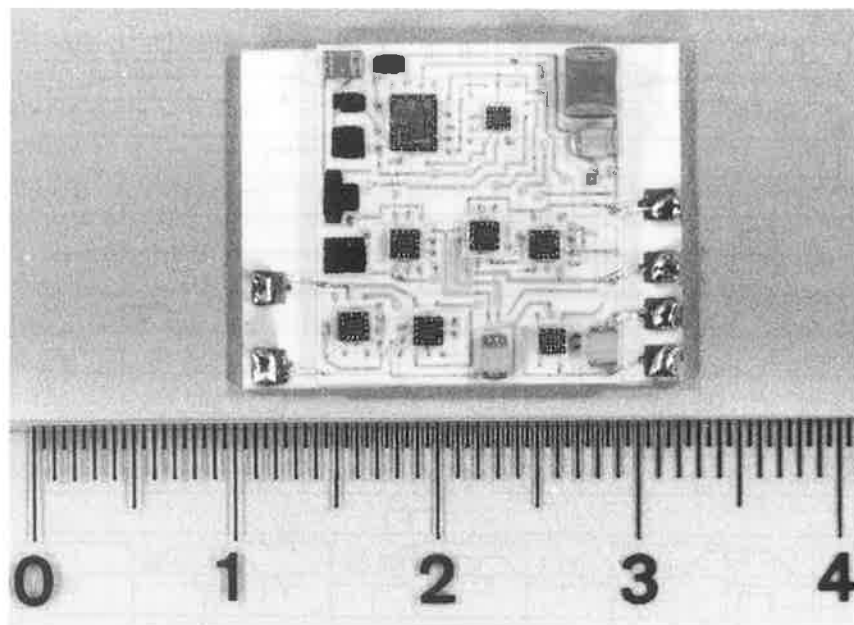


Fig. 4 . Thick film multilayer hybrid circuit of the dual channel implant.

MEASUREMENTS AND CONCLUSION

Measurements of the electronics show that the stimulating parameters are independent of axial and radial dislocation of the antenna, with the exception of the amplitude which decreases for 20 % at 15 mm axial dislocation and for 10 % at 15 mm radial dislocation. The amplitude is constant with loads from 0 to 1 kOhm, except at the maximal amplitude (10 mA) which decreases for 20 % with 300 Ohms to 1 kOhm load. This disadvantage could be reduced by increasing the output energy of the external controller.

With the wide spectrum of stimulating parameters, the new dual channel implantable stimulator is suitable for a variety of applications by simply modifying the electrode arrangement.

REFERENCES

1. Waters RL, McNeal DR, Clifford B, Faloon W (1984) Long-term follow-up of peroneal NMA patients, Proc. of 8th Int. Symp. on ECHE, 471-474.
2. Jeglič A (1972) Two-channel implant approach to an orthotic device, Proc. of 4th Int. Symp. on ECHE, Dubrovnik, 647-656.
3. Bogataj U, Maležič M, Filipič D (1987) Preliminary testing of a dual-channel electrical stimulator for correction of gait, Journal of Rehab. Res. and Dev. Vol. 24 No. 3, 75-80.

IMPLANTABLE STIMULATOR FOR FUNCTIONAL ELECTRICAL STIMULATION OF THE PERONEAL NERVE

J. ROZMAN, B. KELIH, U. STANIČ, M. KLJAJIĆ

J. Stefan Institute, E. Kardelj Univ., Ljubljana, Yugoslavia

INTRODUCTION

This paper describes the development of an implantable stimulator for peroneal nerve stimulation. The RF coupled stimulator system IPPO2 Fig. 1. has a passive receiver implanted under the skin in the region of the fossa poplitea, behind the head of the fibula, with the platinum stimulating electrodes and an external antenna transmitting power to the implanted receiver. In the past five years about 40 bipolar implants, as shown in Fig. 1, with monophasic voltage stimulation pulses frequency of 28 Hz, pulse width from 50 to 500 μ s and direct coupled stimulating electrodes, were implanted; six of them have been subsequently replaced (4). The implant shown in Fig. 2 was a 5 mm thick epoxy resin disc with a diameter of 17 mm. The electrodes were made from platinum wire (99 % purity), diameter 0,7 mm. The anode and cathode were of equal shape and had a geometric area of 37 mm². The passive receiver receives signals with a carrier frequency of 2 MHz from the stimulator and converts it into a train of electrical pulses with charge density of less than 0,1 μ C/mm²(geometric). The electrodes could also be used as fixation loops during the surgical procedure.

MATERIAL AND METHODS

An implantable stimulator has been modified for excitation of the common peroneal nerve with a monopolar epimysial electrode as shown in Fig. 2. As the stimulator is radio-frequency powered and controlled, the system utilizes a 2 MHz radio frequency link to transmit both power and stimulus information. The implant stimulator converts the RF power into DC supply for the implant hybrid electronic circuitry which detects information into stimulating pulses. The stimulating electrode made of pure platinum foil is designed as a little disc to be epineural electrode. The lead to the nerve consists of a multistranded stainless steel lead wire isolated with silicone tube and an epimysial stimulating platinum cathode embedded with medical grade silicone (e.g.: Dow Corning type A medical adhesive) and

reinforced with Dacron mesh. The length of the lead wire depends on the dimensions of the patient's lower extremity. The 'real' surface of the stimulating platinum cathode is the area actually available for charge injection and is about 52 mm^2 . The 'real' differs from the geometric area (37 mm^2) due to the roughness of the surface (factor for smooth platinum is about 1,4 (1,2,3)). The lifetime of the electrode and/or its lead may be the most important limitation in the development of motor prostheses. Placing a stimulating cathode on the perineurium of the common peroneal nerve on the optimal position results in better selectivity. The implant body flexible in the tissue obviates the need for suture fixation, allowing for very small variations in nerve position and relatively free exchange in interstitial fluid, which are important stipulations for long term prosthetic application as indicated in Fig. 2. The neutral electrode is a platinum part of the surface of the implant body with the 'real' surface of about 150 mm^2 as shown in previous figure. Packaging the hybrid electronic circuit and connecting to the electrode involves the utilization of the unique properties of several biomedical materials. The use of these materials is necessitated by the constraints imposed by the stimulator electronics including: nonmetallic encapsulation due to RF coupling and minimum 5 year working lifetime after implantation. The circuit is secured in the

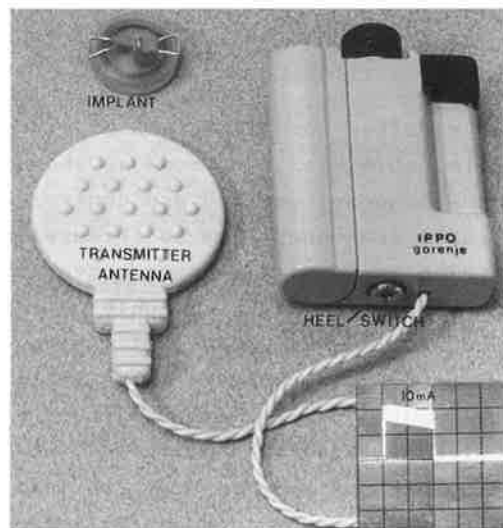


Fig.1. IPPO2 system for peroneal nerve stimulation.

capsule of special wax. Encapsulating material is HYSOL medical grade epoxy resin C8-W795 and hardener WH796. At present the capsule top is coated using medical grade silicone (e.g.: Dow Corning type A medical adhesive). A thin coating is applied by repeated dipping of the stimulator in a bath of silicone thinned with n-heptane followed by air drying. Since the electrochemical reactions depend mostly on the range of electrode-electrolyte voltage over which the electrode cycles from pulse to pulse, the potentials of electrodes during pulsing were measured. Dummy platinum electrodes with the same shape and geometric surface as the real electrodes were connected to the receiver circuitry and immersed in 0,9 % NaCl solution. The potentials were measured versus a Ag/AgCl reference electrode using a high impedance digital voltmeter, type HP 3456A. The separation between receiver and transmitter antenna, frequency of pulses and pulse widths were 1 cm, 28 Hz and 200 μs , respectively.

RESULTS

The implantable stimulator for functional electrical stimulation of the common peroneal nerve was constructed with all the advantages of the former monophasic implantable stimulator and improvements such as new hybrid electronic circuitry with biphasic charge balanced current controlled stimulation pulses, monopolar epimysial stimulating cathode and changed fixation in the tissue, as shown in Fig. 2 were introduced. Biphasic pulses were of exponential decay type.

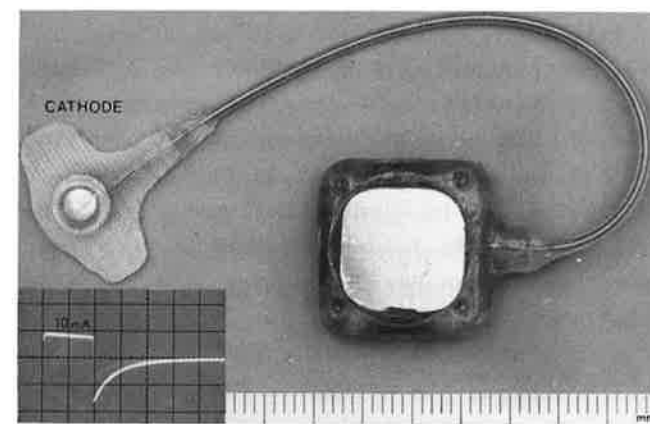


Fig. 2. Implantable stimulator with a monopolar epimysial electrode.

To achieve the appropriate current waveform, a current output stage was added to the electronic circuitry. The delay between the primary (cathodic) and secondary (anodic) pulses were zero. Beside the parameters of the implantable stimulator the observed range of anodic and cathodic potentials, measured in 0,9 % NaCl solution, are shown in Table I. Potentials of electrodes were considerably lower than the potential limits for oxygen evolution on the anode (+1230 mV NHE-normal hydrogen electrode) and for hydrogen evolution on the cathode (-830 mV NHE) (4).

TABLE I

PARAMETERS OF MONOPOLAR BIPHASIC IMPLANTABLE STIMULATOR MEASURED IN 0,9 % NaCl SOLUTION.	
Geometric surface of the common anode	90 mm ²
Geometric surface of the stimulating cathode	37 mm ²
Frequency of pulses	28 Hz
Pulse width	200 μs
Stimulating current	10 mA
Charge density	0,047 μC/mm ²
Ea*	350 mV
Ec*	370 mV

Ea*, Ec*-anodic and cathodic potentials durin pulsing.

REFERENCES

1. Brummer, S.B. & Turner, M.J.: Electrical stimulation with Pt electrodes: 1-A method for determination of "real" electrode areas. *IEEE Trans. Biomed. Eng.* 24:436-439, 1977.
2. Donaldson, N. de N., Donaldson, P.E.K.: Where are Actively Balanced Biphasic ('Lilly') Stimulating Pulses Necessary in a Neurological Prosthesis? II Historical Background; Pt resting potential; Q studies. *Med. & Biol. Eng. & Comput.* 24:41-49, 1986.
3. Mortimer, J.T.: Motor prostheses. In *Handbook of Physiology, The Nervous System II*, Vernon B. Brooks (Ed.), John M. Brookhart, Vernon B. Mountcastle (section Eds.), American Physiolog. Soc., Ch. 5, 155-187, Williams & Wilkins, Baltimore 1981.
4. Rozman, J., Kelih, B., Pihlar, B.: Potentials of Platinum Electrodes Versus a Ag/AgCl Reference electrode, in *Proc 2nd Vienna, Int. Workshop on Functional Electrostimulation, Vienna, Austria, 121-124, September 21-24, 1984.*

SENSITIVITY, SELECTIVITY AND BIOACCEPTANCE OF AN INTRANEURAL MULTI ELECTRODE STIMULATION DEVICE IN SILICON TECHNOLOGY

W.L.C. RUTTEN, H.J. VAN WIER, J.H.M. PUT, *R. RUTGERS AND *R.A.I. DE VOS

Dept. of Biomedical Engineering, Twente University, 7500 AE Enschede

*Laboratory for Pathology and Microbiology, 7512 AD Enschede, The Netherlands

INTRODUCTION

The ideal neural stimulatory information transducer must be able to activate individual neural fibres within a fascicular bundle, for example in a sensory or motor nerve. Basically, the activation process of a myelinated fibre starts by imposing a sufficiently large voltage gradient over the nodes in a fibre in the axial direction (1). As the neural tissue is to be characterized as a inhomogeneous, anisotropic and capacitive volume conductor and the nodes have variable internode distances, this is not an easy task. In a local approach using microelectrodes it is sufficient to apply current pulses to one node in order to reach the stimulatory threshold of the so-called activating functions (2). To this end a multi electrode array in silicon technology is being inserted into a fascicle. This report focuses on three aspects: sensitivity, selectivity and bioacceptance of such a neuro electronic interface, implanted in a motor nerve of a rat.

MATERIALS AND METHODS

The intraneural stimulation device.

Figure 1 shows a schematic drawing of the tip of the silicon device, the twelve Platinum stimulation sites upon it and the positioning of the device in a fascicle. Not shown is the Si₃N₄ insulation cover layer over the tip. The tip length is 840 μm, its thickness 45 μm. The length dimension has been chosen on basis of the fascicle diameter of about 0.5 to 1.0 mm in man as well as in rat. The interelectrode distance (50 μm) follows from the fibre diameter of about 10 to 20 μm and the number of about 300 to 600 efferent motoric α fibres in a population of 1000 to 2000 fibres in an average fascicle of the Peroneus Communis Nerve of the rat. For more information about the design and fabrication see (5).

The tip was inserted in the exposed peroneal nerve of the anaesthetised rat during acute experiments in order to stimulate the Extensor Digitorum Longum muscle of the right hindleg. After insertion the nerve was immersed in parafin oil or vaselin. Rectangular current pulses were used to elicit single twitch contractions of the muscle under isometric conditions. Pulse patterns (see next section) had a repetition interval of 1127 ms. Each force response was the averaged result of 16-64 twitches.

Sensitivity of a single electrode in the array.

If a monopolar extracellular electrode is close to a node n (compared to the internode dis-

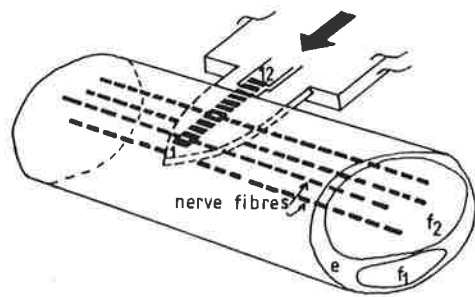


Fig. 1 The silicon stimulation device and the way its tip is inserted into fascicle f_2 . The array has 12 Platinum electrode sites ($10 \times 50 \mu\text{m}$) at interdistances of $50 \mu\text{m}$. e: epineurium. f: fascicle.

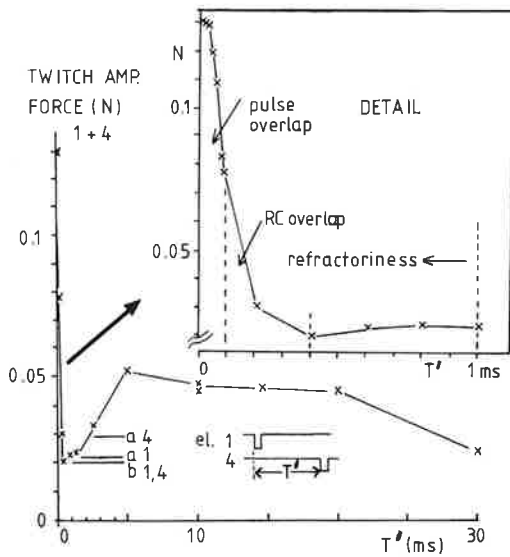


Fig. 3 Force versus time interval T' between cathodic pulses at two electrodes, 1 and 4. Force levels for stimulation at only one electrode (1 or 4) before and after the experiment (b1,4 and a1,4) are also drawn. In the inset "DETAIL" three regions are sketched: pulse overlap ($0-100 \mu\text{s}$), RC overlap ($100-400 \mu\text{s}$) and refractory ($< 1 \text{ms}$) region.

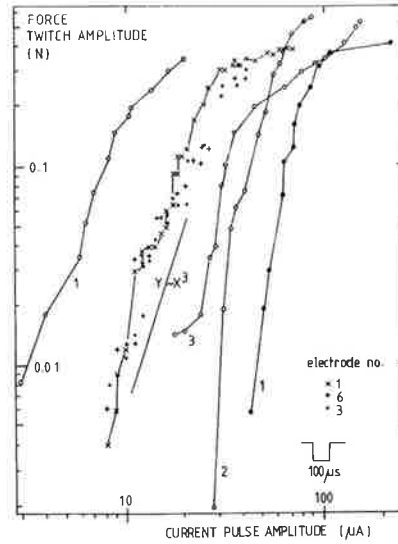


Fig. 2 Selection of recruitment curves for monopolar cathodic stimulation at electrodes no. 1, 2, 3 and 6 in several animals.

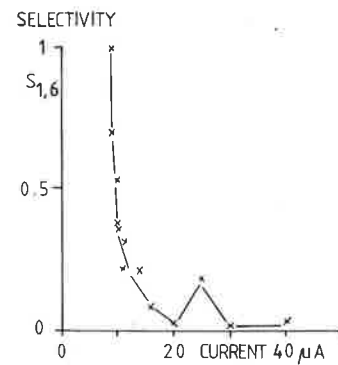


Fig. 4 Selectivity $S_{1,6}$ versus stimulus current. For definitions of selectivity see the text. $T' = 400 \mu\text{s}$.

tance), one can put the two potentials at nodes $n-1$ and $n+1$ equal to zero in the activating function

$$f = V_{e,n-1} - 2V_{e,n} + V_{e,n+1}$$

In a homogeneous, isotropic medium one has for the potential at distance R

$$V_{e,o} = \rho_e I / 4\pi R$$

in which ρ_e is the resistivity of the external medium (Ωm) and I is the current. Solving the RC membrane network model of McNeal (1) for the condition given above yields

$$V_o(t) = -0.19(1 - e^{-T/\tau})I/R$$

in which $V_o(t)$ is the membrane potential minus its rest value. Excitation occurs when $V_o(t)$ reaches the threshold voltage V_d . Defining R_o as the distance from electrode to node beyond which no excitation occurs and for pulsewidth $T = 100 \mu\text{s}$, one can derive (1,2)

$$R_o = 2K I_o \quad (1)$$

with $K = 6.5 \text{ m/A}$. I_o is the rheobase for that distance R_o .

The spherical stimulation volume with radius R_o contains $4\pi N R_o^3 / 3$ nodes, in which N is the nodal density (m^{-3}). This number of nodes excites the same amount of motor units, yielding a total twitch force amplitude of $F_t 4\pi N R_o^3 / 3$ (F_t is the average twitch force amplitude of a motor unit). With eq (1) this leads to a cubic force versus current relationship

$$F = 4F_t 4\pi N K^3 I_o^3 / 3 \quad (2)$$

A selectivity test for intraneural stimulation

Selectivity is maximal when each electrode excites one specific nerve fibre. In practice, with increasing current stimulus fields will expand and overlap with neighbouring fields. A measure for selectivity, which is valid within the refractory period (see below), is

$$S_{i,j} = \frac{F_{i+j} - F_j}{F_i} \quad \text{or} \quad S_{j,i} = \frac{F_{i+j} - F_i}{F_j}$$

in which F_i (or F_j) is the force due to electrode i (or j) separately and F_{i+j} is the force due to stimulation at both electrodes. In the latter case S will have a value between zero and one, provided the stimulus timing fulfills three requirements. First, the pulse at electrode j must have no temporal overlap with that at electrode i . Secondly, the pulse at j must be separated in time from the pulse at i to let the membranes be fully discharged. Thirdly, the two pulses must arrive both within the absolute refractory period of 1 ms. The optimal separation must be derived from experiment.

Bioacceptance

Bioacceptance was tested by chronic implantation of the device tip in the peroneal nerve of the rat. Five animals were implanted. The tip remained in the nerve for 1,2,3,4 and 8 weeks. After these periods the nerves were removed over a length of 1 cm and kept under natural stretch in buffered formalin. They were imbedded in plastic (JB4) and serial sections were cut, $3 \mu\text{m}$ thick. The sections were stained with Haematoxylin and eosin, Kluver-Barrera (myelin), Elastica von Gieson (connective tissue, elastic), and Bielchowsky (axon cylinders). In most

cases the tip was removed before or during sectioning.

RESULTS

Sensitivity

Experiments were performed in six rats. A representative selection of force versus current curves in four animals is given in figure 2. Figure 2 shows saturation of the recruitment curves to about 0.5 N in all cases. Stimulation starts at the lowest attainable force level, varying between 0.002 and 0.015 Newton. These levels are probably single motor unit levels. Recruitment curves are sampled series, no attempt was made to find all possible (discrete) force levels. For comparison the F versus I^3 relation (eq. 2) is drawn also in this figure. The five left most curves obey this relationship, while the two rightmost curves are steeper in the low F range. Other experiments (not shown) in which current was fixed and pulse width T varied, yielded that $\tau = 70 \mu\text{s}$ is a realistic experimental value. The application of equation (2) to the most sensitive curve in fig. 2, with $T = 100 \mu\text{s}$, $K = 6.5 \text{ m/A}$ and $F_t = 0.01 \text{ N}$, gives an estimate for the nodal density: $N = 8 \times 10^{12} \text{ nodes/m}^3$. This implies an internode distance of 0.5 mm (nerve diameter 1 mm, fibre diameter $10 \mu\text{m}$, a relative abundance of 30% of motoric fibres and the closest possible packing).

Selectivity

Figure 3 shows the force as a result of stimulation with fixed currents at two electrodes of the array, no. 1 and no. 4 (interdistance $150 \mu\text{m}$) as a function of pulse separation T' . For $T'=0$ the combined force is 0.13 Newton which is far more than just the summation of two times 0.02 N, but still below a factor $2^3 = 8$ times 0.02 N. It indicates that the current fields of these two electrodes almost completely overlap. This is corroborated by the decrease of the force to the single electrode level at $T' \approx 400 \mu\text{s}$. Beyond about 1 ms the stimulated nodes are no longer refractory, so mechanical addition of twitches occurs up to the maximal possible value of 0.05 Newton (apparently the force levels drift upward during the experiment, see the figure, a(fter)4 and a1). Beyond a separation of 20 ms the addition is less effective as this time interval is that of the maximum of a twitch. Beyond $100 \mu\text{s}$ and below $400 \mu\text{s}$ the membranes still contain enough charge to enable currents to raise the membranepotential above excitation threshold. This lead us to a choice of $400 \mu\text{s}$ between two pulses. Figure 3 is representative for the bad selectivity we obtained, also at low stimulus levels, up to electrode separations of $200 \mu\text{m}$. Only beyond $250 \mu\text{m}$ selectivity reaches values of one, at low currents (figure 4).

Bioacceptance

In all cases the implant site of the device tip was easy recognizable in the stained sections by a histiocytic (giant cell) reaction with some eosinophils (fig. 5). In the surrounding of the tip some pigmented material (silicon particles) together with a histiocytic reaction was seen. In all cases the nerves showed a proliferation of Schwann cells, new blood vessels, fibroblasts and tissue edema. After one week this reaction was moderate, after 2-4 weeks strong and after 8 weeks (one case) possibly a slight decrease occurred. There seemed to be a slight mastcell proliferation

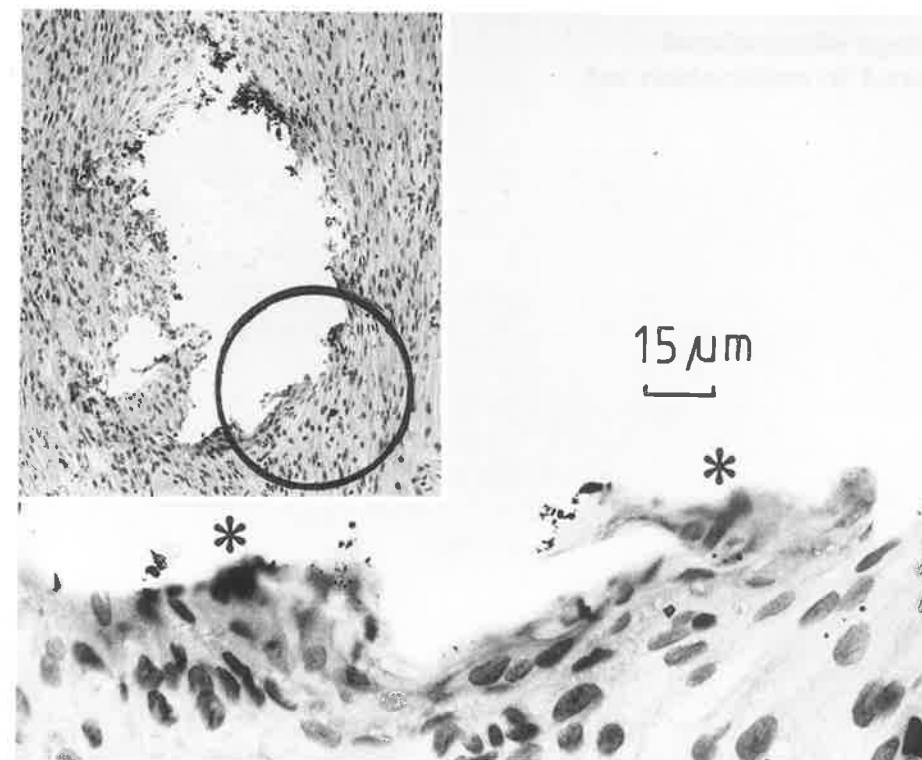


Fig. 5 Longitudinal section ($3 \mu\text{m}$ thick) of the peroneal nerve through the region of the implanted tip (Haematoxyline staining). Inset above left shows an overview after the tip has been removed, 8 weeks after implantation. The region within the circle has been enlarged below. Small black particles are Silicon grains (artefacts). Giant cells are indicated by the * symbol.

and some degree of demyelination. No axon destruction was observed. The epi- and perineurium showed also inflammation reactions, adhesions and probably a slight increase of connective tissue. During the implantation period the motoric behaviour of the rats was also observed. Not any outer sign of disfunctioning of the implanted hindleg was seen.

REFERENCES

1. McNeal D (1976) IEEE Transactions on Biomed Engineering 23:329-337
2. Rattay F (1987) J Theoretical Biology 125:339-349
3. Edell DJ (1986) IEEE Transactions on Biomed Engineering 33:203-214
4. Prohaska OJ, Olcaytug F, Pfunder P, Dragaun H (1986) IEEE Trans. BME 33:223-229
5. Veltink P, Rutten WLC (1986) In: Lodder CJ (ed) Sensors and Actuators, micr technology for transducers. Kluwer, Deventer Netherlands pp 229-239

**Implantable systems
for restoration of function**

IMPLANTABLE NEUROSTIMULATORS

THE PHRENIC PACEMAKER - Technology and rehabilitation strategies

HERWIG THOMA, H.GERNER, W.GIRSCH, J.HOLLE, W.MAYR, H.STÖHR

Institute for Biomedical Engineering and Physics, 2nd Surgical
Clinic Univ. Vienna, Sensengasse 8/19, A 1090 Vienna, Austria

1. INTRODUCTION

The application of modern technology in medicine is controversial nowadays. Enormous costs, high degree of redundancy, loss of patients personality, unjust distribution of resources (regional as well as international) and not least functional and practical faults give rise to partly justified criticism /1/.

The application of highly technicalized methods is particularly difficult in chronic diseases. Nowhere, not even in the field of intensive medicine, the patient-specific technology is so complex and pose so many problems - depending of course on the degree of disability - as in chronic cases.

The goal of this article is not only to describe the present state of technology of implantable neurostimulators but also to explain at least the basic criteria of a functional rehabilitation. For this purpose we describe the extreme situation where a phrenic pacemaker is applied in a patient with complete tetraplegia and additional respiratory paralysis. The first part of this article deals with the technology of our implantable multichannel neurostimulators, the second part describes a structured rehabilitation which allows the patient to reach the optimum of life quality. Consequently we come to the conclusion that the optimal rehabilitation means the optimum of patients self-treatment, sole responsibility and independence. Patients satisfaction and will to live is guaranteed when he is convinced at having reached everything within the bounds of his handicapped possibilities.

2. PRESENT TECHNOLOGY OF THE RESPIRATORY PACEMAKER

The components of a (proper) respiratory pacemaker (fig.1) are the following:

- (1) a battery-powered control unit (8 channels),
- (2) an external high frequency (27 MHz) transmission coil for control and power supply of the implant,
- (3) the electronic implant (thin film technology with a receiver coil and connector pairs (8 channels),
- (4) leads for electrodes,
- (5) ring-shaped electrodes (stainless

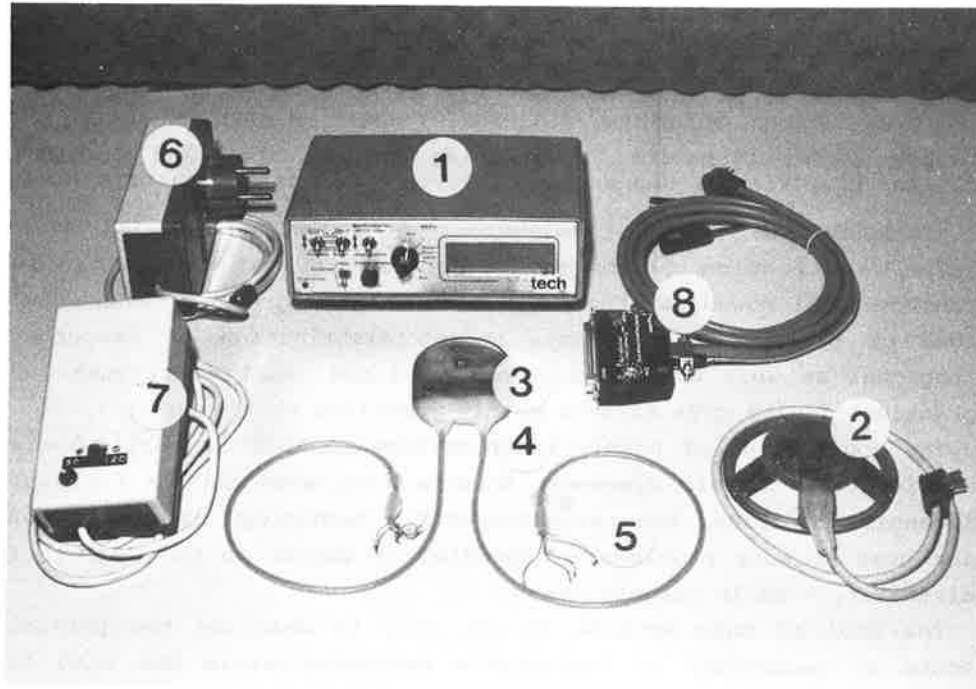


Fig. 1. Components of the respiratory pacemaker

steel 316, 1 mm diameter). Peripheral devices required are a (6) main supply, (7) a supply using car batteries, and (8) a trigger unit for the respirator for training purposes. The features of the respiratory pacemaker are:

1. An external control device with rechargeable batteries for 24 hour operation; a built in "round-about electrode" circuit, with free programming of 16 combinations /2/; control of the constant current source between 0-8 mA, resolution 0,25%; impulse duration variable from 0,1 to 1 ms; impulse frequency variable from 10-40 Hz; adjustment of respiratory rate in the range of 5-60 per minute; adjustment of duration of inspiration from 0,5-6 sec
2. Transmission coil with single turn antenna (27 MHz) and operational range between 0 and 100 mm due to digital

transmission

3. Eight-channel implant - 4 electrodes for each nerve, utilizing thinfilm hybrid technology with connectors for the electrodes.
4. Leads for electrodes in 316-stainless steel, polyfil (12 x 0,05 mm)

Extensive studies were done to achieve standardization of our stainless steel electrode /3/. The electrode lead consists of 12 monofilaments with a diameter of 0,05 mm. The lead is isolated by silicone rubber. The ring-shaped end of the electrode has a diameter of 1 mm. The ring is sutured directly to the epineurium with a 8/0 suture.

For application in infants the implant has been made even smaller. The implant has a shape of a flat, rounded spherical segment. 8 electrodes are led out of its underside.

In the last years great efforts were made to improve the 8-channel implant which has been used in the clinic since 1982. Instead of the thinfilm hybrid technology, the thickfilm technology is applied now. Due to development of custom-specific switching circuits the size of implants could be further reduced despite the thickfilm technology and the increase in number of channels. In order to optimize the application of the implant system for different purposes (respiratory pacemaker, leg pacemaker, hemiplegic patients) a so-called master slave system has been developed /4/. It consists of a minimum of 10 stimulation channels (master implant). An optional number of further units (slave implants) with 10 stimulation channels each can be connected to this unit (maximum number of channels: 80).

Independantly of the distance between the transmission and receiver coils, the implant control is carried out by digital pulses (32 bits per one stimulation puls) of the high frequency carrier, which also supplies energy for the implant. 10-channel implants are tested presently in animals.

For the new implant generation also the external control has been redesigned. The basic idea was to create separable program and control units (through the RS 232 interface). A normal personal computer can be used for programming, the control unit is equipped with the Philips 80C552 microprocessor.

3. APPLICATION OF NEUROSTIMULATORS AS PHRENIC PACEMAKER

The application of the phrenic pacemaker is indicated in the following cases:

- * high-level paraplegia (within the region of C0 to C3)
- * central failures of respiratory center e.g. tumor
- * severe disturbances of the rhythm of respiration e.g. Pickwickian syndrome
- * any other severe respiratory depressions

Contra-indications exist in case of pulmonary diseases. At present, the phrenic pacemaker can be applied only if phrenic nerves function properly. The course of implantation is as follows:

The operation starts with a median skin incision above the upper part of the sternum, followed by a median sternotomy of the upper two thirds of the sternum. The procedures that then follow include: the opening of both pleural cavities, identification of both phrenic nerves in the upper mediastinum, and incision of the pleura sheathing the nerves.

A skin incision in the right upper abdominal wall is made, together with a subfascial pocket for the implant. When the implant is positioned the electrodes are pulled through subcutaneously and underneath the caudal part of the sternum into the upper mediastinum. Fixation of the electrodes (4 to each nerve) to the epineurium of the nerve with 8/0 prolene sutures in a square position is done using microsurgical techniques. First function tests of all electrodes are then carried out. Final steps include insertion of two Bülow-drains into the pleural cavities and wound closure in layers. At the end of the operation, the second and final function tests of the implant are made.

The intrathoracic position of electrodes offers several advantages, but this is by no means a prerequisite for their application. It is advisable to position the electrodes in the cervical region, especially in not chronic cases.

4. NEW REHABILITATION STRATEGY (Fig.2)

The stimulation, i.e. training of diaphragm, starts 10 to 14 days after the implantation. During training of the diaphragm, the respiratory pacemaker can be synchronized with the respirator. For this purpose a special trigger device was developed. The training of auxiliary respiration starts even before operation and is

necessary because of the possibility of failure or improper handling of the respiratory pacemaker. Details of the special physiotherapy for strengthening the auxiliary muscles of respiration have already been published /5/. The aim of this training is to allow the patients unaided respiration via auxiliary muscles over a time span of at least a few hours. Within a minimum of half an hour, the patient is able to be transferred to an ordinary ward. At this time the functional rehabilitation starts with technical environmental aids (e.g. for reading, writing, playing, making telephone calls and computer programming). In the sequence of medical intervention and rehabilitation the patient is able to be discharged from the hospital and stay at home. A major goal of our rehabilitation is to close the tracheostoma. To improve mobility, the patients are trained to use an electrically driven wheel chair via chin controls and also are trained in the handling of alarm systems.

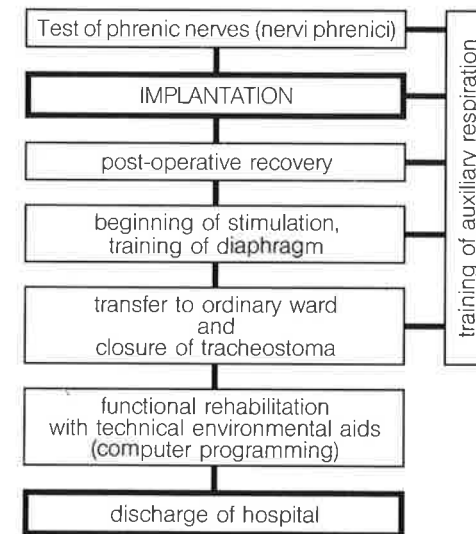


Fig. 2. Sequence of medical intervention and rehabilitation

To demonstrate our rehabilitation strategy upon implantation of the respiratory pacemaker we have made a video film which can be seen by every interested person /6/.

5. RESULTS

Reliabilität

Until 1983 the implant components were mounted on a printed plate. Due to creeping distances the liquid incursion ocured with- in 2 years after implantation and the implants had to be replaced. No implant produced at a later time without a printed plate has failed until today except one failure caused by a defective compo- nent. Despite replacing there were no failures in plug connections of electrodes, leads or electrodes. There good results are conse- quence of our extremely expensive quality test /7/.

Clinical application

Out of our neurostimulators 4 leg pacemakers and 9 phrenic pace- makers have been implanted in patients up to May 88 (Fig. 3).

Table with columns for Patient Initials, Year of Birth, Sex, and years 1982-1988. Rows 1-13 list patient details and events (1-7) marked on a grid.

Fig. 3. Time table with events of 13 patients implanted with the leg and respiratory pacemaker. Events: 1. implantation, 2. failure (implant), 3. infection, 4. dislocation (electrodes), 5. implant change, 7. patient died, 8. reduced function

Our method of round-about stimulation allows fatigue-free stimulation (24 hours per day) of both halves of the lungs at a normal respiratory rate. This advantage enables closing of tracheostoma and, in fact, in all patients discharged of hospital tracheostoma could be closed. All patients considered this at a

great advantage.

In emergency cases the patients attendants use inflating bellows, some patients have "iron lungs"; also the application of a triggered respirator has proved successful since such patients should regularly make an aerosol therapy. One patient with implan- ted leg pacemaker died of cerebellar neoplasm 2 years after the implantation so that the electrodes could be examined (Fig.4) and histologic sections could be made from the transition region electrode/nerve.

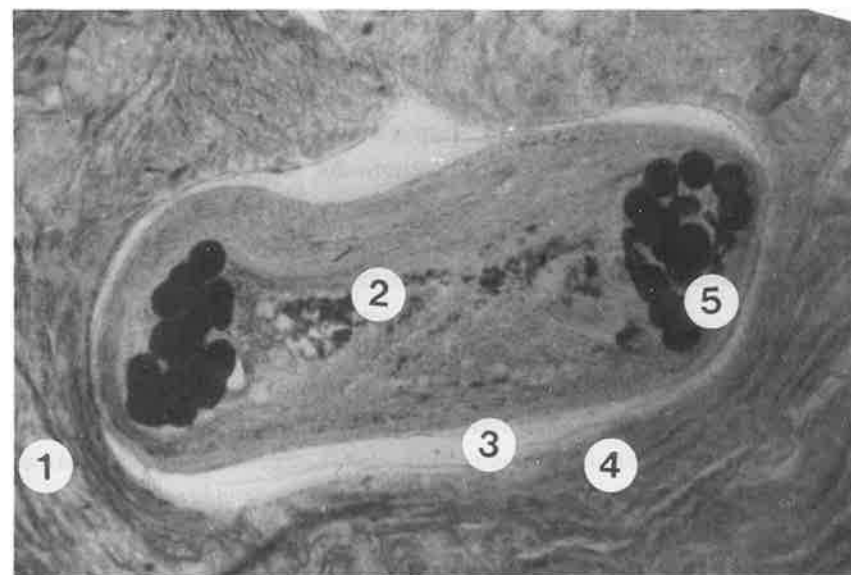


Fig. 4. Cross section of the active non-isolated electrode. 1.connective tissue, 2.round-cell infiltration, 3.liquid, 4.pseudo- sheat, 5.non-isolated electrode

Up to now there are no usable results of experimental implantation of the new generation neurostimulators in animals.

6. DISKUSSION

Electrophrenic respiration - the control of respiration by proper stimulation of phrenic nerves - was first discussed in a publica- tion by Sarnoff in 1948 /8/. Since then, numerous investigators have described in vivo experiments and clinical application /9-13/.

Unlike the cardiac pacemaker, however, the phrenic pacemaker has had no significant success in recent years. Perhaps the modest progress in this field has been a result of the electrically induced fatigue of the nerve-muscle complex. Glenn localized this fatigue in the area of the motor end-plate /10/.

To avoid the electrically induced fatigue mentioned above, in 1973 we developed the so called "round-about electrode" /14/ which solved the problem of fatigue, but poor technologic standards at this time prevented a practicable solution.

Also other groups occupy themselves at present with possibilities of a fibre-selective and locally variable stimulation according to the round-about method protected by our patent.

It is only in the last few years that more complex neurostimulators have been developed and important progress has been made with cochlea stimulators for inner-ear deaf persons. This was possible due to methods of microelectronics (hybrid technology, custom-specific circuits ...) and standardized methods of sealing (hysol sealing, metal cases); also experience gained from research on reliability of electrodes of the heart pacemaker was very important.

Although efforts have been made recently to organize the establishment of the respiratory pacemaker (Tampere, Finland, Oct. 87) we still think that the high developing costs can pay only if the same implant can be used for various goals of neurostimulation. This means that specific solutions for respiratory pacemakers such as (1) safe control system in case of failure, (2) sensor controlled respiration, (3) expiration adopted to the rhythm of speaking, (4) additional stimulation of other groups of muscles, (5) mode for expectoration, will be available for the patient only with a significant delay.

Advantages of our development can be summarized as follows:

- * The method of "round-about stimulation" protected by patent allows fatigue-free stimulation - 24 hours per day - of both halves of the diaphragm at a normal respiratory rate.
- * The epineural application of the electrodes makes the muscle respond softly with minimum exposure of biomaterials at the nerve due to a new kind of electrodes.
- * By means of a new control, which works in a closed loop using a sensor, the respiratory minute volume may be adjusted

individually to the patients.

- * A number of peripheral devices reduce staff expenses and allow safe operation - particularly AT HOME:
 - a) Control adjustment of the respiratory minute volume in a closed loop
 - b) Automatic measuring system (also used for permanent documentation of the stimulation parameters).
 - c) Trigger unit for the respirator during the training period
 - d) Alarm for failures at home (upon request, connected to the PTT network).

Beside the problem of realization of special developments concerning functional substitution of respiration control, as mentioned above, there is in praxis still a number of problems:

During training we observed a period when, although the diaphragm is already trained, the patients still seem to have problems in synchronization with the vocal cord muscles (note that tracheostoma is closed!). A fixed respiratory rate is still used. Although this rate can be changed, e.g. during the night, every fixed respiration rate is unphysiologic. Expectoration is difficult and has to be supported by relatives and other care personnel. The alarm systems are not standardized, more can we guarantee 100% reliability for either alarm-sensors or implants. It turns out that most failures are due to improper handling and at the very least we have to expect complications, e.g. because of infections secondary to a change in pulmonary function.

Analyzing our rehabilitation strategy, we observed the following advantages:

- * Despite the necessity for unaided respiration when using auxiliary muscles, the patient is able to influence his tidal volume arbitrarily.
- * Closing of the tracheostoma offers physiologic respiration conditions with normal verbal communication
- * Not least of all, the reduction of care costs resulting from discharge from ICU to home should be discussed.
- * We found a substantial increase in quality of life for the patients and an increase in comfort of the care-giving personnel resulting from the training in communication aids and outdoor use of an electrically driven wheel chair with a chin control and an alarm system.

* If the patient is able to be discharged from the ICU, there is no question about cost effectiveness: the cost of the respiratory pacemaker is about the same as the cost of staying 3 weeks in the ICU.

ACKNOWLEDGEMENTS

We are grateful for the financial help of the Austrian Research Foundation (FWF), the Lorenz Böhler-Gesellschaft, Jubiläumsfonds der Nationalbank, Ministry of Research and Science, and the Handelsministerium (ERP-Fonds).

REFERENCES

1. Thoma H (1986) *Theoretical Medicine* 7: 305-317
2. Holle J, Moritz E, Thoma H, Lischka A (1974) *Wiener Klinische Wochenschrift*, 86 (1): 23-27
3. Thoma H, Frey M, Holle J, Losert U, Rosenkranz D, Stöhr H (1981) Experiments on the electrode nerve connection, 7th Internat. Symp. on External Control of Human Extremities, Dubrovnik
4. Stöhr H (1986) State-of-the-art of custom designed integrated circuits with respect to implantable stimulation devices, 2nd Vienna Internat. Workshop on Functional Electrostimulation, Proceedings, Vienna, pp 17-20.
5. Gerner HJ, Kluger P (1986) High quadriplegia accompanied by neurogenic respiratory insufficiency, potentialities, limits and outlook, 2nd Vienna Internat. Workshop on Functional Electrostimulation, Proceedings, Vienna, pp 157-161
6. Weber JP, Holle J, Thoma H (1988) Der Atemschrittmacher - medizinischer Eingriff, strukturierte Rehabilitation und Lebensqualität nach Entlassung, Videofilm
7. Schwanda G, Mayr W, Stöhr H, Thoma H (1985) Concepts in quality assurance for implantable neuromuscular stimulators, 5th World Congress ISAO, Chicago
8. Sarnoff SJ, Hardenbergh E, Whittenberger J (1948) *Am. J. Physiol* 155:1
9. Escher DJW, Ashley W, Ertag W, Parker B, Furman S, Robinson G (1968) *Trans Am Soc Artif Int Organs*, 14:192-197
10. Glenn WWL, Holcomb WG, Gee JBL, Rath R (1970) *Ann Surg* 172: 755-773
11. Holle J, Moritz E, Thoma H (1971) *J Anaesthesist* 20:102-106
12. Pengelly LD, Alderson AM, Milic-Emili J (1971) *J. Applied Physiol* 30:797
13. Stemmer EA, Crawford DW, List JW, Heber RE, Connolly JE (1967) *J Thorac Cardiovasc Surg* 54(5):649-657
14. Thoma H (1975) Verfahren und Vorrichtung zur Langzeitstimulation von Nerven und Muskeln, OSPA 330342

FUNCTIONAL ELECTRICAL STIMULATION OF THE POSTICUS MUSCLE IN BILATERAL RECURRENT NERVE PARALYSIS

MICHAEL ZRUNEK*, W. STREINZER*, W. MAYR**, H. GRUBER***; H. THOMA**

* 2nd ENT-Dept., University of Vienna, Alserstraße 4, A-1090 Vienna

** Bioengineering lab., 2nd Surgical Dept., Vienna, Austria

*** Institute of Anatomy, University of Vienna, Austria

INTRODUCTION

In cases of bilateral recurrent nerve paralysis the patient is no longer able to open the glottis sufficiently for inspiration. The disease is most frequently caused by thyroid gland operations. The multitude of treatments shows that a therapy of choice does not exist.

With the goal of achieving a breath correlated glottis opening, our study group is engaged in direct electrical stimulation of the paralyzed posterior cricoarytenoid muscle (PCM) in sheep.

MATERIAL AND METHODS

A one sided paralysis of the recurrent nerve was set by resecting a nerve piece of approximately 2 cm length in three sheep. Bipolar electrodes with skin-feed-through connectors were implanted in the ipsilateral posticus muscle and an intermittent chronic direct electrical stimulation started over an external stimulation unit.

The stimulation parameters were:

+/- 7 mA biphasic exponential pulses, 30msec + 30msec duration, 10 Hz frequency, 1,5 sec stimulation/2 sec rest.

The daily stimulation time was increased from 12 hours per day to 24 hours per day over a period of between 45 to 68 days.

The success of stimulation was documented by means of direct microlaryngoscopic video recording of the abduction degree of the stimulated vocal cord site.

Neuromyography and electromyography of the denervated vocal muscle was performed routinely to make sure that the stimulated muscle was not reinnervated.

After termination of the test the denervated, stimulated and the healthy muscles were removed and examined histo- and biochemically.

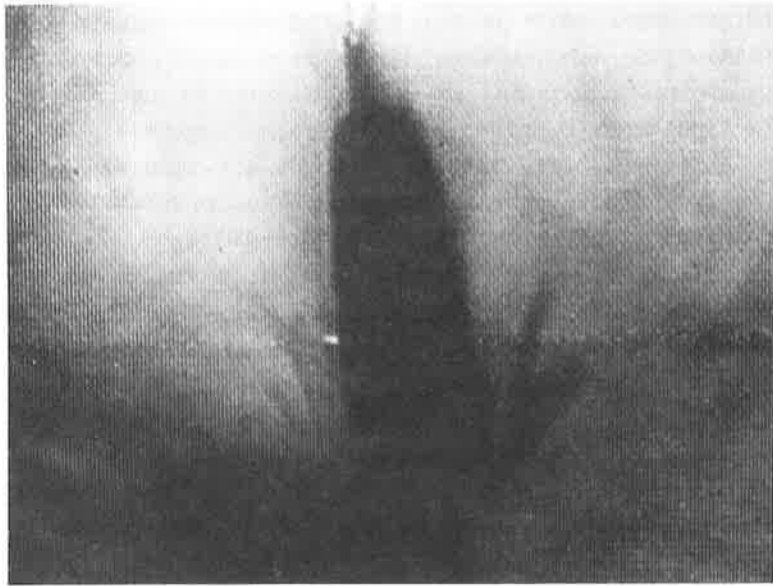


Fig.1. Direct microlaryngoscopic view of a sheep larynx in rest.



Fig.2. Direct microlaryngoscopic view of a sheep larynx during direct electrical stimulation on the right side.

SHEEP 24 CONTROL POSTICUS MUSCLE: fibertyp1=hlw;2=sld

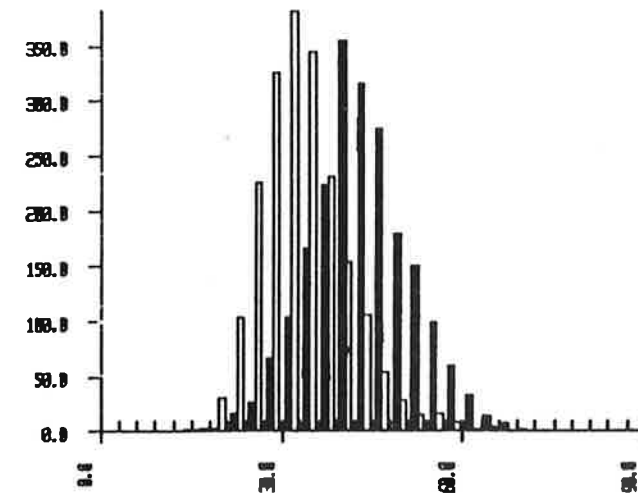


Fig.3. Histogram, sheep no. 24, control PCM, white: slow type I fibers, black: fast type II fibers.

SHEEP 24 POSTICUS den. 15d; sta. 77d; brk. 78d; sta. 62d: fibertyp1=hlw;2=sld

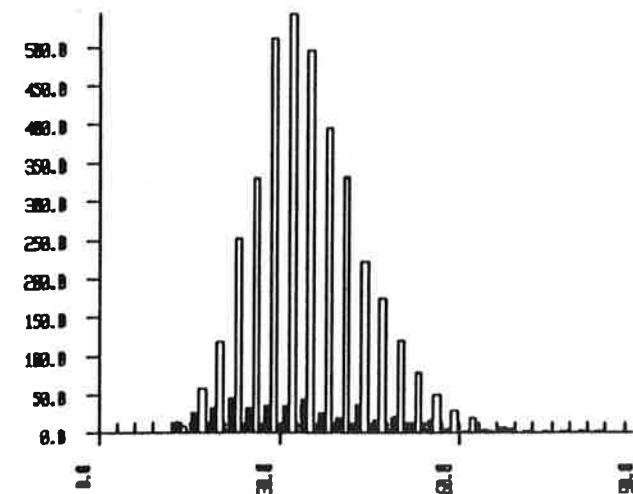


Fig.4. Histogram, sheep no. 24, denervated, stimulated PCM; (denervation: 15 days, stimulation: 2488 hours), white: type I, black: type II fibers.

RESULTS

In all three animals it was possible to keep the denervated PCM irritable by means of direct electrical stimulation. In two animals (S 23, S 24) the PCMs were stimulated 24 hours for 9 days and in one animal (S 25) for 100 days.

The abduction angle of the vocal cords was for sheep S 23, 25°, for S 24, 17° and for S 25, 27° at the end of the experiment which was caused in all three cases by electrode corrosion (Fig. 1 and 2).

The histochemical results show that the denervated, stimulated PCMs of the sheep convert into muscles mainly consisting of slow type I fibers (Fig. 3 and 4).

DISCUSSION

Chronical functional electrical low frequency stimulation of the denervated PCM of the sheep is possible at least for several weeks. The degree of vocal cord abduction was sufficient for an inspiration, the excitation of adjacent nerves was avoided.

For development of an implantable diaphragm-myogram-triggered device, the time-course of the muscle activity of the PCM and the diaphragm in sheep during inspiration and expiration has to be evaluated.

REFERENCES

1. Bergmann K, Warzel W, Eckhardt HV, Gerhardt HJ (1984) *Laryngoscope* 94:1376-1380
2. Obert PM, Young KA, Tobey DN (1984) *Arch Otolaryngol* 110:88-92
3. Zrunek M, Streinzer W, Burian K, Thoma H (1983) In: Thoma H (ed); *Proc. 1st International Workshop on Functional Electrostimulation*, Vienna
4. Zrunek M, Carraro U, Catani C, Szabolcs M, Gruber H, Streinzer W, Mayr W, Thoma H (1986) *Laryng Rhinol Otol* 65:621-627

FUNCTIONAL ELECTROSTIMULATION IN THE TREATMENT OF TRAUMATIC INJURIES OF CERVICAL SPINAL CORD

JERZY KIWERSKI, ROMAN PASNICZEK

Rehabilitation Clinic of Warsaw Medical Academy, Konstancin 05-510,
 Wierzejewskiego 12 /Poland/

INTRODUCTION

Stimulation of the spinal cord has been used as a method of treating pain, syndromes /6,8/ and, since the report by Cook /1/, it has also been used in the treatment of spinal cord diseases. At the same time, at the Rehabilitation Clinic in Konstancin /Poland/, stimulation has been applied to the spinal cord /5/, within the first hours after injury to the spinal cord. Our initial investigations showed beneficial effects of this therapeutic method on injured spinal cord, evident in a markedly quickened regulation of the excretion mechanism and, as it seems, in fuller neurologic and functional improvement, compared to the group of patients treated without stimulation /3/.

The present report presents the effects of direct stimulation of the spinal cord after injury in terms of neurologic improvement and the more rapid formation of bladder automatism.

MATERIAL AND METHODS

50 patients with spinal cord injury in cervical segments have had electrodes implanted surgically. Although an additional 18 patients with injury to the thoracic spinal cord were similarly treated, the present study concerns only the effects of treatment of the cervical spinal cord injuries, since it is the cervical spinal cord segment that we have stimulated most frequently so far, and we were able to select representative groups of patients with equal degree of spinal cord damage. The analysis accounts for 40 patients out of a group of 50 patients. 7 patients died within the first few weeks after injury. In 3 other cases, stimulation was terminated either too early, because of complications which arose during the treatment or due to the failure of the stimulation programming apparatus.

Electrodes were implanted during decompression of the spinal cord via the anterior approach, usually with partial or complete resection of the vertebral body, since our earlier analysis showed that early surgical decompression of the spinal cord yield better results than conservative treatment. After removing fragments of the vertebral body compressing the spinal cord and after forming the bed in the adjacent bodies, the electrodes were inserted under the bone graft or under the adjacent

vertebral bodies. Then a canal was made in the subcutaneous tissue of the neck or in the subclavicular region where the receiver of the stimulator was placed. The implanted stimulators were designed in our clinic and had been used for stimulation of peripheral nerves. The stimulator was supplied externally by electrically coupled circuits, and emits rectangular impulses, duration 0.2-1.2ms, frequency 30-80Hz and amplitude 0-20V. The following parameters are usually used: impulse duration 0.7ms, frequency 45Hz, amplitude individually regulated up to several volts. The stimulation was performed with the use of a specially designed programming device. Series of impulses of 5s. each with intervals 30s. were applied for 10 min. Then a 20 min break followed and the 10-min stimulation was repeated. The daily training lasted 3-4 h and was carried on within 3-4 weeks after surgery.

CLINICAL EVALUATION

Clinical evaluation of the effects of stimulation in spinal-injured patients can only be made in comparison to a group of patients with similar degrees of spinal cord injury who underwent surgical decompression by the same method. The two groups consisted of 20 patients of corresponding age, who had the same kind of decompression and surgical stabilization at the same period of time, but in one group only stimulation of the spinal cord was applied. Each group was divided into subgroups according to the symptoms of complete or incomplete injury to the spinal cord. The average age in the stimulated group was 30.7 years, in the unstimulated group 31.6 years. Table I presents a comparison of neurologic improvement obtained in the group of complete and incomplete injuries of the cervical spinal cord.

TABLE I
NEUROLOGIC IMPROVEMENT

neurologic state		anterior decompression	decompression + stimulation
before treatment	after treatment		
C	3	-	2
C	2	3	5
C	1	3	3
1	3	5	9
1	2	7	4
C	C	14	10
1	1	8	7

These groups were compared with respect to neurological improvement, as determined by 2 independent examiners, and time elapsed from injury to the formation of bladder automatism. In complete injuries there was loss of active movements and of all kinds of sensation from the level of spinal cord injury downwards. Incomplete injuries are traditionally /4/ divided into three groups:

- 1 - Loss of voluntary movements with traceable deep sensation in feet;
- 2 - extensive paresis with active movements of no functional use;
- 3 - paresis of slighter degrees.

Table II presents a comparison of bladder automatism formation in the stimulated and unstimulated groups.

It seems that although the clinical material is not vast yet the presented data clearly show beneficial effects of stimulation on injured spinal cords. Neurologic improvement in the complete spinal cord injury group followed decompression and implantation of stimulators at the earliest possible time after injury within a few or several hours preferably, all within 24 hours after injury.

Table I shows that stimulation influences not only the incidence of neurologic improvement, but leads to a better quality of the improvement. Significant neurologic improvement, i.e., by 2 degrees of our scale at least, was obtained in 43% of stimulated patients, whereas it occurred in only 20% of the unstimulated group.

Table II. Bladder automatism formation in stimulated and unstimulated groups

Automatism formation /weeks/	degree of spinal cord injury			
	complete		incomplete	
	decompr.	decompr. + stimul.	decompr.	decompr. + stimul.
3 - 5	-	5	3	8
6 - 8	4	8	7	8
9 - 12	5	5	7	4
13 - 16	8	2	3	-
17 - 20	3	-	-	-
average, weeks	12.9	7.9	9.1	6.6

The effect of spinal cord stimulation on control of the functions of neurogenic bladder had been reported earlier /2,7/. This effect is also clearly seen in Table II.

REFERENCES

1. Cook AW /1974/ Lancet 1: 869-870
2. Dooley DM, Sharkey J, Keller W /1978/ Med, Prog Technol 6: 1-14
3. Kiwerski J /1979/ Neurol Neurochir Pol 13: 511-516
4. Kiwerski J, Weiss M /1981/ Paraplegia 19: 31-37
5. Kiwerski J, Weiss M, Pańniczek R /1978/ Chir N Ruchu Ortop Pol 43:23-27
6. Nashold BS, Friedman H /1972/ J Neurosurg 36: 590-597
7. Nashold BS, Friedman H /1972/ Arch Surg 104: 195-204
8. Shealy CN /1970/ J Neurosurg 32: 560-564

URINARY INCONTINENCE IN ELDERLY WOMEN - TREATMENT WITH FUNCTIONAL ELECTRICAL STIMULATION

BOŽO KRALJ, ADOLF LUKANOVIČ

University Clinical Center Ljubljana, Department of Gynecology and Obstetrics, Šlajmerjeva 3, 61 000 Ljubljana, Yugoslavia

The last few decades have been characterized not only by a prolonged life-span, but also by an increased activity of elderly persons. The phenomenon is even more pronounced in the female population, in which a greater professional and social activity of persons over 65 is noticeable not only in the developed countries but also in the developing ones. Unfortunately, this activity is often hindered by diseases which accompany the aging process and the old age, and those which progress with the aging process. Urinary incontinence is doubtlessly one of the diseases observed much more frequently in the old population than in the middle-aged one. This holds true in particular of urinary incontinence in women. The rate of incontinent women with urgent need of treatment is estimated to be 5 - 10%, while in the elderly population it increases to 50 - 80%. It is true that urinary incontinence does not represent a fatal danger for elderly women, but it significantly influences their social and professional activities, their life condition, their desire for social contacts-occasionally even their wish to live.

MATERIAL, METHODS AND RESULTS

In order to determine the number of elderly women with urinary incontinence, we made a query among 306 female residents of several homes for the aged. As a criterion for selecting elderly women, the age 65 and more was taken. All of them were capable of independent mobility and self-care and their psychic condition permitted them to take part in the query. Participation in the query was on a voluntary basis, but almost all the women fulfilling the above criteria consented to participate.

TABLE I
DISTRIBUTION OF THE ELDERY WOMEN AND NUMBER OF ELDERY WOMEN WITH URINARY INCONTINENCE BY AGE GROUPS

Age (in years)	No. of women	%	No. of incontinent women	%
65 - 69	54	17,6	26	48,1
70 - 74	67	21,9	46	68,7
75 - 79	84	27,5	53	63,1
80 - 84	65	21,2	34	52,3
over 85	36	11,8	16	44,4
Total	365	100,0	175	57,2

Table shows that the greatest number of women with urinary incontinence (68,7%) is found in the age group 70-74. In the total sample of women over 65, 175 of them (57,18%) manifest symptoms of urinary incontinence.

From the query we found out: stress incontinence in 58 patients (33,1%), urge incontinence in 63 patients (36,0%), and mixed incontinence in 54 patients (30,9%).

Urge incontinence increases with age and in the oldest group it achieves almost twice the rate of the younger groups. This means that with aging increases the need for conservative therapy. If we take into account also mixed incontinence, which requires at least partly conservative treatment, the group of elderly women in need of conservative treatment significantly increases (by almost one third, or 32%). Thus, 66,9% of elderly women need exclusively or at least partly conservative treatment. This is a favourable finding, since the general health status of elderly women, and the condition for safe and efficient surgical interventions deteriorate with age.

Interesting are the elderly women's answers to the question about the degree to which urinary incontinence hinders them at work or in social life. 256 (83,7%) answered they were hindered and 50 women (16,3%) said urinary incontinence caused them no inconvenience either in social life or at work.

The question whether they wanted to be treated was affirmatively answered by 95 (54,3%) incontinent patients.

In the case of most elderly women we have to decide on conservative treatment, both because of the type of incontinence (urge and mixed incontinence 66,9%) and cauterindications for surgical treatment (44,0%).

Patients were treated by stimulators of the pelvic floor muscles. The type of stimulators used depended on the type of incontinence (all the patients with urge incontinence were treated by acute maximal functional electrical stimulation -

AMFES) and the local status of the genitalia. The other patients were treated by stimulators for chronic use. The patients using AMFES stimulators had only five 20-minute stimulations a day. The patients treated by chronic use applied them once or twice a day for 1,5 to 2 hours during a period of three months or more. Stimulators were used either vaginally or rectally. The AMFES stimulators were current limited to 80 mAs, the chronic use stimulators to 35 mAs.

We found out that 78,9% of women would be capable of using conservative treatment by functional electrical stimulation, either independently or with a nurse's help.

The efficiency of treatment by functional electrical stimulation is shown in the next table.

TABLE II

Type of incontinence	Cured/improved	No success	Total
Mixed	29 (93,6%)	2 (6,4%)	31 (100,0%)
Stress	9 (75,0%)	3 (25,0%)	12 (100,0%)
Urge	10 (90,9%)	1 (9,1%)	11 (100,0%)
Total	48 (88,0%)	6 (11,1%)	54 (100,0%)

The table shows that the best results of treatment are achieved in treating urge incontinence: our patients were completely cured in 54,5% and their condition improved in 36,4%. In other words, satisfactory results were obtained in 90,9%. The poorest results were achieved in cases of pure stress incontinence (25,0% failure) which is in accordance with results of treatment in other age groups.

DISCUSSION

Our sample of 306 women might be considered representative as regards distribution of women by age and frequency of urinary incontinence in elderly women, but only for the population of female residents at homes for the aged. The sample is most probably not representative of the total elderly female population, because it does not include women living in their own homes. It may be expected that in the latter group there are more women in a better condition and fewer incontinent women.

CONCLUSION

The number of elderly women (over 65) needing treatment for urinary incontinence is six times higher than in the middleaged population (5-10% : 57,18%). The number of women with urge incontinence increases with age, reaching 47,2% in the age group 75-79. This trend is favourable because of the fact that in 44,0% of elderly women absolute or relative counterindications for surgical treatment are found. Because of the frequency of urge and mixed incontinence, at least 66,9% of elderly patients may be treated conservatively, i.e. by functional electrical stimulation. Elderly women are capable of using stimulators of pelvic floor muscles for treatment by functional electrical stimulation in 78,9%. The results of treatment by functional electrical stimulation are satisfying in 88,9% of cases.

REFERENCES

1. Resnick NM, Scherr P Urinary urgency in community-dwelling elderly, East Boston Community Research group, Harvard Medical School, International Continence Society, Fourteenth Annual Meeting, September 13-15, 1984, Innsbruck (proceedings)
2. Ouslander JG, Raz S, Hepps K, Yale C Clinical and urodynamic characteristics of an incontinent outpatient geriatric population, UCLA School of Medicine, Los Angeles, California. proceedings, International Continence Society, Fourteenth Annual Meeting, September 13-15, 1984, Innsbruck

**Evaluation of functional electrical stimulation
in standing up and walking**

LONGITUDINAL STUDY OF GAIT PATTERN OF HEMIPARETIC PATIENTS
USING SUBCUTANEOUS PERONEAL ELECTRICAL STIMULATION

M. KLJAJIĆ, R. AČIMOVIC¹, J. KRAJNIK¹, E. VAVKEN²,
M. MALEŽIĆ, A. AHLIN, M. GREGORIČ¹

J. Stefan Institute, Univ. "E. Kardelj", Ljubljana, Yugoslavia.

(1) Univerzitetna Rehabilitacija, Ljubljana, Yugoslavia.

(2) Univerzitetna Klinična Centra, Ljubljana, Yugoslavia.

INTRODUCTION

The benefits of functional electrical stimulation (FES) in hemiparetic patients is usually assessed by comparing the gait pattern with and without FES. The gait pattern observed with FES with the implanted stimulator was compared to the gait pattern investigated with surface stimulation, in an attempt to analyse the efficacy of implantable stimulator over a longer period. Fifteen hemiparetic patients participated in the study. During a minor surgical procedure, the peroneal nerve electrode position was selected by moving the implant along the exposed common peroneal nerve until the optimal foot movement was obtained (1). Reliability of electrode positioning during surgery was enhanced by simultaneously monitoring EMG responses of the tibialis anterior, peroneus longus and soleus (2). Prior to, and following the recovery from the surgical procedure gait quality was assessed with force shoes and electrogoniometry. Similar gait patterns were observed in all patients when using surface stimulation prior to surgery and subcutaneous stimulation after implantation of the electrical stimulator. Gait pattern was also assessed each year following surgery.

METHOD

The method of longitudinal evaluation of gait consists of measurements of the vertical component of the ground reaction force and its point of action (POA) on the sole of the measuring shoes (3) together with space and time gait parameters. For this purpose different events on the POA trajectory have been denoted as follows: Hc beginning of POA at first rear transducer, H beginning of POA at heel contact area (first rear transducer excluded), M midfoot area, while T representing POA running through the toe off phase. If the

trajectory of the POA runs on laterally or medially on the sole (out of the marked area), indices l or m are added to the standard notation, as shown in Figure 1. However, the first index in the Table I describing gait events always means foot contact and the last index foot off.

RESULTS AND DISCUSSION

Fifteen hemiparetic patients from the population of 36 already implanted were analysed. General conclusion was found: A time domain analysis of ground reaction pattern indicated three characteristic groups of trajectories: a) a tendency to approach a normal gait trajectory; b) no change in trajectory; and c) following a period of stability in trajectories, some patients exhibited migration of the trajectory to a new undesirable state, suggesting a less functional stimulation. In the four patients who exhibited the response described in c), reimplantation was necessary. Following reimplantation in these patients, similar ground reaction patterns were observed as following the initial implantation. For the illustration, in Fig. 1 gait of right hemiplegic patients, case 10, is shown. Dashed lines represent gait with subcutaneous stimulation while solid lines represent gait without stimulation. On impaired leg, line a and b represent gait measurements from 13.01.1983 (one month after implantation) while c and d measurements from 07.06.1985 one month after reimplantation. Significant improvements of POA curve c with respect to curve a of impaired leg during gait without stimulation, have been observed in this period. Yet, the last measurements show high similarity of POA trajectories during walking with stimulation. There is no change in POA trajectories on left leg during gait with and without stimulation, therefore measurements from 07.06.1985 have been presented only. To illustrate time behaviour and repetitibility of POA trajectories as a function of stimulation events two patients case 1 and 4 are shown in Table I. Different combinations of gait events as defined in Figure 1 can occur for different patients. Therefore any statistics are meaningless. However, initial combination, transient condition and study state are of primary interest. At case 1 main change is manifested on unaffected side when the trajectories of POA migrate toward the normal gait pattern and the difference between the trajectories with and without stimulation disappear. The phenomenon

remains to be explained. The trajectories of POA of affected leg are identical with surface stimulation, implantable stimulation and with stimulation after reimplantation in case 4.

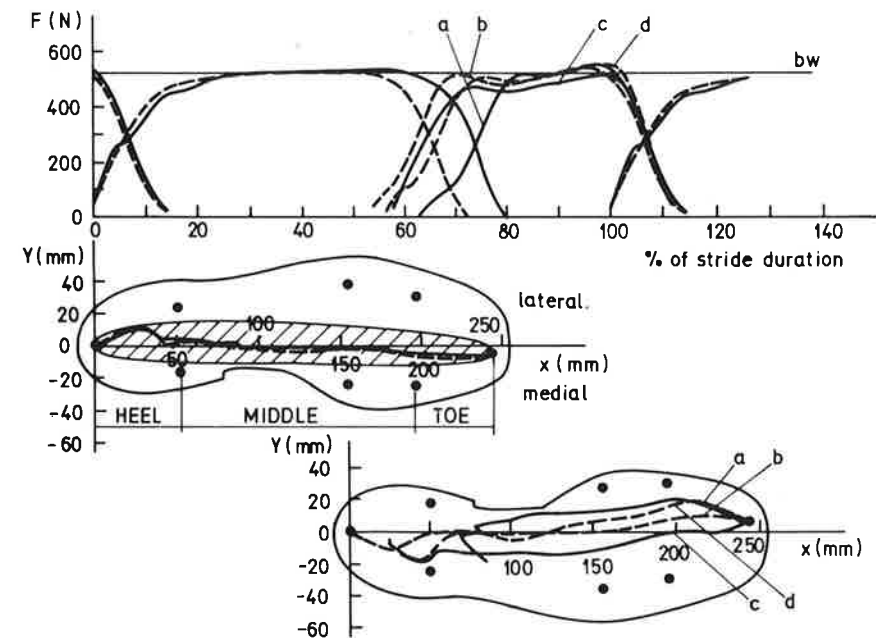


Fig. 1. Average ground reaction force and its POA of gait of a hemiplegic patient without stimulation (solid line) and with stimulation (dashed line). The marked area of the shoe sole represents the region of normal POA.

From observed population following conclusions could be stated:

- (1) with subcutaneous stimulation, when it is indicated, the gait performance could be achieved, at least, as good as with surface stimulation,
- (2) the characteristic of ground reaction pattern caused by single channel peroneal implants are reproducible over time,
- (3) stability of ground reaction pattern are dependent on electrode-nerve fixation,
- (4) in some cases carry over effects were observed.

Though desired foot movements with FES can be adequately predicted with the knowledge of the anatomical structure of the limbs and the implantation methods, the efficacy of the implanted stimulator may change with movement of the peroneal nerve electrode, over a longer period.

TABLE I

TIME BEHAVIOUR OF POA TRAJECTORIES IN FUNCTION OF FES OF HEMIPLEGIC PATIENTS

CASE	DATE OF EXPERIMENTS AND EVENTS		POINT OF ACTION OF UNAFFECTED SIDE		POINT OF ACTION OF AFFECTED SIDE	
			STIM.	NO STIM.	STIM.	NO STIM.
1	03.03.1983	S	Hc,M,T	H,M,T	Ml,T	Ml,T
1	08.03.1983	I				
1	23.05.1984		Ml,T	Ml,T	Hc,M,Tm	Hc,M,Tl
1	18.07.1985		Hc,M,T	H,M,T	Hc,M,T	Hc,M,T
4	07.03.1983	S	M,T	M,T	Hc,M,T	Ml,Tl
4	08.03.1983	I				
4	25.05.1984		Hc,M,T	Hc,M,T	Hc,M,T	H,M,Tl
4	07.03.1985		Hc,M,T	Hc,M,T	Hc,Mm,T	Hc,Ml,T
4	12.03.1985	RI				
4	28.03.1985		Hc,M,T	Hc,M,T	Hc,M,Tm	H,M,Tl
4	23.04.1987		Hc,M,T	Hc,M,T	Hc,M,T	Hl,M,T

Note: Hc: heel contact on first transducer, H: heel contact in the area of heel, first transducer excluded, M: midfoot, T: toe off, l: lateral, m: medial, I: implantation, RI: reimplantation, S: surface stimulation.

REFERENCES

1. Strojnik P, Aćimović R, Vavken E, Simič V, Stanič U (1987) Treatment of drop foot using an implantable peroneal underknee stimulator. *Scand J Rehab Med* 19: 37-43
2. Maležič M, Gregorič M, Kljajič M, Vavken E, Aćimović- Janežič R (in print) EMG Monitoring of Stimulating Electrode Position in Implantation of Subcutaneous Peroneal Stimulator. *Scand J Rehab Med*
3. Kljajič M, Krajnik J (1987) The use ground reaction measuring shoes in gait evaluation. *Clin Phys Physiol Meas* 8: 133-142

PARAPLEGIC LOCOMOTION USING A HYBRID ORTHOSIS: MECHANICAL AND FUNCTIONAL ELECTRICAL STIMULATION OF GLUTEAL MUSCLES WITH IMPLANTED ELECTRODES

JENNINGS SJ, NENE AV AND PATRICK JH

ORLAU, The Orthopaedic Hospital, Oswestry, Shropshire, SY10 7AG. England.

INTRODUCTION

The ParaWalker (hip guidance orthosis) was developed at ORLAU for reciprocal gait in paraplegic children. When applied to taller, heavier paraplegic adults, lateral stiffness is insufficient to fully prevent adduction at the hip. This makes it more difficult to clear the swing leg and as a result greater forces need to be applied through the crutch (1). Electrical stimulation of the gluteal muscles on the stance hip is thought to assist abduction and has been shown to improve walking ability in the ParaWalker (2). In many paraplegics the strength of gluteal muscle contraction is limited because anterior abdominal wall muscle contraction occurs. It was suggested that this was a reflex contraction initiated by depolarisation of afferent axons in the nerve fibre (3). Alternatively it may be a cutaneous withdrawal reflex and could be avoided by using intramuscular electrodes. This was to be tested by inserting percutaneous electrodes into gluteus maximus (g. max.) and gluteus medius (g. med.) in a paraplegic, ParaWalker user.

The Medical Research Council's Neurological Prosthesis Unit, London, has developed an implant system which allows some movement between transmitter and receiver without affecting the output. The amplitudes of the receiver's two isolated outputs can be controlled independently (4,5). A trial of this system using two implanted receivers to stimulate g. max. and g. med. on both sides in a ParaWalker user, is described here.

SUBJECT

The subject was a 29 year old, male, paraplegic with a complete lesion at level T7 following a road accident six years before the beginning of the study. He weighed 63.6 kg, was 1.74 m tall and a proficient user of the ParaWalker. His gluteal muscles had been retrained over a period of 11 months using a surface stimulator. The use of surface stimulation had led to some reduction in the crutch force required. Further reduction could not be achieved since increasing the stimulus strength resulted in anterior abdominal wall muscle contraction.

INTRAMUSCULAR ELECTRICAL STIMULATION

Percutaneous Electrodes

Under sterile conditions pairs of electrodes were inserted into g. max. and

g. med. on both sides.

The electrodes were made from 0.07 mm diameter 80% Pt/20% Ir, coated with an insulating layer of trimel (polyimide). The cathode consisted of two strands, with the end 1 cm of each bent to form barbs and stripped bare of insulator by heating in a flame. The exposed geometric area was 4 mm². The anode consisted of four strands with 2 cm of each bent back and a geometric area of 17 mm² exposed. Consideration was given to the electrode areas required to avoid corrosion or the evolution of harmful chemical products (6). Each electrode was supported in a 125 mm, 18G spinal needle.

For each muscle a cathode was inserted through a 17 mm, 11G canula at motor points, previously identified from the surface, to depth of approximately 2 cm away from the underlying bone. The canula and needle were then removed. The corresponding anodes were similarly inserted at convenient sites approximately 3 cm away from the cathodes. In the laboratory the electrodes were connected to the percutaneous stimulator system. This was set to deliver 25 pulses.s⁻¹ each of duration 0.2 ms and the amplitude of each channel could be adjusted separately, up to 20 V. The cathodes were coupled through a 1000 nF capacitor to prevent net flow of charge. On stimulation g. max. was found to give forceful contractions on either side and g. med. contracted with moderate force. No cross stimulation occurred between muscles and no abdominal wall muscle contraction occurred at any level of stimulation. On removal, four hours after insertion the electrodes emerged cleanly, without breaking.

Implant System

Apparatus. Cooper cables were used to conduct charge from a pair of subcutaneous receivers (diameter 40 mm x 15 mm) on the left and right, lower costal surface. They consist of a triple helix of 0.07 mm diameter, Pt/Ir wire coated in silicone to an outer diameter of 2 mm. Bipolar electrodes are formed from the wires emerging from the distal ends of the cables and inserted into g. max. and g. med. The two outputs are regulated for charge and can deliver up to 0.002 mC per channel, typically with a spike shaped pulse of duration 0.1 ms at 25 pulses.s⁻¹. The external equipment consists of an oscillator/transmitter (70 x 105 x 10 mm) fixed to the skin over each receiver, a control box (60 x 110 x 120 mm, 0.8 kg) attached to the orthosis and a finger switch on each crutch handle. Insensitivity to coil separation, over a radius of 45 mm is achieved by the 3 MHz inductive coupling. The control box, which supplies the oscillator/transmitter is powered by 2 PP3 Ni-Cad batteries which last approximately one hour between charges.

Implant Procedure. Under strict sterile conditions the system was implanted during a four hour operation. All the incisions were below the neurological level and so no anaesthetic was needed. A probe was inserted via a 'U' shaped canula

through an incision between motor points for g. max. and g. med. marked previously on the skin surface. This formed the cathode and the anode was formed by the self retaining retractors holding open the incision. A battery powered stimulator provided 3 pulses.s⁻¹, each of duration 0.35 ms, with amplitude adjustable up to 20 V and coupled through a 0.1 mF capacitor and was used to find a good site to leave the electrode/cable. The probe was replaced with the electrode/cable and the canula withdrawn. The cables were passed, subcutaneously, to a second incision at the lateral mid-line and then to a third on the lower costal surface where they were connected to the receiver and positioned in a pouch prepared for it. This procedure was carried out on both sides and the wounds were closed after careful haemostasis.

Implant Performance. A period of six weeks without any electrical stimulation was allowed for the electrodes to become securely fixed to the surrounding tissue. The wounds were inspected and found to have healed satisfactorily. Muscle training was restarted using the surface stimulator and at four months a second post-operative visit was made by the subject to the laboratory. Good contractions of g. max. and g. med. could be achieved but these were less forceful than when using percutaneous electrodes. No abdominal wall muscle contraction was observed at any level of stimulation. On the left side electrical stimulation could be used to make g. max. or g. med. contract independently but cross stimulation occurred on the right side.

The subject continued to train his gluteii and to use the implant system whilst walking, prior to a third post-operative visit at six months. The gluteii responded to stimulation as before and on this occasion crutch impulse (integral of the vertical force through the crutch with respect to time), walking speed and cadence were measured. The numbers of footfalls and the time taken to walk along a 6.15 m path were used to evaluate speed and cadence. At the same time left or right crutch impulse was derived using measurements from a force platform (Kistler 9261B) set into the floor in the middle of the path. Pairs of walks with left and right impulse measurements were recorded alternately with and without electrical stimulation with the subject resting for one minute between each. From a total of 20 walks the mean (standard deviation) crutch impulse was reduced, when using electrical stimulation from 163 (20) to 156 (37) N.s for the right crutch and from 184 (36) to 159 (16) N.s for the left. At the same time speed increased from 0.36 (0.03) to 0.39 (0.04) m.s⁻¹ with electrical stimulation and cadence from 49.6 (2.0) to 52.6 (2.8) steps per minute.

DISCUSSION

In this subject, intramuscular stimulation has been shown to overcome the limitation to the strength of gluteal muscle contraction imposed by the anterior

abdominal wall muscle contraction found to occur with surface electrodes. This supports the hypothesis that anterior abdominal wall muscle contraction is mediated by a cutaneous reflex.

Use of the implanted system reduced crutch impulse whilst walking in the ParaWalker. The differences were small compared with the variation in the measurement and this reflects the less forceful contractions observed using the implant system compared with the percutaneous. The electronic circuit which separates the two outputs in the receiver limits the charge delivered to approximately 0.002 mC but the percutaneous system was capable of delivering a charge of up to 0.025 mC (assuming a tissue resistance of 390 Ohm). Wider separation between cathode and anode would increase the volume of tissue affected, making siting less critical, but would decrease current density. In this study the best compromise may not have been achieved. At the time of implantation the sites within the muscle were determined using a separate cathodic probe with the anode at the skin surface. This differs from the configuration in use and may give a misleading impression of the best site to leave the electrode/cable.

The improvement in the walking ability of this ParaWalker user, with electrical stimulation was shown to be limited. He normally walks well without putting a great adducting moment onto the orthosis but a heavier, taller subject may be expected to derive greater benefit from the implant system.

REFERENCES

1. Nene AV, Major RE (1987) Dynamics of reciprocal gait of adult paraplegics using the ParaWalker (Hip Guidance Orthosis). *Prosthet Orthot Int*, 11:124-127
2. McClelland M, Andrews BJ, Patrick JH, Freemans PA, El Masri WS (1987) Augmentation of the Oswestry ParaWalker orthosis by means of surface electrical stimulation: Gait analysis of three patients. *Paraplegia*, 25:32-38.
3. Nene AV, Andrews BJ (1986) An assessment of the ParaWalker hybrid orthosis. *Proceedings of Second Vienna International Workshop on Functional Electrostimulation*. Sept: 79-82.
4. Ivall T (1987) Does your coupling coefficient matter? Making inductively-coupled energy less sensitive to coil separation. *Electronics & Wireless World*, 93:577-579.
5. Donaldson PEK (1987) The Janus link: two for the price of one? *Electronics and Wireless World*, 93:1097-1098.
6. Craggs MD, Donaldson NdeN, Donaldson PEK (1986) Performance of platinum stimulating electrodes, mapped on the limit-voltage plane. Part 1, Charge injection in vivo. *Med Biol Eng Comput*, 24:424-430.

CEREBRAL EVOKED POTENTIALS

MILAN R. DIMITRIJEVIĆ

Division of Restorative Neurology and Human Neurobiology, Baylor College of Medicine, Houston, Texas (U.S.A.)

INTRODUCTION

There are two basic methods to carry out non-invasive recordings of cerebral evoked potentials in humans: the first is based on time locked stimulus related brain evoked potentials (1,2) and the second, more broadly, on cerebral event related potentials (3,4). Recently, an entirely different approach has been developed to study brain motor functions by means of transcranial stimulation. It is not a methodological approach to record cerebral evoked potentials. It is rather an approach which leads to the study of the integrity of the brain's descending functions for the first time independently from the patient's cooperation. Indirectly, it is also an electrical event of the brain, but it is elicited transcranially and recorded peripherally (5,6).

STIMULUS RELATED BRAIN EVOKED POTENTIALS

Stimulus related brain evoked potentials can be elicited by stimulation of visual, auditory and sensory nerve structures of the body and result in visual evoked potentials, auditory brainstem potentials and somatosensory cortical evoked potentials (7). All share the feature that brain evoked responses are locked to the stimulus and, in their early phase, appear with a rather constant latency followed by more variable latency and amplitude of positive and negative phases which can be readily applied to different mixed cutaneous nerves, or even to different sizes of nerve fibers. Moreover, in addition to electrical stimulation, a stimulus can be in the form of a mechanical tap, muscle stretch, short lasting vibration, etc. Electrical stimulation, however, is more easily applied.

There is still uncertainty regarding the neurogenerators of cortical somatosensory evoked potentials (CSEP). It appears there are more components than generators. However, it is generally agreed that near-field components N19, elicited by nerve stimulation of the upper extremities, and N37, elicited from the nerves of the lower extremities, reflect multiple and independent thalamocortical projections. Far-field potentials P13 for median and P27 for tibial stimulation are supposed to relay dorsal column nuclei - all other

potentials reflect the electrophysiological changes in the surrounding volume conductor (8,9).

Somatosensory evoked potentials have proved to be a useful diagnostic tool for disorders of the peripheral nervous system, particularly for the detection of focal and peripheral nerve lesions found in inaccessible proximal segments, such as the plexus or spinal roots. Moreover, SEPs have served a useful purpose in the diagnostic evaluation and assessment of dysfunctions of the ascending system in demyelinating diseases, such as multiple sclerosis, hereditary ataxia, spastic paraplegia, as well as in brainstem and hemispheric lesions, coma and brain death.

In our studies of SEP in subacute and chronic spinal cord injury patients we were able to document that the degree of severity of the spinal cord lesion corresponds to the degree of alteration of the SEP (10). Moreover, when we compared quantitative sensory evaluation of vibratory sensibility, temperature, thermal pain sensibility and semi-quantitative testing of light touch with recorded changes in somatosensory evoked potentials, it became obvious that the perception of vibration and touch can be preserved in the absence of SEPs (11).

In another cortical and lumbosacral SEP study carried out in 130 patients with cervical and thoracic chronic injuries, we documented clinically, neurophysiologically and by testing bladder urodynamic functions, that 18 of these patients had additional lumbosacral dysfunctions (12).

The study of quantitative sensory and somatosensory evoked potentials in 13 spinal cord injury patients, who complained of diffuse ongoing dysesthesias below the level of the lesion, burning in quality and usually functionally limiting, helped to demonstrate a relative preservation of dorsal column functions whereas the spinothalamic system mediated functions in such patients were absent (13).

These 4 SEP studies in chronic spinal cord injury patients illustrate the clinical value of such studies for the assessment of residual spinal cord functions and description of the underlying mechanisms of altered sensation, pain and bladder dysfunctions. Moreover, the usefulness of this technique is well recognized in the early assessment of the integrity of spinal cord functions in acute spinal cord injuries and to monitor spinal cord functions during interventions on the spine or spinal cord.

Improvements in instrumentation have made it possible to record somatosensory cortical evoked potentials during voluntary or passive finger movements, or even during gait. Somatosensory evoked potentials can be modified, gated by the performance of motor activity while demonstrably constant stimulation is applied to the nerve trunk. It has been reported that the primary cortical response N20-P30, after stimulating the second finger, are only slightly affected as opposed to the P45-N55 response which is markedly diminished by passive or volitional movement of the finger (14). Similar observations can be made when we elicit cortical somatosensory evoked potentials by stimulating the tibial nerve at the fossa poplitea in healthy subjects while standing and walking (15).

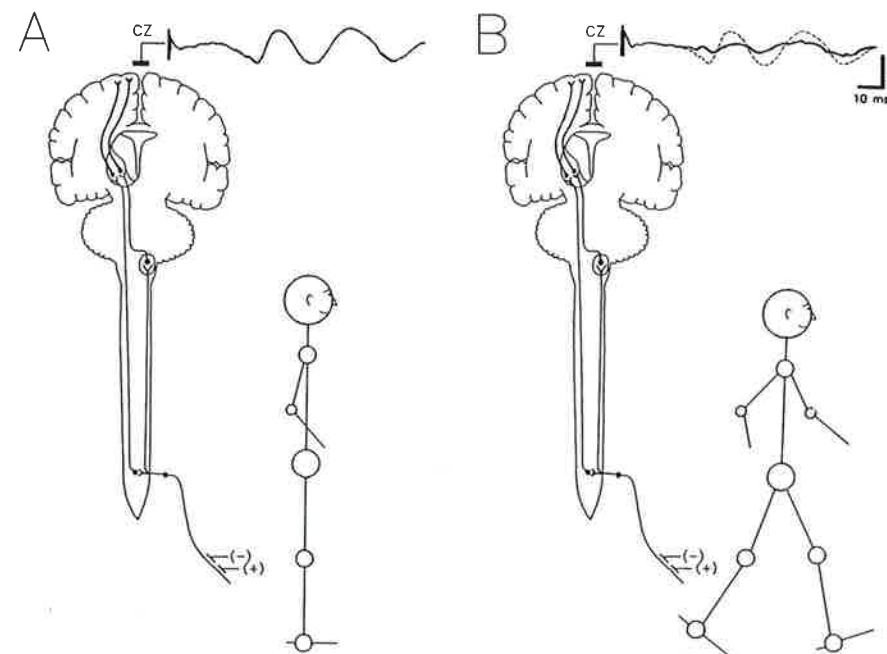


Fig. 1 illustrates the characteristic cortical somatosensory evoked potential after tibial nerve stimulation in healthy adult subjects while standing (1A) and during walking (1B). In both instances, the tibial nerve was stimulated at the fossa poplitea with a frequency of .3 Hz while standing, or every second step while walking (approximately .3 Hz). The stimulus strength was adjusted at the level to generate a well defined H-reflex. The recording from the scalp from Cz and Fz was averaged 100 times. Fig. 1B shows the decrease in the

amplitude of the response with a superimposed response from Fig. 1A. During the recording, the stimulus strength was maintained at a constant level by monitoring the size of the M-wave. The diminished response was a consistent finding on repeated trials and across subjects.

Briefly, the SEP is a widely used neurophysiological technique in diagnostic studies of neurological diseases involving the somatosensory system as well as in studies of the visual system and brainstem functions via auditory brainstem evoked responses. Somatosensory evoked potentials have been found to be a useful procedure to prevent additional injuries to the spinal cord during manipulation of the spine or surgical intervention on the spinal cord. Finally, SEP studies can be used to monitor and evaluate sensory and motor processing mechanisms in the healthy and diseased nervous system by gating sensory processing during volitional or automatic motor activities.

CEREBRAL EVENT RELATED POTENTIALS

Event related potential (ERP) or endogenous potentials occur when the subject is selectively attentive to the stimulus. For instance, ERPs could be elicited when the subject was asked to distinguish one stimulus (target stimulus) from a group of similar stimuli (non-target stimuli). The ERPs depend primarily on the setting in which the target stimulus occurs and are relatively independent of stimulus characteristics (16). Many different components of ERP have been described - with the exception of P3 or P300, the other components are less consistent. In clinical practice, an auditory stimulus is most commonly employed. P300 changes with the deterioration of the intellect and the impairment of cognitive functions such as orientation, judgement and memory.

Another group of ERPs can be recorded under similar recording conditions when a subject is asked to perform a voluntary movement with the hand or foot. These ERPs begin approximately 800 milliseconds before the onset of EMG. The negative potential thus obtained is known as "readiness potential". This potential probably originates from the premotor association area of the cerebral cortex and the medially located supplementary motor area (17).

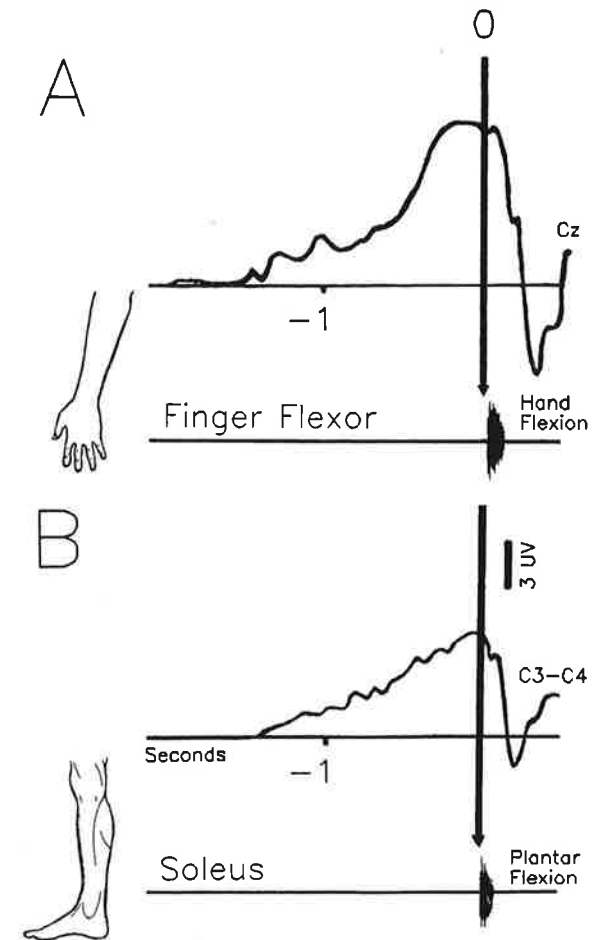


Figure 2 illustrates the human premotor potential recorded from the scalp (Cz-Fz and C3, C4). There are 20 averages during finger flexion (2A) and plantar flexion (2B)

This relatively simple index of preparatory functions before the execution of motor activity is now better understood and is described as motor cortex potential (MCP), a sign of generated response, motor potential, an indicator of pyramidal cell discharge (IMP), premotor positivity (PMP) and as an index of movement initiation.

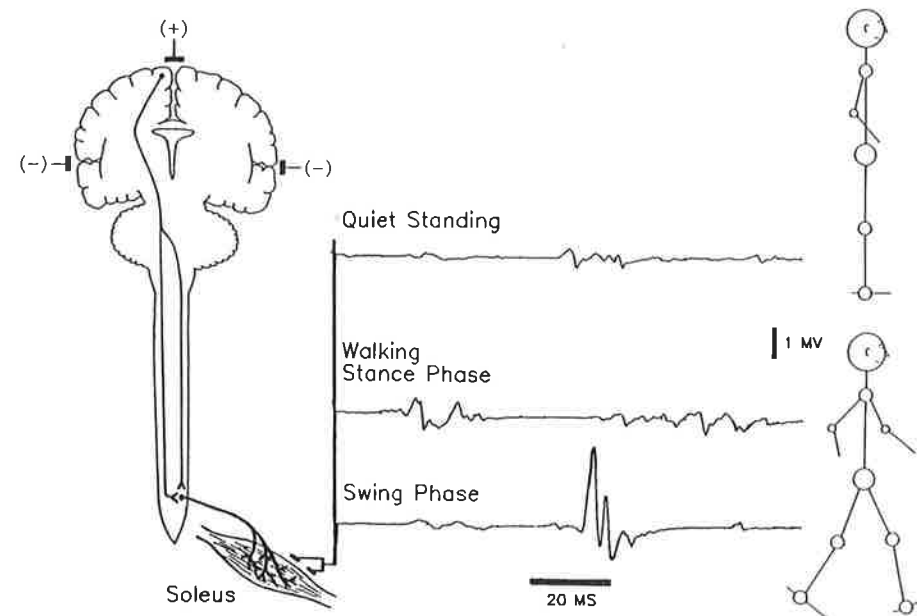
Briefly, human premotor potentials give insight into the preparatory brain functions which set motor performance. Through such studies it is possible to demonstrate the presence of setting mechanisms and their sub-set which can vary independently from the main setting mechanisms. The brain initially specifies the motor task within the motor cells but later the task is individually adjusted according to the sensory information which follows a volitional attempt.

Recordings of premotor potentials in humans have opened the avenue to the analysis of brain events involved in the preparatory functions for the execution of a motor act. This new possibility will play a growing role in the electrophysiology of kinesiology by studying how the brain uses different strategies in programming the same motor act.

TRANSCRANIAL MOTOR CORTEX STIMULATION

When a high voltage single, short stimulus of 50 to 100 microseconds is applied with the anode over the scalp above the motor cortex strip, a muscle twitch of the hand, arm, or lower limb muscles will appear. This motor response can be recorded electromyographically with surface electrodes, thus making it possible to record the time between the cortical stimulus and muscle response as well as the amplitude and duration of the muscle response. Simultaneous contractions of the muscles, which respond to motor cortex stimulation, will enhance the size of the response and also shorten the latency time. Stimuli applied over the motor cortex between both hemispheres will result in muscle responses in the proximal and distal muscle groups of the lower limbs.

In addition to testing the integrity of the corticospinal pathway and of the common final path, cortically induced motor responses of the lower limb muscles in a standing subject will result in a backward movement. When a postural disturbance is induced by a forward or backward sway in a standing subject, simultaneously applied cortical stimulation can augment or diminish the already induced movement. In cases of postural disturbance and automatic motor response, additionally induced cortical motor cortex response reveals its efficacy and can even modify the already established postural response (18).



The prepotency of the cortical spinal induced response over the neurocontrol of gait, as shown in the gait phase, is illustrated in Figure 3. The transcranially stimulated motor cortex elicits a low amplitude motor response in the soleus while the subject is standing which is followed by a silent period and then by another response longer than the first one. While the subject is walking in the stance phase, cortical stimulation results in an early motor response of larger amplitude as opposed to stimulation in the swing phase in which the early response is decreased and the amplitude of the later response is significantly increased.

In this figure, we only show the motor response in the triceps surae which reveal the characteristic early and later responses divided by a long silent period. While the triceps surae contribute to the stance phase, the cortical response is augmented in both phases and these responses are diminished when the triceps surae is in the swing phase. Thus, the underlying motor organization during gait also gates the corticospinal response by modifying the size of the response but not changing the motor effect.

CONCLUSION

Technological advances in instrumentation make it possible to average and recognize among background activity otherwise unrecognized responses which are locked to the stimulus. This new tool to record stimulus related potentials and somatosensory evoked potentials allows us to study the integrity of peripheral and central sensory pathways and, recently, also to examine the modification of such responses during motor acts which will modify and gate such responses. Event related responses open the field of cerebral evoked potentials to studies of cognitive functions and essential premotor, presetting and setting mechanisms before the initiation of motor acts. In the future, these studies will enable us to learn much more about the interaction between the sensory and motor systems when inducing responses to changes in the immediate environment, and how the motor act can be achieved through many different pre-programming strategies. Finally, newly developed transcranial motor cortex stimulation contributes to the field of cerebral evoked potentials the important possibility of examining motor cortex responses without any preprogramming and without the involvement of mechanisms for cognition, as is the case with premotor potentials. Overall, from the present standpoint of methodology of evoked potentials we are able to examine the integrity of the sensory pathways together with studies of gating of motor events on such sensory systems (19). Preprogramming and readiness potential mechanisms have enabled us to understand cerebral events before movement is generated. Finally, we can study motor cortex responses even without the subject's collaboration. This methodology has been developed in different laboratories and has rarely been integrated, but with the help of technology and this new knowledge we expect that there will be a growing number of laboratories that will use all three methods for studies of movement, kinesiology and movement disorders.

ACKNOWLEDGEMENTS

The author wishes to express his appreciation to the members of the Division of Restorative Neurology and Human Neurobiology, Baylor College of Medicine, for their continuous support in his research work. Support was also generously provided by the Vivian L. Smith Foundation for Restorative Neurology, Houston, Texas.

REFERENCES

1. Dawson GD (1954) A summation technique for the detection of small evoked potentials. *Electroencephalogr Clin Neurophysiol* 6:65.
2. Halliday AM (1967) Changes in the form of cerebral evoked responses in man associated with various lesions of the nervous system. *Electroencephalogr Clin Neurophysiol Suppl* 25:178.
3. Donchin, E, Ritter W, McCallum WC (1978) In: Callaway E, Tueting P, Koslow S (eds), *Brain Event-Related Potentials in Man*. Academic Press, New York, p 349.
4. Ritter W, Ford JM, Faillard AWK et al. (1984) Cognition and event-related potentials: I. The relation of negative potentials and cognitive processes. *Ann NY Acad Sci* 425:24.
5. Rothwell JC et al. (1987) Motor cortex stimulation in intact man. I General characteristics of EMG responses in different muscles. *Brain* 110:1173-1190.
6. Merton PA, Morton HB (1980) Stimulation of the cerebral cortex in the intact human subject. *Nature* 285, 227.
7. Starr A (1978) Sensory evoked potentials in clinical disorders of the nervous system. *Ann Rev Neurosci* 1:103.
8. Desmedt JE, Cheron G (1980) Central somatosensory conduction in man: neural generators and interpeak latencies of the far-field components recorded from neck and right or left scalp and earlobes. *Electroencephalogr Clin Neurophysiol* 50:382.
9. Desmedt JE, Cheron G (1981) Prevertebral (oesophageal) recording of sub-cortical somatosensory evoked potentials in man: the spinal P13 component and the dual nature of the spinal generators. *Electroencephalogr Clin Neurophysiol* 52:257.
10. Dimitrijevic MR, Prevec TS, Sherwood AM (1983) Somatosensory perception and cortical evoked potentials in established paraplegia, *J Neurol Sci* 60: 253-265.
11. Beric A, Dimitrijevic MR, Lindblom U (1987) Cortical evoked potentials and somatosensory perception in chronic spinal cord injury patients. *J Neurol Sci* 80:333-342.
12. Beric A, Dimitrijevic MR, Light JK (1987) A clinical syndrome of rostral and caudal spinal injury: neurologic, neurophysiologic and urodynamic evidence for occult sacral lesion. *J Neurol Neurosurg Psychiat* 50:600-606.
13. Beric A, Dimitrijevic MR, Lindblom U (1988) Central dysesthesia syndrome in spinal cord injury patients. *Pain* (in press).
14. Rushton DN, Rothwell JC, Craggs MD (1981) Gating of somatosensory evoked potentials during different kinds of movement in man. *Brain* 104:465-491.
15. Dietz V, Quintern J, Berger W, Schenck E (1985) Cerebral potentials and leg muscle EMG responses associated with stance perturbation. *Exp Brain Res* 57:348-354.

16. Rosler F, Sutton S, Johnson R, Mulder G, Fabiani M, Plooij-Van Gorsel E, Roth WT (1986) In: McCallum WC, Zappoli R, Denoth F (eds), Cerebral Psychophysiology: Studies in Event-Related Potentials. Electroencephalogr Clin Neurophysiol, Suppl 38. Elsevier, Amsterdam, pp 51-92.
17. Rohrbaugh JW, McCallum WC, Gaillard AWK, Simons RF, Birbaumer N, Papakostopoulos D (1986) In: McCallum WC, Zappoli R, Denoth F (eds), Cerebral Psychophysiology: Studies in Event-Related Potentials. Electroencephalogr Clin Neurophysiol, Suppl 38. Elsevier, Amsterdam, pp 189-229.
18. Van der Linden C, Dimitrijevic MR, Eaton WJ, Sherwood AM (1987) Modification of responses to postural disturbances in leg muscles by transcranial motor cortex stimulation in man. Society for Neuroscience Abstracts, Vol. 13, Part 1:346.
19. Dimitrijevic MR, Eaton WJ, Sherwood AM, Van der Linden C (1988) In: Rossini PM, Marsden CD (eds), Non-Invasive Stimulation of Brain and Spinal Cord: Fundamentals and Clinical Applications. Alan R. Liss (in press).

CLINICAL EVALUATION OF PULSED MAGNETIC STIMULATION IN DEGENERATIVE DISEASES OF THE CENTRAL NERVOUS SYSTEM

Katsunori IKOMA, Yukio MANO, Takuya NAKAMURO and Tetsuya TAKAYANAGI
 Department of Neurology, Nara Medical University,
 840 Shijo-cho, Kashihara, Nara 634, Japan

SUMMARY: Pulsed magnetic stimuli were applied to the brain, the cervical region and the lumbar region in patients with Parkinson disease (PD), spinocerebellar degeneration (SCD) and multiple system atrophy and motor central conduction times (MCCTs) were calculated. In some cases of SCD, MCCTs were prolonged, which suggests disorders of the central motor pathways. Magnetic stimuli applied at the head did not solve the frozen gait in patients with PD. The stronger stimuli were applied to the head, the more polyphasic potentials were recorded, which might reflect a variety of the central motor pathways.

Key words: Magnetic stimulation, Motor central conduction time, Spinocerebellar degeneration, Multiple system atrophy, Parkinson disease, Frozen gait

INTRODUCTION

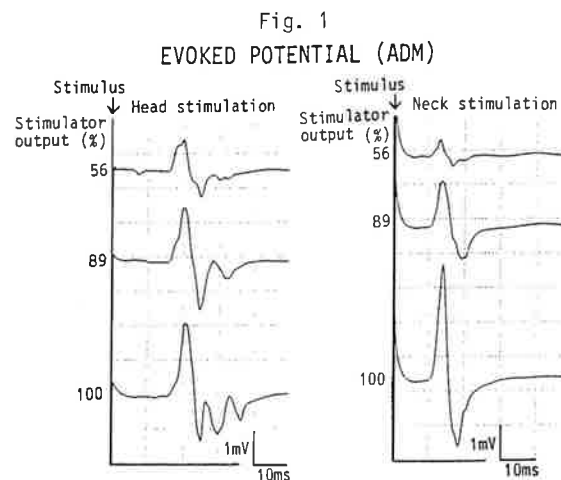
Magnetic stimulation of the human brain through the surface of the head and recording of the resultant muscle evoked potentials has recently been possible (1). This non-invasive technique is expected as a clinically useful examination of the central motor pathways because of being painless and less discomfort than conventional electrical stimulation. We, using pulsed magnetic stimulation, evaluated the muscle evoked potentials and motor central conduction times (MCCTs) in normal subjects and patients with Parkinson disease (PD), spinocerebellar degeneration (SCD) and multiple system atrophy (MSA).

PATIENTS and METHODS

This study was performed on 6 normal subjects (6 sides, 6 men, age range 25-32 years) and on 8 patients with PD (8 sides, 6 men and 2 women, age range 15-62 years), 6 patients with SCD (7 sides, 2 men and 4 women, age range 38-77 years) and 3 patients with MSA (4 sides, 3 men, age range 57-66 years).

The stimulator has high energy capacitors charged to a maximum of 9 kV, which are, by electronic switching, discharged through the flat coil (outside diameter 152 mm, inside diameter 125 mm). As a result of the high flowing in the coil (peak value 10000 A after 180 μ s), a pulsed magnetic field (peak 0.46 Tesla at maximum output) is produced.

Patients and normal subjects were examined in a sitting position, relaxing their muscles. The flat coil was put on the head and pulsed magnetic stimuli were applied to the brain. The resultant muscle evoked potentials from abductor pollicis brevis (APB), abductor digiti minimi (ADM), tibialis anterior (TA) and



abductor hallucis (AH) were recorded by surface electrodes. In the same way magnetic stimuli were applied to the cervical region, then the resultant muscle evoked potentials from APB and ADM were recorded. The lumbar region was also stimulated and the evoked potentials from TA and AH were recorded. Stimulator output was set at maximum ordinarily. Further, in one subject stimulator output was changed at various voltages. Responses were amplified, stored and analyzed with an electromyograph machine (Neuropack 4; bandpass of amplifier 20Hz to 5kHz). At maximum stimulation the latencies of the evoked potentials were measured. MCCTs were calculated as the difference in the latencies elicited from head stimulation and from cervical or lumbar stimulation.

Magnetic stimuli was applied to the head in patients with PD to solve the frozen gait, monitoring their surface electromyograph of lower extremities.

RESULTS

In a subject muscle evoked potentials from ADM in response to magnetic stimuli applied at the head tended to be polyphasic. The stronger stimuli were applied at the head or at the cervical region, the higher amplitudes were measured. Further, the stronger stimuli were applied at the head, the more polyphasic potentials were recorded. On the other hand, evoked potentials at the cervical region were not so polyphasic even when stimuli were increased (Fig. 1).

Measurements of latencies and conduction times from four examined muscles of the 6 normal subjects (6 sides) and 17 patients (19 sides) with PD, SCD and MSA are summarized in Table. There were no significant delays of mean latencies and mean MCCTs in each group of the patients compared with the normal group. But in 2 cases of SCD, which were clinically supposed to

Table
Conduction Times Obtained from the Four Relaxed Muscles Examined (Mean±SD)

Muscle	Measurement	Conduction times (msec)			
		Normal	PD	SCD	MSA
APB	Latency				
	Head to muscle	20.2±1.0	20.1±1.4	22.6±3.3	20.4±2.1
	Cervical region to muscle	11.9±0.8	12.9±1.1	12.6±0.9	12.7±1.4
	Conduction time: head to cervical region	8.3±0.7	7.2±1.0*	10.0±2.7	7.7±1.5
ADM	Latency				
	Head to muscle	19.9±2.4	20.4±1.9	21.4±3.4	20.2±1.9
	Cervical region to muscle	12.0±0.9	12.5±1.1	12.0±1.1	12.4±1.3
	Conduction time: head to cervical region	7.9±2.3	7.9±2.0	9.4±2.9	7.8±2.2
TA	Latency				
	Head to muscle	29.6±3.2	29.7±1.4	28.2±2.1	30.8±3.2
	Lumbar region to muscle	11.8±0.9	13.3±1.6	12.7±1.5	12.2±1.9
	Conduction time: head to lumbar region	16.5±4.6	16.3±2.3	16.1±2.0	18.6±2.6
AH	Latency				
	Head to muscle	37.1±1.7	38.9±1.8	43.9±7.3	38.5±3.0
	Lumbar region to muscle	19.9±1.3	21.4±1.7	20.9±3.1	19.8±2.4
	Conduction time: head to lumbar region	18.5±4.0	17.5±1.1	22.0±8.0	18.7±0.9

*P<0.05 compared with the normal group

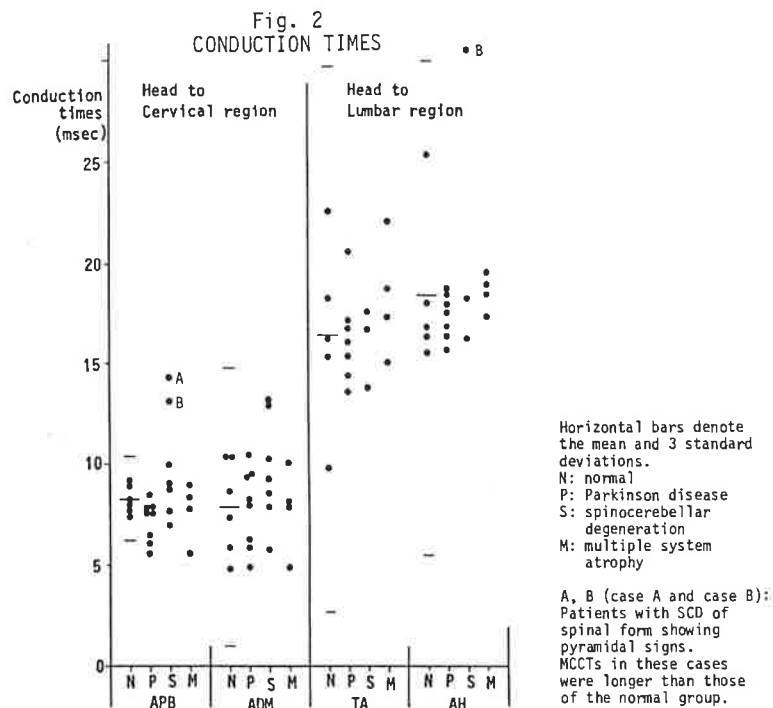
involve the spinal cords predominantly and showed pyramidal signs, delays of MCCTs (head to cervical region and head to lumbar region) were observed compared with the normal group (Fig. 2).

In one case of SCD and one case of MSA, MCCTs were measured bilaterally. Pyramidal signs were found with laterality in these cases and there was laterality of MCCTs, but laterality of MCCTs was not always correlated with laterality of the pyramidal signs.

Magnetic stimuli applied at the head in patients with PD did not change their surface electromyograph of the frozen gait.

DISCUSSION

Using magnetic stimulation, abnormalities of MCCTs in patients with multiple sclerosis have been reported (2,3). In this study MCCTs in patients with PD, SCD and MSA were measured. Mean MCCTs in each patient group were not significantly longer than those of the normal group. But prolonged MCCTs were observed in 2 cases of SCD showing remarkable pyramidal signs, which suggests disorders of the central motor pathways in these cases. MCCTs (especially in head to lumbar region) might change in proportion to the height. Although each subject in this study was not so different in height, investigation considered about height may be



desirable.

Evoked potentials in response to magnetic stimuli applied at the head were polyphasic and the stronger stimuli were applied to the head, the more polyphasic potentials were observed. It suggests that increased stimuli might excite slowly conductible descending tracts, interneuron, etc. in addition to an excitable and fast conductible pyramidal tract.

The beginning of the gait in patients suffering from the frozen gait was not motivated by magnetic stimuli. Magnetic fields were expected to stimulate the association area, but it is considered that magnetic stimuli did not reach to it.

Magnetic stimulation might be clinically available to evaluate the central motor pathways in degenerative diseases of the central nervous system. Studies in more cases are expected.

REFERENCES

1. Barker AT, Jalinous R, Freeston IL: Non-invasive magnetic stimulation of human motor cortex. *Lancet* i: 1106, 1985
2. Barker AT, Freeston IL, Jalinous R, Jarratt JA: Clinical evaluation of conduction time measurements in central motor pathways using magnetic stimulation of human brain. *Lancet* i: 1325, 1986
3. Hess CW, Mills KR, Murray NMF: Measurement of central motor conduction in multiple sclerosis by magnetic brain stimulation. *Lancet* ii: 355, 1986

THE SAFETY OF MAGNETIC STIMULATION

Yukio MANO, Itaru FUNAKAWA, Takuya NAKAMURO, Katsunori IKOMA, Tetsuya TAKAYANAGI, Kyoko MATSUI*

Department of Neurology, Nara Medical University, 840, Shijo-cho, Kashihara, Nara, 634, JAPAN. *National Institute of Neuroscience, Tokyo, Japan.

SUMMARY

The safety of magnetic stimulation on rat brain was examined kinesiological, neurochemically and neuropathologically. There were no significant changes in movement or neuropathology. However, there were some changes at 60 minutes in DA and serotonin metabolism, which returned to the control values in 4 days. These changes were considered to be due to the direct excitation of neurons by stimulation. From our study, magnetic stimulation had no adverse effects.

INTRODUCTION

Pulsed magnetic stimulation of the human brain and the recordings of the resultant muscle action potentials has recently been reported. Unlike electrical stimulation, magnetic stimulation excites the motor cortex without discomfort to the subject; thus, it may be a new clinical test to study the central motor pathway. Although no deteriorating effects have been observed thus far, the safety of this technique has not been established. Therefore, we investigated the safety of frequent magnetic stimulation of rat brain by quantitative kinesiological, neurochemical and pathological analysis.

METHODS

A pulsed magnetic discharge system which consisted of a high voltage capacitor bank and flat circular coil of insulated copper wire, was used for brain stimulation. In a high voltage capacitor bank, it is discharged to a maximum of 900 V, in voltage, a maximum current flow of 8000 ampere and 1637 μ F in condenser capacitance. The flat coil consisted of 9 turns of insulated copper wire, with an external diameter of 105 mm and internal diameter of 65 mm. Its magnetic field is 1.00 Tesla with an inductance of 7 μ H and a peak time of 190 μ s. Sixtyfour normal Wister rats each weighing 200 g were used. The rats were divided into two groups. Rats in one group were given the pulsed magnetic stimulation, 50 times in 0.5 Hz by a flat circular coil, which surrounds the head of the rat 1cm in front of its interauricular line in the long thin plastic circular chamber 5 cm in diameter. Rats in the control

group did not receive the pulsed magnetic stimulation in the long circular chamber. For the kinematic analysis by Animex II, 20 rats (10 with magnetic stimulation and 10 without magnetic stimulation) were put in the measurement cage of an Animex II in a soundproof chamber immediately after magnetic preparation. Animex II, the details of which are described in another paper, is used for this measurement. Twelve rats, 6 given magnetic stimulation and 6 not given magnetic stimulation, were killed by decapitation 1 hour after preparation. Another 12 rats, 6 given magnetic stimulation and 6 not given magnetic stimulation, were killed 4 days after preparation. The cerebral motor cortex, striatum, hippocampus were removed. They were dissected out and placed on dry-ice. Tissues were stored at -80°C until taken for analysis. Prior to analysis, brain tissues were weighed. All tissues were thoroughly disrupted by sonication. The tissue homogenate was then centrifuged at 15,000 rpm for 10 min. Its clear supernatant was injected into a chromatographic system. Quantitative determinations were made by comparing the peak heights of the samples with those given by a known concentration of standards. The measured monoamines were dopamine (DA), homovalinic acid (HVA), noradrenaline (NA), 5-hydroxytryptamine (5-HT) and dihydroxyphenylacetic acid (DOPAC). The analysis of neuropathological state. 10 rats, 6 rats given magnetic stimulation, and 4 rats not given magnetic stimulation, were killed 1 hour after preparation with decapitation after they were anesthetized with intraperitoneal pentobarbital. Ten rats, 6 rats given magnetic stimulation and 4 rats not given magnetic stimulation, were killed by decapitation 4 days after preparation. The brains were removed and they were soaked in formalin. They were prepared for light microscopy using standard methods. Samples were stained with haematoxylin-eosin (H.E.), Nissl, Bodian, Klüver-Barrera.

RESULTS

Results of kinematic analysis

In spectrum analysis by Animex II according to the size of movement, the total length of movement did not show any significant difference for 60 minutes between the two groups. In the analysis of the total length of movement every 10 minutes, there were no statistically significant difference between the two groups.

Neurochemical results

The concentrations of DA, HVA, DOPAC, NA and 5-HT in motor cortex, striatum and hippocampus from control rats and from rats 60 minutes and 4 days after magnetic stimulation are compared. In the motor cortex, the 5-HT level

is decreased at 60 min. In the striatum, the level of the DA metabolite, HVA, is increased at 60 min. In the hippocampus, the 5-HT level is decreased at 60 min. DOPAC level is not increased significantly. This is probably due to the rapid removal of DOPAC from CNS. Four days after magnetic stimulation there were no significant changes. The (DOPAC + HVA)/DA ratio, a useful index of DA metabolism and turnover, was increased by 142 % at 60 minutes in the motor cortex. It was slightly increased at 60 minutes in the striatum. No significant changes in NA levels are noted at any time, although there is a slight tendency of decrease at 60 minutes in the hippocampus. These results indicate that increased dopaminergic and serotonergic metabolism is noted at 60 minutes after magnetic stimulation, and it returns to the normal level at 4 days (table). Neuropathological results in the macroscopical observation, no destruction of tissues, bleeding, or other findings were observed. Microscopically, no changes were observed in the nerve cell, glia, vessels or other tissues. These pathological results indicate that the magnetic stimulation in our study does not induce pathological changes in macroscopic or microscopic observation.

DISCUSSION

In the present kinematic, neurochemical and neuropathological study, we found no significant changes in movement or neuropathology. Although there were some change at 60 minutes in DA and serotonin metabolism, these changed values returned to the control values in 4 days. These changes were reversible. When we excite the neurone, consequently the neurotransmitter is released from the synapse. The observed decrease of DA and serotonin is supposed to be due to the direct excitation of neurone by magnetic stimulation. During magnetic stimulation the muscles of the rat's body are contracted at every magnetic stimulation. However, after the cessation of stimulation, no special movement or contraction is observed at all. This suggests that there is no special release of neurotransmitter as an after effect. The metabolites of neurotransmitters are increased for several hours after their release but these changes do not last long. In this study, the flat coil for magnetic stimulation to the rat is larger relatively. Considering that the intensity of magnetic field falls off at negative third power of the distance, the larger size of the flat coil is supposed to stimulate the brain tissues more deeply, and the rat brain in this study might have been given too much stimulation, compared to the stimulation given to human brain. We usually do not apply repeated cortical magnetic stimulation to humans. Even from this point, the rat brain seems to have been given more

Table

Mean values \pm SE of DA, HVA, DOPAC, NA and 5-HT concentration ($\mu\text{g/g}$ tissue) in motor cortex, striatum and hippocampus samples taken from control rats and from rats 60 minutes and 4 days after magnetic stimulations

[motor cortex]	control	60min	4 days
DA	0.918 \pm 0.258	0.514 \pm 0.127(↓)	1.206 \pm 0.190
HVA	0.149 \pm 0.025	0.111 \pm 0.019	0.132 \pm 0.019
DOPAC	0.121 \pm 0.018	0.104 \pm 0.021	0.165 \pm 0.028
NA	0.342 \pm 0.048	0.277 \pm 0.024	0.443 \pm 0.045
5-HT	0.449 \pm 0.035	0.348 \pm 0.030*↓	0.463 \pm 0.051
[striatum]			
DA	10.206 \pm 0.713	10.700 \pm 0.372	10.687 \pm 0.457
HVA	0.571 \pm 0.045	0.746 \pm 0.052*↑	0.628 \pm 0.034
DOPAC	1.050 \pm 0.065	1.108 \pm 0.055	0.947 \pm 0.034
NA	0.119 \pm 0.017	0.108 \pm 0.020	0.110 \pm 0.019
5-HT	0.389 \pm 0.029	0.402 \pm 0.012	0.402 \pm 0.026
[hippocampus]			
DA	0.058 \pm 0.005	0.060 \pm 0.004	0.049 \pm 0.005
HVA	N.D	N.D	N.D
DOPAC	0.017 \pm 0.002	0.014 \pm 0.002	0.012 \pm 0.002
NA	0.398 \pm 0.077	0.215 \pm 0.024(↓)	0.279 \pm 0.011
5-HT	0.318 \pm 0.038	0.221 \pm 0.006*↓	0.291 \pm 0.037

* : $p < 0.05$

N.D.: not detected

magnetic stimulation. In this study, no definite adverse after effects were observed, but it further studies on memory, behavior and others over longer duration after magnetic stimulation may be necessary.

REFERENCES

- 1) Barker AT, Freeston IL, Jalinous R, Jarratt JA (1986) *Lancet* 1:1325-1326
- 2) Mano Y, Matsui K, Toyoshima E, Ando K (1986) *Acta Neurol Scand* 73:352-358

EVALUATION OF ACETAMINOPHEN (SETAMOL) ANALGESIA BY ARGON LASER INDUCED PAIN RELATED CORTICAL RESPONSES.

ARENDR-NIELSEN, L and BJERRING, P*.
Dept of Medical Informatics, Ålborg University, Badehusvej, DK-9000 Ålborg, * Dept of Dermatology, Marselisborg Hospital, P P Orumsgade, DK-8000 Aarhus, Denmark.

INTRODUCTION.

Clinical evaluations and comparisons of pain alleviation obtained by weak analgesics have been difficult to perform in an objective and quantitative way because 1) clinical practice shows that pain intensity and quality differ between patients, and 2) it is difficult to compare pain perceptions over time.

To standardize the pain conditions (intensity and quality), we have used an argon laser as experimental pain stimulator because it is then possible to induce well defined and reproduceable pain.

Short argon laser pulses can elicit pain related cortical responses, and the amplitudes of these responses are found to correlate with the intensity of the pain perceived (1). This amplitude was in the present study used as a quantitative and objective parameter to monitor changes in the pain perception caused by a weak peripherally acting analgetic (acetaminophen).

MATERIAL AND METHODS.

Volunteers. Participants in the experiment were five females (mean age 29 years, ranging from 22 to 45 years) without known heart-, lung-, liver-, kidney- or neurologic diseases. The II Declaration of Helsinki was respected and informed consent was obtained from all volunteers.

Laser stimulation. The output from an argon laser (Lexel Aurora 150, Cooper Medical, USA) was transmitted via a quartz fibre to a handpiece. The wave lengths were 488 nm (blue) and 515 nm (green). An external laser power meter (Ophir, Israel) was used to measure the dissipated output power. A continuous low energy beam (0.005 W) from the argon laser visualized the stimulation site.

The stimulus duration was 200 ms and the beam diameter was 3 mm. The stimuli were applied randomly at different sites on the dorsum of the left hand within the C7 - dermatome. The laser intensity was increased until the volunteer perceived the stimulus as an intense painful pin prick. This intensity was kept constant during

the experiment.

Recording of cortical responses. The cortical responses were recorded by a platinum needle electrode (Disa 25C04), placed 2 cm behind Cz with reference to ear lobe.

The EEG was filtered (0.5-200Hz) and amplified (Disa 5C01). A microcomputer system was triggered by stimulus onset and 1 second of EEG was collected. A total of 32 responses were averaged. The cortical responses were recorded before 60, 120, and 180 min after administration of acetaminophen. After each recording the volunteer described how the stimuli were perceived.

Analgesia. Oral doses (0, 1, 2g) acetaminophen (Setamol, Pharmacia, Denmark) were given according to a double blind randomized cross-over design. At least 48 h elapsed between the three experiments.

Statistics. Friedmans test was used and statistical significance was accepted at a 5% level.

RESULTS.

The maximum reductions in cortical amplitudes occurred 120 min after ingestion (fig. 1), but only the reduction produced by 2 g acetaminophen was significant in comparison with the initial value. No significant changes or tendencies (fig. 1) were seen in the placebo group.

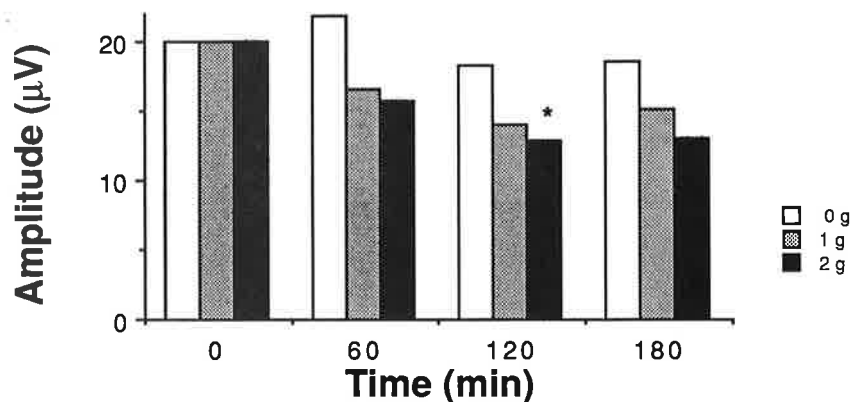


Fig 1. The mean (N = 5) changes in amplitude of the argon laser evoked cortical responses before, 60, 120 and 180 minutes after 0g, 1g or 2g acetaminophen (Setamol). The asterix indicates statistical significance at 5% level. The amplitudes measured before ingestion are normalised to 20 µV.

DISCUSSION.

Different modalities of painful stimuli have been used to elicit pain related cortical responses. The most appropriate stimulation

modality is thermal laser stimulation, because thermoreceptors in the skin can be activated selectively without synchronous activation of mechanoreceptors. Laser pulses activate pain sensitive A δ - and C-fibers in the skin (2) and the perceptions elicited by the laser are described as intense and distinct painful pin pricks often accompanied by a burning after-sensation (2, 3). The pin prick sensation is mediated by thin, myelinated A δ -fibers and the burning sensation probably in C-fibers (4). In clinical studies the analgetic efficiency of acetaminophen (0.65 g) has been evaluated in patients after oral surgery (5) and the maximum pain alleviation was obtained 120 minutes after administration.

In patients who had undergone gynaecological, general or orthopedical surgery, the postoperative pain symptoms were treated with acetaminophen (0.65 g), and maximum pain relief was also obtained 120 minutes after administration (6). The same conclusion was reached by Beaver and McMillan (7) who treated postpartum patients with 1 g acetaminophen.

Cooper et al. (8) used 0.5 g acetaminophen after oral surgery and found maximum pain relief after only 60 minutes. This finding supported the study by Beaver and Feise (9) where 0.6 g acetaminophen was administered to postoperative pain patients.

In the present study, 2 g of acetaminophen resulted in a considerably larger reduction in the amplitude of the cortical response than 1 g. The maximum reductions occurred 120 min after administration.

Clearly, for both low and high doses there is a substantial delay between the time of maximum pain alleviation and the time when the plasma concentration of paracetamol peaks. Peak concentrations are found 30 - 60 minutes after administration of a single peroral dose (10).

It should be emphasized that argon laser induced pain is brief, sharp, and precise without any of the qualities commonly used to describe chronic pain. Therefore the results obtained by the present experimental model can not directly be adopted in the management of chronic pain. However, the amplitude of the argon laser induced pain related cortical response seems to be a reliable parameter for pain relief because it is not attenuated significantly by placebo administration. This may be due to the short duration of the pain, the acute onset, and use of randomised intervals between stimuli.

Recently, pain related cortical responses to argon laser

stimulation have been introduced in anaesthesiology to compare the analgetic potency of a new analgetic cream (EMLA) for topical application and conventional intradermally injected lignocaine. The decrease in amplitude was found to follow the level of analgesia, which was proportional to the cream application time. After the cream had been applied for 2 h the cortical responses were completely abolished and analgesia comparable to lignocaine injection was obtained (11).

In conclusion to these and present findings the laser based experimental model for measuring pain in humans has a wide range of applications where time-effect and dose-response relations may be determined for various analgesics.

REFERENCES.

1. Bjerrring P, Arendt-Nielsen L (1988) J Neurol Neurosurg Psychiat 51: 43-49.
2. Bromm B, Treede R-D (1984) Human Neurobiol 3: 33-40.
3. Arendt-Nielsen L, Bjerrring P (1988) J Neurol Neurosurg Psychiat 51: 35-42.
4. Torebjork H E, Ochoa J L (1980) Acta Physiol Scand 110: 443-447.
5. Cooper S A, Beaver W T (1976) Clin Pharmacol Ther 20: 241-250.
6. Forbes J A, Kolodny A L, Chachic B M, Beaver W T (1984) Clin Pharmacol Ther 35: 843-851.
7. Beaver W T, McMillan D (1980) Br J Clin Pharmacol 10: 215-223.
8. Cooper S A, Engel J, Ladove M et al. (1979) Clin Pharmacol Ther (Abst.) 25: 219.
9. Beaver W T, Feise G A (1978). Clin Pharmacol Ther (Abst.) 23: 108.
10. Forrest J A, Clements J A, Prescott L F (1982) Clinical Pharmacokinetics 7: 93-107.
11. Arendt-Nielsen L, Bjerrring P (1988) Laser-induced pain for evaluation of local analgesia - A comparison of topical application (EMLA) and local injection (Lidocaine). Anesth Analg 67: 115-123.

ELECTROMYOGRAPHY

Electrical activity of motor units and single muscle fibres

MOTOR UNIT TOPOGRAPHY VIEWED BY DIFFERENT EMG TECHNIQUES

ERIK STALBERG

Department of Clinical Neurophysiology, University Hospital,
S-751 85 Uppsala, Sweden

INTRODUCTION

The motor unit comprises a ventral horn cell, a motor axon and all fibres innervated by by this axon. The number of muscle fibres in each motor units varies from about 25 in eye muscles to many hundred in large limb muscles. In each muscle the motor unit size and its cross sectional distribution, territory, varies from 2 to 10 mm. There are no signs of clustering of fibres within the motor unit although animal studies have indicated a tendency for concentration towards its centre (3). In nerve-muscle diseases the function of nerve, motor end-plate or muscle fibre is abnormal. Often also number, size or distribution of muscle fibres in the motor unit is changed by the disease process. EMG techniques are mainly aimed at studying physiological properties but some of the measured parameters are more or less directly reflecting anatomical aspects of the motor unit, (15). This paper will point to some the methods that reveal such information.

SINGLE FIBRE EMG

Single fibre EMG, SFEMG, is used to study of single muscle fibre physiology in normal and diseased muscles. The technique and its major applications have been described in detail elsewhere (18). Two of the parameters, progagation velocity and jitter do not reflect motor unit topography but are of vital importance for the understanding of many EMG phenomena. They are also basic parameters in simulation studies involving motor unit models. They will therefore be introduced briefly.

Propagation velocity

The impulse propagation velocity along a single muscle fibre can be measured by using a multielectrode. The propagation velocity, positively correlated to the muscle fibre diameter, ranges from 1.5 to 6 m/s in the normal muscle. In this sense, the parameter has a direct morphological counterpart. The velocity decreases in many muscle fibres during continuous activity, more at high firing rate. This is the major reason for the shift towards lower frequencies in power spectrum obtained during continuous activity (8). It has been used as a parameter of muscular fatigue although the causal relationship to fatigue, in the sense of decreased force output is not yet clarified. The propagation velocity measurements have mostly been used in research although lately some authors have indicated the value of these measurements in clinical practice (4,5,20).

Jitter

The jitter is defined as the variability at consecutive discharges of the time interval between action potentials from two muscle fibres belonging to the same motor unit, activated voluntarily. The jitter gives quantitative information about the neuromuscular transmission in individual motor end-plates in situ and in the terminal nerve tree. This parameter may even detect subclinical transmission disturbances. In one situation is the jitter parameter directly related to a morphological parameter. This is in the case of very low jitter (less than 5 usec), which indicates recording from two branches of a split muscle fibre.

Fibre density

The fibre density, FD, is a parameter directly reflecting the local topography of muscle fibres within one motor unit. The electrode is positioned to record activity from one muscle fibre in a voluntarily activated motor unit. The number of synchronously active muscle fibres (time locked action potentials) is counted. An average of the results from 20 sites, probably reflecting 10-15 different motor units, is calculated. In order to be accepted, an action potential must have an amplitude exceeding 200 uV and a rise time that is less than 300 usec, which corresponds to an average maximal distance of about 300 um between muscle fibre and the recording electrode

surface. Thus, fibre density is a measure of the number of action potential generators (single fibres) from one motor unit within the uptake radius of about 300 um. FD is normally less than 1.5, differing with muscle and patient age (18).

In muscles in which collateral sprouting has occurred the fibre density is increased. This is seen in histochemically stained muscle biopsies as fibre type grouping. A slightly increased fibre density also occurs in many myopathies.

SFEMG recordings during intramuscular stimulation

By stimulating intramuscular nerve twigs by means of a monopolar needle electrode the jitter can be recorded from individual motor end-plates. The technique is described in detail elsewhere (21). Electrical stimulation can also be used to study the latency of single fibre action potentials. If the nerve is stimulated, the latency is composed of nerve conduction time, neuromuscular delay and muscle fibre conduction time. This result may be difficult to interpret in anatomical terms. In situations when the muscle fibres are directly stimulated, indicated by the absence of jitter between stimulus and response, the latency reflects the conduction time along the muscle fibres, inversely related to fibre diameter. Apart from difficulties to obtain a selective single fibre response, this method may be of potential interest for studies of muscle fibre conduction. This was actually one of the methods used by Buchthal et al (1). Stålberg (14) discussed the technique in conjunction with propagation velocity studies of single muscle fibres, and has later used it, particularly in studies of myopathies. Troni (20) has elegantly showed how this technique can be applied in studies of patients with neuromuscular disorders.

In conclusion, SFEMG may be used to study the relative muscle fibre size by means of propagation velocity of single muscle action potentials during voluntary activity or electrical stimulation, and the local arrangement of muscle fibres.

CONVENTIONAL EMG

Conventional electromyographical studies are performed using needle electrodes, usually either concentric or monopolar. This type of

recording gives useful information in the clinical assessment of neuro-muscular disorders (7,9).

The so called motor unit potential (MUP) is the spatial and temporal summation of action potentials of muscle fibres in the motor unit. The spike component is mainly determined by the 2-12 closest fibres (19) whereas more distant fibres contribute to the slow components of the MUP. In pathological conditions, number, size and distribution of muscle fibres changes. This is reflected by shape changes in the MUP. Typically the MUP is short and polyphasic in myopathies, and of long duration and high amplitude in neurogenic conditions. In order to give better understanding of the relationship between the MUP parameters and motor unit morphology, simulation studies have been performed. In one such study (12) it was shown that the amplitude was to 88% determined by fibres within a radius of 0.5 mm from the electrode tip, the area under the signal by fibres within 2 mm and the duration by fibres within 2.5 mm distance from the electrode. Number of phases increase when the temporal dispersion of individual muscle fibre action potentials increases e.g due to variation in fibre diameter seen in myopathies or early reinnervation. Increased temporal dispersion decrease the amplitude and area slightly but does not affect duration. Thus, the different MUP parameters reflect differently large portions of the motor unit, and therefore give complementary information about its topography.

SIZE OF THE MOTOR UNIT

As discussed above, the MUP as obtained by means of conventional EMG electrode does not usually represent the entire motor unit. Therefore a non-selective method was developed, called Macro EMG (15). The recording is made from the partially insulated cannula of a modified SFEMG electrode. The recording is based on spike triggered averaging. The cannula signals are averaged in dual buffers in the computer. By point-to-point subtraction of the signals in the two buffers and by adding the absolute differences, a value is obtained that indicates the dissimilarity between the averaged signals. When the difference falls below a preset value, the processes is stopped, and the average of the two resulting signals is used for final analysis. This method provides a "quality control" of the averaging process (16).

Simulations have shown that the amplitude and area under the signal are positively correlated to the number of fibres in the motor unit and their individual size but not to the local organisation of the muscle fibres inside the territory (13). In normal muscle, the Macro MUP amplitudes are higher for motor units recruited at higher force levels, the so called size principle. The Macro MUP are usually bi- or tri-phasic. The individual peaks reflect the main electrical front in the motor unit, e.g due to the position of the motor end-plates of fibres in that unit (Fig 1).

With enlargement of the motor unit due to reinnervation, the Macro MUP increases in amplitude.

With information about the electrical size of individual motor units, it should be possible to get an estimate of number of motor units as well. De Koning (1987) evoked a maximal M-response by nerve stimulation and used to Marco EMG electrode for recording. M-amplitude divided by mean Macro MUP amplitude was used as a measure of number of motor units.

Another method to estimate size and number of motor units was developed by McComas et al., (10). It has become known as the method for motor unit counting and is based on surface recordings of muscle response during graded weak nerve stimulation and maximal nerve stimulation. Reports from different authors have demonstrated practical usefulness of the technique which has given many interesting aspects of size and number of functioning motor units in health and disease. This method will not be further described here.

MOTOR UNIT MAPPING

None of the above mentioned techniques give information about the spatial distribution of electrical activity in the motor unit. One technique to obtain this information is called Sanning EMG (16). A SFEMG electrode records action potentials from one muscle fibre in an active motor unit which is used to trigger the computer process. A separate concentric needle electrode is positioned in the same motor unit (synchronous activity from the two electrodes), and is then pulled through the motor unit in steps of 50 um after each discharge. The signal is stored in the computer and displayed in various plots e.g hidden line raster (Fig 1), semi-3-dimensionals plots or as amplitude related grey scales or colourplots. Parameters

such as total length over which the peak-to-peak amplitude exceeds 50 μ V, number of "motor unit fractions", silent areas along the tracking path, amplitude, area and duration of the recorded responses along the motor unit territory are analysed.

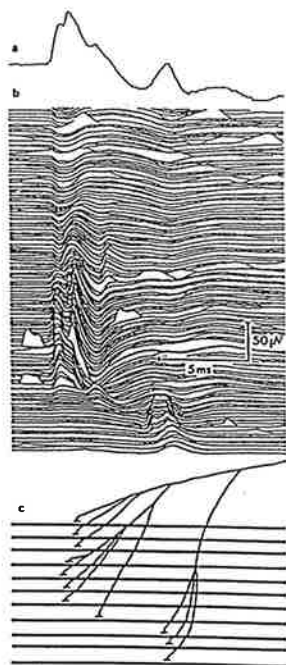


Fig 1. A: Macro MUP obtained by averaging the spike-triggered signal recorded between the shaft of the concentric electrode, inserted through the motor unit and a remote reference electrode. B: Scanning EMG from the same motor unit, obtained by pulling the concentric electrode in 50 μ m steps. Note 2 distinctly separated motor unit fractions. C: Proposed schematic representation of a motor unit giving rise to such a scanning picture. Different delays in the nerve branches and an irregular end-plate zone are assumed to explain the motor unit fractions which also correspond to the peaks in the Macro MUP (from ref 16).

Scanning EMG has been performed in normal muscles and in different types of nerve-muscle pathology, reported elsewhere (6,17).

This method thus gives direct measure of motor unit distribution and also helps to understand the concentric and monopolar electrode recordings.

Another method to study the distribution of the electrical activity in the motor unit, is based on recording from an array of surface electrodes (5,11). In this way the wave front from individual motor units is obtained. This gives information about motor end-plate zone, the gross arrangement of muscle fibres in a motor unit and the average velocity of action potentials of a motor unit.

FINDINGS IN THE PATHOLOGICAL MOTOR UNIT

The motor unit organisation and microphysiology becomes altered in neuromuscular diseases. Typical patterns of abnormality occur in different types of diseases (Fig 2).

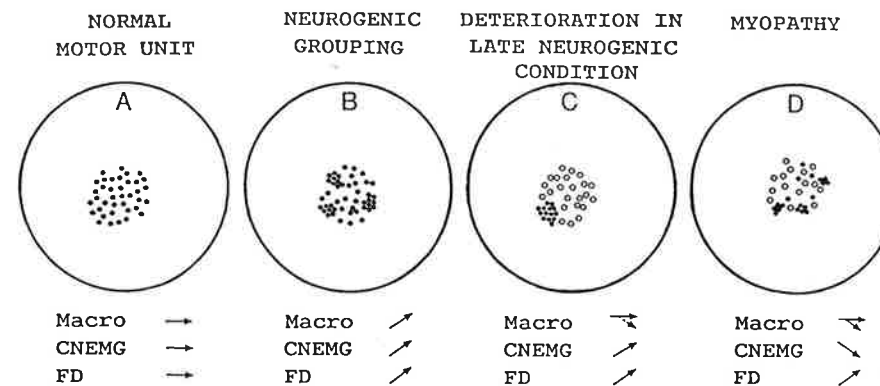


Fig. 2. Schematic findings with Macro EMG, concentric muscle EMG (CNEMG) and fibre density measurements (FD) in different types of motor units. In the normal muscle, Macro EMG signal may differentiate between normal small and large motor units.

Reinnervation

Reinnervation usually takes place as collateral sprouting. New sprouts are formed by surviving nerve twigs, innervating neighbouring denervated muscle fibres. In this way, muscle fibres from the same motor unit will occur more closely packed and the total number of fibers in this motor unit will increase.

This change is seen in SFEMG as increased FD already with very slight degree of reinnervation. In concentric needle EMG the enlarged motor units is reflected by increase in amplitude, area and duration. Macro EMG typically shows an increased MUP amplitude (Fig 2B). A combination of findings with increased FD, prolonged concentric EMG MUPs and normal Macro is interpreted as patchy grouping of fibres with clusters of fibres in some areas adjacent to empty areas within the same motor unit (Fig 2C). This is seen in rapidly progressive motor neurone disease. Scanning EMG usually shows dense motor units with mainly unchanged cross sectional length. This seems to indicate that the reinnervation process mainly takes place within the fascicles where the reinnervating motor unit was originally represented.

Primary myopathies

In many cases of muscular dystrophy SFEMG shows increased ED (15). This is contradictory to the conventional EMG findings which has been considered to suggest loss of fibres. The increased fibre density may indicate small groups of fibres e.g. due to fibre splitting or regeneration or new innervation of sequestered muscle fibre segments (Fig 2D). Other areas of the motor unit, deprived of fibres by the disease are instead locally electrically silent, seen in Scanning EMG. The concentric EMG electrode may detect an average loss of fibres within some areas of the muscle.

Macro EMG often shows normal or slightly reduced Macro MUP amplitudes.

SUMMARY

By means of electromyographic techniques it is possible to obtain information about some morphological parameters of the motor unit reflecting the topographical organisation of its muscle fibres. A combination of selective and non-selective recording methods give more information than each of them alone. Their main characteristics is summarized below.

<u>METHOD</u>	<u>PARAMETER</u>	<u>REFLECTS</u>
SFEMG	fibre density	# fibres in one MU within 300 um
CNEMG	amplitude	activity close to the electrode tip
	duration	# fibres within a part of the MU
SCANNING EMG	distribution	spatial and temporal distribution of activity in a corridor through the MU
MACRO EMG	amplitude	number and size of fibres in the entire MU

ACKNOWLEDGEMENTS

Supported by the Swedish Medical Research Council (Grant 135).

REFERENCES

- Buchthal F, Guld C, Rosenfalck P (1955) Propagation velocity in electrically activated muscle fibres in man. *Acta Physiol. Scand.* 34:75-89
- Koning P (1987) Estimation of the number of motor units based on Macro EMG (Thesis, University of Utrecht, The Netherlands) 105-123
- Edström L, Kugelberg E (1968) Histochemical composition, distribution of fibres and fatiguability of single motor units. *J Neurol Neurosurg Psychiat* 31:424-433
- Gruener R, Stern LZ, Weisz RR (1979) Conduction velocities in single fibres of diseased human muscle. *Neurology*, 29: 1293-1297
- Hilfilker P, Meyer M (1984) Normal and myopathic propagation of surface motor unit action potentials. *Electroenceph. clin. Neurophysiol.* 57:21-31
- Hilton-Brown P, Stålberg E (1983) The motor unit size in muscular dystrophy, a Macro EMG and Scanning EMG study. *J Neurol Neurosurg Psychiat* 46: 996-1005
- Kimura J (1983) *Electrodiagnosis in Diseases of Nerve and Muscle: Principles and Practice.* F.A. Davis, Philadelphia
- Lindström L, Petersen I (1981) Power spectra of myoelectric signals: motor unit activity and muscle fatigue. In: Stålberg E, Young RR (eds) *Neurology: Clinical Neurophysiology*, Butterworths, England, 66.
- Ludin HP (1980) *Electromyography in Practice*, Georg. Thieme Verlag, Stuttgart, New York.
- McComas AJ, Fawcett PRW, Campbell MJ, Sica REP (1971) Electrophysiological estimation of the number of motor units within human muscle. *J. Neurol. Neurosurg. Psychiat*, 34:121-131
- Masuda T, Miyano H, Sadoyama T (1985) A surface electrode array for detecting action potential trains of single motor units. *Electroencephalography and Clinical Neurophysiol*, 60:435-443
- Nandedkar S, Sanders DB, Stålberg E, Andreassen S (1988) Simulation of Concentric Needle EMG Motor Unit Action Potentials *Muscle & Nerve* 11:151-159
- Nandedkar S, Stålberg E (1982) Simulation of macro EMG Motor Unit Potentials, *Electroencephalography and Clinical Neurophysiol*, 56: 52
- Stålberg E (1966) Propagation velocity in human muscle fibres in situ. *Acta Physiol Scand* vol 70 suppl 287 1-112

15. Stålberg E (1986) Single Fibre EMG, Macro EMG and Scanning EMG. New Ways of Looking at the Motor unit CRC Press Inc, Florida, USA. vol 2, issues 2: 125-167
16. Stålberg E, Antoni L (1983) Computer-aided EMG analysis. In Desmedt JE (ed) Computer-Aided electromyography, Prog clin Neurophysiol, Karger Basel, 10, 186.
17. Stålberg E, Sanders DB (1984) The motor unit in ALS studied with different neurophysiological techniques. In Clifford RF (ed) Research Progress in motor neurone disease. Pitman Book Ltd, London, 105.
18. Stålberg E, Trontelj JV (1972) Single fibre electromyography. Woking, Surrey: Mirvalle Press
19. Thiele B, Boehle A (1978) Anzahl der Spike-Komponenten im Motor-Unit Potential. EEG-EMG 9: 125
20. Troni W (1984) Human muscle fibre conduction velocity in clinical application. In: Pinelli P, Pasetti C, Mora E (eds) Neurophysiological contributions for assessing rehabilitation in lower and upper motor neuron diseases. Liviana Editrice, Padova
21. Trontelj JV, Mihelin M, Fernandez JM, Stålberg E (1986) Axonal stimulation for end-plate jitter studies, J Neurol Neurosurg Psychiat 49:677-685

POWER SPECTRA OF MUSCLE FIBER EXTRACELLULAR POTENTIALS

GEORGE V. DIMITROV, ZOE C. LATEVA, NONNA A. DIMITROVA

Bulg Acad Sci, Ctr Biol, CLBA, G. Bonchev str, bl.105, 1113 Sofia (Bulgaria)

INTRODUCTION

The spectral analysis of the surface EMG is a widely used method¹⁻⁵. The results, however, have been interpreted on the basis of the theoretical investigations of the power spectrum (PS) of extracellular potentials (EPs) produced by an infinite excitable fiber⁶⁻⁸. Lindström⁸ supposed that the finite length of the muscle fibers affected the low frequency part of the spectrum towards decreasing spectral densities. On the other hand, in order to represent the muscle fiber signal source as two travelling waves propagating in opposite directions from the innervation point Lindström⁷ introduced factors 2 or 1 in the case of great radial distances (surface electrodes) or small ones (intramuscular electrodes), respectively.

Dimitrova⁹ showed that, when the waves of the intracellular action potential (IAP) reached the muscle fiber ends, a terminal positive phase (TPPh) was formed over the fiber, and a terminal negative phase - outside the fiber ends. The shape of these phases is similar to that of the IAP. The proportion between the amplitudes of the terminal phases and of the basic phases of the EPs is determined by the relationship between the fiber length, the IAP wavelength and the radial distance from the excited fiber axis to the point of observation¹⁰.

The aim of this paper is to investigate the sensitivity of the spectral characteristics of EPs produced by a skeletal muscle fiber to changes in the propagation velocity (PV) or in the IAP duration (T_{1n}).

METHOD

The EPs produced by a skeletal muscle fiber were obtained on the basis of the mathematical model proposed by Dimitrova⁹ by means of the method described by Dimitrov¹¹. The cylindrical muscle fiber length was supposed to be 80 mm (typical of *m. biceps brachii*) and the end-plate - in the middle of the fiber. The EPs were normalized by a factor $k = a^2 \cdot \sigma_a / 4 \cdot \sigma_e$, where a was the fiber radius, and σ_a and σ_e were the conductivities of the intra- and extracellular space, respectively. The extracellular space was supposed to be an isotropic and homogeneous one. The EPs were computed at points located at 20mm axial distance from the end-plate and at different radial distances from the fiber ($y = 0.1\text{mm}; 2\text{mm}; 15\text{mm};$ and 25mm). The PS of EPs were computed by means of a FFT algorithm with decimation in time.

RESULTS

The results reveal that the sensitivity of the spectral characteristics of EPs produced by a muscle fiber to changes in PV or T_{in} depends considerably on the radial distance from the excited fiber to the point of observation.

At small radial distances ($y < 0.2\text{mm}$) and aside of the end-plate and of the fiber ends the PS is a smooth curve which resembles the IAP shape. The spectral power distribution depends weakly on changes in PV. However, when T_{in} changes the spectrum shifts along the frequency axis approximately in inverse proportion to the changes in T_{in} . The excitation waves' origin and attenuation have no effect on the PS.

At middle radial distances ($0.2\text{mm} \leq y \leq 10\text{mm}$) the muscle fiber finite length starts to influence the EPs and correspondingly the PS (Fig. 1). Though small, TPFh is noted in the EP, and the PS is not so smooth as in the former case. Weak oscillations occur in the PS. The spectral power distribution depends on changes both in T_{in} and in PV.

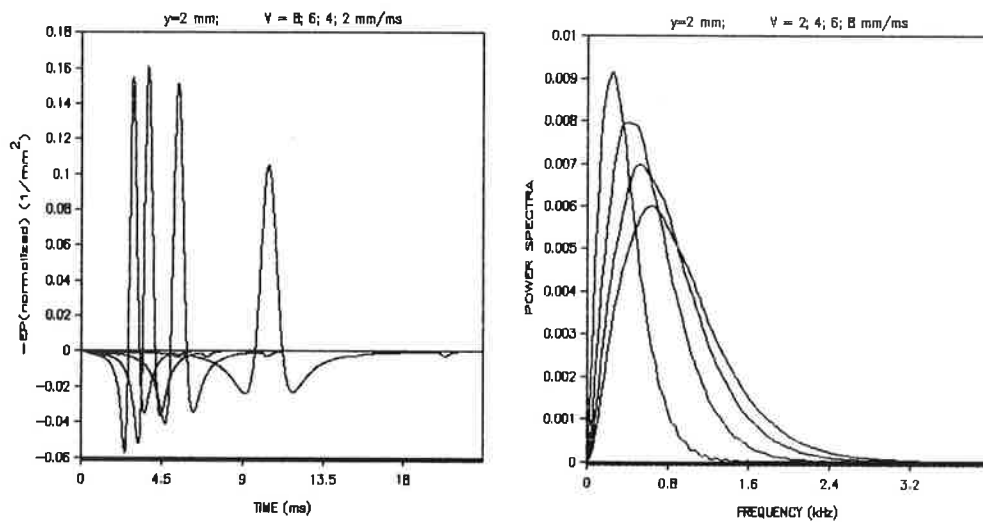


Fig. 1. Normalized extracellular potentials and their spectra calculated for different PV at 2mm radial distance ($T_{in}=1.25\text{ms}$)

At great radial distances ($y > 10\text{mm}$) both the EPs and their PS are influenced by the following features: 1) the excited fiber finite length, 2) the presence of two waves propagating from the end-plate to the fiber ends, and 3) the commensurability of the distance from the excited fiber to the point of observation with the distances from the latter to the end-plate and to the fiber ends (Fig. 2). The amplitude of the TPFh of EPs produced by a

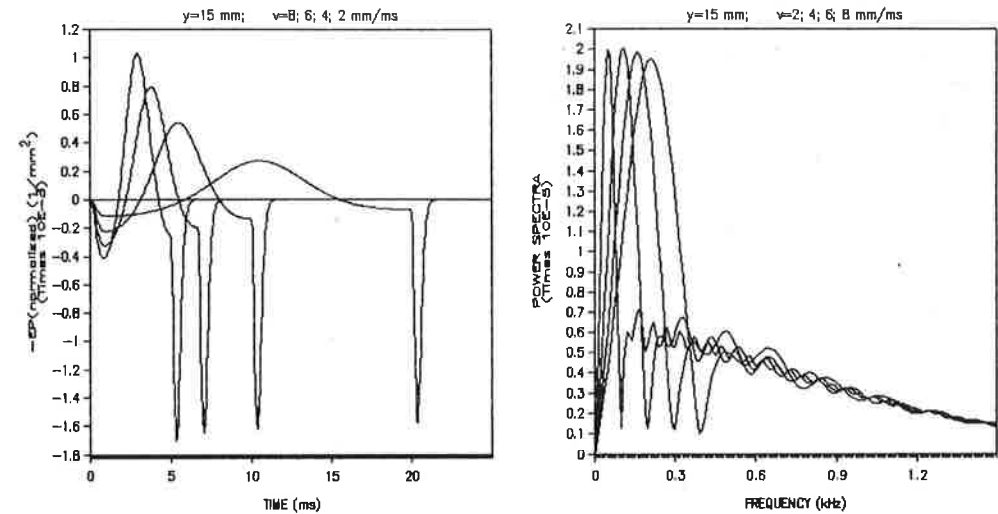


Fig. 2. Normalized extracellular potentials and their spectra calculated for different PV at 15mm radial distance ($T_{in}=1.25\text{ms}$)

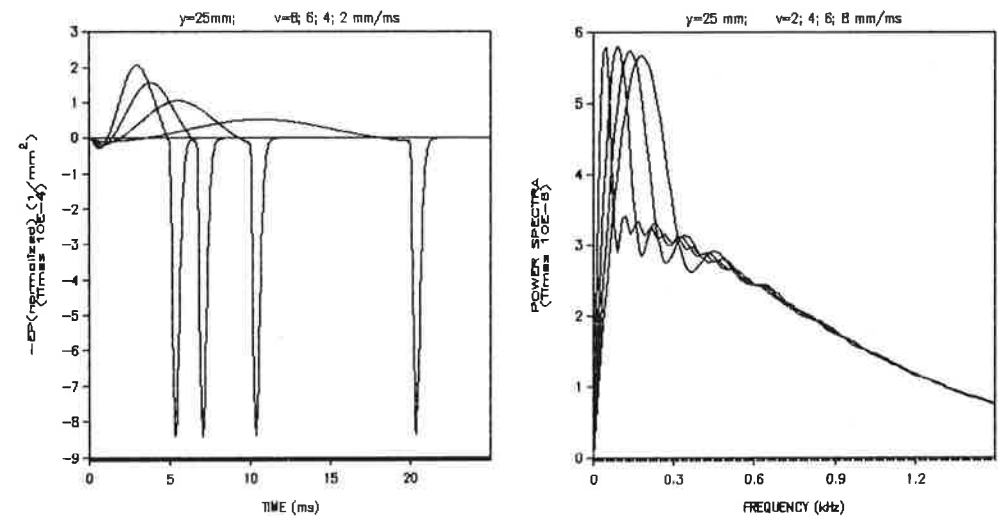


Fig. 3. Normalized extracellular potentials and their spectra calculated for different PV at 25mm radial distance ($T_{in}=1.25\text{ms}$)

single fiber can be greater than the amplitude of the basic EP negative phase. The oscillations in the PS become greater. The PS is formed by two components. The first is a lower frequency one and it reflects the basic phases of the EP. The second component is a higher-frequency one and it

reflects the TPPH. A change in PV does not alter the TPPH duration and, therefore, the spectral power distribution of the PS second component is not modified when PV changes. However, the durations of the individual basic phases of the EP are modified and, respectively, the spectral power distribution of the PS first component is modified as well. Furthermore, the PS first component shifts along the frequency axis approximately proportionally to changes in PV.

At greater radial distance ($y=25\text{mm}$) the relative contribution of the PS second component to the PS increases (Fig. 3) for the reason that the relation between TPPH and the basic phases of the EP increases.

When T_{in} changes the durations of the individual basic phases of the EP are not practically modified at great radial distances. The duration of TPPH, however, is modified proportionally to the changes in T_{in} (Fig. 4). As a result the spectral power distribution of the PS first component does not change, but the spectral densities of the lower frequency part of the PS second component rise when T_{in} increases.

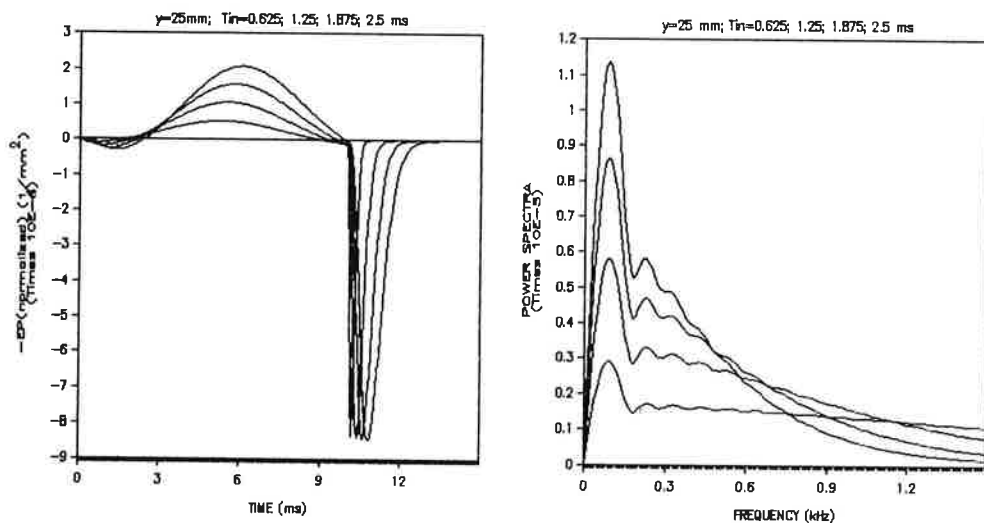


Fig. 4. Normalized extracellular potentials and their spectra calculated for different T_{in} at 25mm radial distance ($PV=4\text{ mm/ms}$)

DISCUSSION

At small radial distances corresponding to SFEMG (aside the end-plate and of the fiber ends) the sensitivity of the spectral characteristics of EPs of a finite length fiber to changes in PV or in T_{in} is the same as that in the case of an infinite fiber¹²⁻¹⁴. At middle distances corresponding to needle

electrode recording, there are inessential differences in the spectra of EPs of a finite and of an infinite fiber. However, at great radial distances corresponding to surface electrode recording, the differences are essential, especially in the case of an anisotropic volume conductor. The radial distance in an isotropic volume conductor corresponds to $\sqrt{K_{an}}$ times smaller distance in a case of an anisotropic volume conductor¹⁵. In the case of $K_{an}=10$ the radial distance of 25mm corresponds to an actual distance of about 8mm in the anisotropic conductor.

In this paper a comparatively long fiber typical of *m. biceps brachii* is studied. In a case of shorter fibers¹⁰ the relative contribution of the second component to the PS may increase at a great radial distance. The negative after-potentials typical of muscle fibers can rise still more the contribution of the second component to the PS because they affect the lower frequency components towards increasing their densities.

The positive phase (TPPH) of a compound EP recorded with surface electrodes, is not so pronounced as that shown in the present paper. This can be a result of desynchronization in excitation of fibers, that alters mainly TPPH through increasing its duration and decreasing its amplitude¹⁶.

Shoshina et al.¹⁷ give an experimentally obtained PS of surface led potentials of *m. biceps brachii*. In the figures the two components and oscillations in the PS, described in this paper, can be distinguished.

REFERENCES

1. Agarwal GC, Gottlieb GL (1975) IEEE Trans Biomed Eng, BME-22:225-229
2. Lindström L, Magnusson R (1977) Proc IEEE 65:653-662
3. Sato H (1982) Electomyogr clin Neurophysiol 22:459-516
4. Hermens HJ, Boon KL, Zilvold G (1984) Electomyogr clin Neurophysiol 24:243-265
5. De Luca CJ (1984) CRC Crit Rev Biomed Eng 11:251-279
6. Krakau CET (1957) Kungl Fysiogr Sällsk i Lund Förhandl 14:177-183
7. Lindström L (1970) Res Lab Med Electr, Chalm Univ, Techn Rep 7:70
8. Lindström L (1973) Res Lab Med Electr, Chalm Univ, Techn Rep 5:73
9. Dimitrova NA (1974) Electomyogr clin Neurophysiol 14:53-66
10. Dimitrov GV, Dimitrova NA (1978) Agressologie 19:176-186
11. Dimitrov GV (1987) Electomyogr clin Neurophysiol 27:243-249
12. Dimitrov GV, Lateva ZC, Dimitrova NA (1988) Effects of changes in asymmetry, duration and propagation velocity of intracellular potentials on the power spectrum of extracellular potentials produced by an excitable fiber, Electomyogr clin Neurophysiol (in the press)
13. Dimitrov GV, Lateva ZC, Dimitrova NA (1988) Power spectra of extracellular potentials generated by an infinite homogeneous excitable fiber, Med Biol Eng & Comp (in the press)
14. Lateva ZC (1988) Dependence of quantitative parameters of the extracellular potential power spectrum on propagation velocity, duration and asymmetry of action potentials, Electomyogr clin Neurophysiol (in the press)
15. Dimitrov GV, Dimitrova NA (1974) Electomyogr clin Neurophysiol 14:423-436
16. Dimitrov GV (1978) Electomyogr clin Neurophysiol 18:361-376
17. Shoshina M, Gonen B, Wolf E, Mahler Y, Magora A (1986) Electomyogr clin Neurophysiol 26:513-520

POSSIBLE MECHANISMS OF BIOELECTRIC PHENOMENA ASSOCIATED WITH DISORDERS OF NEUROMUSCULAR TRANSMISSION

NONNA A. DIMITROVA, GEORGE V. DIMITROV

Bulg Acad Sci, Ctr Biol, CLBA, G. Bonchev str, bl. 105, 1113 Sofia (Bulgaria)

INTRODUCTION

Disorders of neuromuscular transmission accompanying myasthenia gravis, Lambert-Eaton syndrome, botulinum or certain antibiotic intoxication, lead to a reduction of the end-plate currents (EPC) as compared with these typical of normal conditions. Changes in the extracellular potentials (EPs) produced by motor units or by a muscle under their voluntary or electrical activation are thought to be a result of blocking of a number of muscle fibres in which propagating intracellular action potentials (IAPs) fail to develop^{1,2}. The increase of jitter that is typical of these disorders, is thought to be a result of slowing the rising slope of the EPC, combined with the firing threshold fluctuations in muscle fibres². On the other hand, Dimitrova and Dimitrov³ have shown that the propagation velocity (PV) of the IAP wave in a fibre of finite length, under a slightly suprathreshold electrical stimulation, can become considerably higher (or even negative) than that which is typical of a substantially suprathreshold stimulus strength. The shorter the fibre, the stronger the effect. Variations in PV may change the IAP profile formed along the fibre length and, thus, the EP value.

The aim of the present paper was to elucidate whether the reduction of EPC can induce variations in the magnitude of EPs generated by a relatively short fibre, before the failure of muscle fibre action potential occurs.

METHOD

Mathematical modelling was used to study IAPs and EPs generated in response to a single rectangular electrical pulse of current applied in the middle point of a cylindrical fibre terminated by insulated ends. The fibre radius was 30 μm , and its length was 8 mm. The stimulus pulse duration was 200 μs and its strength (I_{st}) was either slightly higher (less than 1 per cent) than the threshold value (I_{thr}) or substantially above it (50 per cent). EPs were calculated on the basis of the mathematical model proposed by Dimitrova⁴, while the intracellular potential profile was calculated on the basis of the Hodgkin-Huxley⁵ model by the method of Joyner et al.⁶

The fibre geometry used in the present paper was an approximation of a skeletal muscle fibre geometry, where the site of stimulus application and the insulated ends corresponded to the end-plate and tendons, respectively.

RESULTS

1. Substantially suprathreshold stimulus strength

IAPs arose after a short latency and propagated from the site of stimulation to the fibre terminations (Fig.1-bottom-left). The membrane potential profile formed along the fibre length (Fig.1-bottom-right) was pronounced. The EPs corresponded to those typical of short muscle fibres⁷. At small radial distances the EPs were negative-positive above the end-plate, positive-negative-positive above the middle portion of the fibre (closer to the end-plate) and positive-negative in the region of fibre termination and behind it (Fig.1-top-left). At greater radial distances the region where the EPs were negative-positive, became wider at the expense of the region where the EPs were triphasic (Fig.1-top-middle and right).

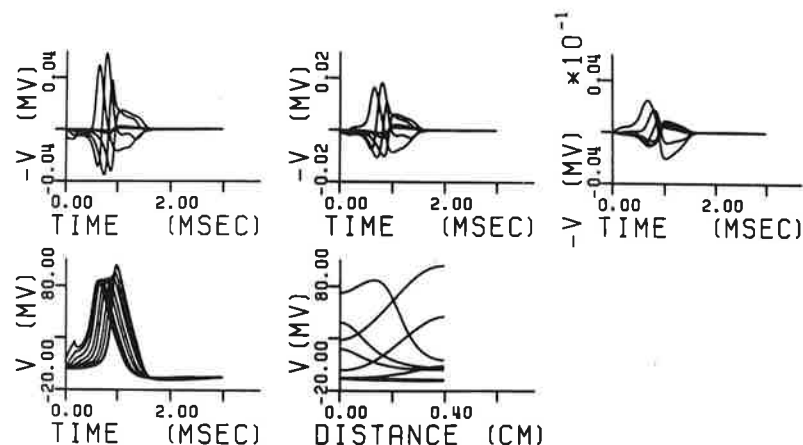


Fig.1. Intracellular (bottom) and extracellular (top) potentials. IAPs in the time domain are shown for 9 equidistant (0.5 mm) points along the fibre semilength. IAPs in the distance domain are shown for moments of time 0.25-2.5 ms at every 0.25 ms. The EPs (from left to right) are for radial distances $y=0.125; 0.5; 2$ mm, respectively. The axial distances (x) of the points of observation are 1-6 mm at every 1 mm and are the same for all radial distances. EPs calculated above the motor end-plate ($x=0$) are not shown because of large stimulus artifact. Stimulus strength $I_{st}=1.5 I_{thr}$.

2. Slightly suprathreshold stimulus strength

A. I_{st} exceeded I_{thr} by 0.62 per cent. After a long latency the whole fibre membrane fired almost simultaneously³ (Fig.2-bottom-left). The IAP duration was practically unchanged, but the PV considerably increased. As a result, the potential profiles formed along the fibre length, were less pronounced (Fig.2-bottom-right) and the EP amplitudes were considerably lower (Fig.2-top) than those obtained under the stronger stimulus.

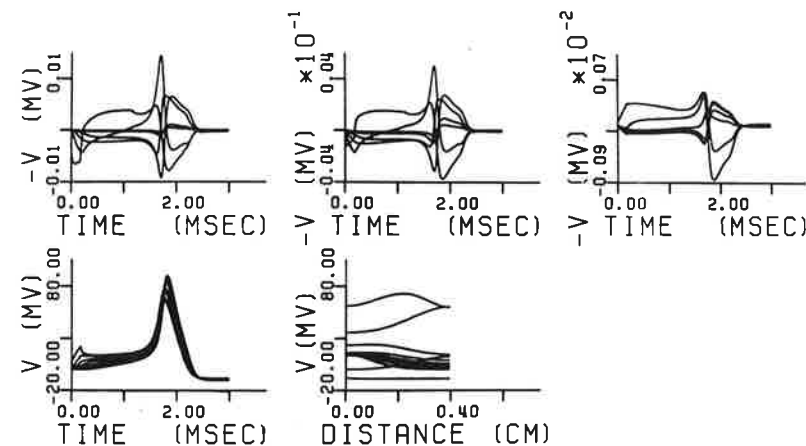


Fig.2. The same as Fig.1, but I_{st} exceeds I_{thr} by 0.62 per cent

B. I_{st} exceeded I_{thr} by 0.58 per cent. After a long latency IAP arose first at the fibre terminations³, instead at the site of stimulation, and then it propagated to the end-plate (Fig.3-bottom-left). The PV was negative, but its absolute value was commensurable with that described above (in p.1). The IAP duration was practically unchanged. As a result, the potential profiles (Fig.3-bottom-right) were more pronounced and the EP amplitudes (Fig.3-top) were higher than those described in p.2a. The polarity of the EPs was, however, opposite to that described in the preceding cases. The EPs were positive-negative above the end-plate and negative-positive in the regions of the fibre terminations and behind them.

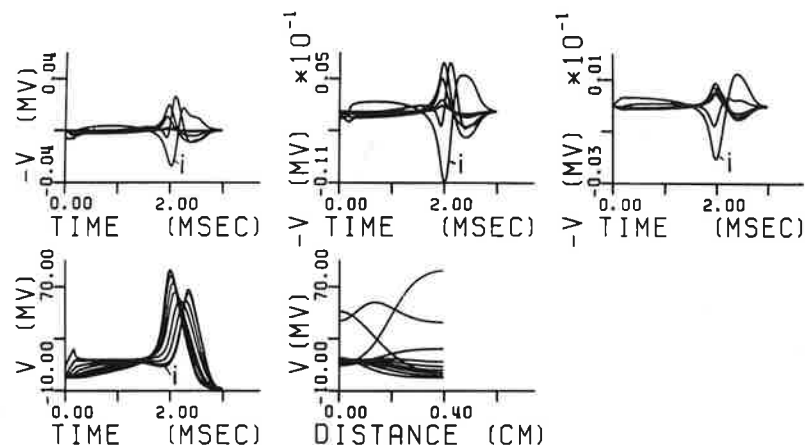


Fig.3. The same as Fig.1, but I_{st} exceeds I_{thr} by 0.58 per cent. Symbol "i" corresponds to the IAP calculated at the point of stimulation, and to the EPs calculated at points of volume conductor having axial distance $x=1$ mm.

DISCUSSION

The results obtained in the present paper show that reduction of stimulus strength to a slightly suprathreshold value can lead to the following electrophysiological phenomena: reduction of the EP amplitude or abnormal sequence of phases of EPs generated by short fibres having uniform membrane properties up to their insulated ends.

In these conditions, if the end-plate is not in the middle point of the fibre, an abnormal IAP will arise first at the fibre termination that is nearer to the end-plate, and will propagate to the other end. This will also result in abnormal EPs generated above the shorter "semilength" of the fibre and above a portion of the fibre next to the end-plate, but at its other side.

When compound EPs are recorded, the decrease in their amplitudes can be a result of a reduction of EPs produced by individual fibres and of subtraction of abnormal EPs.

Stimulus effect can be changed through variation of either stimulus amplitude or its duration³ and, as a first approximation, of its area. Thus alterations in IAPs, EPs, latency (and, respectively, in jitter) can be due to changes not only in rising but also in falling phase of the end-plate currents.

In contrast to normal conditions when EPCs substantially exceed the threshold value, influence of currents of other active fibres on processes of the fibre excitation is facilitated under slightly suprathreshold EPCs.

The results of the present paper demonstrate that dramatic changes can be expected not only in jitter², but also in amplitude of a single fibre or of compound EPs generated by muscles that include or consist of short fibres before impulse blocking occurs and thus before symptoms of neuromuscular disorders are present.

REFERENCES

1. Desmedt JE (1973) In: Desmedt JE (ed) *New Developments in Electromyography and Clinical Neurophysiology* S. Karger, Basel, v. 1, pp 305-342
2. Stalberg E, Trontelj JV (1979) *Single Fibre Electromyography*. The Mirvalle Press Ltd, Old Working, Surrey, pp 1-244
3. Dimitrova NA, Dimitrov GV (1988) *Electroenceph Clin Neurophysiol* (in the press)
4. Dimitrova NA (1974) *Electromyogr Clin Neurophysiol* 14:53-66
5. Hodgkin AL, Huxley AF (1952) *J Physiol (London)* 117:500-544
6. Joyner RW, Westerfield M, Moore JW, Stockbridge N (1978) *Biophys J* 22:155-170
7. Dimitrov GV, Dimitrova NA (1978) *Agressologie* 19:176-186

ACTIVITY OF SINGLE MUSCLE FIBRES RECORDED AT KNOWN DISTANCES

W. WALLINGA, B.A. ALBERS, J.H.M. PUT, W.L.C. RUTTEN, AND P. WIRTZ¹

University of Twente, Department of Electrical Engineering, Biomedical Engineering Division, P.O. Box 217, 7500 AE Enschede (The Netherlands).

INTRODUCTION

Simulations of extracellular single fibre action potentials (SFAP's) with a structure based model (1,2) show how parameters concerning the structure of the tissue and the conductivity properties of the tissue components can determine the relations between SFAP-characteristics and recording distance.

Here we present data of our experimental research of the SFAP. Stimulation and labelling of a single muscle fibre, together with labelling of the recording electrode, enable a morphometric derivation of the recording distance. The number of SFAP's recorded at known distances is rather restricted. Other SFAP's are considered here as well. Some aspects of the discrepancies between experiment and theory are discussed.

MATERIAL AND METHODS

Muscle preparation

All experiments were done with the m. extensor digitorum longus (EDL) in the hind limb of the rat (Wistar, adult males). The rats were anaesthetized intraperitoneally with pentobarbital sodium. The muscle was *in vivo* as described before (3). The muscle temperature was 36-38°C. The length of the muscle was set at optimum twitch length.

Micropipette electrode

The micropipette electrodes were produced from glass-capillaries with an inner filament (Clark Electromedical Instruments, type GC 150F-15). The tip diameter of the electrodes was 1 to 2 μm . The micropipette was filled with Lucifer Yellow dissolved in a 0.5 M LiCl solution (4). The intracellular resting membrane potential was often stable (about -70 mV). Activity of the penetrated fibre was evoked with a hyperpolarizing current pulse. The muscle fibre responded with one up to five responses after the current pulse.

Labelling of a fibre was done by iontophoresis of the Lucifer Yellow with hyperpolarizing current pulses with a low amplitude and a duty cycle of 50%.

¹Affiliated to the University of Nijmegen during the research.

Wire electrodes

The wires had a stainless steel core with a diameter of 25 μm , isolated with a 4 μm Karma coating. The tip was cut obliquely. Fourteen wire electrodes were inserted in the muscle. The spatial arrangement aimed at the recording of the response of the stimulated single fibre, preferably at more than one radial distance and at two to three locations along the muscle fibre.

Electrophysiological procedure

The SFAP's were sampled with 100 kHz. When one or two electrodes showed SFAP-amplitudes above 1 mV, Lucifer Yellow was iontophoretized. Thereafter the position of the tips of the recording electrodes with sufficient amplitudes were marked by a silver deposition. The micropipette was removed, the wire electrodes too except the marked ones. These were cut above the muscle surface. Signal analysis was applied to threephasic SFAP's for derivation of - the top-top amplitude (V_{tt}), - the amplitude of the first positive phase (V_1), - the time between the first positive and the negative peak (Δt), - the moment of crossing the baseline of the transient between the first positive and the negative peak (figure 1).

Morphologic data

The muscle was frozen preserving its length and stored at low temperature. The frozen muscle was cut in 10 μm thick sections. No fixation was applied. The autofluorescence of the Lucifer Yellow was detected microscopically. The fibres were labelled up to about 4 mm, but not along their whole length. In its non-fluorescent part, the fibre was followed up to and including the sections containing the recording electrodes. The recording distance was determined. The histochemical character of the labelled fibres was type Y (fast, glycolytic) or type J (fast, slightly more oxidative) in the scheme of Wirtz et al. (5).

Material and methods are described in detail in (6).

RESULTS

In twentyfive muscles the technique described above was applied. In eleven cases the fluorescent fibre was detected. In seven experiments the recording distance(s) (ranging from 70-300 μm) were considered reliable (main factor restricted damage around the electrodes). A lot of SFAP-recordings were made. The small set of recordings at known distance had characteristics which appeared to be normal with respect to V_{tt} , V_1/V_{tt} and Δt . In figure 2 the amplitude of the first positive peak (V_1) is plotted against the top-top amplitude (V_{tt}) of about eighty triphasic SFAP's. Figure 3 shows two SFAP's of the same fibre recorded at two distances. In figure 4 the values of V_1/V_{tt} are plotted against the recording distance. The experiments are indicated with different symbols. Note the variable behaviour. The Δt -values of the SFAP's range from 50 to 170 μs . In four out of five cases with two recordings at known distances, the Δt increased with distance.

The conduction velocities were determined from the longitudinal distance between two electrodes and the time period between the moments of crossing the baseline of the transient in the two AP's (best time reference point, ref. 7). The velocities varied from 1.1 to 8.5 m/s. This is a range with lower and higher values than expected.

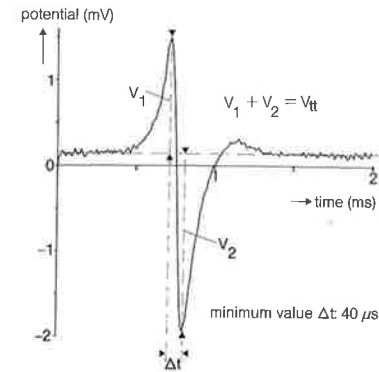


Fig. 1. SFAP with indication of V_{tt} , V_1 and Δt .

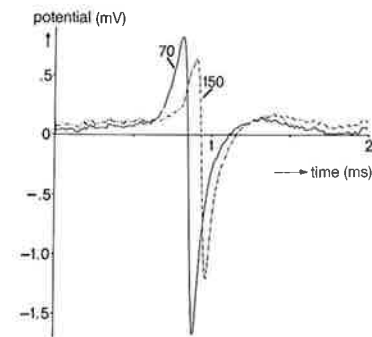


Fig. 3. SFAP's recorded at 70 and 150 μm distances from the same stimulated fibre.

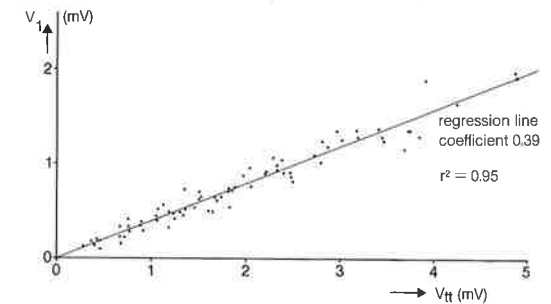


Fig. 2. The amplitude of the first positive phase (V_1) versus the top-top amplitude (V_{tt}) for 80 SFAP's.

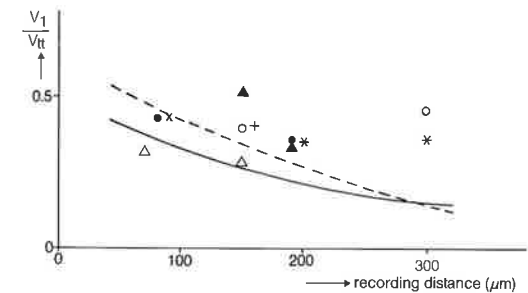


Fig. 4. V_1/V_{tt} versus actual recording distance. Measurements of one fibre have the same symbol.

Once we derived from simultaneous recordings at three positions along one fibre three values of conduction velocity: 5.0 ± 0.3 ; 4.2 ± 0.2 and 2.5 ± 0.3 m/s. These values could indicate variation of the conduction velocity in the longitudinal direction of the muscle fibre or a less reliable recording position than expected. We found that the size of this fibre stayed constant within 10%. The rather limited set of observations did not enable yet statements on the relation between the fibre size and the conduction velocity. When after a stimulus the fibre responded with some AP's, the SFAP's recorded at different electrodes changed parallel in Δt . Increased, decreased and constant values of Δt were observed in a train of SFAP-responses.

DISCUSSION

SFAP's recorded some mm away from stimulation site and tendinous tissue are nearly always triphasic (80 out of 83). The amplitude of the first positive phase / the total amplitude (V_1/V_{tt}) does not depend on the SFAP-amplitude (fig. 3). This suggests a flat plot of V_1/V_{tt} versus recording distance. Figure 4 is consistent with that.

In simulations with homogeneous and inhomogeneous models (6), however, the quotient V_1/V_{tt} decreased apparently with recording distance (see figure 4). Additional experiments and simulations are necessary to study this intriguing point.

The Δt often varies within a train of responses after one stimulus. A change of conduction velocity can reasonably be the starting point of this (7), but then it is amazing that the sign of change is so variable.

Quantitative analysis of SFAP's needs higher filter settings and higher sample frequencies than often used. A sample period of 10 μs , as used in this study, limits already the accuracy of the conduction velocity. Reliable derivation of the conduction velocity (comparison of AP's of comparable amplitude is necessary) combined with labelling of the stimulated fibre will offer direct data for the description of the relation between conduction velocity and fibre size, in contrast to the experimental results described before.

ACKNOWLEDGEMENTS

The authors wish to thank Ms. T. van der Reijden and Ms. H. Loermans for carrying out the morphological and histochemical part of this work. The work was supported by the Netherlands Organization for Scientific Research (NWO).

REFERENCES

1. Albers BA, Rutten WLC, Wallinga-de Jonge W, Boom HBK (1986) A model study on the influence of structure and membrane capacitance on volume conduction in skeletal muscle tissue. *IEEE Trans Biomed Eng* 33: 681-689
2. Albers BA, Rutten WLC, Wallinga-de Jonge W, Boom HBK (1988). Frequency domain modeling of volume conduction of single muscle fibre action potentials. *IEEE Trans Biomed Eng* 35: 328-332.
3. Wallinga-de Jonge W, Boom HBK, Boon KL, Griep PAM, Lammeree GC (1980) Force development of fast and slow skeletal muscle at different muscle lengths. *Am J Physiol* 239: C98-C104
4. Stewart WW (1978) Functional connections between cells as revealed by dye-coupling with a highly fluorescent naphthalimide tracer. *Cell* 14: 741-759
5. Wirtz P, Loermans HMT, Peer PGM, Reintjes AGM (1983) Postnatal growth and differentiation of muscle fibres in the mouse. I A histochemical and morphological investigation of normal muscle. *J Anat* 137: 109-126
6. Albers BA (1987) Microscopic volume conduction of myo-electrical activity. Thesis, University of Twente
7. Stålberg E (1966) Propagation velocity in human muscle fibers in situ. *Acta Physiol Scand* 70 (suppl. 287): 1-112

Surface EMG: Modelling and effect of electrode-configurations

VOLUME CONDUCTOR MODELING OF MOTOR UNIT ACTION POTENTIALS IN THE
SURFACE ELECTROMYOGRAM.

T.H.J.M. GOOTZEN', H.M. VINGERHOETS", D.F. STEGEMAN"

'Lab. of Medical Physics and Biophysics,
"Dep. of Clinical Neurophysiology (Institute of Neurology),
University of Nijmegen P.O.Box 9101, 6500 HB Nijmegen, The Netherlands

INTRODUCTION

In the interpretation of surface EMG (SEMG) recordings not all factors contributing to the EMG waveform are quantitatively known. The conduction velocity of the muscle fibre action potentials, the distance of the motor units to the surface electrodes, other spatial characteristics and the firing frequency of the motor units in the muscle certainly do influence the SEMG signals. No satisfactory physical descriptions of the SEMG characteristics, especially in terms of volume conduction phenomena on motor unit level were available.

To study these factors, we analysed surface EMG and intramuscular concentric needle EMG simultaneously obtained. When the intramuscular EMG signal is decomposed with the ADEMG technique, developed by McGill and others [1], the firing times of the motor units become available for the motor unit level analysis of the surface EMG signal. Both intramuscular recorded MUAPs and surface MUAPs can then be compared with simulated MUAPs.

METHODS

From healthy volunteers the EMG signals from the vastus medial muscle were recorded by using a concentric EMG needle electrode as well as six standard disk surface electrodes at a fixed percentage of maximum voluntary isometric contraction (MVC). After localizing the motor zone by means of surface electric stimulation, the surface electrodes were placed between the motor zone and the distal tendon of the muscle, in two rows lying parallel to the (expected) orientation of the muscle fibres (fig. 1).

The needle electrode was inserted between the two rows, a few mm distal from the most proximal surface electrodes. A surface electrode on the knee was used as common reference, making all recordings monopolar, including the needle tip signal. Ten seconds of each signal were stored, sampled with a frequency of 10 kHz. The ADEMG decomposition technique [1] was used to decompose the needle signal into the contributions of different motor unit action potentials (MUAPs) and their corresponding firing times. These firing times were used to obtain averaged MUAPs of the same motor units from both the needle tip and the surface electrode signals. Two ways to analyse the data are presented. (1) From the resulting MUAP averages from each signal and the firing times, EMG signals were synthesized. The

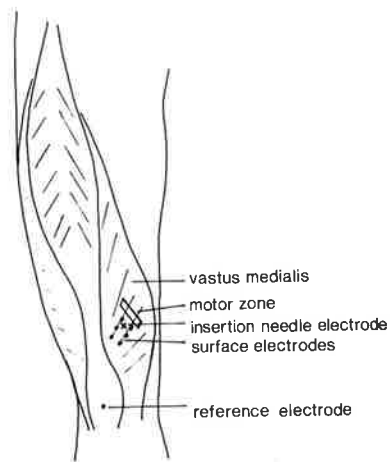


Fig. 1. Electrode locations on the vastus medialis muscle

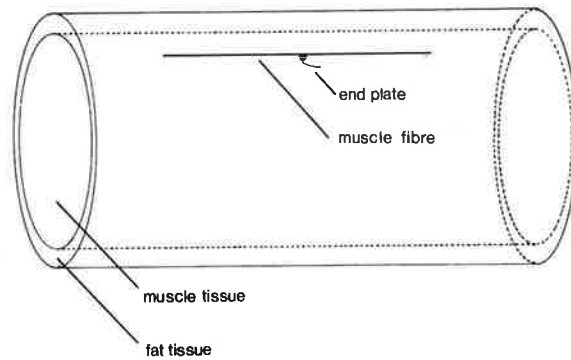


Fig. 2 Volume conductor geometry including muscle and subcutaneous fat tissue.

estimated signals were compared to the original signals by the root-mean-square (RMS) amplitude of the signals. (2) The MUAPs were compared to simulated MUAPs from a newly developed volume conductor model.

THE VOLUME CONDUCTOR MODEL

The volume conductor consists of two concentric cylinders, the inner cylinder representing muscle tissue, the region between the two cylinders representing the subcutaneous fat lying over the muscle. The outer cylinder is assumed to be surrounded by air (i.e. conductivity zero). (fig. 2) Parameters are adapted to the geometry of the leg. The volume conduction problem is solved analytically [2]. Within the muscle compartment muscle fibres of finite length are placed randomly. Innervation is somewhere halfway the fibres. MUAPs are simulated after choosing proper distributions for the fibre diameters, the muscle fibre locations and the end plate locations.

RESULTS AND DISCUSSION

About 6 MUAPs (range 3-9) are detected by the ADEMG technique at force levels of 12 to 36 % MVC. Fig. 3 shows in the upper trace 0.2 seconds of the needle signal recorded at 12 % MVC at an insertion depth of 15 mm. From this signal the MUAP averages and corresponding firing times were used to synthesize the signal in trace 2 of fig. 3. A large part of the (high frequency) spike components caused by motor unit activity close to the needle tip has been recognized. The RMS-value of the synthesized signal is 40 % of the RMS-value of the original signal increasing to 60 % at higher force levels. The remaining, still large part of the needle tip



Fig. 3. Trace 1 needle EMG signal, trace 2 synthesized signal from averaged MUAPs, trace 3 surface EMG signal, trace 4 superposition of needle and surface EMG signal.

signal in a monopolar montage originates from motor units not detectable by ADEMG.

Trace 3 of fig. 3 shows the corresponding interval of one of the surface electrode signals. In this signal no motor unit spikes can be distinguished from the total activity recorded by the surface electrode. The RMS-value of a signal synthesized from surface MUAPs (SMUAPs) only reaches 15 to 30 % of the original surface signal RMS-values. The percentages decrease monotonically with increasing insertion depth of the concentric needle. The observation common for both the needle and surface recordings is the (unexpected) large amount of activity in these monopolar signals which cannot be attributed to detected motor units, apparently originating from a large fraction of the muscle. The latter can be concluded from trace 4 in fig. 3 where the needle signal and the surface signal are superimposed, and where a striking resemblance appears in the low frequency components of both signals.

Although the individual motor unit spikes cannot be recognized in the surface EMG, the number of firings detected from the needle signal is sufficient to obtain averaged SMUAPs with an acceptable signal to noise ratio. Fig. 4 A shows a needle tip MUAP and two SMUAPs and fig. 4 B shows a needle tip MUAP and three SMUAPs. From the averaged surface MUAPs the propagation of the action potential can be seen clearly from the time shift of the negative peak to larger latencies. However not only propagating peaks appear in the SMUAPs. In both columns 4A and 4B a peak with constant latency is visible.

To illustrate the origine of the signal components in the averaged SMUAPs a simulated needle MUAP and corresponding SMUAPs with approximately the same geometrical conditions under which the MUAPs from fig. 4B were recorded are shown

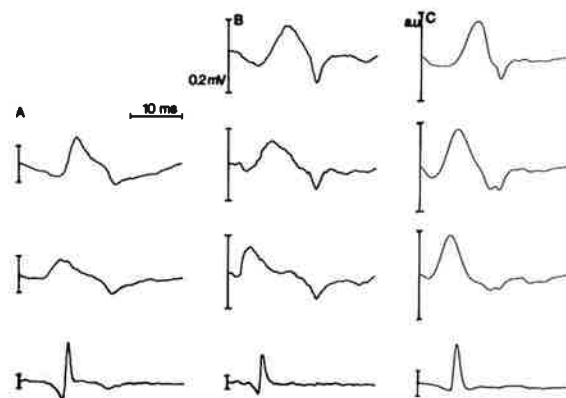


Fig. 4A and 4B averaged needle and surface MUAPs, 4C simulated MUAPs under approximately the same conditions as the recording of 4B. (a.u.=arbitrary units)

in fig. 4 C. We simulated a motor unit, lying with its centre 15 mm below the skin surface. The total length of the fibres was taken 100 mm, with the endplate zone 10 mm from the middle of the fibres. In fig. 4C the simulated needle MUAP and three surface MUAPs are shown. Both the shifting negative peak and the constant latency positive peak can be seen. From the results from this volume conductor model we conclude that the latency of this peak corresponds to the moment at which the muscle fibre action potentials reach the end of the muscle fibres. This is the first time the large spatial spread of these positive peaks of blocking action potentials is simulated with a MUAP simulation model. Their amplitude characteristics are mainly determined by the finiteness of the volume conductor [3].

Fig. 4 shows that the different components of surface MUAPs can well be understood by comparing them to the modeled MUAPs. The appearance of positive peaks may explain the observation of non-moving components in surface EMG recordings used for conduction velocity measurements [4]. The observations made in fig. 3 suggest a large take-up area for monopolar recordings. From the depth dependence of the RMS-values of the synthesized signals obtained by using the ADEMG algorithm [1] the contributions of the individual motor units to the EMG at other sites can be estimated. In combination with results from the volume conductor simulation model a new, simpler procedure for estimating the total number and the size of motor units comes into view.

REFERENCES

- [1] McGill, K.C. et al, (1985) IEEE Trans. Biomed. Engin. 32:470-477
- [2] Gootzen et al, (1988) in preparation
- [3] Stegeman et al, (1987) Electroenceph. Clin. Neurophysiol. 67:176-187
- [4] Broman et al, (1985) IEEE Trans. Biomed. Engin. 32:341-343

A STOCHASTIC MODEL FOR SIMULATION OF SURFACE EMG PATTERNS

H.J. HERMENS, T.A.M. v. BRUGGEN, W.L.C. RUTTEN, G. WILTS, K.L. BOON,
 W. WALLINGA- DE JONGE, G. ZILVOLD

Rehabilitation Centre het Roessingh, Enschede, The Netherlands
 University of Twente, Enschede, The Netherlands
 Hospital De Stadsmaten, Enschede, The Netherlands

INTRODUCTION

A measuring set-up has been realised, which involves a standardized way of recording and analysing surface EMG (1). This set-up is used frequently to study the course of specific disorders and to evaluate the effect of treatment.

In order to improve our understanding of surface EMG a simulation model was developed. This model generates action potential trains and adds these trains in order to obtain interferenced EMG patterns.

Special attention was paid to obtain characteristics of MUAPs recorded with surface electrodes in order to make simulation as realistic as possible.

METHODS

1. Concepts of the model

We based our model on the one of Person and Libkind (2), described in more detail by De Luca (3). It assumes that a motor unit action potential (muap) train can be generated by filtering a train of delta pulses. The train simulates the firing of the motor unit. The filter process generates the MUAP as it is observed by an electrode. The EMG signal of the muscle is now generated by a linear summation of a large number of MUAP trains.

Instead of using a single synthetic shape of the MUAP a library is created in which a number of MUAP shapes of standardized amplitude and duration is present. These may be measured MUAPs extracted from EMG registrations and/or synthetically obtained shapes. In this way a large flexibility is obtained to study various effects of the MUAP shape on the power spectrum.

In order to get a MUAP that can be used in a MUAP train the library shapes are multiplied both with a time and an amplitude factor. These factors are obtained from a Gaussian distribution in order to simulate the wide range of amplitudes and durations of motor units that are found in EMG. Within a train the MUAP's shape, amplitude and duration remain constant, but among trains these factors can be changed.

The interpulse intervals of the MUAPs within a train are assumed to have a Gaussian distribution.

In order to simulate synchronization between a number of MUAP trains the

firing moments of the first train are used to link the firing moments of others.

2. Determination of MUAP shapes

In order to extract MUAP-shapes from surface EMG registrations at moderate contraction levels a single fibre electrode, positioned inside the muscle is used as a trigger to average the surface EMG signal.

All EMG signals are obtained from the M. Biceps Brachii of male, healthy subjects, 20-35 years of age. For recording and averaging we use a Medilog Mystro. To enable bipolar recordings with different electrode distances an electrode configuration is applied with three electrodes parallel to the muscle fibres. These electrodes are placed between motor endplate region and distal tendon with distances of 20 mm. For monopolar recordings the electrodes are used separately, with the reference electrode placed on the elbow.

The subject is asked to exert a constant force and then the needle is manipulated to find either a single fibre signal (amplitude > 0.2 mV, rise time < 0.3 ms) or a signal composed of several single fibre signals of the same motor unit. Once detected, it is used as a trigger to average the surface signal at least 250 times. To increase the reliability of the responses each averaging process is carried out twice.

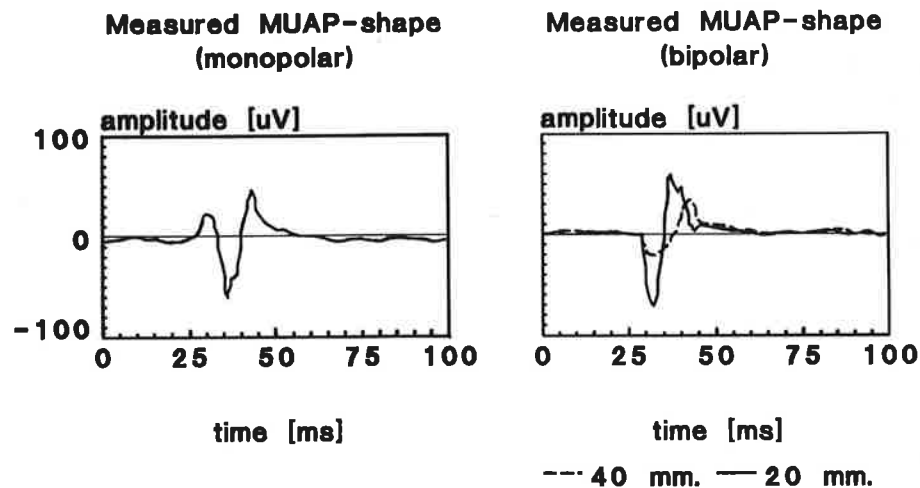


Figure 1. Typical examples of MUAP-shapes recorded with different electrode configurations.

RESULTS

MUAP shapes found with single fibre needle triggering

Some typical examples of recordings are shown in figure 1. Generally the monopolar derivations show a tri-phasic shape, whereas the bipolar derivations show a bi-phasic shape. The range of values of the peak-to-peak duration of the bipolar action potentials is 3.9-18.1 ms. The range of peak-to-peak amplitudes is 25-158 μ V (40 mm el. distance). In figure 2 the distribution of both quantities is given. There is a difference in peak-to-peak duration between shapes measured with electrode distances of 20 mm and 40 mm.

The bipolar shapes can also be calculated by subtracting the two monopolar recordings, shifted in time according to electrode distance and conduction velocity. This offers the possibility to calculate the mean muscle fibre conduction velocity by finding the best fit between the calculated and bipolar recorded shape.

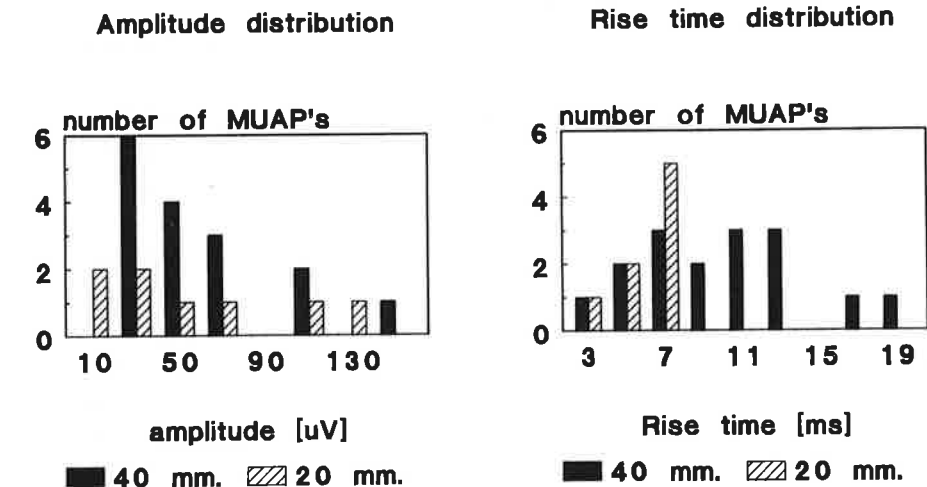


Figure 2. Distribution of peak-to-peak amplitude and rise time (time between the two peaks) of MUAP-shapes recorded with bipolar electrodes. Electrode distances are 20 mm and 40 mm.

Simulation of interferenced EMG patterns

The simulated EMG patterns are analysed in the same way as the signals recorded, to enable comparison of both patterns. Figure 3 illustrates normalized power spectra of a recorded signal and a simulated signal, in which a MUAP shape of the same person and the rise time distribution of figure 2 are used.

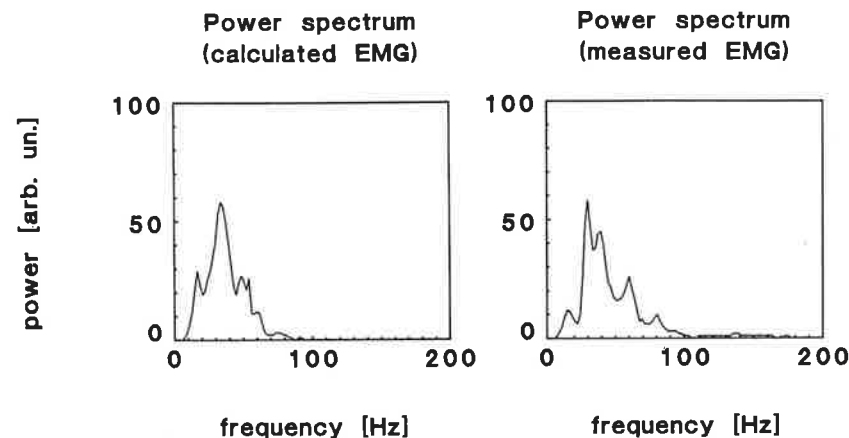


Figure 3. Spectra of recorded and simulated EMG-signals.

DISCUSSION

In this paper we presented a brief description of the model as well as the surface MUAP characteristics found with needle EMG triggering.

The model offers the possibility to investigate the influence of various MUAP and firing characteristics on the EMG patterns. First EMG patterns are calculated with MUAPs of healthy men and compared with actual recordings, using parameters of the power spectrum.

Simulation and literature indicate that the power spectrum is divided into two parts; the lower frequency part, merely determined by the firing characteristics and the main part, determined by the MUAP characteristics. A first impulse has been given to obtain the MUAP characteristics, like shape and distribution functions of MUAP amplitude and duration. Further investigation is necessary to determine the characteristics in a more reliable way as well as a possible correlation between these functions. The first results however indicate no such correlation.

REFERENCES

1. Hermens HJ, Boon KL, Zilvold G (1984) The clinical use of surface EMG. *Electromyogr clin Neurophysiol* 24:243-265
2. Person RS, Libkind MS (1970) Simulation of electromyograms showing interference patterns. *Electroenceph clin Neurophysiol* 28:625-632
3. De Luca CJ (1979) Physiology and mathematics of myoelectric signals. *IEEE Transactions on biomedical engineering* 26: 313-325

SURFACE EMG: THE EFFECT OF ELECTRODE-CONFIGURATION PARAMETERS

J.A. de Kreek, J. Harlaar, H. Bakker.

Free University Hospital
 Dept. of Rehab. Med.
 P.o. box 7057
 1007 MB Amsterdam
 The Netherlands

INTRODUCTION

Standardization on instrumentation in human kinesiological-electromyography will attribute to a further progress in this field. In the near past, ISEK has set a first step towards standardization by means of well defined report-terms to abandon erroneous communication (Winter, 1980).

Concentrating on instrumentation, a complete standardization can be reached on general agreement. However, de facto standards emerge, and the aim of this study is to assist this process.

In electrophysiological kinesiology a class of studies deals with surface electromyography during human movement. The (de facto standard) instrumentation in these applications is:

- bipolar lead-off, with various electrode-configurations
- electrode mounted preamplifiers (state of the art electronics eliminates the effects of disturbing signals: RTI-noise < 2uV)
- a high-pass filter to suppress movement artefacts
- EMG-preprocessing by rectifying and smoothing with a low-pass filter (several cut-off frequencies have been reported).

In this study the effect of the electrode configuration on the quantified surface EMG is evaluated.

METHODE AND MATERIALS

The electrode configuration parameters 'diameter' and 'distance' are evaluated independently using the following three tests:

- D=C test

electr. diameter = constant	(6 mm)
rim to rim electr. distance = variable	(6 - 48 mm)
- R-R=C test

rim to rim electr. distance = constant	(24 mm)
electr. diameter = variable	(2.5 - 12.5 mm)
- C-C=C test

centre to centre electr. distance = constant	(30 mm)
electr. diameter = variable	(2.5 - 12.5 mm)

To realize the different bipolar electrode configurations, two-sided self-adhesive tape (1.6 mm thick) was used with holes of the desired sizes at the various distances. These holes were filled up with ECG electrode jelly to contact skin and electrodes, which consist of tin coated copper.

The signals were recorded by K-Lab SPA 10 preamplifiers and

bandpass filtered (20 - 10 kHz) by a Medelec AA6T amplifier. The EMG's of the M.Rectus femoris and the M.Biceps femoris were sampled at 1000 Hz. In all recordings isometric contractions were performed at a knee angle of 70 degrees flexion. Force was measured by means of a Kin/Com dynamometer with the hip fixed at 65 degrees flexion. The lever-arm of the force-transducer was the same (30 cm) for all subjects.

After a maximal voluntary contraction, the subjects were instructed to ramp the force linearly from 0 to 50 % MVC in 2.5 s. A force curve on a monitor provided a visual feedback. All the subjects were trained for some time.

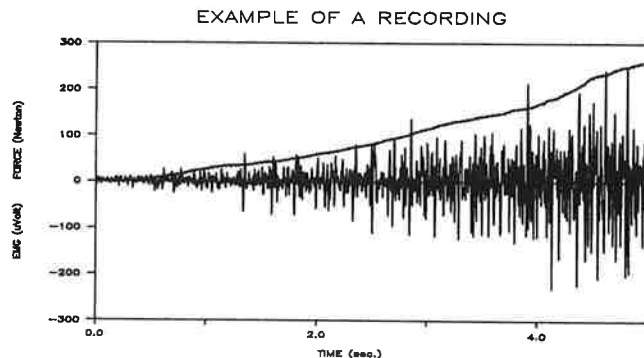


Fig. 1. EMG and Force recording.

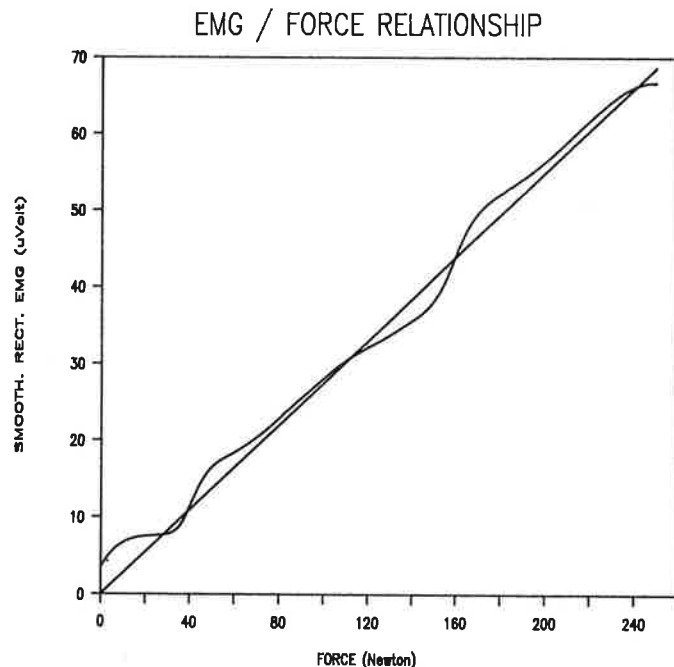


Fig. 2. Measured and calculated EMG-Force relationship

Twelve electrode configurations (4 per test-item) were evaluated on 5 subjects (ageing 25 - 31). Two registrations were performed on each configuration with one minute rest between successive trials. The three tests of this study were handled in a randomized order. Figure 1 shows an example of a typical recording.

The EMG of the Rectus was full wave rectified and low-pass filtered bidirectionally with a third order Butterworth filter (2.5 Hz cut-off freq.). The force was filtered in the same way. A EMG/Force Ratio (EFR) was obtained from the filtered data by means of first order curve fitting (fig. 2).

From the both EFR's found for each configuration, the mean was taken and normalized on the average over the 4 values per test-item. This was done for each subject and each test-item. Finally these values were ensemble averaged over the subjects. The median-frequency was computed from the power spectrum of the 'raw' EMG after applying a Hanning window. The median frequencies were processed in the same manner as the EFR's. The EMG recordings of the Biceps were used to obtain qualitative information about co-contraction.

RESULTS

Figure 3 shows the average and standard error of the normalized EFR's for the 5 subjects in the three different tests. This figure suggests that the EFR increases with an increasing rim to rim distance (D=C test). The same conclusions can be found in the literature. Vigreux (1979) reported an increasing IEMG of the M.Biceps brachii with an increasing electrode distance (23 - 120 mm) on both sides of the center of the muscle belly. This phenomenon was explained by the bipolar recording, causing a reduction of in phase signals.

No clear trend is seen from the R-R=C and the C-C=C test where electrode diameters are varied. Kramer (1972) studied the EMG at various electrode diameters with a constant centre to centre distance (77 mm) and found no significant differences. With a small centre to centre distance, there was a significant change in EMG, because of an important change in rim to rim distance. With a small rim to rim distance he found no significant differences between the EMG in recordings with various electrode diameters.

In this study, no clear trends were found from the median frequency computations.

Even with the same electrode position, it was difficult to obtain reproducible recordings (Siegler, 1985). There was a great variability in the reproducibility over the subjects. This can be caused by the fact that isometric ramping isn't a very 'natural' movement, which results in various contracting strategies of the subject, with more or less co-contraction. In spite of a firm fixation, changes in the length of the Rectus can also disturb the recordings. In two subjects it was found that a second order curve fit resulted in a great reduction of the least square error. It is difficult to compute a EFR from these recordings.

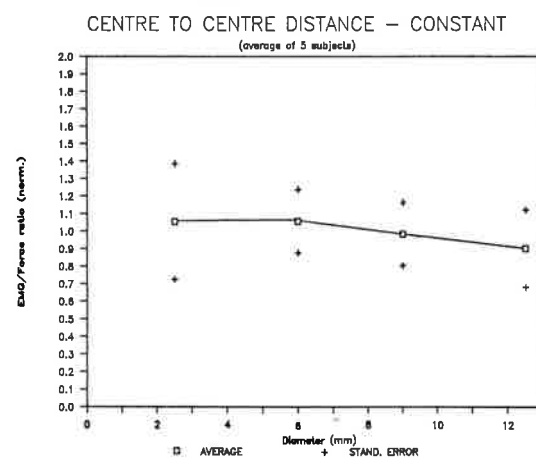
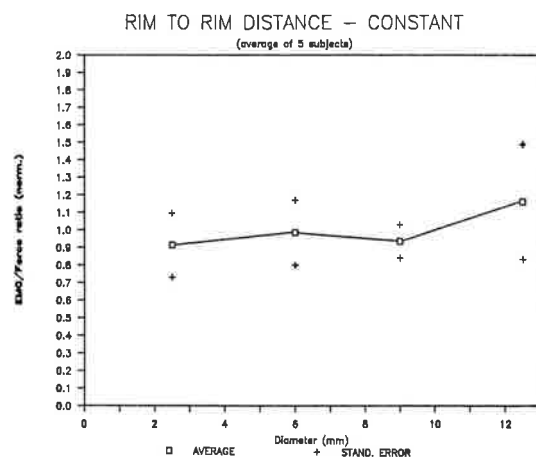
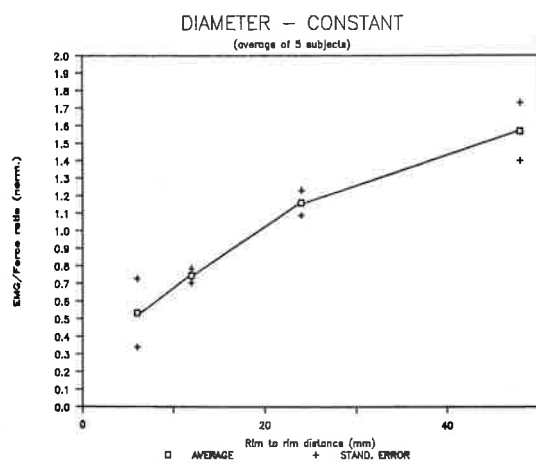


Fig. 3. Normalized EMG/Force ratio's in 3 tests.

There are some indications that the M.Vastus lateralis or medialis will overcome some of the disadvantages mentioned above.

CONCLUSIONS

This study suggests that the rim to rim distance is the most important electrode configuration parameter. The electrode diameter is of minor importance especially when larger electrode distances are applied.

There is a need for reproducible methods to obtain an EFR in the range of 0 - 100 % MVC. These methods are necessary for reliable calibration recordings. This is obligatory when different subjects have to be compared in kinesiologic studies.

It is recommended that several classes of electrode configurations for different human kinesiologic electromyographic studies will be defined, serving different purposes. On the long term full standardization can be achieved. ISEK should encourage this.

REFERENCES

- Kramer, H. et al, 'Die Beeinflussung des mittels Oberflächenelektroden abgeleiteten Elektromyogramms durch ableitetechnische Variablen', Acta biol.germ., Vol. 28, 1972, pp 489-496.
- Siegler, S. et al, 'The effect of myoelectric signal processing on the relationship between muscle force and processed EMG', Electromyogr. clin. Neurophysiol., Vol 25, 1985, pp 499-512.
- Vigreux, B. et al, 'Factors influencing quantified surface EMG', Eur. J. Appl. Physiol., Vol 41, 1979, pp 119-129.
- Winter, D.A. et al, 'Units, terms and standards in the reporting of EMG research', Report by the ad hoc committee of the International Society on Electrophysiologic Kinesiology., 1980.

**Endplate position, conduction velocity
and fibre type proportion**

INNERVATION ZONE AND DELAY DENSITY ESTIMATES

STEPHEN W. DAVIES

Defence Research Establishment Atlantic, Dartmouth, N.S., Canada

PHILIP A. PARKER

Department of Electrical Engineering, University of New Brunswick, Fredericton, N.B., Canada

1. INTRODUCTION

Pioneering work in innervation zone and propagation velocity in human muscle was done by Buchthal et al, [1], in the 1950's. Work by Hilfiker and Meyer, [2], used cross-correlation measurements from several electrode positions to isolate the innervation zone in both health subjects and patients with progressive muscular dystrophy. Masuda et al, [3], employed an electrode array and cross-correlation to recover an innervation histogram from surface myoelectric signals. It is desired to develop a technique for innervation zone estimation that combines the accuracy of histological measurements with the non-invasiveness of the aforementioned myoelectric measurements. Our work in conduction velocity distribution estimation, [4], suggested that the innervation density information was extractible from dual electrode measurements. Specifically, we studied the distribution of myoelectric fiber signal delays between the two electrodes. The estimator of delay density was

$$\hat{f}_T(\tau) = F^{-1}[\hat{\Phi}_{u_1 u_2}(f) / \hat{\Phi}_{u_1 u_1}(f)] \quad (1)$$

where $\hat{f}_T(\tau)$ is the delay density estimate, $\hat{\Phi}_{u_1 u_2}(f)$ is the cross-spectral estimate between electrode 1 (u_1) and 2 (u_2), $\hat{\Phi}_{u_1 u_1}(f)$ is the auto-power spectrum estimate at electrode 1 and F^{-1} is the inverse Fourier Transform. As we shall show in the remainder of this paper, the delay density carries innervation information when one or both of the electrodes lie in the innervation zone. The results reported here are preliminary with much work still to be done, particularly in regards to experimental verification and understanding the various sources of error.

2. DELAY DISTRIBUTION WITH INNERVATION ZONE EFFECTS

Propagation along a muscle fiber is initiated at the innervation point and spreads in both directions away from the innervation point. Therefore, the direction of propagation under an electrode site may be distal or proximal depending on the electrode's position relative to the innervation point. Figure 1 is a stylized representation of the innervation zone and adjacent regions. The solid dots are the innervation points and the parallel lines represent muscle fibers. Let there be two electrodes placed along the muscle fibers with electrode 1 to the left of electrode 2. If both electrodes lie in region R, all fiber signals travel in the direction from electrode 1 to electrode 2 and the delays of the signals received at electrode 2 are positive relative to electrode 1. On the other hand, if both electrodes lie in region L, all fiber signals travel in direction from electrode 2 to 1. Therefore, the delay measured at electrode 2 relative to electrode

l must be negative.

We now consider the effect of placing an electrode in the innervation zone. We will allow electrode 1 to enter the innervation zone while keeping electrode 2 in region R. First, we note that, for all fibers that are innervated to the left of electrode 1, the direction of propagation under both electrodes is the same as when both electrodes are in region R. Thus, the delay associate with each fiber is described by just the electrode separation, Δ , and the fiber velocity, v , as in $\tau = \Delta/v$. However, fibers innervated to the right of electrode 1 present a new situation. For these fibers, the direction of propagation under electrode 1 is opposite to the direction of propagation under electrode 2. For example, if electrode one is a distance a to the left of an innervation point and electrode 2 is a distance, Δ , to the right of electrode 1 the relative delay is

$$\tau = \frac{\Delta - a}{v} - \frac{a}{v} = \frac{\Delta - 2a}{v}$$

Thus, the measured delay is less than the true propagation delay for Δ and v by $2a/v$. Also, if the innervation point is closer to electrode 2 than electrode 1 then $a > \Delta/2$ and the measured delay, τ , will be negative.

From these comments, we may progress to the general placement situation for electrode 1 to the left of electrode 2 and all delays measured to electrode 1. Those fibers innervated to the left of electrode 1 will have positive delays of magnitude Δ/v . Fibers innervated between electrode 1 and electrode 2 but closer to electrode 1 will have positive delays of magnitude less than Δ/v . Fibers innervated between electrodes 1 and 2 but closer to electrode 2 will have negative delays of magnitude less than Δ/v . Fibers innervated to the right of electrode 2 will have negative delays of magnitude Δ/v .

3. DELAY PROBABILITY DENSITY FUNCTION

The measurement delay of the k -th fiber, τ_k , is the difference in the delays in propagation from the innervation point to the two electrodes. These innervation point to electrode delays, T_1 and T_2 , are functions of the conduction velocity random variable and the random variable describing the location of the innervation point; a fiber represents a single realization of these random variables. The procedure for determining the measurement delay pdf uses the given innervation and velocity pdfs to determine the joint density function for the electrode delays. The measurement delay pdf is then obtained from the electrode delay joint density function and the equation describing the measurement delay as the difference of the electrode delays.

The innervation position pdf, $f_y(y)$, will be described relative to the position of Electrode 1. For an innervation point at y , the electrode delays are

$$T_1 = |y|/v \quad \text{and} \quad T_2 = |y-\Delta|/v \quad (2)$$

where v is the fiber conduction velocity.

The measurement delay probability density, $f_{\tau}(\tau)$, evaluated at $\tau=0$ can be shown, [6], to be given by

$$f_{T_2-T_1}(\tau) \Big|_{\tau=0} = \frac{\mu}{2\Delta} f_y(\Delta/2) \quad (3)$$

where μ is the mean conduction velocity. Equation 3 gives a scaled measure of the innervation pdf at the point halfway between the electrodes. It is clear that one can measure the innervation position pdf by sliding the electrodes along the muscle while recording the zero-delay pdf value and the electrode centre position.

4. EXPERIMENTAL RESULTS

The theoretical results of this paper were examined through a simple experiment. A surface electrode pair assembly with an electrode separation of 20mm was moved in 20mm increments from proximal to distal along the short head of biceps brachii. At each position the subject sustained a moderate contraction for a non-fatigueing length of time. The EMGs were sampled at 2kHz, recorded and used to obtain averaged estimates of the myoelectric cross and auto-power spectra. Simple rectangular windows of 32ms were used and 100 of these segments were averaged. Then, the basic ratio estimator of (1) was used to obtain an estimate of the delay pdf.

The results are presented in Figure 2. Note how the first two estimates are virtually identical; the discrepancies are due to noise and other measurement errors and artifacts. This is consistent with the remarks of Section 2 with respect to the independence of delay density to position when outside the innervation zone; there are significant delay densities on just one side of zero delay. In the third curve, the effects of entering the innervation zone show clearly. There are significant delay densities on both sides of zero delay; both negative and positive delays are present as there is propagation in both directions. The spike at $\tau = 0$ is proportional to the innervation position pdf value at the center of the electrodes according to Equation [2]. In the last curve, we have moved past the core of the innervation zone. All the significant delay density values now occur at negative delays. As expected, the shape of the delay density is very similar to that of curves one and two with the delay axis reversed; outside the innervation zone, the shape of the delay density depends only on the velocity distribution and electrode separation.

5. DISCUSSION

The gross features of Figure 2 support the theoretical derivations of this paper. However, some features of these experimental curves are artifacts of the delay distribution estimation process. In particular, the negative values of the estimate are not valid as a probability density function can only be positive. In [4], it is shown that the negative undershoots are due to the high-pass filter action of this form of estimator to signals from high conduction velocity fibers.

More important to the estimation of innervation density are effects felt at zero delay. The zero-delay density values in Figure 2 are significant even outside the supposed innervation zone. A possible explanation for this is cross-talk between the electrodes due to conduction on the skin surface; or zero-delayed components of the myoelectric signal.

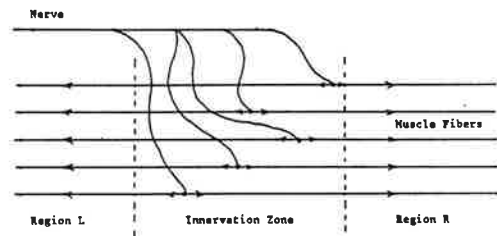


Figure 1 - Innervation zone and adjacent regions.

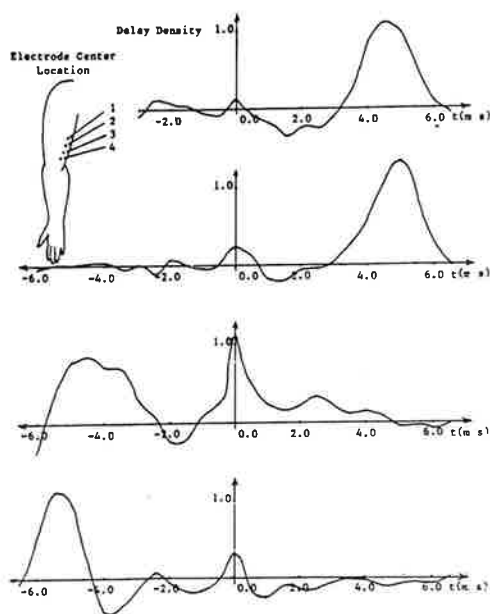


Figure 2 - Measured delay densities from short head of biceps brachii.

REFERENCES

1. Buchthal, F., Guld, C., Rosenfalck, P., "Innervation Zone and Propagation Velocity in Human Muscle", *Acta Physiologica Scandinavica*, V.35, 1956, pp. 174-190.
2. Hilfiger, P., Meyer, M., "Normal and Myopathic Propagation of Surface Motor Potentials", *Electroencephalography and Clinical Neurophysiology*, V. 57, pp. 21-31, 1984.
3. Masuda, T., Miyano, H., Sadoyame, "The Position of Innervation Zones in the Biceps Brachii Investigated by Surface Electromyography", *IEEE Trans. Biomedical Engineering* V.BME-32, N.1, pp. 36-42, 1985.
4. Davies, S., Parker, P., "Estimation of Myoelectric Conduction Velocity Distribution", *IEEE Trans. Biomedical Engineering*, Vol. BME 34, No. 5, pp.365-374, 1987.
5. Davies, S., "Estimation of Myoelectric Conduction Velocity Distribution", M.Sc. Thesis, University of New Brunswick, 1985.

NONINVASIVE INVESTIGATION OF THE EXCITATION OF SINGLE MOTOR UNITS BY MEANS OF MULTI-LEAD ELECTRODE ARRAYS

G. RAU, J. SCHNEIDER, J. SILNY

Helmholtz-Institute for Biomedical Engineering,
 Pauwelsstr., D-5100 Aachen, FRG

INTRODUCTION

The application of conventional noninvasive EMG techniques for the measurement of single motor unit activity is limited by spike interference caused by the low spatial and temporal resolution of the recordings. Our research has focused on modified noninvasive recording techniques to overcome this limitation.

The low spatial and temporal resolution can be attributed to the large size of the electrode pick-up area. This can be reduced by the application of bipolar /1/ or more complex /2,3/ electrode configurations. The size of the pick-up area then becomes a function of the interelectrode distances. Improvements in resolution require small interelectrode distances of only a few millimeters. Inevitably this leads to a far reduced contact size with high electrode skin impedances. Good results were obtained by using arrays of novel pin electrodes, which penetrate the upper, particularly high impedance skin layers when placed on the skin surface above a muscle. High impedance amplifiers were integrated within the electrode unit to ensure high signal quality.

PRINCIPLE OF SPATIAL FILTERING RECORDING TECHNIQUE

This multi-electrode system can be theoretically described as a spatial filter acting on the potential distribution at the skin surface /2,3/. The output signals are formed by the weighted summation of the signals picked up by different electrode contacts. These input signals can be regarded as samples of the spatial potential distribution on the skin surface at a given moment. The filter output can be calculated as the convolution between the filter impulse response and the spatial potential distribution, which becomes a function of time as the excitation is propagated along the muscle fibres.

By varying the number of electrodes and the weighting factors the performance of such a recording arrangement can be adapted to a specific task. Fig. 1 shows some simple realisations. A common property is that the sum of the weighting factors equals zero so that an equal input signal at the electrode does not lead to an output signal. This is important for suppression of a number of disturbances. The simplest configuration is formed by the well-known bipolar derivation. A more complex configuration uses three equidistant electrode contacts located in a line parallel to the muscle fibres. We call this configuration double differentiating, because for short interelectrode distances of only a few millimeters the configuration performs a double differentiation of the spatial potential distribution. Another, two-dimensional configuration uses five electrode contacts. The center electrode is weighted

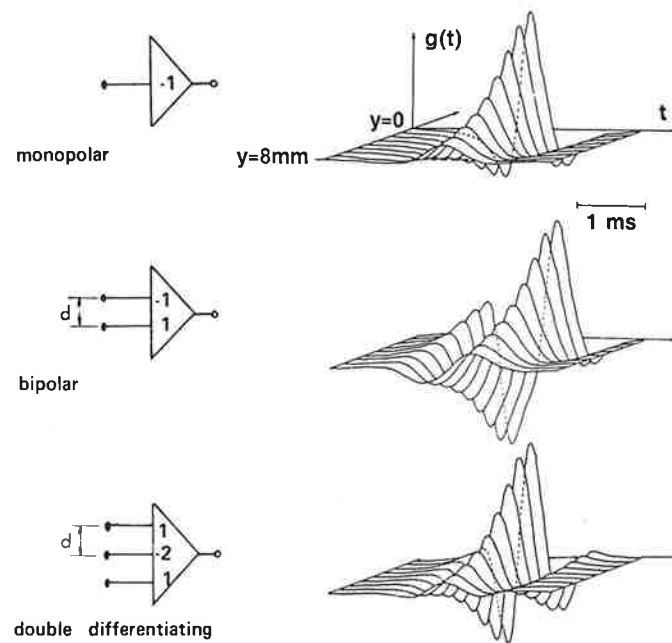


Fig. 1. Theoretical performance of spatial filtering recording arrangements. Left column: Connection schemes. Right column: Filter output signal $g(t)$ with the electrode center just above the excited fibres ($y=0$) and shifted sideways to $y=-1, -2, \dots, -8$ mm. The excited motor unit is modelled by a tripole. Mean fibre depth 3 mm, muscular conduction velocity 4 m/s, interelectrode distance $d = 2.5$ mm.

by a factor of -4 and the surrounding neighbours by a factor of $+1$. The performance of this arrangement is similar to that of the double differentiating one, but the differentiation is calculated in both tangential directions. The arrangement is therefore called normal double differentiating.

Such differentiating electrode configurations are characterized by an enhancement of the EMG signals of those motor units located close to the filter axis, while the signals from distant motor units are attenuated. The effect was theoretically deduced by a tripole model to describe the excitation of a single motor unit. The curves in the right column of Fig. 1 show the filter outputs when the electrode center is located directly above the excited motor unit ($y=0$), and when the electrode center is shifted laterally by 1 to 8 mm. Compared to the monopolar arrangement, the differentiating configurations show sharpened signal peaks and a higher amplitude attenuation when shifted sideways. This performance is strongly affected by the interelectrode distance. We found that for recording single motor unit activity at the superficial lower arm and hand muscles good results could be obtained with distances of 2.5 or 5.0 mm.

APPLICATIONS

Investigations of single motor unit excitation were performed with a multielectrode array containing 19 electrode contacts with equal electrode spacings of 2.5 mm. This electrode array was used to form seven channels of normal double differentiated output signals, five with their recording centers located in a straight line, the others laterally on both sides at a distance of 2.5 mm. Due to the reduced pick-up area of the normal double differentiating configuration, it records only action potentials that are generated within a small part of the muscle close to the recording electrode. Therefore, when placed on the skin on top of a voluntarily contracted superficial muscle, the recordings show less activity compared to the conventional noninvasive monopolar or bipolar ones. Fig. 2 shows a recording derived from the M. abductor pollicis brevis at an isometric contraction level of about 30 % MVC. In the spatially filtered channel the spikes generated by a single motor unit can be easily separated, thus allowing for the investigation of motor unit firing patterns. The monopolar signal in fig. 2 was recorded simultaneously from the center electrode of the spatial filtering arrangement. The large size of the monopolar pick up area makes the extraction of single action potentials impossible.

The multi-channel recordings open the opportunity to study the excitation propagation within single motor units. An example is given in Fig. 3. The multielectrode was placed on top of the M. brachioradialis with the longitudinal axis in the fibre direction. The figure shows 6 normal double differentiated channels located in the fibre axis with equal spacings of 2.5 mm. The endplate position can be found here by analysing the peak shape. The initial upward deflection of the peaks in channel 3 and 4 indicates that these channels are close to the innervation zone. The appearance times of the peak maxima in the other channels indicates, too, that the endplate is located here between channels 3 and 4. This example shows that the precision of the endplate position estimation lies in the range of the channel distance which is only 2.5 mm.

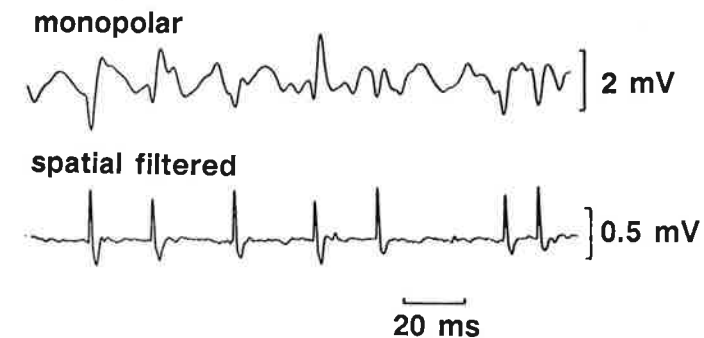


Fig. 2. Effect of spatial filtering on EMG signal. Both signals were simultaneously recorded from the M. abductor pollicis brevis.

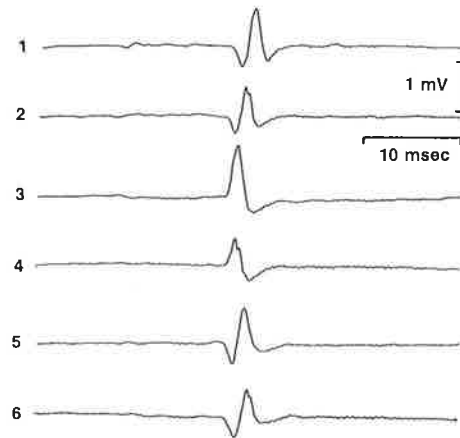


Fig.3. Propagating action potential of single motor unit. 6 channel, spatially double differentiated recording from the M. brachioradialis. Recording centers are located in a straight line with spacings of 2.5mm. The signals indicate location of the endplate position between channels 3 and 4.

Knowledge about the endplate position is important when studying the conduction velocity in muscle fibres (MCV). With the signals in Fig. 3 this parameter can be detected from the peak delay times between channels 1 and 2 or between channels 5 and 6. The conduction velocity can not be investigated too close to the endplate /4/, because the action potential form changes rapidly while the excitation develops on the fibre membrane. Therefore, the analysis of the wave forms is essential for the muscular conduction velocity measurements to ensure an electrode position outside the innervation zone.

This technique for determination of the MCV does not supply a global parameter that characterizes a whole muscle /5/, but is measured for a single excitation of a single motor unit. This creates the opportunity to study the MCV in more detail, especially the influence of physiological parameters such as muscle temperature and firing frequency.

REFERENCES

1. Masuda T., Sadoyama T. (1986): The propagation of single motor unit action potentials detected by a surface electrode array, *EEG clin Neurophysiol* 63: 590-598
2. Reucher H., Rau G., Silny J. (1987): Spatial filtering of noninvasive multielectrode EMG: Part I - Introduction to measuring technique and applications, *IEEE Trans Biomed Engg* 34(2), 98-105
3. Reucher H., Silny J., Rau G. (1987): Spatial filtering of noninvasive multielectrode EMG: Part II - Filter performance in theory and modelling, *IEEE Trans Biomed Engg* 34(2), 106-113
4. Roy S.H., De Luca C.J., Schneider J. (1986): Effects of electrode location on myoelectric conduction velocity and median frequency estimates, *J. Appl. Physiol.* 61:1510-1517
5. Sollie G., Hermens H.J., Boon K.L., Wallinga-de-Jonge W., Zilvold G. (1985): The boundary conditions for measurements of the conduction velocity of muscle fibres with surface EMG, *EMG clin Neurophysiol* 25: 45-56

NONINVASIVE MEASUREMENT OF CONDUCTION VELOCITY IN MOTOR UNITS INFLUENCED BY TEMPERATURE AND EXCITATION PATTERN.

J. SCHNEIDER, J. SILNY, G. RAU

Helmholtz-Institute for Biomedical Engineering
 Pauwelsstr, D-5100 Aachen, FRG

INTRODUCTION

Muscular conduction velocity (MCV) measurements have been established within the last years for detecting muscle fatigue. Similar good results have not yet been reported for applications of MCV measurements in the clinical diagnosis of neuromuscular diseases. One of the reasons can be seen in the poor reproducibility of the MCV measurements. While fatigue experiments use only the changes in MCV during relatively short time intervals, clinical diagnosis requires long-term reproducibility of the MCV measurements. This may be feasible by controlling more precisely those physiological parameters which influence the MCV.

The commonly applied noninvasive MCV recording techniques are not well suited for studying these parameters. They give only global MCV values, as the signals recorded contain activity of numerous muscle fibres belonging to different motor units and having different fibre characteristics, diameters and MCVs. The MCV in a single motor unit (MU) can be expected to be more consistent. The examination was therefore based on action potentials (AP's) recorded from single motor units (MUs).

METHODS

Recording arrangement

The noninvasive recording of single MU activity was made possible by a technique which utilizes a spatial filter multi-lead electrode configuration /1,2/. The EMG signals were recorded by a noninvasive multielectrode with small pin contacts and interelectrode distances of only 2.5 mm. This electrode array was placed on the skin on top of a superficial muscle. The signals from the electrode contacts are preamplified within the electrode unit and then fed into a bandpass amplifier (30-1200Hz). A special signal processing unit performs for each channel a weighted summing of the signals picked up by five electrode contacts. The central electrode is weighted by a factor of -4, the four surrounding electrodes by a factor of +1. This configuration performs a spatial double differentiation of the potential distribution on the skin surface in both tangential directions. As a result of the spatial differentiation, the spatial resolution is improved compared to monopolar recordings. The acquisition system used allows for the recording of seven spatially filtered channels. Five of them have their centers located along a straight line with equal spacings of 2.5 mm. The two others are located with the same distance laterally, one on each side. The seven spatially filtered signals were sampled at a rate of 10 kHz per channel and stored on an AT-compatible microcomputer that was also used to perform the signal evaluation. The high spatial

resolution of the recording arrangement enables a good separation of single APs from the activity of the whole muscle and forms a prerequisite to estimate the exact position of the excitation center. Such an estimation of the excitation position and time is the basis for calculating the propagation velocity.

Detection of conduction velocity

The MCV was calculated from the time shift between the APs recorded at different positions along the muscle fibres. Different signal parameters for definition of this time shift were tested: the peak maximum, the left and right zero crossing of the main peak, and the left and right points of inclination of the main peak. Because of the limited sampling rate of 10 kHz per channel, the sampled signals were interpolated by approximating cubic splines whose approximation characteristic was adapted to the signal qualities. The standard deviation of the MCV values calculated for consecutive APs recorded from a single MU was chosen as an indicator of the CV reliability. Lowest standard-deviation values were obtained when using the main peak maximum for calculating the time shift. Therefore, this parameter was utilized to detect the MCV for the examination of the temperature and firing rate influence.

Temperature influence

The effect of temperature was studied with three normal subjects and MUs of the *M. palmaris longus*. The lower arm was cooled down by the application of an ice package. When the subject felt uncomfortable, the ice was removed and the temperature on the skin surface measured by a fast electronic thermometer. The muscle was contracted moderately while the surface electrode was placed close to the thermometer probe and moved to a position where the signals indicated a steadily firing MU with the endplate lying outside the

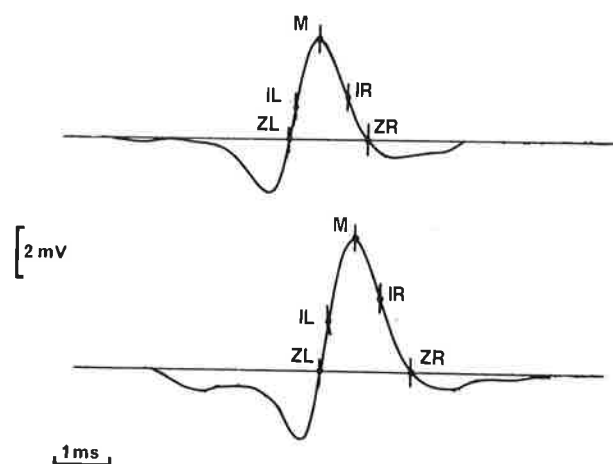


Fig.1. Parameters for definition of time delays between action potentials recorded in adjacent channels for calculation of muscular conduction velocity. M = peak maximum, IL (IR) = left (right) point of inclination, ZL (ZR) = left (right) zero crossing.

electrode region. The signal was recorded for one second and the skin temperature was noted. As the skin temperature increased, several recordings from the same MU were performed. To reach skin temperatures higher than 32 degrees centigrade, the lower arm was heated by an infrared lamp up to 36 degrees centigrade skin temperature. This technique allowed variation of the skin temperature in the range of about 26 to 36 degrees centigrade. The recorded signals were evaluated by calculating the mean values from the CVs detected for the single APs.

Influence of firing rate

To study the influence of firing rate on the MCV, the firing rate of a recorded MU was voluntarily varied, controlled by oscilloscope feedback. The effect was studied for stationary firing rates, keeping the firing rate nearly constant for a number of seconds. The recordings were performed at four MUs of the *M. brachioradialis* of one normal subject. The firing rate could be varied in the range of 5 to 20 per second. To avoid effects of muscle fatigue, the different firing rates were adjusted in a random sequence.

RESULTS

Temperature influence

The MCV values showed a high correlation with skin temperature. In all three subjects the rate of increase was about the same: 0.13, 0.13 and 0.14 m/s per degree centigrade were measured. Fig. 1 shows a plot of the values from one of the measurements with the regression line drawn.

Firing rate influence

In all experiments the MCV increased with increasing firing rate. In contrast to the temperature influence, the rate of change varied considerably. The values measured were 0.057, 0.057, 0.028 and 0.064 m/s per s⁻¹. Fig. 2 shows the values and the regression line for one of the measurements.

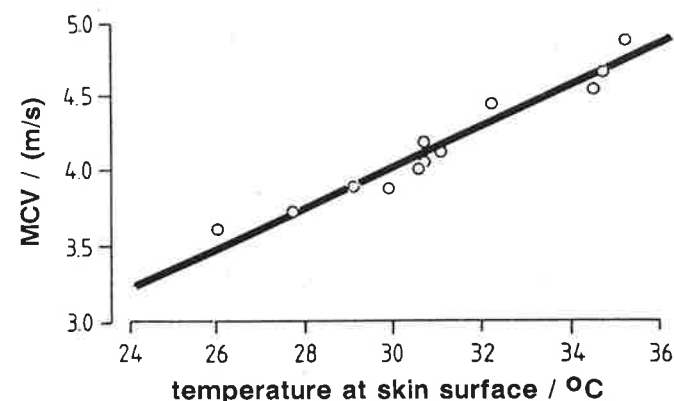


Fig.2. Influence of temperature on muscular conduction velocity of a single motor unit. Skin temperature was measured on skin surface above the muscle. Recording from the *M. palmaris longus*. The slope of the regression line is 0.13 m/s per degree centigrade.

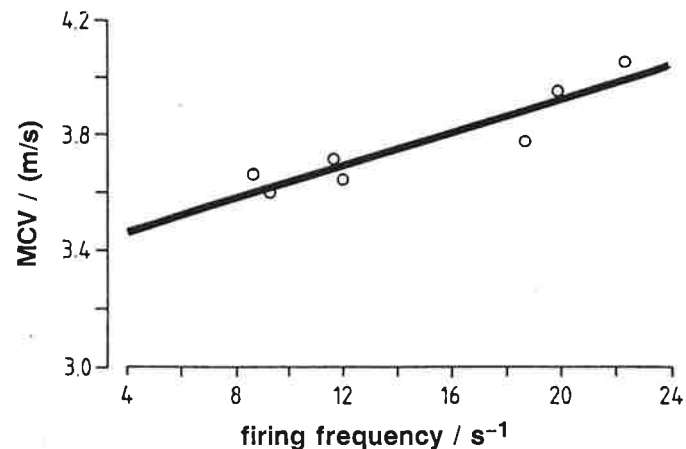


Fig.3. Influence of firing rate on muscular conduction velocity of a single motor unit. In each measurement the firing rate was held constant for several seconds. Recordings performed at the M. brachioradialis. The slope of the regression line is 0.028 m/s/s⁻¹.

DISCUSSION

The results indicate that the MCV is markedly affected by temperature as well as firing rate changes. In this study, to keep the noninvasive character of the measurements, the temperature was recorded at the skin surface, not near the muscle fibres. Obviously the temperature changes at the fibre level are in a smaller range than the changes at the skin surface. This means that the temperature influence would be even more pronounced when recording muscle temperature instead of skin temperature. The differences in the rate of change detected for the firing frequency dependency may be due to different fibre types of the MUs [3]. One can conclude from these findings that in applications of MCV measurements the temperature as well as the firing rate need to be controlled. The technique of spatial filtering surface EMG recording, in conjunction with skin temperature measurement, enables the noninvasive performance of such examinations. The proper temperature can be easily adjusted by infrared heating or ice cooling. The control of the firing rate may be possible with biofeedback, although this may be problematic with patients. An open problem is the necessity to localize the same MU in repetitive examinations.

REFERENCES

1. Reucher H., Rau G., Silny J. (1987): Spatial filtering of noninvasive multielectrode EMG: Part I - Introduction to measuring technique and applications, IEEE Trans Biomed Engg 34(2), 98-105
2. Reucher H., Silny J., Rau G. (1987): Spatial filtering of noninvasive multielectrode EMG: Part II - Filter performance in theory and modelling, IEEE Trans Biomed Engg 34(2), 106-113
3. Stalberg E. (1966): Propagation velocity in human muscle fibers in situ, Acta Phys Scand 70, Suppl 287, 1-112

A CLOSE RELATIONSHIP BETWEEN MEAN POWER FREQUENCY AND FIBRE TYPE PROPORTION

KARIN HENRIKSSON-LARSEN, BJÖRN GERDLE AND MARIE-LOUISE WRETTLING

National Institute of Occupational Health, Box 6104, S-900 06 Umeå and Department of Clinical Physiology, University of Umeå, Sweden

INTRODUCTION

Many studies in recent years have been concerned with the relationship between mechanical performance and fibre type proportion and area. The use of an invasive technique, such as muscle biopsy, increases the risk that the number of participants will be low. If mean power frequency could be used as a non invasive method for determination of fibre type proportion it would be of great value in ergonomic studies. Studies of muscular fatigue have resulted in weak (significant) correlations between the degree of decrease in mean power frequency (MPF) and fibre type proportion (1,2,3). We have in two earlier studies of isokinetic knee extensions found a close relationship between mean power frequency and fibre type proportion (4,5). The closest correlation was found when single maximal isokinetic contractions were used ($r=0.93$). In these studies we have presented two different equations for fibre type estimation from the mean power frequency.

The aim of this study was to evaluate the validity of one the earlier described equations.

MATERIAL AND METHODS

Subjects

One woman (age 30 years, weight 60 kg, height 167) volunteered to participate in the study. She was going to take part in a training study. Prior to the test she went through a structured interview and medical examination. She had not had any complaints from the lower limb during the last 6 months and was clinically healthy.

Method

Isokinetic and electromyographic methods. Dynamic knee extensions were performed using an isokinetic dynamometer (Cybex II, Lumex INC, New York). The subject made 3 maximum knee extensions at 1.57 rad/s. Electromyographic (EMG) signals were obtained from the two vastii (medialis and lateralis) and the rectus femoris muscle. Silver-

Silverchloride surface electrodes (Medicotest, Ølstykke, Denmark) were used (center to center distance: 20 mm). Before the application of the electrodes the skin area were dry shaved and rubbed with alcohol and ether (4:1).

The three raw-EMG signals, the angle and the torque signals from the dynamometer were simultaneously recorded on a 7-channel tape recorder (TEAC-FM recorder). The EMG signals were sampled with a frequency of 4 kHz and analog to digital converted with a 12 bit accuracy over the signal range ± 5 V. The signals were pretreated by trend removal and Hamming windowing. The power spectral density function (PSDF) was obtained using Fast Fourier Transform Technique (FFT). The mean power frequency (MPF) was computed. For further details concerning the isokinetic and electromyographic methods see Gerdle et al 1988 (in press).

Muscle biopsies. Several days after the isokinetic test an open surgical muscle biopsy was taken from the right m vastus lateralis under local anaesthesia. The specimen was transversely oriented with OCT embedding compound (Ames Tissue-Tek) on a piece of cardboard and lowered into liquid nitrogen-cooled propane. The specimen was stored at -80°C until sectioning. In a cryostat at -20°C serial cross-sections 10 μm thick were cut. The sections were treated for routine myofibrillar ATPase (pH 9.4, 4.6 and 4.2) (6).

Fibre type classification into type 1 (slow twitch), type 2A, type 2B and type 2C (fast twitch) was carried out, at least 400 fibres were classified.

Prediction of type 1 fibre proportion. The equation used for prediction is earlier described by us (5).

$\% \text{ type 1 fibres} = 87.1 - (0.55 * \text{MPF})$ ($r=0.93$)
based on the results from nine women who went through the same test and muscle biopsy procedure as described below.

RESULTS

Muscle morphology

All histochemically stained sections contained tightly packed polygonal muscle fibres in well preserved fascicles and no oathological signs were seen.

The section from the biopsy contained 46% type 1 fibres and 54% type 2 fibres.

Electromyographic variables

The mean power frequency was 77 Hz in the vastus lateralis and

81 Hz in the vastus medialis which were about 10 Hz lower than in the rectus femoris muscle (88 Hz).

Predictions of type 1 fibre proportion

The mean power frequency of 77 Hz was used to predict the proportion of type 1 fibres with the use of the above equation. The calculated type 1 fibre proportion was 45% (see figure).

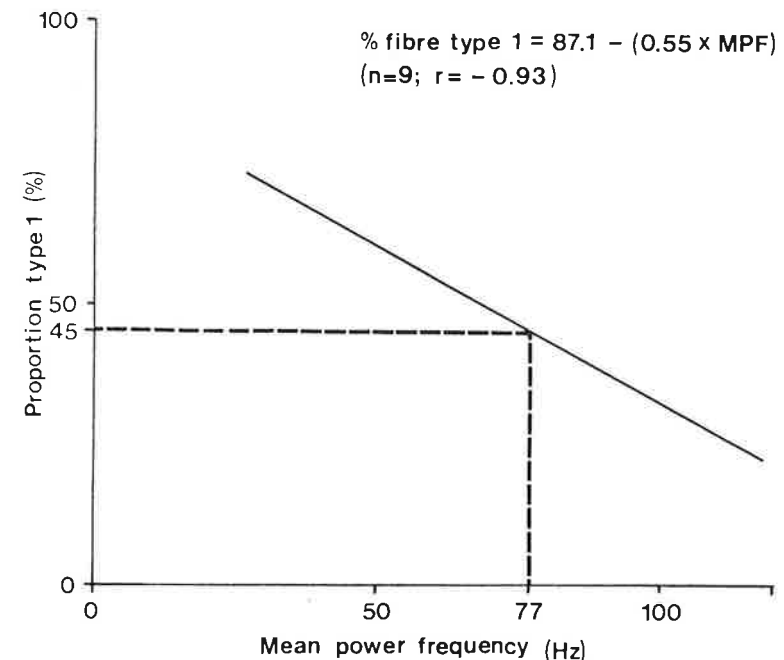


Figure 1. The prediction of type 1 fibre proportion from the mean power frequency of the EMG is shown. The equation given, has earlier been described (5).

DISCUSSION

It has recently been suggested by us and others that the electromyographic technique might be used as a non invasive method for determination of the fibre type proportion (4,5,7). Studies of fatigue have partly confirmed this suggestion by showing significant, though weak, correlations between relative decrease of mean power frequency and the fibre type proportions and areas (1,2,8). The mean power frequency of non-fatiguing static contractions at 50% of MVC correlated to a higher extent ($r=0.80$) with the fibre type proportion in the gastrocnemius muscle (3). In our previous

studies of isokinetic knee extension at 1.57 rad/s the mean power frequency registered was highly correlated with the proportion of type 1 fibres ($r=0.87$ and $r=-0.93$ respectively (4,5)). In the present study we show that the equation of the regression line from these studies (4,5) could be used to predict the proportion of type 1 fibres from mean power frequency, with 1% accuracy. Further studies of the relationship between the fibre type proportion and the mean power frequency would elucidate if this is also valid for larger groups of women, and for men.

In conclusion our results indicate, at least for untrained women, that the mean power frequency can be used as a non-invasive method for fibre type determination.

REFERENCES

1. Tesch PA, Komi PV, Jacobs I, Karlsson J, Viitasalo JT (1983) *Acta Physiol Scand* 119:61-67
2. Häkkinen K & Komi PV (1985) *Eur J Appl Physiol* 55:588-596
3. Moritani T, Gaffney FD, Carmichael T, Hargis J (1985) In: Winter DA, Norman RW, Wells RP, Hayes KC, Patla AE (Eds) *Biomechanics IX-A*, pp287-292
4. Wretling ML, Gerdle B, Henriksson-Larsén K (1987) *Acta Physiol Scand* 131:627-628
5. Gerdle B, Wretling ML, Henriksson-Larsén K. Do fibre type proportion and angular velocity influence the mean power frequency of the electromyogram? *Acta Physiol Scand* (In Press)
6. Dubowitz V and Brooke MH (1973) In: *Muscle Biopsy: A Modern Approach*. WB Saunders, London, pp 5-33
7. Basmajian JV & DeLuca CJ (1985) In: *Muscles alive - their functions revealed by electromyography*. Williams & Wilkins, Baltimore, USA
8. Häkkinen K & Komi PV (1986) *Electromyogr Clin Neurophysiol* 25:319-330

CROSTALK ASSESSMENT IN HUMAN THIGH MUSCLES

M. KNAFLITZ† R. MERLETTI† F. CATANI†

† CLINICA ORTOPEDICA II - ISTITUTO ORTOPEDICO RIZZOLI - BOLOGNA - ITALY
† DIPARTIMENTO DI ELETTRONICA - POLITECNICO DI TORINO - TORINO - ITALY
and NEUROMUSCULAR RESEARCH CENTER - BOSTON UNIVERSITY - BOSTON - U.S.A.

INTRODUCTION

Surface myoelectric signal (SMES) detection is preferred to indwelling electrode techniques when *global* information about muscle activity is desired. A major drawback of the surface detection techniques is their poor spatial resolution. When a muscle is activated action currents associated with the action potentials generated by active muscle fibers flow through the volume conductor. Moreover, the action currents may generate a signal detected by electrodes placed at some distance from the source which may be erroneously interpreted as generated by fibers below the detection electrode. This signal is usually referred to as *crosstalk*, and according to previous experiences [2], [3], [1], [4], its importance is often underestimated. Our interest in evaluating crosstalk among human thigh muscles was elicited by a recent study [5] in which co-contractions between muscles of the thigh and hip needed to be clearly identified. As co-contraction evaluation was mainly based on SMES, it was crucial to discriminate between volume conducted potentials and signals due to the activation of the observed muscles. De Luca and Merletti [1] demonstrated that SMES detected on peroneus brevis having a peak to peak value of up to 16.6% of a signal detected over tibialis anterior may be due to crosstalk rather than to activation of the muscle below the electrode. In a preliminary evaluation Emley et al. [4] measured crosstalk between thigh muscles and concluded that up to 12% of the signal amplitude detected over a thigh muscle may be attributed to an adjacent or antagonist muscle. Starting from the results presented above further investigations have been carried out to obtain a more reliable quantitative evaluation of crosstalk between thigh muscles.

MATERIALS AND METHODS

All the experiments were carried out on volunteer subjects with no history of orthopaedic or neurological diseases. Two different experimental protocols were followed: a first set of experiments has been carried out to investigate the relationship between crosstalk index (CI) and stimulus intensity. Results obtained during these experiments allowed us to determine the proper stimulation level to be administered during the second set of experiments, performed to obtain a quantitative evaluation of CI between thigh muscles.

Crosstalk evaluation was performed by means of electrical stimulation of the main muscle motor point. The neuromuscular stimulation and recording system was developed by the authors and is described elsewhere [7]. Signals were simultaneously recorded over the stimulated muscle and over an adjacent or antagonist muscle by means of two four-bar electrodes. As reported in literature [1] the double differential technique [6] is particularly suitable for crosstalk evaluation as allows to discriminate signals produced by depolarized zones travelling along muscle fibers below the pick-up, and signals generated by the activation of a neighboring muscle and recorded at some distance from the activated muscle itself. Dedicated software was developed for the IBM XT personal computer to manage the experiment as well as to

sample SMES during the contraction and to process data. Six analog channels (one Single Differential (SD) and two Double Differential (DD) signals for each pick-up) were collected by a 12 bit A/D card with a sampling rate of 1024 Hz. Stimulation frequency was set at 20 Hz. M-waves were averaged over time epochs lasting one second each and the averaged M-wave was then processed by means of zero padding in the frequency domain to increase time resolution up to 122 μ s. The peak to peak value (PP), the average rectified value (ARV) and the root mean square value (RMS) were then computed for each averaged M-wave. Each contraction lasted 10 s. For each contraction three tables were prepared respectively containing the time series of the PP, ARV and RMS values of the six collected channels, and of the CI (defined as the ratio between the SD signal detected over the neighboring muscle and the SD signal detected over the stimulated muscle). According to previous experience [1] volume-conducted signals were identified as those generating a DD signal below 30% of the PP value of the SD.

Eight preliminary experiments were carried out in different days on four volunteer subjects (one female and three males) in order to investigate the relationship between stimulus intensity and CI, and to assess result repeatability. Subjects were comfortably seated in a chair with hip, knee and ankle joints at approximately 90 degrees. Vastus Lateralis (VL) and Lateral Hamstrings (LH) shapes were carefully outlined and VL motor points were identified and marked. The main motor point was defined as the one producing the strongest contraction. The stimulation level producing the maximal M-wave was identified and eight stimulations at four different levels (producing an M-wave amplitude of about 25%, 50%, 75% and 100% of the maximal), five minutes apart, were administered.

A second set of experiments was then carried out in the same experimental conditions on eight volunteers (four females and four males) in order to quantify CIs between thigh muscles. VL, Vastus Medialis (VM), Rectus Femoris (RF), LH and Medial Hamstrings (MH) shapes were carefully outlined and VL and VM motor points were identified and marked. Stimulus intensity was set separately for each stimulated muscle to obtain an M-wave amplitude of about 50% of the maximal value. Eight electrically elicited contractions lasting 10 s each, five minutes apart, were obtained by stimulating VL and recording volume conducted potentials over RF, VM, LH and MH and then by stimulating VM and recording volume conducted potentials over RF, VL, LH and MH. A first probe was positioned over the stimulated muscle and its position carefully adjusted to obtain two DD signals as similar as possible and trying to maximize SD and DD signal amplitude. The second probe was positioned over the observed muscle between the lowest motor point and the distal tendon. Three result tables were obtained for each contraction.

RESULTS and DISCUSSION

Results obtained during the first set of experiments are reported in fig. 1. Each subject is identified by a line style. For all the subjects intraexperiment repeatability was excellent. As shown in fig. 1 interexperiment repeatability was good only for subject # 1. In particular it may be noted that for the subject # 1 CI was almost independent of stimulation level. In both the experiments, when stimulation amplitude was increased from 25% to 50% subject # 2 showed a strong reduction of CI, while a less evident decreasing trend was obtained with increasing the stimulation level from 50% to 100%. Subject # 3 showed a strong reduction of CI in the first experiment, while in the second experiment CI was much smaller and in-

	VASTUS LATERALIS			
	RF	VM	MH	LH
BM (F)	10.2	4.3	5.4	15.6
AMC (F)	5.9	1.5	2.6	2.0
BG (F)	18.2	7.7	7.8	16.9
VF (F)	7.8	2.4	(0.8)	7.1
KM (M)	4.8	2.0	1.6	2.2
MC (M)	0.4	0.6	0.4	0.8
BG (M)	1.4	0.6	0.5	1.2
LP (M)	(0.8)	(0.5)	(0.3)	(0.6)
	VASTUS MEDIALIS			
	RF	VL	MH	LH
BM (F)	0.6	1.3	0.5	0.9
AMC (F)	8.6	10.7	4.9	3.5
BG (F)	1.0	3.0	(0.2)	0.9
VF (F)	1.5	1.8	0.7	0.9
KM (M)	0.7	1.4	0.6	0.5
MC (M)	1.8	1.6	0.4	0.4
BG (M)	0.6	1.7	(0.1)	0.2
LP (M)	0.9	1.7	(0.3)	(0.3)

TABLE 1. Percent crosstalk of SMES detected on RF, VM, VL, MH and LH during stimulation of VL (upper table) and VM (lower table).

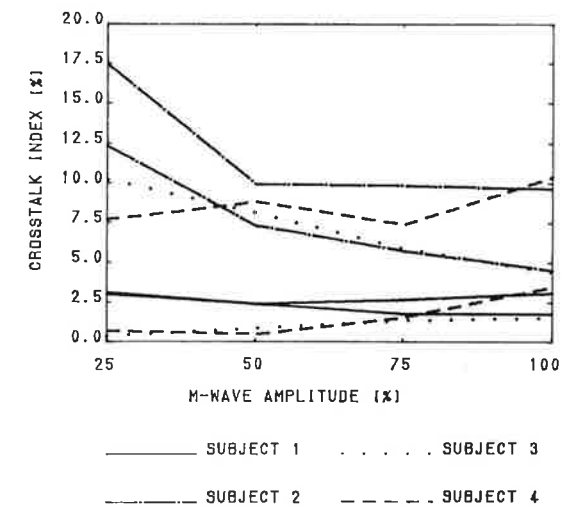


FIG. 1. Correlation between crosstalk index and normalized M-wave amplitude.

creased with the stimulus amplitude. Subject # 4 showed an increasing trend of CI in both the experiments with a remarkable difference of CI values. A possible explanation of these findings is that subject # 1 had well defined and separated VL motor points, while the other two subjects had motor points poorly defined and separated. These anatomical differences might be responsible for poor interexperiment repeatability, because in subjects with poorly defined and separated motor points even small displacements of the stimulation electrode may cause major variations of the pool of active muscle fibers. Moreover, these anatomical differences might also explain the different behavior showed by the subjects when the stimulus amplitude was increased: if motor points are well defined and separated, increasing the stimulation level increases the number of recruited motor units, and if their muscle fibers are randomly distributed within the same part of the muscle, CI should not change significantly. This situation is particularly evident in subject # 1. If motor points are not well defined and separated, motor units of different motor points may be progressively recruited when stimulation level is increased. This produces a significant geometrical variation of the signal source that causes CI variations. In subject # 2 this behavior is quite evident when the stimulation level is increased from 25% to 50%. In subjects # 3 and # 4 a similar behavior is present. These results indicate that if the geometry of the signal source within the stimulated muscle does not change, when stimulation level is increased CI may be regarded as independent of the M-wave amplitude.

In table 1 the results obtained during the second set of experiments are reported. By stimulating VL higher CIs were found in females than in males. A similar behavior may be observed by stimulating VM. The observed differences between females and males may be explained by the different subcutaneous tissue structure. The results reported in the table agree with those of De Luca and Merletti [1] for the shank, and Emley et al. [4] for the thigh. Emley et al. [4] reported CI up to 12% between adjacent thigh muscles. Our data show CI up to 18.2% between VL and RF, and up to 16.9% between VL and LH. When stimulating VL the lowest CIs were obtained over VM and MH. This is not surprising considering that the full diameter of the thigh and the femur separate the muscles. When stimulating VM the highest CIs were generally found on the VL. As in previous works [1], [4] no relationship was found between limb circumference and CI.

In conclusion our data support previous findings, and indicate that a signal detected by means of surface probes over a muscle of the thigh cannot be assumed as entirely generated by the muscle itself. These results suggest that caution should be exercised when interpreting SMES when several muscles are active as during walking or stairclimbing, and confirm that the double differential technique is effective in crosstalk assessment.

ACKNOWLEDGMENTS

This work was performed at the Department of Electronics of Politecnico di Torino (Torino - Italy), in cooperation with the NeuroMuscular Reserch Center of Boston University (Boston - U.S.A.) and Clinica Ortopedica II of Istituto Rizzoli (Bologna - Italy). Major support was provided by the Italian Ministry of Education within the framework of the national project on Rehabilitation Engineering and within the doctoral program of Dr. Marco Knafitz. Partial support was provided by the Liberty Mutual Insurance Company.

REFERENCES

1. C.J. De Luca and R. Merletti, "Surface EMG crosstalk between muscles of the leg", *Electroencephal. Clin. Neurophysiol.*, (in press)
2. J.W. Morrenhof and H.J. Abbink, "Crosscorrelation and crosstalk in surface elentromyography", *Electromyography Clin. Neurophysiol.*, vol. 25, pg. 73-79, 1985
3. R.P. Nielsen, L.F. Hayward, R. S. Hutton, *Concomitant (Reciprocal Excitation?) short latency EMG reflexes in triceps surae and tibialis anterior muscles: volume conduction as a confounding variable*, Abstracts of the Neuroscience Meeting, 12, pg. 682, 1986.
4. M. Emley, F. Catani, S. Roy, M. Knafitz, "Myoelectric crosstalk in antagonist muscles of the human thigh", Proceedings of the Ninth Annual Conference of the IEEE EMBS, vol. 4, pg. 2016-2017, 1987
5. F. Catani, A. Hodge and R.W. Mann, "Hip dynamics in level walking and stairclimbing", Accepted ASME, December, 1987
6. H. Broman, G. Bilotto and C.J. De Luca, "A note on non-invasive estimation of muscle fiber conduction velocity", *IEEE Trans. Biomed. Eng.*, vol. BME-32, no. 5, pg. 341-344, 1985
7. M. Knafitz and R. Merletti, "Suppression of stimulation artifacts from myoelectric evoked potentials recordings", *IEEE Trans. on Biomed. Eng.*, (in press)

CROSTALK OF THE INTRINSIC LUMBAR BACK MUSCLES

H.A.M. DAANEN¹, P.VINK²

¹ Interdepartmental Research Group of Kinesiology, Rijksuniversiteit, Mezenstraat 2a, 2333 VT Leiden (The Netherlands),

² Stichting Arbouw, P.O. Box 8114, 1005 AC Amsterdam (The Netherlands).

INTRODUCTION

In kinesiological research the electrical activity of contracting muscles is recorded by wire- and surface electrodes. Unfortunately, the myoelectrical signal (EMG) is not restricted to anatomical borders. This implicates that the electrodes also pick up activity from other muscle(part)s than they are meant for. This phenomenon is called crosstalk (fig.1).

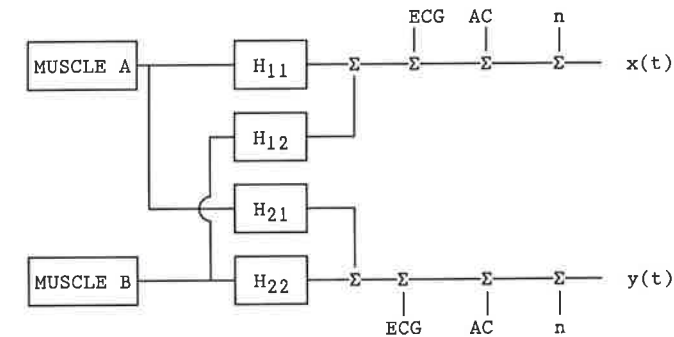


Fig. 1. Schematic representation of crosstalk. Each electrode records a summation of desired EMG and EMG of neighbouring muscles (crosstalk). The electrocardiogram (ECG), AC-components (AC) and Noise (n) are also present in the measured signals (x(t) and y(t)). H is a transferfunction influenced by skin resistance, muscle temperature etc.

Although crosstalk is present in wire-EMG (1), most problems with crosstalk exist in surface-EMG, because the pick-up area of the electrodes is larger.

The cross-correlation coefficient function (CCCF) can be used as an estimator of the amount of crosstalk if two electrodes are used. Let x(t) be the signal from the electrode for muscle A and y(t) be the signal from the electrode for muscle B, then the CCCF can be represented by (2):

$$\rho_{xy}(\tau) = \frac{R_{xy}(\tau)}{\sqrt{(R_{xx}(0) R_{yy}(0))}}$$

in which:

$$R_{xy}(\tau) = \frac{1}{T} \int_0^T x(t) y(t+\tau) dt$$

$$R_{xx}(0) = \frac{1}{T} \int_0^T (x(t))^2 dt$$

$$R_{yy}(0) = \frac{1}{T} \int_0^T (y(t))^2 dt$$

For all τ , the quantity $\rho_{xy}(\tau)$ satisfies $-1 \leq \rho_{xy}(\tau) \leq 1$.

The CCCF is used to investigate the specificity of three columns of the Intrinsic Lumbar Back Muscles (ILBM): the medial, intermedial and lateral column (3).

MATERIAL AND METHODS

Surface EMG of the ILBM has been recorded in 8 healthy subjects. They were asked to exert isometric forces of 10% and 60% MVC.

electrodes Bipolar surface electrodes were placed, bilaterally, 30, 60 and 90 mm from the processus spinosus of L1 and 30 and 60 mm from the spinal processus of L3. The electrodes consisted of gold plated brass cores with a diameter of 7.5 mm and a bipolar distance of 21,5 mm.

signal processing The signal was led through a differential preamplifier (gain: 100, impedance 100 MOhm, cmmr > 20.000), attached to the subject and to a main amplifier with a variable gain up to 1000. After high-pass (10Hz, 3dB/oct) and low-pass (1000Hz, 24dB/oct) filtering the signal was sampled at 2000Hz. The CCCF was calculated with a microcomputer.

RESULTS AND DISCUSSION

The noise, AC-components and ECG must be minimal to make the CCCF a good estimator for crosstalk.

Noise and AC-components In our investigation the RMS of the noise was .0007 mV. The lowest RMS level of the EMG was always more than 10 times higher. Even at the lowest EMG-level the power density spectrum showed no peaks at 50 or 100 Hz, thus AC-components were absent.

ECG With a digital low-pass filter the QRS-complex of the ECG could be detected in the EMG of 10% MVC at the L1 level of the left side of the body. CCCF was calculated in the data without the QRS-complex. If this 'gating' was omitted an overestimation of crosstalk of more than .1 could be the result. The use of powerful subtraction techniques (5,6) to remove the ECG may also improve the results.

Channel Acquisition Time In the calculation of the CCCF the signals must be sampled at the same time. The channel to channel acquisition time (CAT) gives a time shift which results in underestimation of the CCCF. In the medial ILBM 99% of the total power of the power density spectrum occurred below 372 Hz. At this frequency the error in the CCCF in two succeeding channels is less than 5% if the CAT is less than .136 ms. This is the case for the most available AD-boards.

Crosstalk The CCCF was calculated over a time span of 0.512 seconds. The maximal CCCF of unrelated EMG's at 60% MVC was calculated to be $.21 \pm .02$. This is called the lower limit value (LLV).

TABLE I
Mean Maximal CCCF of the ILBM (\pm SD).

level distance (mm) parts	L1 30 med-int	L1 30 int-lat	L1 60 med-lat	L3 30 med-int
10% MVC	.47 \pm .14	.63 \pm .13	.25 \pm .07	.55 \pm .15
60% MVC	.38 \pm .14	.53 \pm .15	.23 \pm .06	.57 \pm .14
t-test	P <.01	P <.05	N.S.	N.S.

Force level The maximal value of the CCCF was higher at 10% MVC compared to 60% MVC for the electrodes with an interspace of 30 mm at L1 (Table I). This may be due to the fact that at 10% MVC only part of the motor-units are recruited. Moreover, Vink et.al.(7) showed that at force levels below 10% MVC the signal to noise ratio was so unfavourable that an increase in CCCF could result.

Distance The maximal values of the CCCF were highly dependent on the distance between the electrode pairs. The electrodes which were separated by 60 mm had a mean correlation of .23 (SD .06), which was not significantly different from the LLV (Table I). This means that the EMG of the medial and lateral parts of the ILBM at L1 are unrelated.

The maximal CCCF of the electrodes with an interspace of 30 mm was .38 to .63. This is significantly higher than the LLV. Although the correlation between the neighbouring muscles is high, the registrations still contain specific information, which is demonstrated by an entirely different EMG to force relationship at 30, 60 and 90 mm from the lumbar spine at L1 (4).

Conclusion In locating the EMG-electrodes the CCCF can be a useful technique. If the maximum CCCF is not different from the lower limit value no crosstalk is present. If the maximal CCCF exceeds a certain limit value transposition of the electrodes must be considered. Determining this limit is difficult. This experiment points out that the EMG of the ILBM contains specific information even when the maximum CCCF amounts to .63.

REFERENCES

1. Mangun GR, Mulkey RM, Young BL, Goslow GE (1986) Electromyogr Clin Neurophysiol 26:443-461
2. Bendat JS, Piersol AG (1986) Random Data: Analysis and Measurement Procedures. Wiley & Sons, New York
3. Andersson BJG, Jonsson B, Ortengren R (1974) Scand J Rehab Med Suppl 3:91-108
4. Vink P, vd Velde EA, Verbout AJ (1988) Electromyogr Clin Neurophysiol 27:517-525
5. Bloch R (1983) J Appl Physiol 55:619-623
6. Levine S, Gillen J, Weiser P (1986) J Appl Physiol 60:1073-1081
7. Vink P, Daanen HAM, Verbout AJ (1988) Human Movement Science In Press

Spectral parameters during muscle fatigue

MUSCLE FIBER CONDUCTION VELOCITY AND EMG SPECTRAL PARAMETERS IN VOLUNTARY AND STIMULATED CONTRACTIONS

R. Merletti† M. Knafitz† C. J. De Luca‡

†DIPARTIMENTO DI ELETTRONICA - POLITECNICO DI TORINO - TORINO - ITALY
‡NEUROMUSCULAR RESEARCH CENTER - BOSTON UNIVERSITY - BOSTON - U.S.A.

INTRODUCTION

Muscle fiber conduction velocity (CV) is defined as the propagation velocity of the depolarized zone along muscle fibers. Correlation between CV and spectral parameters (SP) (mean and median frequency) during voluntary contractions has been shown in both theoretical (8) and experimental (1,2,3,4,5,11) work, and is particularly evident when the surface electrodes used to detect the signal are located away from the innervation zone (10). This study was undertaken to investigate the relationship between myoelectric signal CV and SP during electrically-elicited and voluntary isometric contractions of the human tibialis anterior (TA) muscle using surface stimulation and detection techniques.

MATERIALS AND METHODS

Thirty two experiments were performed on 22 healthy subjects. The ankle joint was restrained in an isometric brace. Visual feedback of contraction level during voluntary efforts was provided. Voluntary contractions were performed at 20% and 80% MVC. Stimulated contractions were elicited with a monopolar technique using a small electrode (2x3 cm) placed on the most proximal motor point of the TA, and a large electrode (10x12 cm) placed on the gastrocnemius. Rectangular current pulses of 0.1 ms width and 20 Hz repetition rate were applied between the two electrodes with intensities suitable to elicit submaximal (25% of maximal) and maximal M waves. The two modalities are referred to as low and high level stimulation, respectively (LLS and HLS). Force feedback and voluntary myoelectric signals were not present during stimulation.

Artifact removal, signal detection, and conditioning techniques have been described elsewhere (7). Conduction velocity was obtained from the ratio of the interelectrode distance to the delay between the double differential signals provided by the four bar pasteless electrode system described by Broman, Bilotto, and De Luca (3). The delay was estimated with the algorithm of McGill and Dorfman (9). Spectral parameters (mean and median frequency) estimates were computed from the single differential signal. Both CV and SP were computed on 20 one second epochs for each contraction. The electrically elicited responses were averaged over each epoch (20 events). SP and CV estimates were computed from the averaged responses. Each contraction was repeated twice in all the experiments. Each experiment was repeated twice on different days on 10 of the 22 subjects.

The time series of 20 values of each parameter was fitted with a linear and an exponential regression curve. The intercept of the curve with the smallest residual standard deviation was taken as the initial value.

RESULTS

At LLS and HLS force was respectively $4.23\% \pm 3.7\%$ and $16.24\% \pm 4.9\%$ MVC, indicating that only a part of the TA was activated rather than the entire anterior compartment

as during voluntary contractions.

Fig. 1 shows samples of results from one experiment. Repeatability within the same experiment was within a few percent. Time fluctuations of SP and CV estimates were much smaller during electrically elicited contractions than during voluntary contractions. Mean and median frequency had statistically identical behavior and often showed percent decrease greater than that of CV.

The initial values of either SP or CV at 80% MVC were always greater than at 20% MVC whereas it was not so for LLS and HLS contractions. Fig 2 shows the initial values of mean frequency and CV for 20% MVC, 80% MVC, LLS and HLS. With increasing level of stimulation SP and CV both increased in 17 cases, SP decreased and CV increased in 5 cases, SP increased and CV slightly decreased in 3 cases, SP and CV both decreased in 7 cases. Five out of the ten subjects on which the experiment was repeated presented different behaviors in the two experiments indicating the critical role of electrode positioning and the consequent poor interexperiment repeatability. Fig.3 shows the time course of mean frequency and CV values normalized with respect to their initial value. Very similar and highly correlated variations are evident. In most cases, however, SP showed a larger decrement than CV.

DISCUSSION

It is known that during voluntary muscle contractions, recruitment progresses from units with smaller fibers (low CV) to units with larger fibers (high CV). Therefore, SP and CV should increase with increasing muscle force. Our results show this expected behavior and support previous findings (3,10).

Three factors may play a role in determining the order of recruitment (as indicated by muscle fiber CV changes) during surface electrical stimulation: a) the size of the motoneuron (known to be related to the excitability threshold, the size of the motor unit and the average size of its muscle fibers), b) the size of the motoneuron branches (whose diameter is related to excitability threshold) and, c) the location and the direction of the motoneuron branches in the current field. Fig. 2 shows that in most cases (69%) electrically elicited recruitment proceeded in increasing order of CV, and that, in fewer cases (31%) it proceeded in decreasing order of CV, indicating that the electrical excitability threshold of the motoneurons (or of their terminal branches) is not always a dominant factor, or that larger motoneurons have branches smaller than those of small motoneurons.

On the other hand, the depth of a motor unit in the muscle would highly affect SP and only marginally affect CV estimates. The significantly different ($p < 0.05$) and opposite changes observed in type 2 behavior (5 cases) for SP and CV indicate that increasing stimulation level recruited progressively faster and deeper motor units whose contribution to the myoelectric signal power spectrum was band-limited by the tissue low pass filtering function. This interpretation is supported by Henriksson-Larsen et al.'s data (6). They found a higher percentage of large fibers in the deeper parts of the human tibialis anterior. The case described in Fig 1 clearly shows this behavior. Units recruited at HLS show higher values and higher drop rates of CV than those recruited at LLS. The latter, however, show higher SP values.

The higher decrease of SP with respect to CV during a sustained contraction shown in some cases seems to indicate that SP are affected by other factors beside CV. Decrease of axonal branches CV would increase the duration of the MUAP and lower the SP. Either

changes of length or of potential distribution of the depolarized zone might have a similar effect. These factors deserve further investigation.

In conclusion, we believe that the two paradigms of voluntary and stimulated contractions may provide tools for non invasive characterization of muscle structure and architecture.

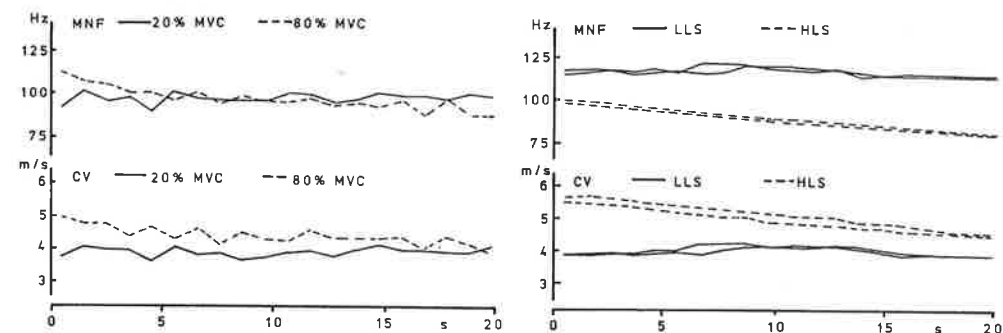


Fig. 1. Time course of mean frequency and conduction velocity during 20s contractions at 20% MVC, 80% MVC, LLS and HLS (20 Hz). One contraction at 20% and one at 80% are shown. Two contractions at LLS and two at HLS are shown to indicate repeatability.

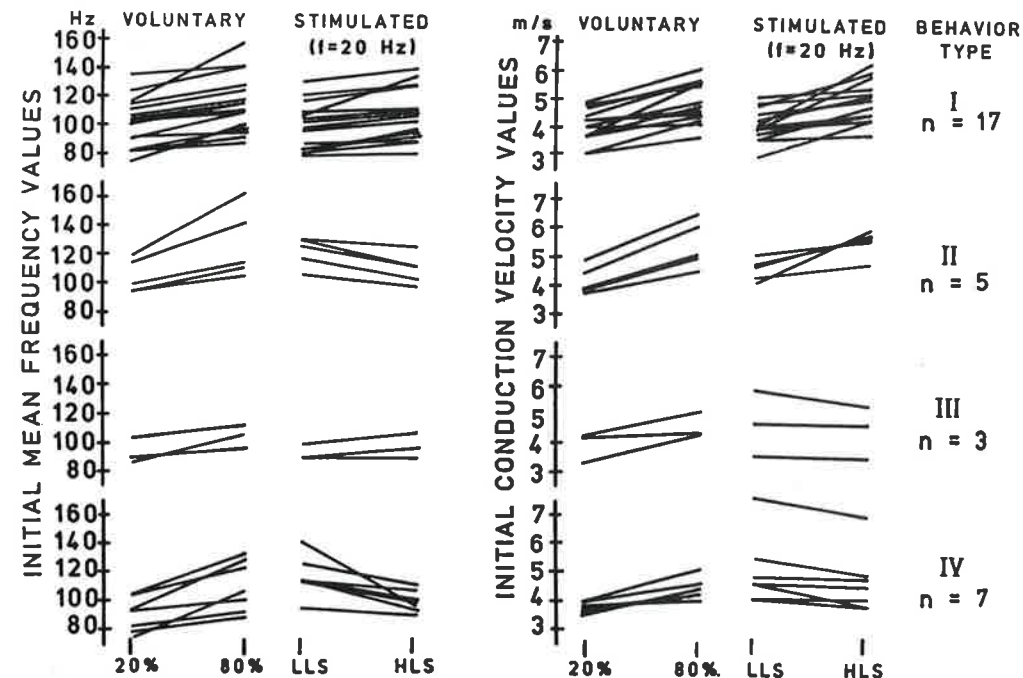


Fig. 2. Initial values of mean frequency and conduction velocity at 20% and 80% MVC and at LLS and HLS (20 Hz). All 32 experiments show the same behavior during voluntary contractions. Four different behavior types are identified during stimulated contractions.

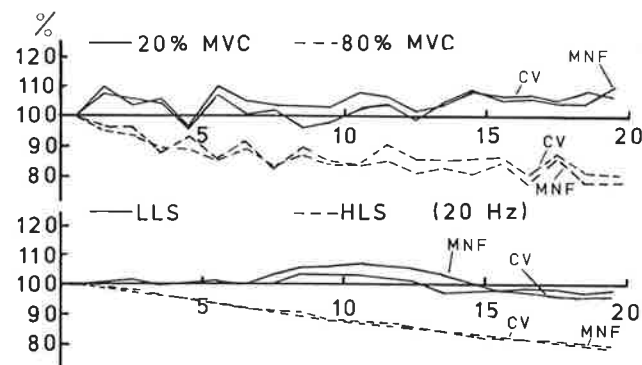


Fig. 3. Percent variation (with respect to the first value) of mean frequency and conduction velocity during 20% 80%, LLS and HLS contractions at 20 Hz.

ACKNOWLEDGMENT

This work was performed at the NeuroMuscular Reserch Center of Boston University in cooperation with the Department of Electronics of Politecnico di Torino, Italy. Major support was provided by Liberty Mutual Insurance Company. Partial support was provided by the Italian Ministry of Education within the framework of the national project on Rehabilitation Engineering and within the doctoral program of Dr. Marco Knaflitz.

REFERENCES

1. Arendt Nielsen L., K.R. Mills, The relationship between mean power frequency of the EMG spectrum and muscle fiber conduction velocity. *EEG and Clinical Neurophysiology*, 60,130-136, 1985.
2. Bigland Ritchie B., E.F. Donovan, C.S. Roussos, Conduction velocity and EMG power spectrum changes in fatigue of sustained maximal efforts. *J. Appl. Physiol.* 51, 1300-1305, 1981.
3. Broman H., G. Bilotto, C.J. De Luca, Myoelectric signal conduction velocity and spectral parameters: influence of force and time., *J. of Applied Physiology*, 8, 1428-1437, 1985.
4. De Luca C.J., Myoelectric manifestations of localized fatigue in humans., *CRC Crit. Rev. Bioeng.*, 11, 251-279, 1984.
5. Eberstein A., B. Beattie, Simultaneous measurement of muscle conduction velocity and EMG power spectrum changes during faigue, *Muscle and Nerve*, 8, 768-773, 1985.
6. Henriksson-Larsen K, J. Friden , M. Whetling, Distribution of fiber sizes in human skeletal muscle. An enzyme histochemical study in muscle tibialis anterior. *Acta Physiol. Scand.*, 123, 171-177, 1985.
7. Knaflitz M., R. Merletti, Suppression of stimulation artifacts from myoelectric evoked potential recordings. *IEEE Trans. on BME.* (in press)
8. Lindstrom L. , R.I. Magnusson, Interpretation of myoelectric power spectra: a model and its applications., *Proc. IEEE* 65, 653-662, 1977.
9. McGill K., L. Dorfman, High resolution alignment of sample waveforms, *IEEE Trans on BME*, 31, 462-468, 1984.
10. Roy S.H., C.J. De Luca, J. Schneider, Effects of electrode location on myoelectric conduction velocity and median frequency estimates., *J. of Applied Physiol.* 61, 1510-1517, 1986.
11. Sadoyama T., T. Masuda , H. Miyano, Relationships between muscle fiber conduction velocity and frequency parameters of surface EMG during sustained contraction., *Eur. J. Appl. Physiol.* 51, 247-256, 1983.

STATIONARITY OF VOLUNTARY AND ELECTRICALLY ELICITED SURFACE MYOELECTRIC SIGNALS

G. BALESTRA†

M. KNAFLITZ†

R. MERLETTI†

‡ DIPARTIMENTO DI AUTOMATICA E INFORMATICA - POLITECNICO DI TORINO - ITALY

† DIPARTIMENTO DI ELETTRONICA - POLITECNICO DI TORINO - TORINO - ITALY
and NEUROMUSCULAR RESEARCH CENTER - BOSTON UNIVERSITY - BOSTON - U.S.A.

INTRODUCTION

During either voluntary or electrically elicited sustained contractions, muscle fatigue induces a decreasing trend of muscle fiber conduction velocity (CV), a progressive compression of the surface myoelectric signal (SMES) power spectrum toward the lower frequencies, a progressive decrease of mean and median frequency (MNF, MDF), a progressive widening of the main lobe of the autocorrelation function (ACF) and, in general, an increase of signal RMS, as shown by theoretical and experimental work [1], [4], [5], [3], [8]. The signal may therefore be assumed as stationary only for short time intervals.

This study was undertaken (a) to identify tools for assessing signal stationarity and (b) to assess the limits of a SMES model to predict the behavior of signal parameters at different levels of voluntary and stimulated contractions.

Since the mean value of the SMES is zero (and any DC component due to the electrodes is removed by the instrumentation), wide sense stationarity (WSS) implies only the time invariancy of the autocorrelation function (ACF) [6]. Since the SMES has real values, ACF time invariancy implies power spectrum (PSD) time invariancy and vice-versa. *If MNF or MDF or RMS are not time independent the ACF will not be time independent.* In general the converse doesn't hold. Previous researchers [8] showed that a linear relationship exists between SMES MNF and/or MDF variations and CV variations. If fatigue related spectral changes are considered, such relationship allows to state that *if MNF and MDF and RMS are time independent PSD may be considered time independent too.*

Run Test (RT) [7] at 5% confidence level was used to test time independency of the observed parameters.

MATERIALS AND METHODS

Twenty experiments were performed on the tibialis anterior (TA) of ten volunteer subjects. Each experiment consisted of two initial isometric constant torque voluntary contractions at 20% MVC and at 80% MVC, ten electrically elicited contractions with monopolar supramaximal stimulation of the TA's main motor point, ten submaximal (M-wave amplitude = 25% of maximal) contractions and two final voluntary contractions at 20% and 80% MVC. Visual feedback of the contraction level was provided during voluntary contractions. Electrical stimulation was applied to relaxed muscles with current pulses of 0.1ms width and frequency of 20, 25, 30, 35, 40 Hz. Each contraction was repeated twice, three minutes apart, and lasted 20 s. The following parameters were estimated on 20 one-second signal epochs: power spectrum mean (MNF) and median (MDF) frequency, average rectified value (ARV) and rms (RMS) value, muscle fiber conduction velocity (CV) and joint torque (T). The instrumentation used has been described in a previous paper [5].

Time independency of MNF, MDF, and RMS was tested by detecting the presence or absence

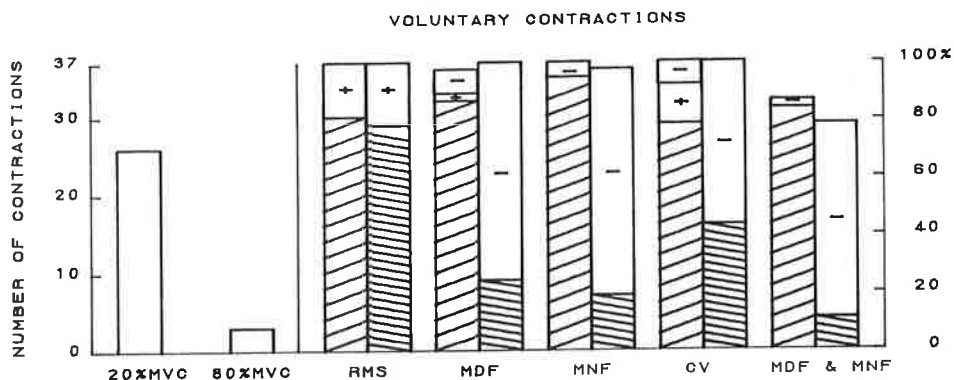


Figure 1: A) Number of contractions generating WSS SMES; B) Number and percentage of voluntary contractions showing no trend [///], positive trend [+], negative trend [-] of RMS, MDF, MNF, CV and MDF & MNF at 20% MVC (left bar) and at 80% MVC (right bar).

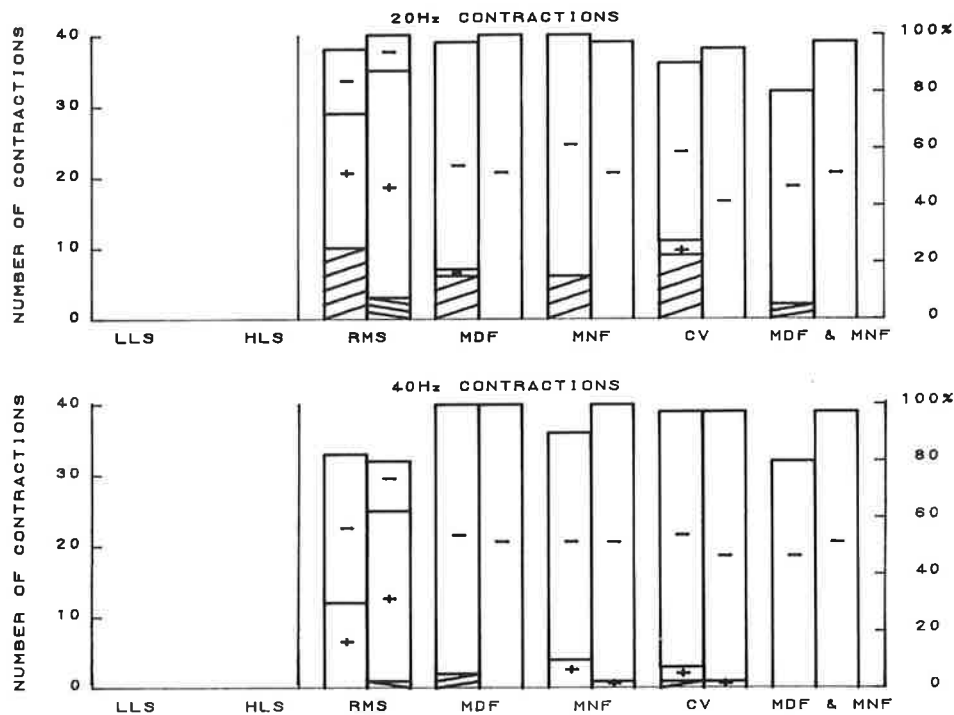


Figure 2: A) Number of contractions generating WSS SMES; B) Number and percentage of stimulated contractions showing no trend [///], positive trend [+], negative trend [-] of RMS, MDF, MNF, CV and MDF & MNF at LLS (left bar) and HLS (right bar).

of trends at 5% confidence level by means of the RT and the direction of the observed trends was evaluated by means of linear fitting.

RESULTS

Voluntary contractions

According to the stationarity requirements (MNF, MDF and RMS all trendless during the 20 s contraction) the contractions generating a WSS myoelectric signal were 26/37 at 20% MVC and 3/37 at 80% MVC. Overall results are presented in fig.1.

Stimulated contractions

In only 1/200 case at LLS and 0/200 cases at HLS SMES was classified as WSS according to the stationarity definition given in the introduction. Random variations of spectral and amplitude parameters were much smaller than during voluntary contractions (probably due to the fixed firing rate imposed by stimulation) and therefore trend detection by RT was more efficient. Overall results are presented in Fig.2 and 3 for stimulation at 20 Hz and at 40 Hz respectively.

DISCUSSION

It is evident from Fig.1 that most contractions at 20% MVC were stationary as well as a few contractions at 80% MVC level. Contractions should therefore be sustained for longer than 20 s if detectable fatigue has to be induced at 80% MVC in all cases. It is also evident from Fig.1 that the behavior of RMS was similar at 20% MVC and at 80% MVC, indicating that this parameter is not a good fatigue indicator and it changes less than predicted by Lindstrom's model. A very similar behavior (no statistically significant difference) of MNF and MDF is indicated in Fig.1. Both parameters show a number of negative trends at 80% MVC higher than RMS and are good fatigue indicators. CV shows trend in only 21/37 cases at 80% MVC, indicating, as suggested by previous results [4], that spectral parameters are affected by factors other than CV variations. Decrease of axonal branch CV, changes of length and/or potential distribution of the depolarized zone, synchronization of motor units might contribute to the spectral shift. These factors deserve further investigation.

Fig.2 and 3 show the behavior of the parameters at 20 Hz and 40 Hz stimulation. Contractions generating WSS SMES were present neither at 20 Hz nor at 40 Hz. At HLS and 20 Hz the trends are those predicted by Lindstrom's model. Longer contractions would probably have shown the same behavior at LLS. The predicted pattern is even more evident at 40 Hz, however, the initially positive trend of RMS becomes negative before the end of the contraction in most cases, both at LLS and HLS. At 40 Hz RT detected 12/40 LLS and 24/40 HLS contractions generating an increasing trend of RMS, however, looking at RMS time series it is evident that in most cases RMS reverses its initial positive trend before the end of the contraction. In average (80 cases, 40 Hz LLS and HLS) RMS value starts decreasing after 11.05 s ($\sigma = 4.96$). The model predicted behavior seems to apply well in controlled conditions (constant firing rate, stable motor unit pool) and when fatigue is not so intense to reverse the positive trend of RMS.

During stimulated contractions, as both MNF and MDF variations are generally strictly monotonic, the appropriate duration for studying fatigue by applying RT as described above seems to depend only on RT itself. At least 10 values of the sequence are needed to obtain reliable results by applying RT [7]; as MNF and MDF values are computed on 1 s time

epochs, 10 s should be sufficient for trend detection. As during voluntary contractions MNF and MDF behavior is not strictly monotonic, contractions longer than 20 s are needed at 20% MVC and sometimes at 80% MVC too.

The decreasing behavior of RMS during highly fatiguing stimulated contractions deserves further investigation. Major changes of either excitability (drop out of motor units) or of action potential shape may provide possible explanations.

In 27/40 LLS and in 24/40 HLS contractions at 40 Hz T showed an increasing trend, while the same behavior was evident in only 19/40 LLS and in 12/40 HLS contractions at 20 Hz. No clear relationship was found between RMS and T during stimulated contractions.

The RT has been shown to be an effective method to study stationarity during time intervals of at least 10s. Short term stationarity of SMES produced during voluntary contractions is better studied by observing the behavior of the ACF. Monotonic widening of the main lobe of the SMES ACF has been observed during stimulated contractions whereas random fluctuations of the shape and parameters of the ACF have been observed during voluntary contractions using 1s signal epochs. A method for describing *short term* stationarity is presently being investigated.

ACKNOWLEDGMENTS

This work was performed at the NeuroMuscular Reserch Center of Boston University in cooperation with the Dept. of Electronics of Politecnico di Torino, Italy. Major support was provided by Liberty Mutual Insurance Company. Partial support was provided by the Italian Ministry of Education within the framework of the national project on Rehabilitation Engineering and within the doctoral programs of Dr. G. Balestra and Dr. M. Knafitz.

REFERENCES

1. Arendt Nielsen L., K.R. Mills, "The relationship between mean power frequency of the EMG spectrum and muscle fiber conduction velocity" *EEG and Clinical Neurophysiology*, 60,130-136, 1985.
2. M. Knafitz and R. Merletti, "Suppression of stimulation artifacts from myoelectric evoked potential recordings" *IEEE Trans. on BME*, in press.
3. L. Lindstrom and R.I. Magnusson, Interpretation of myoelectric power spectra: a model and its applications., Proc. IEEE 65, 653-662, 1977.
4. H. Broman, G. Bilotto, C.J. De Luca, "Myoelectric signal conduction velocity and spectral parameters: influence of force and time.", *J. of Applied Physiology*, 8, 1428-1437, 1985.
5. L. Lindstrom, R. Magnusson, I. Petersen, "Muscular fatigue and action potential conduction velocity changes studied with frequency analysis of EMG signals", *Electromyography*, vol. 10. pp. 341-356, 1970
6. A. Papoulis, *Probability, random variables, and stochastic processes*, McGraw-Hill, 1984
7. L. Sachs, *Applied Statistics*, Springer-Verlag, 1982
8. F.B. Stulen and C.J. De Luca, "Frequency parameters of the myoelectric signal as a measure of muscle conduction velocity", *IEEE Trans. Biomed. Eng.*, vol. BME-28, 7, pp. 515-523, 1981

RECOVERY FROM SEVERE ISOMETRIC, CONCENTRIC OR ECCENTRIC CONTRACTIONS IN THE HUMAN BICEPS MUSCLE

G.W. KROON AND M. NAEIJE

Department of Masticatory Function, Academic Centre Dentistry Amsterdam, ACTA, Amsterdam, The Netherlands.

INTRODUCTION

Heavy muscular contractions induce muscular fatigue. In order to evaluate muscular fatigue force and endurance capacity are used as muscular physiological indices (Stull 1974). Muscular fatigue is also reflected in changes in the surface EMG signal (Lindström et al. 1977; Petrofsky and Lind 1980; Naeije and Zorn 1981). Subsequent to a fall in muscular strength during the exercise phase (Clarke and Stull 1969; Edwards et al. 1977) its recovery is initially rapid and completed within a relatively short period of time, ranging from 10 minutes to a few hours depending upon the experimental protocol. The recovery of the endurance capacity needs a longer period of time (Funderburk et al. 1974). In contrast to this, studies indicate, that the recovery in the EMG signal takes only a few minutes (Mills 1982; Kroon et al. 1986). Thus, the recovery in the muscle physiological indices seems to take a longer period of time than the recovery in the EMG signal (Hara 1980). However, in most of these studies the recovery in either the muscular function or the EMG signal was studied. In a recent study (Kroon and Naeije 1988) regarding the simultaneous recording of the recovery in the muscular physiological indices and in the EMG signal following alternating concentric and eccentric contractions until exhaustion it was shown that 25 hours after the exercise both the muscular function and the EMG signal were not fully recovered yet. These results suggest, that the recovery has to be studied for a longer period of time than just 25 hrs. Eccentric muscular contractions induce longer lasting fatigue effects upon the muscular force than concentric or isometric contractions (Sargeant and Dolan 1987). Whether this is also true for the EMG signal is still unknown. Therefore, the aim of this study was to investigate the changes in the muscular force, the endurance capacity and the EMG signal until complete recovery after exhaustive eccentric, concentric or isometric contractions.

MATERIAL AND METHODS

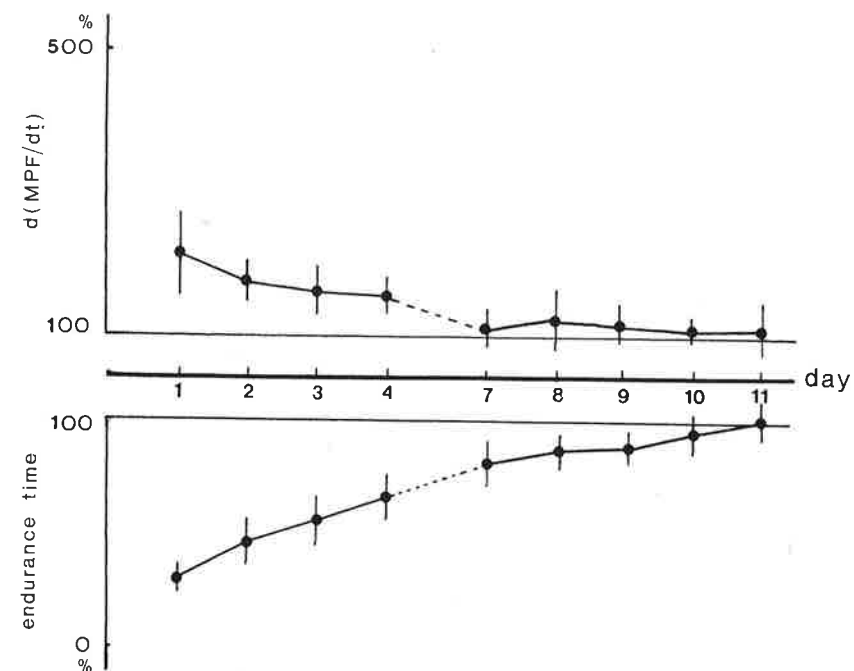
Five healthy untrained male subjects participated in the experiment. EMG recordings were obtained using a pair of silver amalgam surface electrodes. The electrodes were applied to the skin parallel to the main direction of the muscle fibres of the common belly of the biceps muscle of the left arm. The electrode positions were marked on the skin enabling accurate repositioning of the electrodes on subsequent days.

With an interval time of three weeks muscular fatigue was induced by exhaustive isometric, concentric or eccentric muscle contractions. The maximum voluntary contraction force (MVC) and the endurance capacity for a 40% isometric contraction were used to evaluate muscular fatigue. The EMG signal was recorded during 30 second isometric contractions at 40% of the pre-fatigued MVC. The Mean Power Frequency and Root Mean Square value at the start of each contraction and the rate of change in the MPF value ($d(\text{MPF})/dt$) during the contraction were calculated.

Each experiment consisted of three phases. In the first phase, the pre-exercise phase, reference values for the different indices were obtained. In the second phase, the exercise phase, muscular fatigue was provoked. The subjects were instructed to perform 3 second contractions followed by 2 second rest periods at 50% (isometric) or 40% (concentric or eccentric) of the pre-fatigued MVC. At exhaustion the load was reduced to 40% and 30% respectively and once again the contractions were performed until exhaustion. In between sets of 10 contractions there was an extra 1 minute rest period. During the third phase, post-exercise phase, the muscular physiological indices and the EMG signal were recorded at regular intervals until complete recovery.

RESULTS

There was a similar rate of recovery in the muscular physiological indices and as in the parameters of the EMG signal (see figure). The recovery following the eccentric contractions took a longer period of time (7 days, $p < 0.005$) compared to the recovery following the isometric (2 days) or concentric (1 day) contractions.



Mean standardized values with the standard errors of the mean of the rate of frequency shift of the EMG signal ($d\text{MPF}/dt$) and the endurance time following muscular exhaustion by eccentric contractions.

DISCUSSION

In contrast to other studies (Hara 1980) this study indicates that there is not a great difference in the recovery rate of the muscular physiological indices and of the EMG signal following muscular contractions until exhaustion. It is also shown that eccentric muscle contractions induce longer lasting effects compared to either isometric or concentric contractions. Especially these eccentric contractions are harmful to the muscle. They may evoke long lasting changes in the histochemical and morphological components of the muscle (Friden et al. 1981; Bobbert et al. 1986). Damage of the muscular cell (Hough 1902; Abraham 1977) acts upon the electrical properties of the muscular cell membrane and may be the reason for the longlasting changes in the EMG signal.

REFERENCES

- Abraham W. M. (1977). Factors in delayed muscle soreness. *Med Sc Sports* 9: 11-20
- Bobbert M. F., Hollander A. P. and Huijting P. A. (1986). Factors in delayed onset muscle soreness of man. *Med Sci Sports Exerc* 18: 75-81
- Clarke D.H. and Stull G.A. (1969). Strength recovery patterns following isometric and isotonic exercise. *J Mot Behav* 3:233-243
- Edwards R. H. T., Hill D. K., Jones D.A. and Merton P.A. (1977). Fatigue of long duration in human skeletal muscle after exercise. *J Physiol* 272: 769-778
- Friden J., Sjöström M. and Ekblom B. (1981). A morphological study of delayed muscle soreness. *Experientia* 37: 506-507
- Funderburk C.F., Hipskind S.G., Welton R.C. and Lind A.R. (1974). Development of and recovery from fatigue induced by static effort at various tensions. *J Appl Physiol* 37: 392-396
- Hara T. (1980). Evaluation of recovery from local muscle fatigue by voluntary test contractions. *J.Human Ergol.*,9:35-46
- Hough T. (1902). Ergographic studies on muscular soreness. *Am J Physiol* 7: 76-81
- Kroon G. W., Naeije M., and Hansson T. L. (1986). Electromyographic power-spectrum changes during repeated fatiguing contractions of the human masseter muscle. *Arch Oral Biol* 31: 603-608
- Kroon G. W. and Naeije M. (1988). Recovery of muscle physiological and EMG parameters following exhaustive dynamic exercises. *Eur J Appl Physiol* (Submitted)
- Lindström L., Kadefors R., Petersen I. (1977). An electromyographic index for localized muscle fatigue. *J Appl Physiol Resp Environ* 43 (4) 750-754
- Mills K.R. (1982). Power spectral analysis of electromyogram and compound muscle action potential during muscle fatigue and recovery. *J Physiol* 326: 401-409
- Naeije M. and Zorn H. (1981). Changes in the power spectrum of the surface electromyogram of the masseter muscle due to local muscular fatigue. *Arch Oral Biol* 26: 409-412
- Petrofsky J.S. and Lind A.R. (1980). Frequency analysis of the surface electromyogram during sustained isometric contractions. *Eur J Appl Physiol* 43: 173-182
- Sargeant A.J. and Dolan P. (1987). Human muscle function following prolonged eccentric exercise. *Eur J Appl Physiol* 56: 704-711
- Stull G.A. (1974). Recovery of muscular endurance following rhythmic or sustained activity. *J Mot Behav* 6: 59-66

THE INFLUENCE OF FORCE AND CIRCULATION ON THE AVERAGE MUSCLE FIBER CONDUCTION VELOCITY DURING LOCAL MUSCLE FATIGUE

M.J. ZWARTS (1) AND L. ARENDT-NIELSEN (2)

(1) Dept. of Neurology, University Hospital, PO Box 30.001 Groningen, The Netherlands and (2) Dept. of Medical Informatics, Aalborg University, 9000 Aalborg, Denmark

INTRODUCTION

The rapid occurrence of local muscle fatigue during static contractions, is generally believed to be the consequence of a high metabolic demand combined with an impeded blood flow (1). The force level influences to a high degree the endurance time (2) and the metabolic changes in the muscle (3). So far, no systematic studies have been done on the change in sarcolemmal function as measured by muscle fiber conduction velocity (MFCV) in relation to force level and muscle blood flow. We investigated the changes in MFCV during static contractions in relation to the force level in two experiments.

METHODS

Two approaches were used to investigate if the change in MFCV during fatigue of isometric voluntary contraction was sensitive to changes in the intramuscular pressure and hence the level of ischaemia. The force was measured with strain gauges. The m. vastus lateralis and m. biceps brachii were chosen for the experiments since the fibre orientation is such that the length of fibers distal to the motor point is accessible for MFCV determination. The electrodes were placed in a bipolar array with the centre electrode common, parallel to the fibre axis and distal to the motor point. The electrode distance was 15 mm for m.vastus lateralis and 10 mm for m. biceps. The two EMG signals were amplified and digitized. Cross-correlation was performed off-line.

Two series of experiments were accomplished. The first experiment was done both with the blood flow in the leg intact and occluded with a pneumatic tourniquet (300 mm Hg) around the upper leg confirmed by the persistent absence of a palpable peripheral pulse.

Volunteers were five healthy males (mean age 32 years, range 26-39). Target forces from 10 to 100% MVC were chosen in random order and at least 24 hr. elapsed between contractions. The duration of contraction was varied such that the product of relative force (% MVC) and time was constant; hence 10% MVC was maintained

for 400 s; 100% MVC for 40 s etc. When the endurance point was reached the volunteers still tried to maintain the maximal possible force.

The second experiment was done to study the change in MFCV during a maximal voluntary contraction. Volunteers were 3 healthy male aged 34, 29 and 31 years. During maximal elbow flexion measurements of MFCV were done on the biceps brachii every 13 seconds, until at least 5 measurements were done. This procedure was repeated 5 times on different days for each volunteer.

RESULTS

Experiment 1

During low contractions (10 and 20% MVC) the muscle fiber conduction velocity increased slightly in both ischaemic and non-ischaemic muscles. However, the increase was significantly higher in the experiment without ischaemia (Wilcoxon's test, $p < 0.05$). In the 30 and 40% MVC experiment MFCV decreased significantly more in ischaemic than non-ischaemic muscles. Above 40% MVC no significant differences in MFCV could be observed between the two experiments (Fig 1). MFCV measured at the beginning of the contraction were found to increase for increasing force.

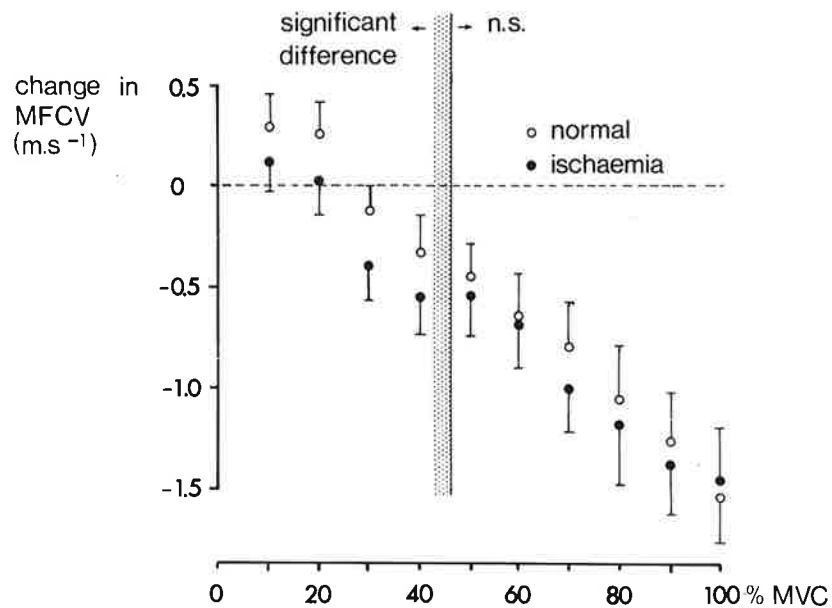


Fig. 1 The decline in conduction velocity as a function of the contraction level in normal and occluded conditions.

Experiment 2

The change in MFCV was always maximal at the third to fourth measurement after 26-39 seconds. The maximal percentage decline (\pm SD) was then 58.6 \pm 5.7; 58.0 \pm 8.4 and 59.6 \pm 4.5. The decline in force was always maximal at the last contraction and was for the 3 subjects: 50.8 \pm 3.6; 42.0 \pm 7.9 and 31.6 \pm 6.6 (expressed in %). At the end of the contraction, generally at force levels of 30 - 50% MVC, the decline of the MFCV reversed, and an increase occurred for the next 13 s, until the experiment was terminated (Fig. 2).

DISCUSSION

Increase in MFCV at higher force has been described previously (4, 5) due to the higher conduction velocities of the motor units that are recruited at higher force levels.

At 30 and 40% MVC a significantly larger decrease in MFCV was found between the contractions with occluded circulation as compared with the normal situation, indicating that at these force levels the m.vastus lateralis is not working in total anaerobic conditions.

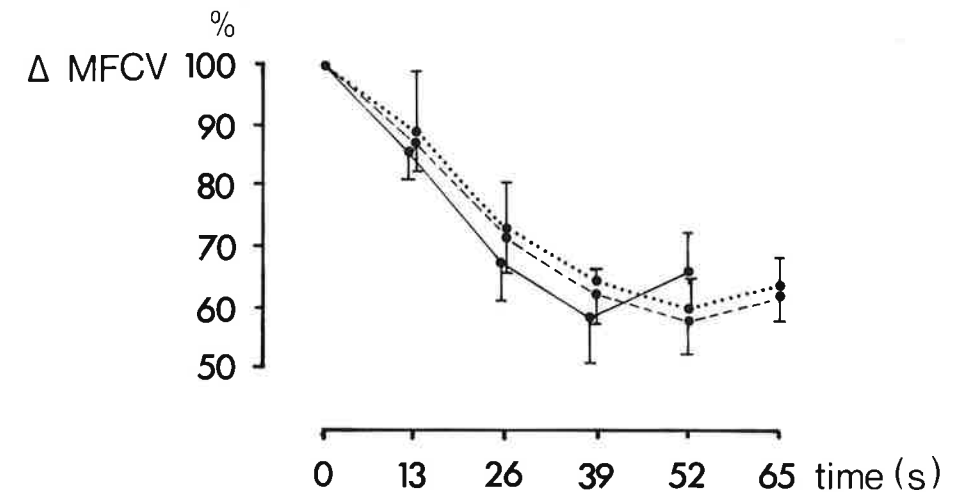


Fig. 2 Changes in conduction velocity during maximal contractions. The data are the mean values (\pm SD, $n=5$) of 3 controls.

Above 40% MVC no differences could be found between the two experimental situations. An obvious explanation is that the muscle must be regarded as working in anaerobic conditions, so the

tourniquet ischaemia cannot longer worsen the metabolic situation of the muscle. But at high levels fatigue changes result also from a too high metabolic demand irrespectively of the blood flow. Possibly, at high force level the force loss could be the result of a reduction in the rate of ATP turnover (6).

The second experiment supplements the findings from experiment 1. At the end of the contraction the decline in MFCV is reversed, despite a continuous loss in force, indicating that different mechanisms could be responsible for the loss of force and the change in sarcolemmal function. The fact that this occurs between 30-50% MVC strongly suggests that a partial restoration of blood flow is responsible for the restore in MFCV. A fast wash-out of lactate and accumulated extracellular potassium could result in the raise in MFCV, while the force generation continues to decline due to a too high energy demand.

Together, the two experiments indicate that the force level and the consequent intramuscular blood flow are important for the change in MFCV at fatigue of static contractions higher than 30% MVC. At high force levels the loss in force is probably caused by different mechanisms than those responsible for the change in MFCV.

REFERENCES

1. Edwards RHT (1981) Human muscle fatigue: physiological mechanisms. Ciba foundation symposium 82. London, pp 1-18
2. Rohmert (1960) Int Z Angew Physiol Einschl Arbeitsphysiol 18: 123-164
3. Ahlborg et al. (1972) J App Physiol 33: 224-228
4. Zwarts MJ, Van Weerden TW, Links TP, Haenen HTM, Oosterhuis HJG (1988) Muscle and Nerve, 11: 166-173
5. Andreassen S, Arendt-Nielsen L (1987) J Physiol 391: 561-571
6. Fitch C, Chevli R, Petrofsky JS, Kopp Js (1978) Life Sci 23: 1285-1292

ELECTROMYOGRAPHY IN WALKING OF PATIENTS WITH INTERMITTENT CLAUDICATION

A.L. HOF, G.J.J. BONGA, W.D. KUIPERS*, A.A. WOUDA* and L. DE PATER.

Laboratory of Medical Physics and (*) Department of Internal Medicine, University of Groningen, Bloemsingel 10, 9712 KZ Groningen (The Netherlands)

INTRODUCTION

Intermittent claudication is a symptom of an obstruction of arteries to a leg. Atherosclerosis is the cause in the majority of cases. In the intermittent claudication stage the blood (and especially oxygen) supply to the leg is sufficient at rest but cannot cope with the increased demand of active muscles. Typical symptoms are painful cramps in the leg, very often in the calf muscles, after a limited distance of walking. The pain disappears quickly after a short rest.

The usual explanation of these phenomena (1,2) is that the lack of oxygen supply keeps the muscles in an anaerobic condition, even in light exercise. This, combined with the insufficient waste removal due to the low blood flow, leads to an accumulation of acid byproducts which results in the typical pain, which may be interpreted as a fast and acute form of fatigue.

The process of muscular fatigue has been extensively investigated by means of electromyography. It is commonly observed (3) that a sign of fatigue is a decrease of the mean or median frequency of the EMG power spectrum. This effect may be explained by a slowing down of the conduction velocity of the muscle fibres due to an increasing intramuscular acidity (lower pH).

On the above grounds a marked effect on the EMG median frequency would be expected in the course of an exercise leading to claudication.

METHODS

Subjects, procedure

The subjects were two male patients, aged (1) 62 and (2) 75, who took part in walking exercise program (4). They walked together with one of the investigators up and down a 25 m

corridor, paced at a speed of 6 km/h and a stride frequency of 1.0 stride/s (120 steps/min). Under the circumstances of this walking test, the distance until claudication is reproducible within 25 m. It amounted to 200 and 500 m for subjects 1 and 2, respectively.

Instrumentation

Surface EMGs of MM. soleus, gastrocnemius medialis and gastrocnemius lateralis and goniometer angles of ankle and knee were recorded from the leg that showed the strongest claudication effects. The signals were transmitted by an FM telemetry system (5) that allows transmission of the "raw" EMG signals (30-600 Hz), stored on tape, AD converted and processed afterwards on a PC with ASYST software. Single EMG bursts in walking were sampled over 512 points at 1024 Hz. Power spectra and median frequency were obtained by FFT over these epochs.

RESULTS

The angular movements of ankle and knee did not change noticeably in a bout of walking until claudication (Fig. 1a). Neither was this the case for the EMG linear envelope (Fig. 1b).

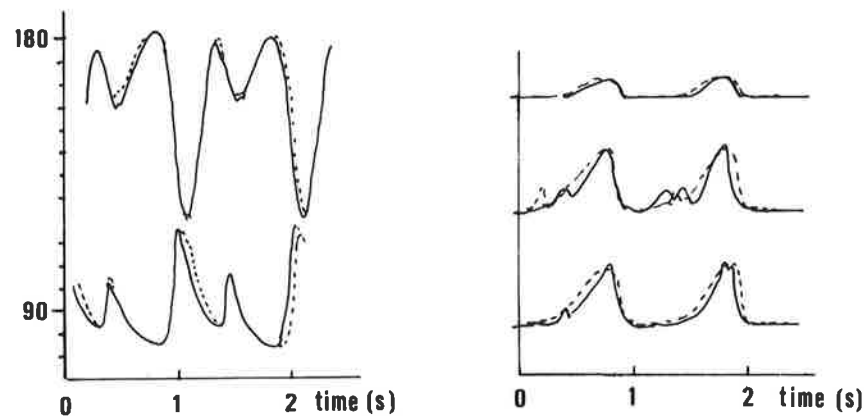


Fig. 1a. Knee angle (upper) and ankle angle (lower) of steps 2 and 3 (solid) superimposed by the 4th and 3rd step before the walk had to be terminated because of claudication pain. Fig. 1b. Envelopes of rectified EMG of (from top to bottom) mm. soleus, gastrocnemius medialis and gastrocnemius lateralis for the same steps as Fig. 1a. The main difference between solid and dashed curves in both figures is the duration of the second step.

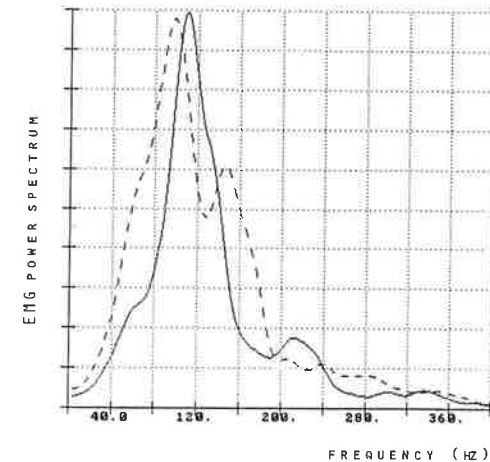


Fig. 2. Power spectrum of m. gastrocnemius medialis of subject 1 at the onset (solid) and in the final stage (dashed) of walking until claudication. Spectrum smoothed over 20 Hz in the frequency domain.

Figure 2 gives the EMG power spectra of m. gastrocnemius medialis for two steps, one from the beginning of the walk and one from the stage when claudication pain was already severe, just before the walking had to be interrupted. For all three muscles the median frequencies at the same two steps have been given in Table 1.

TABLE 1

MEDIAN FREQUENCY (Hz) OF CALF MUSCLES AT BEGIN OF EXERCISE AND JUST BEFORE STOPPING DUE TO CLAUDICATION. SUBJECT 1

muscle	begin	end	% change
soleus	191	173	- 10%
gastrocnemius med.	115	110	- 5%
gastrocnemius lat.	117	95	- 20%

DISCUSSION

The effects of claudication, drastic as they may be to the patient, are hardly reflected in the EMG or the gait registrations. The present results can only be preliminary, therefore. Either a more refined analysis may reveal slight but

significant changes, or the absence of these should be confirmed in a much larger number of patients.

Possible changes in the walking pattern are so slight that they do not change the sagittal leg movements (Fig. 1a) or the calf muscle EMG envelope (Fig. 1b). As a consequence, the force and work output of these muscles will not have changed in the process of increasing claudication complaints (6). One might have anticipated that the muscles would have reduced their output, to be taken over by other muscle groups. Important in this respect is, however, that our patients were paced, they were not allowed to slow down as the pain came up.

The shifts in EMG median frequency (Fig. 2, Table 1) are minor, from 5 to 20%. The standard error in the median frequency can be estimated at 10% for these short epochs. Whether the spectral changes are significant therefore remains questionable, although a detailed analysis may show more conclusive results. A number of factors may have contributed.

First, the calf muscles largely consist of slow oxidative muscle fibres and therefore may not show the EMG-fatigue effects as pronounced as muscles of a mixed fibre composition. Second, in the few studies of others on EMG spectral changes in dynamic contractions, these effects were less than those reported for the usual static endurance experiments. This may be attributed to the rise of temperature in working muscle, which causes an increase of conduction velocity, that counters the decrease due to a lowering pH (7). There are, finally, indications that calf muscle pH shows only a minor decrease during exercise in healthy subjects and patients with a mild degree of claudication (2).

REFERENCES

1. O'Donnell TF (1975) *Lancet* 2:533
2. Hands LJ, Bore PJ, Galloway G, Morris PJ, Radda GK (1986) *Clin. Science* 71:283-290
3. De Luca CJ (1986) *CRC Crit. Revs. Biomed. Eng.* 11:251-279
4. Andriessen MPH (1986) Thesis (in Dutch) State University Groningen
5. Hof AL, Bonga GJJ, De Pater L and Swarte FGJ (1987) Abstract XI Congress of Biomechanics
6. Hof AL, Geelen BA, Van den Berg JW (1983) *Journal of Biomechanics* 16:523-537
7. Petrofsky JS (1979) *Eur. J. Appl. Physiol.* 41:1-15

AN ALL-POLES MODEL FOR THE STUDY OF THE MUSCULAR SOUND

MARISA MARANZANA-FIGINI, ANTONINO PIZZINO, BERTRAND DIEMONT

Centro di Teoria dei Sistemi CNR, Dipartimento di Elettronica, Politecnico di Milano, Milan (Italy)

INTRODUCTION

The contracting muscle generates sound. Although this phenomenon was known more than one and a half century ago, only recently /1/ its study has been resumed leading to a number of questions concerning the nature of this signal which are still open.

A compared spectral analysis of the Sound MyoGram (SMG) and the EMG Signal /2/ has shown that at low contraction levels the SMA spectral density distribution is unimodal and very narrow. These findings suggest to describe the SMG signal following a time series approach.

Aim of this work is to model the SMG by means of an Autoregressive (AR) model and to compress the information into the poles which can be derived from the estimated AR parameters.

This approach allows modelling of the system considered, independent of the knowledge of the internal physical mechanisms, taking into account only the output of the System (the SMG signal). As input a white noise is postulated. Any temporal epoch of the SMG is seen as part of a realization of a stochastic process.

MATERIAL AND METHODS

The SMG Signal

The study has been carried out on 7 male subjects (age 22-24 years). The angle between arm and forearm was maintained between 90° and 115° in order to ensure activation of the arm flexors only. The force was measured by a strain gauge and trasduced into an electric signal in order to provide visual feedback to the subject. The contraction level was 20% Maximum Voluntary Contraction (MVC): no fatigue was present. The SMG signal was recorded by a contact sensor (HP 21050/A; bandwidth 0.02 - 2000 Hz) located on the Biceps Brachii belly by means of a sphigmomanometer. After amplification (HP 8802/A) and low-pass filtering at 100 Hz, the signal was sampled at 1024 Hz because of constraints set by the surface EMG signal which was contemporary recorded. Three phases were considered: rest before the contraction, activation of the muscle, rest after the contraction. Epochs of 2s were digitized for each phase, corresponding to 2048

points records. A number of epochs from 13 to 19 were memorized for the active period and only 3 to 4 for the rest period.

Signal Processing

The signal sample sequence is considered as part of a realization of a stochastic process; of this process the dynamic representation (1) is given:

$$y(t) = \sum_{i=-\infty}^t W(t-i) \xi(i) \quad (1)$$

where $\xi(t)$ is the white noise, $W(\cdot)$ the impulse response of the system, $y(t)$ the signal.

In practice $W(\cdot)$ is replaced by the transfer function $G(z)$ of a discrete dynamic system /3/

In this work the AR class of models was selected which describes the signal as follows:

$$y(t) = a_1 y(t-1) + a_2 y(t-2) + \dots + a_n y(t-n) + \xi(t)$$

with a_i the AR parameters, n the order of the model.

The transfer function $G(z)$ becomes (2). The poles p_i of $G(z)$ can be obtained from the AR parameters, yielding (3).

$$G(z) = \frac{z^n}{z^n - a_1 z^{n-1} - \dots - a_n} \quad (2) \quad G(z) = \frac{z^n}{(z-p_1)(z-p_2)\dots(z-p_n)} \quad (3)$$

A crucial point in this approach is the selection of the optimal model order. This was done by means of three criteria and the Final Prediction Error (FPE), Akaike Information Criterion (AIC), Rissanen (RIS) /4/. The Anderson and Portmanteau tests were adopted to check the whiteness of the residual.

RESULTS

The first record of the rest phase before activation; the first, the central and the last record of the active phase; the first record of the rest phase after activation have been processed. The main problem was to find the appropriate sampling frequency to compress into few parameters (low AR model order) the useful information of the SMG signal. Identification was carried out for the original time series s_0 and for s_1 and s_2 obtained by discarding one sample every 10 and 20 samples, respectively.

The optimal model order for s_0 was higher than 30; this confirmed oversampling of the original signal. For s_1 the model order was generally 4 and for s_2 a second order model was found to be the optimal AR model.

Fig. 1 shows the position of one of the two complex conjugate poles of the AR(2) model in the complex plane, in the case of one subject for different epochs (Fig. 1a) and of all the subjects for the first epoch of the active phase (Fig. 1b), respectively. The frequency corresponding to the position of the 2 complex conjugate poles in the complex plane ranges from 8.6 Hz to 9.8 Hz for the first epoch of the active phase in all subjects while the average value of all active phases ranges from 8.5 Hz to 10.7 Hz.

In the rest phase the AR(2) model is not the optimal model. A much higher model order is requested to identify the signal in this phase. The poles of the AR(2) model are real (Fig. 1a: poles 1 and 18). The dynamic of the signal in this case is much more complex than that of the SMG signal in the active phase (Fig.1a: poles 4, 10, 17).

DISCUSSION AND CONCLUSION

After careful selection of the sampling frequency, parametric identification of the SMG signal has been carried out adopting the AR model class. Corresponding to a sampling frequency of 51 Hz, the AR(2) model was found to be the optimal model for the signal during the active phase, whereas a much higher

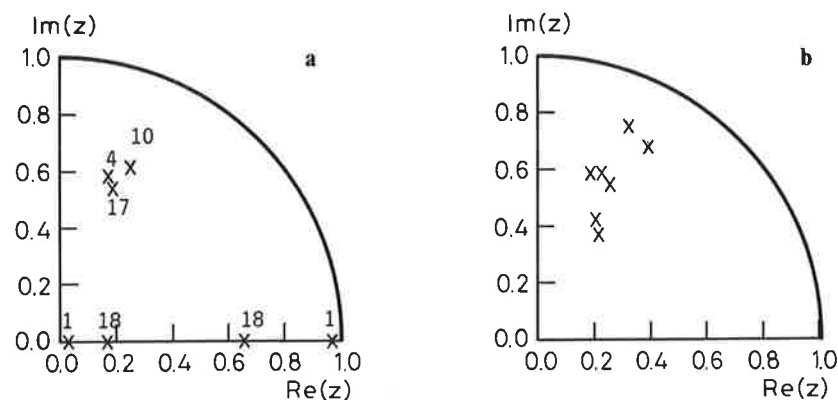


Fig. 1 - Poles of the AR(2) model: epochs 4, 10, 17 of the active phase and 1 and 18 of the rest phase in the case of one subject (a); first epoch of the active phase for all 7 subjects (b).

model order, different from one record to the other and from one subject to the other, was required for the rest phase.

From the AR parameters the two complex conjugate poles were computed allowing estimation of the related frequency in the active phase. When all the subjects were considered, a very low variability was found (<7%) for the frequency which ranged from 8.5 Hz to 10.7 Hz. The voluntary contraction level of 20% MVC was selected in this work in order to refer to a well-established pattern of fibre activation. It is known that at 20% MVC the firing frequency of the activated motor units ranges from 8 Hz to 18 Hz (fibre type I).

The study of the pole location has led to results which confirm the findings of /2/. However the methodology adopted here yields a better representation of the dynamics of the SMG signal. This seems particularly fit to investigate the phenomenon of fatigue /5/ and changes in the motor unit activation pattern corresponding to different contraction levels, which involve type I or/and type II fibers.

In conclusion the results of this work allow to state that parametric identification of the SMG yields a very efficient compression of the signal information by means of the position of the poles computed from the estimated AR parameters.

ACKNOWLEDGEMENTS

The authors wish to thank Prof. A. Veicsteinas and his Research Group, at Istituto di Fisiologia Umana, Facoltà di Medicina e Chirurgia, Università di Brescia, Italy, for allowing use of the SMG data.

REFERENCES

1. Oster G. (1984) Muscle sounds Scientific American 3: 250-260
2. Diemont B., Maranzana-Figini M., Orizio C., Perini R., Veicsteinas A. (1986) Compared Spectral Analysis of Muscular Sound at Fatigue IEEE/Eighth Annual Conf. of the Engineering in Medicine and Biology Society Dallas USA Nov. 1986 3: 3022-3024.
3. Bittanti S. (1981) Parametric Identification (in Italian) CLUP Milan Italy
4. Maranzana-Figini M., Molinari R., Sommariva G. (1984). The parametrization of the electromyographic signal: an approach based on simulated EMG signals Electromyog. Clin. Neurophysiol. 24: 47-65.
5. Paiss O. and Inbar (1987) G. Autoregressive Modeling of Surface EMG and its Spectrum with Application to Fatigue IEEE Transactions on Biomedical Engineering MBE-34 : 761-770

A STUDY OF FATIGUE BY THE CROSS SPECTRUM OF MUSCULAR SOUND AND SURFACE EMG

B. DIEMONT^o, M. MARANZANA FIGINI^o, C. ORIZIO^{oo}, R. PERINI^{oo}, A. VEICSTEINAS^{oo}

^o Centro di Teoria dei Sistemi, Dipartimento di Elettronica, Politecnico di Milano, Milan, Italy

^{oo} Istituto di Fisiologia Umana, Facoltà di Medicina e Chirurgia, Università di Brescia, Brescia, Italy

INTRODUCTION

It is known since the nineteenth century that the contracting muscle produces a sound in the low frequency range. In more recent studies Oster and Jaffe (4), using the autocorrelation method, observed that the dominant frequency of the SoundMyoGram (SMG) during isometric contraction is about 25 Hz. In similar experimental conditions the mean frequency was found to be about 15 Hz at the Maximal Voluntary Contraction (MVC) (5) and about 11 Hz at 20% MVC (3).

When fatigue is monitored by means of the Power Spectrum Density (PSD) of the Surface ElectroMyoGram (SEMG), possible changes in the Motor Unit (MU) activation pattern are difficult to retrieve. This information is confined in the low frequency range, where it is masked by the information concerning the morphology of the MU potential. The mechanical nature of the SMG is probably related to dimensional changes of the activated muscle fibers. Its PSD can therefore provide an additional tool to study the firing mechanisms of the two types of MUs, whose firing frequencies range from 8 to 18 Hz and from 15 to 30 Hz, respectively.

Aim of this work is to study the activation pattern at fatigue by means of the behavior in time of the mean frequency of consecutive recordings of SMG and SEMG, and the Cross Spectrum of SMG and SEMG of the same consecutive recordings.

MATERIAL AND METHODS

Experimental procedure

Seven healthy sedentary male subjects (age 22-26) volunteered for this study. A contact sensor transducer (HP 21050A, bandwidth 0.02-2000 Hz) was placed on the belly of the right biceps brachii, using a sphygmomanometer cuff, for the detection of the SMG signal. The SMG signal was amplified, low pass filtered at 100 Hz and recorded. The SEMG signal was recorded with a bipolar electrode placed immediately above and below the contact sensor. The SEMG signal was amplified and low pass filtered at 400 Hz. Because of the system memory

limitation, only 2 out of every 4 seconds of activity were acquired with a sample frequency of 1024 Hz.

Each subject performed an isometric contraction at 80% of his MVC up to exhaustion, maintaining a constant angle of 115° between arm and forearm by means of visual feedback. If the resulting variations were larger than $\pm 1\%$, the experimental data were discarded.

Spectral analysis

Two methods have been adopted to estimate the Power Spectrum Density (PSD):

1. Fast Fourier Transform (FFT). First the periodogram was obtained by FFT from the sampled signal; by inverse FFT the AutoCorrelation Function (ACF) estimate was computed. The ACF was multiplied by a Papoulis window to increase statistical stability and again transformed to yield the final PSD estimate.
2. Maximum Entropy Spectrum Estimation (MESE). The applied MESE method has been developed according to Burg's algorithm (2). This method suggests that the estimated ACF should be predicted beyond the data limited range. The principle used for this prediction process is that the PSD estimate must be the most random, i.e., must have the maximum entropy of any power spectrum which is consistent with the sample values of the ACF. The objective is to add no information as a result of the prediction process. The MESE method is equivalent to the least squares fitting of an autoregressive model to the process.

A relevant problem is the choice of the order of the model. In general a low order model results in a global PSD estimate and is biased by the highest peaks; a high order model results in a peaky PSD estimate of which the peaks may be spurious. The selected optimal order was appointed by the middle one of the three adopted criteria: the Final Prediction Error, the Akaike Information Criterion and the Rissanen Minimum Length.

To describe adequately the SMG and the SEMG signals and to determine the behavior of the consecutive records, the mean frequency was calculated from the PSD estimates. The PSD of the SMG and the SEMG signals as well as the Cross Spectrum were estimated.

RESULTS AND DISCUSSION

Spectral analysis of SMG

The PSD estimates of consecutive recordings of the SMG signal from the onset of contraction up to fatigue of a representative person are shown in Fig. 1. The

optimal order of the MESE model found by the criteria ranged from 4 to 6. The presence of information in the 1 to 4 Hz range of the PSD estimates is due to this low optimal order. The amplitude in this range can be reduced by increasing the model order, while the frequency parameters of interest will not be influenced significantly.

The trend of the mean frequency of the SMG signal of all seven subjects is shown in Fig. 2-top. The average value of this parameter is depicted by the solid line and it can be seen that it is increasing from 10 to 40% of the total time, it is decreasing between 40 and 80% and levels off when exhaustion is approaching. This general trend can also be seen in the 2 SMG spectra of Fig. 1.

Spectral analysis of the Cross spectrum

The PSD estimates of consecutive recordings of the Cross spectrum of SMG and SEMG are shown on the right hand side of Fig. 1. In time the Cross spectrum becomes more enriched, the frequency band is embroadening and finally shifts towards the lower frequencies. The great amplitude of the 16 Hz peak of the fifth epoch masks the presence of information in other frequency bands.

The trend of the mean frequency of the Cross spectrum (solid line in Fig. 2-bottom) is similar to that of the SMG autospectrum. However, the trend of mean frequency of the SEMG is decreasing in time from the onset of contraction in accordance with the literature (1). The relative variation of the mean frequency for both SMG and Cross spectrum from onset of contraction up to exhaustion is about 20%, while it is about 35% for the SEMG spectrum.

Many phenomena are related with muscular fatigue, like increasing MU frequency discharge, MU synchronization and reduction of conduction velocity (1). The time at which these phenomena occur and their relative influence on both SMG and SEMG, because of their different nature, can explain the different trends of the spectra of the two signals in time.

We have found that the related bandwidth is present in the low frequency range, where in the SEMG spectrum the information of firing frequency is masked by the information concerning the morphology of the MU potential. This result and the similarity between the Cross spectrum and the SMG spectrum suggest that the latter could contain the major part of firing pattern information. In conclusion we suggest that the SMG spectrum can be used to follow the firing pattern changes during sustained contraction.

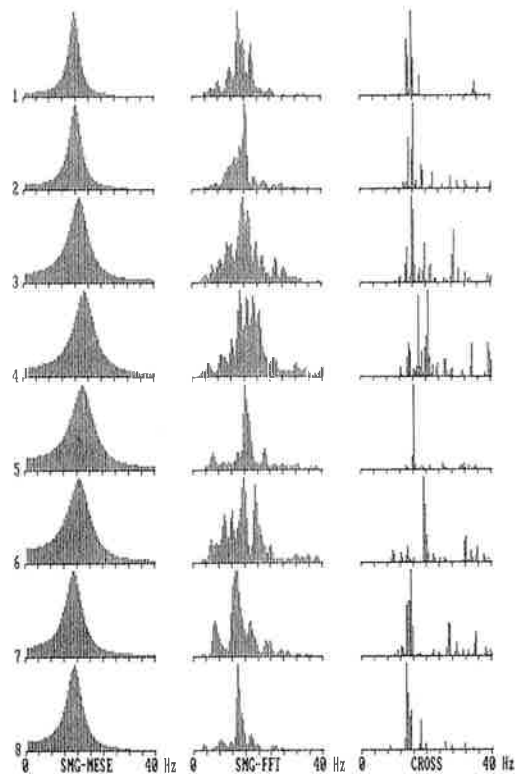


Fig. 1. Spectra of consecutive recordings from the onset of contraction up to exhaustion of a representative subject: Left: spectrum of SMG (optimal order MESE) Middle: spectrum of SMG (FFT) Right: cross spectra of SMG and SEMG (FFT)

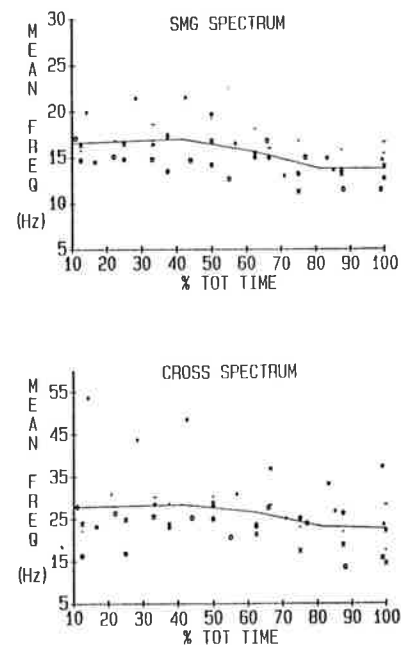


Fig. 2. Trend of the mean frequency in time from the onset of contraction up to exhaustion of all subjects for SMG (top) and cross spectrum (bottom).

REFERENCES

1. Bigland Ritchie B, Woods JJ (1984) Changes in muscle contractile properties and neural control during human muscular fatigue. *Muscle & Nerve* 7:691/699
2. Burg JP (1975) Maximum Entropy Spectral Analysis. Ph.D. Dissertation, Dept. of Geophysics, Stanford University, Stanford California
3. Diemont B, Maranzana Figini M, Orizio C, Perini R, Veicsteinas A (1987) Correlated spectral analysis of EMG and muscular sound for the study of motor unit firing pattern. Proc. of the IEEE/IEBS 9th Annual Conference, Boston
4. Oster G, Jaffe JS (1980) Low frequency sounds from sustained contraction of human skeletal muscle. *Biophys. J.* 30:119/128
5. Rhatigan BA, Kenneth CM, Lomsdale E, Stern LZ (1986) Investigation of sounds produced by healthy and diseased human muscular contraction. *IEEE Trans. Bio. Eng.* BME 33:967/971

Surface EMG in occupational health studies

SURFACE ELECTROMYOGRAPHY IN WORK-PHYSIOLOGICAL FIELD STUDIES FOR THE ANALYSIS OF MUSCULAR STRAIN AND FATIGUE

ALWIN LUTTMANN, MATTHIAS JÄGER, WOLFGANG LAURIG

Institut für Arbeitsphysiologie an der Universität Dortmund
Ardeystr. 67, D-4600 Dortmund 1, Germany (Fed. Rep.)

INTRODUCTION

Work-physiological field studies conducted at actual workplaces are essential for practice-oriented research in occupational health. The classical indicators of stress and strain used in work physiology, such as energy expenditure and heart rate, are adequate measures where large muscle groups are involved and a clear increase in energy expenditure and cardiovascular activity is consequently induced. If, on the other hand, only individual muscles or small muscle groups are active (for example, in assembly work), a method should be employed which allows the local strain of these particular muscles to be measured. Electromyography is suitable for this purpose. This method has been developed to such an extent in recent years that it can be employed under field conditions for investigations covering whole shifts as well as in the laboratory [1,2].

METHOD

A schematic diagram of the concept and the equipment designed for application in work-physiological field studies is shown in fig. 1. Both the electromyograms (EMG) of relevant muscles and the electrocardiogram (ECG) are derived from the subject with the aid of adhesive surface electrodes. After amplification the signals are sent to a receiver using a portable transmitter and are recorded on a magnetic tape. Evaluation of electromyograms requires a precise workload protocol regarding the person's activity and knowledge of the sequence of operations. The protocol is produced by an observer who uses a numerical keyboard to input the activity of the

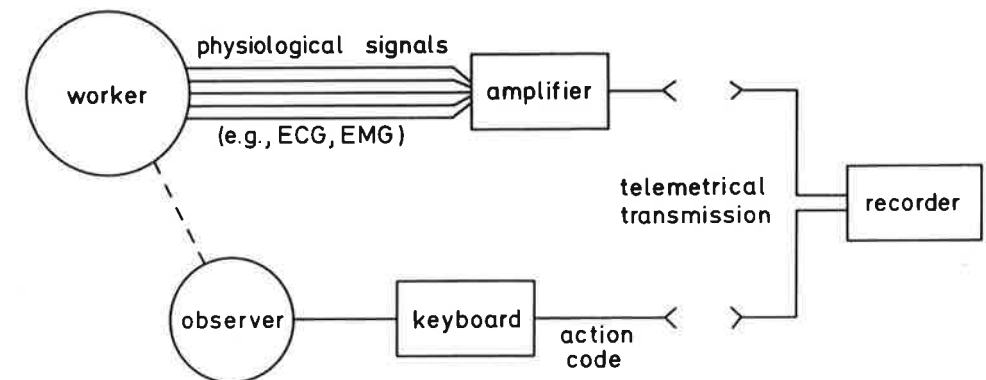


Fig. 1. Schematic diagram of a telemetrical measurement method for application in work-physiological field studies

subject according to a predetermined code. This action code is transmitted to the recording station and recorded parallel to the physiological data. The code signal enables, for each point in time, recording of the important load values, such as for posture, the person's activity, and the type and mass of the objects moved by the person, and comparison with the physiological reactions.

APPLICATION OF ELECTROMYOGRAPHY

Determination of muscle strain

The application of electromyography in field studies will be demonstrated taking an example from a weaving mill [3]. The activity under examination is termed creeling. The worker has the task of lifting bobbins with a mass of about 10 kg out of a transporter and placing them in a so-called beamer on pegs positioned at a height of between 30 and 190 cm. The electromyograms were derived for both arms from the biceps muscle and the finger flexor. The original recording of 2 sections, each lasting about 3 minutes, is shown in fig. 2. The time lapse between the sections amounts to about half an hour. The so-called Electrical Activity (EA) is derived from the electromyograms by means of rectification and subsequent continuous averaging. The lower trace provides an example of such EA for the left finger flexor. The markings below the recordings denote sections in which a bobbin is lifted. The time and duration of these lifting periods are determined using the action code. In the sections shown in fig. 2 the highest EMG-amplitudes, and therefore the highest strain for all the examined muscles, occur during lifting. Comparison between the left and right portions of fig. 2 shows that the peak values of EA are higher in the second section than in the first, even though the same activity was involved. Such an increase in EA for similar load indicates tiring of the muscle under examination in the course of the activity.

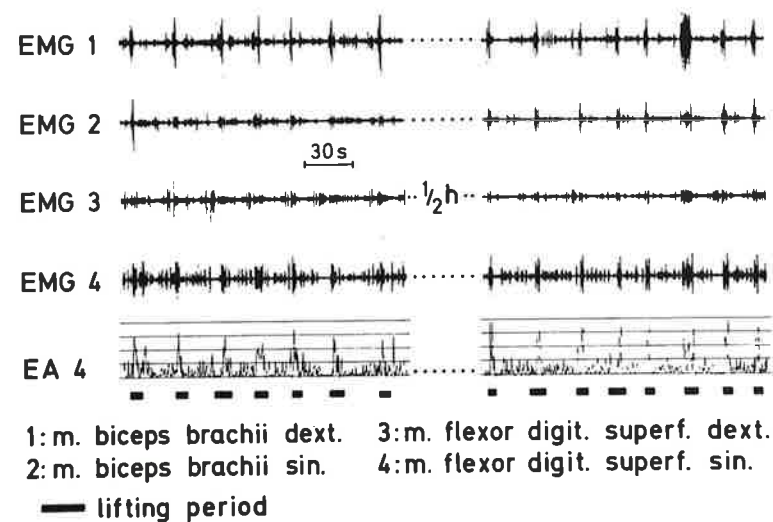


Fig. 2. Original recording of electromyograms (EMG) and Electrical Activity (EA) taken during the pegging of bobbins in a weaving mill

Determination of muscle fatigue

Fig. 3 shows the evaluation of a shift section lasting about 50 minutes in which bobbins were continuously moved. Two activity sections can be observed in alternation: transfer and pegging. In the transfer stage the bobbins are loaded from a large transport container into a smaller one. In pegging the bobbins are taken out of the small container and positioned in the beamer. The number of bobbins pegged per unit of time, this acting as a measure of working speed, is shown in the lower section of fig. 3. After reaching a maximum in the second section, working speed decreases as time progresses. The highest values for heart rate (middle diagram) are reached during transfer. During pegging the heart rate follows, to a large extent, the course for working speed, that is to say,

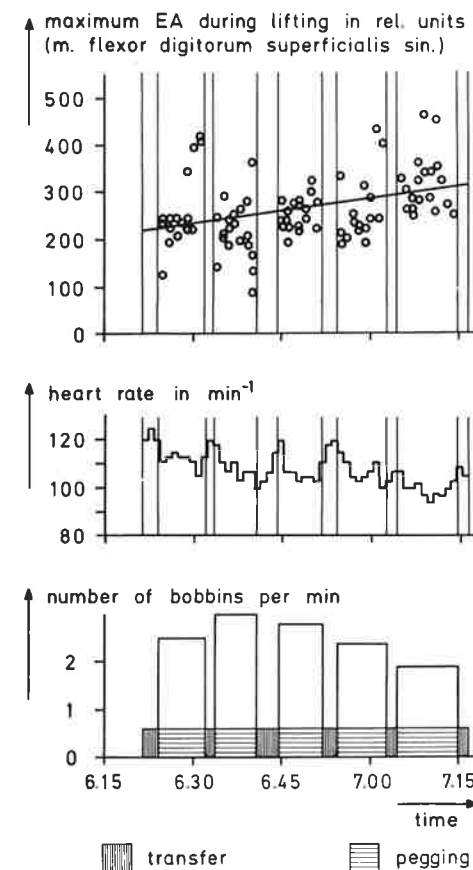


Fig. 3. Time courses for working speed (lower) and heart rate (middle), and the peak values of Electrical Activity for the left finger flexor (upper) during the creeling of bobbins

like working speed it decreases as time progresses. The upper portion of fig. 3 shows an evaluation of the Electrical Activity for the left finger flexor. From the EA time courses, examples of which are presented in fig. 2, the maximum was established for each lifting period and shown as a dot in fig. 3. As time progresses, the EA peaks become larger in spite of the activity remaining the same and the working speed actually falling. Both the increase in EA and the decrease in working speed indicate that muscle fatigue occurs and that the activity can only be carried out for a limited period of time. In fact, the person in this example stopped working after about 50 minutes and took an arbitrary break. In a similar manner a total of 11 activity sections were examined for 3 persons and the increase in EA and the duration of continuous activity were established in each case.

In fig. 4 a comparison with earlier laboratory studies was undertaken in order to examine whether termination of the activity could be explained by muscle fatigue. In this reference was made to a connection between an increase in EA and endurance time as determined by Laurig [4,5]. The laboratory findings are indicated by the open symbols, the regression line, and the confidence interval. In fig. 4 the value pairs for EA-increase and duration of continuous activity

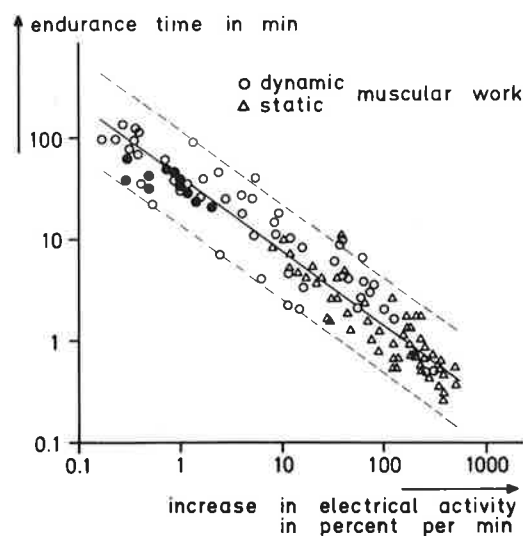


Fig. 4. Connection between length of continuous activity and increase in Electrical Activity (extended version of a diagram taken from Laurig [4,5]) closed symbols: field-study data [3] open symbols: laboratory data, for ref. s. [6]

CONCLUSIONS

Electromyography is a suitable method for measuring the local muscle strain in work-physiological field studies. A telemetrical procedure, in which an action code is recorded parallel to the physiological variables, has proven itself in field studies. The level of Electrical Activity (EA) permits quantification of muscle strain. A time-related increase in the EA in spite of continuity in the activity serves as an indicator of fatigue. The steepness of rise permits prognoses regarding the maximum duration of work. The example taken from the weaving mill shows how findings from field studies can be used in the planning and design of work according to ergonomic criteria.

REFERENCES

1. Ballé W, Smolka R, Luttmann A (1982) *Zbl Arbeitsmed* 32:214
2. Luttmann A, Laurig W (1986) In: Schäcke G, Mayer P (eds) *Berufliche Schädigung des Nervus ulnaris*. Haefner, Heidelberg, pp 75-84
3. Luttmann A, Kylian H, Laurig W, Jäger M (1985) *Arbeitsmed Sozialmed Präventivmed* 20:261
4. Laurig W (1974) *Beurteilung einseitig dynamischer Muskelarbeit*. Beuth, Berlin
5. Laurig W (1975) In: Komi PV (ed) *Biomechanics V-A*. University Park Press, Baltimore, pp 219-230
6. Laurig W, Luttmann A, Jäger M (1987) In: Asfour SS (ed) *Trends in Ergonomics / Human Factors IV*. Elsevier, Amsterdam, pp 685-692

derived from the field study are shown as closed symbols. Since the values lie near to the regression line it can be assumed that the termination of the activity really is a result of muscle fatigue. Consequently, in order to prevent damage to health, the breaks which have hitherto been taken arbitrarily should be legalized and a system of breaks ensuring that the length of working sections does not exceed 40-60 minutes should be introduced.

The investigations presented here apply to bobbin masses of approximately 10 kg. The maximum duration for continuous activity will presumably decrease when bobbins of greater mass are used. According to a recently performed estimate [3,6], a shortening of the working sections to less than half is to be expected as a result of increasing the bobbin mass to 15 kg.

QUANTITATIVE AND QUALITATIVE ELECTROMYOGRAPHY IN THE EVALUATION OF ERGONOMIC MEASURES

BENGT JONSSON

Work Physiology Unit, National Institute of Occupational Health, Box 6104, S-900 06 Umeå, Sweden.

INTRODUCTION

Two important principles for ergonomic measures are to decrease the level of the peak loads and to avoid long lasting static muscular load. Pure static loading, i.e. continuous isometric contraction of one load level, however, is a rare occurrence in actual work situations. In reality the activity pattern is more likely to be intermittent, i.e. that there occurs variation between differing activation levels. In many jobs, however, load levels during an extended period of work seldom if ever decrease to full muscular relaxation. To the lowest level of muscular activation during the work period we may attribute the "static" component of muscular activation (5). Load levels above this static level (in a varying load level reading) may then be referred to as the "dynamic" component of muscular activation.

It has been suggested (3) that the static load level ought not to exceed 5% maximal voluntary contraction (MVC) for work tasks of long duration, and that the peak load levels ought not to exceed 50-70% MVC.

Amplitude probability distribution analysis of normalized and RMS-detected myoelectric signals will offer a possibility to quantitatively as well as qualitatively analyse the static and dynamic components of muscular activation during work and to evaluate the effects of different ergonomic measures in specific work situations. By citing examples from a few actual work situations this paper is intended to provide an illustration to the use of amplitude probability distribution analysis in ergonomic work.

METHODS

Of the neck and shoulder muscles the upper, descending portion of the trapezius muscle was examined in all studies to be presented here. In some of the studies the anterior portion of the deltoid muscle and/or the infraspinatus muscle were examined in addition to the examination of the trapezius muscle.

The myoelectric activity was recorded by means of disposable bipolar surface electrodes placed with an interelectrode distance of approximately 2 cm. The preamplified myoelectric signals were transmitted with telemetry and recorded on a multichannel tape recorder. Simultaneously with the tape recording the signals were also monitored on an oscilloscope and with an ink writer.

To facilitate a comparison of the EMG activity in a subject's different muscles and the activity in specific muscles between individuals, the EMG was normalized. A ratio, % RVC (per cent of reference voluntary contraction), was obtained, in most cases in the following way: the percentage of the EMG levels recorded during the different work tasks were calculated in relation to the activity level recorded during an isometric maximum voluntary test contraction performed for each muscle in a standardized position (1).

The amplitude distribution of the RMS-detected normalized myoelectric signals obtained during the different work tasks was analyzed by means of a microcomputer. From the amplitude distribution histograms the static, median, and peak load levels (corresponding to probability levels .1, .5, and .9, respectively) were determined (2, 3, 4).

EXAMPLES OF ELECTROMYOGRAPHIC EVALUATION OF ERGONOMIC MEASURES

Control sticks in forestry machines

One study (6) concerning the effect of redesigning the control sticks in forwarders and forest harvesters clearly showed that both the static load level and the peak load levels in the upper portion of the trapezius muscle could be substantially reduced by a fairly simple redesign of the controls (Fig. 1).

Cash registers in a post office

Another ergonomic study aimed at studying the effect of redesigning the cash registers in a post office. Ten healthy female cashiers were examined while performing a standardized work using two different types of cash registers. There were no differences in trapezius, deltoid or infraspinatus muscle activity when comparing the two different types of cash registers (Fig. 2).

Job rotation

Job rotation means that the worker is changing between different tasks as an attempt to create variations in the work situation and to reduce the effects of harmful muscular loads associated with

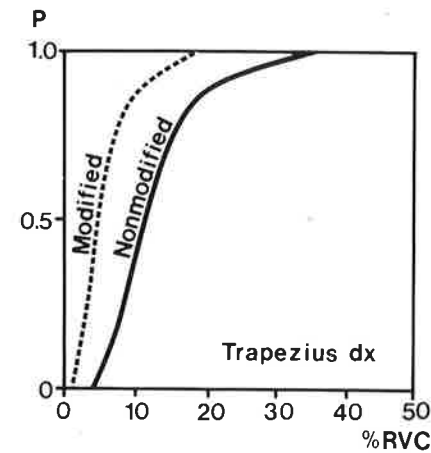


Fig. 1. Amplitude probability distribution curves from the upper portion of the trapezius muscle when operating a modified and a nonmodified forwarder. Mean of 8 subjects. Marked reduction in muscular load after the modification.

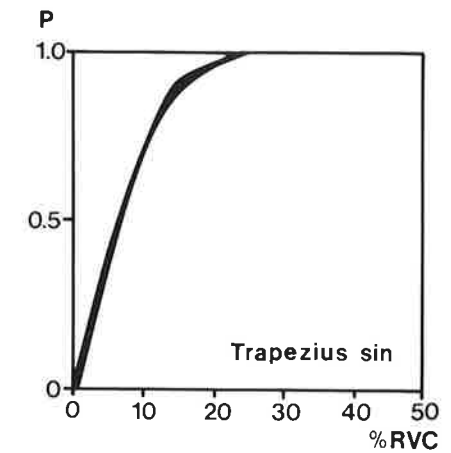


Fig. 2. Amplitude probability distribution curves from the upper portion of the trapezius muscle when working with two types of cash registers. Mean of 10 subjects. No difference in muscular load between the two job situations.

individual tasks. In a number of work situations where job rotation had been introduced the myoelectric activity in some shoulder muscles was analysed during the different tasks (5). The electromyographic results from the trapezius, infraspinatus and deltoid muscles during performance of light assembly work in electronic industries showed that there were quantitatively as well as qualitatively only minor differences in muscular activity levels between different tasks (Fig. 3). Jobs perhaps best able to benefit from job rotation seemed to be those of a more dynamic character such as mining work (Fig. 4) and glass blowing.

CONCLUSIONS

The muscle physiological effect of different ergonomic measures may be measured and analysed with myoelectric methods using amplitude probability distribution analysis to evaluate the static and dynamic components of the work performed.

REFERENCES

1. Hagberg C (1987) Electromyography and bite force studies of

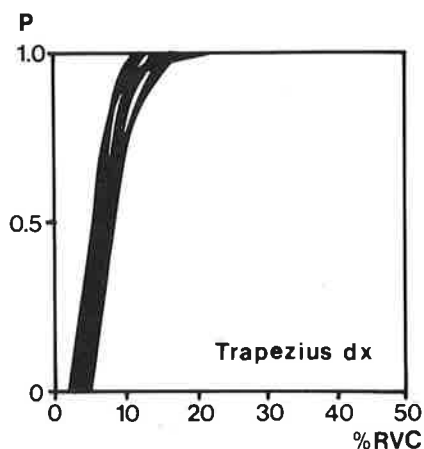


Fig. 3. Amplitude probability distribution curves from the upper portion of the trapezius muscle during seven different tasks in assembling telephones. No meaningful effect of the job rotation.

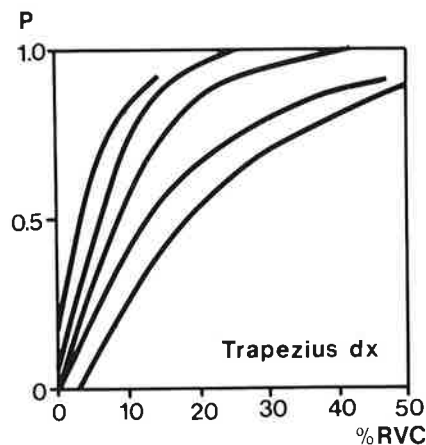


Fig. 4. Amplitude probability distribution curves from the upper portion of the trapezius muscle during five different tasks in mining work. Mean of 5 subjects. Substantial differences in muscular load between the tasks.

muscular function and dysfunction in masticatory muscles. Swedish Dent J (Suppl 37) Thesis.

- Hagberg M (1981) On evaluation of local muscular load and fatigue by electromyography. *Arbete och Hälsa*, National Board of Occupational Safety and Health, Stockholm 1981:24, Thesis.
- Jonsson B (1978) Kinesiology. With special reference to electromyographic kinesiology. *Contemporary Clinical Neurophysiology* (EEG Suppl No 34) 417-428.
- Jonsson B (1982) Measurement and evaluation of local muscular strain in the shoulder during constrained work. *J Human Ergol* 11:73-88.
- Jonsson B (1988) The static load component in muscle work. *Eur J Appl Physiol* 57:305-310.
- Jonsson B, Brundin L, Hagner IM, Coggman, I, Sondell J (1985) Operating a forwarder: An electromyographic study. In Winter DA, Norman RW, Wells RP, Hayes KC, Patla AE (eds) *Biomechanics IX-B*. Human Kinetics Publ, Champaign, pp 21-26.

INFLUENCE OF WHOLE BODY VIBRATION ON NECK AND SHOULDER MUSCLE ACTIVITY

EIICHI MACHIDA, BENGT JONSSON, ULF LANDSTRÖM AND LARS BRUNDIN

Work Physiology Unit, National Institute of Occupational Health, Box 6104, S-900 06 Umeå, Sweden.

INTRODUCTION

In many occupations the workers are exposed to whole body vibration. Many groups of drivers are exposed to whole body vibration while they are in the sitting posture. It is well known that the character and localization of sensations during exposure to whole body vibration varies both with the frequency and with the amplitude of vibration (5). On the other hand the local electromyographic reactions to whole body vibration are not well known.

The aim of the present investigation was to examine if the frequency of whole body vibration has any significant effect on the myoelectric activity in some neck and shoulder muscles in a seated subject performing precision work with one hand.

MATERIAL AND METHODS

Subjects. In ten healthy male subjects (age 22-35 years, stature 175-189 cm, body weight 66-85 kg) the upper portion of the trapezius and the anterior portion of the deltoid muscles were examined bilaterally.

Experimental procedure. The subjects were seated (upright position with the upper arms vertical and the elbow joints in 90° of flexion) on a driver's seat mounted on a vibrator (5). The seat was exposed to a marked vertical sinusoidal vibration with frequencies of 0 (no vibration), 1.5, 3, 6, 12 and 24 Hz, respectively. The level of exposure was 115 dB (relative to 1 $\mu\text{m/s}^2$). The vibration was continuously recorded with an accelerometer placed between the seat and the subject.

Each exposure had a duration of 15 minutes. The order of frequencies of vibration was selected at random. There was a 15 minutes break between each exposure. Before the onset of vibration the subject started a precision job (moving a cursor on a screen in front of the subject) by means of a joystick operated with the right hand (left hand in one lefthanded subject). The other hand

was held passively on another joystick. This precision job was performed continuously for 15 minutes. The joysticks were attached to the base of the seat and its position could be adjusted for the individual subject. The joysticks vibrated with the seat.

Electromyographic procedure. Electromyographic activity was recorded from the four muscles by disposable surface electrodes placed with an interelectrode distance of approximately 2 cm. The preamplified myoelectric signals were transmitted with telemetry and recorded on a multichannel tape recorder. Simultaneously with the tape recording the signals were also monitored on an oscilloscope and with an ink writer.

To facilitate a comparison of the EMG activity in a subject's different muscles and the activity in specific muscles between individuals, the EMG was normalized. A ratio, % RVC (per cent of reference voluntary contraction), was obtained in the following way: the percentage of the EMG levels recorded during the experiment were calculated in relation to the activity level recorded during a sustained isometric maximum voluntary test contraction performed for each muscle in a standardized position (1).

The amplitude distribution of the RMS-detected normalized myoelectric signals obtained during the experiments was analyzed by means of a microcomputer. From the amplitude distribution histograms, the static, median, and peak load levels (corresponding to probability levels .1, .5, and .9, respectively) were determined (2, 3, 4).

For each of the six examined frequencies of vibration the electromyographic analysis was performed for:

- precision job before the onset of vibration (3 minutes),
- precision job during the first 3 minutes of exposure to vibration,
- precision job during the 5th to 10th minutes of exposure to vibration,
- relaxation when still exposed to vibration (3 minutes).

RESULTS

The electromyographic activity when performing the precision job increased when the exposure to whole body vibration started (Fig. 1). There was a tendency for the myoelectric signal level to increase during the five first minutes of exposure. This tendency was most marked for exposure to 12 and 24 Hz whole body vibration.

For that reason the mean EMG activity level during the 5th to 10th minutes of exposure was used as a measure of the effect of vibration. There was usually a marked decrease in myoelectric signal level when the subject tried to relax after the precision job while still exposed to whole body vibration.

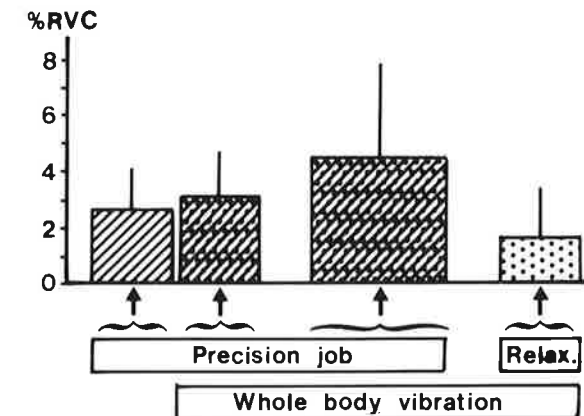


Fig. 1. Mean relative muscular load (% RVC) on the right trapezius muscle during precision job before vibration (3 minutes), and during the first 3 and the 5th-10th minutes of vibration, as well as when relaxing during exposure to vibration (3 minutes). 12 Hz whole body vibration. Mean from ten subjects.

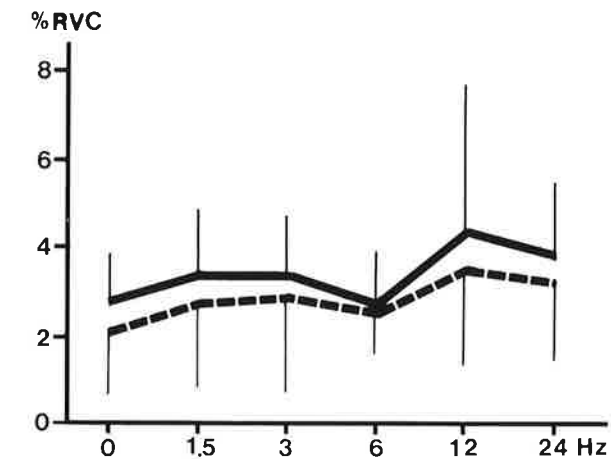


Fig. 2. Mean relative muscular load (% RVC) on the upper portion of the trapezius muscle on the "working" side (solid line) and the "passive" side (dashed line) when exposed to whole body vibration with different frequencies (0 Hz = no vibration). Mean from ten subjects.

The EMG activity during precision job with the joystick proved to be highest at 12 and 24 Hz (Fig. 2). The lowest levels of EMG activity was recorded at 6 Hz and without exposure to vibration. The effect of vibration both on the trapezius and the deltoid muscles was more pronounced on the right ("working") side compared to the left ("passive") side. The effect of vibration was quantitatively roughly the same for the static level of contraction ($P=.1$), the median level of contraction ($P=.5$) and the peak load level of contraction ($P=.9$) as that for the RMS value of the EMG signal amplitude.

REFERENCES

1. Hagberg C (1987) Electromyography and bite force studies of muscular function and dysfunction in masticatory muscles. Swedish Dent J (Suppl 37) Thesis.
2. Hagberg M (1981) On evaluation of local muscular load and fatigue by electromyography. Arbete och Hälsa, National Board of Occupational Safety and Health, Stockholm 1981:24, Thesis.
3. Jonsson B (1978) Kinesiology. With special reference to electromyographic kinesiology. Contemporary Clinical Neurophysiology (EEG Suppl No 34) 417-428.
4. Jonsson B (1982) Measurement and evaluation of local muscular strain in the shoulder during constrained work. J Human Ergol 11:73-88.
5. Landström U, Lundström R (1986) Sensations, perception thresholds and temporary threshold shifts of whole body vibrations in sitting and standing posture. Journal of Low Frequency Noise & Vibration 5:68-77.

THE EFFECTS ON EMG LOAD LEVELS OF DIFFERENT KINDS OF PAUSES IN VDT WORK

GUNNEVI SUNDELIN (1,3) MATS HAGBERG (2) ULF HAMMARSTRÖM (1)

National Institute of Occupational Health, Box 6104, 900 06 Umeå (1) and 171 84 Solna Sweden (2). Dept. of Occup. Med. Region Hospital, 901 85 Umeå Sweden (3).

INTRODUCTION

The rapid growth of office automation and the use of VDTs have given rise to several issues in the work environment. Some are connected to the operators' health while others are linked to the physical characteristics of the workplace and to the organization of the work. Limitations to the length of the work period, pauses and breaks are emphasized. Little is known about the effects of pauses on muscular load in sedentary work situations. The aim of this EMG field study was to investigate whether different kinds of pauses introduced into sedentary work have an effect on the muscular load.

MATERIALS AND METHODS

Operators

Twelve secretaries, well-trained in the use of VDT word processors volunteered to participate in the field study. Their mean age was 33.1 years, ranging from 21-48 years.

Work task

The secretaries were working at their ordinary workplaces typing from a written manuscript. They typed during three work periods lasting 30 minutes each.

Intervention

Pauses were introduced into the work every sixth minute lasting 15-20 seconds. Three kinds of pauses were introduced; passive pauses (the operator leaned backwards in the chair closing her eyes during the pause), active pauses (the operator performed pause gymnastic movements while sitting in the chair during the pause), and diverting pauses (the operator left the work place for a short walk in the corridor). No pauses were allowed other than the ones which were introduced.

EMG measurements

Electromyographic measurements were conducted during the entire typing time and during the pauses with surface electrodes connected to the right side. Three pairs of electrodes were attached; the cervical and the lateral parts of the trapezius muscle, pars descendens, and the superficial part of m levator scapulae. The surface electrodes had a contact diameter of 6 mm and an inter-

electrode distance of 3 cm. Small Medinik amplifiers with a bandwidth of 5-500 Hz were used for amplification of the myoelectric signals. The amplified signals were recorded on a TEAC R -71 tape recorder with a bandwidth of DC 1250 Hz.

Measurement of RVC

Before the EMG field recordings started, a maximal contraction force of the right shoulder elevators was performed, here called RVC (reference voluntary contraction). The measurements were made in two steps. 1) The operator performed a slow maximal shoulder elevation lasting 15 seconds in order to measure RVC. The reason for performing the shoulder elevation slowly was to avoid a jerk which could result in a muscle tear. The RVC maneuver was repeated three times in order to get a measure of the reliability. The highest value was regarded as the RVC value and the difference between the three measurements was not to be more than 10 percent to be considered reliable. 2) After the RVC measurement a slow shoulder elevation also lasting 15 seconds was performed reaching up to 30 percent of RVC. EMG activity was simultaneously recorded to get the EMG-force relationship. Thirty percent of RVC was chosen because the EMG-force relationship is approximately linear up to this level (1).

Analysis of the EMG amplitude

The myoelectric signals were r.m.s. (root mean square) detected by an AD 536A processor with a time constant of 100 ms and then A/D converted and stored on a floppy disk. The sampling frequency was 1 Hz and the number of samples per work period was thus 1800. During the RVC measurement a sampling frequency of 7 Hz was used with a time constant of 100 ms. The number of samples were 105. In the analysis of the r.m.s. detected signal, the amplitude probability distribution function, described by Hagberg 1979 (2), was used and thus an estimate of the static, median and peak muscular load could be computed. A mean of the r.m.s. values in three minute intervals was computed to get a measure of the variation of the amplitude.

RESULTS

The load levels during different percentages of the registration time in relation to the percentage of RVC are illustrated in table 1. for one of the operators. The activity during 90-99 percent of the registration time reflects the static load level, indicating that the amplitude has reached above or up to this level during 90-99 percent of the registration time. Fifty percent of the registration time corresponds to the median level and 1-10 percent corresponds to the peak load. The greatest differences are found at the peak load level, reflecting the activity during the pause.

Table 1

LOAD LEVELS

The load levels as percentages of the registration time in relation to RVC during the three periods with different kinds of pauses introduced into VDT work for one operator.

P=passive pause, A=active pause, D=diverting pause.

		Percent of RVC								
Reg.time %		trap.lat.			trap.cerv.			lev.scap.		
		P	A	D	P	A	D	P	A	D
99	stat.	0.8	1.1	1.2	0.7	0.8	1.0	0.3	0.5	0.3
90	level	3.7	4.1	3.6	5.0	6.4	7.5	3.4	3.8	3.5
50	median level	7.8	7.9	7.3	15.5	16.8	17.5	7.4	8.0	6.0
10	peak	14.1	14.5	13.4	25.5	27.2	28.0	12.4	13.7	12.2
1	level	23.2	32.1	23.4	35.2	39.5	45.1	18.5	24.1	20.0

In a previous study (3) we found no significant differences in muscular load between work periods with introduced passive pauses and work periods with spontaneously taken pauses. However, there was a significant negative correlation between the number of spontaneous pauses and static muscular load on the upper trapezius muscle. Some of the operators regarded the introduced pauses as being disturbing for their work and expressed that they would rather themselves take pauses whenever needed. In an education program in the show industry where we had emphasized the importance of pauses for reduction of the static muscular load (4), we found that changing the work organization is not easily done. A follow-up study of the program showed no changes in the pause pattern among the workers. A mean of the r.m.s. detected signal in three minute intervals during work periods with active and passive pauses are shown in figure 1. for one operator. A variation of the activity during the work period with pause gymnastic movements is more obvious than with passive pauses.

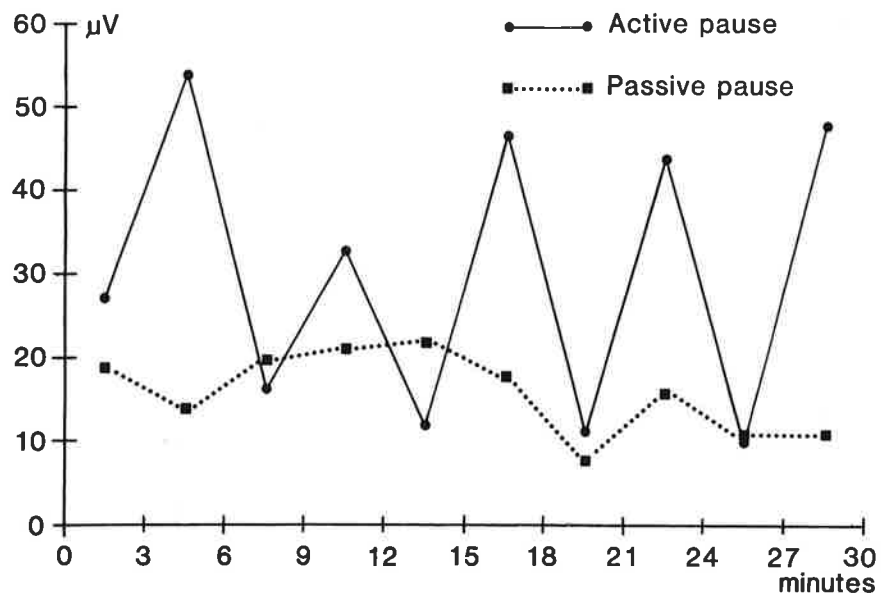


Fig 1. Mean in three minute intervals for the r.m.s. values for trapezius pars descendens, the lateral part, during work periods with active and passive pauses. Values for one operator are illustrated.

ACKNOWLEDGEMENTS

The Swedish Work Environment Fund is gratefully acknowledged for their financial support of this project.

REFERENCES

1. Chaffin D B, Lee M, Freivalds A (1980) Muscle strength assessments from EMG analysis. *Med. Sci. Sports Exercise* 12:205-211.
2. Hagberg M (1979) The amplitude distribution of surface EMG in static and intermittent static muscular performance. *Europ. J. Appl. Physiol.* 40: 265-272.
3. Hagberg M and Sundelin G (1986) Discomfort and load on the upper trapezius muscle when operating a work processor. *Ergonomics* 29:1637-1645.
4. Sundelin G, Hagberg M, Kolmodin-Hedman B (1988) Education in Ergonomics in shoe industry - Experiences and evaluations. Part III. *Arbete och Hälsa* 10:37-47. In Swedish.

EMG AND MECHANICAL PERFORMANCE DURING SHOULDER FORWARD FLEXIONS AT DIFFERENT ANGULAR VELOCITIES

BJÖRN GERDLE, JESSICA ELERT and KARIN HENRIKSSON-LARSÉN

National Institute of Occupational Health, Box 6104, S-900 06 Umeå, Sweden.

INTRODUCTION

The primary aim of this study was to analyze if the EMG of the deltoid and the trapezius muscles were dependent on the angular velocity during single or repeated dynamic maximum shoulder forward flexions.

MATERIALS AND METHODS

21 clinically healthy females (20-30 years) performed dynamic shoulder forward flexions using an isokinetic dynamometer (CYBEX II, Lumex Inc, New York). The subjects were seated in a specially constructed chair with a harness. This was used to ensure that the position adopted for the tests would be maintained throughout. Great care was taken to align the gleno-humeral flexion/extension axis with the movement axis of the dynamometer for the investigated range of motion. The arm was held with the elbow extended and the hand pronated, gripping a handle. The length of the lever arm was adjusted for each person to achieve an optimal position with an extension in the elbow joint. Electromyographic (EMG) signals were obtained from the descending part of the right trapezius and the anterior part of the right deltoid using silver-silver chloride surface electrodes (centre to centre distance 20 mm). The EMG signals and the signals from the dynamometer (torque and angle) were simultaneously recorded on a tape-recorder. For each shoulder forward flexion the following variables were determined: Peak torque (Nm), Work (Joule), the signal amplitudes (RMS) of the EMG and the mean power frequency [(Hz; i.e. mean spectral frequency) of the EMG (for details concerning the methods see: Gerdle et al. (1)].

Single maximum contractions were performed at 0, 0.52, 1.05, 2.09 and 3.14 rad/s. During the static contraction the lever arm of the dynamometer was positioned in the middle of the used range of motion (68° of shoulder forward flexion). Between each single

maximum contraction and between each step in angular velocity subjects rested 1-2 minutes.

Endurance tests consisting of 150 repeated maximum contractions were performed at 0.52 and 1.05 rad/s, respectively. The order in which the tests were performed was randomized. The two tests were performed at 2 weeks interval. Each contraction cycle started with the lever arm of the dynamometer against the thigh. After having performed a shoulder forward flexion (from 45° to 90°), subjects were instructed to relax completely and in so doing passively extend, using gravitation torque. For every 10th contraction the subjects rated their perception of muscular fatigue in their shoulder muscles using a 10-graded scale (2).

RESULTS

Single maximum contractions: Peak torque, work and the RMS of the two muscles were significantly lower at 3.14 rad/s than at 0.52 rad/s (peak torque 16%, work 30%, trapezius 25% and deltoid 7% lower, respectively). No significant change in mean power frequency occurred with increasing angular velocity in the deltoid (85-94 Hz) and the trapezius (77-88 Hz).

Repeated maximum contractions: The mechanical output (work) decreased during the first 40-50 contractions at both angular velocities (figure 1).

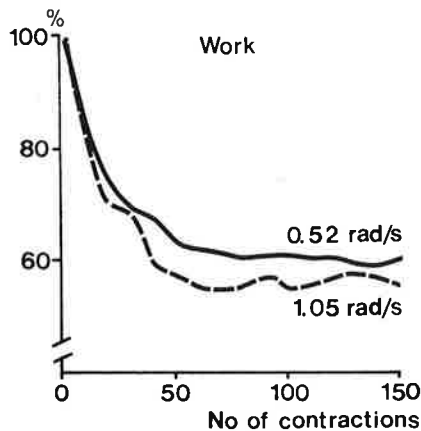


Fig. 1. Work (%) and no of contractions.

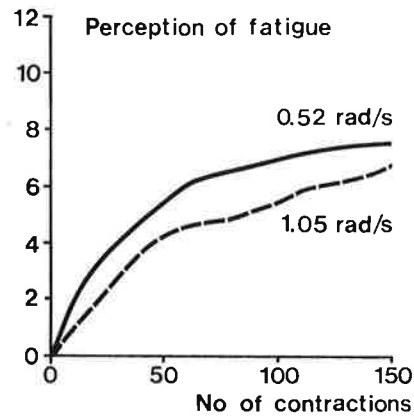


Fig. 2. Perception of fatigue and no of contractions. (10 denotes very, very strong fatigue).

Thereafter steady-state levels were established without any further significant change. The relative steady-state levels were similar for the two angular velocities. The feeling of fatigue increased throughout the tests, even though the rate of increase was fastest during the first 40-50 contractions (figure 2). The mean power frequencies of the two muscles decreased during the first 40-50 contractions at both angular velocities and then reached a steady-state level. The relative mean power frequency steady-state levels of the deltoid (0.52 rad/s: 71% and 1.05 rad/s: 70%) were lower than for the trapezius (0.52 rad/s: 78% and 1.05 rad/s: 77%).

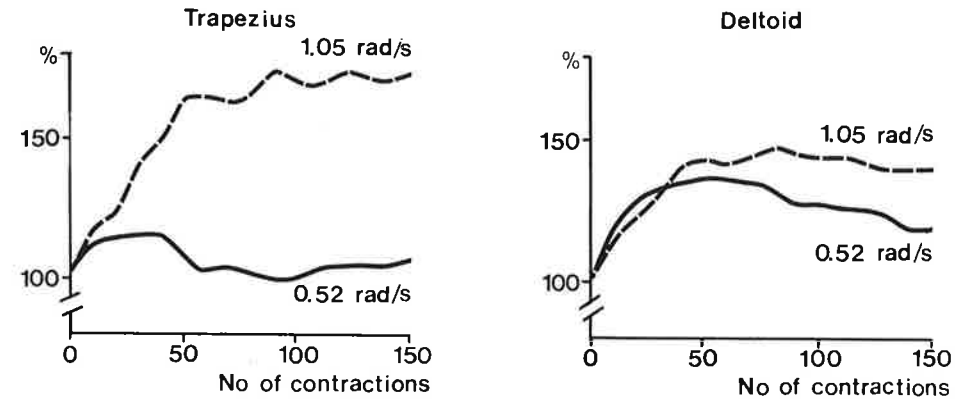


Fig. 3. RMS-values (%) of the trapezius and no of contractions

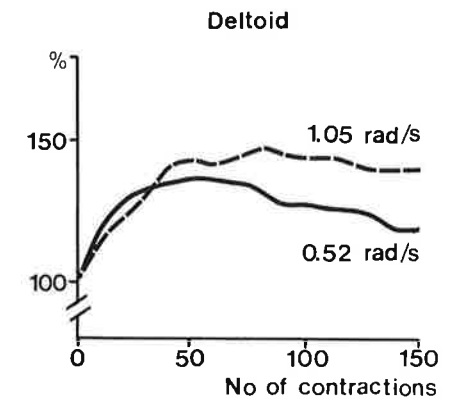


Fig. 4. RMS-values (%) of the deltoid and no of contractions.

The signal amplitudes of the trapezius and the deltoid increased during the first 40-50 contractions at both angular velocities (figure 3 and 4). At 1.05 rad/s this (increase) was followed by a steady-state level, while at 0.52 rad/s it was followed by a gradual decrease. As a consequence of this significantly higher relative levels were found between contractions no 60 to 150 at 1.05 rad/s than at 0.52 rad/s. From individual time series analyses, concerning the initial 50 contractions, it was found that the mean power frequency of the deltoid and the trapezius muscles significantly reflected muscular fatigue (i.e. decrease in work). The RMS values of the two muscles during the first 50 contractions generally had lower degrees of correlation with work.

COMMENTS

The use of EMG techniques in studies of dynamic repetitive work in different ergonomic situations has been limited. One prerequisite for an increased use of EMG techniques in field studies of dynamic contractions, for example during fatigue, is that the behaviour of the EMG with respect to the angular velocity is known. In particular, the power frequency spectrum of the EMG has to be systematically investigated in this respect. We can conclude from the present study that the mean power frequency of the deltoid and the trapezius were independent of the angular velocity during single (non-fatiguing) shoulder forward flexions. These observations agree with observations from the quadriceps femoris muscles during maximum knee extensions at different angular velocities (3).

The mechanical output during the repeated contractions followed a pattern with two phases. This has been described in muscles of the lower limb (4, 5). An important finding of the present study was that the mean power frequency, according to the individual time series analysis, was a better indicator of the decrease in work (fatigue) than the signal amplitudes of the two muscles.

REFERENCES

1. Gerdle B, Eriksson N-E, Hagberg C (1988) *Eur J Appl Physiol* 57:404-408
2. Borg G (1982) *Med Sci Sports Exercise* 14:377-381
3. Gerdle B, Wretling ML, Henriksson-Larsén K (1988) *Acta Physiol Scand*, accepted for publication
4. Gerdle B, Hedberg R, Jonsson B, Fugl-Meyer AR (1987) *Acta Physiol Scand* 130:501-506
5. Johansson C, Gerdle B, Lorentzon R, Reiz S, Fugl-Meyer AR (1987) *Acta Physiol Scand* 131:203-209

 RELATIONS BETWEEN ELECTROMYOGRAPHIC SIGNS OF FATIGUE DURING WORK
 AND OCCUPATIONAL MYALGIA IN THE SHOULDER REGION

 GÖRAN HÄGG¹ AND JAAN SUURKÜLA²
¹Department of Physiology, National Institute of Occupational Health, S-171 84 Solna, Sweden

²Industrial Health Care Unit, ABB, Box 701, S-771 01 Ludvika, Sweden

INTRODUCTION

Myalgia in the shoulder region related to monotonous strain on the muscles is today a severe problem in industrial work. The causative factors as well as the nature of these injuries are incompletely known. A widespread hypothesis is that regular local muscular fatigue during work would be an etiological factor. One method to study muscular fatigue is to measure electromyographic signs of fatigue (ESF) which appear as spectral shifts towards lower frequencies. Although a complete physiological explanation of ESF still is lacking this is one of the few measurable parameters available to study the progression of muscular fatigue during work. If the hypothesis mentioned above is true ESF may be used as a predictor of occupational myalgia.

The study presented here is a part of a larger project covering also other aspects of occupational myalgia. The project was designed as a longitudinal study of workers exposed to monotonous muscular work over two years. The EMG measurements of this project is a continuation of the work presented by Suurküla and Hägg⁴ based on short test contractions (TC:s) using zero crossing technique for the estimation of ESF, the FTC-method (Frequency analysis of Test Contractions), described by Hägg et al². Suurküla and Hägg⁴ showed that workers who already have contracted shoulder myalgia show greater ESF than healthy workers performing the same task. If the hypothesis mentioned above is true, these differences in ESF would have been found even before the injuries occurred. However, it is also possible that the injury itself is associated with more pronounced ESF. The aim of this work was to elucidate these relations.

MATERIAL AND METHODS

Subjects

The 58 subjects were all female and were recruited from a newly established assembly plant making electrical cable bundles, mainly for cars. None of the subjects had been employed for more than two years.

Measurements

Measurements were performed at the start of the project (year 0) and after 1 and 2 years. EMG was detected with surface electrodes from m. trapezius desc. and m. infraspinatus, bilaterally. The following measurements were performed:

- * TC:s every 10 minutes during ordinary work for 2 hours starting at the beginning of the working day²
- * An endurance test in the TC position driven to exhaustion.

These measurements were accompanied by a thorough medical examination of the shoulder/neck status where local as well as general muscular disorders were classified.

EMG analysis

EMG from the TC registrations was analysed according to Hägg et al² yielding a value, nz (normalized zerocrossings) for each TC. As an estimation of the mean ESF during work for each muscle the nz values were averaged as \bar{nz} . The \bar{nz} values from all four muscles were averaged as a general index, \bar{nz}_g of the mean ESF for each subject.

The EMG recordings from the endurance test were analysed with the continuous zero crossing technique according to Hägg¹ and Hägg et al². As an index of the progression of ESF the time constant of an applied exponential model according to Lindström et al³ was used.

Statistical analysis

All statistical analysis is done with Spearman's rank-order correlation as the medical variables probably are not normally distributed.

RESULTS

The correlation between EMG parameters from both the endurance test and the TC measurements from year 0 vs muscle impairment from year 0 to year 1 and 2 was analysed. No significant correlations were found.

The same kind of analysis was performed only including \bar{nz} values <1. In this case significant ($p < 0.01$) positive correla-

tion was found between \bar{nz}_g and general muscular impairment from year 0 to year 2. A corresponding analysis of \bar{nz} values >1 showed no significant relations.

The correlation between EMG parameters from year 2 and muscular disorders year 2 was analysed. Here the endurance test parameters showed no significant correlations or trends but the TC measurement parameters showed a trend towards negative correlation with muscular disorder. Of 70 possible such correlation pairs 56 showed negative coefficients. 10 of these had $p < 0.10$. The remaining 14 positive were far from significant.

DISCUSSION

The central question to be answered is whether any of the EMG parameters from year 0 can predict the muscular impairment revealed year 1 and 2. The hypothesis can be described graphically as in Figure 1 (straight line). It should be pointed out

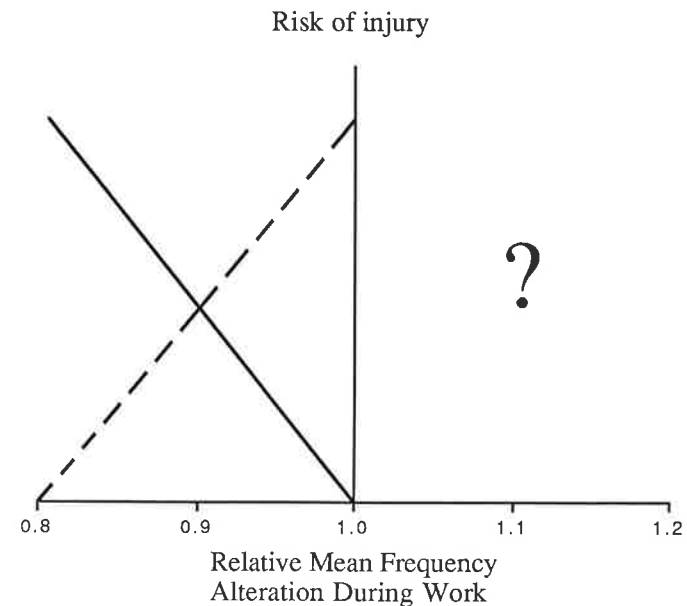


Fig. 1. Graphical illustration of the hypothesis (straight line), and indication of some of the results (dashed line).

that spectrum shifts towards higher frequencies during work which also was found by Suurkula and Hägg⁴ as \bar{nz} values >1 are not included in the hypothesis as they can not necessarily be interpreted as 'negative fatigue'. According to the results none of the EMG parameters from year 0 seem to have any predictive value for the muscular impairment, at least not when local ESF is related to muscular impairment of the same muscle. The correlation between $\bar{nz}_g < 1$ and the general muscular impairment is positive which corresponds to the dashed line in Figure 1. This finding completely contradicts the original hypothesis (straight line in Figure 1). It also suggests that \bar{nz} values >1 should not be seen as 'negative fatigue' but as some other physiological phenomenon.

Our interpretation of these results is that these muscular disorders are caused by static loads below the threshold generating ESF and that the injury is caused by the the static conditions as such independent of load level. A more dynamic working style inducing ESF may perhaps reduce the risk for injury.

The trend of negative correlation coefficients between \bar{nz} values year 2 and muscular disorders year 2 indicate the same kind of relation as found by Suurkula and Hägg⁴, however not as pronounced probably due to the fact that the relative number of severely injured subjects in this study was much less than in the former study. It is remarkable that no corresponding relations were found for the endurance time constants. It is possible that the ESF detected during an endurance test of 5-10 minutes reflects other physiological phenomena than the ESF detected with the FTC method during two hours of work.

REFERENCES

1. Hägg G (1981) Electromyographic fatigue analysis based on the number of zero crossings. Pflügers Archiv 391:78-80
2. Hägg GM, Suurkula J, Liew M (1987) A worksite method for shoulder muscle fatigue measurements using EMG, test contractions and zero crossing technique. Ergonomics 30:1541-1551
3. Lindström L, Kadefors R, Petersén I (1977) An electromyographic index for localized muscle fatigue. Journal of Applied Physiology 43:750-754
4. Suurkula J, Hägg GM (1987) Relations between shoulder/neck disorders and EMG zero crossing shifts in female assembly workers using the test contraction method. Ergonomics 30:1553-1564.

REHABILITATION

Training and evaluation in rehabilitation

EVALUATION IN REHABILITATION

G. ZILVOLD * en R. BAUMGARTNER**

* Roessingh Rehabilitation Centre & Twente University, Enschede,
(The Netherlands)

** Westfälische Wilhelms-University, Münster, (Fed.Rep.of Germany)

An understanding of rehabilitation medicine at the interface of clinical medicine and activities aimed at the restoration of functional abilities can be obtained by looking at the dynamics of disease, its consequences for life and potential interventions (1).

Disease may result in spontaneous or man-induced recovery or death. Recovery may be incomplete and leave residual impairments. Impairments may be reduced by the use of pharmacological or surgical methods. If still remaining impairments interfere with the desired level of functional ability, some form of disablement is present. Moreover a large proportion of the population will live long enough to become susceptible to the chronic diseases of later life, often resulting in some form of disability (2).

Illness-related phenomena are consequently:

disease → impairment → disability → handicap

These dimensions of the effects of disease need to be defined (3).

Wood formulated the following definitions:

Impairments: any loss or abnormality of psychological, physiological or anatomical structure of function.

Disability: any restriction (resulting from an impairment) or lack of ability to perform an activity within the range considered normal for a human being.

Handicap: a disadvantage for a given individual resulting from an impairment or a disability that limits or prevents the fulfilment of a role that is normal (depending on age, sex, and social and cultural factors) for that individual (4).

The surviving trauma victims from two world wars created an impetus for the development of medical rehabilitation services. Also changing attitudes in society have influenced the goals of rehabilitation and social policy making for the disabled. Health has come to be considered as a basic human right and disability is no longer accepted as an inevitable consequence of life (5).

The World Health Organisation defines rehabilitation as 'the combined and co-ordinated use of medical, social, educational and

tions of disorders already diagnosed e.g. in an institute for medical rehabilitation.

THE PARAMETERS TO DESCRIBE SURFACE EMG.

I. Parameters that are related to the amplitude.

Surface EMG is generally, at least with healthy subjects, a rather noisy signal. This means that the parameters that describe the properties of such a signal are basically statistical ones.

The pattern of the surface EMG of a healthy person is dominated by noisy fluctuations. The statistical behaviour of the amplitude only, can be described by means of the amplitude distribution function (a.d.f.). This function describes the chance of occurrence of each amplitude. The a.d.f. can be estimated by sampling the EMG and by constructing a histogram of the measured samples. Such a histogram is an estimation of a probability density function, if enough independent samples are taken into account.

If we consider the EMG as a superposition of many independent motor unit action potentials it can be shown mathematically that such a superposition leads to a Gaussian distribution.

In our case the expected mean value is always zero and therefore the standard deviation is the only parameter of interest to us.

Two parameters are directly related to the standard deviation. These are:

- the EMG-force gradient: EFG. This parameter provides information about the "efficiency" of force generation.

By measuring the EMG at different low forces (in order to avoid fatigue) a gradient can be defined that indicates the increase of EMG activity at the increase of force. This gradient is called the EMG-force gradient (EFG) and it is defined as the increase of the standard deviation of the surface-EMG signal divided by the increase of the isometric force. Note that in case of nonlinearly between standard deviation and exerted force this parameter is dependent on the exerted force.

RIC: the reciprocal innervation coefficient.

This parameter is related to the activity of two muscles and it is defined as the quotient of the standard deviation of antagonist activity and the standard deviation of agonist activity. Therefore the RIC provides information about the balance between the activities

of these two muscles.

II. Parameters that are related to time/frequency

Besides the statistical behaviour of the amplitude we can consider the statistical behaviour of the fluctuations in time of the EMG signal. Stochastic signal analysis shows that the estimation of the power spectrum provides relevant information. Based on our experience the median frequency and the minus 10dB frequency are the most valuable parameters.

Measuring set-up

Flexors and extensors of the forearm or leg are examined. The activity of the muscles is measured during isometric contractions (Figure 1).

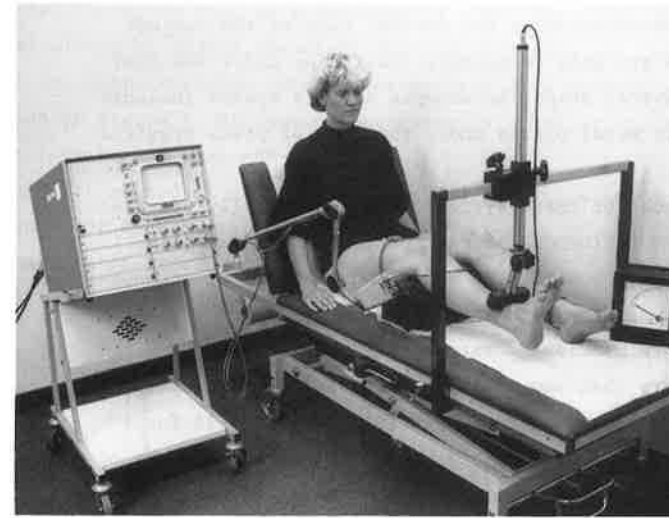


Figure 1. Measuring set up

GAIT ANALYSIS SYSTEM

Gait analysis is used at many institutes to provide a complete understanding of the aspects of locomotion. Other than the scientific approach, gait analysis is used in clinical environments to form an objective judgment on the walking capability of a patient and the progress in it during rehabilitation.

Despite the differences in methods and systems used, it is

generally accepted that for a complete analysis of gait, the following parameters should be incorporated in the measurements: 1) time and distance factors; 2) forces; 3) angles of the joints; 4) muscle activity; and 5) metabolic balance. The most commonly used gait analysing methods are dealing with the measurement of time and distance factors.

Recently, several methods have been developed to measure the forces under the feet. With a Kistler force plate based on piezo crystals, one can measure the total vertical force as well as the horizontal reaction forces of one foot during one stance phase (8). Another measuring system is the Palrod Pelmobarograph system. By means of a transparent force plate, the pressure distribution under the feet can be visualized for one stance phase. Usually such force plates are embedded in the floor; the patient is instructed to place the designated foot in the proper way while walking on this platform. Due to the forced walking pattern, this results in measurements which are not likely to be representative of the natural gait of the subject.

Only a few systems are able to measure the forces under the feet dynamically during several steps. An example of this system includes strain gauges glued to metal plates under the shoe of piezo crystals attached to the shoe.

The disadvantage of most of these systems is that specially prepared shoes are required and influence the gait pattern of the subject. Furthermore, it is hardly possible to measure the effect of orthopedic shoes on the gait pattern with these systems.

To overcome the afore mentioned restrictions a force measuring system with transducers that can easily be attached to and removed from the subject's own shoes was developed (9). In total, 16 force transducers are used with a surface of about 10 sq cm each. Eight of these transducers will cover the surface of the sole. The data are stored on disc after the measurement is completed and can be recalled to present the data on screen, or on paper by means of a plotter. Force transducer number 1 is located at the heel, number 8 at the toe. When the two sets of force curves are compared, differences between the two feet can be easily detected.

The time course of the eight forces for each foot in relation to each other is shown in figure 2.

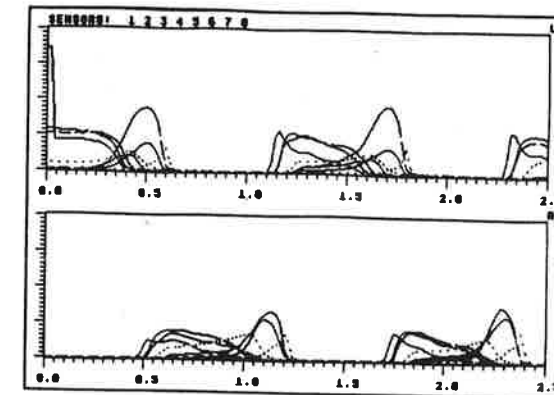


fig. 2: Time course of the eight separate forces measured under the left foot (upper) and the right foot (lower).

Another useful method of data presentation on paper is drawing the total force per foot as a function of time. The total force is calculated by adding the eight individual forces per foot. An example of the characteristic total force pattern of a healthy person can be seen in figure 3. Maximum values normally occur at the moments of heelstrike and push-off.

The last method of presenting the measured forces is to calculate the center of force $(x(t), y(t))$ of the eight forces of one foot as a function of time.

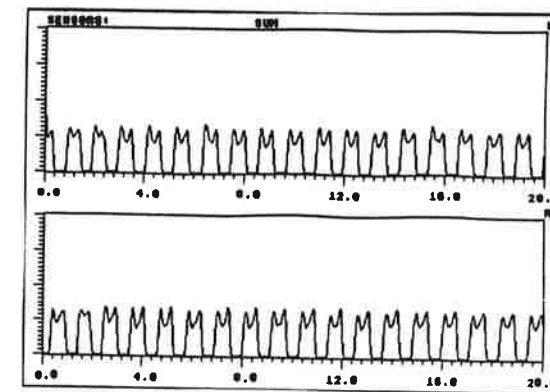


fig. 3: Time course of the total vertical reaction force for left and right foot.

This is done for each set of samples measured at the same time. The line connecting the calculated points of one stance phase is called the gait line and it shows how the center of the force distribution moves under the foot during the stance phase. Gait lines can be plotted in the outline of a foot for a single step or for several steps (figure 4). The gait line gives a good visual presentation of the measured forces per foot, and therefore this presentation is often used when the results are used by the medical staff. The system can be completed with possibilities to measure the angles of the joints and the surface EMG of muscles the clinician wants to be assessed.

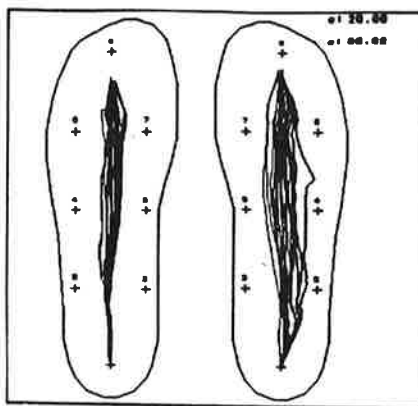


fig. 4: Gait lines of left and right foot for several steps.

CARDIAC CONDITION

Both the heart rate (HR) and the product of HR and systolic blood-pressure (BP) (double product) are good (noninvasive) estimators for myocardial oxygen consumption and therefore for the cardiac energy load. We defined the peak cardiac load as the peak heart rate (HR max) that could be obtained during graded exercise testing without subjective or objective cardiac problems. During graded exercise testing the workload gradually can be increased, resulting in an increased HR. The test is stopped when exercise-induced cardiac problems will be observed in the electrocardiogram (ECG) (two leads: CC5, CM5), or because of general fatigue.

Because amputees obviously are unable to bicycle, one can use a specially designed graded-exercise-testing device (rowing ergometry) based on arm and trunk work (figure 5). To detect exercise-induced

arrhythmias and ST-segment changes a specially developed computer system for ECG analysis is used (10).

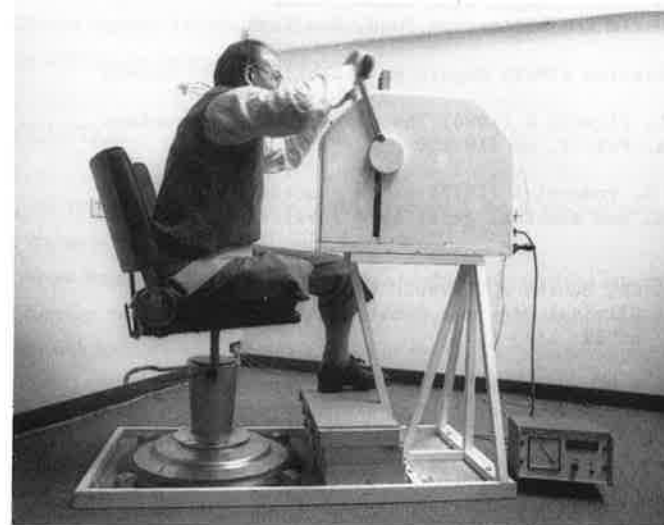


figure 5: Rowing ergometry

The aim of exercise testing is to obtain a maximum safe HR in all amputees (11).

From the measurements of cardiac load one can conclude that the patients adapt their walking speed and distance to their capabilities. Excessive cardiac loads will not be found. In amputees with peripheral vascular disease, graded exercise testing can be used to estimate the attainable walking performance and to detect patients with a Pmax (peak workload) limited by previously unrecognized cardiac problems (12).

REFERENCES

1. Lankhorst GJ Rehabilitation medicine and the assessment of functional abilities. In: Rehabilitation in the Netherlands Ed. by Association of Rehabilitation centres in the Netherlands P.O. Box 9696, 3506 GR Utrecht, the Netherlands, pp 9
2. Sokolow J, Silson JE, Taylor EJ, Anderson ET, Rusk HA (1961): A new approach to the objective evaluation of physical disability. J.Chon Dis 15, pp 105-12
3. Wood PHN (1980) Appreciating the consequences of disease: the International Classification of Impairments, Disabilities and Handicaps. WHO Chronicle, 34, pp. 376-380

4. Wood PHN, Badley EM (1985) The origins of ill-health. An appraisal of strategy for health for all and its implications. Recent Advances in Community Medicine no. 3. (ed. Smith A.), Churchill Livingstone, Edingburgh
5. Wood PHN, Badley EM (1981) People with disabilities. Monograph no. 12. World Rehabilitation Fund, New York
6. World Health Organisation (1969) Report on Rehabilitation, Geneva
7. Hermens HJ, Boon KL, Zilvold G (1986) The Clinical use of surface EMG, Medica Physica, Vol. 9, pp 119-130
8. Boccardi S, Chiesa G, Pedotti A (1977) A New procedure for evaluation of normal and abnormal gait, Am J Physical Med; 56 (4): 163-182.
9. Hermens HJ, de Waal CA, Buurke J, Zilvold G (1986) A New Gait Analysis System for Clinical Use in a Rehabilitation Center, Orthopedics Vol. 9, nr 12: 1669-1675.
10. Alsté JA van, la Haye MW, Huisman K, Vries J de, Boom HBK (1985) Exercise electrocardiography using rowing ergometry suitable for leg amputees: Int Rehabil Med &: 1-5.
11. Baumgartner R (1973) Beinamputationen und Prothesenversorgung bei arteriellen Durchblutungsstörungen, Ferd.Enke Verlag Stuttgart.
12. Cruts HEP, de Vries J, Zilvold G (1987) Lower Extremity Amputees with peripheral vascular disease: Graded Exercise Testing and Results of Prothetic Training, Arch Phys Med Rehabil vol. 68: 14-19.

BELGRADE ACTIVE A/K PROSTHESIS

DEJAN POPOVIC, LASZLO SCHWIRTLICH*

Faculty of Electrical Engineering

*Rehabilitation Institute "Dr Miroslav Zotovic"

University of Belgrade, Belgrade, Yugoslavia

1. INTRODUCTION

Gait restoration of Above-Knee (A/K) amputees is one of the first successful integration of artificial organs in biological system.

Above-Knee Prosthesis (AKP) cannot be unambiguously classified into passive and active ones. Such solutions as the polycentric knee mechanism (Cappozzo et al., 1980), the polycentric knee mechanism with hydraulic valve (Radcliffe, 1980) or the AKP with friction type breaking device (Aoyama, 1980) satisfy some of the required performances. Logically controlled hydraulic valve represents a further bridge between purely passive and fully active controllable assisting devices (Tomovic et al., 1982, James et al., 83). All above mentioned prostheses satisfy the stance phase requirements as well as the minimum power consumption principle. However the amputee is not able to extend the knee in the stance phase once it has been flexed. Flexion in the swing phase is not controlled. Extension of knee in swing phase is usually obtained by higher energy consumption due to hip movement or circumduction. The flexion during swing is usually not adequate, the toe clearance is too low for normal gait pattern and circumduction is involved.

In order to overcome mentioned deficiencies, AKP having fully controllable knee joint motions were developed (Popovic, 1984, Koganczawa, 1984, Kuzhckin, 1984, Flowers, 1978 etc). It has to be pointed that the only self contained device is Belgrade active AKP, and that even that device has a number of disadvantages for the practical use (energy consumption, noise, reliability of sensors, inadequate adaptivity to patient needs etc).

2. CONTROL SYSTEM FOR AKP CONTROL

Following diagram presents the actual organisation of the expert system (Tepavac, 86):

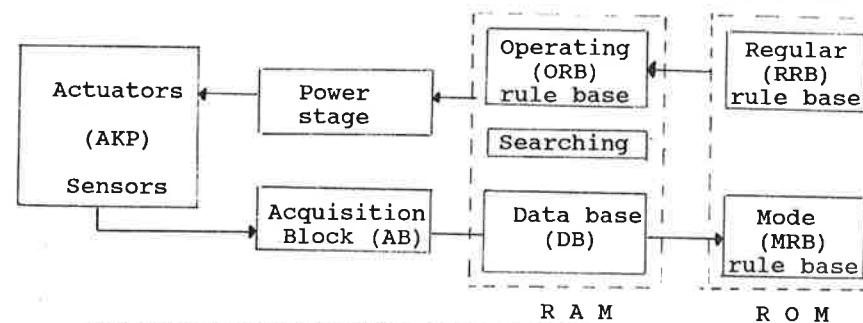


Fig.1 Schematic presentation of the software organisation

Software realization of the production control system consists of following blocks: data acquisition (AB and DB), inference engine (SEARCHING), working memory (ORB), general rule base (RRB and MRB) 1).

The sensory input vector formed through acquisition procedure (AB) is stored using FIFO algorithm in the data base (DB). DB contains a sequence of previous sensory vectors, so called prehistory of artificial leg behavior. In our application sensory input vector is formed with four components: knee potentiometer output, pendulum potentiometer output providing displacement of the shank towards vertical line, toe and heel zone force transducers (Kljajic' et al. 1985). Software provides the angular velocities of the shank and knee joint.

General rule base has two subsets of rules (regular and mode rules). Rules are represented by logical expressions.

The RRB contents regular rules, but also the Hazard Rule Base (HRB), for unexpected situations and hardware limitations.

"Firing" the rule from regular rule base change the actuator state, i.e. locking, damping or extension - flexion are engaged.

"Firing" of a rule from a mode base produces transition of the set of rules from regular mode base to working base.

This specific control method, because it relies on some similarities with biological reflex loops is called Artificial Reflex (AR).

Artificial reflex is the name for non-numerical method for the control of movements. The artificial reflex is sensory driven algorithm based on knowledge representation (production rule based system).

Artificial reflex reflects some rudimentary features of reflex loop reactions in the nature:

- Externally powered and controlled joint is activated by artificial proprioceptive and exteroceptive sensors;
- Sensory input to the joint controller is used for recognition of bionic patterns. The pattern can be recognized by non-numerical, logical expressions;
- Recognized sensory patterns are directly matched to one of the actuator states: damping, locking, flexion - extension.

More details about control are presented elsewhere (Tomovic, 87, Popovic, 88).

3. EXPERIMENTAL WORK WITH BELGRADE AKP

We will concentrate now to experimental results. We used skeletal standard US prosthesis with specific artificial foot, which enables controlled stiffness and elasticity of ankle joint. The construction relies on two elastic straps and hard rubber support (Fig 2). The ankle angle is adjustable as well as the forces in straps in resting position of the foot. The foot sole is equipped with force transducers, one in the metatarsal zone, and one in the heel zone (Fig 3). Semiconductor strain gauge bridge as bonded to steel support (Kljajic, 85). Linear output from 0 to 1400 N is achieved. Knee joint is equipped with motor unit, called Cybernetic Actuator (CA). CA is based on

two independent regulators, the motion and the stiffness controller. Motion control is done by electrically driven telescopic mechanism (Fig 4). Motor provides maximum angular velocity of 6 rad/s. Maximum torque acting on knee joint is limited by construction of gears and ballscrew to $M_{max}=82$ Nm. Nominal torque is 24 Nm. Stiffness control is applied by DC controlled drum brake mechanism. In recent use it operates in on-off mode. DC motor provides low consumption and fast response. On - off transition is $t_r=16$ ms. The leg is equipped with sensors described earlier.

The patient (male, 51 years old, 176 cm, 78 kg) is wearing Otto Bock standard skeletal prosthesis for more than 10 years. The length of the stump is about 35% of normal thigh length. The patient was trained for several weeks to use skeletal prosthesis with hydraulic damping unit (Henschke - Mauch unit) and Belgrade active prostheses.

We measured ground level walking with variable speed and walking on the slope (-10° , $+10^\circ$). Goniometric and TV system are used for gait kinematics recording. Oxygen consumption has been recorded for different types of gait. Battery consumption is measured for Belgrade leg, during locomotion.

Assuming that patient was able to walk with all three prostheses equally efficient and comparably safe and comfortable we figured that there are differences in gait patterns, as a result of different devices which are applied. Ground level walking didn't limited patient's locomotion and he was able to perform gait up to 1.8 m/s. Walking on the slope was analyzed with speeds between 0.6 to 1.1 m/s. Down the slope walking introduced a number of problems in both conventional prosthesis, but patient performed the task. The interesting conclusion is that gait symmetry really does not show very much, because the sound leg is performing totally different pattern than one in normal subject. The amputee is compensating all the imperfections of the artificial legs. Comparison with the normal subject is equally unreliable because AKP does not have an ankle joint in all applied devices.

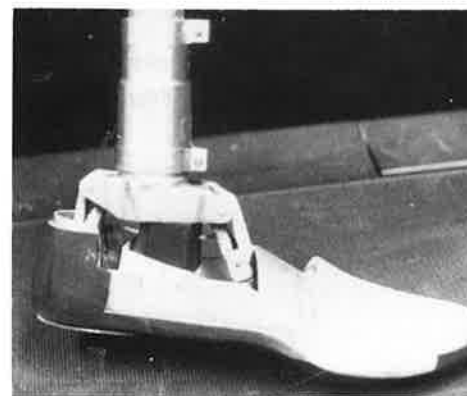


Fig 2. Artificial foot

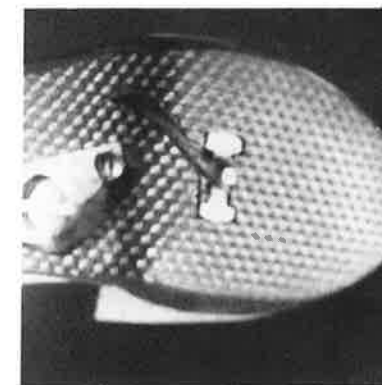


Fig 3. Force transducers in sole of the foot

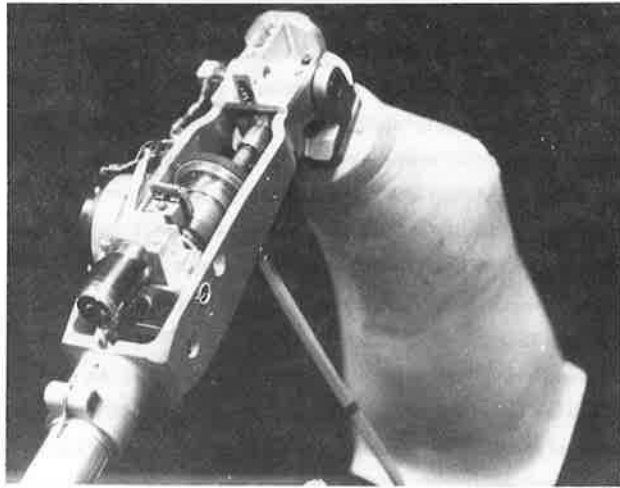


Fig 4. Cybernetic actuator in Belgrade AKP

Angular changes in ground level walking are presented in order to discuss the most interesting result (Fig 5). Table 1 shows the ratio of energy consumption in amputee to energy used by normal subject, biomechanically very similar. The table is self explained.

	AKP									
v(m/s)	0.6	0.7	0.8	0.9	1.0	1.1	1.2	1.3	1.4	1.5
E/E ₀	2.9	2.9	2.8	2.6	2.5	2.6	2.8	3.0	3.4	3.7
E/E ₀	2.6	2.6	2.5	2.2	2.3	2.4	2.6	2.9	3.1	3.2
E/E ₀	1.8	1.8	1.8	1.7	1.6	1.5	1.6	1.7	1.8	1.9

Table 1. E is metabolic energy used with use of AKP, E₀ is metabolic energy used in normal subject, Type 1 is Otto Bock, Type 2 is hydraulic damping control of knee mechanism, and Type 3 is Belgrade AKP. Average result is presented for 5 minutes of performance with each type of prostheses.

The application of the AKP on the slope shows even more difference in gait consumption, specially walking downstairs (Table 2)

	AKP					
$\dot{\alpha}$ (°)	5	8	10	-5	-8	-10
E/E ₀	3.0	3.4	4.0	3.2	3.7	4.5
E/E ₀	2.9	3.2	3.6	3.1	3.3	3.8
E/E ₀	1.9	2.1	2.2	2.0	2.1	2.4

Table 2. The fixed velocity was performed, v = 0.8 m/s, for the period of 5 minutes

One of the results which are important is the force exerting the sound leg and the prostheses during gait. This force is acting to the stump in prosthetic side, but it also act to the hip joint (Fig 6). The results presented here are single subject results., so we would not like to predict final conclusions of a complete clinical evaluation of the externally powered legs but we can suggest that external power:

- increase the toe clearance,
- allows better performance on the slope,
- decrease the energy consumption of amputee,
- decrease the heel force and collision effects, and
- match better the gait to the "normal" pattern.

In the same time we must point out that engaging of external power and control introduce a number of technical problems, like external energy (we are using 12 V batteries, 4 Ah, and they are good for approximately two hours of continuous use), external controller with efficient control algorithms (we are using Artificial reflex method which relies on application of an Expert system), noise, reliability etc.

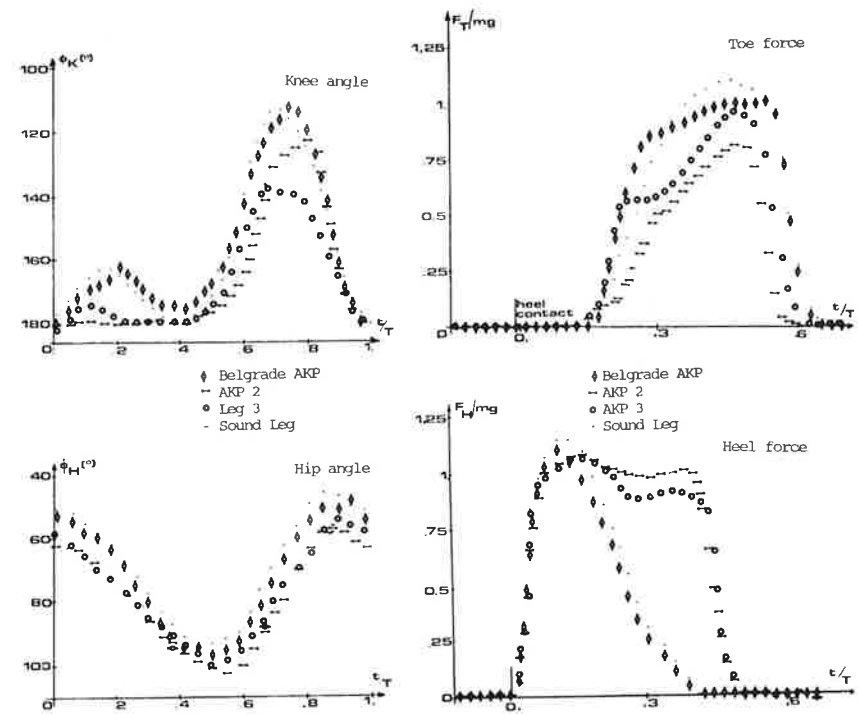


Fig 5. Angular changes in application of AKP

Fig 6. Ground reactions in AKP application

4. CONCLUSION

This paper presents the application of the self-contained, externally powered AKP. The active AKP may find best application in patients with limited hip control and strength and in bilateral A/K amputations. Artificial reflex control, meets some of the requirements of modern rehabilitation. Presented material demonstrate some of main futures of active AKP. Decrease of energy consumption, reduction of compensating movements of the hip, variety of gait modes and decrease of jerking and impulse forces are recorded in use of Belgrade AKP in comparison with some other conventional prostheses. It should be mentioned that external powering has a number of disadvantages. It decrease reliability, and complicate the maintenance. Most of the amputees, including the patient who is presented, if they are performing dissent gait without external power will use conventional AKP. There are several technical problems as well, like noise, dimensions, weight, wiring and similar which is not acceptable for some of handicapped human's.

5. REFERENCES

- Aoyama, F. et al. (1980), Lapoc System Leg, Proc. of the Rehabilitation Engineering Seminar REIS '80, Tokyo, Japan, 59 - 67
- Cappozzo, A. et al. (1980), A Polycentric Knee-Ankle Mechanism for Above-Knee Prostheses, J. of Biomechanics, 13, 231-239
- Flowers, W. Mann, R.B. (1977), An Electro-hydraulic Knee-Torque Controller for a Prostheses Simulator, Transaction of ASME, J. of Biomechanical Engineering, 3-8
- James, K.B. (1983), Improved knee joints for Above Knee Amputees, Fragment, Fall, 56 -57
- Kljajic, M. et al. (1985), Relevance of ground reaction pattern for gait analysis and its measurement by force shoes, In Biomechanics IX-B, edited by D.Winter et al., Champaign, IL, Human Kinetics, 195-200
- Koganczawa, K. Kato, I. (1984), A Development of A/K Prosthesis Adaptable to Voluntary Walking Period, Advances in External Control of Human Extremities VIII, Published by Yugoslav Committee for ETAN, Beograd, 343 - 355
- Kuzhikin, A.P. et al. (1984), Subsequent Development of Motorized Above Knee Prosthesis, in Advances in External Control of Human Extremities, Published by Yugoslav Committee for ETAN, Beograd, 525-530
- Popovic, D. et al. (1984), Technical and Clinical Evaluation of the Self-Fitting Modular Orthoses, Progress Report, NIH, Washington D.C., Project No 432
- Popovic, D. et al. (1988), Control Aspects on Active A/K Prostheses -in print, Int. Journal of Man-Machine Studies, Canada
- Popovic, M., Popovic, D. (1983), Cybernetic Actuator for Orthosis / Prosthesis, Proc. of the XXVII Yugoslav Symp. for ETAN, pp II.285 - 292, Beograd,
- Radcliffe, C.W. (1980), Biomechanical Basis for the Design of Prosthetic Knee Mechanisms, Proc of the Rehabilitation Engineering International Seminar REIS '80, Tokyo, Japan, 68 -88
- Tepavac, D., Tomovic, R., Popovic, D (1986), Knowledge Base for Reflex Control, Proc. of the XXIX Yugoslav Conference for ETAN, pp IV.232- 239, Beograd
- Tomovic, R., Turajlic, S., Popovic, D. (1981), Active Modular Unit for Lower Limb Assistive Devices, in Advances in ECHE VII, Published by Yugoslav Committee for ETAN, Beograd, 1-15
- Tomovic, R., Popovic, D. et al. (1982), Bioengineering Actuator with Non-Numerical Control, Proc. of the IFAC Conference on Orthotics and Prosthetics Columbus, Ohio, 145 -156, Pergamon Press
- Tomovic, R., Popovic, D., Tepavac, D. (1987), Adaptive Reflex Control of Assistive Systems, in Advances in External Control of Human Extremities IX, 207 - 214, Beograd
- Tomovic, R., Bekey, G., Carplus, W. (1987), A Strategy for the Synthesis of Grasp with Multifingered Robot Hands, Proc. of the 1987 Conference IEEE on Robotics and Automation, Vol 3, 85 - 99
- Wagner, E.M., Catranis, J.G. (1954), New Developments in Lower-Extremities prosthesis, in Human Limbs and Their Substitution, National Academy of Science, Washington, D.C., Chapter 17

AN ELECTROPNEUMATIC PLATFORM FOR A COGNITIVE APPROACH IN REHABILITATION OF HEMIPLEGIC PATIENTS

A. Pepino (*), M. Bracale (*), M. Iocco (**), N. Misasi (**)

(*) Electronic Dept., Faculty of Engineering, Univ. of Naples
"Nucleo di Ingegneria Medica e della Riabilitazione" CNR Naples (I)
(**) Orthopaedic Clinic, II Faculty of Med. and Surg. Univ. of Naples (I).

INTRODUCTION

The Neurological principles, which Cognitive Rehabilitation is based on, can be summarized as follows: (Bracale 1985)

- The plasticity of function within the CNS .
 - Cerebral cortex as "open system" (highly maleable and adaptable)
- From a therapeutic point of view the restoration of function can be seen as a learning process; the motor rehabilitation, for example, can be considered as the learning process of new motor skills. Three sequential steps have been postulated in the development of motor learning: a) Cognitive phase, b) Fixation phase, c) Automation phase
- In cognitive phase the subject sketches a sort of prototype of the motor skill to be learned (Marteniuk 1979) especially to create new cinesthetic channel to control new motor activity.

In fixation phase a period of continuous reorganization of motor behaviour can be observed, in this phase Robb (Robb 1972) observed the great importance of biofeedback mechanisms; of course the biofeedback patterns have to be correctly provided to the patient, otherwise a negative effect could be obtained. (Bracale 1985). Finally in automation phase the motor skill has progressively improved to become more coordinated. Obviously this step comes necessarily after the previous two.

P.E.R.M.: ELECTROPNEUMATIC PLATFORM FOR MOTOR REHABILITATION

The platform P.E.R.M. is a therapeutic tool for a cognitive approach in motor rehabilitation of hemiplegic patients.

The platform consists of a basculant plane moved by four pneumatic pistons; they are driven through a microprocessor based device. The platform is provided of pressure and position sensors for closed loop control; several I/O interfaces are available for all control needs, a video section allows visual biofeedback outputs via a video-monitor.

Two working modes are allowed, a) Active mode b) Passive mode:

In mode (a) the platform the operator can control from the console the position of the platform, or the pressure distribution inside the pistons, to provide the patient with appropriate mechanical stimuli.

In mode (b) the pistons under the platform are preliminary charged at a reference pressure level, and the patient has to provide by himself voluntary actions on the platform.

Position or pressure are recorded and displayed in graphical and numerical form on a TV screen (Fig. 1), as position or force, visual biofeedbacks. We consider the possibility to use mode (a) for cognitive phase, and mode (b) for fixation and automation phase.

CLINICAL ASPECTS

Two type of exercise have been tested:

a) Recognizing jobs, in which the patient has to provide his attention on the external mechanical stimuli coming from the platform.

b) Voluntary jobs in which the patient has to perform a voluntary control in simple or complicated tasks, with support of visual biofeedback patterns.

The platform works under the plegic patients, the subject can work standing or sitting; (Fig.2) Typically voluntary movement are performed in standing position, while recognizing job in sitting position.

At the RESET the video display reports a command menu to select the right mode:

1)Position Monitoring 2)Pressure Monitoring 3)Position Control
4)Pressure Control 5)No Console Control

For example if the job is: "the patient has to recognize the amount of a position change": the operator selects point 1 followed by point 3. In such way the operator can control the position and receives a visual display of the position, on the monitor (Fig.1). The patient is explained about that, the therapist places the plegic side under the moving platform, then through a joystick, progressively makes a change of the position of the platform. As soon as the patient feels the position change under the



Fig. 1

foot, he calls the attention of the therapist.

The therapist at the same time records the numerical value of the position, displayed on the monitor. This value can be used to quantify the exercise, infact it's reasonable to say that it depends by the capability to use sensorial and cinesthetic informations.

In similar way it's possible to propose to the patient voluntary tasks (selecting point 1 & 5 in command menu) in which he uses video monitor as a force (or position) biofeedback device (Fig.1); of course, now, the displayed value could quantify the capability of voluntary loading on the plegic side.

PRELIMINARY RESULTS

This method to quantify these particular therapeutic jobs is

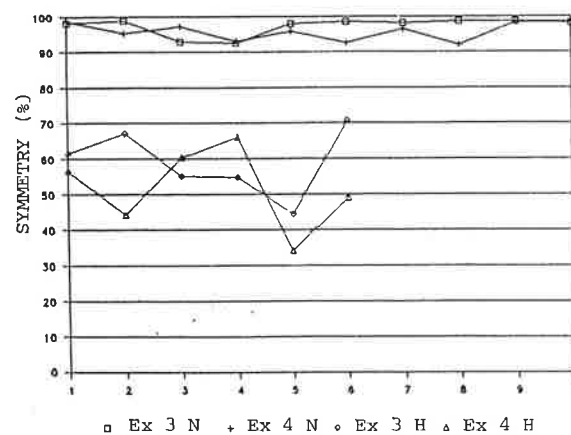


Fig. 3

affected by "human error"; for this reason the therapist usually repeats each task for five times, (the average of the five experiments is calculated offline). Another aspect regards the normalization problems due to the Antropometric characterists of each individual. We make the choice to normalize by using symmetry coefficients of the values recorded for health and plegic side. The recognizing exercise (ex 3) and the voluntary exercise (ex 4) has been tested on 10 normal subjects and 6

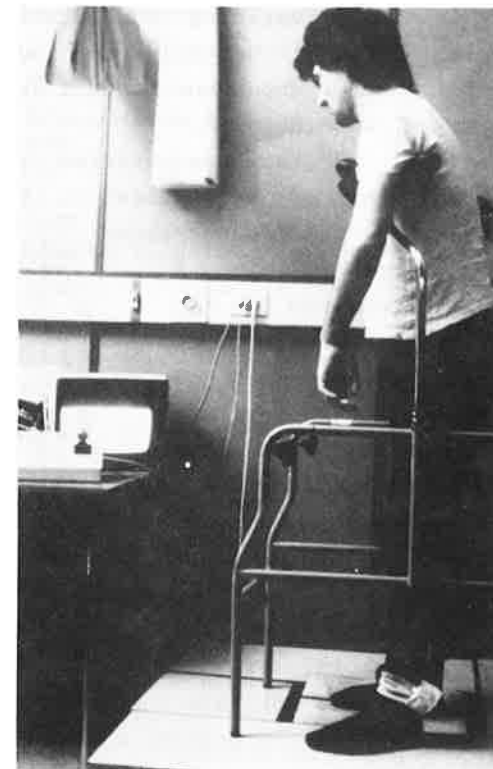


Fig.2

hemiplegics, verifying the statistical separation of the groups ($p < .1$) (Fig.3) Secondly a group formed by four hemi patients received for about one month a therapeutic treatment in which the P.E:R.M. was included.

For all of them we verified the possibility to monitor the improvement of the patient in the "short time" by using symmetry parameters provided as above

For example in fig. 4 is reported the symmetry trend in time during one month of therapeutic treatment of a stabilized patient (1 year accident). In exercise 3 (recognizing task) we observe a significant

improvement; on the contrary in ex. 4

trendt we do not have the same, probably for the short observation time. For all the patient a correlation between the symmetry trendt and clinical story has been observed. A longer observation time and a larger group of patient, are necessary to have more accurate and definite results about the therapeutic effects of this treatment.

BIBLIOGRAPHY

-Bracale M.: The use of Electronic Games as informatic aids in the cognitive rehabilitation. In Special Session "Ausili informatici per disabili" pp.93-106.

Proceedings of the Congresso A.I.C.A. 9-11/10/1985, Florence.

-Clein M.I., Stone W.J.: Physical education and the classification of educational objectives: psychomotor domain. Physical Educator, 34-35 (1970)

-Marteniuk R.G.: Motor skill performance and learning: Consideration for Rehabilitation Physiotherapy Canada, 31, 187-202. (1979)

-Robb M.D.: Man and Sports: the acquisition of skill. in Christina R.W., Shaver L.G. (eds.): Biological and Psychological perspectives in the Study of Human Behaviour, Kendall/Hurst, Dubuque Iowa (1972).
This work is financially supported by MPI 40% "Motor Rehabilitation Engineering", and C.N.R. "Nucleo di Ingegneria Medica e della Riabilitazione.

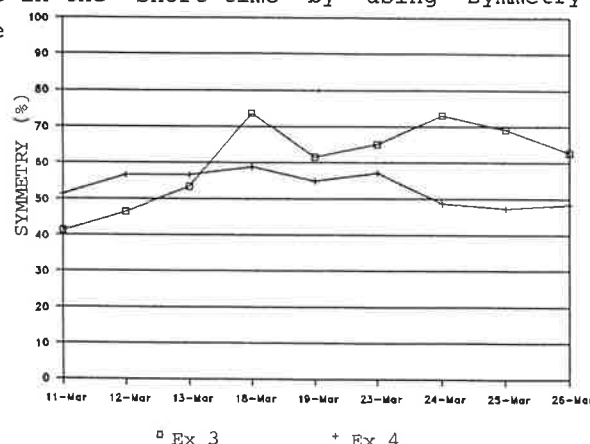


Fig. 4

QUANTIFIED MYOFEEDBACK IN MUSCLE (RE)EDUCATION BY COMPUTERIZED VIDEO GAMES.

R. SOERJANTO AND R. PHILIPS.

University Hospital Leiden, Department of Rehabilitation Medicine
10 Rijnsburgerweg, 2333 AA Leiden, Netherlands.

INTRODUCTION.

Biofeedback is the use of modern instrumentation to give a person better moment to moment information about a specific physiological process that is under control of the nervous system but not clearly or accurately perceived (1).

Myofeedback (MFB) is the kind of biofeedback by which the electromyogram (EMG) is applied as feedback signal.

MATERIAL AND METHODS.

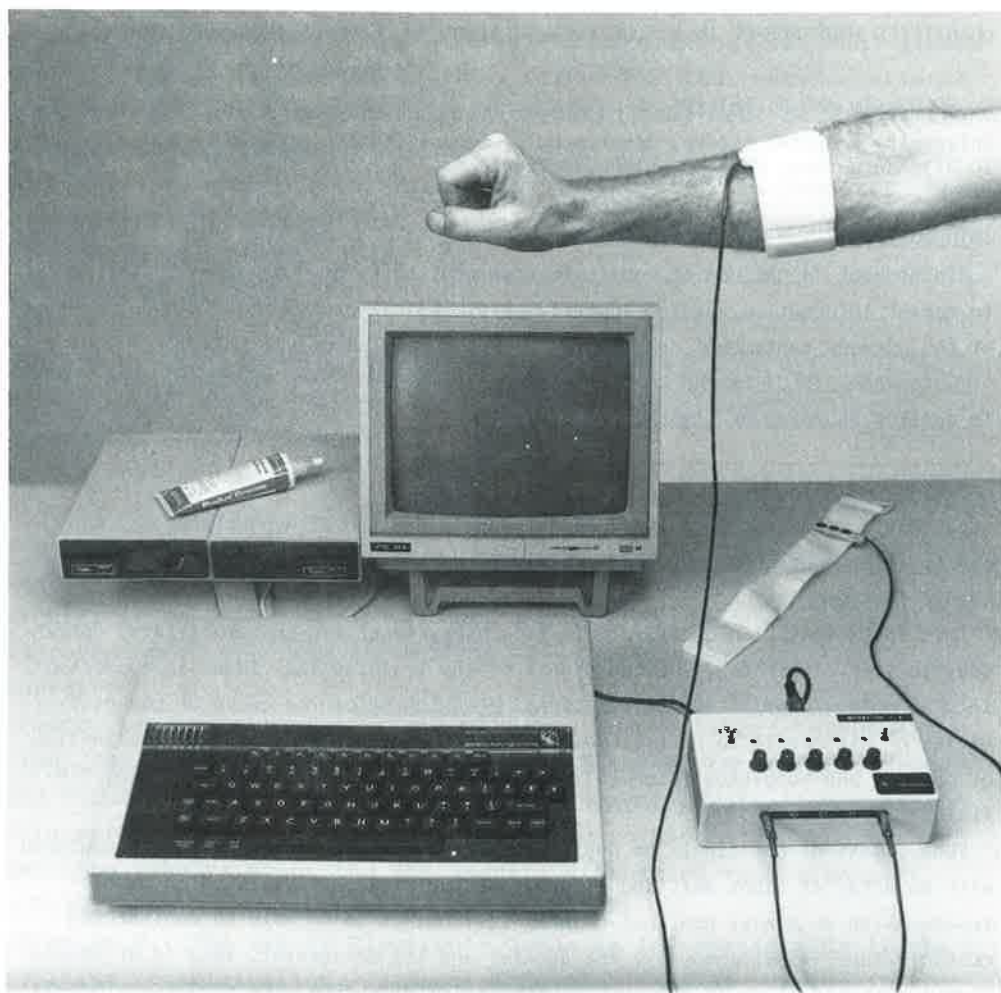
As mentioned in the definition we are mostly dealing with physiological phenomena which cannot be perceived clearly or accurately without the help of electronic instrumentation.

This instrumentation usually consists of very sensitive EMG amplifiers, operated via skin-electrodes. The EMG signal of the training individual is converted into an optical and/or acoustical signal by which he can be aware of the activities of his muscle to be trained. In practice it appeared that the combination of optical and acoustical signals are preferred by the patients performing MFB-training.

Today, most of the single or dual-channel MFB training instruments are equipped with an array of light emitting diodes, one for each channel. Used in muscle-re-education we always use dual-channel instruments to be able to monitor two muscle(groups) simultaneously: the agonist and its antagonist. This is of essential importance since in whatever neuromuscular disorders, the normal reciprocal innervation is disturbed (2).

From our experiences in training many patients during the past 17 years, we learned that MFB-training actually is a monotonous way of a learning process by only watching and listening to the signals produced by the training instrument. Therefore, after developing one of the first MFB-instruments with a double array of led's, called the Myodisplay (3), especially for the children, a dual-channel EMG-controlled model train was linked to this device. Even this model train that thus could be moved forward and backward by a muscle(group) and its antagonist respectively, could not sufficiently keep the attention of youngsters performing EMG-training.

The latest development therefore, is the application of the well-known numerous video games as a mean of never boring MFB-training.



The MYOSTICK, linked to a standard, inexpensive homecomputer, with which commercially available video games can be controlled by up to 5 muscle(groups), whether or not in combination with the common joystick and/or any other kind of switch.

A five-channel homecomputer (Commodore, MSX, etc.)-based instrument has been manufactured by KRD-Electronics, by which each known and commercially available video game can be played. This device is called the Myostick and enables myoelectric control of video games by muscle action (4, 5).

Instead of the 5 regular functions of the well-known joystick (X-Y function plus "fire"-button) the game can be played with up to 5 muscles or musclegroups, whether or not in combination with the common joystick. Or even with 10 muscles with appropriate soft-ware.

The greatest advantages of this method over those using the instruments mentioned before, are:

1. Prevention of boredom because of the nearly unlimited number of commercially available video games;
2. Possibility of objective quantification of the training results by the scoring system of the game concerned, displayed on the monitor screen;
3. Diversion of the attention of the training individual from (difficult) control of his muscle(s) to the playful control of the game on the screen;
4. Possibility to play a competition with an opponent, this being a healthy individual or another MFB-trainee;
5. Because of the relative low price of the instrument, the patient can resume his training at home while his inmates can join him in playing, thus augmenting the effect of training in a playful manner. (The training sessions in hospitals and rehabilitation centers usually are limited to 20-30 minutes per day).

REFERENCES.

1. Miller NE (1974) Biofeedback: evaluation of a new technique. *New England J. Med.*, 290, pp 684-685.
2. Soerjanto R (1974) Myoelectric training of congenital below-elbow stumps in children. *Inst. Med. Phys. TNO*, Progress rep. 4, pp 18-22.
3. Kwee HH, Prenger JAM and Brekelmans FEM (1976) Myodisplay: An EMG biofeedback apparatus for functional neuromuscular training. *Inst. Med. Phys. TNO*, Progress rep. 5, pp 25-29.
4. Soerjanto R (1987) Moderne toepassingsmogelijkheden voor de biofeedback trainingmethode (deel 1). *Soma & Psyche* (ed. Ciba-Geigy) Jg. 13/3 pp 45-50.
5. Soerjanto R (1988) Moderne toepassingsmogelijkheden voor de biofeedback trainingmethode (deel 2). *Soma & Psyche* (ed. Ciba-Geigy) Jg. 14/1 pp 30-35.

EFFECTS OF SPECIFIC MUSCLE POWER INCREASE IN CASE OF FLAT-FOOT

CRIVELLINI M., DACQUINO G., DIVIETI L., SANTAMBROGIO G.C., STUCCHI M.

Dipartimento di Elettronica, Politecnico di Milano, 20133 Milano, Italia.

INTRODUCTION

The foot presents a series of longitudinal and transverse arches forming a vault as shown in Fig. 1; such a vault has a chief importance both for gait and standing. From a biomechanical point of view the foot arches act like springs and their weakening causes the so called flat-foot. The anatomical structures that are responsible for maintaining the foot arches are the ligaments and the muscles acting to bear the weight in all conditions. An insufficient action of such muscles is followed by a lengthening of the ligaments and a weakening of the foot arches which are thus flattened.

Clinical treatment of flat-foot is commonly based, when surgical intervention is not the primary solution, on both the use of orthopaedic insole and the execution of physiokinetic exercises suitable for powering those muscles involved in restoration of the foot arches. The aim of the present paper is to illustrate and discuss the results obtained in the treatment of flat-foot by applying sinusoidal electrical stimulation for selective powering of the arch rising muscles.

METHODS AND EQUIPMENT

Electrical Stimulation

The best known method to increase muscle power is to perform strong voluntary contractions repeatedly many times each day. An improving of both muscle force and contraction velocity can also be obtained by electrical stimulation which allows a stronger single muscle contraction without stressing the patient and with a more specific muscle selection (1). Although many current waveforms can be used to induce contraction, a 2500 Hz sinusoidal current applied 20 min per day for 15 days (see Fig. 2 for details on muscle force improvement during treatment) has been adopted to increase power of the lombricals, interossei and adductor hallucis muscles which act to reduce flattening of the foot arches.

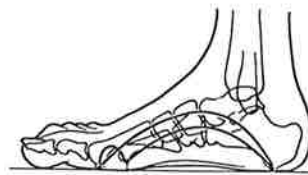


Fig. 1. Scheme of the foot arches.

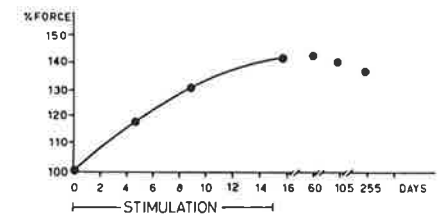


Fig. 2. Muscle force improvement.

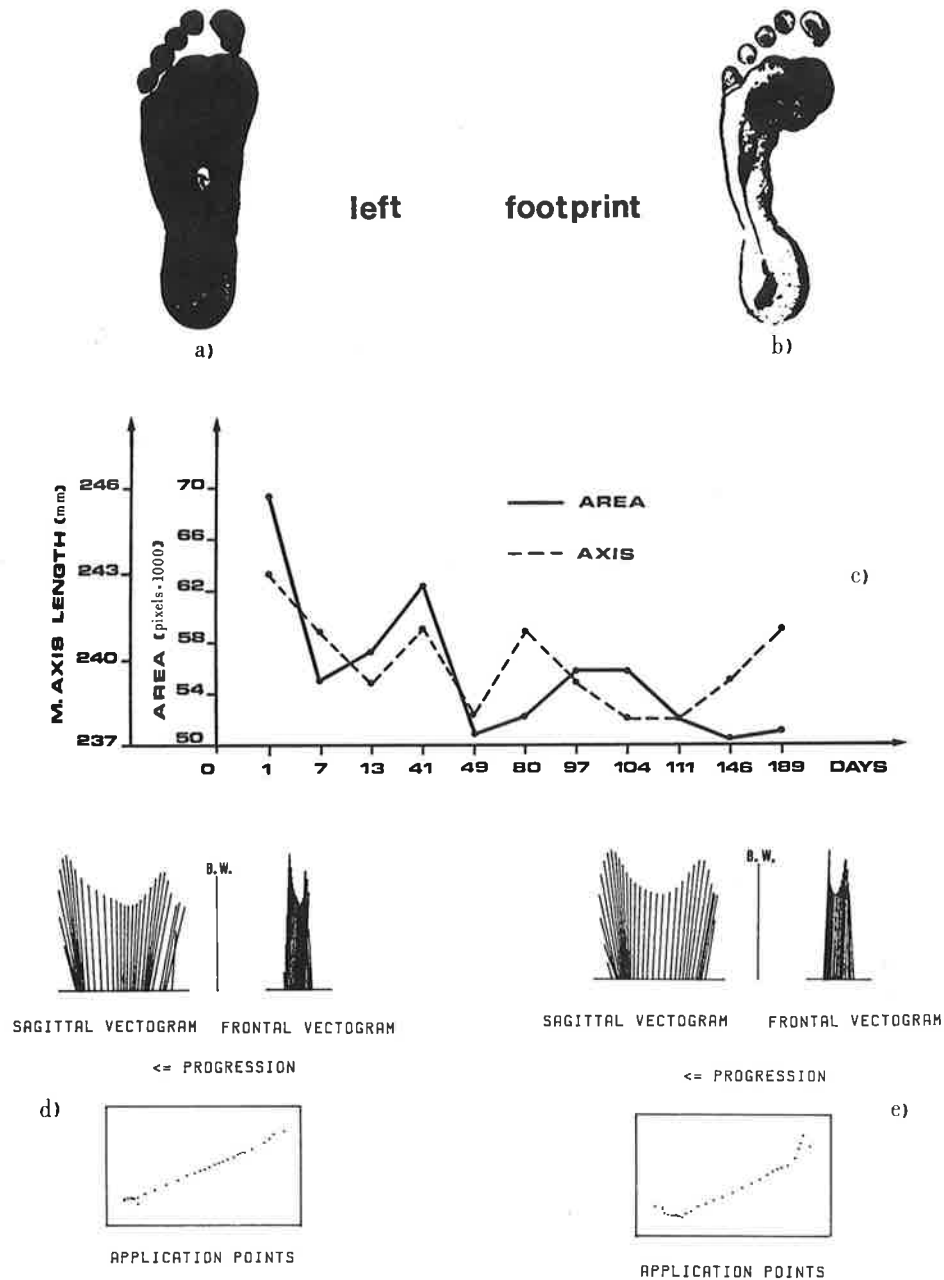


Fig. 3. a) and b) are the footprints of the left foot taken before and after treatment. c) is the course of the footprint area and the length of the major axis. d) and e) shows the mean ground reaction evolution measured before and after treatment.

The electrodes are usually placed on the dorsal and plantar mid-foot area but, when further stimulation is needed, another couple of electrodes can be applied higher up on the leg to contract the tibialis posterior, peroneus longus, flexor hallucis and flexor digitorum longus muscles. Further details on theory and application of sinusoidal electrical stimulation are reported in (1, 2).

Footprint Measurement

To provide non-invasive documentation about the morphological changes induced by the treatment in the plantar surface, footprint has been taken with the patient in orthostatic condition. From this picture, two parameters have been measured: footprint surface and the so called major axis length defined as the straight segment joining the two farthestmost points on the footprint contour.

Gait Analysis

The static measurement described above gives impressive information about the plantar morphology which, however, is not sufficient for quantification of functional efficiency. Such an evaluation needs a more detailed analysis involving also dynamics of gait. To this purpose the Vector Diagram Technique (3) for the analysis of the ground reaction evolution during the stance phase of a step has been used. A more complete description of theory, experimental set-up and procedure is reported in the references (1, 3).

Although the crude representation of the ground reaction evolution provides useful information on the gait efficiency, a further analytical approach has been made to quantify the locomotor changes induced by treatment. Such an approach, whose mathematical description is reported in (1), is based on a statistical estimation of the differences occurring between two groups of ground reaction patterns. The coming out findings can be synthesized through the so called Pathological Level Index (PLI) which provides the percentage of the stance-phase that is featured, at one and five per cent level of significance, by abnormal results with respect to a basal data collection. P.L.I. can be adopted for the evaluation of both the whole ground reaction evolution and the course of each variable associated with the ground reaction: vertical component of force (F_z), horizontal components of force (F_x and F_y) and linear coordinates (P_x and P_y) of the application point in the sagittal and frontal plane respectively.

RESULTS

A significant example of the flat-foot recovery obtained by using sinusoidal electrical stimulation is illustrated in the results of Fig. 3.

Postural Changes

Figures 3 a and b show the footprints of the left foot (the most damaged) taken before (a) the beginning of muscle powering and after (b) six months (the

whole treatment was formed by two stimulation cycles in the first three months). The impressive recovery of the foot arch morphology is also proved by the results shown in Figure 3 c where the course of the major axis length and the related footprint area are illustrated. The effects of muscle powering are particularly evident after the second stimulation cycle (after the day hundred in the graph) when a lower value of the major axis and a relevant mid foot concavity associate with a successful foot arch restoration. After the second stimulation cycle, both the footprint area and the major axis length last around values significantly better than at the beginning of treatment. Also X-ray response (not included here because of paper length limit) shows an excellent recovery to normal shape of the foot arches.

Walking Changes

Figures 3 d and e show the vectorial representation of the ground reaction evolution (averaged over five steady-state trials performed at 108 steps/min and taken before (d) and six month after (e) the treatment) along the sagittal, frontal and horizontal planes. If compared with normal results available in literature (1, 3), the pre-treatment pattern presents some abnormalities that are confirmed by the P.L.I. values reported in Table 1. After treatment both the general shape of the diagrams and the P.L.I. (see in particular the values of Fz which was the most abnormal) remark an improvement of gait efficiency according with the findings from static data and the previous experiences on foot arch restoration by means of sinusoidal electrical stimulation (1).

Table 1. Partial and total values of P.L.I.

Level of Significance	P.L.I. Fz	P.L.I. Fx	P.L.I. Fy	P.L.I. Px	P.L.I. Py	P.L.I. Tot
B E F O R E T R E A T M E N T						
0.01	87.11	40.62	0.39	21.48	7.42	31.41
0.05	88.67	51.56	3.13	34.36	10.94	37.73
A F T E R T R E A T M E N T						
0.01	30.86	28.91	1.18	19.92	5.86	17.34
0.05	38.28	48.05	2.34	40.63	11.33	28.12

REFERENCES

1. Divieti L, Santambrogio GC (1986) Changes in muscle characteristics: basic principles and applications. In: Sensorymotor plasticity: theoretical, experimental and clinical aspects. INSERM 140: 367-384.
2. Divieti L, Salice F (1982) Threshold characteristics for sinusoidal electrical stimulation. Proc. of the 5th ISEK Congress, Ljubliana.
3. Pedotti A (1977) Simple equipment used in clinical practice for evaluation of locomotion. IEEE Trans. BME 24: 456-461.

ASSESSMENT OF MUSCLE FUNCTION IN HEMIPLEGIC AND HEALTHY SUBJECTS
BY KINESIOLOGIC EMG-REGISTRATION DURING REPETITIVE MOVEMENTS.

J.BECHER, J.HARLAAR, T.W.VOGELAAR, H.BAKKER.

Dept. of Rehabilitation Medicine, Free University Hospital
Amsterdam, De Boelelaan 1117, 1081 HV Amsterdam, The Netherlands.

INTRODUCTION

In hemiplegia, alteration of motor-function of the muscles can be expressed in negative symptoms, positive symptoms and modified symptoms. Negative symptoms include loss of strength and dexterity, positive symptoms include hyperreflexia and spasticity and modified symptoms are abnormal responses to cutaneous stimuli. In spite of many investigations, no generally accepted method of measurement, monitoring muscle-function in hemiplegia is available. As a loss of ability to rapid and isolated muscle-activation characterises central paresis syndromes, repetitive movements (RM) in a joint seems an adequate and easy performing method to assess the level of impairment of motor-function of a muscle. The purpose of the present study is to examine the usefulness of repetitive movements as a method of assessment of muscle-function in hemiplegia.

METHOD

Performance : To assess muscle-function, voluntary movement in the ankle-joint is studied. Two ways of performance are considered :

1. Free Frequency Repetitive Movement (FFRM) : The patient is instructed to move the foot alternating plantarward and dorsalward with the maximal range of motion and in the maximal frequency. Thirty seconds of movement are registered.

2. Imposed Frequency Repetitive Movement (IFRM) : The patient is asked to move the foot alternating dorsalward and plantarward in the rhythm of a metronome with visual and acoustical control, also 30 seconds are registered.

Ankle-movements are registered by a potentiometer based goniometer. Muscle-activity is recorded by Surface Electromyography (EMG) of the Tibial Anterior Muscle (TAM), Soleus Muscle (SM) and the Gastrocnemius Muscle (GCM). For the bipolar lead off, the electrodes are placed in the direction of the muscle-fibres, at the most central part of the palpable muscle-belly. Rim-to-rim distance is 23 mm, the effective lead-off surface of the electrodes (disposable Medi-Trace Pellet Electrodes) is 1 cm².

Data Processing : The EMG is pre-amplified with an electrode-mounted preamplifier (gain 100x, CMRR > 100dB) and highpass-filtered to remove movement-artefacts (20 Hz). After final amplification, the signal is rectified and smoothed (lowpass-filtering at 25 Hz, 18 dB/oct) to obtain the Smoothed-Rectified EMG (SR-EMG). The SR-EMG and goniometersignal are on-line stored by means of A/D-conversion in a micro-computersystem.

Off-line, the SR-EMG is filtered by a digital low-pass filter at a frequency of 4 times the frequency of movement in the joint (4' order Butterworth, zero-lag). Furthermore, all signals are ensemble-averaged (triggered on the crossing the median angle of the range of motion in the joint) to obtain a plot. Also, mean

values and variance are calculated.

Parameters: The following parameters are used to describe muscle-function :

1. Performance : The performance is expressed in the score of ankle-movement, the frequency of movement and the range of motion (ROM) in the joint.

2. Voluntary Muscle Activity (VMA) : VMA is expressed as the difference of the average maximal and minimal SR-EMG of the muscle.

3. Paresis. The level of the Low-Output Paresis (LOP) is expressed in the percentage of VMA, at the affected side in relation to the healthy side. Subtraction-Paresis (SP) is expressed in the value of SR-EMG of the antagonist as percentage of the maximal SR-EMG of the agonist of movement.

4. Cocontraction (CC) : The level of cocontraction is defined as the SR-EMG of the antagonist of movement minus the minimal SR-EMG of the antagonist at the moment of maximal SR-EMG of the agonist.

5. Minimal Muscle Activity (MMA) : The MMA is expressed as the percentage minimal SR-EMG of the maximal SR-EMG of that muscle of the averaged values of a cyclus of movement.

TABLE 1.

Comparison of the results of Free Frequency and Imposed Frequency Repetitive Movement of a healthy subject. (N = 20).

Parameter.	FFRM				IFRM			
	RIGHT		LEFT		RIGHT		LEFT	
	mean	2sd	mean	2sd	mean	2sd	mean	2sd
Score.	4268	1220	4127	1128	1783	142	1602	224
Freq. Hz	2.6	0.7	2.3	0.3	0.9	0.1	0.9	0.1
TA VMA uV	261	60	273	46	295	90	263	102
GC CC uV	10	4	8	2	16	9	8	3
TA MMA %	9	4	3	2	0.4	1	0.3	1
LOP %	95				89			
S.P. %	23		5		6		4	

Explanation of the parameters : see text.

RESULTS

1. Test-retest investigation.

Table 1 summarises the results of test-retest investigation of a healthy subject, both at FFRM and IFRM. At IFRM, only voluntary muscle-activity is observed in the TAM. The GCM and SM remain relaxed during plantar-flexion, expressed by a low level of SP at IFRM. The lower scores are not only caused by a lower frequency, but also by a lower ROM in the ankle-joint, as the plantar-flexion is diminished. The relaxation of the TAM at IFRM is also improved, expressed in a lower percentage of MMA. In IFRM, the variance in score shows a strong correlation with the ROM (Pearson's rho = 0,98.). The correlation of the level of VMA of the TAM with the score reaches no significant value. This suggests a major influence of mechanical properties of the muscle on the variance of the score. As at FFRM the parameters show an irregular pattern of variation, at IFRM a learning-effect is detectable. The fourth measurement is the most reliable. In both methods, the intra-individual variance of the VMA is considerable, the other parameters show a limited variance.

TABLE 2.

Results of FFRM of 10 patients (N=1).

Parameter	1	2	3	4	5	RHO
Score	1018	668	1141	371	2282	.30
Freq. Hz	0.9	0.77	1.12	0.62	0.80	.79
ROM	19	15	20	10	48	.22
TA VMA uV	164	71	63	15	52	.73
GC CC uV	2	7	4	1	1	.30
TA MMA %	7.8	31.7	22.2	72.7	3.7	-.46
LOP %	N.A.	40.5	45.0	8.6	23.3	1.00
S.P. %	3.9	15.3	14.8	7.3	3.7	-.22
GC VMA uV	57.0	12.0	28.0	1.0	8.0	.52
GC MMA %	8.0	42.8	22.2	75.0*	11.1	-.29

	6	7	8	9	10	RHO
Score	252	441	1289	2473	442	1.00
Freq. Hz.	0.75	0.66	0.90	0.89	0.63	.51
ROM	7	12	24	46	13	.99
TA VMA %	3	17	63	50	36	.53
GC CC uV.	8	1	1	1	1	
TA MMA %	85	22	19	40	32	-.52
LOP %	19.2	12.2	37.2	28.6	25.3	.30
S.P. %	510	22	6.4	9.5	1.8	-.36
GC VMA uV	16	5	1	18	0	.29
GC MMA %	85	44	*80	28	*100	-.68

Explanation parameters: see text. NA =Not Available.

* high percentage caused by low values in uV.

TABLE 3.

Results of IFRM of 2 patients (N =15) and 5 healthy subjects, both sides (N =25).

Pat.1.	SCORE	FREQ	ROM	TA.VMA	GC.CC	TA.MMA	LOP	SP
A.S mean	591	.98	13	239	5	6	84	4
2sd	300	.1	5	55	3	10		
UA.S mean	1327	.84	27	283	8	2		4
2sd	426	.01	8	74	4	3		
Pat.2.								
A.S mean	757	.85	16	60	5	16	40	20
2sd	198	.1	4	15	4	7		
UA.S mean	1714	.90	35	148	10	4		10
2sd	440	.1	9	55	4	2		
H.S.								
R.S mean	1534	.92	31	211	9	2	99	6
2sd	248	.10	6	68	6	1		
L.S mean	1779	.87	37	210	9	2		
2sd	468	.08	10	114	10	2		6

A.S.=Affected side. UA.S.=Unaffected side. H.S = Healthy Subject.

R.S / L.S = Right/Left Side. Explanation parameters : see text.

2. Assessment of muscle-function in hemiplegic patients.

Table 2 shows the results of FFRM of 10 patients with an at least 2 years existing hemiplegia. All were community-walkers. Differences in motor-performance are detectable : - Loss of

dexterity is represented by a low level of VMA of the TAM, score, frequency and LOP (patient 4, 7, 10). Pearson's correlation coefficient for the LOP with the other parameters is shown in table 2, upper part.

- Tonic hyperreflexia of the GCM is only registered in patient 6 (SP, MMA of the GCM). As the level of CC of the GCM is not raised, there is a tonic hyperreflexia of the GCM throughout the cyclus of motion.- Tonic hyperreflexia of the TAM is present in patient 4, 9 and 10, represented by the MMA of the TAM. Patient 6 shows a high level of MMA of the TAM, caused by a very low level of VMA. The correlation of the defined parameters with the score are also taken up in table 2, lower part. Testing the differences between the affected and unaffected side, significant levels are obtained for all parameters, except the SP ($P < 0,01$, T-test). Table 3 shows the results of test-retest investigation of patient 1 and 2, affected side and unaffected side ($N=15$). The features of motor-performance are stable.

CONCLUSION

Repetitive movement in the ankle-joint is a reproducible method for assessment of the characteristics of disturbance of motor-activation patterns in hemiplegic patients. The performance with Imposed Frequency Repetitive Movement (0.9 Hz) represents the ability to selective muscle-contraction more sensitive than Free Frequency Repetitive Movement. The values, derived from the SR-EMG after ensemble-averaging of the cycles of motion, can be described both by absolute and relative parameters.

DISCUSSION

Large inter-individual differences in the registered levels of SR-EMG limits the clinical use to comparison of the affected side with the unaffected side or before-treatment with after-treatment. Also, the technical equipment, the way of performance and data-processing and the patient-conditions are influencing the results. The method of measurement as described, is a relatively simple method for objectifying motor-function of a muscle. The costs of the technical equipment is low. These are important conditions for extended clinical use. Further investigation to the validity of this method of measurement by evaluating the results of therapeutic regimes and correlation with clinical scores of muscle-function and walking-ability will be performed.

ACKNOWLEDGEMENT

This study was supported by the Dr.W.M.Phelps Foundation for spastic patients, The Netherlands.

REFERENCES

1. Delwaide DJ, Young RR (1985) Clinical Neurophysiology in Spasticity. Elsevier, Amsterdam.
2. Hopf HC, Struppeler A (1974) Electromyographie. Georg Thieme Verlag Stuttgart.

THE CUMULATIVE VIBRATORY INDEX OF THE SOLEUS H-REFLEX: A NEW QUANTITATIVE MEASURE FOR SPASTICITY.

L.J. BOUR, B.W. ONGERBOER DE VISSER

Dept. of Clinical Neurophysiology, Academic Medical Centre, AZUA, Amsterdam
(The Netherlands)

INTRODUCTION

In the past attempts have been made to characterize quantitatively spasticity by means of the H/M ratio and the vibratory index of the Soleus H-reflex (1). The H/M ratio is defined as the ratio between the maximum H-reflex response and the maximum M (motor) response. The vibratory index expresses the amount of H-reflex suppression induced by vibration of the Achilles tendon and is defined as the ratio between maximum H-reflex during vibration and the maximum H-reflex without vibration. The H/M ratio is supposed to be a measure for the excitability of the soleus motoneuron pool, while the vibratory index is a measure for the amount of presynaptic inhibition of I-a afferent volleys. These two measures have demonstrated a quite reproducible value for every subject. However, the inter-individual differences of H/M ratio's appeared to be too large in order to discriminate adequately between healthy subjects and spastic patients (2). It was found that vibratory indices tended to be larger for spastic patients than for control subjects.

A disadvantage of the "classical" index is first of all that it may compare two H-reflex amplitudes (with and without vibration), that have been measured at different stimulus intensities. Secondly the "classical" index only reflects the amount for suppression at one stimulus intensity level of maximum H-reflex response. As a last disadvantage this index is subject to an extra variability, since the variance of the ratio between H-reflex amplitude with and without vibration is equal to the sum of the variance of each H-reflex amplitude separately. In order to overcome these disadvantages of the "classical" vibratory index a new quantitative measure has been developed, called the cumulative vibratory index. This index is defined as the ratio between the surfaces that fall under the two H-reflex recruitment curves, measured with and without vibration. This ratio is a function of stimulus intensity and as a consequence compares two surfaces up to the same intensity level. The cumulative vibratory index represents the integrated effect of vibration up to a certain stimulus level, such that the effects of vibration at lower intensity levels are also incorporated in this index. The variance of each individual ratio at a certain intensity level is more or less averaged out in the cumulative vibratory index, since it represents the sum of all ratio's up to a certain stimulus intensity

level.

SUBJECTS AND METHODS

The control group consisted of 46 healthy individuals while a total of 16 subjects with hypertonia, hyperreflexia and a Babinski response due to upper motoneuron lesions were selected. Registration of the H-reflex occurred by means of the procedure recommended by Hugon (3). H-reflexes were elicited with arbitrarily randomized intervals and at least 30 seconds elapsed between successive stimuli. H/M recruitment curves were measured under normal condition and during vibration of the Achilles tendon. The amplified signals were digitized and stored in the computer with a sample frequency of at least 10 kHz. Peak to peak amplitude as well as area values for the M-response and H-reflex were automatically calculated in an off-line procedure. In addition, recruitment curves of both the M-response and H-reflex were generated. The H/M ratio, the "classical" vibratory index and the cumulative vibratory index were computed from the recruitment curves. The cumulative vibration index I_{cv} is defined as:

$$I_{cv} = \frac{\sum_{i=ithr}^s \{ H_{vibrated}(i+\Delta i) + H_{vibrated}(i) \} \times \Delta i}{\sum_{i=ithr}^s \{ H_{unvibrated}(i+\Delta i) + H_{unvibrated}(i) \} \times \Delta i} \times 100\%$$

i = stimulation intensity
 $ithr$ = threshold intensity level
 Δi = variable inter-intensity interval

This formula expresses the ratio between the surface under the H-reflex recruitment curve with vibration and the surface under the H-reflex recruitment curve without vibration. The ratio is a function of the stimulus intensity, s , up to which integration is carried out. The formula is based on a linear interpolation between two successive measured points of the H-reflex recruitment curve.

Although the I_{cv} is calculated as a function of intensity, statistical analysis was only performed on three intensity levels, that were determined on the basis of the unvibrated recruitment curve i.e.: 1, at the H-max intensity level (S1); 2, at the 0.5 H-max intensity level (S2); 3, at supramaximal intensity level yielding H-total (S3).

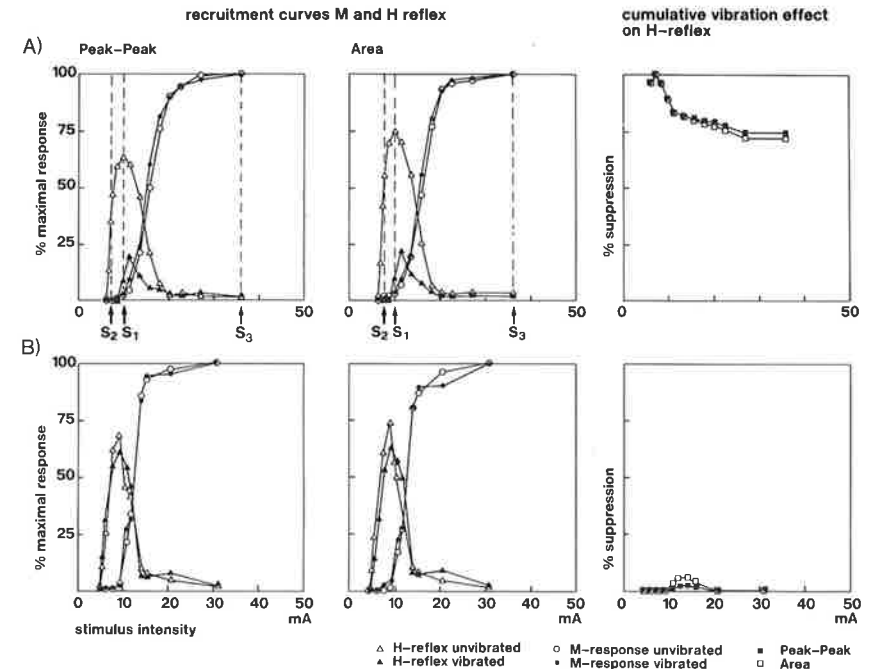


Fig. Representation of M-response and H-reflex recruitment curves with and without vibration for peak to peak values (left panels) and area values (middle panels). The right panels show the cumulative effect of vibration. Upper panels (A) and lower panels (B) refer to a control subject and a patient respectively. S₁, S₂ and S₃ indicate stimulus intensity levels (see text).

Since both peak to peak+area values of the H-reflex were computed, six I_{cv} 's were obtained, i.e., $I_{cv}(S1)PP$, $I_{cv}(S2)PP$, $I_{cv}(S3)PP$ for the peak to peak (PP) values and $I_{cv}(S1)AR$, $I_{cv}(S2)AR$, $I_{cv}(S3)AR$ for the area (AR) values. In addition to the "classical" index I_v , $I_v(AR)$, H/M ratio (PP) and H/M ratio (AR) were also included. This resulted in a total of 10 variables calculated per individual subject.

A stepwise discriminant analysis was performed (BMDP, P7M) in order to investigate which of the 10 variables measured, yielded the best discrimination between the healthy subjects and the patient group. The discriminant analysis yields for every variable, that significantly contribute to a discrimination, a coefficient by which for each case a canonical variable is computed. Classification of both groups is based on this canonical variable. Moreover, a regression analysis with age for the control group was performed on those variables that gave the best classification.

RESULTS

The stepwise discriminant analysis demonstrated that controls and patients could be separated much better with the new cumulative vibratory index than with the "classical" index. The cumulative index Icv(S1)PP gave the best results. Additional information could successively be obtained from the H/M ratio (PP) and Icv(S1)AR. After a discrimination based on these three variables the other variables did not contribute significantly anymore. In this way 100% of the control subjects were correctly classified and 15 of the 16 selected patients (94%) could be correctly classified into the patient group. Mean values and standard deviations for the Icv(S1)PP of the control group and the selected patients are $21\% \pm 16\%$ and $72\% \pm 18\%$ respectively. For the H/M ratio (PP) these values are $49\% \pm 20\%$ and $75\% \pm 26\%$ respectively and for the Icv(S1)AR these values are $23\% \pm 17\%$ and $70\% \pm 18\%$ respectively.

The regression analysis for the control group between age and the variables Icv(S1)PP, H/M ratio (PP) and Icv(S1)AR demonstrated a highly significant ($P < 0.005$) correlation of .41, -.53 and .43 respectively. This means that the amount of H-reflex suppression during vibration and the H/M ratio diminishes with age. Classification of the patient group only on the basis of Icv(S1)PP especially may become difficult at older age due to the increase of this index with age. Conversely, the H/M ratio (PP) decreases with advanced ages and, therefore, this ratio provides additional information for the discrimination between patients and controls.

Mean values of the cumulative index at 0.5 H-max intensity level (S2) in the control group were found to be lower than the indices at the H-max intensity level (S1), while in the patient group mean values of the cumulative vibratory indices at the two intensity levels were practically the same. However, the standard deviations in the patient group for Icv's at S2 stimulus intensity were higher, which consequently caused a somewhat larger overlap for these indices between both groups than for the Icv's at S1 intensity level. In the control group mean values of the cumulative vibratory index at supramaximal intensity level (S3) were higher than those at the S1 intensity level, while again for the patient group both values were of the same magnitude. Therefore, overlap between the patient and control group is considerably large for Icv's at S3 intensity level. The results for these latter cumulative vibratory indices were comparable with the values found for the "classical" index Iv.

DISCUSSION AND CONCLUSIONS

The present study demonstrates that the cumulative vibratory index at H-max intensity level has a much greater discerning power than the "classical" vibratory index in distinguishing between the selected patients and the

control subjects. This difference is mainly due to the fact that, in contrast to the "classical" vibratory index, the cumulative vibratory index represents the integrated effect of vibration up to a certain stimulus level, such that the effects of vibration at lower intensity levels are also incorporated in the calculation.

In the control subjects the cumulative vibratory index related to stimulus intensity (Fig.) shows that with a decrease of stimulus intensity vibration becomes more effective in suppressing the Soleus H-reflex. Since the vibratory effects at lower intensities are integrated in the cumulative vibratory index at H-max, mean values of this index for the control group are found to be about 15% less than the mean values of the "classical" vibratory index. However, the mean values for both indices in the patient group are about the same. This results in a better discrimination between the patient and control group for the cumulative vibratory index. An increased effect of vibration on the Soleus H-reflex in calf muscles at lower intensity levels has also been reported by Van Boxtel (4),

Another interesting result is that the H/M ratio may contribute to the classification of the selected patients. Matthews (2) reported that the inter-individual variability of the H/M ratio in control subjects was too large in order to achieve a quantitative distinction between healthy subjects and spastic patients. However, we have found a significant correlation of the H/M ratio with age and we have demonstrated that, especially at advanced ages, the H/M ratio provides additional information to the quantitative classification of patients with upper motoneuron diseases.

REFERENCES

1. Delwaide PJ (1971) Etude expérimentale de l'hyperreflexie tendineuse en clinique neurologique. Bruxelles: Editions Arsica
2. Matthews WB (1966) Ratio of maximum H-reflex to maximum M-response as a measure for spasticity. *J Neurosurg Psychiatry* 29:201-204
3. Hugon M (1973) In: Desmedt JE (ed) New developments in electromyography and clinical neurophysiology. Karger, Basel pp 508-522
4. Van Boxtel A (1986) Differential effects of low-frequency depression, vibration induced inhibition, and posttetanic potentiation on H-reflexes and tendon jerks in the human soleus muscle. *J Neurophysiol* 55:551-568

MEASUREMENT OF BIOMECHANICAL AND MYOELECTRICAL PROPERTIES OF ELBOW MUSCLES WITH PENDULUM TEST

DAMIJAN MIKLAVČIČ, STANISLAV REBERŠEK, NUŠA GROS*
Faculty of Electrical Engineering, Tržaška 25, Ljubljana (Yugoslavia)
*University Rehabilitation Institute, Linhartova 51, Ljubljana (Yugoslavia)

INTRODUCTION

The function of upper extremities is of great value for a man, one can create works of art, manage tools and perform indispensable daily living movements. It also represents a very important part in human locomotion(1). Some of these performances can be objectively evaluated through different biomechanical measurements.

Biomechanical properties of the elbow joint are interesting from many different points of view such as the state of muscle tonus and reflex activity, fatiguability and joint contractures. In this paper an earlier used pendulum test(2,3,4) applied for the first time on the elbow joint is introduced. This method is classified among measurements of biomechanical parameters where gravity is used for excitation. The object of interest is the position of the forearm and its time derivations. To implement results, electromyographic activity of biceps and triceps brachii is recorded as well.

The aim of this study was to find out whether the pendulum test can be used for clinical measurements of some biomechanical parameters indicating passive muscle properties, reflex responses and range of motions.

MATERIAL AND METHODS

Before performing the pendulum test on the elbow joint in spastic patients, we implemented the model represented by Jackson et.al.(5) in order to verify whether the achieved angle velocity will be of such value which assures the provoking of stretch reflex. The angle velocity achieved was about 400 Deg./sec at the starting angle 115 Deg. which was confirmed by measurements of healthy subjects as well. So, during the pendulum test reflex activities of the elbow joint in spastic patients can be observed besides its passive properties.

Measurement Method

A subject sits on a chair and is fastened on it with wrapper around his shoulders so that he remains in the upright position during the measurement. The arm to be measured hangs freely beside the trunk. Between the trunk and the arm a specially designed panel is placed to avoid possible knocking of the arm against the trunk. The upper arm is fixed for 20 Deg. in retroflexion and slightly abducted. This positioning was chosen in order to enable better swinging. Apart from that, m.biceps brachii is extended in the glenohumeral joint which gives it better efficiency in the elbow joint. During the pendulum test the forearm lightly slides along the panel. In order to decrease this friction and to eliminate the influence of wrist rotation(6) a volar splint is used. A goniometer is placed in the elbow axis to measure the absolute elbow joint angle which is calibrated as 0 Deg. at full elbow extension. Ag-AgCl (diameter 1cm) surface electrodes for the detection of EMGs are placed 2,5 cms apart (center to center distance) longitudinal to the trunk of m.biceps and triceps brachii. The resistance of <10 kilohms between electrodes is assured by means of the contact paste and previous cleaning of the skin. The subject is asked to relax. The examiner grasps the forearm and brings it slowly (angle velocity < 10 Deg./sec) to a predicted position (apr. 100 Deg.). After a few seconds of relaxation in these position the forearm is left to swing freely. Each measurement contains ten tests.

TABLE 1 : GENERAL DATA OF MEASURED SUBJECTS

Initials	Sex	Age	Diagnosis	Time post CVI	Measured upper extremity
M.O.	F	37	Hemipar.sin.	2 months	S
F.Z.K	M	59	Hemipar.sin.	7 years	S
S.C.	M	67	Hemipar.sin.	10 years	S
M.L.	F	22	Healthy	-	D
T.G.	F	25	Healthy	-	D
N.J.	F	21	Healthy	-	D
D.M.	M	25	Healthy	-	D
N.G.	F	51	Healthy	-	D
R.K.	F	24	Healthy	-	D
D.K.	M	26	Healthy	-	D

The measurement was performed on 7 healthy subjects and 3 patients with hemiplegia. In the Table 1 their general data are given.

RESULTS

First an integrated rectified EMG (iEMG) was calculated over a time of period 0-1,252 secs. The average value with standard deviation is given in the Table 2 for each subject. On the basis of the smallest deviation from the average iEMG a typical pendulum test for presentation is chosen. A peak to peak values of EMGs are listed in Table 2 as well. Both parameters characterise the pattern of the muscle activity provoked by passive movement. In the case of the patient S.C. quite a strong tonus in m.biceps and triceps can be observed. Exaggerated phasic activity is observed as well, while in the case of the patient M.O. no reflex activity is present. In the case of the healthy subjects N.G. and D.M. it is necessary to mention that they were already accustomed to the procedure and measurement while the h.sub. D.K. was not able to relax himself. Generally no reflex activity was observed in healthy subjects, which means the velocity was too small to provoke stretch reflex in them.

TABLE 2: RESULTS

	M.biceps brachii:				M.triceps brachii:				R (-)	RPRM (%)	Max. Velocity (Deg./s)
	iEMG (uVs)	STD (uVs)	PP (uV)	STD (uV)	iEMG (uVs)	STD (uVs)	pp (uV)	STD (uV)			
M.O.	5.6	0.2	24.0	6.8	3.3	0.1	14.1	1.4	1.05	73	248
F.Z.K.	10.8	1.9	367.3	188.8	3.0	0.2	22.6	6.4	1.53	82	441
S.C.	14.5	2.2	231.8	77.6	12.6	0.4	81.5	10.6	1.19	72	352
M.L.	5.8	0.2	27.1	3.0	8.9	0.2	64.1	25.1	2.07	100	315
T.G.	6.8	0.3	43.3	9.2	9.4	0.2	53.0	10.5	1.99	100	311
N.J.	6.7	0.4	65.5	49.2	9.2	0.6	66.9	37.7	1.99	114	305
D.M.	1.8	0.2	16.0	6.9	4.7	0.3	23.6	4.1	2.10	105	352
N.G.	1.5	0.2	13.1	6.4	4.6	0.3	28.2	15.5	1.74	101	409
R.K.	6.6	0.2	37.0	4.4	11.8	0.1	83.5	30.5	1.97	94	379
D.K.	10.0	0.8	64.0	13.1	11.5	0.3	49.4	5.2	4.16	100	461

In order to evaluate biomechanical properties of the elbow an amplitude ratio R and the relative passive range of motion were defined. The former is calculated by means of equation 1 and the latter by means of equation 2. Values of both are given in Table 2 as well and they show the possible abnormal properties of the elbow joint and its muscles.

$$R = \frac{\phi_0 - \phi_{\min}}{\phi_0 - \phi_{\max}} \quad (1) \quad \text{RPRM} = \frac{\phi_0 - \min(\phi)}{\phi_0} \cdot 100 \quad (2)$$

To present the arm swinging graphically, a phase diagram (4) is used. In the Fig.1 a comparison between the patient's diagram (solid line) and the healthy

subject (dotted line) is given. The difference in pattern between them is evident.

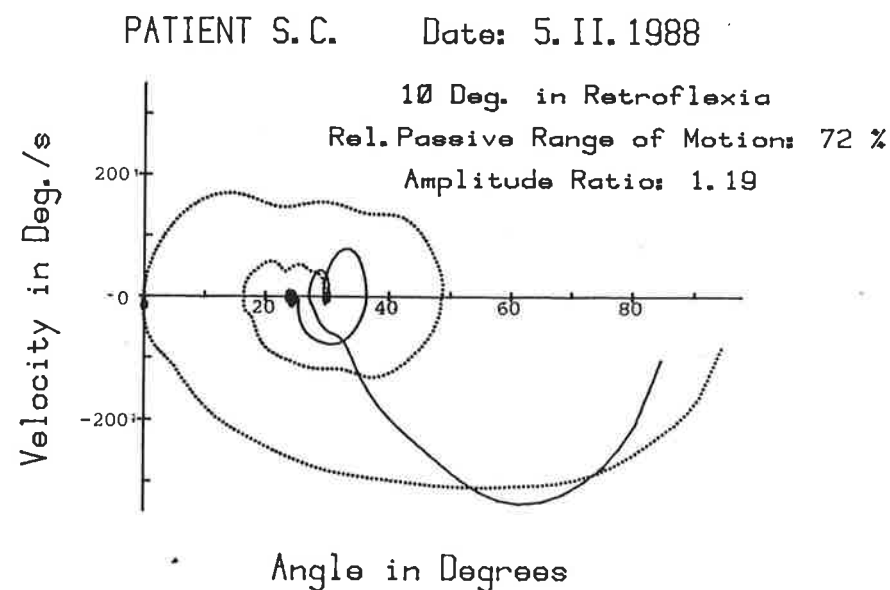


Fig. 1. Phase Diagram

At the end it is to point out that even though the pendulum test is limited due to unadequate velocity course during swinging it still has clinical value for simple objective testing which has now been extended to the upper extremity.

REFERENCES

1. M.L.Fernandez-Ballestreros, F. Buchthal, F. and P. Rosenfalck (1965), The pattern of muscular activity during the arm swing of natural walking, *Acta. Physiol. Scand.*, 63, pp. 296-310
2. R. Wartenberg (1951), Pendulousness of the legs as a diagnostic test, *Neurology*, 1, pp. 18-24
3. T. Bajd, L. Vodovnik (1984), Pendulum testing of spasticity, *J. Biomed. Eng.*, Vol. 6, pp. 9-16
4. T. Bajd (1985), Graphical representation of spasticity measurement data, In: *Electrical Stimulation in restorative neurology*, Progress report for 1984, Ljubljana REC
5. K.M. Jackson, J. Joseph, S.J. Wyard (1978), A mathematical model of arm swing during human locomotion, *J. Biomechanics*, Vol. 11, pp. 277-89
6. D.G. Simons, E.N. Zuniga (1970), Effect of wrist rotation on the XY-plot of averaged biceps EMG and isometric tension, *American J. of Physical Med.*, Vol. 49, No. 4, pp. 253-6

QUANTITATIVE ASSESSMENT OF PATELLAR TENDON REFLEX USING AN ANGULAR ACCELEROMETER

MICHAEL K. YOSHIDA, LARRY W. LAMOREUX, M. ELISE JOHANSON, ROGER ST. HELEN, STEPHEN R. SKINNER, AND R. KIRKLIN ASHLEY

Orthopaedic Biomechanics Laboratory, Shriners Hospitals for Crippled Children, 1701 19th Ave. San Francisco, CA 94122 (USA)

INTRODUCTION

Spasticity is defined as a state of sustained contraction or an increase of muscle tonus. The assessment of spasticity in the clinical setting is usually attempted by tapping the muscle tendon with a hammer or by passive movement of the extremities. At present, a number of therapeutic options are available to treat spasticity, but it is difficult to assess their effectiveness except by subjective impression. An objective measurement of spasticity is urgently needed to assess the efficacy of various treatments which are intended to affect spasticity. In this study, quantitative measurement of the muscle tendon reflex response was performed. This measurement employed an electro-mechanical hammer to produce consistent stimulus forces and an angular accelerometer which allowed free movement of the leg during the reflex response.

METHOD

Angular Accelerometer (Fig. 1). Two linear accelerometers, firmly fixed on a light aluminium frame, were taped to the leg. The entire weight of the angular accelerometer was about 100 grams. The accelerometers were oriented with their sensitive axes parallel to each other, so that, if the proximal acceleration is subtracted from the distal one and divided by the distance between these two accelerometers, an angular acceleration can be calculated.

Electro-mechanical hammer (Fig. 1). An electro-mechanical hammer was constructed from a voice-coil type of linear actuator with a stroke of 2.8 cm. A force transducer was mounted at the tip of the actuator ram to measure the force of the hammer blow. The moving mass of the linear hammer was 75 grams.

Data processing. As shown in Fig. 2, the hammer blow triggered data collection for EMG and acceleration data. The angular acceleration data were processed by digital filtering to remove initial noise caused by direct action of the hammer blow. From the filtered angular acceleration, the first onset of sustained positive acceleration was also displayed. The area under the positive acceleration curve and the peak value of positive acceleration were calculated. The area is expressed as radians/second, and is equivalent to maximal angular velocity. It is hypothesized that the area of positive angular acceleration will be a reliable measure of the magnitude of the muscle stretch reflex response. Two Beckman silver-silver chloride surface electrodes were also applied over the vastus medialis muscle. The latency time between hammer tap and the onset of EMG, and the peak-to-peak value of a single twitch, were measured from the recorded electromyographic data.

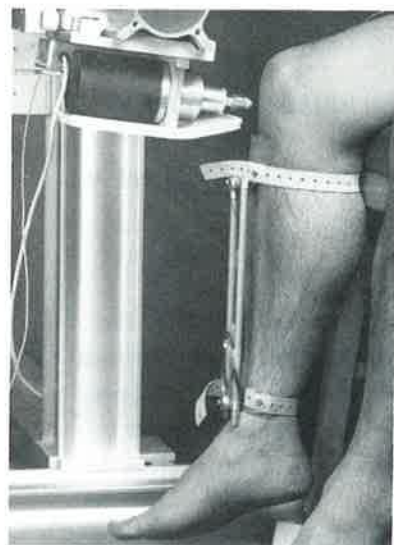


Fig. 1. Electro-mechanical hammer and angular accelerometer

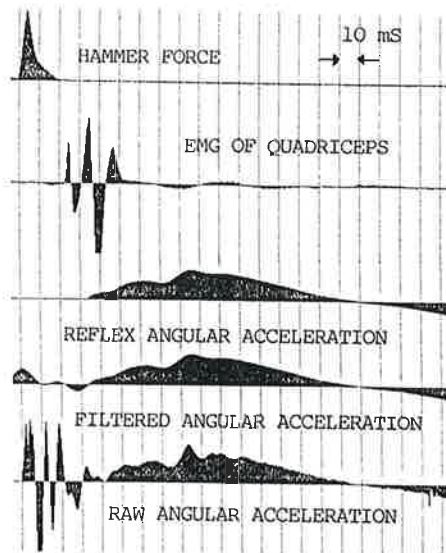


Fig. 2. Hammer force, EMG and Reflex angular acceleration

SUBJECTS

Five normal adults (from 30 to 59 years old) consisting of three females and two males were assessed. Normal subjects were the investigators, staff members of our laboratory, and faculty members of University of California at San Francisco. None of them had any known neurological or musculo-skeletal diseases. Five spastic spinal cord injured children also were chosen for study. Of these, three were males and two were females (from 15 to 20 years old). The average time after their spinal cord injury was 5.6 months, ranging from 2 months to 12 months.

PROTOCOL

All subjects sat in a wheelchair with their legs hanging down freely. The angular accelerometer was attached to the anterior surface of the leg. The linear actuator type electro-mechanical hammer was precisely positioned perpendicular to the right patellar tendon at a distance of 7 mm. The hammer's force can be varied electrically from 0 to 40 Newtons. At least twenty taps were made in each test session. All the data were analyzed statistically. The experiment was conducted in a controlled, quiet environment.

RESULTS

Table 1 shows the average, one standard deviation, and the total number of taps for five normal subjects. Approximately the same hammer force was used for all the normal subjects (mean is 26 N, ranging from 25 to 28 N). The average positive area among five subjects was 1.06 rad/sec.

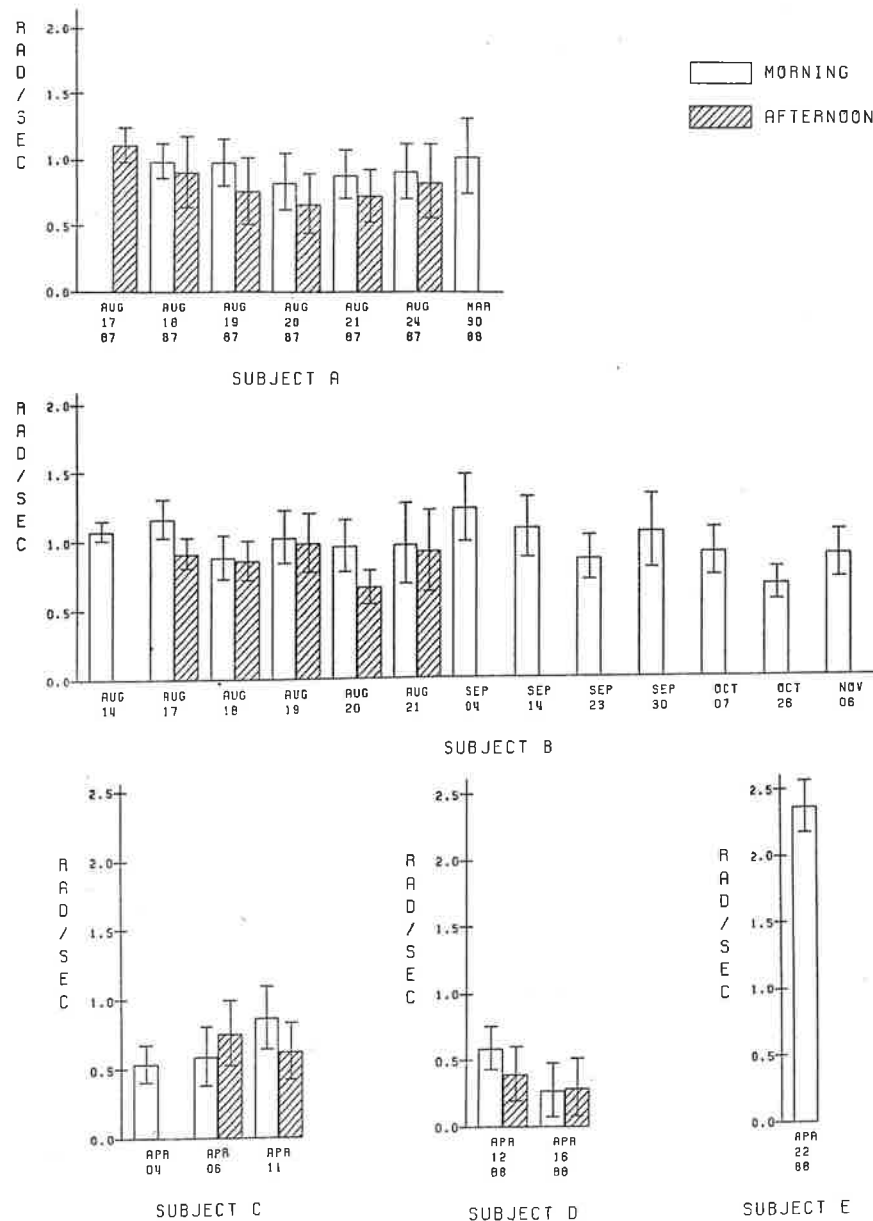


Fig. 3. Physiological fluctuation of five normal subjects.

However, the results varied widely from subject to subject. For example, the ratio of the smallest response to the largest was about 1 to 6.

TABLE 1
RESULTS OF FIVE NORMAL SUBJECTS

Subject	A	B	C	D	E	Average of five subjects
Hammer force (N)	25	26	28	26	26	26
Mean (rad/sec)	0.91	0.93	0.70	0.39	2.37	1.06
Standard Dev.	0.28	0.25	0.24	0.23	0.20	0.24
Count	266	400	114	100	25	181

For normal subjects the results fluctuated within the same day and from day to day. Within the same day and on consecutive days, this fluctuation was not statistically significant. However, subjects A and B showed significant variation between two non-consecutive days (Fig. 3).

Auditory stimulation had no significant enhancing effect in all subjects. Jendrassik's maneuver showed a significant effect in two subjects (D and E), but the other three had no enhancements (Fig. 4).

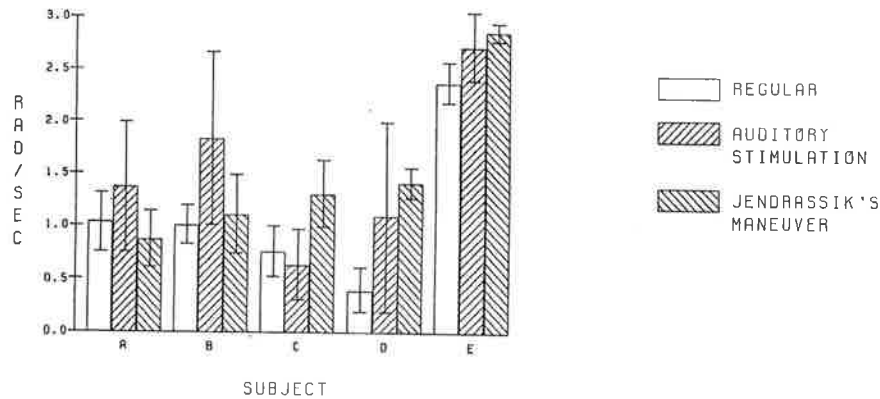


Fig. 4. Effect of auditory and Jendrassik's maneuver enhancement on PTR of five normal subjects.

Five spastic subjects were examined. Table 2 shows the results for these spastic subjects. The average standard deviation is larger among spastic patients than normals. Subject 2 shows a very low reflex even though this subject had severe spasm of both lower extremities and trunk muscles. Subject 2 has hypertonic muscles, but no hyperreflexia. This illustrates the limitation of this method; only the hyperreflexic component of spasticity can be measured. Three subjects showed a

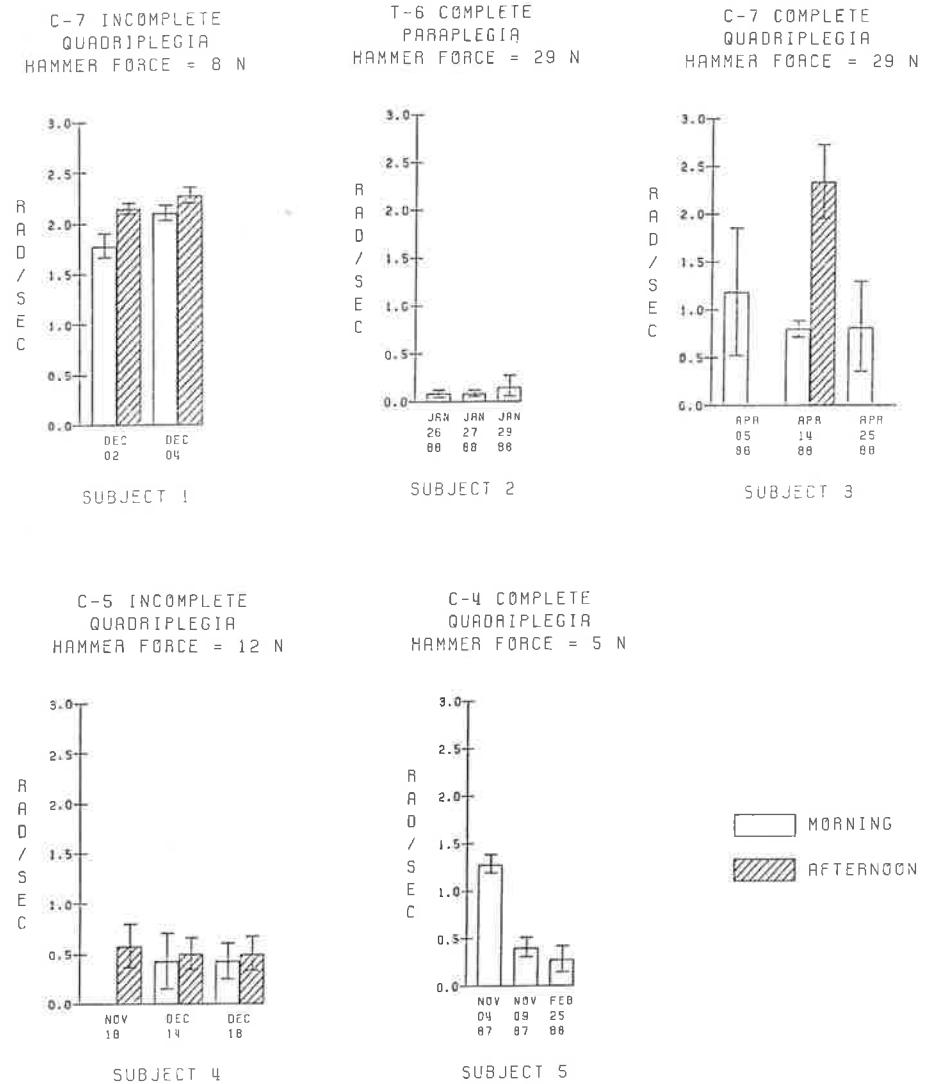


Fig. 5. Daily fluctuation of five spastic patients.

large magnitude of reflex, therefore, the hammer force had to be reduced to produce a moderate reflex.

TABLE 2
RESULTS OF FIVE SPASTIC SPINAL CORD INJURY PATIENTS

Subject	1	2	3	4	5	Average of five patients
Hammer force (N)	8	29	29	12	5	16.6
Mean (rad/sec)	2.07	0.11	1.22	0.49	0.63	0.90
Standard Dev.	0.20	0.07	0.70	0.21	0.45	0.33
Count	86	84	120	114	66	94

The daily fluctuation among SCI patients was greater than among normal subjects (Fig. 5).

CONCLUSION

The use of an angular accelerometer for quantitative assessment of the muscle tendon reflex is a new and valid technique. The greatest advantages of this technique, rather than the use of EMG or a force transducer, are that: 1) it does not prevent the normal reaction movement of the leg; 2) it can be used with the extremities in any position; 3) the accelerometer is light and small, so that the measurement does not appreciably affect the reaction itself; and 4) the size of the entire apparatus is small and it is easily attached to a human's extremity. In normal subjects the average maximal angular velocity was 1.06 rad/sec with 26 N average hammer force and it fluctuates physiologically, usually insignificantly. Jendrassik's enhancement maneuver was effective only in two among five subjects. In spastic subjects, only the hyperreflexia could be measured. The average maximal angular velocity was 0.9 rad/sec with an average hammer force of 16.6 N. Tap to tap and daily fluctuations were significantly large.

ACKNOWLEDGEMENTS

We gratefully acknowledge the support of Shriners Hospitals for Crippled Children.

REFERENCES

1. Simons DG, Dimitrijevic MR (1972) *Am J Phys Med* 51:240-263
2. Simons DG, Lamonte RJ (1971) *Am J Phys Med* 50:72-79
3. Kroll W (1968) *Am J Phys Med* 47:292-301
4. Clarke, AM (1967) *J Neurol Neurosurg Psychiat* 30:34-42

COMPARISON BETWEEN PHENOLISATION OF THE MOTOR POINTS OF THE GASTROCNEMIC MUSCLE AND PHENOLISATION OF THE TIBIAL NERVE

D. WEVER, M. SCHLECHT, H.J. HERMENS

Rehabilitation Centre het Roessingh, Roessinghsbleekweg 33, 7522 AH Enschede, The Netherlands

INTRODUCTION

The arguments whether a phenolisation will be performed by blocks of the motorpoints of the gastrocnemius muscle or by blocks of the tibial nerve are described. The subjects, the method of phenolisation, the criteria of evaluation and the (preliminary) results are described and compared.

I. PHENOLISATION OF THE MOTOR POINTS OF THE GASTROCNEMIC MUSCLE

In our rehabilitation centre, we have performed percutaneous phenolblocks in order to decrease the activity of spastic muscles for several years with reasonable success. The following study was set up to evaluate the results by means of objective criteria.

PATIENTS

A group of 16 hemiplegic patients was treated for a spastic equinovarus foot after a period of at least 6 months succeeding the cerebrovascular accident. This time span eliminates effects due to the improvement of the neurologic disorder.

METHOD OF PHENOLISATION

The motor point was localized with a skin electrode in the traditional way. After this the motor endplate zone was searched with a needle. Upon each stimulus the EMG response of the muscle was registered. The position of the needle that caused a clear biphasic response at low amplitude (1 mA) of stimulation was the most suited to inject phenol solution. When such an optimal point was found, a small amount of phenol solution (\pm 0.25 cc) was injected. After this other optimal points within the endplate zone were investigated until no responses were found anymore on surface EMG (1).

METHOD OF EVALUATION

During the phenolisation procedure the total amount of phenol solution used was recorded as well as the EMG-response to every injection with 0.25 cc. It was possible to note side-effects.

In order to investigate the short term results a number of tests were

performed immediately before and after the phenolisation; clinical determination of the clonus and the achilles tendon reflex and determination of the T-response. This is the EMG response to performing the tendon reflex elicited by means of a special hammer (connected with the EMG apparatus).

In order to investigate the long term effects we used:

1. Clinical function tests: by means of the leg function test we quantified the ability to perform plantar and dorsal flexion in a 4 point scale.
2. Gait analysis: we determined the symmetry of gait and the walking speed.
3. Surface EMG: By means of standardised EMG registration and analysis we determined the maximal activity of the gastrocnemius muscle and its antagonist, the anterior tibial muscle (2).

These tests were repeated 2 weeks, 2 months, 6 months and 1 year after the phenolisation.

RESULTS

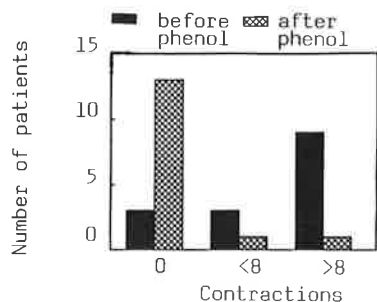


fig. 1. The clonus

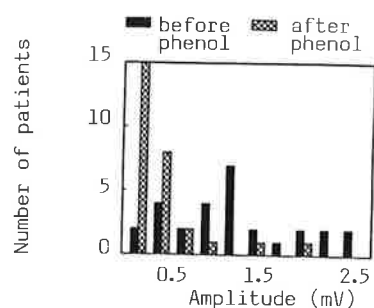


fig. 2. The T-response

Short term effects: (3)

The achilles tendon reflex, the clonus (number of contractions) (fig. 1) and the T-response (fig. 2) showed a clear decrease.

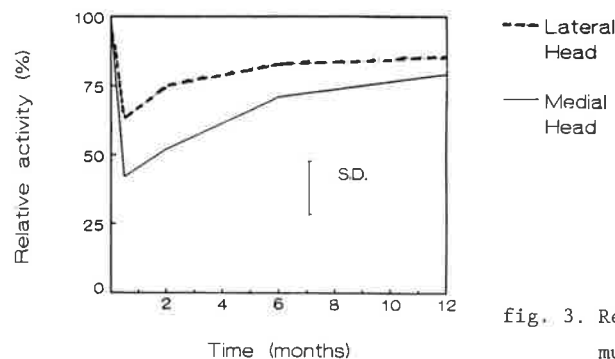


fig. 3. Recovery of the gastrocnemius muscle.

Long term effects: (3)

The clinical function tests (dorsal and plantar flexion) showed no changes. The walking velocity and the symmetry in swing phase did not show a clear difference before and after the phenolisation.

Surface EMG: The maximal activity of the musculus gastrocnemius showed a significant decrease up to 12 months. The activity is noted as a percentage of the activity before the phenolisation (fig. 3). The activity in the anterior tibial muscle showed no significant change.

CONCLUSIONS

It is obvious that the short term effects are better than the long term effects. The short term effects might have been caused by a local anaesthetic effect, the long term effects by a neurolytic action of phenol solution. Probably we did not succeed in blocking motor points with a destroying neurolytic action in some cases (4).

The EMG registrations are more sensitive to changes than the leg function test and the gait analysis.

There is a large difference in effect among the individual patients. No side effects were found.

2. PHENOLISATION OF THE TIBIAL NERVE

We decided to start a new study with phenolisation of the tibial nerve. We chose this technique because of the following reasons:

1. with 1 block all innervated muscles are treated.
2. only 1 place has to be blocked instead of 2.
3. a smaller amount of phenol is needed.
4. it is easier to find the nerve than the motorpoints.

METHOD OF PHENOLISATION

Basically the same method is used as the one described before. The injection of phenol solution is done more carefully because of the possibility of neuralgia.

PATIENTS

The same selection criteria are used.

METHODS OF EVALUATION:

The short term results were not evaluated again. The long term results were evaluated by means of the following examinations:

1. Inquiry form.

2. Ashworth scale.
3. Standardised EMG measurements.
4. Gait analysis: measurements of the angle of the spastic equinusfoot, EMG measurement of the gastrocnemius and the anterior tibial muscle and time-distance factors.

PRELIMINARY RESULTS

Inquiry form:

Overall result: all 4 patients responded positive.

Walking: 4 patients walked easier.

Clonus: 3 patients had no clonus anymore after the phenolisation. The other one had no clonus before.

Side-effects: 1 patient got an obvious neuralgia, 1 patient had disturbances of sensibility during 2 weeks.

Ashworth scale:

no change.

Surface EMG:

After 2 and 8 weeks 3 patients did not show any EMG-activity during passive dorsal flexion in the gastrocnemius muscle. 1 Patient (with spastic activity only in the posterior tibial muscle) did neither show any activity during passive dorsal flexion after 2 and 8 weeks. The activity in the anterior tibial muscle and the peroneal muscle showed no clear change.

Gait analysis:

All the patients showed a decrease of activity in the gastrocnemius muscle during stance and swingphase (fig. 4). As a result of this the activity in the anterior tibial muscle decreased too (during swingphase). Probably this is due to a better balance between the two muscles. At the same time the angle of the ankle showed more dorsal flexion during stance phase.

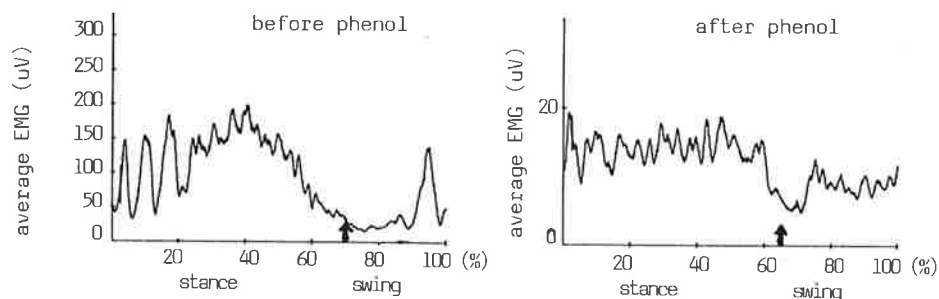


fig. 4. Average EMG of gastrocnemius muscle during 1 gait cycle

CONCLUSIONS

Compared to the first method of phenolisation (motorpoints) the following conclusions can be drawn:

No objective comparison is possible because of too few patients in the second too short follow-up study.

The second method of phenolisation is less time consuming.

It seems that there are more side effects in the second study.

In the second study the EMG activity in the gastrocnemius muscle during standardized EMG measurements decreased too.

EMG measurements during walking seem to give good information about the balance between gastrocnemius and anterior tibial muscle.

The study will be continued to get more objective and reliable data.

REFERENCES:

1. Zilvold G, Hermens H.J., Boon K.L., Wever D. (1982): Treatment of spastic muscles by means of phenol blocking: EMG analysis before and after treatment. Proceedings 5th Congress of ISEK, Ljubljana, Journal of Slovenian Medical Society: 143-144.
2. Hermens H.J., Boon K.L., Zilvold G. (1984): The clinical use of surface EMG. *Electromyogr. clin. Neurophysiol.*, 24: 243-265.
3. Wever D, Buurke J., Hermens H.J., Zilvold, G. (1985): Evaluation of the effect of phenolisation by means of a quantitative follow up-study. Proceedings 6th Congress of ISEK, Tokyo: 5-4-3.
4. Felsenthal G. (1974): Pharmacology of phenol in peripheral nerve blocks: a review. *Arch. Phys. Med. Rehab.*, 55: 13-16.

NEUROMUSCULAR DISEASES

Therapeutic methods and fundamental research

EFFECTS OF ELECTRICAL STIMULATION ON MUSCLES OF PATIENTS WITH PROGRESSIVE MUSCULAR DYSTROPHY

MILAN GREGORIČ*, VOJKO VALENČIČ**, ANTON ZUPAN*, ANA KLEMEN*

*University Rehabilitation Center Ljubljana, **Faculty of Electroengineering, E. Kardelj University, Ljubljana (Yugoslavia)

INTRODUCTION

Low frequency electrical stimulation of dystrophic muscles may improve some biochemical and contractile properties of the affected muscle fibers^{1,2}. In the present study we wished to analyse the effects of long-term electrical muscle stimulation with two different frequencies (8 and 20 Hz) on the muscle strength and fatiguability in patients with various types of muscular dystrophy.

PATIENTS AND METHODS

13 patients with an established diagnosis of progressive muscular dystrophy were included in the study (12 boys and one girl). 5 patients had Duchenne, 4 limb-girdle, 3 Becker and one facioscapulohumeral type of muscular dystrophy. They were 8 - 21 years old, on average 14.2 ± 4.2 years. Functional ability classified after the Vignos and Archibald's scale³ was 1 - 9, on average 3.9 ± 2.9 .

The isometric muscle strength during maximal voluntary contraction (MVC) in the direction of the dorsal flexion of the foot was measured by means of a special brace for measuring torques of the ankle⁴. Fatigue resistance was measured during one minute of maintenance of MVC (Fig.1).

Changes in the amplitude of the EMG responses, recorded by surface electrodes over the tibial anterior muscle and evoked by prolonged repetitive supramaximal stimulation of the peroneal nerve, were also studied (Fig.3). The duration of impulses was 0.3 ms. The periods of stimulation lasted one minute at each stimulation frequency - 50 Hz and 20 Hz. All measurements were performed on both legs.

When the measurements were completed long-term electrical stimulation of the tibial anterior muscle on the right leg was introduced. The left leg served as a control. The stimulator generated two-phase voltage pulses occurring cyclically in trains - each pulse train lasted 5 sec. and was followed by a 5 sec. pause. Pulse width was 0.2 ms, pulse frequency was 8 Hz in 8 patients and 20 Hz in the other 5 patients. The intensity of stimulation was adjusted individually to the level where an appropriate visible contraction was obtained. The patients stimulated their muscles 2-3 times daily for one hour. After 2-3 month of regular muscle stimulation all the described measurements were repeated.

RESULTS

The results of torque measurements on MVC and fatigue testing are shown in Fig.1., Fig.2. and Table I.



Fig.1. Recording of torques at the ankle and EMG activity of the tibial anterior muscle on three trials of isometric MVC in the direction of dorsal flexion (left) and fatigue testing on one minute maintenance of MVC (right).

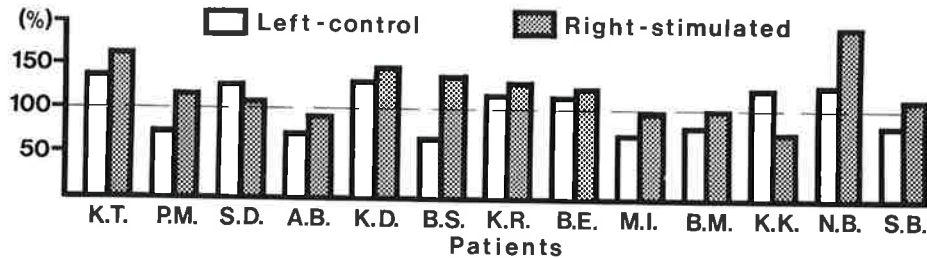


Fig.2. Histograms showing torques on MVC after long-term muscle stimulation expressed in the percentage values of the initial torques, measured before the stimulation.

TABLE I.

The mean torques (+SD) on MVC in the direction of the dorsal flexion of the foot and fatigue indices* on the stimulated right leg and on the control left leg, before and after a long-term stimulation of the right tibial anterior muscles, in 13 patients with muscular dystrophy.

N = 13	Mean torques on MVC		Fatigue indices	
	Before	After	Before	After
Stimulated Leg (Nm)	4.53 +- 4.11	5.92 +- 5.85	0.72 +- 0.2	0.68 +- 0.13
Control Leg (Nm)	4.42 +- 4.26	4.62 +- 4.30	0.78 +- 0.14	0.69 +- 0.13

* Torques at the end of measurement divided by torques at the beginning of one minute of maintenance of MVC.

Voluntary EMG activity was also recorded but not yet analysed in detail.

No obvious relationship between the effects of the muscle stimulation on its strength, measured as torques on MVC, and the applied pulse frequency of the long-term stimulation (8 Hz or 20 Hz) was observed.

The mean changes of the amplitude of the EMG responses of the tibial anterior muscle evoked by prolonged repetitive stimulation of the peroneal nerve at two different frequencies (50 Hz and 20 Hz) are shown in Fig. 3 and Table II.

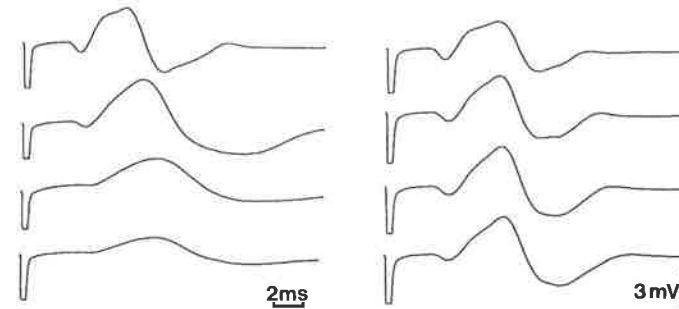


Fig.3. EMG responses of the tibial anterior muscle evoked by prolonged repetitive stimulation of the peroneal nerve. 32 responses were averaged at the beginning of the stimulation and after 20, 40 and 60 sec. of continuous stimulation with 50 Hz (left) and 20 Hz (right).

TABLE II

Mean percentage changes (+SD) of the amplitude of averaged EMG responses calculated from the first to the last averaged responses (32 averages) in one minute periods of stimulation.

Stimulation frequency	50 Hz		20 Hz	
	Before	After	Before	After
N = 13				
Stimulated Leg (%)	-55.8 +- 18.6	-62.5 +- 25.0	0.3 +- 25.7	23.1 +- 35.5
Control Leg (%)	-55.3 +- 19.0	-58.2 +- 25.4	27.7 +- 47.3	27.6 +- 37.7

DISCUSSION AND CONCLUSIONS

The increase in the isometric voluntary strength of the tibial anterior muscle was observed in 10 of 13 investigated patients after long-term stimulation of this muscle in comparison to the initial values before stimulation. A pronounced increase in the torques during maximal voluntary contraction was observed after the stimulation programme only in one patient with a mild form of limb-girdle muscular dystrophy.

In severely disabled patients, especially in boys with Duchenne muscular dystrophy, the improvement of muscle strength after prolonged stimulation was very slight, functionally insignificant and often only relative in comparison to the initial values or results on the unstimulated leg. It seems reasonable to believe that early use of electrical muscle stimulation in mildly affected patients with progressive muscular dystrophy may show better results than in the later stages of the disease.

Long-term muscle stimulation did not effect the results of fatigue testing. No significant influences on the decremental or incremental behaviour of the electrically evoked EMG responses (post-tetanic exhaustion or potentiation) were observed on testing with prolonged repetitive stimulation.

No differences in the effects of the pulse frequency (8 Hz or 20) of the long-term muscle stimulation could be demonstrated. The optimal frequency and other stimulation parameters for achievement of possible therapeutic effects on dystrophic muscles are not yet firmly determined.

The results of the present study, revealing mild improvement in the strength of the stimulated muscle and no significant changes in fatiguability, are in agreement with the findings reported by Scott et al.².

However, the essential questions, whether an early use of chronic electrical muscle stimulation could delay degenerative or support regenerative processes, remain unanswered and demand further, more extensive studies with a long-term follow up of the treated patients.

REFERENCES

1. Vrbova G, Ward K (1981) Observations on the effects of low frequency electrical stimulation on fast muscles of dystrophic mice. *J Neurol Neurosurg Psychiatr* 44: 1002-6
2. Scott OM, Vrbova G, Hyde SA, Dubowitz V (1986) Responses of muscles of patients with Duchenne muscular dystrophy to chronic electrical stimulation. *J Neurol Psychiatr Neurosurg* 49: 1427-1434
3. Vignos PJ Jr., Archibald KC (1960) Maintenance of ambulation in childhood muscular dystrophy. *J Chron Dis* 12: 273-290
4. Trnkoczy A (1978) Functional Electrical Stimulation of Extremities: It's Basis Technology and Role in Rehabilitation, *Automedica* 2: 59-100

THE VALUE OF LIGHT-WEIGHT ORTHOSES IN THE PREVENTION OF SCOLIOSIS IN DUCHENNE MUSCULAR DYSTROPHY

ELIANA B RODILLO, MD; ESTHER FERNANDEZ-BERMEJO; JOHN Z HECKMATT, MB ChB MRCP MD; VICTOR DUBOWITZ, MD BSc MRCP DCH.

Department of Paediatrics, Hammersmith Hospital, London, U.K.

INTRODUCTION

All boys with DMD lose independent walking by 13 years of age. Once wheelchairbound, progressive scoliosis is the most serious complication and occurs in over 90% of boys

Prolongation of ambulation in full length ischeal weight-bearing orthoses was first described in 1962 (1) and it has been suggested that this may prevent progressive scoliosis, although at present there is no definite confirmation.

In this study we tried to establish whether rehabilitation in orthoses had been effective in preventing scoliosis.

PATIENTS AND METHOD

93 boys with DMD (aged 6-12 years) were rehabilitated in light-weight knee-ankle-foot orthoses at the time of loss of ambulation between 1977-1987 at Hammersmith Hospital. The scoliosis data was analysed cross-sectionally and longitudinally.

(1) Cross-sectional analysis. 84 of the boys had had at least one spinal X-ray, and when there was more than one X-ray, the latest was analysed. The severity of the scoliosis was measured by the Cobb method.

We found there was a sharp rise in the Cobb angle data at 13 years and so the boys were divided in two groups. Group I: 39 boys, aged 9 to 12 years 11 months. Group II: 45 boys, aged 13 to 20 years. Linear regression analysis was performed for each group separately to determine the relationship between the Cobb angle and the age, the time spent wheelchairbound and the age of loss of ambulation in the orthoses. Group II was also subdivided according to whether the boy stopped walking in orthoses before 13 years of age (26 boys) or after 13 years of age (19 boys), and the difference in the Cobb angle analysed using the Mann-Whitney U-test.

(2) Longitudinal analysis. 38 boys had had 2 or more X-rays, 6 months apart, which allowed measurement of the rate of progression of the scoliosis. The rate of progression was analysed for three age ranges: A) 10-12 years 11 months B) 13-14 years 11 months C) 15-18 years. The rate of progression for the age ranges (B) and (C) was calculated separately for those boys who stopped walking in orthoses before 13 years of age and those who continued walking after 13 years.

RESULTS

Of the 93 boys, 77 were no longer ambulant in the orthoses having walked for a period ranging from 0 to 72 months (mean 21 months) in them. There was no relationship between the age at rehabilitation and the duration of ambulation. Seventeen boys are still ambulant in the orthoses on average 25 months after rehabilitation.

(1) Cross-sectional analysis. There was no significant relationship between the Cobb angle and the boy's age in either group. There was a highly significant relationship between the Cobb angle and the time spent wheelchairbound (0.01 in each group) and an inverse relationship between the Cobb angle and the age of loss of ambulation in the orthoses (p 0.05 in each group). In group II there was a highly significant difference in the Cobb angle between the 26 boys who stopped walking in orthoses before 13 years of age (mean 62 degrees) and the 19 boys who walked beyond 13 years of age (mean 32 degrees) (p 0.005).

(2) Longitudinal analysis. Longitudinal analysis showed the mean rate of deterioration in the Cobb angle in four of the five groups was similar ranging from 0.5 to 0.95 degrees/month including the mean rate between 13 and 14 years 11 months in 14 boys who were ambulant in the orthoses beyond the age of 13 years. In contrast the mean rate between 13 and 14 years 11 months in 13 boys who had stopped walking in orthoses before 13 years of age, was significantly higher at 2.5 degrees/month (p 0.001). Fig shows the raw data.

DISCUSSION

This study clearly shows that the most rapid rate of deterioration in scoliosis occurs during puberty (13 to 15 years of age), a feature also observed in other forms of scoliosis (2). The longitudinal data showed markedly slower rate of progression of scoliosis at this age in boys who walked in orthoses beyond 13 years of age. The cross-sectional data confirmed the same findings by showing much less scoliosis in boys who walked in the orthoses beyond the age of 13 years. 22% of boys walked beyond 13 years in the orthoses and none could have done so without the orthoses.

Despite the use of the orthoses, scoliosis developed in the majority of boys with DMD because they stop walking before puberty or in early puberty. The effect of the orthoses is to delay the onset of scoliosis for 2 years (on average) and thereby delay the need for spinal stabilization. If the boy manages to walk during puberty with orthoses, scoliosis is effectively prevented. However, if the boy does not walk during puberty this delay is probably valuable as it effectively postpones the need for spinal stabilization (Luque procedure). This is important as the Luque procedure may have a finite life (3).

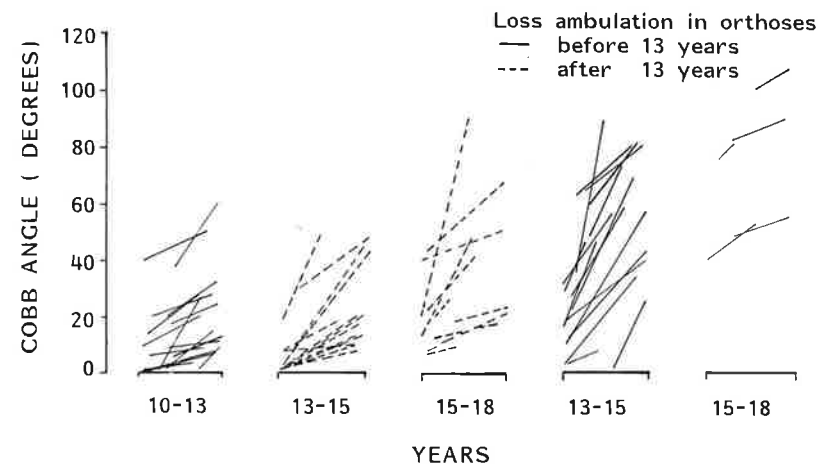


Fig. Longitudinal data showing the rapid rate of progression of the curve between 13-15 years in the boys who stopped walking in the orthoses before 13 years of age.

BIBLIOGRAPHY

- (1) Spencer GE, Spencer JR, Vignos PJ (1962). *The Journal of Bone and Joint Surgery* 44A: 234-242.
- (2) Duval Beaupere G (1972). *Acta Orthopaedica Belgica* 38: 365.
- (3) Herndon WA, Sullivan JA, Yngre DA, Gross RH, Dehren G (1987). *Journal of Bone and Joint Surgery* 69A: 851-859.

FORCE OF DYSTROPHIC MOUSE HINDLEG MUSCLES AND THE EFFECT OF EARLY IMMOBILIZATION.

L. BROCKS H. JANSSEN W. WALLINGA-DE JONGE [x] and P. WIRTZ.
Department of Cell Biology, Univ. of Nijmegen, St'Adelbertusplein 1,
6525 EK Nijmegen, [x] Department of Electrical Engineering, Univ. of
Twente, 7500 AE Enschede, The Netherlands.

INTRODUCTION

Muscular dystrophy in the mouse strain ReJ 129 is an inherited progressive disease. There is a continuous loss of muscle fibers, partly compensated through regeneration.

The first signs of necrosis (death of single fibers and small groups of fibres) are found during the second week postnatally¹. Early immobilization postpones and reduces the progression of the disease, provided the procedure is started before necrosis is observed². The effects of early immobilization on the force characteristics of dystrophic muscles can be studied only when we know how force characteristics change during the development of normal and dystrophic muscles, that is without immobilization. Force characteristics of developing normal and dystrophic extensor digitorum longus (EDL) muscles are described here in detail. The effect of early immobilization on the force characteristics of normal and dystrophic EDL is shown for a limited number of animals.

MATERIALS AND METHODS:

Mice

In this study mice of the strain ReJ 129 were used. The dystrophic mice were bred from heterozygous (Dy/dy) animals. As controls either normal heterozygous animals or mice of a homozygous (Dy/Dy) line were used. The animals were in the range of 20-80 days of age.

After weighing, the animals were given an atropine sulfate solution (0.05 mg/ml) to prevent excessive mucus secretion in the respiratory organs. Subsequently they were anaesthetized with pentobarbital sodium (10 mg/ml). The mice were placed upon a heated table (35 °C) to control body temperature.

Immobilization

Animals of 7 days old were anaesthetized with ether and the left hindleg was immobilized by fitting a plastic cast around the leg and

foot. The cast, fixed with plaster tape, was fitted in such a way that the calf muscles were in a relaxed, and the EDL in a lengthened position. All littermates of heterozygote (Dy/dy) parents were treated. The immobilization lasted for one week, adapting the casts to the size of the leg every other day. After this period remobilization was achieved by removing the cast.

Force measurements

Force measurements (twitch and tetanus) were carried out in vivo on the EDL of the left and right hindleg. The EDL was exposed leaving the blood supply and innervation intact. First the EDL of the left leg was prepared and measured, second the EDL of the right leg. The femur was fixed in a clamp as proximal to the knee as possible. The distal tendon was tied to an isometric force transducer (Sensotec, 500 mN). Muscle temperature was controlled by a constant flow of warm, moist air (muscle temperature, 36.0 ± 1.0 °C). The n. peroneus, innervating the EDL, was stimulated via a bipolar stimulating electrode. Stimulation was supramaximal (pulse width 50 μ s). The characteristics studied at the optimal twitch length were: the amplitude, contraction and half relaxation times of the twitch; the amplitude of a 200 Hz tetanus during 200 ms. Normal and dystrophic muscles show a smooth, stable force plateau upon such a stimulation pattern.

Dystrophic muscles are very susceptible to extension. Lengthening of dystrophic EDL beyond a critical length appeared to irreversibly damage the muscle. Force (twitch and tetanus) collapsed, when muscles were stretched to a length a little above this critical length (which was found to be about comparable with the optimal twitch length). Therefore the optimal twitch length could only be approximated, approaching it from short length. When active force did not increase substantially upon lengthening, further extension was stopped to prevent surpassing the critical length.

Morphometry

After completion of the physiological measurements, the muscles (left and right EDL) were excised and frozen in isopentane (-150 °C). The largest cross sectional area of the muscle was measured, using serial frozen cross sections (10 μ m).

RESULTS

Body-weights of the dystrophic animals were compared with those of normal littermates. In control mice growth was considerable during

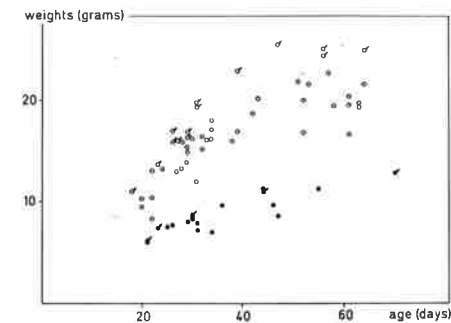


fig. 1: Body weights (in grams) of dystrophic and normal mice at various ages; \blacksquare = dystrophic male, \bullet = dystrophic female, \square = normal male, \circ = normal female.

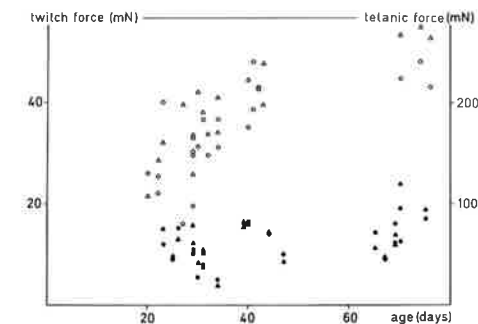


fig. 2: Absolute twitch and tetanic forces of normal and dystrophic EDL of mice at various ages, expressed in mN; \bullet = twitch of dystrophic muscle, \circ = twitch of normal muscle, \blacktriangle = tetanus of dystrophic muscle, \triangle = tetanus of normal muscle.

the postnatal period of 20 to 50 days of age. Dystrophic mice weighed significantly less than their normal counterparts for all ages studied (fig. 1).

The twitch and tetanic force of normal EDL increased strongly during this period. The twitch and tetanic force of dystrophic EDL remained below normal EDL even at an age of 23 days (fig. 2). Also twitch and tetanic forces, as related to the largest cross sectional area, were lower in dystrophic EDL, compared with normal EDL (fig. 3).

The twitch contraction time of dystrophic EDL seemed to be a little prolonged when compared with normal EDL, but the differences were not significant. The twitch contraction time of dystrophic EDL

was 8.8 ± 1.2 ms (mean \pm SD, $n=22$) in dystrophic EDL compared with 8.0 ± 0.9 ms ($n=27$) in normal EDL. The twitch half relaxation time of dystrophic EDL was 12.4 ± 4.7 ms ($n=22$) and of normal EDL 8.7 ± 2.0 ms ($n=27$).

As a result of early immobilization, the tetanic force of the remobilized dystrophic EDL of adult mice appeared to be higher than of the dystrophic EDL of the contralateral, non-treated leg. The effect of immobilization on twitch force was less clear (fig. 4).

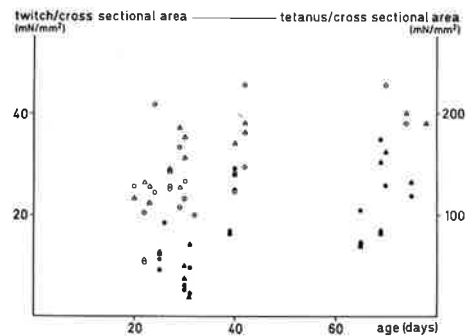


fig. 3: Twitch and tetanic forces relative to cross sectional area of normal and dystrophic EDL muscles of mice at various ages, expressed in mN/mm^2 ; ● = twitch/cross sectional area of dystrophic muscle, ○ = twitch/cross sectional area of normal muscle, ▲ = tetanus/cross sectional area of dystrophic muscle, △ = tetanus/cross sectional area of normal muscle.

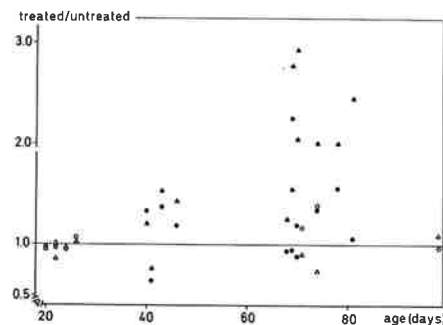


fig. 4: The effect of early immobilization on the twitch and tetanic forces of normal and dystrophic EDL muscles of mice at various ages. The ratio between the treated and non-treated leg of an animal is expressed against its age. ● = twitch ratio dystrophic EDL, ○ = twitch ratio normal EDL, ▲ = tetanus ratio dystrophic EDL, △ = tetanus ratio normal EDL. The drawn line expresses the non-effect level. A point above this line means a positive effect of the treatment.

DISCUSSION

It has to be noted that different strains of mice vary in onset and progression of the disease, therefore we only can compare our work with that of Douglas and Baskin¹ keeping in mind that they made their measurements in vitro.

In our experiments the isometric contractile force of dystrophic EDL was weaker than that of normal EDL, also when expressed relative to the largest cross sectional area. Douglas and Baskin¹, too, showed that force in dystrophic EDL is reduced related to normal muscles in mice at ages of 1 to 12 weeks. Body-weights of our animals as well as twitch and tetanic forces of the dystrophic and normal EDL are in agreement with the results of Douglas and Baskin¹.

The contraction and relaxation times of dystrophic EDL appeared a little prolonged with respect to normal EDL, but the differences were not significant, in accordance with Douglas and Baskin¹, who revealed a slight but non-significant prolongation of contraction time of dystrophic EDL. On the other hand they showed that relaxation time was significantly prolonged (30.6%).

As an effect of early immobilization, the muscles had an increased tetanic force compared with untreated muscles. Surprisingly we could not find the same effect for the twitch force. We need further experimental information to find an explanation for this, and to link the present results to the positive effect of immobilization on the functioning of the dystrophic leg muscles⁴.

REFERENCES

1. Douglas WB and Baskin RJ (1971) *Am J of Physiol* 220:1344-1354
2. Loermans H and Wirtz P (1983) *Br J exp Path* 64:225-230.
3. Wirtz P, Loermans HMTh, Peer PGM and Reintjes AGM (1983b) *J Anat* 137:127-142.
4. Wirtz P, Loermans H and Wallinga-de Jonge W (1986) *Br J exp Path* 67:201-208.

GLYCOGEN DEPLETION OF FAST GLYCOLYTIC MOTOR UNITS IN MOUSE SKELETAL MUSCLE.

A.F. Evenhuis, W. Wallinga—de Jonge, P. Wirtz* and H.M.Th. Loermans*
Biomedical Engineering Division, Twente University, P.O. Box 217, 7500 AE Enschede
and * Department of Cytology and Histology, University of Nijmegen, 6500 HB Nijmegen
(The Netherlands).

INTRODUCTION

Conventional methods for the stimulation of individual motor units, i.e. via split ventral roots are technically demanding, especially in small animals like the mouse^{1,2,3}. Histological examination of glycogen depleted motor unit fibres has not been carried out due to neuromuscular failure at tetanic stimulation².

An easier way to stimulate a single motor unit is by low amplitude stimulation of the nerve^{1,4}. In this way only the first motor unit that responds can be studied in detail with respect to electrical and mechanical responses. Glycogen depletion of the motor unit cannot be achieved under these circumstances due to unstable stimulation conditions (own, unpublished data).

In this paper we describe an experimental set up that enables glycogen depletion of a single motor unit in the m. extensor digitorum longus (EDL) of the mouse, using the epimuscular microstimulation method⁵.

MATERIALS AND METHODS

Preparation.

The electrophysiological measurements were carried out *in vivo*, on the EDL in the right hind leg of twenty five adult mice (Bar Harbor strain ReJ Dy/Dy; both male and female; 121 ± 31 days old; weight 29.6 ± 3.8 g). The animals were anesthetized intraperitoneally with pentobarbital sodium (Nembutal). Body and muscle temperatures were kept at about 35 and 33 °C, respectively. Muscle temperature was controlled by a warm, humid air flow across the muscle surface.

Physiological methods.

All measurements were made at optimum twitch length of the muscle. An isometric force transducer (Sensotec 50 g, stiffness 4.10^4 Nm^{-1} , sensitivity 20 VN^{-1}) was used to measure the force of the muscles and the motor units.

The electrodes used to record motor unit action potentials were trimell—coated karma wires of 25 μm diameter, the tip bevelled at an angle of about 45 °.

The stimulation electrodes used consisted of two Pt Ir (10% Ir) teflon—coated wires, diameter 15 or 25 μm. The tip of the negative electrode was positioned on the muscle surface in the end plate region. Due to its flexibility the electrode followed the movement of the muscle during contraction. The positive electrode was placed on a nearby muscle.

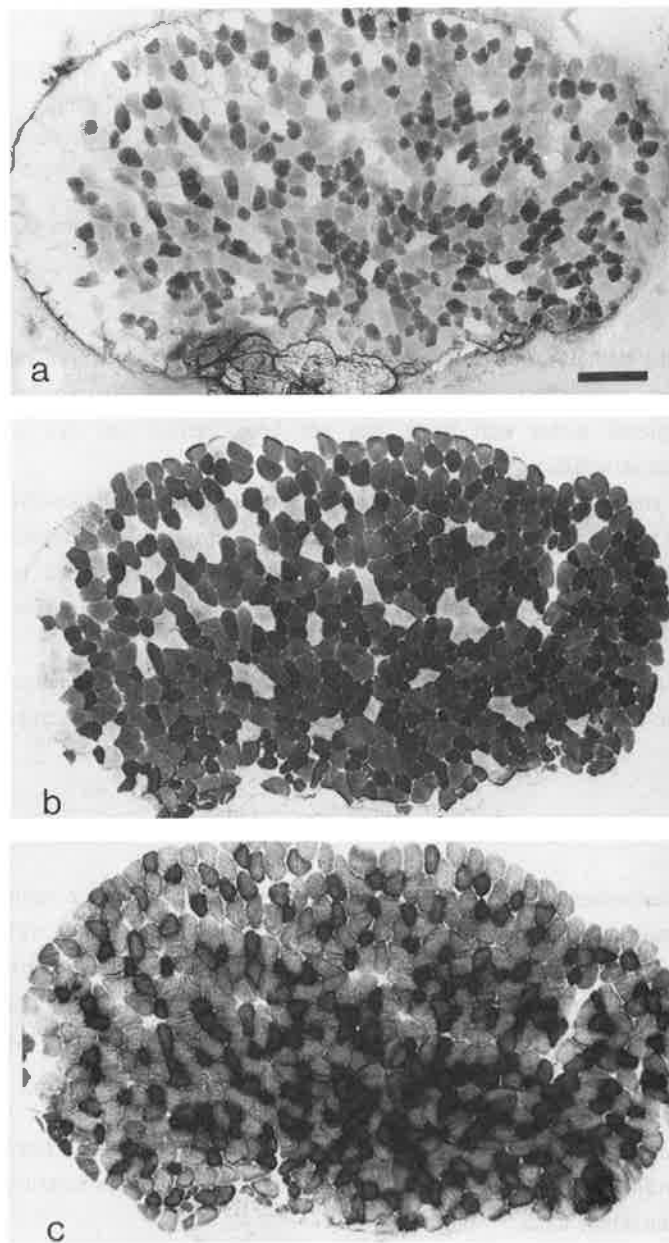


Fig.1. Serial cross-sections through the EDL muscle of a mouse with one motor unit depleted of its glycogen. a. PAS-staining b. α -glucan-phosphorylase reaction c. succinate dehydrogenase reaction. The lightly stained fibres at the left border of the sections are artefacts introduced by the method of controlling temperature and humidity during the experiment.

Glycogen depletion procedure.

Glycogen depletion of a single motor unit was initiated only if, at single current pulse stimulation, the current amplitude, the pulse width or both could be increased by a factor 1.5–2.0 times the threshold value, without activating additional motor units. The motor unit should give a perfect all-or-nothing force and EMG response if the stimulus amplitude is adjusted close to the threshold values. When the motor unit is not active, there should be no activity of (directly stimulated) muscle fibres. During stimulation the force and EMG of the motor unit were monitored. A continuous 10 Hz stimulation was used in all experiments. Quite often it was necessary to increase the stimulus amplitude and/or pulse width during the depletion. The criteria to decide to stop the stimulation are given in the legend of table I.

After termination of the stimulation the muscle tendons were glued to a staple bent at an appropriate length. The tendons were cut, the muscle was immersed in a white of egg and rapidly frozen in isopentane chilled with liquid nitrogen to about -90°C within three minutes after the stimulation had stopped. The temperature was lowered to -140°C within three minutes. The muscle was stored at -95°C .

Histochemistry.

Serial frozen cross sections of $10\ \mu\text{m}$ were cut at regular intervals through the muscle. In the area where EMG electrodes had been positioned all consecutive sections were collected on microscope slides. PAS and α -glucan-phosphorylase stainings were used to localize glycogen depleted fibres of the motor unit⁶. Histochemical fibre typing was carried out using the method of Wirtz et al.⁷.

RESULTS AND DISCUSSION

In seven of twenty five experiments depletion was successful. The way the twitch amplitude diminished varied, but the fibre type was in all cases fast-glycolytic. During exhaustion the MUAP's slowed down, again in a variable way. Their amplitudes decreased in relation to a prolongation of the action potential.

No consistent relation was found between the alteration of force and MUAP parameters during the stimulation and the ultimate effect of the depletion. The gradual changes in the twitch and MUAP patterns indicated that one single motor unit had been stimulated throughout the depletion procedure for the seven motor units described here.

All muscles showed histochemical artefacts due to the airflow system used. By means of a time-consuming morphological investigation (studying the depleted fibres at many levels of the muscle) it was possible to determine the exact number of fibres in the depleted motor unit. The number of fibres of exp.026 is exact, the other numbers in table I are minimum values.

Figures 1 and 2 present the typical histochemical fibre type of a fast glycolytic motor unit (exp.026). The depleted motor unit fibres (lightly stained in figures 1a and 1b) appear to lay

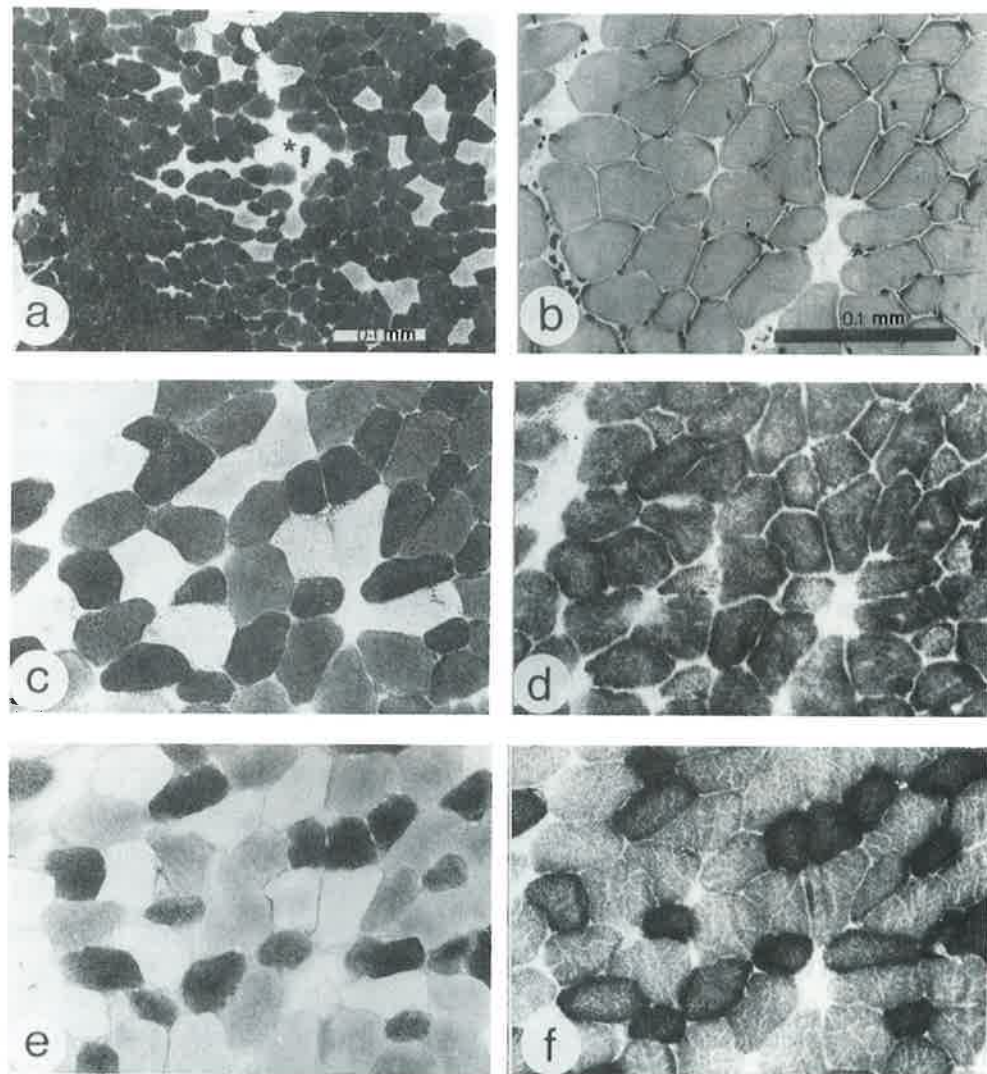


Fig. 2a Position of one of the EMG electrodes (*) in relation to the surrounding depleted motor unit fibres (α -glucan-phosphorylase reaction). The section was taken from another level of the muscle than the sections shown in figure 1.

- 2b to f Detail of the same series of sections as shown in figure 1, processed for:
- b. haematoxylin-eosin
 - c. α -glucan-phosphorylase
 - d. α -glycerol-phosphate dehydrogenase
 - e. PAS
 - f. succinate dehydrogenase.

Morphological and histochemical profile of the depleted motor unit fibres of the fast-glycolytic type.

scattered throughout the section. No slow fibres were present at this cross-sectional level (not shown in picture).

TABLE I.

Summary of motor unit data and stimulation conditions applied to introduce depletion of the motor unit fibres. If one of the following three criteria was fulfilled the stimulation was stopped.

EMG : EMG and force responses failed

force: force response < 20 % of initial level

time : no changes in MUAP characteristics and twitch response were observed during some minutes.

Experiment	016	019	020	025	026	071	074
optimum twitch length (mm)	13.5	11.9	12.6	14.3	13.5	13.9	14.5
motor unit twitch force (mN)	3.8	4.5	4.0	2.7	5.5	1.1	5.8
twitch contraction time (ms)	7.8	8.5	11.2	6.7	8.2	6.7	6.6
% force reduction	85	80	70	15	90	86	87
% EMG amplitude reduction	25	13	23	16	28	45	95
criterion stimulation stopped	EMG	force	EMG	time	force	EMG	EMG
stimulation period (min.)	$3\frac{1}{2}$	$16\frac{1}{2}$	$5\frac{1}{2}$	$17\frac{2}{3}$	2	2	3
minimum number of depleted fibres	27	30	30	20	50	60	45

The method described in this paper has certain disadvantages. The percentage successful experiments is low and sometimes it takes rather a long time before a motor unit has been traced that fills the criteria for adequate stimulation. It cannot be ascertained that there is no activity of directly stimulated fibres during the depletion stimulation.

The major advantages of the method are that preparation takes little time and that, as a result, both animal and muscle remain in good condition during the entire experiment. This is especially important when examining mice suffering from muscular dystrophy, since these animals generally have a poor condition.

REFERENCES

1. Taxt T (1983) Cross-innervation of fast and slow-twitch muscles by motor axons of the sural nerve in the mouse. *Acta Physiol Scand* 117: 331-341
2. Lewis DM, Parry DJ, Rowleson A (1982) Isometric contractions of motor units and immunohistochemistry of mouse soleus muscle. *J Physiol* 325: 393-402

3. Bateson DS, Parry DJ (1983) Motor units in a fast-twitch muscle of normal and dystrophic mice. *J Physiol* 345: 515-523
4. Law PK, Caccia MR (1975) Physiological estimates of the sizes and the numbers of motor units in soleus muscles of dystrophic mice. *J Neurol Sci* 24: 251-256
5. Griep PAM, Pool CW, Lammeree GC, Wallinga-de Jonge W, Seeder T, Donselaar YC (1980) Intramuscular and epimuscular microstimulation of single motor units. *Neuroscience Letters* 17: 191-196
6. Wirtz P, Loermans HMTh, Peer PGM, Reintjes AGM (1983) Postnatal growth and differentiation of muscle fibres in the mouse. I. A histochemical and morphometrical investigation in normal muscle. *J Anat* 137: 109-126
7. Wirtz P, Wallinga-de Jonge W, Vermorken AJM (1983) An improved technique for the demonstration of glycogen depleted skeletal muscle fibres. *Histochemistry* 79: 141-143.

Evaluation of muscular dystrophies

COMPARISON OF CLINICAL EVALUATION METHODS AND SURFACE EMG IN A FOLLOW-UP
STUDY OF PATIENTS WITH DUCHENNE DYSTROPHY

A.H.SCHAARS, H.J.HERMENS, M.C.SCHLECHT, G.ZILVOLD

Rehabilitation centre Het Roessingh, Roessinghbleekweg 33, 7522 AH Enschede,
The Netherlands

INTRODUCTION

Quantification of clinical changes is a wellknown problem, especially in diseases with a slowly progressive picture. The loss of functions in each stage of the disease often is clinically compensated without the appearance of serious defects. At the end of a certain stage nevertheless, suddenly compensation of loss of function may be no longer possible and serious defects may appear. In progressive muscular diseases like Duchenne dystrophy a striking example of a rather suddenly starting defect is the transition from walking to wheelchair dependency. The use of technical appliances may diminish the defect; for example ambulation can be prolonged by the use of long leg braces with an average of 20 - 24 months (1). Since among others by their weight and construction these long leg braces also may reduce the functioning of the patient, it is of great importance to be able to objectivate as good as possible the moment of their prescription.

An important condition for this is the ability to assess the course of the muscular disease in an objective and quantitative way. During our follow up study a number of tests were applied in order to investigate whether they would meet these requirements.

This paper deals especially with surface EMG measurements in relation to the functional classification according to Vignos (2).

MATERIAL AND METHODS

The patients were examined every three months. After each investigation the obtained data were gathered in a database for further analysis. Also the dates of delivery of appliances were added.

The long leg brace used is a light weight knee-ankle-foot orthosis made of carbon re-inforced resin with light weight steel side supports and with knee hinges of type Kelly. The thigh cuff has a high lateral support and a postero-medial lip to encourage ischial seating.

The following tests were used:

1. Measurement of the muscle force according to the MRC scale. The force was measured of: knee flexors and extensors, ankle dorsal and plantar flexors, hip abductors and extensors.

2. Functional classification according to the Vignos scale (2)
3. Surface EMG measurements

Standardized protocols are applied describing the position of the patient and the localisation of the EMG electrode (Medelec EL210) with respect to anatomical reference points. Surface EMG is recorded during two seconds at maximal isometric effort. The measurement and analysis procedures are described by Hermens et al. (3). In this paper only the standard deviation of the EMG signal at maximal effort (SDm) is used. EMG recordings (both sides) are made of: M.Rectus fem., M.Gluteus med., M.Gluteus max., M.Tibialis ant., M.Gastrocnemius.

Patients

This follow-up study was performed with 7 boys with Duchenne dystrophy (at the start: 6.5 - 9.4 years old). At the start of the study all patients were able to walk and none of the patients had contractures that might influence their functionality. By using night splints prevention of equinus is started when a passive dorsiflexion of less than 10 degrees is found.

All patients and their parents gave their informed consent to cooperate in this study.

RESULTS

The course of the Vignos score is shown in figure 1. Note that due to the definition an increase of its scale means a decrease of functional level.

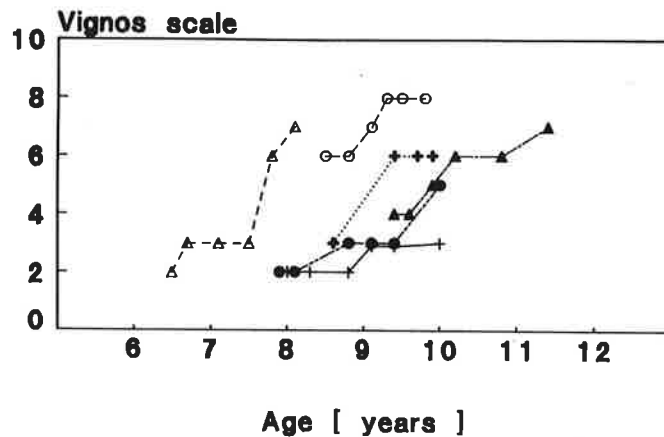


Figure 1. The course of the functional classification according to the Vignos scale with 6 patients with Duchenne dystrophy.

Although the course is related to the age of the patients it is not meant to suggest a general relation between the two parameters for all patients. The non-existence of such a course becomes clear from the figure.

As could be expected all patients showed a decrease of functional level. Note that the transition to level 6 indicates the moment that long leg braces are applied and the transition to level 7 indicates that the patient starts using a wheelchair.

Figure 2 shows the course of the standard deviation of the EMG signal at maximal effort of the Rectus femoris, with 6 patients with Duchenne muscular dystrophy (follow up for more than one year). This muscle was chosen because of its critical function concerning walking.

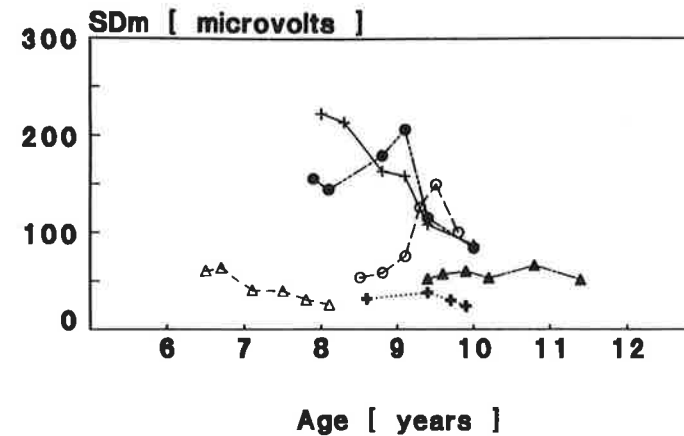


Figure 2. The course of the standard deviation of the EMG signal at maximal effort (SDm; mean values of both M.Rectus femoris) with 6 patients with Duchenne muscular dystrophy.

Note the large differences between the individual courses: with three patients a slight or no decrease of SDm is found, with one patient a rather strong decrease. With two patients a remarkable 'temporary' increase of the activity is found, followed by a decrease of SDm.

DISCUSSION

In this follow up study we investigated the use of different tests to quantify the course of muscular dystrophy and to assess an appropriate timing of prescription of long leg braces.

The advantage of clinical tests and the classification according to Vignos is that they can be applied by the physician himself in a minimum of time.

According to our results the muscle strength test (MRC-scale) however seems not sensitive enough to be useful.

The functional classification, according to the Vignos scale, is a very helpful way to describe the course of the functional level of the patient. A disadvantage in clinical use is its lack of standardization. This makes the scale subjective and therefore less suited for comparison to several tests.

Surface EMG provides a tool to quantify muscle activity. Yet interpretation is made difficult by the increase of activity that may occur. This increase, probably due to muscle regeneration, did not either correlate with an increase of functional level nor with an increase of force.

Our first results indicate that when the value of SDm of the Rectus femoris muscles is less than 100 μ V (approximately 1/3 of the lower limit of the normal range) this is the appropriate moment to prescribe long leg braces.

This needs further investigation, in which we will combine EMG measurements with quantitative force measurements. For the timing of the prescription of the braces the Siegel-test (4: antigravity hip and knee extension lag test) will be added.

REFERENCES

1. Hyde SA, Scott OM, Goddard CM, Dubowitz V. (1982): Prolongation of ambulation in Duchenne muscular dystrophy by appropriate orthoses. *Physiotherapy* Vol 68 Nr 4:105-108
2. Vignos PJ and Archibald KC (1960): Maintenance of ambulation in childhood muscular dystrophy. *J. chron. dis.* Vol 12 Nr 2:273-290
3. Hermens HJ, Boon KL, Zilvold G (1984): The clinical use of surface EMG. *Electromyogr. clin. Neurophysiol.* 24:243-265
4. Siegel LM (1982): Maintenance in ambulation in Duchenne muscular dystrophy. *Clinical pediatrics* 19:383-388

AUTOMATIC ANALYSIS OF EMG INTERFERENCE PATTERN IN PATIENTS WITH PROGRESSIVE MUSCULAR DYSTROPHY (PMD)

NORINA MARCELLO, FIORELLA ORTAGGIO, ADA LANFRANCHI, DONATA GUIDETTI

Divisioni di Neurologia e Pneumologia, Arcispedale "S. Maria Nuova", Viale Risorgimento, 80 - 42100 Reggio Emilia (Italy)

INTRODUCTION

Automatic analysis of the Number of Turns (NT) and Mean Amplitudes (MA) of the EMG Interference Pattern (IP) in Progressive Muscular Dystrophy can be useful, if combined with quantitative and functional evaluation of muscular strength and pulmonary tests, for detecting different findings between the Duchenne and Becker type. If applied to longitudinal studies, TA analysis could allow us to define the changes occurring in disease progress.

MATERIALS AND METHODS

Study population. 20 male subjects, aged between 5 and 41 (mean age 14.4) were included in our study. 13 affected by Duchenne (DMD) and 7 by Becker Muscular Dystrophy (BMD), nosologically defined according to the classical criteria. They were examined in a longitudinal study for data collection of the disease natural history (1).

Muscular strength of quadriceps f. muscle by myometer, motor performance (possibility to walk) and pulmonary function test (Vital Capacity-V.C.-in percentage values) were evaluated in each patient. Data are summarized in Table 1.

Electromyographic procedure and force determination. Automatic analysis of Turns/sec and Mean Amplitudes/turn in the Electromyographic Interference Pattern (EMG-IP) was carried out using concentric needle electrodes and applying the "TA" program developed by E. and S. Stalberg for EMG equipment Medelec MS92 and PC Apple IIe (1982). Three points of the vastus medialis on the dominant side were examined during variable voluntary effort. Before EMG examination in each patient the force of maximum voluntary contraction at the right quadriceps muscle was evaluated by Penny and Giles Transducer myometer recording the best value out of 3 measurements. During EMG examination

assessment of isometric contraction for force determination the patient was respectively made lie on the bed and placed in sitting position with 90° hip and knee flexion. Also in younger patients good collaboration was obtained by training them to the frequent determination of muscular strength.

RESULTS

The average values from myometry, NT and MA of EMG-IP are summarized in Table 1.

BMD Pts-Years	GENETIC DATA	GAIT	MYOMETRY (Newton)	N° TURNS	MEAN AMPL. (µvs)	VC %
F.C.11	sporadic *	ambulant	151	414	538	110
F.A.15	familiar	ambulant	55	311	388	79
D.F.16	familiar	ambulant	68	274	370	92
V.S.17	familiar	ambulant	150	482	706	116
R.M.23	sporadic *	ambulant	206	472	457	111
P.J.39	sporadic *	ambulant	54	566	242	84
A.S.41	sporadic *	not ambulant	19	263	310	66
DMD						
Pts-Years						
I.M.5	familiar	ambulant	57	235	290	66
B.P.7	familiar	ambulant	58	249	273	82
P.M.7	familiar	ambulant	45	261	271	80
P.G.7	sporadic *	ambulant	32	222	248	78
T.V.7	sporadic *	ambulant	37	48	142	75
G.A.10	familiar	ambulant	62	178	174	84
Z.A.10	sporadic *	ambulant	49	264	200	90
I.D.10	familiar	ambulant	32	93	153	66
S.D.10	familiar	not ambulant	29	244	286	77
E.E.11	sporadic *	not ambulant	18	349	307	73
C.G.13	-	ambulant	17	132	174	84
F.F.13	not evaluated	ambulant	45	231	266	-
V.G.16	-	not ambulant	27	69	139	17

* mother with high CK

In the thirteen DMD patients mean NT is 198.16 ± 88.35 and mean MA- 225.08 ± 62.31 . In all of them, even the strongest, data points of each TA diagram plot are found under the cloud in the lower quadrant. In DMD NT and MA values decrease with age. In the seven BMD patient mean NT is 397.52 ± 116.98 and mean MA is 430.37 ± 154.82 . Also in the BMD population mean NT and MA decrease with age, but at a slower rate than in DMD. TA analysis in BMD patients shows values that exceed the DMD averages even in later stages of the disease when the patient is confined to the wheelchair. (See case A.S.41 - Table 1).

The computation of Student t test for significant differences between mean values of myometry, NT and MA in DMD and BMD patients shows high significance for NT and MA ($p < 0.001$); myometry has lower significance ($p < 0.05$) (Fig. 1).

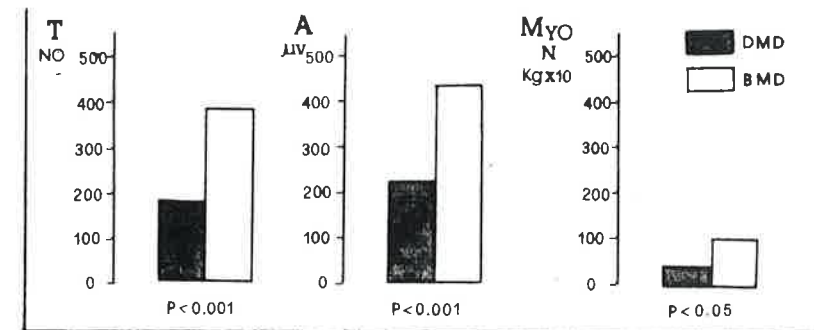
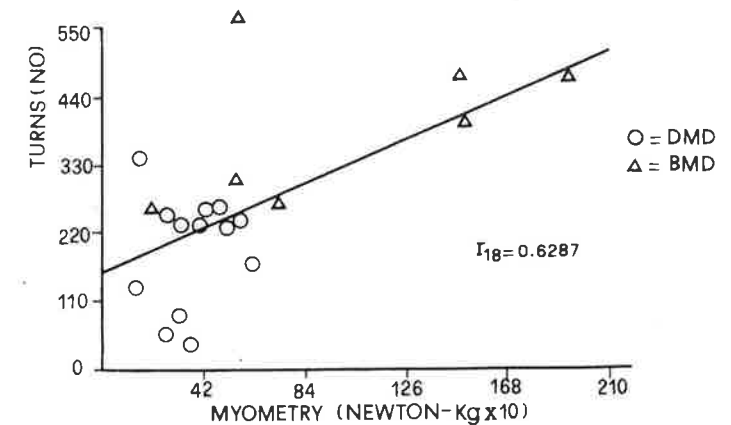


Fig. 1 Mean values of NT, MA and Myometry and the significance of their differences between the DMD and BMD patients.

A significant correlation is found between maximum voluntary contraction, measured by myometer, and NT values. In DMD patients NT values are lower than in BMD (Fig. 2).

Fig. 2 Correlation between NT and Myometry values in all patients.



DISCUSSION

Numerous variations and modifications have been introduced to the earlier Willison's method to analyse Turns-Amplitude in EMG-IP. Stålberg. and Antoni have also modified it for EMG detection independently of force evaluation (2).

Several Authors have tried to differentiate among the types of Progressive Muscular Dystrophy and Spinal Muscular Atrophy using different method of quantitative EMG.

In our study the two populations are differentiated by genetic, clinical, myometric and spirometric findings. The correlation between clinical diagnosis and TA analysis is very high and shows that the latter enlarges the diagnostic yield in Progressive Muscular Dystrophy. The method's sensitivity may be linked to the possibility of analysing the EMG Interference Pattern resulting from a weak effort because it is impossible to sustain valid contraction in later stages of DMD (3). When muscular power decreases to a very low level of force contraction, also NT and MA decrease.

It is generally accepted that NT increases with greater muscular strength. In later stages of DMD, apart from the severe loss in force contraction, the NT decrease may be due to diminished amplitude so that the turns are below the threshold of analysis. (4 - 5).

Nevertheless in BMD patients the highest values of NT and MA could not be linked to greater muscular effort but could reflect the underlying stage of less pathological involvement.

This may be in accordance with the preservation of a larger number of regenerating fibres in BMD than DMD muscles in which regeneration occurs for the most part in earlier stages, as demonstrated by recent studies with the fetal myosin method (6).

ACKNOWLEDGEMENTS

The Authors wish to thank Prof. C. Angelini from Centro Regionale per le Malattie Neuromuscolari - Università di Padova, for valuable advice as well as Miss D. Riccò for the technical cooperation.

REFERENCES

1. Angelini C, Ringel SP, Micaglio G, Trevisan C (1986) Ital.J. Neurol.Sci. 3:137-142
2. Stålberg E, Chu J, Brill V, Nandedkar S, Stalberg S and Ericsson M. (1983) EEG Clin. Neurophysiol. 56:672-681
3. Edwards R H T, Chapman S.J., Newham D J and Jones D A (1987) Muscle & Nerve 10:6-14
4. Haridasan G, Sanghvi S H, Joshi V M, Pandya S S and Desai A D (1980) J. Neurol.Sci. 48:353-365
5. Fuglsang-Frederiksen A (1987) Electromyogr.Clin.Neurophysiol. 27:327-333
6. Galassi A, Battilana M, Schiaffino S, Piccaluga A, Angelini C (1986) Ital. J.Neurol.Sci. 7:286

EMG QUANTITATIVE ANALYSIS OF MUSCLE FATIGUE IN MYOTONIC DYSTROPHY

B. ROSSI, G. SICILIANO, M. ANGELOTTI, R. RISALITI
Institute of Neurological Clinic, Pisa, Italy.

INTRODUCTION

Myotonic Dystrophy (MD) is a multisystemic disorder characterised by concomitant involvement, other than voluntary muscles, of central nervous system (CNS). Dystrophy and myotonia contribute, with different mechanisms, in provoking motor impairment. CNS involvement is revealed by mental retard, apathy, inertia and brain generalised atrophy at C.T. scan.

Aim of this work is to assess in this disease, the aspects of fatigue mechanisms by quantitative analysis of EMG surface activity during isometric contraction. Particularly, we investigated the respective roles of central and peripheral mechanisms of muscle fatigue.

METHODS

We compared the E.M.G. pattern of 18 male patients (age 32 ± 8 yr.) affected by MD to that of 18 normal subjects, matched with age and sex. Each of them performed an isometric contraction of biceps brachii muscle at 50% of maximal voluntary contraction (MCV). MCV was considered as the mean value of force measured during 5 contractions, each lasting 10 seconds, during which patient was asked to carry the maximum voluntary effort. Force was recorded by a strain gauge connected to an oscilloscope for on line monitoring and to a A/D converter for storage on floppy disk.

During recording subjects were sitting in a chair, with their trunk straight, their upper arm abducted of 90° resting on a table fixed to the strain gauge. Elbow was flexed at 90° and fixed to the same table. Forearm and arm were maintained in a position intermediate between pronation and supination. This position was found as the better one that avoided co-contraction of synergic muscles. Patients received visual feedback of force. Endurance time was monitored.

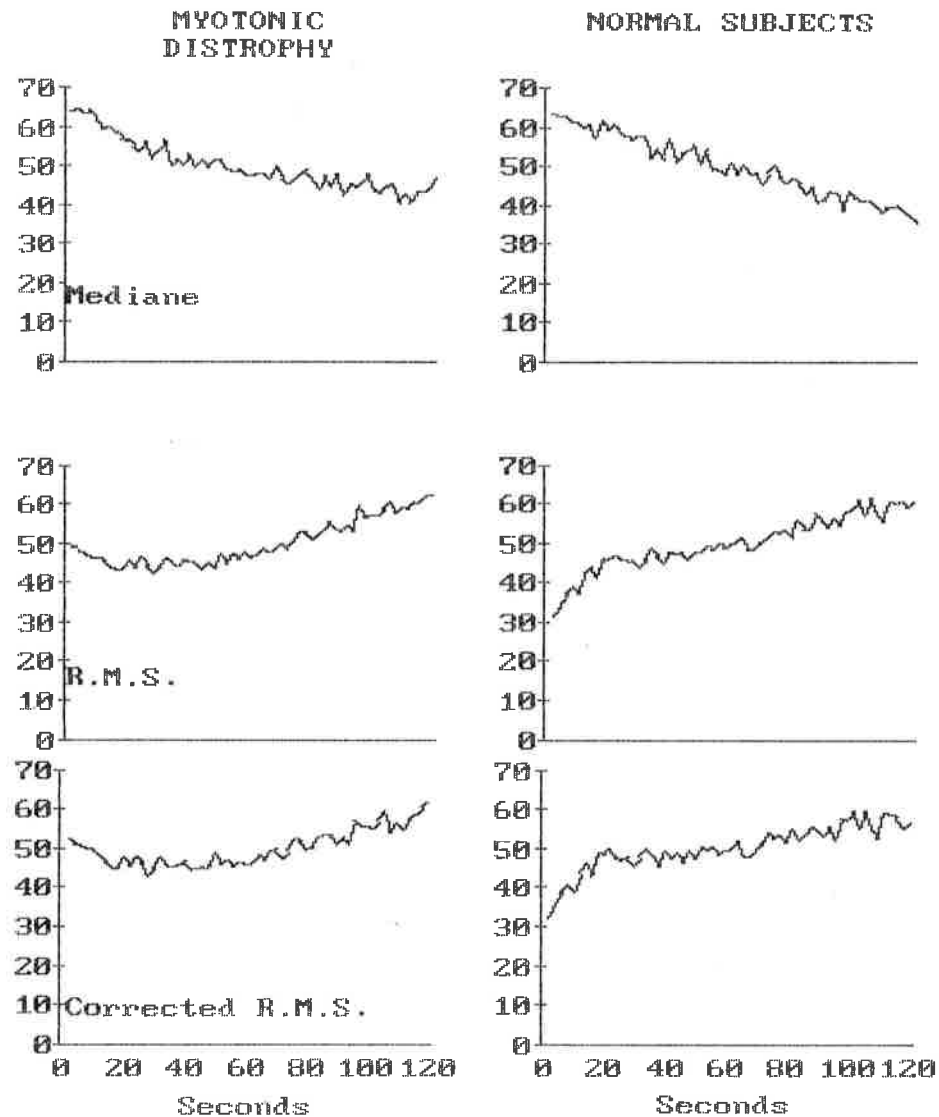


Fig. 1: Mediane, Root Mean Square, and Corrected Root Mean Square plotted as a function of contraction time. All data are normalized as in (1) (see text). Left column: Myotonic Patients. Right column: Normal subjects.

EMG activity was recorded through two silver electrodes: the first was placed on the belly of the muscle, the second 30 mm. distally. Signal was filtered at 1-512 Hz., digitised with a sampling rate of 1024 Hz. and stored on floppy disk. Analysis was performed off-line: only the first 120 sec. were examined, because it was the shorter endurance time observed in our patients. 70 segments of EMG signal, lasting 500 msec. each, were sampled and for each of them root mean square of signal (RMS), mediane frequency of power spectrum (Fm) and the product of RMS and square root of Fm were calculated. The last value represents an index of the generalised firing rate as described by De Luca (1979) subsequently modified by Kranz e coll. (1985).

RESULTS

Force exerted was 16.04 Kg. in normal subjects and 8.37 Kg in patients affected by MD ($p < 0.05$).

Endurance time, considered as time during which subjects succeeded in maintaining a contraction 50% of MVC was 126 ± 17 sec. in patients and 186 ± 62 in controls ($p < 0.05$).

Mediane Frequency

No significant difference was found in the initial mediane value (65 ± 20 in MD, 73 ± 8 Hz in controls, n.s.).

In order to avoid inter individual variations all data were normalized using the formula:

$$1) Fm'(t) = 50 + 10 * (Fm(t) - \text{mean}) / S.D.$$

where $Fm'(t)$ represents the normalized value of $Fm(t)$, $Fm(t)$ is the mediane frequency at time t , mean is the mean value of Fm during the entire period examined, and S.D. is the standard deviation during the same period. In this way, we were able to examine the trend of variation of Fm during contraction. As represented in fig. 1 no significant difference was found between the two groups.

Root Mean Square

Absolute values of RMS in MD were similar to normal ones at the beginning of the test (8.0 ± 2.0 vs. 8.1 ± 0.9 ; n.s.).

The same formula as in (1) was used to examine the trend of RMS. In the first 10 seconds, a significant difference in the trend of the curves was observed: MD presented a decrease of normalized RMS values, while normal subjects showed an

increase. After the 10th second of contraction a progressive increase was found but no significant difference appeared between the two groups (fig.1).

Corrected Root Mean Square

No significant difference (63 ± 15.6 vs. 71 ± 7.2 ; n.s.) was found between the two groups as far as concerned absolute values. The trend of variation of normalized values were similar to that observed in RMS curve(fig.1).

DISCUSSION

As described by De Luca, several modifications of EMG pattern appears during prolonged contraction and some of them are correlated with fatigue. A reduction of Fm is constantly described in literature as the main parameter of fatigue.

In order to explain the abnormal fatiguability in MD we studied this parameter and we observed that, even if a reduction of Fm is present in these subjects, it is not different from control values. Therefore the alterations of muscular membrane excitability in MD cannot be directly related to the decrement of endurance time.

The possibility of a reduction of a motoneuronal drive, considered as a sign of "central fatigue" was investigated through the examination of two parameters: RMS and corrected RMS normalized values. A significant difference in MD with respect to controls was present during the first 10 seconds of contraction, which could be related to the abnormal spontaneous activity provoked by myotonic phenomena at the beginning of contraction. After this time the trend in the two groups was similar. The absence of any substantial difference in the electric pattern between patients and normal subjects suggests the hypothesis that other factors like excitation contraction coupling or contractile mechanisms can be involved in the abnormal muscular fatigue in MD.

BIBLIOGRAPHY

De Luca C.J. (1979) Physiology and mathematics of Myoelectric signals. IEEE Trans. Biomed. Eng. 26:313-325

Kranz H., Cassel J.F., Inbar G.F. (1985) Relation between electromyogram and force in fatigue. J. Appl. Physiol. 59:821-828

Evaluation of other neuromuscular diseases

ISOKINETIC STRENGTH EVALUATION AND STRENGTH EXERCISE IN SPINAL MUSCULAR ATROPHY

CLAUDIA GRANATA (1), LUCIANO MERLINI (2), MAURO COLOMBARI (2), STEFANO DELLA VILLA (2), FAUSTO BOMBARDI (3)

Rehabilitation Unit (1), Muscle Clinic (2), Istituto Ortopedico Rizzoli, and Research Center (3), Officine Rizzoli, Bologna, Italy

INTRODUCTION

Measurement of muscle strength is important in the assessment and evaluation of treatment for patients with muscle disorders. Spinal Muscular Atrophy (SMA) is an hereditary disorder of the spinal motoneurons causing atrophy and weakness in the skeletal muscles. The mild form of SMA, Kugelberg-Welander disease, has clinical onset in childhood, with muscle atrophy and weakness mainly confined to the muscles of the pelvic girdle and the thighs causing a variable difficulty in walking and climbing stairs. Apart from few cases with a progressive course the majority of patients remain quite stable for several years. EMG and muscle biopsy are compatible with a denervative-reinnervative process with enlargement of the remaining motor units and fiber type grouping. The objective of this study was to determine whether an appropriate isokinetic strengthening program allows the maintenance or improvement of muscle strength in very weak patients affected by SMA.

MATERIAL AND METHODS

We studied 3 patients affected by the mild form of SMA. In order to assess whether an appropriate strengthening program was effective, after a bilateral test with a isokinetic dynamometer (LIDO ACTIVE SYSTEM, Loredan), only the weakest leg was exercised for 1 month so as to use the other limb as a control. The strengthening program consisted of 12 sessions in one month, 3 times weekly. Each session included a 5 minute warm-up on a stationary bike and 10 minutes of isokinetic training with active movements during the CPM (continuous passive motion) program and active concentric exercise when possible.

RESULTS

Case N. 1. This 48-year-old woman had a right quadriceps weaker than the left. Data are shown in Table 1. A very marked improvement was obtained in the right leg.

Table 1.

	Initial Test		Retest		Improvement	
	($^{\circ}$ /sec)		($^{\circ}$ /sec)		($^{\circ}$ /sec)	
	100	240	100	240	100	240
KNEE EXT						
R (trained)	9	7	18	17	100%	143%
L (untrained)	72	48	72	51	0%	6%
KNEE FLEX						
R (trained)	16	24	39	35	144%	46%
L (untrained)	33	26	36	28	9%	8%

Case N. 2. This 23-year-old-man had a slightly weaker right quadriceps at 60 $^{\circ}$ /sec. His manual muscle test was 2/5 bilaterally. In this case some improvement was also observed in the untrained leg.

Table 2.

	Initial Test		Retest		Improvement	
	($^{\circ}$ /sec)		($^{\circ}$ /sec)		($^{\circ}$ /sec)	
	60	100	60	100	60	100
KNEE EXT						
R (trained)	5	9	14	13	180%	44%
L (untrained)	7	5	8	8	14%	60%
KNEE FLEX						
R (trained)	15	14	21	16	40%	14%
L (untrained)	16	13	15	14	- 6%	8%

Case N. 3. This 17-year-old boy had a slightly weaker left leg. Manual muscle test of the quadriceps was 1/5 bilaterally. Initial test and retest were done using the CPM program because he was too weak to move the lever arm actively in the concentric flex-ext program. After 6 training sessions he was able to exercise the left knee actively in the concentric program.

Table 3.

	Initial Test		Retest		Improvement	
	($^{\circ}$ /sec)		($^{\circ}$ /sec)		($^{\circ}$ /sec)	
	60	100	60	100	60	100
KNEE EXT						
R (untrained)	5	6	6	6	20%	0%
L (trained)	4	5	6	4	50%	- 20%
KNEE FLEX						
R (untrained)	12	13	16	11	33%	- 18%
L (trained)	14	12	23	19	64%	58%

COMMENT

Isokinetic evaluation is feasible also for very weak patients with muscle strength less than gravity. This can be done using an isokinetic dynamometer with gravity compensation and with torque recording in CPM program. Isokinetic muscle exercise performed with isokinetic dynamometers which monitor strength even as the patient exercises, is very helpful in regulating the amount of work which will maximize muscle strength improvement while avoiding excessive muscle fatigue. Strength training in patients with SMA allows an increment in the peak torque at various angular velocities.

A complete assessment and management program for mild SMA patients should include isokinetic test and appropriate isokinetic therapeutic exercise.

ACKNOWLEDGEMENTS

This study was supported by the grant N. 1/25/1988 from the Istituto Ortopedico Rizzoli, Bologna, Italy.

ABNORMAL FATIGUE IN MYOTONIA CONGENITA

M.J. ZWARTS AND T.W. VAN WEERDEN

Department of Neurophysiology, Neurological Clinic, University Hospital. PO Box 30.001, Groningen, The Netherlands

INTRODUCTION

It is well known that Myotonia Congenita (MC) patients suffer from an inability for sudden movements, resulting in frequent falls. Generally, this has been thought to be caused by "bouts" of myotonic stiffness. On the other hand "transient paresis" after physical rest is described (1). In the present study we investigated the changes in muscle membrane function during voluntary maximal contractions with surface EMG.

METHODS

Three male patients with recessive Myotonia Congenita (MC), and 3 healthy male controls were studied.

A longitudinal array of three electrodes was used for EMG recording, the distance between the electrode centres being 10 mm. Care was taken to place the electrode parallel to the direction of the muscle fibre between the motor point and the tendon. The two EMG signals were digitised with a sample rate of 6024 Hz over a signal period of 0.34 s. every 0.44 s. The conduction velocity was calculated by the cross correlation method.

The experiments were done after 10 minutes rest of the arm. The subjects were exhorted to sustain a maximal flexion of the forearm during 10.3 s. This was done 5 times with 13 s recovery between the contractions.

RESULTS

At the start of the contraction of the controls, the MFCV* rose (mean: 12.5%) and the power spectrum shifted to the higher frequencies. The course of both variables was identical for every contraction despite a lowering of the initial value due to fatigue, (fig. 1). The second (fatiguing) phase was characterised by a slight decline in force, the IEMG* did not change much. In contrast, MFCV and Fmed* both declined.

During the first contractions of the MC patients a sharp decline in MFCV, Fmed and IEMG occurred. The change in force was generally

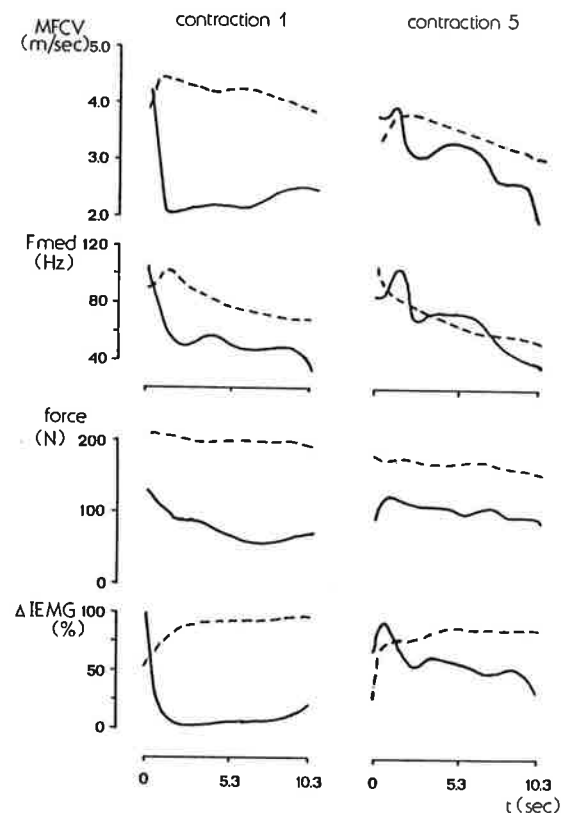


Fig. 1 Typical force and Surface EMG changes of a MC patient. The broken line is the mean value of 3 controls.

slower. The abnormalities lessened with consecutive contractions. The MFCV declined maximal with 32-56% in 1-1.5 s.

In some measurements, especially in the second and third, large fluctuations of the variables could occur within seconds (fig. 2). A significantly linear relation was found between the MFCV and Fmed of the power spectrum (fig. 3). Generally, force and IEMG changed simultaneously in the MC patients, but the change in force was usually less than the decline in IEMG, especially in the first contractions, resulting in a non-linear relation.

DISCUSSION

The changes in the surface EMG and force of the MC patients can be interpreted as follows. Initially, the muscle fibres behave normally, but after the occurrence of several action potentials the membrane properties start to change. This results in a fast decline of the average MFCV indicating that all fibres undergo the same change. Consequently, the power spectrum shifts to the lower frequencies as can be seen from the decline in Fmed. During the first contractions, the majority of the muscle fibres subsequently undergo a depolarisation block. This can be deduced from the near-total disappearance of the EMG signal. As a result, the force declines. Possibly, accumulation of tubular potassium is responsible for a depolarisation of the surface membrane (2).

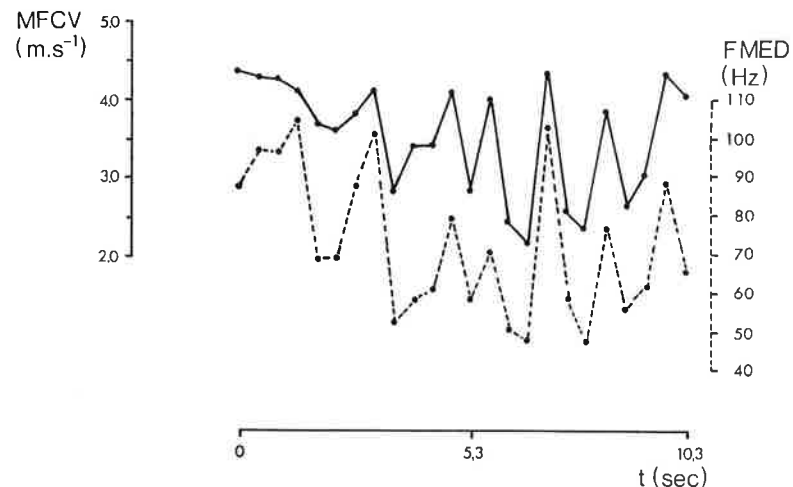


Fig. 2 Example of the fast changes during the second contraction of a MC patient

The discrepancy we have found between the larger decline in IEMG as compared with the force could be due to the depolarisation of the muscle membrane resulting in action potentials of lower amplitude (3), thus disturbing the normal, more or less linear relation between force and IEMG. Further, the important change in the frequency content of the signal could also alter the relation between force and IEMG. Since the surface electrodes act as a high-pass filter depending on the electrode separation the change of the signal to a lower frequency content will result in the transfer of

less energy. The fast changes in the course of the contractions could be explained by firing of muscle fibres in a cyclic way during the course of the contraction: after being depolarised, restart with initially a normal conduction velocity and amplitude, only to drop out again. The changes of force in the MC patients can also be described in terms of fatigue, since it fulfils the definition of fatigue: the loss of the described or expected force. Furthermore, this loss in force is accompanied by EMG changes normally seen in fatigue, though in a grossly exaggerated form. The decrease of the MFCV to 2.1 m/s is lower than ever seen in controls. In conclusion, transient paresis in MC can be described as pathological fatigue caused by membrane changes resulting in a dramatic fall in MFCV and subsequent depolarisation block. Our findings support the notion that the disability of the MC patients result predominantly from transient paresis and not from stiffening of the extremities due to myotonic discharges.

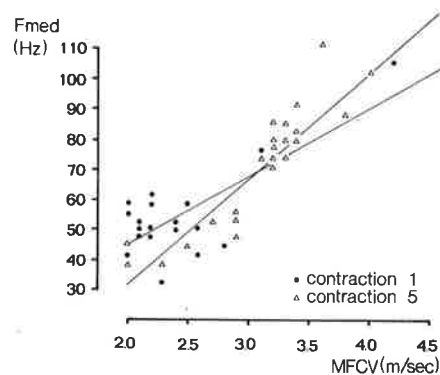


Fig. 3 Relation between conduction velocity and median frequency during 2 contractions of a MC patient ($r=0.75$ and 0.9 , $p<0.001$).

REFERENCES

1. Ricker K, Meinck H-M (1972) *European Neurology*, 7, 221-227
2. Adrian RH, Bryant SH (1974) *Journal of Physiology (London)*, 240, 505-516
3. Trontelj JV, Mihelin M, Stralberg E (1987) *Journal of Electroencephalography and Clinical Neurophysiology*, 66, S106

* ABBREVIATIONS

MFCV = muscle fiber conduction velocity
 Fmed = median frequency
 IEMG = integrated EMG

ANALYSIS OF THE SURFACE ELECTROMYOGRAM IN PATHOLOGIC FATIGUE

J.P. BRAAKHEKKE, D.F. STEGEMAN, E.M.G. JOOSTEN, S.L.H. NOTERMANS

Institute of Neurology, University of Nijmegen, P.O. Box 9101, 6500 HB Nijmegen, The Netherlands

INTRODUCTION

The analysis of the myoelectric signal of exercising muscle has greatly contributed to our knowledge of human muscle fatigue. Already in 1921 an increase in EMG activity and a shift of the EMG frequencies towards lower values with fatigue have been reported (1). Since then, many papers on this subject appeared, confirming the existence of these myoelectric characteristics of fatigue, and dealing with its origins (see 2).

The main complaint in many metabolic disorders of skeletal muscle is pathologic fatigue. Studies on myoelectric aspects of fatigue in patients with these disorders are rare. Yet, there are two reasons to hypothesize that such studies are valuable: 1) it might unravel some of the pathophysiological aspects of these disorders, and 2) such studies might add to our understanding of the myoelectric phenomena occurring in physiological fatigue. We are studying the surface EMG (SEMG) signal in patients with metabolic defects of skeletal muscle during exercise.

MATERIAL AND METHODS

When one seeks to examine pathologic fatigue, testing conditions have to be chosen that provoke it. The actual role of the various metabolic routes in skeletal muscle in energy supply depends on the intensity and duration of exercise (3). So, a disorder of glycogenolysis will become manifest during ischemic forearm exercise, or during the first 20 minutes of submaximal prolonged exercise, whereas prolonged, submaximal exercise is needed to examine disorders of lipid metabolism. For several reasons we chose bicycle ergometry to study pathologic fatigue: a) in The Netherlands almost everyone is accustomed to cycling, even patients with muscle disorders, b) large muscle masses are involved, c) with appropriate workloads and exercise durations, the various metabolic pathways can be stressed, and d) factors that might be important in the pathophysiology of pathologic fatigue (circulation, ventilation), or that might be related to changes in the myoelectric signal (e.g. lactate) can be studied with routine techniques.

The SEMG signal is obtained from the musc. vastus lateralis. Around the midpoint of the line joining the greater trochanter and the patella, two silver disc electrodes (diameter 7 mm) are placed 5 cm apart over the belly of that muscle. The signal is fed in a differential amplifier and stored on tape (Fig. 1). The

quality of the thus obtained signal is good, considering the signal-to-noise ratio and the absence of movement artifacts (Fig. 2).

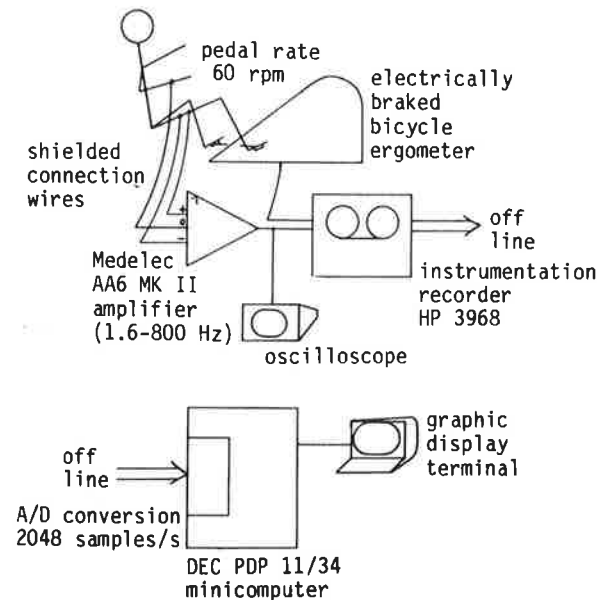


Fig. 1. Schematic representation of experimental arrangement for detecting, recording and analysing the myoelectric signal from the m. vastus lateralis during bicycle ergometry.

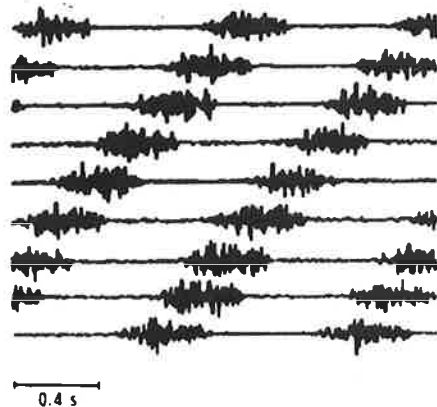


Fig. 2. A trace of raw EMG signal. Bursts of myoelectric activity occur at each pedal rotation when the m. vastus lateralis contracts. Pedal rate has to be maintained at 60 rpm, so 55-65 bursts are found per minute.

As we were not aware of studies in which the myoelectric aspects of fatigue were studied during actual cycling, we developed methods to analyse this signal (4). We chose the standard deviation of the amplitude distribution as a measure of EMG activity, the median frequency (MF) of the power density spectrum (PDS) is used as a measure of the frequency content of the SEMG signal.

In this paper results will be shown that have been obtained in patients with McArdle's disease, and in a patient with carnitine deficiency (CD). Subjects exercised at $30\% \dot{V}O_{2max}$, during two hours, after an overnight fast.

RESULTS

Results are presented in figure 3. In patients with McArdle's disease, a transitory increase in SEMG activity occurs during the first 10-20 min. of exercise, paralleling transient feelings of fatigue. During this epoch, the MF shows no consistent change (not shown here, see 4). Lactate formation does not occur in these patients (4). In the patient with CD, SEMG activity increases with ongoing submaximal exercise as do his feelings of discomfort and fatigue. However, the MF shifts towards higher frequencies. In this patient, disproportionate amounts of

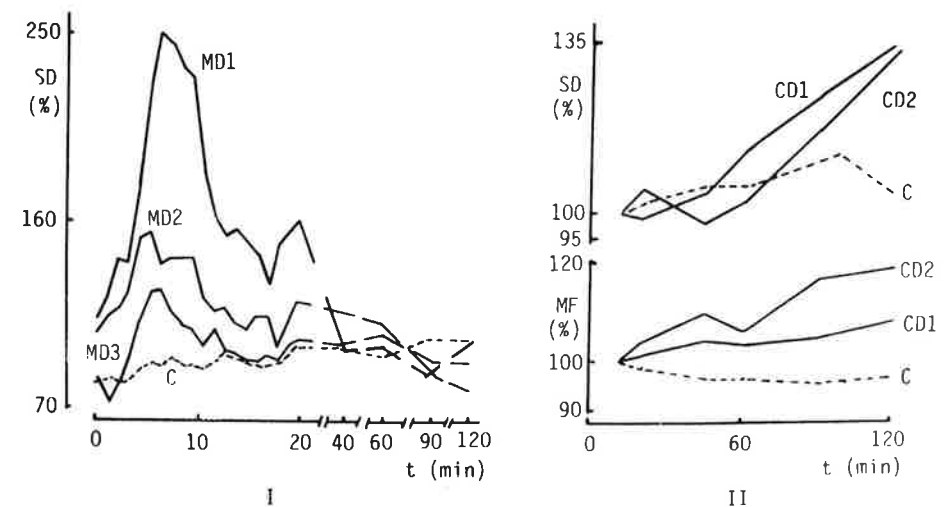


Fig. 3. Standard deviation (SD) of the amplitude distribution, and median frequency (MF) of the power density spectrum of the surface EMG, from the m. vastus lateralis during bicycle ergometry ($30\% \dot{V}O_{2max}$, 2h) in I) 3 patients with McArdle's disease (MD1, MD2, MD3), and II) in a patient with carnitine deficiency who exercised twice (CD1, CD2). The McArdle data are presented in percentages of the average value during the last 80 min of exercise, CD data are given in percentages of the value at min. 10 of exercise. As trends among the 3 control subjects (C) appeared to be identical, only mean values are shown for that group.

lactate are formed during this exercise (5).

DISCUSSION

Papers on pathophysiological aspects of metabolic muscle disorders mainly focus on biochemistry, and, to a lesser degree, on ventilatory and circulatory mechanisms (see 4 for references). Neurophysiological mechanisms have been neglected. Our studies indicate that motor control is important in those disorders. Recruitment of more (McArdle's disease and CD), and of other, type II fiber (CD), motor units might compensate to a certain degree for the metabolic disorder (4,5).

Myoelectric aspects of skeletal muscle fatigue have mainly been studied in healthy subjects. It is widely accepted, that 1) EMG activity increases and the frequency content decreases with fatigue, 2) these changes are interrelated, and 3) are due to lactate formation. The latter has been proven not to be true, as in McArdle's disease the MF decreases even faster than in healthy subjects (6). Our results show that the first 2 points of view are questionable, too.

We conclude that our hypothesis is valid: SEMG studies in patients with metabolic disorders of skeletal muscle contribute to our understanding of the pathophysiology of these disorders, and cast new light on the myoelectric aspects of fatigue.

ACKNOWLEDGEMENTS

The studies mentioned in this paper are part of the research program "Disorders of the Neuromuscular System" of the University of Nijmegen, and were financially supported by the "Prinses Beatrix Fonds".

REFERENCES

1. Von Weizsäcker (1921) Dtsch Z Nervenheilk 70:115-130
2. De Luca CJ (1984) CRC Crit Rev Biomed Eng 11:251-279
3. Felig P, Wahren J (1975) N Engl J Med 293:1078-1084
4. Braakhekke JP, De Bruin MI, Stegeman DF, Wevers RA, Binkhorst RA, Joosten EMG (1986) Brain 109:1087-1101
5. Braakhekke JP, Stegeman DF, Joosten EMG, Wevers RA, Ruitenbeek W, De Bruin MI, Binkhorst RA (1988) Can J Sport Sc in press
6. Mills KR, Edwards RHF (1984) Electroencephalogr Clin Neurophysiol 57:330-335

BIOMECHANICS

Biomechanics of the spine and shoulder

DYNAMIC ANALYSES OF LIFTING

Andersson, G.B.J., Schipplein, O.D., Trafimow, J.H., Andriacchi, T.P.
Department of Orthopedic Surgery, Rush-Presbyterian-St. Luke's Medical Center,
1653 West Congress Parkway, Chicago, Illinois 60612

INTRODUCTION

Low back pain is a frequent, costly problem in the industrialized world. One frequent cause of low back pain is injury due to lifting. Several investigators have studied lifting to determine safe, effective lifting techniques in order to reduce injury rates. Education in lifting techniques is also quite common.

Traditionally, workers have been instructed to use a squat technique (primarily bending the knees), rather than a stoop technique (primarily bending the hips and spine). However, injury rates have not been significantly reduced by those measures. Further, workers often do not lift using the recommended technique.

The studies on which this report is based were undertaken to provide basic information about lifting. To that purpose, we have defined lifting technique in terms of parameters which can be analyzed. The parameters were divided into 2 groups: positions of various joints and limb segments, and forces and moments acting on these joints. All parameters are functions of time. Position data permit calculation of velocities and accelerations. The addition of forces permits the determination of forces and moments acting on the body.

The purpose of this report is to explore the effects of changes in various factors on the technique of lifting. It is based on 4 different studies, each of which dealt with somewhat different factors.

MATERIAL AND METHODS

Ten healthy male subjects with no history of back pain or trauma and normal physical findings participated in each of the four studies, which were done at different times. Each subject was asked to lift a box weighing 20 N from the floor to a shelf set at knuckle height directly in front of him. The box had two fixed handles placed symmetrically 27 cm above the bottom. The foot and load positions were constant throughout the study, with the load always positioned 37 cm in front of the subject's feet. The lift was performed as sagittally symmetrically as possible.

In Study 1, three lifting techniques (back or stoop lift, leg or squat lift, and free style lift) and three speeds (fast, normal, and slow) were used to lift

150 N. In Study 2, leg lift and free style techniques and 2 speeds (normal and fast) were used to lift each of 5 different loads (50 N to 250 N in 50 N increments). In Study 3, the same 5 loads were lifted before and after fatiguing the quadriceps. In Study 4, 0 N, 150 N, 250 N, and 300 N were lifted, with and without the subject knowing the weight he lifted.

Motion was recorded using an optoelectronic system (Selspot), to measure the three-dimensional position of six light-emitting diodes. These diodes were placed on the right side of the body at: the lateral aspect of the fibular malleolus, the midpoint of the lateral joint line of the knee (just posterior to Gerdy's tubercle), the tip of the greater trochanter, the iliac crest in line with the two previous diodes with the subject standing straight, the acromion process, the middle of the dorsal aspect of the third metacarpal. The position of each diode was recorded at 50 Hz.

A piezoelectric force plate (Kistler), was used to determine the ground reaction force. Calculations of moments and kinematic data were made using a dynamic, 5 link rigid body model. Anthropometric data and inertial properties were approximated from Dempster and Gaughran (1957). Moment magnitudes were normalized by expressing them as a percentage of body weight multiplied by height.

Repeated Measures Analysis of Variance or paired t tests, as appropriate, was used for statistical analyses.

RESULTS

In Study 1, peak lumbosacral moment and peak velocity of lift were calculated for specific speeds of lift and for specific lifting techniques. Increasing peak velocity was associated with increasing lumbo-sacral moment. This effect was particularly strong for back or leg lift, while the increase in moment with increasing lifting speed was less while lifting free style.

In Study 2, peak lumbosacral moment and peak velocity of the lifts were calculated for specific lifting techniques, speeds, and loads. Lumbosacral moment increased with increased load for normal speed. At fast speed the curve was essentially parallel to the one at normal speed, but at a higher level. With free style technique the moment was consistently higher than with leg lift technique. Peak velocity of the load decreased with increasing load during fast speed lifts but not with normal speed lifts. At the knee, however, the moment decreased with increasing load; and angular velocity increased.

With increase in load from 50 N to 250 N, L5/S1 moment increased only 60%, indicating that a large fraction of the moment is needed to lift the body, and a relatively smaller amount is used to lift the weight.

Study 3 showed that with quadriceps fatigue the hips are kept in more extension and the lumbosacral spine in more flexion. The knee motion does not change significantly. A strong statistical trend is present for the quadriceps moment integral to decrease with increasing demand on the quadriceps. The integral was taken over time from liftoff to time of maximum height of the load.

Study 4 showed statistically significant differences at 0 N in peak L5-S1 and knee moments, and in peak trunk and hand velocities. A smaller but still significant difference was present in trunk velocity at 15 kg. Each of these parameters was larger when the subject did not know how much he was lifting.

At 250 N, there were no statistically significant differences, and at 300 N peak acceleration of the trunk was greater when the load was known.

DISCUSSION

The first two studies concentrated on the L5 moment. The effects of changing speed, technique, and load were observed. Peak L5 moment increased with increased speed and with increasing load. The effect of lifting technique was somewhat unexpected. One might have expected the back lift to produce the highest peak moment because of the increased moment arm produced when the trunk is horizontal. However, the moment was actually least.

This may not be a proper comparison, however, because the experimental conditions precluded the subject from bringing the feet close to the load when using the squat or free style techniques. However, in industry one often must lift a bulky box, or there may be obstructions. In these cases, also, the feet cannot be brought close to the center of mass of the load. The squat lift may not be the best way to avoid high peak moments at the lumbo-sacral articulation.

The last 2 experiments focused on multiple parameters to characterize lifting. Studies 2 and 3 showed that knee moment integral decreased and peak knee moment decreased with increasing demand on the quadriceps. Angular velocity at the knee increased.

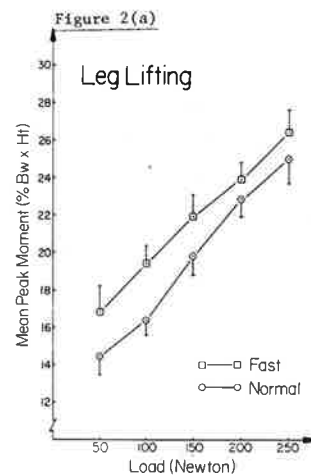
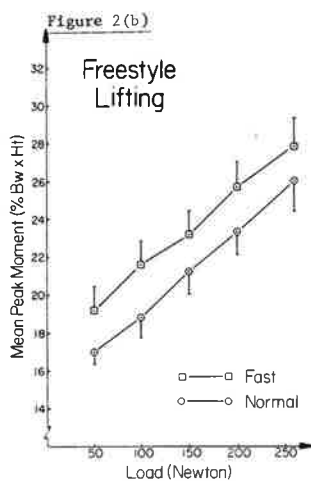
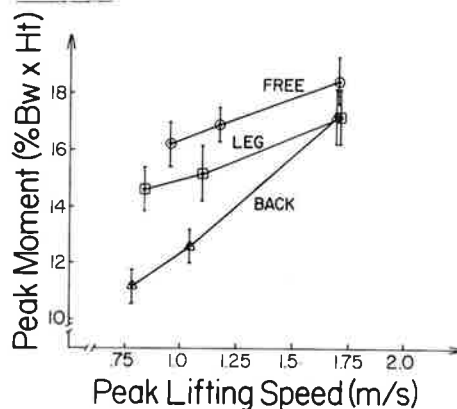
The change in lifting technique can be divided into 2 parts: changes in moments, and changes in joint positions as lift progresses. The two are not independent; for example, by proper positioning the center of mass be placed more nearly over the knees, decreasing the moment needed.

The subject certainly has a certain amount of choice of joint positions during a lift. The data indicate that this choice is used to decrease the demand on the knee extensors. The subject may also be able to choose which muscle force pattern to use, e.g. when the subject accelerates the load upward, he/she may choose to accelerate the weight upward with more force from the hip

extensors and less force from the quadriceps, or vice versa. He/she can therefore change lifting technique both by change of positions and by change of muscle force patterns so as to decrease the demand on the quadriceps. The subject may compensate differently for increased load as compared to increased fatigue.

The results of last study indicate that there is a pre-lift buildup of momentum in the lifter's body which requires knowledge of load to be appropriate. He will lift the same load differently if his estimate of the weight changes.

Figure 1



Acknowledgement: NIH (NIAMS) AR07375 (Grant).

References:

1. Buseck, M., Schipplein, O.D., Andersson, G.B.J., Andriacchi, T.P.: (1988) Spine. In Press.
2. Bush-Joseph, C., Schipplein, O.D., Andersson, G.B.J., Andriacchi, T.P.: (1988) Ergonomics 31:211-216.

A SPATIAL DYNAMIC BIOMECHANICAL MODEL FOR THE ANALYSIS AND ASSESSMENT OF LUMBAR STRESS DURING WHOLE BODY MOVEMENTS

MATTHIAS JÄGER, ALWIN LUTTMANN

Institut für Arbeitsphysiologie an der Universität Dortmund
Ardeystr. 67, D-4600 Dortmund 1, Germany (Fed. Rep.)

INTRODUCTION

The risk of pain and irreversible damage to the skeletal and locomotor systems is always present in load handling. Persons who manipulate loads professionally - such as transport workers, foundry workers, and construction workers - complain of low-back pain more frequently than, for instance, bank employees [1]. Occupational health and ergonomics consequently have the task of describing quantitatively the spinal stress during load manipulation. Those activities and activity sections causing a high level of spinal stress can thereby be recognized and possibly avoided in future. Spinal load has been determined in a series of investigations by measuring the pressure within a lumbar intervertebral disc [2]. This measurement method is invasive and, as a result, makes heavy demands on clinical medicine. In occupational health and ergonomics non-invasive methods are to be preferred for routine examinations. Biomechanical model calculations of appropriate comprehensiveness represent one such non-invasive method.

SPATIAL DYNAMIC BIOMECHANICAL HUMAN MODEL

The biomechanical human model presented in this paper permits calculation, in time, of the kinetic quantities force, torque and pressure at the five intervertebral discs in the lumbar spine for both symmetrical and unsymmetrical load-manipulation in the sagittal plane.

Skeletal system

The model comprises a total of 19 segments. It is represented as a "rod chain" in the schematic diagram in fig. 1a. The segments are linked at punctiform joints which only permit rotational movements. As shown in fig. 1a, the model includes a total of 18 joints at the ankle, knee, hip, neck, shoulder, elbow, wrist, as well as at the height of the 5 lumbar intervertebral discs. The thoracic discs are not assumed to be joints since the amount of movement in the thoracic spine is far smaller than in the lumbar spine. The cervical spine is also assumed to be rigid since its movement is unimportant for the investigations here into lumbar load. A neck joint enables movement of the head. The head and neck are included together in one segment. Lengths and weights of body segments, as well as the position of their centres of gravity within the segments have been taken, for the main part, from the literature (for ref. see [3]). All body segments are assumed to be cylindrical or conical in shape. The joints are, in part, provided for on the longitudinal axis of the assumed cylinder or conical frustum (e.g., in the case of the forearm) and, in part, on the surface

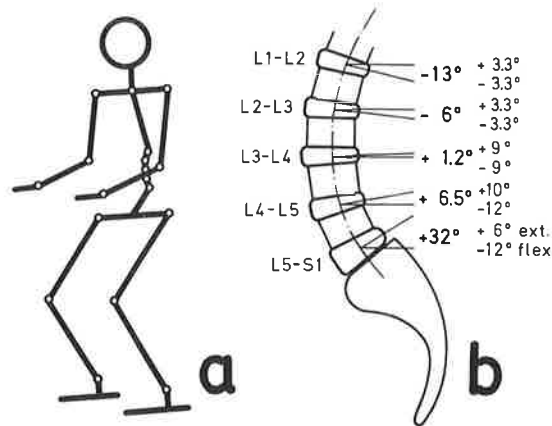


Fig. 1. Scheme of the 19-segment, 18-joint human model (a) and of the lumbar region with values of inclination and mobility for the discs (b)

area (trunk segments). Mass distribution within the body segments is in each case assumed to be homogeneous.

The lumbar region is shown in somewhat more detail in fig. 1b than in fig. 1a. As a result of the natural lumbar lordosis, the lumbar discs in the sagittal plane are inclined in relation to the longitudinal axis of the body. The values, for example, 13° for L1-L2 or 32° for L5-S1, are calculated from information provided by the literature [4,5]. Fig. 1b also contains information about sagittal mobility due to the discs' elasticity [4]. Consideration of extension and flexion in the bio-

Trunk muscles and intra-abdominal pressure

In the biomechanical model presented here the muscular system in the lower trunk is simulated by a total of eight muscles, four for each side of the body: m. erector spinae for the back, m. rectus abdominis, m. obliquus externus abdominis, and m. obliquus internus abdominis for the abdominal wall. The external muscle from one side of the body combines with the internal muscle from the opposite side to form, via a tendinous network, the diagonal banding of the abdominal wall. The effect of the rectus abdominis is antagonistic to that of the back musculature. The position of the stomach muscles relative to the spine, and therefore of the lever arms of the stomach-muscle forces in the sagittal, frontal and transversal planes, were estimated. The lever arms of the resultant forces of the back muscles were determined, with the aid of electromyographical measurements, on the basis of the activity maximum of the muscles parallel to the spine [6].

Contraction in the stomach and pelvic musculature results in the "abdominal press". This pressure has a supportive effect on the spine during frontal load manipulation. Measured values for intra-abdominal pressure [7] are considered in the biomechanical model in this paper.

APPLICATION OF THE BIOMECHANICAL MODEL

An application for the biomechanical model is shown in fig. 2. Fig. 2a shows the time courses for compressive force, section b the courses for shear force at the 5 lumbar discs during the lifting of a load of 20 kg, according to a back-lift lasting 1.5 s in total, performed by a person of 1.73 m and 69 kg. In this example the straightening of the trunk is accompanied by the bending of the arms at

the elbow joints. At the end of the lift the load is held in front of the body in straightened forearms. The course for movement is simulated in the example. The body segments are accelerated out of the rest position at the beginning. At the end of the lift body and load are again at rest. The acceleration and retardation phases are assumed to be of equal length here, in each case 0.75 s [8]. The assumption made about the acceleration is that the rotational acceleration of the body segments corresponds to the positive part of a sinus curve in the acceleration phase and to the negative part in the retardation phase. Accordingly, the curves for angular velocity represent in principle sinus square curves. The total angle traversed by the particular body segment between the initial and final position depends on the movement simulated.

Comparison of the maximum values for compressive and shear forces in figs. 2a and b shows that the compressive forces are about 7 times greater than the shear forces in this example. This is due to the fact that in back lifts the sagittal forward torque is, for the main part, offset by the back musculature. In the lumbar region the erector spinae follows the lumbar lordosis and only has a small dorsal lever arm. Consequently, the lumbar discs are compressed by the back muscles. Shear forces occur in this example through the weight and inertia forces due to the load, trunk, head, and the arms. However, their components at the respective disc level are far smaller than the forces exerted by the back muscles. The compressive force on the L5-S1 disc in fig. 2a reaches a maximum later than the courses for the other lumbar discs. This is due to the significantly greater sagittal inclination of L5-S1 (fig. 1b). Furthermore, fig. 2b shows that the shear forces at the cranial discs change direction towards the end of the lift; they first reveal a ventral tendency (pos. sign), and later a dorsal one (neg. sign; cf., fig. 1b).

LUMBAR ULTIMATE COMPRESSION STRENGTH

In structural mechanics it is customary to compare actual loads with the maximum load-carrying capacity of the component or structure in order to allow for a sufficient safety margin before damage occurs. An insufficient number of tests have been conducted to date to permit statements

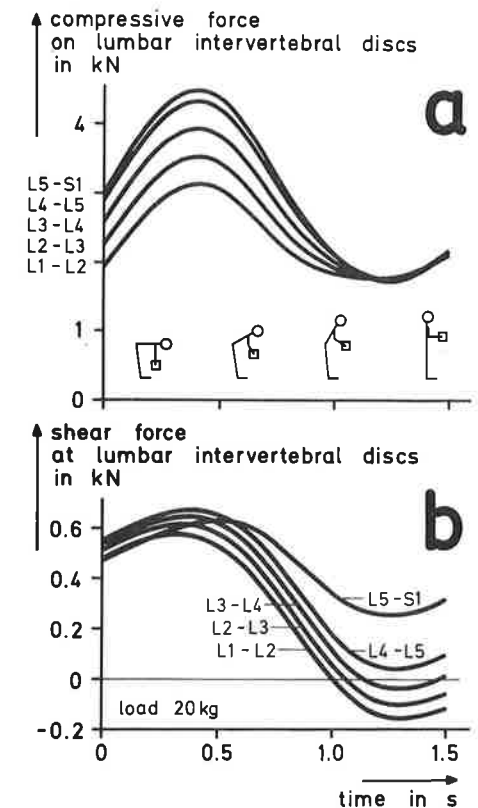


Fig. 2. Compressive force (a) and shear force (b) at the lumbar discs during a 20-kg back lift

about the maximum strength of the human spine with regard to tensile, shear or torsional loads. To date mainly compression characteristics of autopsy preparations have been examined. Values for the ultimate compression strength of lumbar segments of various lengths, i.e., in part taken from complete lumbar spines and in part from vertebrae in isolation, are provided in table 1. Only values from preparations not displaying signs of degeneration are included. The average for the 307 preparations in total amounts to 4.36 kN, the standard deviation being 1.88 kN. The relatively high scatter is presumably a result of a variety of influences, e.g., age, sex, and the cross-sectional area of the preparations. These influencing variables are currently being examined. On the whole, the values in table 1 demonstrate that the load on the spine during the execution of load-manipulation tasks (cf., fig. 2a) falls within the range for the compression strength of the human spine.

REFERENCES

1. Junghanns H (1979) Die Wirbelsäule in der Arbeitsmedizin II: Einflüsse der Berufsarbeit auf die Wirbelsäule. Hippokrates, Stuttgart
2. Nachemson A, Morris JM (1964) J Bone Joint Surg 46 A: 1077
3. Jäger M (1987) Biomechanisches Modell des Menschen zur Analyse und Beurteilung der Belastung der Wirbelsäule bei der Handhabung von Lasten. VDI, Düsseldorf
4. Farfan HF (1973) Mechanical disorders of the low back. Lea and Febiger, Philadelphia
5. Orne D, Liu YK (1971) J Biomechanics 4: 49
6. Jäger M, Luttmann A, Laurig W, Puhlvers E (1983) In: Del Pozo F, Hernandez C, Fernandez G (eds) Actas del II Simposium de Ingeniera Biomedica, Madrid, pp 51-56
7. Morris JM, Lucas DB, Bresler B (1961) J Bone Joint Surg 43 A: 327
8. Jäger M, Luttmann A (1987) In: Bergmann G, Kölbel R, Rohlmann A (eds) Biomechanics: Basic and Applied Research. Nijhoff, Dordrecht, pp 473-478
9. Wyss T, Ulrich SP (1954) Vierteljahresschrift Naturforsch Ges Zürich 99: 3/4
10. Brown T, Hansen RJ, Yorra AJ (1957) J Bone Joint Surg 39 A: 1135
11. Perey O (1957) Acta Orthop Scand 25: Suppl
12. Decoulx P, Rieunau G (1958) Rev chir orthop 4: 254
13. Evans FG, Lissner HR (1959) J Bone Joint Surg 41 A: 278
14. Eie N (1966) J Oslo City Hosp 16: 73
15. Hansson T, Roos B, Nachemson A (1980) Spine 5: 46

TABLE I

Lumbar ultimate compression strength

Mean [kN]	SD [kN]	n	ref.
5.89	2.24	8	[9]
5.20	0.54	5	[10]
5.20	2.05	119	[11]
4.41	1.14	9	[12]
3.51	1.22	11	[13]
3.28	1.22	11	[14]
3.74	1.20	35	[4]
3.85	1.71	109	[15]

DISPLACEMENT OF THE SPINE DURING LIFTING

ISSACHAR GILAD

Faculty of Industrial Engineering and Management, Technion - Israel Institute of Technology, Haifa 32000 (Israel)

INTRODUCTION

Angular displacement of the spinal segments which determine the curvature of the human torso during work is an important biomechanical measure in the study of manual materials handling. A general concern in the field of occupational biomechanics is to determine, at high level of accuracy, how the contour is created by the vertebral column while changing its geometry during lifting. The search for this geometrical determination of the vertebral column helps to understand the phenomena of body balance due to momentary external forces and counter forces created due to "in vivo" reactions on vertebrae segments. The questions of importance are: how does torso geometry really differ during different methods of lifting, i.e.: torso lifting, leg lifting, as postural arrangement for weight handling. More complex are the issues of the reflection of object size on lifting kinematics and the biomechanical differences between male and female during the act of lifting.

Recent biomechanical evaluations of lifting have indicated that small changes in spinal column configurations while lifting can cause major changes in spinal column forces (Nordin et al¹). There is wide agreement among researchers that the quantitative assessment of torso motion is diagnostically important for biomechanical research and the health care industry (Chaffin et al²) and ergonomically - as an assessment tool for occupational behavior (Ayoub et al³). Tichauer stated that the ever increasing number of low back injuries in industry has created the need for development of methods for the measurement of the response of the spinal column to lifting stress (Tichauer⁴). The effects of lifting stresses on the vertebral column are highly dependent on postural configuration, and vice versa. accuracy of measurements, matter of data evaluation, and its practicability for the study of spinal kinesiology are essential factors for an biomechanical diagnostic method. These significant factors led the author to develop the measuring system for the study of spinal configuration. The proposed measuring devices and procedure were developed into a biomechanical assessment tool at the Center of Ergonomics at the University of Michigan.

METHOD

A miniature inclinometer detection system was developed for continuous measuring of angular displacement of 3 spinal regions (cervical, thoracic and lumbar) during the performance of lifting.

The inclinometer detection system is based on small angular detectors manufactured by "Spectron". The detector is an electromechanical miniature device consisting of a single axis electronic resistance potentiometer. It requires an AC excitation signal, and provides a proportional voltage output as the unit is tilted relative to the vertical gravity vector. The inclinometers were designed by the manufacturer to control the gradient output while being subjected to a variety of motions and vibrations. The original user of this device was to input geometrical signals in missile guidance systems. The detector is a one piece glass enclosure, approximately one centimeter in diameter. The device provides a signal which is directly proportional to the inclination of the transducer from the horizontal plane. The frame of reference is relative to the gravity vector. Changes in the curvature of torso will then be measured as changes in the angle between the horizontal and the tangent to the spine at each point of reference. The inclinometer is cylindrically shaped, about the size of a pencil eraser, which enables it to be easily attached to the subject's skin.

A methodological study of the biomechanics of lifting was designed to assess the angular displacement of the three main spinal regions. This employed a wide scale of lifting parameters, such as: object's weight and size, horizontal distances, vertical heights, subject's characters and different methods of lifting. A factorial setup of lifting experiments was conducted, which makes the management of data an important issue vital to the investigation. To control the various parameters assigned to the lifting study, a video recording system was employed parallel to the angular detection system. Video Camera and Video Cassette Recorder (VCR) on line with a computer-video synchronizer and effect generator (Telecomb-1000) attached micro computer impose the lifting assignment parameters on a video control monitor. The multi lifting parameters and the lifting motion picture are synchronized, presented and recorded by the VCR. This method enables the researcher to relate the obtained list of geometrical values, for momentary torso posture, to the assigned set of lifting parameters, and at the same time observe the continuous changes of the torso segments. Figure 1 outlines the layout of the components during the lifting study.

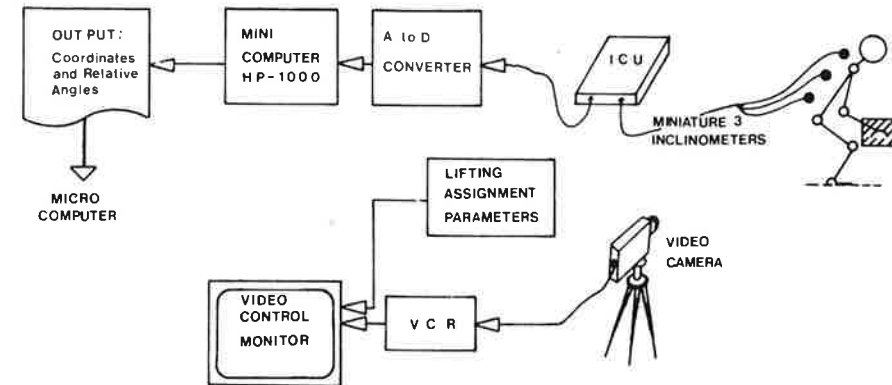


Fig. 1. Components layout of the inclinometer detection and the video control systems.

RESULTS

Momentary angular displacement values of each body segment over time can then be evaluated using simple programming and graphical presentation by using a microcomputer. Figure 2 presents the angular displacement for one of the torso's 3 main regions. This angular presentation is of a female subject who performed dynamic liftings with straight back - flexed knees, floor to knuckle height, lifting weight of 7kg, with maximum horizontal reach distance between torso and weight. In order to describe the various trends in angle trajectory of torso kinematics during lifting, the motion sequence is divided into 5

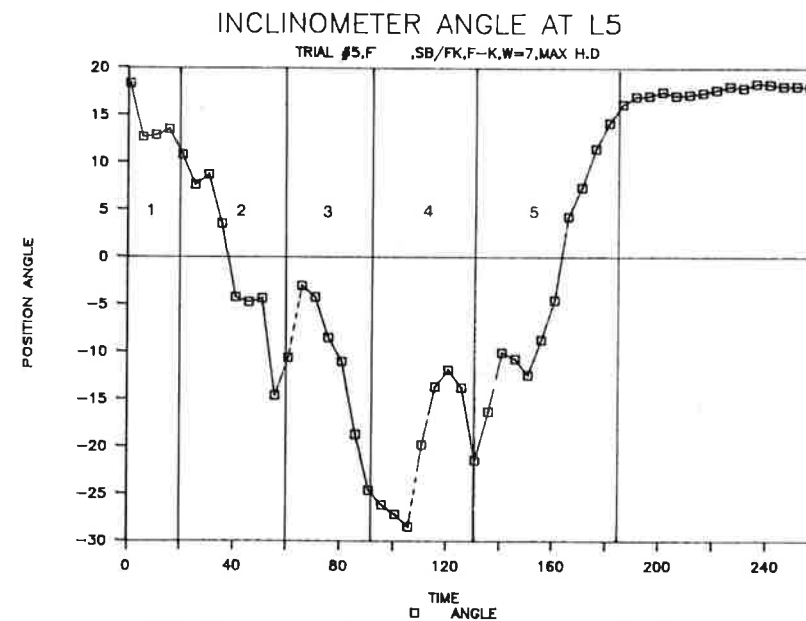


Fig. 2. Graphical presentation of the lumbar angular displacements during 5 phases of the lifting act.

phases: 1. Preload phase, 2. Bending to origin of weight, 3. Lifting to destination, 4. Return weight to origin, 5. Back to preload phase.

DISCUSSION

From the analysis of the complete set of lifting diagrams, various points of interest are recognized: The frequent angular changes of the cervix and the thoracic, especially in the "straight back - flexed knees" lifting posture, indicate the role of the head and the cervical region, which acts as a counterbalance weight for body stability. Different kinesiology behavior was observed in male lifting comparing to female for the same lifting tasks under similar weight assignments. The differences in lifting kinematics, as demonstrated in this study, is the biomechanical output of anatomical differences existing between the sexes. The skeletal architecture of the female shows a forward tilt of the pelvis which results in a different pelvic motion during the lifting act. The new technique proved to be a very accurate and simple to use procedure. Advantages of the technique and the study of systems evaluation is described at length in Gilad et al⁵.

ACKNOWLEDGEMENTS

This study was partially supported by research gifts from both GenCorp and Owens Corning Fiberglass Corporation. The electronic inclinometers were provided by Hoggan Health Industries. The author thank Prof. Don B. Chaffin and Chuck Woolley from the Center for Ergonomics of the University of Michigan for providing research support in the study.

REFERENCES

1. Nordin M, Ortengren R, Andersson GBJ (1984) Measurement of trunk movements during work, . Spine 9(60), PP 465-469.
2. Chaffin DB, Herrin GD, Keyserling WM (1978) Preemployment strength testing. J. of Occup. Med. 20(6), pp 403-408.
3. Ayoub MM, El-Bassoussi MM (1978) Dynamic biomechanical model for saggital plane lifting activities. In: Drury CG (ed), Safety in Manual Handling. DHEW (NIOSH) Publication No. 78-185, pp 88-95.
4. Tichauer ER (1977) The objective corroboration of back pain through thermography. J. Occup. Med. 19(11), pp 727-731.
5. Gilad I, Chaffin DB, Redfern M, Byun SN (1986) A system comparison study of two methods for measuring angular displacement of torso during dynamic lifting. Tech. Report No. G/2/86, Work Study Lab., Technion.

Activity of trunk and back muscles

EMG ASSESSMENT OF MUSCULAR DEFICITS ASSOCIATED WITH CHRONIC LOW BACK PAIN

SERGE H. ROY, CARLO J. DE LUCA, DAVID A. CASAVANT, MARK S. EMLEY

NeuroMuscular Research Center, Boston University, 44 Cummington Street,
Boston, Massachusetts 02215, U.S.A.

INTRODUCTION

Current information regarding chronic lower back pain (LBP) indicates that many cases are suspected of having a significant muscular insufficiency associated with their disorder. Despite this fact, presently available diagnostic techniques and prescribed treatments are often ineffective in detecting and remedying this common component of LBP. Improved methods for assessing back disorders could help to diminish the problem and alleviate the financial burden of this disabling condition. This paper describes the results of a surface electromyographic (EMG) technique used to objectively evaluate muscular disorders associated with chronic LBP. We have developed and are implementing a technique to provide the clinician with an objective index with which to measure treatment outcome for lower back musculature. This technique quantifies the fatigue rate of contracting muscles by measuring the shift occurring in the frequency spectrum of the surface EMG signal [1]. The dynamic interaction of back muscles during fatiguing contractions can be represented by "fatigue patterns" created by the frequency shifts occurring in the different muscles. Differences in these patterns associated with lower back disorders may represent functional disturbances in back muscles.

MATERIAL AND METHODS

Instrumentation

To implement this technique, a computer-aided Back Analysis System (BASTM) was designed and constructed [2]. The BAS consists of 1) a postural restraint device to isolate the back muscles and stabilize the pelvis and lower limbs; 2) a force acquisition system with video feedback to monitor the trunk extension torques; and 3) an IBM-PC Muscle Fatigue Monitor (MFMTM) for real-time computation and display of the median frequency of the EMG power spectrum [3].

Methods

BAS assessment of lumbar back muscles in control subjects and patients with chronic back pain have been performed in two preliminary studies to date. One study tested 24 sedentary individuals and the other tested 23 athletes from a male varsity crew team. The sedentary group, all males, consisted of 12 patients with chronic LBP without radiographic evidence of spinal abnormality. An equal number of closely matched control subjects without a history of chronic back pain were tested according to the same protocols given the back patients. Subjects performed constant-force, isometric trunk extension at 40%, 60%, and 80% of their maximal voluntary contraction (MVC). These contractions were sustained for a maximum of 1 minute with a 15 minute rest period between contractions.

The varsity crew members, of whom 6 have a chronic back pain history (also non-structural), were further categorized into port (n=13) and starboard (n=10) rowers on the basis of their rowing side. This additional grouping was included to determine whether the fatigue measurement would be sensitive to possible contralateral muscle imbalances associated with asymmetrical tasks. The crew members were tested only at 80% MVC for 30 seconds followed by periodic, short-duration contractions of 5 seconds duration to investigate recovery from fatigue. Recovery from fatigue was monitored by measuring the percentage return of the median frequency to its baseline, pre-fatigue value.

Analysis for the data collected from the sedentary population consisted of a multivariate analysis of variance and covariance (ANOVA) to determine whether significant differences were present between the patient and control groups on the basis of the EMG parameters measured. The interactive effects of load (%MVC), laterality (right and left sides), and location of detecting electrode (L1, L2, L5 spinal levels) were also studied by this analysis.

The analysis for the crew team data emphasized whether the EMG variables could correctly categorize subjects into a "back pain" or "no pain" category and whether port and starboard groupings could be similarly identified. A two-group, stepwise discriminant analysis was conducted for this set of data.

RESULTS AND DISCUSSION

Figures 1 and 2 summarize the results for tests on the sedentary subject population. The initial value of the median frequency (IMF) was significantly lower for patients when compared to control subjects for the L1 electrode location (Fig. 1).

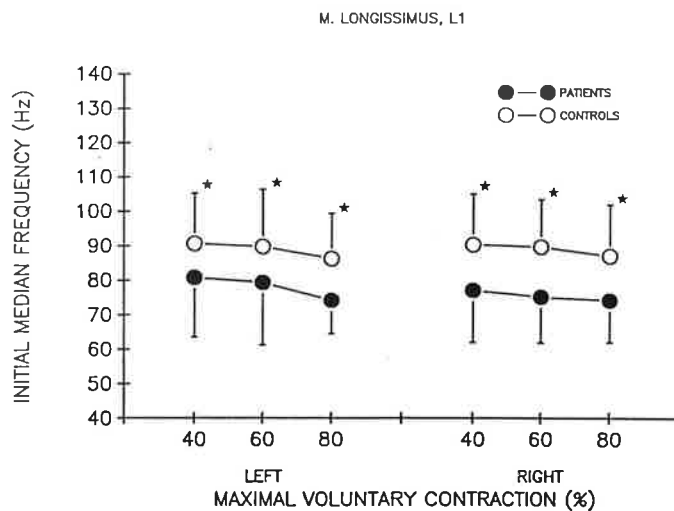


Fig. 1 Mean initial median frequencies (IMF) for patients (●) and control (○) subjects. Results are presented separately for left and right side of the L1 electrode location. (* significance level $p < .05$)

These differences were present bilaterally for all force levels tested. The IMF value also decreased as a function of the force level, particularly at the L2 and L5 electrode locations (not shown). This finding suggests that the Type II muscle fibers, normally recruited at high force levels, are smaller in diameter than the Type I fibers. This peculiarity of back muscles has been reported in histological studies [4]. The smaller IMF values in patients compared to control subjects may suggest smaller diameter muscle fibers which can occur with disuse atrophy or a predominance of Type II muscle fibers.

The rate of decay of the median frequency was greater for back patients when compared to control subjects. This difference was significant only for the 80% MVC force level for bilateral L5 (Fig. 2) and L2 (not shown) electrode locations. Higher rates of median frequency decay are suggestive of either an increase in Type II muscle fiber activity and/or the presence of compromised blood flow [1]. The MVC values for the patient and control groups were not significantly different, indicating that muscle strength was not related to back pain in this study. The patient group did have a higher mean body weight than the control group (84.8 kg versus 71.1 kg) which may be associated with differences in daily activity levels.

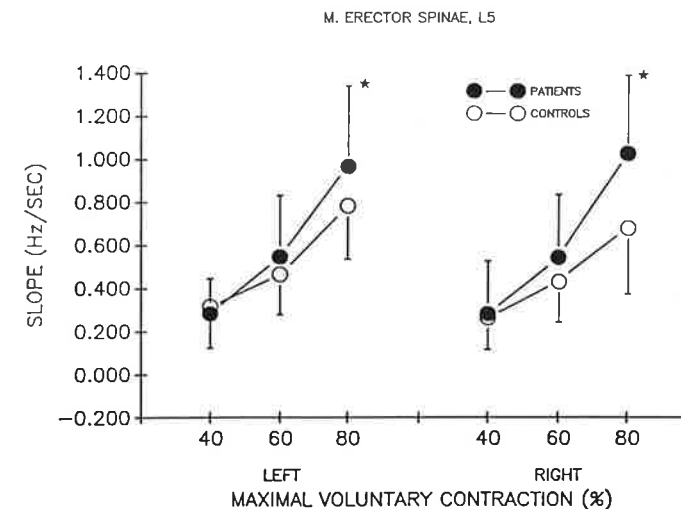


Fig. 2. Mean slope values of median frequency for LBP patients (●) and control (○) subjects. Results are presented separately for left and right L5 electrode location. (* significance level $p < .05$)

Table I summarizes the results of the two-group discriminant analysis for the crew team data. The two-group analysis between all port and starboard rowers correctly classified 91% of the port rowers and 70% of the starboard rowers for the L2 electrode location. The parameters of percent recovery (REC), slope and IMF from the right side of the back, in order of decreasing discriminating power, were identified as variables which classified port and starboard rowers.

Two of the three starboard rowers incorrectly classified had previously been port rowers and had recently switched to the starboard position. The two-group discriminant analysis at L5 significantly classified the rowers into groups of individuals with and without LBP. REC from both the left and right sides of the back were used to correctly identify 83% of the subjects with LBP and 77% of the subjects without LBP. The analysis at L5 revealed one false negative. Although this subject met our pain criteria, he had recently returned to rowing activities and had not experienced LBP in 6 months.

TABLE I :
RESULTS FROM TWO-GROUP STEPWISE DISCRIMINANT ANALYSES

LUMBAR LEVEL (groups)	PERCENT CORRECT CLASSIFICATION	VARIABLES USED IN CLASSIFICATION
L2 (port, starboard) n = 13, n = 10	91% port 70% starboard	REC(R) IMF(R) SLOPE(R)
L5 (NLBP, LBP) n = 17, n = 6	77% NLBP 83% LBP	REC(R) REC(L)

(R), (L) = right side, left side

LBP = with low back pain, NLBP = without low back pain

Future studies are being planned to accumulate a larger data base including other sub-categories of back patients and to conduct prospective studies to determine whether this technique has validity as a method of pre-screening candidates for back pain.

ACKNOWLEDGEMENTS

The financial support of the Veterans Administration Rehabilitation Research and Development Service and the Liberty Mutual Insurance Company are gratefully acknowledged. Our appreciation to Ronda Crenshaw, Juliann Lyons, Lynn Snyder-Mackler and the B.U. Varsity Crew Team for their assistance in conducting the rowing study.

REFERENCES

1. De Luca CJ (1985) *CRC Critical Reviews in Biomed Eng* 11/4 pp 251-279
2. Roy SH, De Luca CJ, Gilmore LD (1986) *Proc of 8th Ann Conf IEEE-EMBS* p 1886
3. Gilmore LD, De Luca CJ (1985) *IEEE Trans Biomed Eng BME-32* pp 75-78
4. Sirca A, Kostevc V (1985) *J Anatomy* 141:131-137

SENSORY NERVE ENDINGS IN THE POSTERIOR LIGAMENTS OF THE LUMBAR SPINE

HOCINE YAHIA, MARC ST-GEORGES and NICHOLAS NEWMAN*

Biomedical Engineering Institute, Ecole Polytechnique, P.O. Box 6079,
Station "A", Montreal, Quebec, CANADA

* Dept. of Orthopaedic Surgery, Hôtel-Dieu Hospital, Montreal, CANADA

INTRODUCTION

The spinal ligaments are thought to play an important role in the lumbar spine mechanism. They provide stability and protection for the vertebral joints while allowing physiological movements of the spine⁹. In addition, they might perform sensory functions, influencing or initiating postural and/or protective muscular reflex activity. This view of spinal ligaments as sensors for the central nervous system was first postulated by Floyd and Silver⁴. They suggested that receptors in the ligamenta flava and other ligaments are stimulated when these ligaments are stretched, and the afferent impulses from the stretch receptors cause reflex inhibition of the erectores spinae muscle. Other evidence has more recently surfaced to support a neurosensory role in spinal ligament function^{1,5,8}. According to Gracovetsky⁶, the stress is minimized and equalized at each vertebral joint by a spinal control system. This author assumed the existence of stress sensors in the posterior ligamentous system which feed stress information to the central nervous system. Bogduk⁷ showed that the posterior ligaments received a dual innervation from the dorsal rami and the sinuvertebral nerve. However, the question of the existence of receptors within the ligaments was not addressed.

The present study was undertaken to determine whether sensory nerve endings are present in the posterior ligamentous structures of the lumbar spine.

MATERIAL AND METHODS

Surgical specimens of the supraspinous ligament, interspinous ligament, yellow ligament and lumbodorsal fascia were obtained from the lumbar region of 20 patients undergoing surgery for disc herniation.

The tissue samples were stained in bulk using the Zimny's modification of the gold chloride technique¹¹. After staining, the samples were frozen and sectioned at 100 micrometers. The sections were floated in alcoholic gelatin, mounted on slides, dehydrated and overlaid with a cover-slip. Serial sections were examined with a light microscope.

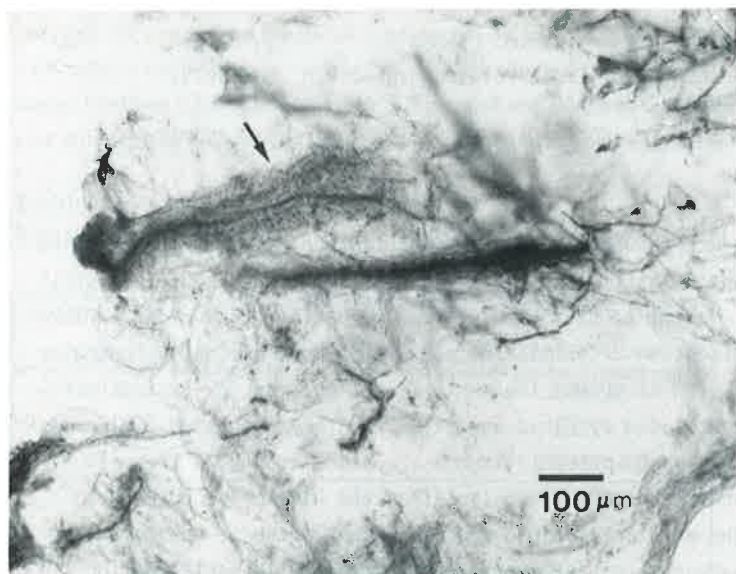


Fig. 1. Light micrograph showing a Paciniform corpuscle in the supraspinous ligament (L2/L3, 39 years).

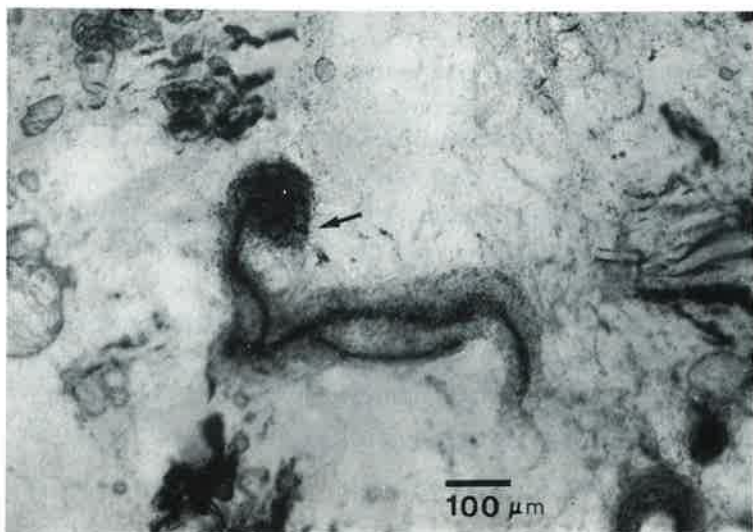


Fig. 2. Light micrograph showing a Ruffini corpuscle in the interspinous ligament (L4/L5, 44 years).

RESULTS

After gold chloride impregnation, abundant neural elements appeared in the posterior ligamentous structures. Consistent with earlier studies of ligament innervation, three types of nerve endings could be readily recognized as Pacini receptors, Ruffini corpuscles and Ruffini end-organs^{2,10,12}.

Paciniform receptors are characterized by encapsulated corpuscles which lie singly or in group of up to five. They are supplied by myelinated afferent axons measuring 4-8 micrometers in diameter (Figure 1). The Paciniform receptors are predominantly found at the junction between the supraspinous ligament and the lumbodorsal fascia.

Ruffini corpuscles consisted of an afferent axon and a globular capsule (Figure 2). These corpuscles are about 80 μm in maximum diameter and 35 μm in minimum diameter. The Ruffini receptors are found abundantly in the interspinous ligaments and in lesser number in the yellow ligaments. In the interspinous ligament, they are located peripherally near the insertions of the longissimus.

Ruffini end-organs resembling the Golgi tendon organs are found in the supraspinous and interspinous ligaments. They are longer than the Ruffini corpuscles and display individual variations in morphology (Figure 3). In the interspinous ligament, they are oriented preferentially in the antero-posterior direction.

DISCUSSION

Our observations demonstrate the presence of at least three mechanoreceptors in the posterior ligamentous structures: Paciniform corpuscles, Ruffini corpuscles and Ruffini end-organs. Their morphology is similar to that of nerve endings described by Zimny et al.¹² in the knee joint ligaments. The function of these receptors has been described by several authors^{2,7}. In the posterior ligaments of the lumbar spine, they may be involved in the spinal control system postulated by Gracovetsky and Farfan⁵.

The Paciniform corpuscles have a low threshold of excitability and adapt rapidly to a stimulus⁷. Their location between the supraspinous ligament and the lumbodorsal fascia is suitable for the assessment of sudden increased stresses during weight lifting.

The Ruffini corpuscles have also a low threshold of excitability but adapt slowly to a stimulus³. These receptors, occurring mainly in the interspinous ligament, could be responsible for the control of the reflex inhibitory mechanism postulated by Floyd and Silver⁴ to explain the flexion-relaxation phenomenon of the erectors spinae.

Finally, the Ruffini end-organs are also slow-adapting mechanoreceptors but uniquely sensitive to in-plane axial stresses². In the interspinous ligament,

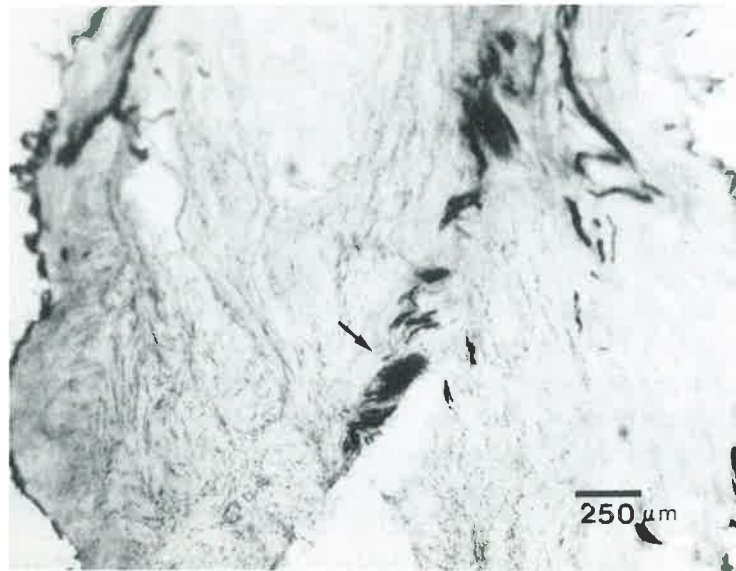


Fig. 3. Light micrograph showing a Ruffini end-organ in the supraspinous ligament (L4/L5, 19 years).

they are oriented parallel to the spinous processes, i.e. in the preferred orientation of the collagen fibers. They are strategically located to monitor the interspinous ligament tension during a contraction of the abdominal muscles.

ACKNOWLEDGEMENTS

This research was funded by the IRSST, Quebec, CANADA, grant #RS-86-22.

REFERENCES

1. Bogduk N (1983) *Spine* 8:286-293
2. Boyd IA (1954) *J. Physiol* 124:476-488
3. Eklund G, Skoglund S (1960) *Acta Physiol Scand* 49:184-191
4. Floyd WF, Silver PHS (1951) *Lancet* 260:133-134
5. Gracovetsky S, Farfan H (1986) *Spine* 11:543-573
6. Gracovetsky S (1988) *In the Spinal Engine*, Springer-Verlag
7. Halata Z, Badalamente MA, Dee R, Propper M (1984) *J. Orthop Res* 2:169-176
8. Hirsch C, Ingelmark BE, Miller M (1963) *Acta Orthop Scand* 33:1-17
9. Panjabi NM, Gohl VK, Takata (1982) *Spine* 7:192-203
10. Stilwell DL (1956) *Anat Rec* 127:139-169
11. Zimny ML, St-Onge, Schulte M (1985) *Stain Technol* 60:305-306
12. Zimny ML, Schulte M, Dabezies E (1986) *Anat Rec* 214:204-209

DIFFERENT EMG - FORCE RELATIONSHIPS OF THE LOW-BACK MUSCLES DURING STANDING AND SITTING

L.J. MOUTON, S. BESSELING, A. HIDDING, J. van der BIJ

Department of Anatomy and Embryology and Department of Rehabilitation,
 University of Groningen, The Netherlands

INTRODUCTION

It is often stated that low-back pain is caused by bad work postures and/or heavy workloads (1,2). However, to be able to investigate the relation between work posture, workload and low-back pain it is necessary to have a valid, reliable and usable method to measure the load on the back of an individual in work situations. Besides the use of biomechanical models electromyography seems useful for this purpose (3). However, more information is needed about the possibilities and restrictions on the use of emg in this field.

This study examines the effect of static backload on the myoelectric activity of the backmuscles in different symmetric postures. It focuses attention on the EMG - muscular moment relationship of the low-back muscles during brief isometric contractions while standing and sitting.

MATERIALS AND METHODS

Subjects

Eight subjects participated (4 male and 4 female, age between 20 and 30). All were healthy and had no history of backpain.

Electromyographic recording

Myoelectric signals were picked up by two pairs of bipolar surface electrodes (ConMed, Ag/AgCl ECG electrodes) placed 3 cm. to the left and to the right of the midline of the spine at the L3 level (interelectrode distance 38 mm.).

Raw EMG signals were amplified (differential amplifier, passband 3.5-600 Hz) and recorded on tape (Bell & Howell VR3200, tapespeed 7.5"/second) simultaneously with the force signal. During experiments EMG signals were monitored on a 2 channel memory oscilloscope (Philips, PM3302).

Recording of force and posture

Subjects were placed in a reference frame, sitting or standing; the pelvis fixed with a Veleron strap to a wooden board at the level of the anterior superior iliac spines. To enable measurement of exerted moments of the back muscles a harness was strapped around the chest, just under the arms. A chain connected the harness via a force transducer (range 0 - 2000 Newton) to the wall 90 cm. in front of the subject. For each subject and each position care was taken that the chain ran horizontally. The harness was not removed during an experimental session.

It is assumed that forces measured this way reflect the moments resulting from isometric extension forces of the erector spinae. Force levels were controlled by the researchers by means of a digital multimeter (Philips PM 2519). Subjects received feedback on their force levels by means of an oscilloscope (Tektronix 502A). To get an indication of the erector spinae length distances from Th1 to L3 and Th1 to L5 were measured for each subject in each position.

Experimental design

Experimental series were divided into two parts: first measurements of EMG and force signals and muscle lengths in upright standing were executed, secondly measurements in upright sitting were carried out.

In each position subjects performed 3 Maximal Voluntary Contractions (MVC) with 2 minutes rest after each exertion. Thereafter the subjects performed two identical series of isometric contractions at 0,10,20,...90%MVC. Contractions lasted 5 seconds each and were followed by 10 seconds of rest.

Data processing

Signal analyses was done by means of a PDP11/34 computer. For each short isometric contraction 3 seconds of the EMG signals were A/D converted (sampling rate 2048 Hz.), rectified and averaged. Force signals were digitized and averaged over the same 3 second intervals. Results from each pair of electrodes, from each subject in each position were represented graphically. To evaluate the relation between EMG and force regression analysis was used.

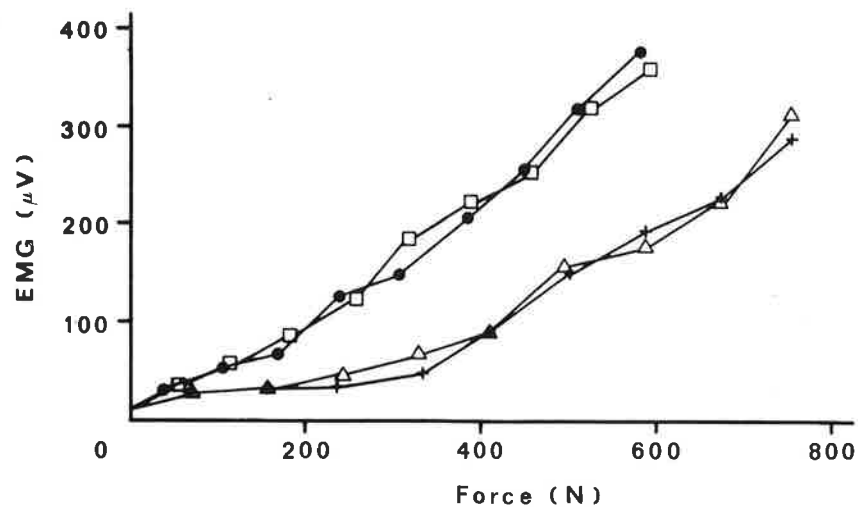


Fig. 1. Data from subject 1: The rectified averaged EMG (μV) measured at the electrode 3 cm. right of L3, as a function of measured forces (Newton). Highest force level represents 90%MVC for each position.

series 1 \bullet and series 2 \square in upright standing
series 1 \blacktriangle and series 2 \triangle in upright sitting

RESULTS

Although interindividual differences are present, results show that for all subjects the EMG-force relationship of the low-back muscles is different during standing and sitting (see figure 1.). Most remarkable is the fact that in all cases the EMG value at a particular force is far lower in sitting than in standing posture; several graphics show EMG-values in standing three times higher than the EMG-values in sitting at the same force level.

Next to this the data make clear that for all subjects the maximal force exerted in sitting is higher than in standing: mean maximal force over the eight subjects in standing is 581 N. (range 401-748). In sitting this is 775 N. (range 594-940). In contrast to this maximal EMG-values in sitting are in all cases far lower than in standing: mean EMG-value at MVC in standing is 439 μV . (range 281-601). Mean EMG at MVC in sitting is 297 μV . (range 206-425).

Regression analysis indicates a high correlation between force and EMG both in standing and in sitting (correlations between .90 and .99). In several cases, mainly in sitting, a quadratic curve gives a better fit than a linear curve. By comparing series 1 and 2 of each person in each posture it is concluded that the reproducibility of the force - EMG curves is good.

Measurements of the Th1-L3 and Th1-L5 distances are presented in table 1.

subject	Ls	Lz	Ls - Lz	Ds	Dz	Ds - Dz
1	44	44	0	49	53	+4
2	48.5	46.5	-2	54.5	51.5	-3
3	44	45	+1	49	51	+2
4	44	42	-2	50	48.5	-1.5
5	42	41.5	-.5	48	48	0
6	47	45	-2	-	-	-
7	40	39	-1	45	46	+1
8	42	41	-1	48	49	+1

Ls = distance Th1 - L3 in standing (cm.)
Lz = distance Th1 - L3 in sitting (cm.)
Ds = distance Th1 - L5 in standing (cm.)
Dz = distance Th1 - L5 in sitting (cm.)

Table 1. Results of distance measurements

DISCUSSION

Till now little attention has been paid to the influence of posture on the EMG-lumbar moment relationship. In several studies EMG of the low-back muscles in standing and sitting postures was compared. However, these concerned mainly

unloaded situations (4,5,6). In these studies similar activity levels have been recorded in standing and sitting. Schultz et al.(7) measured EMG of the back muscles in standing and sitting while subjects had to resist a flexion force of 15 kg. (load applied to a chest harness fixed just beneath the arms). Their results show that the electrical activity during this task in sitting was about 25% lower than in standing (EMG as mean over 4 electrode locations and 4 subjects).

Present results are in agreement with these studies. Present findings, however, indicate that at higher force levels the differences in EMG between standing and sitting are far bigger and are clearly subject dependent. So it is concluded that if EMG is used as an indicator of backload, standard measurements of EMG and load first have to be made for each subject in each posture.

A difference in EMG - force curves in standing and sitting was expected because of muscle length dependency of EMG - force relationships reported earlier (8,9) and the assumption that from standing to sitting back muscle length increases. Yet, the latter assumption is not supported in this study: intervertebral distances change only little and show lengthening in only part of the cases (table 1.). It is considered that either the difference in EMG - force curves has other causes than a muscle length change, or the measured distances are not good indicators for muscle length. Further research on this will be done.

ACKNOWLEDGEMENTS

This study was initiated and financially supported by the Directorate-General of Labour of the Dutch Ministry of Social Affairs and Employment. The authors would like to thank Dr. A.L. Hof for his support and the helpful comments on the manuscript.

REFERENCES

1. Westgaard RH, Aaras A (1984) *Appl Ergon* 15:162-174
2. Frymore JW, Mooney V (1986) *J Bone Joint Surg* 68A:469-474
3. Andersson GBJ (1982) In: White AA, Gordon SL (eds) *Symposium on idiopathic low back pain*. Mosby Company, St. Louis, pp 220-251
4. Andersson BJG, Ortengren R (1974) *Scand J Rehab Med (suppl)* 3:73-90
5. Andersson BJG, Ortengren R (1974) *Scand J Rehab Med (suppl)* 3:91-108
6. Rosemeyer B (1971) *Arch Orthop Unfall Chir* 69:59-70
7. Schultz A, Andersson G, Ortengren R, Haderspeck K, Nachemson A (1982) *J Bone Joint Surg* 64A:713-720
8. Vredenburg J, Rau G (1973) In: Desmedt JE (ed.) *New developments in electromyography and clinical neurophysiology*, vol 1. Karger, Basel, pp 607-622
9. Grieve DW, Pheasant ST (1976) *Electromyogr Clin Neurophysiol* 16:3-21

ELECTROMYOGRAPHIC INVESTIGATION OF TRUNK CONTROL IN THE SITTING POSITION

M. ELISE JOHANSON

Shriners Hospital for Crippled Children, Orthopaedic Biomechanics Laboratory, 1701 Nineteenth Avenue, San Francisco, California, USA

For many individuals sitting is a position of function. Trunk control, independent mobility, and balance may be facilitated if the wheelchair or seat is designed properly. Therefore, an understanding of the normal kinematics of functional and static sitting postures is needed. The purpose of this investigation was to measure the normal range of EMG output of selected trunk musculature in sitting. Subjects performed voluntary trunk movements, responded to disturbed balance, and maintained relaxed sitting in selected chair configurations. Relative measurements of motion were recorded to describe normal movement patterns of the trunk and pelvis in the sitting position.

METHOD

Nine normal, female subjects between the ages of 20 and 35 were recruited for the study. Muscle activity from the right erector spinae at the levels of the ninth thoracic vertebra and the third lumbar vertebra, and the right external and internal abdominal oblique muscles was recorded with silver-silver chloride surface electrodes. Measurements of lumbar curve depth, pelvic tilt, and trunk movements in the sagittal and frontal planes documented position changes relative to erect, unsupported sitting.

EMG Data. The amplitude of muscle activity was calculated from integrated EMG and expressed as a percent of a maximum voluntary contraction. A mean value was calculated for the nine subjects in each position and expressed as "Mean % EMG". To determine differences in muscle activity for the same muscle in each position, one-way analyses of variance (ANOVA) with repeated measures were performed for each muscle. The positions were grouped into 3 categories; voluntary movements, equilibrium responses, and supported sitting. Each category included EMG data recorded in erect, unsupported sitting for comparison. Neuman-Keuls post hoc analyses were performed on all significant results.

Motion Data. Data needed to calculate changes in subject position were recorded in erect, unsupported sitting, and in the final position (after each movement or position change). By subtracting the value recorded for each parameter in erect sitting from the final position, movements that occurred during the test could be estimated. Pelvic tilt in the sagittal plane was measured by subtracting the heights of the anterior and posterior spines of the pelvis from the chair seat, dividing by the distance between the anterior and posterior spines measured by calipers, and calculating the degree of tilt trigonometrically (Figure 1-A).¹ Flattening or deepening of the lumbar curve was estimated by placing a strip of plastic vertically along the lumbar spine. A ruler mounted perpendicular to the plastic could be pushed inward until it contacted the skin over the 3rd

lumbar vertebra, indicating the depth of the lumbar curve. Angular measurements of the trunk-thigh angle estimated sagittal plane movement, and lateral deviation of the shoulders and pelvis from horizontal estimated trunk and pelvic movement in the frontal plane. These measurements were taken from video tapes of the subject with a goniometer (Figure 1-B, 1-C).

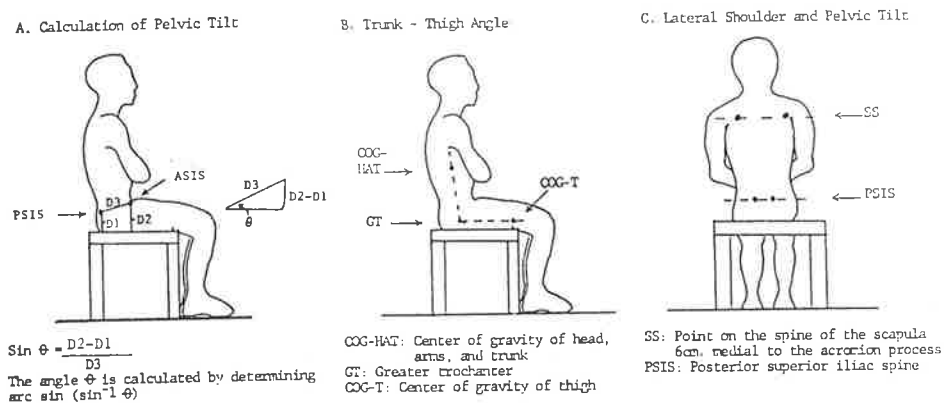


Figure 1.

Each subject assumed the erect, unsupported sitting position, with arms folded across the chest, shoulders and pelvis level, and hips, knees, and ankles at approximately 90 degree angles. Subjects were directed to assume this position before each movement was performed or the chair dimensions were changed. Muscle activity from each muscle was recorded so that all of the subsequent changes in EMG output could be compared with erect, unsupported sitting. Sitting balance was challenged with the subject on an equilibrium board (a square board with rockers attached to 2 sides). The board was tipped as far as possible forward, backward, right and left. Subjects were informed when they would be tipped and in what direction. Voluntary trunk movements of forward flexion, extension, lateral flexion, and rotation to either side were performed in an adjustable chair with the back removed. The chair back was replaced and three relaxed, supported sitting positions were maintained. These included: erect supported sitting; with the seat horizontal to the floor and seat-to-back angle at 90 degrees, reclined sitting; with the seat inclined 20 degrees, keeping the 90 degree seat-to-back angle, and semi-reclined sitting; with the seat horizontal and the back reclined 20 degrees, making a 110 degree seat-to-back angle.

RESULTS AND DISCUSSION

In erect, unsupported sitting all but one of the nine subjects sat with the pelvis in slight posterior tilt and all nine had a lordotic posture of the lumbar spine. The shoulders and pelvis

were horizontal. The mean percent of EMG output for each muscle in erect, unsupported sitting is presented in Figure 2.

Voluntary Movements. During forward flexion, anterior tilting of the pelvis and flattening of the lumbar curve were observed for all subjects. Most subjects tilted the pelvis posteriorly during lateral flexion to either side and anteriorly during trunk rotation. Lumbar curve measurements suggest there was a deepening of the lumbar curve during trunk rotation and flattening during lateral trunk flexion.

Significant increases in muscle activity relative to erect, unsupported sitting were recorded for the thoracic erector spinae during trunk extension (from full flexion) and trunk rotation to the right; for the lumbar erector spinae during trunk extension; for the external oblique during lateral flexion to the right and trunk rotation left; and for the internal oblique during trunk rotation right ($p < .01$). These findings are in agreement with studies of the same muscles in the standing position or during exercises.

Equilibrium Responses. During the forward and backward tipping of the equilibrium board, the pelvis tilted in the opposite direction of the board for most of the subjects. The motions of the pelvis and lumbar spine recorded during the tip right or left appeared to be independent of each other and variability was observed between subjects. The degree of the lateral tilt of the shoulders was equal to the lateral tilt of the pelvis, which occurred in the opposite direction.

In contrast to the voluntary trunk movements, muscle activity recorded during the equilibrium responses was not statistically greater for any of the muscles studied than the activity recorded in erect, unsupported sitting. Adequate support from passive structures or deeper muscles of the pelvis and spine may be effective in maintaining the body's center of gravity over its base of support. When the pelvis is tilted during walking, vertical alignment of the head and trunk is maintained due to the natural curvatures of the spine and ligamentous attachments. A muscle pull lateral to the spine produces a double convexity of the thoracic and lumbar spine, coiling the vertebral column in a naturally occurring scoliosis.² Mechanically coiling the spine may be one mechanism for reducing the amount of muscle activity needed to adjust to changes in pelvic position in sitting as well as standing. Other investigators have reported the function of the deep, transversospinal muscles, which adjust the motion between individual vertebrae, and the multifidus, function to stabilize the vertebral column.³ The action of the psoas may also be important to balance the trunk between flexion and extension.⁴ These muscles are inaccessible with surface electrodes, but should be of interest in further studies of trunk musculature in sitting positions.

Supported Sitting. In all of the supported sitting positions the pelvis was tilted posteriorly with few exceptions. Muscle activity recorded from the lumbar erector spinae was greater during erect,

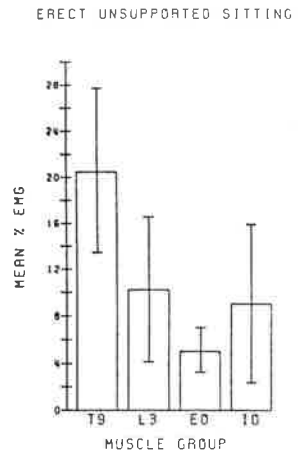


Figure 2.

supported or unsupported sitting than when the seat-to-back angle of the chair was increased from 90 degrees to 110 degrees ($p < .05$). Tilting the chair, but keeping the same seat-to-back angle had no significant effect.

The significant reduction in muscle activity in the lumbar erector spinae during semi-reclined sitting is probably due to a transfer of body weight to the backrest of the chair, not the posterior tilt of the pelvis. A posterior tilt has been associated with a reduction in muscle activity in the erector spinae in other studies that reported a greater degree of tilt than was measured in this study. No reduction in muscle activity was recorded when the entire chair was reclined 20 degrees (keeping the hip and knee angles at 90 degrees). Simply reducing the effects of gravity may not be as effective as changing the backrest inclination of the chair.

The results of this study demonstrate the position of the pelvis and possibly the lumbar spine can be modified or controlled by the subject. The considerable pelvic motion recorded during the voluntary movements and equilibrium responses suggests the trunk muscles may be acting on the pelvis and not the thorax. Andersson et al.⁵ reported subjects in the sitting position can influence the movements of the pelvis and lumbar spine by contracting anterior or posterior muscles, or leaning the trunk forwards or backwards. An independent lumbar-pelvic relationship may be occurring as an important part of balancing the trunk in the sitting position.

For non-ambulatory individuals, it is important to consider sitting as a position of function. Understanding the normal kinematics of "functional sitting" can result in improved chair designs that facilitate normal trunk movements and balance in addition to providing a well supported sitting position for tasks requiring visual control or manual skill.

ACKNOWLEDGEMENTS

Boston University, Sargent College of Allied Health Professions, Boston, Massachusetts, USA.
Therapeutic Equipment Center, W.E. Fernald State School, Waltham, Massachusetts, USA.

REFERENCES

1. Sanders G, Stravakas P: *Phys Ther*, 61, 49-50, 1981
2. Basmajian J, MacConaill M: *Muscles and Movements*. Philadelphia, Williams and Wilkins, 1969
3. Basmajian J, Donish E: *Am J Anat*, 133, 25-36, 1972
4. Nachemson A: *Acta Orthop Scand*, 37, 177-190, 1966
5. Andersson G, Murphy R, Ortengren R, Nachemson A: *Spine*, 4, 52-58, 1979

SITTING POSTURE: BALANS CHAIR VS. CONVENTIONAL CHAIR

PAUL ANDERSON, DEBORAH BELK, ANDREA CONNORS, CHARLENE LEVITAN,
ELLEN MAGUIRE, KELLY MCNAMARA, TOBA SHAPIRO AND CAROL SHELTON

University of Maryland, Department of Physical Therapy,
32 S. Greene Street, Baltimore, MD 21201, USA

INTRODUCTION

In recent years the number of alternative chair designs on the market has increased dramatically. These chairs proclaim decreased musculoskeletal disorders and fatigue associated with prolonged sitting. Much of the focus has been directed towards different chair angles, postural alignment, and weight distribution. Many manufacturers have claimed that specially designed chairs were beneficial for several reasons; including the reduction of stresses on muscles and joints, facilitation of maximal flexibility, and improvement of circulation and breathing due to an "ideal" position. No objective data was found to support these claims.

The Hag Corporation, manufacturer of the Balans chair (BC) Model #6020, has made several public claims as to the benefits of their product even though they could not be substantiated by published research. According to Hag, the chair aligns the body in a more natural posture than a Conventional Office Chair (COC). The BC's design supposedly causes the individual to maintain an upright posture. The chair positions the back in an upright position with the hip and knee joints at an angle of 60 degrees of flexion. The company also states that the chair places less stress on the muscles and joints of the vertebral column thereby decreasing or eliminating low back pain.

In an effort to provide data on the effect of these new chair designs on the individual it was the purpose of this experiment to compare the BC to a COC. Specifically, this study investigated physiological variables (heart rate, breath frequency, mets, tidal volume), angles (hip, thoracic and cervical intervertebral joints), and the electromyography (EMG) of the lumbar erector spinae and vastus lateralis muscles.

Twelve subjects with no prior history of musculoskeletal disorders participated in the study. Beckman miniature Ag-AgCl surface electrodes were placed 1cm apart over the mid-belly of the four muscles. Standard preparation procedures reduced skin impedance below 5K ohms. The EMG signal was passed through a Hewlett-Packard 8 channel 8811A bioamplifier with upper and lower cutoff frequencies at 3 Hz and 10 K Hz respectively. The CMRR was 126 db at 60 Hz. Gain was adjusted for each channel to maintain an adequate signal without distortion. The reduced data was corrected for differences in amplification. The raw EMG signal was recorded on FM tape, sampled digitally then full wave rectified and integrated by computer. The data were in millivolt seconds after integration. A 2-lead EKG was then applied to monitor heart rate. A facemask connected to the metabolic cart was placed over the subject's mouth and nose. Earphones were placed over the subject's ears in an attempt to minimize extraneous noise. The subject was randomly assigned to either the BC or a COC and given a 10 minute adjustment period. During this period, the subject was videotaped. Cervical thoracic and hip angles were measured from the tape using a goniometer. All angles were measured from the vertical. After the adjustment period, the subject typed several paragraphs to simulate an office-related activity. During the task physiological, joint angles and EMG data were collected: initially, at minute one, and every other minute thereafter for 15 minutes totaling nine sampling periods. The subject was then given a 10 minute rest period. The above protocol was repeated for the other chair.

An analysis of variance with a confidence level of 95% was employed to analyze the physiological, joint angles and EMG variables. The data from each subject's nine sampling periods for each chair represented the repeated measure factor in the analysis. Significant F ratios were further analyzed by a Student Newman Keuls Post Hoc test.

DISCUSSION

The results revealed there was no difference physiologically between a task performed in the BC or in the

COC ($F_{0.05, 1,47} df=3.16$). However, collapsed data across chairs, revealed heart rate and breath frequency significantly changed over time whereas tidal volume and METS did not ($F_{0.05,8,384} df = 16.45$).

The thoracic and cervical angles of the BC did not differ significantly from those found in the COC. However, the difference between the 60 degree hip angle in the BC and the 90 degrees found in the COC was significant ($F_{0.05,2,36} df = 32.39$). The variance in hip joint angle can be attributed to the clear difference in chair architecture and was expected.

Data analysis established that the total EMG value collapsed across all four muscles while typing in the BC was significantly greater than the EMG values for the COC ($F_{0.05,1,47} df=192.08$). These results indicate that the examined muscles exhibited a greater amount of electrical activity in the BC as compared to the COC. It can be assumed the greater muscle activity was necessary to maintain the posture required by the BC and therefore the subject could fatigue faster.

Other researches have also examined EMG activity while sitting. Floyd and Roberts (1958)¹ found that small changes in position altered the electrical activity of the trunk musculature. They also reported that the erector spinae worked harder and tended to fatigue more when sitting without back support. They concluded that a backrest may reduce this fatigue factor. Since the present study found more erector spinae EMG activity in the BC ($F_{0.05, 1,36} df=21.69$) without a backsupport, these data appear to be in agreement with Floyd and Roberts.¹

The data presented above as well as the opinions of the subjects did not support the company's advertisements. The BC did not appear to align the subjects in an upright or more natural position as verified by insignificant vertebral column angles between chairs. Also the significantly greater muscle activity demonstrated in the BC than the COC would tend to suggest that the subjects had to work harder to maintain the same position. Subjectively, all the subjects felt more uncomfortable in the BC. The subjects felt pain and fatigue

after only a short time period in the BC. The volunteers stated they felt as if they were "slumping" into a position of comfort as the amount of time and fatigue increased even though the angle data did not verify this feeling.

CONCLUSION

It was concluded that the results of this study do not support the claim of the Hag corporation that the Balans chair reduces low back fatigue. Chair construction alone may not be the sole determinant of sitting posture. One needs to examine the body's posture, the respective working muscles and the physiological work.

ACKNOWLEDGEMENTS

The authors wish to thank the Back Center (Vertech) of Baltimore, MD for donating a Hag Corporation Balans Chair for this study.

REFERENCES

1. Floyd WF, Roberts DF (1958) Anatomical and Physiological Principles in Chair and Table Design *Ergonomics*, 7:1-16

THE PREDICTION OF HUMAN WALKING PATTERNS

H.F.J.M. KOOPMAN, H.J. GROOTENBOER, H.J. DE JONGH

Biomechanics Group, Department of Mechanical Engineering, University of Twente
P.O. Box 217, 7500 AE Enschede (The Netherlands)

INTRODUCTION

One of our subjects of study is the construction and use of exoprostheses for the lower extremities. In this study, the Department of Rehabilitation of the University of Groningen and the rehabilitation centre 'Het Roessingh', Enschede, are participating.

Although many studies describe prosthetic gait, little is known about the underlying mechanics. It is, for example, evident that during normal level walking the muscles of the lower extremities are used in a more or less optimal way. This need not be the case in prosthetic walking. We believe that, by gaining insight in the mechanics of prosthetic gait, the prosthesis and the alignment of the prosthesis can be improved by adapting them more closely to the functional abilities of the patient. It is essential to know how an amputee uses his remaining muscles during walking, how this is affected by the mechanical characteristics of the prostheses, and what these characteristics should be to obtain an optimal walking pattern. To achieve this, one would like to be able to predict how an amputee will walk with a certain prosthesis.

The model we are developing simulates human walking in three-dimensional space. It has three applications: To reconstruct the movement in space when only the joint rotations in the sagittal plane are measured, to predict the movements when no measurements are available and to analyse the walking pattern. In the following, the model is applied to normal level walking.

METHODS

Movement analysis

The part of the model, where the movement is analysed, can be divided in three sub-models: A segments model, a kinematics model and a kinetics model. In the segments model, the human body is modelled as a coupled system of rigid bodies (segments), consisting of segments for upper legs, lower legs, feet and pelvis (including head, arms and trunk). With some measured antropometrical data, the local frames of the segments and the position of the joints in these frames are defined. The mechanical properties of each segment are calculated using the regression relations of Chandler et al.¹ Finally, the muscle attachment model of Brand et al.², consisting of 47 leg muscles, is defined in the local frames. With these methods, we are able to model each specific indivi-

dual.

The input of the kinematics model consists of the joint rotations as functions of time. With these rotations, the rotation tensors of each segment as functions of time are constructed. This tensor defines the relation between local segment frame co-ordinates and absolute frame co-ordinates. Since any arbitrary movement can be used as an input of the model, it must be checked whether the constraints of the movement are met. These constraints are the demands that joint rotations must not exceed maximum values and that the feet must remain on or above the floor, for the stance and the swing phase of the leg respectively. If necessary, the input rotations are corrected to fulfill these demands, as reported earlier.³ Finally, the forward walking velocity is calculated.

In the kinetics model, the ground reaction forces, the joint forces and the joint moments of force are calculated by solving the equations of motion, a method usually referred to as 'inverse dynamics'. During double stance, the system is underdetermined, so the ground reaction forces can not be solved uniquely. This is met by assuming that the point where the resulting ground reaction force applies gradually moves from one foot to the other.

Movement prediction

With optimization routines, (part of) the movement can be predicted. These optimization routines are based on the minimization of an objective function, such as the energy consumption of walking or a function that is a measure for the forces acting on the stump. For every arbitrary input rotation, the value of this objective function is calculated as a result of the movement analysis.

Since gait is continuous and periodical, it is advantageous to impose these properties on the movements. We have incorporated this in the model by representing the input rotations as finite Fourier series. Furthermore, the Fourier coefficients can be used as optimization variables. This leads to a different approach in modelling: Instead of the commonly used time discrete modelling, we have a global approach where the variables are time functions valid for the complete walking cycle. This results in a very fast computation scheme, necessary to reduce the computation time in optimization. In the optimization, the Fourier coefficients of the input rotations are gradually varied to minimize the objective function, so that at the end of the process the rotations reflect an optimal movement.

RESULTS

As an example, the model is applied to a 3-dimensional 7-segmental model with 21 independent degrees of freedom. The input rotations consist of measured hip, knee and ankle rotations in the sagittal plane only, the walking

pattern is assumed to be symmetrical. The joint rotations are measured with the movement analysis system of 'Het Roessingh'. With the constraints, this movement is made consistent, and the forward velocity is calculated, resulting in the stick diagram of figure 1. For clearness' sake, only one leg is plotted during swing, stance and again swing. The two hip joints, the knee joint and the ankle joint are represented by circles. To be able to model the roll-over of the foot during stance, which is an important mechanism of walking, the foot is modelled as an ellipsoid.

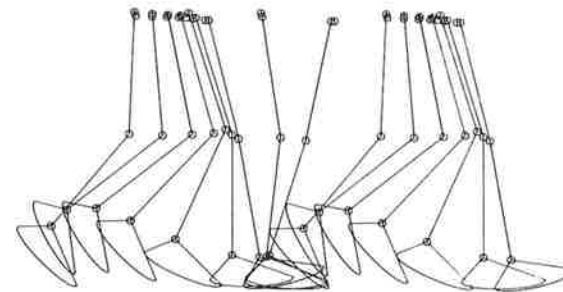


Fig. 1: Stick diagram.

Figure 2 shows the calculated ground reaction forces, normalized with body weight, in forward, vertical and lateral direction. There is good agreement with measured data in literature.⁴ However, in the first part of the stance phase, the vertical ground reaction force is a little too low, which can be explained by the relatively low walking velocity of 0.8 m/s and by the shape of the modelled foot, that lacks a pronounced heel.

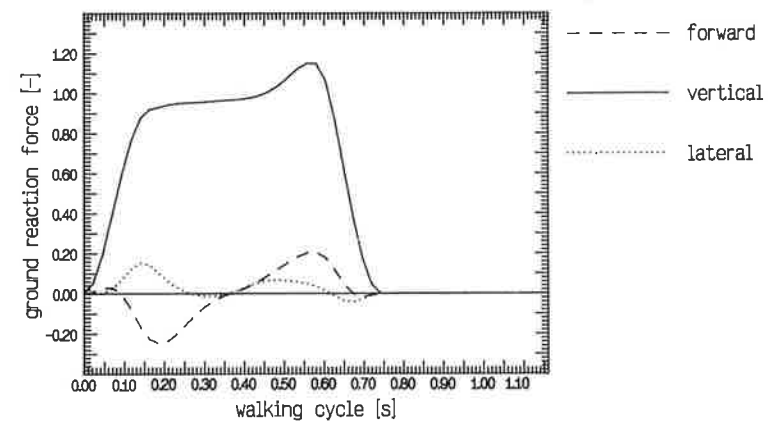


Fig. 2: Normalized ground reaction forces.

In the kinetics model, moments of force in the contact point between foot and floor are assumed to obtain equilibrium. However, in reality these moments can not exist. By optimizing the pelvic rotation around the lateral axis and the hip ad- and abduction, with an objective function based on the magnitude of the moments, they could strongly be reduced. Figure 3 shows the resulting pelvic rotations. The rotations around the forward and vertical axes are necessary to fulfill the demands set by the constraints, and show good agreement with data found in literature.⁴ The rotation around the lateral axis is predicted with the optimization: A slight leaning forward during walking.

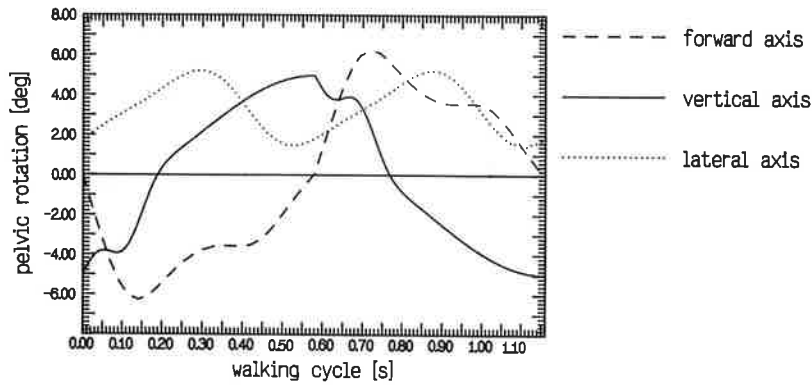


Fig. 3: Pelvic rotations

Future developments involve the implementation of a muscle model to calculate muscle forces and energies and the implementation of a more realistic model of the foot. Since the energy consumption during walking is relatively low, it seems profitable to develop objective functions, based on the muscle and segment energies, to predict the complete walking movement.

REFERENCES

1. Chandler RF, Clauser CE, Mc Conville JT, Reynolds HM, Young JW (1975). Investigation of inertial properties of the human body. Report DOT HS-801230, National Technical Information Service, Springfield Virginia
2. Brand RA, Crowninshield RD, Wittstock CE, Pedersen DR, Clark CR, van Krieken FM (1982). A model of lower extremity muscular anatomy. J Biomech Eng 104-4:304-310
3. Koopman HFJM, Grootenboer HJ, de Jongh HJ (1987). A three dimensional model of human walking. In: Proceedings XI ISB congress, Amsterdam (in print)
4. Inman VT, Ralston HJ, Todd F (1985). Human walking. Williams & Wilkins, Baltimore

MODELLING AND SIMULATION OF HUMAN GAIT IN THREE DIMENSIONS USING MULTIBOND GRAPHS AND IMPLICIT INTEGRATION ROUTINES

P.C. MATTHIJSSE, P.C. BREEDVELD

University of Twente, Electrical Engineering Department,
P.O. Box 217, 7500 AE Enschede (the Netherlands)

ABSTRACT

In order to simulate human gait, a proper model of the human body has to be derived. In this paper multibond graphs are used to model the dynamics of the human body. The equations derived from a multibond graph can be solved with implicit integration routines.

INTRODUCTION TO BOND GRAPHS

Modelling with the use of bondgraphs starts with a description of the physical system in ideal elements, like masses, springs, dampers, etc. In figure 1, the Ideal Physical Model (IPM) of a physical system is shown, which consists of a mass, attached by two strings to a point with a given constant velocity (v_{ref}). Spring properties are assumed in both strings and in the second one damping is assumed too. Only vertical displacement is considered. From the IPM a bond graph is systematically derived by attaching the ideal elements with bonds to a connection structure (fig. 1). A bond, depicted by a half arrow, is the representation of an energetic relation, i.e. power, between elements. Power can be written as the product of force and velocity. There are two kinds of connection structures: a 1-junction at which the forces of the attached bonds are summed and the velocities are equal to ensure power-continuity and a 0 junction at which velocities are summed and the forces are equal. The equations describing the dynamics of the system can be derived by

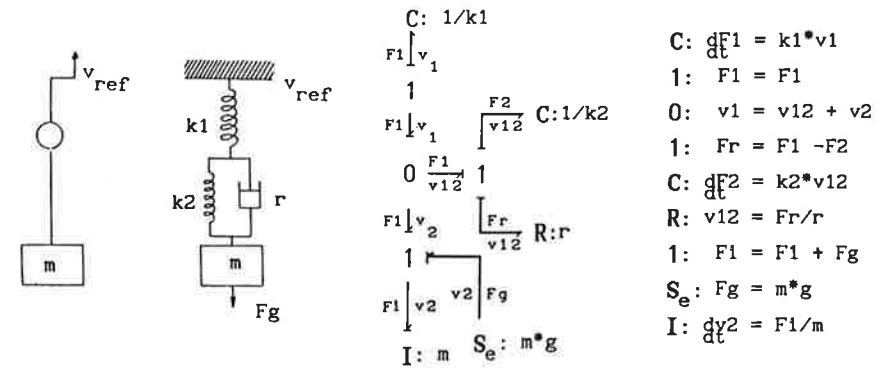


Fig. 1a Physical system. Fig. 1b Ideal Physical Model. Fig. 1c Bond graph. Fig. 1d Equations.

writing the constitutive relations of the elements in the bond graph (fig.1). The thus derived set of differential equations can also be derived by application of methods based on Newton-Euler laws or Lagrange equations. The method of bond graphs is systematic and therefore less error prone and appropriate for computer implementation. Moreover, changes in the model can be easily adapted and the topological structure of the bond graph shows resemblance with the physical system. These advantages of the use bond graphs are especially important in the modelling of large physical systems like the human body. For further and detailed description of bond graphs, see [1],[2].

MODELLING AND SIMULATION OF HUMAN GAIT

Ideal physical model

The dynamics of the human body can be modelled as a mechanical system which consists of rigid bodies interconnected by different types of joints (fig.2). The model has to be three dimensional to take into account lateral stability problems and the influence of walking aids like crutches. In this case, each unconnected body has 3 rotation and 3 translation possibilities. Due to the connection of bodies by joints the possibilities of rotation and translation are constrained. In the joints damping and compliance properties can be exhibited and driving forces or torques can be attached. The dynamics of a body is described in coordinates of its own body-fixed reference frame w.r.t an inertial frame. Only in body-fixed frames parameters, as for example rotational inertias, are constant. In the joints variables have to be transformed from one body-fixed frame to another body-fixed frame. In the body are translational velocities and forces transformed from the body-fixed frame to the inertial frame v.v., because Newton's law is only valid in an inertial frame. If the body-fixed frame has a rotational velocity w.r.t. the inertial frame, gyroscopic torques arise.

Multibond graph

Multibond graphs (MBG's) are used to model systems of rigid bodies. MBG's are an expansion of the single bond graph notation described in the previous section and comparable to an expansion from scalars to vectors. The MBG of the total system is the connection of MBG's, describing the dynamics of a single freely moving body, by MBG's of different type of joints. In fig. 2, a MBG for the single support phase in human gait is shown, in which only one of the 13 MBG's of a body and one example of a MBG of a joint, i.e. spherical joint, is written out. The shaded characters of the elements in the MBG's represent the multiport character. Underscoring expresses an array character. The **MTF** represents a coordinate transformation. Gyroscopic torques are represented by the **MCY** element. The **TF**'s transform rotational velocities/ torques in the

upper part of the MBG into translational velocities/forces in the lower part of the MBG v.v. For further description of the MBG of a body, see [3]. In a spherical joint there are no translational velocity differences between the connection points and thus only an **MTF** arises in the lower part of this MBG. However, in all directions are rotational velocity differences, depicted by the upper **1** in the MBG. **C**- and **R**-elements can be attached at this junction to express compliance and damping properties. The **S_e** represents the resultant muscle torques or other driving torques. Contact of the foot with the ground is modelled as a single point contact. The ground on which the inertial frame is attached, is modelled as an **S_f** (velocity source) and assumed to have zero-velocity. All translational velocity differences between foot and ground are constrained to zero by an **S_f** with zero-velocity.

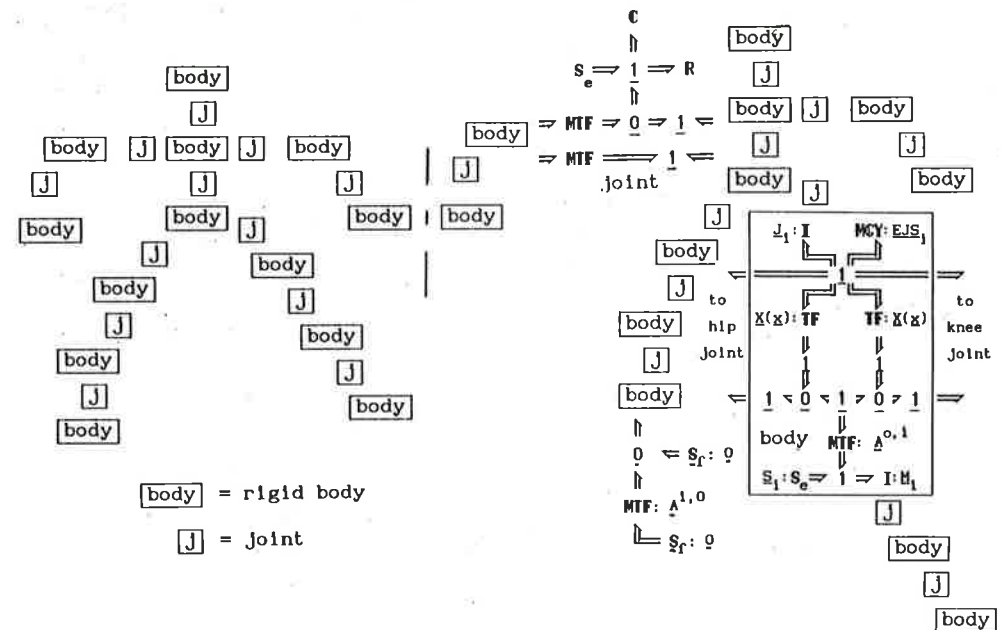


Fig. 2a Ideal Physical Model of a system of rigid bodies. Fig. 2b Multibond graph of the single support phase in human gait.

Equations and computational problems

The dynamics of a system of n bodies can be described by 6n differential equations. The constraints (x) between the bodies restrict the real number of independent differential equations to 6n - x. The MBG will therefore yield an implicit set of equations. Numerical problems will arise if the equations are solved by routines for explicit differential equations. In the MBG these (and other) computational problems can be made visible by so-called causal analysis [1] without actually writing the equations. Various methods are used to solve these problems. Often a set of explicit differential equations is derived by

using a description in generalised coordinates or by inserting stiff springs into the constraints. These solution techniques can also be applied within a bond graph approach. However, they have the disadvantage, besides specific disadvantages in solving the equations numerically, of changing the topological structure of the model. Bos [3] has demonstrated that the implicit equations derived from a MBG with the same topological structure as the IPM can be written as a set of Differential and Algebraic Equations (DAE's), which can be solved using implicit integration techniques. Application of implicit integration routines to solve a DAE-set from a MBG efficiently, is discussed in [4]. With the use of Lagrange multipliers, another conventional method, a DAE-set is formed too. However, solvability of this set equations with implicit integration routines is not guaranteed [3].

Computational problems due to constraints between the bodies arise both in the single and double support phases of human gait. However, during double support additional implicit equations arise due to the closed kinematical loop between the two contact points. These implicit equations can be inserted within the set of DAE's and thus solved with implicit integration routines. For the simulation of one walking cycle, two models, one for the single and double support phase have to be used. Ground reaction forces can be predicted both during single and double support if the point(s) of application is (are) known. Simulation of testproblems with the use of implicit integration routines are currently being performed.

CONCLUDING REMARKS

The use of multibond graphs in the modelling and simulation of systems of rigid bodies has great advantages. The method is systematic and therefore appropriate for computer implementation, less error-prone and easy adaptable to changes in the model. Computational problems, as for example due to constraints and closed kinematic loops, can be detected in an early stage and solved by implicit integration routines without changing the model.

REFERENCES

- [1] Breedveld PC (1986) In: Vansteenkiste GC, Kerckhoffs EJH, Dekker I, (eds) Proc. of 2nd European Simulation Congress. Antwerp, pp 38-44
- [2] Karnopp DC, Rosenberg RC (1975) System Dynamics: a unified approach. Wiley, New York
- [3] Bos AM (1986) Modelling multibody systems in terms of multibond graphs, Ph.D. thesis, University of Twente, Netherlands
- [4] Petzold LR (1982) In: Proc. 10th IMACS congress, Montreal, 1:430-432

BIOMECHANICAL MODEL OF QUADRUPED WITH FLEXIBLE SPINE

E.V.BIRJUKOVA(*), M.DUFOSSE(**), A.A.FROLOV(*), M.E.IOFFE(*), J.MASSION(**)

(* Institute of Higher Nervous Activities and Neurophysiology, USSR Academy of Sciences, Moscow, USSR

(**) Laboratoire de Neurosciences Fonctionnelles, CNRS, Marseille, France

INTRODUCTION

Biomechanical model of quadruped animal body was developed and used for analysis of cat motion during postural adjustment. In experiments the animal stood on the horizontal platform. In response to a conditional signal the animal lifted a forelimb. The main purpose of postural adjustment consisted in transfer of center of gravity (CG) so that it should be projected in a support triangle, formed by the other three limbs. The aim of the biomechanical analysis was identify the co-ordinated changes of movements parameters (synergies, according to N.A.Bernstein) during CG transfer.

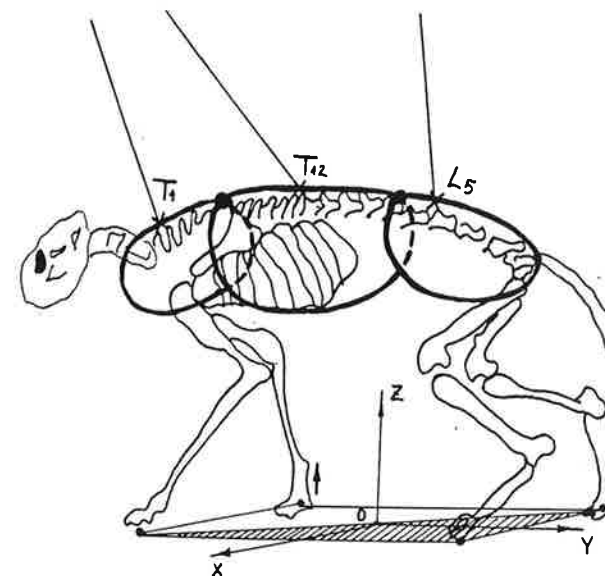


Fig.1 The gross-body model of a cat. OXYZ is the stationary system. Solid circles are the support points and centers of the spine joints. ↑ marks the lifting limb.

MODEL DESCRIPTION

The model consists of 12 rigid bodies (3 links of the trunk, 2 links of each limb, the head) (Fig.1). They are connected by frictionless hinges, which are

the models of animal joints: elbow, humeral, knee, pelvic, joints of the neck and the spine. Muscles are modelled by weightless threads with changing lengths and strengths. The number of the muscles is 29. The masses and dimensions of the links and the positions of the muscles attachment points were based upon the anatomical data [1].

Under the above experimental conditions the model has 16 degrees of freedom. The kinematics and dynamics of the model are described with the aid of tensor formalism [2]. Two sets of coordinates are introduced: generalized coordinates η^λ , $\lambda = 1, 2, \dots, L$, where L - number of degrees of freedom, and so-called base coordinates ξ^p , $p = 1, 2, \dots, 6M$, where M is the number of bodies in the model. ξ^p are the coordinates of CG and Euler angles of each link in a stationary system. Kinematics equations are presented in the standard form:

$$\xi^p = \xi^p(\eta^\lambda) \quad (1)$$

Dynamics equations are the Lagrange equations of the second kind presented in the form of tensor convolution:

$$C_{\lambda\mu}\ddot{\eta}^\mu + C_{\lambda,\mu\nu}\dot{\eta}^\mu\dot{\eta}^\nu = Y_\lambda + \Pi_\lambda, \quad \lambda, \mu, \nu = 1, 2, \dots, L \quad (2)$$

In equations (2) summation over repeated indexes is implied;

$C_{\lambda\mu} = b_{pq} \frac{\partial \xi^p}{\partial \eta^\lambda} \frac{\partial \xi^q}{\partial \eta^\mu}$ is the covariant metrical tensor of the system (b_{pq} is a function of masses and Euler angles, $\frac{\partial \xi^p}{\partial \eta^\lambda}$ is the structural matrix of the

system); $C_{\lambda,\mu\nu} = \frac{1}{2} \left(\frac{\partial C_{\lambda\mu}}{\partial \eta^\nu} + \frac{\partial C_{\lambda\nu}}{\partial \eta^\mu} - \frac{\partial C_{\mu\nu}}{\partial \eta^\lambda} \right)$ is the three indices Kristoffel symbol of the first kind, Y_λ - are generalized external forces, Π_λ - are generalized control forces.

This method of description of gross bodies dynamics doesn't impose any restriction on the kind of connections in the joints and allows to write the equations in compact form for the systems with great number of degrees of freedom. In comparison with other methods [3] this description is convenient to program and needs less computer memory.

If the movement of animal is given (e.g. as a function of joint angles of time) it is possible to calculate the resultant of muscle forces and elastic ligaments forces to perform it. The model has been verified by the comparison of vertical components of support pressure forces calculated by means of the model and measured in the experiment [4].

MOVEMENT RECONSTRUCTION

To measure movements of the cat's body three needles were implanted in selected vertebrae (T1, T12 and L5) (Fig.1). The cat's movements were filmed

from lateral and posterior viewpoints. The methods have been described in details earlier [5].

Three coordinates in stable system OXYZ (Fig.1) of each needle base and tip as well as ears tips were obtained from the movies using frame by frame analysis. The values of these coordinates permit to calculate all generalized coordinates and joint angles.

RESULTS OF MOVEMENTS ANALYSIS

The main conclusions from the experimental data analysis are the following: CG transfer is carried out by the translational transfer of the whole animal trunk. Besides, the stereotyped rotations around vertical axe in the spine joints were found: the moving spine has a form of letter S (S) consisting of three segments (Fig.2,b). The angles between spine segments are related by linear dependence.

CG transfers due to this bending are small. Two variants with the same values of CG transfer were compared: translational movement of the trunk and S-like bending of the spine. In the second case the resultant forces of the spine muscles were two fold. Therefore the bending of the spine is much less effective for CG transfer than the translational movement of the trunk.

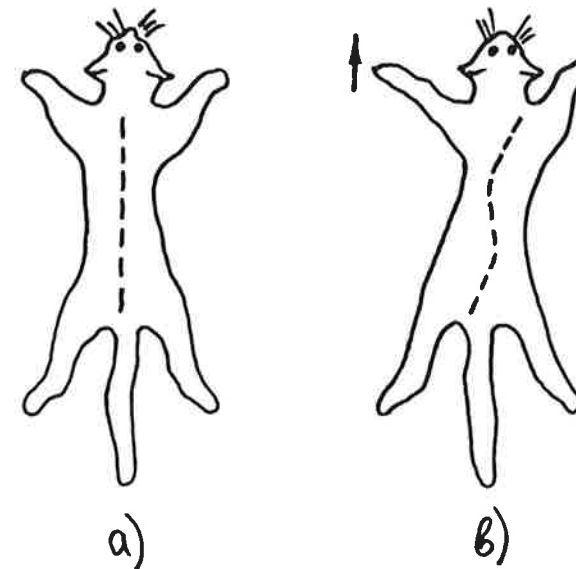


Fig.2 a) the form of the spine with strong muscle tone before learning; b) the form of the spine with lower muscle tone after learning, \uparrow marks the lifting limb.

Nevertheless, during learning to lift the limb the latter movement is replaced by the former one [5] (Fig.2). One of the possible explanation is the following. The muscle forces calculations by means of mechanical model does not allow to take into account the coactivation forces characterizing muscle tone which may be significant to provide high stiffness of the body. Possibly, muscle tone decreases during learning and, in spite of the fact that the resultant forces providing spine bending increase, the total energy expenditures decrease.

The quadruped body may be modelled as a flexible bar, fixed on four supports. If the muscle tone is small, the process of S-like bending may be partly passive as a consequence of stiffness loss after the support falling. Such using specific mechanical properties of the system may also lead to energetic expenditures decrease. This explanation is in accordance with the ideas of N.A.Bernstein about movement coordination perfection [6]: in perfect coordination the muscles are maximally weakened at the expense of external and reactive forces.

CONCLUSIONS

1. The biomechanical model is an effective tool for analysis of quadruped movement: from the description of movement of several points on the animal body, obtained in the experiment, the values of joint angles and correspondent resultant forces are calculated.
2. Co-ordinated movements in the spine joints were found. We assume that this co-ordination is due to the increasing role of passive forces relative to active ones during learning. It agrees with N.A.Bernstein ideas about learned co-ordinations.

REFERENCES

1. Manter JT (1938) *J Exp Biol* 15:522-540
2. Korenev GV (1979) *Goal-oriented mechanics of guided manipulators (in Russian)*. Nauka Publishing House, Moscow
3. Hollerbach JM (1980) *IEEE Trans Syst Man Cybern* 11:730-736
4. Frolov AA, Birjukova EV, Ioffe ME (1988) In: Gurfinkel VS, Ioffe ME, Massion J, Roll JP (eds) *Stance and motion: facts and concepts*. Plenum Press, New York, pp ... (in press)
5. Dufosse M, Macpherson J, Massion J (1982) *Exp Brain Res* 45:38-44
6. Bernstein NA (1966) *Essays on movement physiology and physiology of activity (in Russian)*. Medgiz, Moscow

MUSCLE COORDINATION IN ELITE AND TRAINED SPEED SKATERS

J.J DE KONING, G DE GROOT AND G.J. VAN INGEN SCHENAU

Faculty of Human Movement Sciences, Vrije Universiteit,
 P.O. Box 7161, 1007 MC Amsterdam (The Netherlands)

INTRODUCTION

Differences in performance level in ice speed skaters appear to be related to differences in push-off mechanics (1).

During push-off the upper and lower leg are extended in order to increase the velocity of the mass center of the body with respect to the ice. The amount to which rotation of a segment contributes to this acceleration, depends on simple geometric factors (2) and on temporal aspects of muscle activation (3).

The aim of the present study is to gain more insight on the relationship between muscle activation, movement pattern and performance in ice speed skating.

METHODS

A group of eight young elite and eleven young trained speed skaters were subjected to a biomechanical analysis, incorporating measured push-off forces, cinematographic data and link segment modelling together with simultaneous EMG tracings of ten lower limb muscles during speed skating at speeds typical for 1500 meter races.

Surface electromyographic signals of m. semitendinosus, long head of m. biceps femoris, m. gluteus maximus, m. rectus femoris, m. vastus lateralis, m. vastus medialis, m.gastrocnemius lateralis, m. gastrocnemius medialis, m. soleus and m. tibialis anterior were obtained telemetrically (Glonner, Biomes 80). The signals were full wave rectified, integrated and normalized to the maximum value attained during the stroke.

The push-off force was registered by means of special skates provided with strain gauge measuring elements. During the strokes the push-off force signals were stored in a portable computer carried on the skaters back. The speed skaters were simultaneously filmed (16mm, 100 fps) from a frontal and a sagittal view. Each frame was analyzed, digitized and low-pass filtered (Butterworth 4th order with a cutoff frequency of 20 Hz).

With the use of a link segment model the instantaneous net moments of force and power about hip, knee and ankle joint were calculated.

RESULTS

Comparing the push-off of the elite group with the trained group, a significant difference in maximum velocity difference between ankle and hip (1.59 m/s vs. 1.10 m/s) was found, while the push-off time of the two groups was the same. Moreover, the net power output at hip and ankle joints is larger in the group of elite speed skaters than in the group of trained speed skaters (fig. 2). This larger net power output is also reflected in the larger push-off force necessary for the higher acceleration of the mass center of the body in the elite group (fig. 3).

In coordinational pattern of joint movements we found no difference between the two groups. For both groups these patterns appear to be completely tuned to the constraints inherent to the transformation of rotation in joints into translational velocity of the mass center of the body (2-3): hip extension starts before knee extension, while knee extension starts before plantar flexion. The electromyographic signals also show this sequential pattern (fig. 4). The hip extensors attain their peak in activation before the

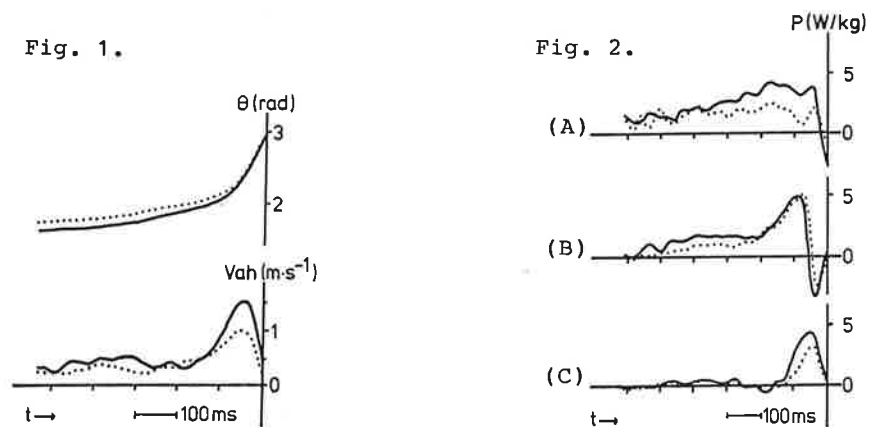


Fig. 1. Mean curves of knee angle (θ) and the velocity difference between ankle and hip (V_{ah}) of the elite group (solid lines) and the trained group (dotted lines) of speed skaters. The vertical axis indicates the end of push-off.

Fig. 2. Mean curves of normalized net power output at hip (A), knee (B) and ankle (C) joints of the group of elite speed skaters (solid lines) and the group of trained speed skaters (dotted lines). The vertical axis indicates the end of push-off.

knee extensors and the knee extensors attain their peak before the ankle flexors.

DISCUSSION

To minimize the external ice and air friction force that has to be overcome, the trunk as well as the foot should be kept in a more or less horizontal position during the speed skating push-off. The purpose of the push-off is to transform the rotational upper and lower leg movements into a high as possible translational velocity of the mass center of the body. Due to geometrical and anatomical constraints (2), the velocity difference between ankle and hip falls to zero if the knee approaches full extension (fig. 1). The decreasing velocity causes a termination of the push-off before the knee is completely extended. As a consequence of this the acceleration of the mass center of the body takes place in a short time (150 ms.).

Caused by the absence of complete extension of the hip and an absence of plantar flexion of the foot, there is a limitation in power production of the hip extending and plantar flexing muscles.

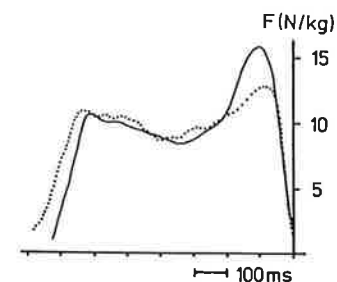


Fig. 3. Mean curves of the push-off force of the group of elite (solid line) and the group of trained (dotted line) speed skaters. The vertical axis indicates the end of push-off.

These muscles can not shorten over their full length range. The difference in power output between the elite group and the trained group can be explained by the smaller hip and knee angle in the elite athletes at the start of the push-off. With these smaller angles they can displace the mass center of the body over a larger distance, in that way they accelerate the mass center of the body over a longer period, which implies a larger power output.

The sequential pattern of joint movements contribute to an optimal power production. Since the bi-articular m. rectus femoris can

transport power produced by the hip extensors to the knee joint till the end of the push-off. In this sequential pattern no difference is found between the two different groups.

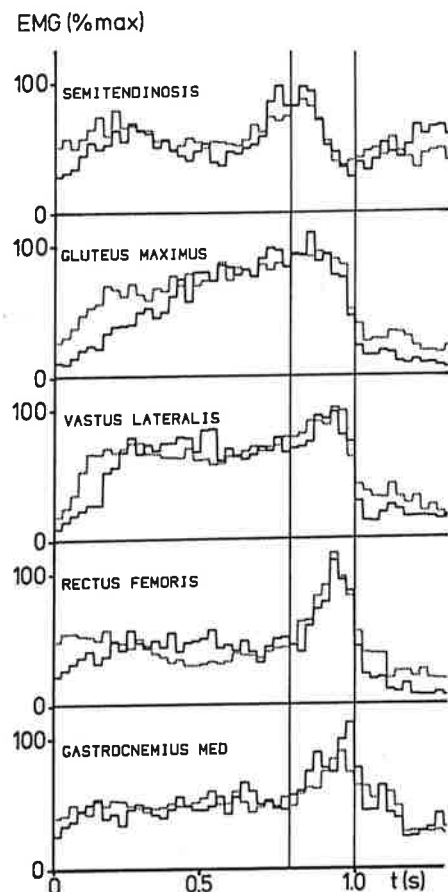


Fig. 4. Mean curves of full wave rectified, integrated and normalized electromyography of m. semitendinosus, m. gluteus maximus, m. vastus lateralis, m. rectus femoris and m. gastrocnemius medialis of the group of elite speed skaters (solid lines) and the group of trained speed skaters (dotted lines). The period between 0.8 and 1.0 sec. indicate the push-off.

REFERENCES

1. Boer, R.W. de, Schermerhorn, P., Gademan, J., Groot, G. de, and Ingen Schenau, G.J. van. (1986). Characteristic stroke mechanics of elite Trained Male speed skaters. *International Journal of Sport Biomechanics* 2:175-185.
2. Ingen Schenau, G.J. van, Bobbert, M.F., and Rozendal, R.H. (1987). The unique action of bi-articular muscles in complex movements. *Journal of Anatomy* 155:1-15.
3. Bobbert, M.F., and Ingen Schenau, G.J. van. (1988). Coordination in vertical jumping. *Journal of Biomechanics* 21:249-262.

EMG AND MOVEMENT PATTERN IN MANUAL WHEELCHAIR PROPULSION.

H.E.J.VEEGER, L.H.V.van der WOUDE, R.H.ROZENDAL, H.J.BIELEMAN & J.A.PAUL

Department of Functional Anatomy, Faculty of Human Movement Sciences, Vrije Universiteit Amsterdam, The Netherlands.

INTRODUCTION

Tilted rear wheels or camber are a widespread feature in racing wheelchairs. Next to a higher stability as the result of an increased wheel base, their advantage supposedly lies in an easier reach of the handrims and less hampered arm movements during push and recovery movement (1). A study on wheelchair characteristics during the 1980 Paralympics showed a trend of decreasing camber with decreased succes of the athlete (2). The objective of this study was to study the effect of camber on EMG, movement pattern and physiological parameters.

METHODS

Eight non-wheelchair users participated in this study. All subjects gave written 'informed consent'.

The experiment consisted out of four twelve-minute wheelchair exercise tests in which camber varied from 0 to 3, 6 and 9 degrees. Within each test the belt speed increased every three minutes (.56, .83, 1.11, 1.39 m.s⁻¹). The corresponding external power outputs were set at .17, .26, .35 and .44 Watts/kg_{total weight} respectively. Prior to testing subjects performed a five minute warm up (speed 1.11 m.s⁻¹) followed by a five minute rest.

For all subjects EMG (DISA 15C01, filter 10-500 Hz) of long head of biceps brachii (BB), lateral head of triceps brachii (TB), descending part of trapezius (TR), anterior and medial parts of deltoid (DA and DM), costal part of pectoralis major (PM) and forearm flexors and extensors were registered by surface electrodes and analysed qualitatively. During the third minute of every run three consecutive strokes were filmed (DBM-55, Teledyne camera systems, 60 f/s) perpendicular to the sagittal plane of the subject. To enable motion analysis in the frontal plane a mirror was used. From film the following timing parameters were derived: time over which the rim is pushed (pushtime PT); time over which the arms return to the starting position (recovery time RT); cycle time CT being the sum of PT and RT; the radius over which the rim is pushed (push angle PA) being the difference between the start and end angles of the push (SA and EA, defined with respect to the horizontal). The abduction or outward travel of the upper arm (OT) was determined as projected in the frontal plane. For one subject film data of the

four camber conditions and the highest velocity also including sagittal information were combined with EMG data.

During each test physiological analysis took place (Oxycon Ox-4; Mijnhardt). Oxygen uptake ($\dot{V}O_2$, STPD) and respiratory exchange ratio (RER) were automatically determined. Heart rate (HR) was monitored with a Lectromed cardiograph according to Woude et al³. External power output was determined in a drag test (3). Gross mechanical efficiency (ME) was derived from oxygen consumption and external power output. The physiological data of one subject were discarded due to the fact that he used anti-diuretics.

Statistical analysis comprised two way ANOVA with repeated measurements (N=8) or appropriate alternatives.

TABLE 1. ANOVA RESULTS

PARAMETER	(units)	CAMBER	BELT SPEED	INTERACTION
Rolling resistance (N)		3.21*	(-)	(-)
Max. OT recovery (rad.)		1.34	4.03*	1.34
Max. OT push (rad.)		3.80*	3.68*	1.48
Min. OT push (rad.)		.64	.82	1.36
Cycle time CT (s)		.12**	42.40**	.40
Push time PT (s)		5.73	137.40**	1.50
Recovery time RT (s)		.93	5.44	.95
Start angle SA (rad.)		5.42**	1.17**	1.29**
End angle EA (rad.)		2.24**	12.71**	3.31
Push angle PA (rad.)		10.50	5.62	2.19*
Heart rate HR (b/min)		1.48	87.99**	2.91**
Oxygen consumption $\dot{V}O_2$ (l/min)		.13	364.50**	2.00
Mechanical efficiency ME (%)		.63	38.68**	1.47

** < .01

* < .05

RESULTS

The change in camber did result in a minor but significant difference in rolling resistance between 0 and 9 degrees camber (8.74 N vs. 7.55 N; Table 1). To exclude possible effects on the results, the variations in rolling resistance were compensated for in every condition by correction of the imposed power output.

Figure 1 shows a typical example of the EMG of the shoulder muscles involved, combined with segment angles at a belt speed of 1.39 m.s⁻¹ and 0 and 9 degrees camber. As can be seen, during the first part of the push BB is actively engaged in elbow flexion; thereafter TB is involved. DM's main activity is found during the second half of the recovery and not, apart from a brief burst at the end of the push, during the push phase. There is no substantial difference in activity between 0 and 9 degrees camber. Both PM and DA have their major activity during the push phase; DA usually somewhat sooner

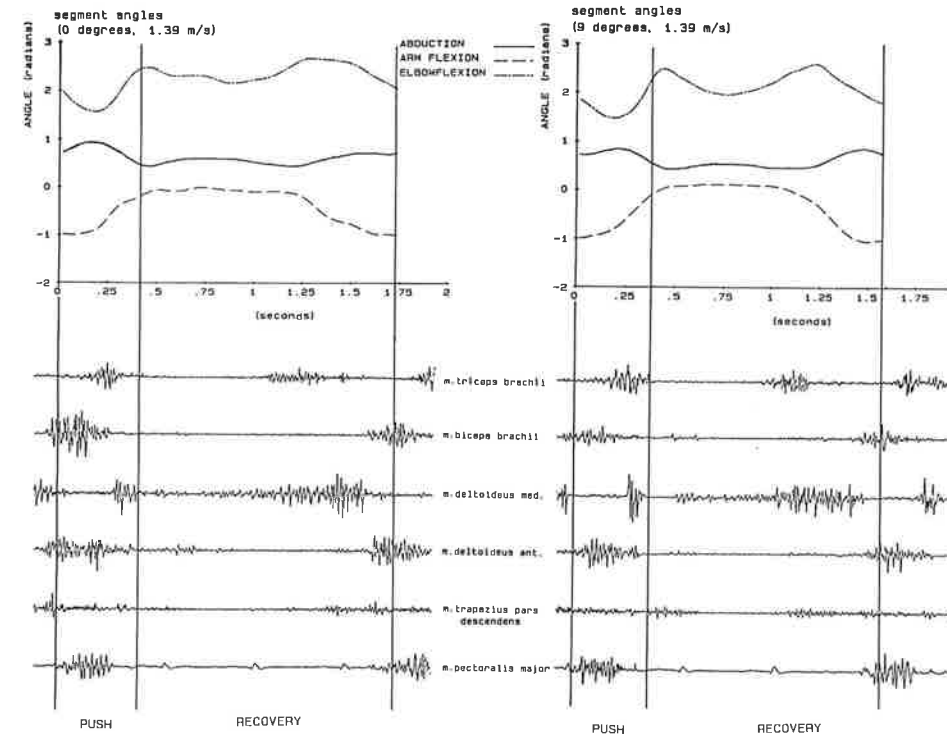


Fig. 1. Typical example of EMG recordings and segment angles (1.39 ms⁻¹, 0 and 9 degrees camber).

than PM. In all subjects PM showed no activity during recovery. TR and DA (during recovery) were inter-individually less consistent. In some subjects TR had a silent period during the push, in others during recovery.

During the push phase no differences in the minimal OT were found. Maximal OT decreased with increasing camber (Table 1). Maximal OT during recovery was not dependent on camber. PA was largest for the 6 degrees camber and smallest at 3 degrees. The latter is mainly caused by a smaller SA; the rims are grabbed further backward; and probably also by a larger EA; the hands follow the rims longer. The differences in EA did not reach the significance level, nor did CT or RT. PT however was significantly longer at 6 degrees. The physiological parameters HR, $\dot{V}O_2$ and ME were not dependent on camber.

DISCUSSION

EMG results showed a generally consistent intra- and interindividual pattern. The results were consistent with those of Cerquiglini et al⁴ on an ergometer and Tanaka⁵, but contrary to Harburn and Spaulding⁶. Of the muscles discussed TR seems to have a mainly stabilising role, while PM, DA, BB and TB

are the prime movers. The function of DM probably lies in controlling the arm OT during recovery (Figure 1).

The kinematic results do not confirm the expectation that increasing camber facilitates arm movements: SA and PA did not (curvi-)linearly change with camber but showed a strong difference between 3 and 6 degrees; minimal OT during the push and maximal OT during recovery did not change significantly. This was not expected, especially since the top-to-top distance of the wheels decreased from 555 to 475mm with increasing camber.

EMG results showed that during the push phase, despite the occurring outward travel of the arm DM is not active. Apparently OT is a side-effect of the activity of DA and PM and the forced trajectory of the hands on the rims. The smaller maximal OT during the push at 9 degrees camber seems thus not to be related to a difference in muscle activity but to a change in trajectory of the hands with camber. The varying top-to-top distances might thus have been the cause of significant differences. DM activity for 0 versus 9 degrees camber underlines the suggestion that the differences in top-to-top distance were not yet large enough for a forced OT.

The results described are supported by the fact that no physiological effects of camber were found (Table 1).

In this project no kinematic or physiological advantages or a slight advantage in rolling resistance were found. Since wheelchairs with cambered wheels have a better static stability, cambered rear wheels are probably preferable.

REFERENCES

1. Clarke R (1982) Technique and training in athletics wheelchair sports. Woodhead-Faulkner Ltd, Cambridge.
2. Higgs C (1983) Res Quarterly for Exercise and Sport 54 (3):229-233
3. Woude LHV van der, Ingen Schenau GJ van, Rozendal RH, Hollander AP (1986) Ergonomics 29: 1561-1573.
4. Cerquiglini S, Figura F, Marchetti M, Ricci B (1981) In: Morechi A, Fidelin K (eds), Biomechanics VII-A, Univ Park Press Baltimore, 410-419.
5. Tanaka O, Iijima H, Oi S, Ito M, Ando N, Ito T (1982) Sogo Rehabilitation 10: 251-257.
6. Harburn L, Spaulding S (1986) Am J Occup Ther 40: 629-636.

DYNAMIC CHANGES OF THE MEDIAL ARCH OF THE FOOT IN CHILDHOOD DURING WALKING

HIROAKI FUJII, NOBUOU MATSUSAKA*, MASAAKI FUJITA*, TOSIHARU NORIMATSU*, and RYOHEI SUZUKI*.

National Sanatorium Nagasaki Hospital, Department of Orthopaedic Surgery, 6-41 Sakuragi-cho, Nagasaki, 850, JAPAN.

*Nagasaki University School of medicine, Department of Orthopaedic Surgery, 7-1 Sakamoto-machi, Nagasaki, 852, JAPAN.

INTRODUCTION

The human foot is structurally well adapted for prolonged bipedal walking and standing. In particular, the structure and function of the planter vault of the foot are very important. For analyzing the structure and function of the arch of the foot under static conditions many studies were performed, but there was no experiment which was done for analyzing the changes of the arch of the foot during walking in childhood. To assess the characteristics of the gait in childhood, much research was done from different viewpoints and many different results have been reported such as Sutherland⁴, Beck¹, and Noguchi³. The purpose of this study is to analyse the medial arch of the foot in childhood and to estimate the period of gait maturation from the viewpoint of changes of the medial arch of the foot.

MATERIAL AND METHODS

The gaits of forty-six normal children between the ages of seven and twelve years were studied (table.1).

TABLE.1

DISTRIBUTION OF SUBJECTS

Age	7	8	9	10	11	12
No.	5	7	5	8	11	10

The changes of the medial arch are measured by special equipment which we call an "electro arch gauge" (EAG). It is made from a strong straight wire, an aluminium tube and a thin elastic steel plate with a strain gauge attached to the middle part. Elastic steel plate makes a bridge between the wire and tube (Fig.1). The anterior part of the EAG was attached to the medial side of the

first metatarsal head and the posterior part to the calcaneus area 1cm behind the medial malleolus and 3cm above the sole. The change of the medial arch and the ground reaction force were recorded simultaneously. The mean patterns of individuals and each age group were analysed with a microcomputer. The data of the children and the adults was altered so that measurements of each group were 25cm in foot length and 45kg in weight.

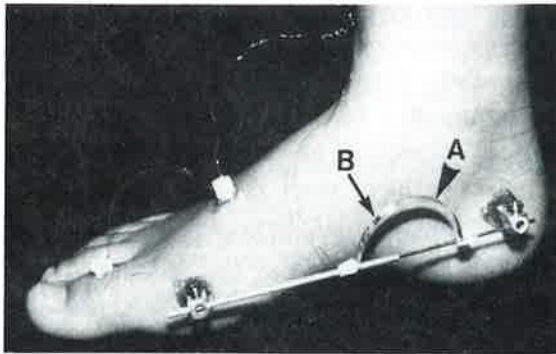


Fig.1. Electro Arch Gauge (E.A.G.)
A: A thin elastic steel plate 5mm in width and 0.5mm in thickness.
B: A strain gauge attached to the middle part of a steel plate.

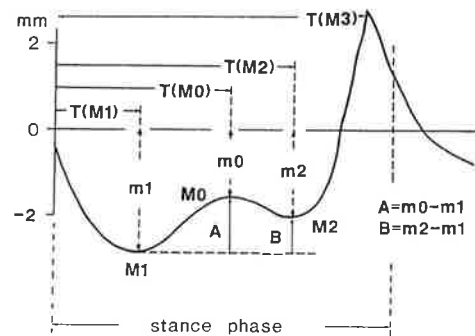


Fig.2 Points of Measurement in the Medial Arch of the Foot.

RESULTS

According to Kayano², in adult customary gait, the medial arch stretched rapidly just after heel-strike and became longest at the early period of the foot-flat phase(M1), then shortened gradually until about heel-off(M0), after that it stretched slightly(M2) and shortened rapidly just before toe-off(M3). Points of measurement in the medial arch of the foot are shown in Fig.2 .

Duration from heel-strike to M1, M0, M2 and M3 are statistically unchanged with age.

The first peak of lengthening(m1) shortened with age up to eight years of age and became almost the same as the adults at nine years of age ($P < 0.01$) (Fig.3).

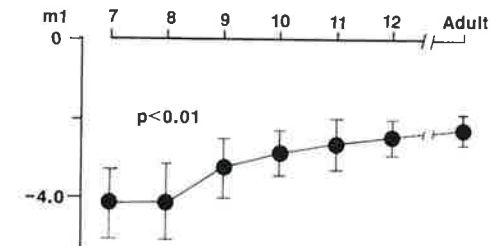


Fig.3 Relationship between the Medial Arch of the Foot and Age. Amplitude of the first peak of lengthening(M1): m1. The length of the medial arch(m1) shortened with age and became almost the same as the adults at nine years of age.

In the late stages of the stance phase, the difference ($m0 - m1$ (A)) between amplitude of the first peak of shortening(M0) and of the first peak of lengthening(M1) decreased with age up to eleven years of age and became almost the same as the adults at twelve years of age ($P < 0.01$) (Fig.4). And the difference ($m2 - m1$ (B)) between amplitude of the second peak of lengthening(M2) and of the first peak of lengthening(M1) also decreased with age up to eleven years of age and became almost the same as the adults at twelve years of age ($P < 0.01$) (Fig.5).

DISCUSSION

Dynamic changes of medial arch occur by a complex relationship of body weight, bone structure, ligaments and muscular force². The first peak of lengthening(M1) was caused mainly by the vertical

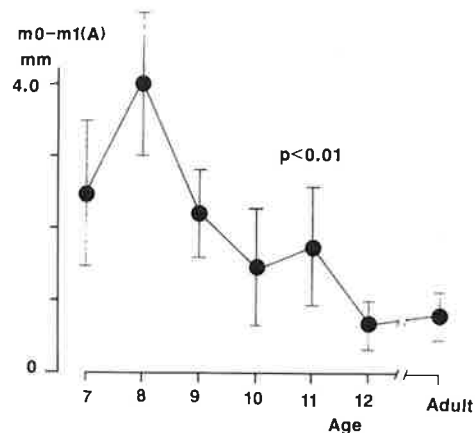


Fig.4. $m_0-m_1(A)$ decreased with age and became almost the same as the adults at twelve years of age.

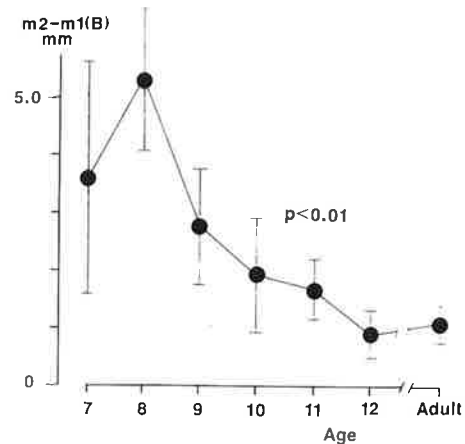


Fig.5. $m_2-m_1(B)$ decreased with age and became almost the same as the adults at twelve years of age.

force on the foot (body weight)², and became almost the same as the adults at nine years of age. It is suggested that the medial arch of the foot during walking is well established in foot flexibility at the age of nine years. The first shortening (m_0) occurred initially due to a decrease in the vertical force and later due to activation of the arch supporting muscles, and the second lengthening (m_2) was caused by an increase in the vertical force and the calf muscle action which was resisted by the arch supporting muscles². m_0 and m_2 became almost the same as the adults at twelve years of age. It is suggested that the medial arch of the foot during walking is transformed into an adult pattern at the age of twelve years in relationship to foot flexibility and muscle force.

REFERENCES

1. Beck, R.J.: Changes in the gait patterns of growing children. *J. Bone Joint Surg.*, 63-A: 1452-1457, 1981.
2. Kayano, J.: Dynamic function of medial foot arch. *J. Jpn. Orthop. Ass.*, 60: 1147-1156, 1986.
3. Noguchi, M., Hamamura, A., Matsusaka, N., Fujita, M., Norimatsu, T., Ikeda, S. & Suzuki, R. Development of gait in childhood. In: *Biomechanics IX-A*, 462-467, Human Kinetics Publishers, Champaign, 1985.
4. Sutherland, D.H.: The development of mature gait. *J. Bone Joint Surg.*, 62-A: 336-353, 1980.

THE DYNAMIC CHANGES OF THE MEDIAL ARCH OF THE FOOT DURING SLOPE WALKING

SUMITAKA TAKESAKO

Department of Orthopaedic Surgery, Nagasaki University School of Medicine, Nagasaki

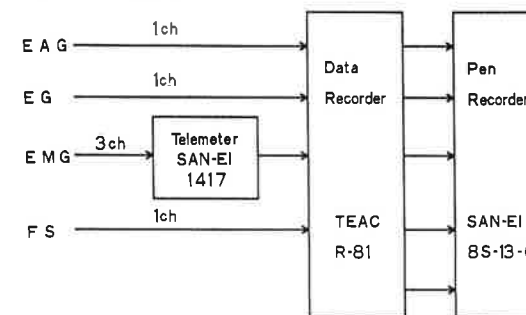
Introduction

The human foot is structurally well adapted for prolonged bipedal walking and standing. In particular, the structure and function of the plantar vault of the foot are very important as a cushion, and its disorder is due to various foot pains and gait disturbance.

Despite the fact that many researchers have investigated the role of bone structure, ligaments and muscles, the mechanism of maintenance of the arches in the foot is still controversial. We still have little knowledge of the dynamic function of the arches, because many studies of their changes have been performed under static conditions.

The purpose of this study is to analyse with our multi-recording system⁸⁾ the dynamic changes of the medial arch of the foot during slope walking.

MATERIAL AND METHODS



The examinees were 15 normal adults whose age range was 23 to 38 years.

A flow chart of the data used is shown in Fig.1. Each subject was asked to walk more than twenty times in his customary gait on the five types of the slope (0°, 5° up and down, 10° up and down) (Fig.2). The dynamic changes of the medial arch of the foot, angular changes of the first metatarsophalangeal (MTP) joint, electromygrams (EMG) and foot switch

Fig.1 Flow Chart of data

signals (FS) were recorded simultaneously. The change in length of the medial arch was measured with a special instrument which we called an "electro arch gauge" (EAG).⁶⁾ It was made from two strong straight wires 12 cm long and 0.24 cm in diameter and a thin elastic steel plate 7 cm long and 0.6 cm wide with a strain gauge attached to the middle part. The steel plate was bridged by the wires. The gauge was made to move in only one direction (Fig 3).

The anterior part of EAG was attached to the medial side of the first



Fig.2 The walkway of the slope

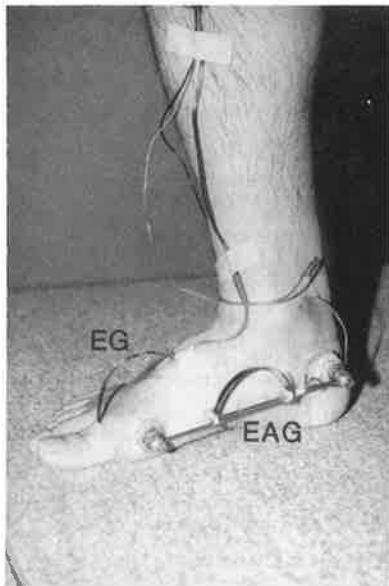


Fig.3 The EAG and EG attached to the foot

metatarsal head and the posterior part to the calcaneus area 1 cm behind the medial malleolus and 3 cm above the sole (Fig.3). The change in length of the EAG was transmitted to both ends of the arc-shaped steel plate and was measured by the strain gauge.

Angular changes of the MTP joint during walking were measured with a specially designed electrogoniometer

(EG),²⁾ which was made from a thin elastic steel plate 10 cm long and 0.6 cm wide with a strain gauge attached to the middle part. This formed a bridge across the MTP joint by binding the two ends into the dorsum of the foot and the big toe (Fig.3). Foot switches made of lead were attached to four points of the sole: the heel, first and fifth metatarsal heads and distal phalanx of the big toe.

Action potentials of the tibialis anterior muscle (TA), peroneus longus muscle (PL), and triceps surae muscle (TS) were picked up by surface electrodes and the electromyographic recordings were transmitted by a four-channel telemeter (NEC, SAN-EI, Japan) attached to the subject. The data was analyzed by a micro-computer (PC-9801-F, NEC, Japan).

Before starting gait examinations each barefooted subject was seated on a chair with his ankle in a neutral position and his knees flexed 90 degrees. The value of the amplitude demonstrated by the EAG in this posture was set at 0 and the value in the erect posture was recorded.

Result

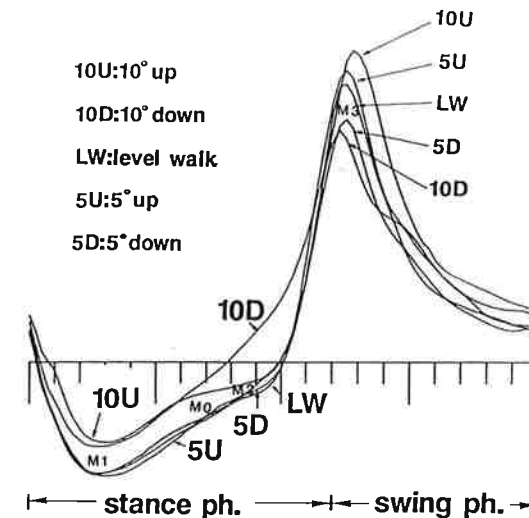


Fig.4 Mean patterns of the Medial arch during each slope walking

Mean patterns of the medial arch during each slope walking were shown in Fig.4. In level walking, the medial arch was stretched (M1) rapidly just after heelstrike and shortened (M0) gradually until heel-off. It was then stretched (M2) again and then shortened (M3) rapidly just before toe-off. And the other mean patterns (four types of slope) had a similar curve. Comparing these curves, the medial arches of the 10° up and down slope type became high and those of level walking and 5° up and down slope type became similarly low.

Discussion

The arches of the human foot are very stable and there have been many discussions of what supports them. The various hypotheses on this subject are classified into three groups: the first is that the arches are mainly supported by muscular force, the second attaches importance to the ligaments and bone structures, and the third is a combined theory of the muscular force, ligaments and bone structure. Mortor⁷⁾ concluded that bones and ligaments are normally sufficient for the maintenance of the medial arch, although muscles can play an active role if there is a structural defect. Jones⁵⁾ reported that much the greater part of the stress on the foot is borne by the plantar ligaments, but the short plantar muscles also contribute to this support. Basmajian¹⁾ reported that the first line of defense of the arches is ligamentous. The muscles form a dynamic reserve called upon reflexively by excessive loads which included the take-off phase in walking. In summary, changes in the medial arch in the stance phase are divided into four phases (M1, M0, M2, M3). The author considered the followings: M1 was caused mainly by the body weight and M2 was stretched by the body weight and the calf muscle action which is resisted by the arch and M3 was mainly caused by the windlass action³⁾⁴⁾ of the plantar aponeurosis.

ACKNOWLEDGEMENTS

I wish to express my gratitude to Prof. Ryohei Suzuki for his guidance in this research and to Dr.Gouji Chiba, Dr.Toshiharu Norimatsu, Dr.Masaki Fujita and Dr. Nobuo Matsusaka for their assistance.

REFERENCES

- 1) Basmajian, J.V.: The role of muscles in arch support of the foot. *J. Bone Joint Surg*, 45-A:1184-1190, 1963.
- 2) Fujita, M.: Motion and role of the MTP-joints in walking. *Biomechanics*, VIII-A: 467-470, 1982.
- 3) Hick, J.H.: The Mechanics of the Foot II. The Plantar Aponeurosis and Arch. *J. Anat.*, 88:25-30, 1954.
- 4) Hick, J.H.: The foot as a support. *Acta Anat.*, 25:34-45, 1955.
- 5) Jones, R.L.: The human foot. An experimental study of its mechanics, and the role of its muscles and ligaments in the support of the arch. *Am. J. Anat.*, 68:1-39, 1941.
- 6) Kayano, J.: Dynamic function of medial foot arch. *J. Jpn. Orthop. Aso.*, 60:1147-1156, 1986.
- 7) Morton, D.J.: *The Human Foot*. Columbia University Press, New York, 199, 1935.
- 8) Suzuki, R.: Simultaneous multirecording system for gait analysis. *Biomechanics*, VII-B:176-183, 1981.

KINESIOLOGY**Analysis of standing up, squatting and walking**

KINESIOLOGICAL ANALYSIS OF STANDING-UP MOVEMENT

Yukio MANO, Toshimasa SAKAKIBARA, Tetsuya TAKAYANAGI

Department of Neurology, Nara Medical University, 840, Shijo-cho, Kashihara, Nara, 634, JAPAN.

INTRODUCTION

The purpose of clinical kinesiology can be classified into the following categories ; 1) analysis of movement of joint, 2) analysis of sway of movement, 3) analysis of muscle discharge in movement, 4) analysis of how to produce the movement, and 5) analysis of function of movement.

The movement is analyzed by a qualitative method or a quantitative method. The qualitative method involves a fairly subjective measurement and its reliability is a problem. Quantitative measurement has limitations in methods and instructions. The method of measurements from outputs of movements include electromyogram, goniometer, stabilometer, force measurements etc. Recently the process-oriented analysis of the results becomes more important than the product-oriented analysis. In our study of voluntary movement in Parkinson's disease, ataxic patients and normal controls, surface EMG recordings of muscles of lower legs, sway of body gravity and displacement in position of parts of the body after given a light signal are analyzed during the rapid standing-up movement in a more process-oriented manner. A new type of position sensor system is tried to detect the movement.

METHODS

The subject is sitting on the chair, which is outside the balance analyzer with both feet on the balance analyzer. The two feet are 20 cm apart. The subject starts in a standing-up movement immediately after given the light signal. After standing for 15 seconds, he sits down again on the chair. He repeats this movement 6 times every 10 seconds resting on the chair between movements. The sways of body balance measured by a balance analyzer is recorded along with surface EMG recording from muscles of trunks and lower extremities and the recording of joint position. The EMG reaction time, the movement reaction time and the reaching time are measured. Since the earliest reactive muscle in EMG recordings is the discharge from tibialis anterior muscle, the EMG reaction time is measured from the signal to the discharge of tibialis anterior muscle.

As the earliest change of parameters in a balance analyzer is the change of anterior-posterior(A-P) sway in balance analyzer, the movement reaction time is measured from the signal to the start of change in A-P sway. The reaching time is measured from the start of change in A-P sway to the time in reaching the erect standing. The movement reaction time plus the reaching time is also measured for analysis. The changes by repetition of movement are evaluated. Before this study, we tested the influence of foot position on standing balance. The area was smallest and total length of sway of body gravity shortest in standing with the feet 20 cm apart. We continued this study with the feet 20 cm apart on this base.

In some of the subjects, comparisons were made for different chair heights, different speed of standing-up movement voluntarily, standing-up movement by one foot, standing-up movement with and without a warning sound before the light signal, and the standing-up movement with and without other movement concomitantly combined.

The position sensor system, which we try to use in this study, has a highly sensitive detector(PSD). The PSD is a planar type PIN silicon photodiode with very uniform layers formed on both the top and bottom surfaces. At opposite edges on both surfaces, electrodes are provided to sense X and Y axis signals.

When the light spot from a light-emitting diodes(LED), which is attached to the subject, is focused via lens system on the active surface of the PSD, a photo current is generated at the spot position in the PSD. Portions of this current are collected at each of the electrodes through both resistive layers. The proportion of current at each electrode is determined by the resistance between the spot position and each electrode, i.e., the distance between them.

The clinical signs and symptoms, and disability of standing-up movement among the ADL items are evaluated in Parkinson's disease and spinocerebellar degeneration(SCD).

The data from the balance analyzer are connected to the computer. Total length, total area, X axis and Y axis histogram, velocity and acceleration in eight director analysis, time course of length, area, X data, Y data, velocity and acceleration, and power spectrum of X and Y axis are analyzed by using the program for balance analysis (S-EGG-01 Patella KK and PC-9801VM2 NEC).

RESULTS

Standing-up movement was easy for normal subjects, but it was difficult

to complete in 44.2 % of 52 cases with Parkinson's disease and 27.3 % of 22 cases with SCD, moderately difficult in 36.5 % and 59.1 % respectively and slightly difficult in 5.8 % and 9.1 % respectively. Only 13.5 % of the patients with Parkinson's disease and 4.5 % of those with SCD showed normal standing-up movement.

Among the 36 items of ADL the "sitting from supine" movement was most correlated with the standing-up movement. Signs and symptoms of disease were not correlated with the other items of ADL.

In normal subjects, the muscle discharge of the tibialis anterior muscle is observed first after the signal, followed by the muscle discharge of the triceps surae muscle in lower extremities.

The movement in anterior-posterior sway starts at the same time or slightly after the discharge of the tibialis anterior muscle in normal subjects.

At the end of the discharge of tibialis anterior muscle, the phasic discharge of the triceps surae muscle starts, which is immediately after the erect standing position is attained. At the erect standing position the point passing the base line from the posterior to anterior is intercepted. The reciprocity in discharges between the tibialis anterior muscle and triceps surae muscle is preserved in normal subjects.

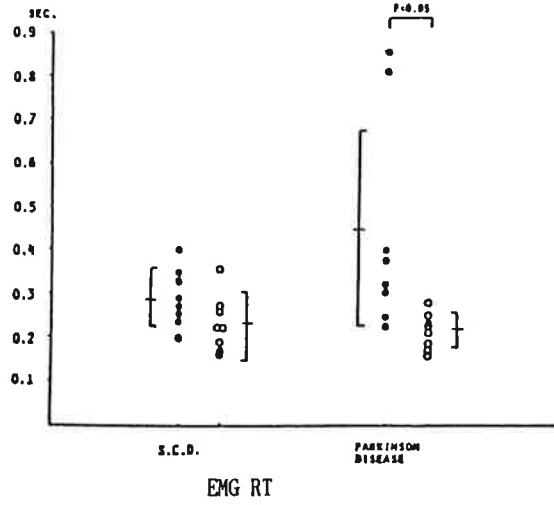
In half of the patients with Parkinson's disease, there is no significant delay in EMG reaction time or movement reaction time. However in some patients with Parkinson's disease there is a marked delay in EMG reaction time and movement reaction time. The reciprocity in muscle discharges is not present. The reaching time is significantly delayed, which is one of the characteristics of Parkinson's disease. The persistent discharge of tibialis anterior muscle is observed in the standing position in some cases of Parkinson's disease(figure 1, 2, 3).

In patients with SCD, there is no delay in EMG reaction time or movement reaction time. There are two peaks in muscle discharge of tibialis anterior muscle in initial phase and there is a phasic muscle discharge of triceps surae muscle between these peaks, this point is close to the point obtained at the erect standing position.

In EMG reaction time and movement reaction time, two out of 8 cases of Parkinson's disease show marked prolonged. By contrast, the cases of SCD show a normal EMG reaction time and movement reaction time.

All 8 cases of Parkinson's disease show prolonged reaching time, and 3 of

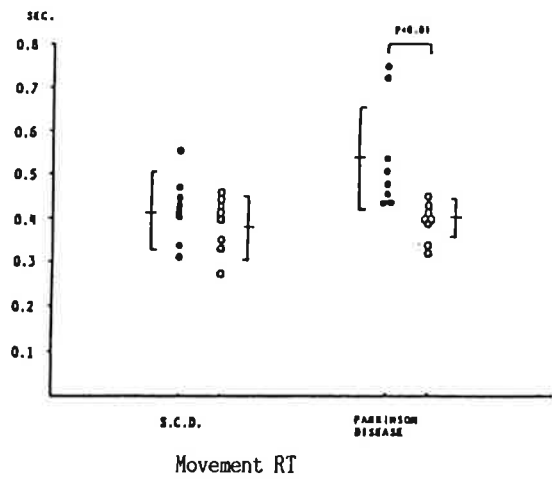
Figure 1



time from the signal of light to the start of muscle discharges from tibialis anterior muscle

closed circles denote cases with diseases
open circles denote normal controls

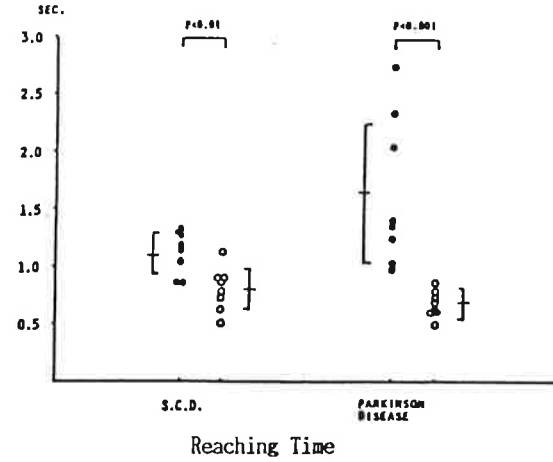
Figure 2



time from the signal of light to the start of standing-up movement

closed circles denote cases with diseases
open circles denote normal controls

Figure 3



time from the start of standing-up movement to the point of erect position

closed circle denote cases with diseases
open circles denote normal controls

Table 1

The time delay (sec) in standing-up movement in Parkinson's disease and clinical symptoms

	EMG RT (signal-TA)	movement RT (signal-movement)	reaching time (movement-erect)	total reaching time (signal-erect)	rigidity	akinesia	tremor	pulsion	freezing
47 yo male	<u>0.81</u>	0.75	0.99	1.74	+ 1	+ 1	-	±	-
51 yo male	0.32	0.44	1.39	1.84	±	±	-	+ 2	<u>+ 3</u>
54 yo female	0.40	0.44	<u>2.05</u>	2.49	+ 2	<u>+ 2</u>	+ 1	+ 2	+ 1
59 yo female	0.23	0.51	1.06	1.56	+ 1	±	-	+ 1	-
63 yo female	0.33	0.45	<u>2.35</u>	2.80	+ 3	<u>+ 2</u>	+ 1	+ 2	+ 1
64 yo female	0.38	0.48	1.42	1.89	+ 1	-	+ 1	-	-
66 yo female	0.25	0.53	<u>2.76</u>	3.48	+ 1	<u>+ 3</u>	-	+ 1	-
68 yo male	<u>0.86</u>	0.61	1.27	1.79	+ 2	+ 1	+ 1	+ 1	±

Figure 4

EMG reaction time (msec) in standing-up movement,
depending on the height of chair

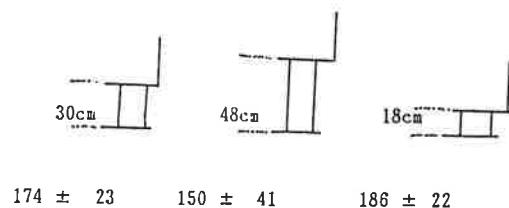
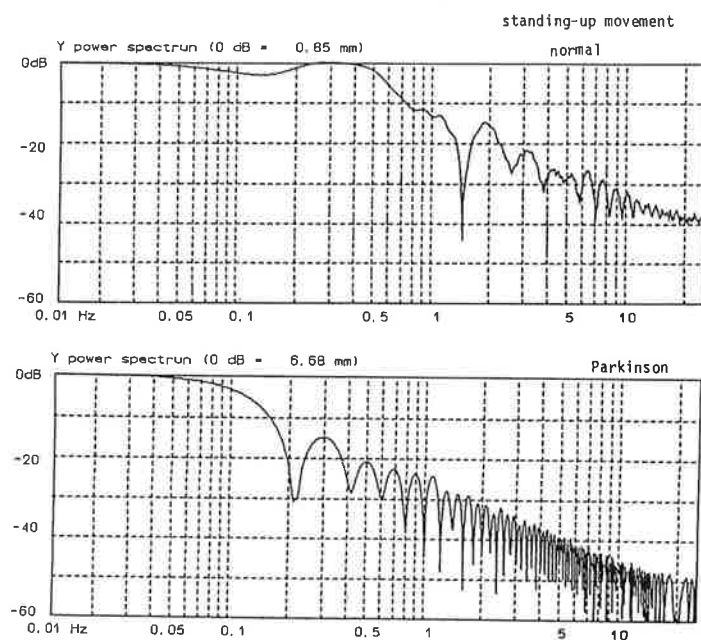


Figure 5



them show markedly prolonged times; they manifested the marked akinesia, and were different from the 2 cases of prolonged EMG and movement reaction time (table 1).

The total time of movement reaction time and reaching time were markedly increased in all cases of Parkinson's disease and slightly increased in the cases of SCD. Total movement time until a relatively stable standing state was reached in SCD was increased and a marked sway of body gravity continued after standing up.

From the clinical point of view, the patient with a freezing gait does not show the prolonged EMG reaction time or the prolonged movement time and freezing gait is supposed to be affected by other problems. Akinesia is well correlated with prolonged movement time. The group in which the reaction time was increased might have problems in premovement central neural processing such as motor planning system, alert system or recognition system.

The prolonged reaction time decreased after 2-3 repetitions of the standing-up movements, and the integrated EMG become relative constant after a few trials of movements in normal subjects and patients. Most of the patients had more difficulty in standing-up movement from a lower chair. When the chair height was elevated to 48 cm, the EMG reaction time decreased. The facilitatory position seemed to be present even during the standing-up movement (figure 4). It was hard to manipulate the speed of standing-up movement in normal subjects and patients. The EMG reaction time was not much different between ballistic movement and slow standing-up movement by their will. It was also very hard for the patient to change the pattern of movement in the middle of a movement. The standing-up movement by one foot was very hard to perform for most of the patients. The reaction time for the standing-up movement with one foot, was not different from that for the movement on both feet.

The new type of position sensor helps us to detect the change in the position in joint or other part of body, compared with the electro-goniometer. Even the angle of the joint does not move, the position sensor catches the movement of the joint itself which might suggest that the total alignment of the body is changing. In Parkinson's disease the position of body does not change in length of X axis or Z axis, and the speed of change is slow. In SCD, the duration of change of position is prolonged with the zigzag sway.

The sway during standing-up movement by balance analyser was input to a computer for analysis. A-P sway was shorter in Parkinson's disease. The

velocity and the acceleration were low in Parkinson's disease compared with controls. The power spectrum of A-P sway showed a big peak at 1 to 2 Hz in standing-up movement in normal subjects, they show many peaks in Parkinson's disease, especially in around 0.2 Hz and higher frequencies in 3 to 10 Hz. These changes might reflect the slowness in movement and fine tremorous movement during the movement (figure 5).

DISCUSSION

Time delay in doing the voluntary movement involved several levels of changes. In Parkinson's disease, one of the main symptoms is akinesia, which is compatible with prolonged movement time. However the delay of reaction time is observed and its impairment is independent of the delay of movement time. In the case of frozen gait, the EMG reaction times is not prolonged. These changes seem to be independent of each other. Therefore, there are at least three types of delay in voluntary movements in Parkinson's disease.

In the standing-up movement, once initiated, control of these movement units is largely ballistic, i.e., feed-forward control. It does not need the visual feedback in initiation of movement until erect standing position. However, after the standing-up movement is completed, feed-back control is necessary to stabilize the postural equilibrium; the somatosensory, visual and vestibular inputs are used for the feed-back control.

The reaction time in initial trial is long and it becomes shorter after 3 or 4 repetitions. It is supposed to be a short-term motor learning, but it does not last as a memory for along time. The effect of learning disappears within several hours when the movement is stopped. The mechanism of this short-term learning is supposed to be due to another short circuit.

When one performs a new movement in response to a signal, the signal stimulates the sense organ first and its signal is perceived in the primary sensory cortex, and we recognize the meaning and plan the new movement and then our primary motor cortex starts to work and finally the motor units start to be discharged. However, when we repeat the movements, we do not need the exact recognition or the exact motor planning of the movement in will, and a more automatic movement would be repeated. Probably this is the mechanism of short-term motor learning (figure 6).

We may divide the slow performance into several categories. One is the delay in reaction time and another is the delay in movement time. In Parkinson's disease Lee defines akinesia as the difficulty in initiation of

the movement, i.e., delay in reaction time. By contrast, the bradykinesia is defined to be delay in movement time, although the terminology is not clear. The warning signal is observed to shorten the reaction time.

The warning signal gives the person the attention and the state of preparation for the following movement, which might stimulate the arousal system in brain and make him more alert for recognition and for planning the motor program.

As I mentioned previously, the slowness in standing-up movement is caused by the following problems: 1) problem in perception of the signal, 2) problem in recognition, 3) problem in initiation of movement (problem in making the motor program), 4) problem in executing the movement, and 5) problem in postural reaction.

Patients with Parkinson's disease seem to have a problem in both recognition system and efferent system, although originally they were considered to have only problems in efferent system. In SCD, the control of the postural response is impaired markedly, the afferent and recognition are fairly well.

The height of chair changes the reaction time, which suggests that the facilitatory position is also present in the standing-up movement. The facilitatory position is frequently used in the neurofacilitatory method in physical therapy. There is no description about it in the standing-up position. These findings are interesting for the future treatment to improve standing-up movement of patients with these diseases.

During one-foot standing, the equilibrium is more impaired than during the movement of standing-up on both feet. There action time was not different between these two situations. This means that the dysequilibrium induced by one-foot standing is the problem in postural reactions, not the problem in motor programming.

The analysis of the effect of other movements during standing-up movement showed that the elevation of arm does not interfere with the standing-up movement in normal subjects. This mean that the motor programming for arm elevation differs from that of standing-up movement. However in Parkinson's disease we observed slower execution during concomitant movements.

The polygraphic EMG recordings showed that the muscle discharges of tibialis anterior muscle appeared first in standing-up movement. Then if the subject continues to contract the tibialis anterior muscle before the standing-up movement, the reaction time in standing-up movement is delayed, possibly due to the use of the same pathway in planning and execution of

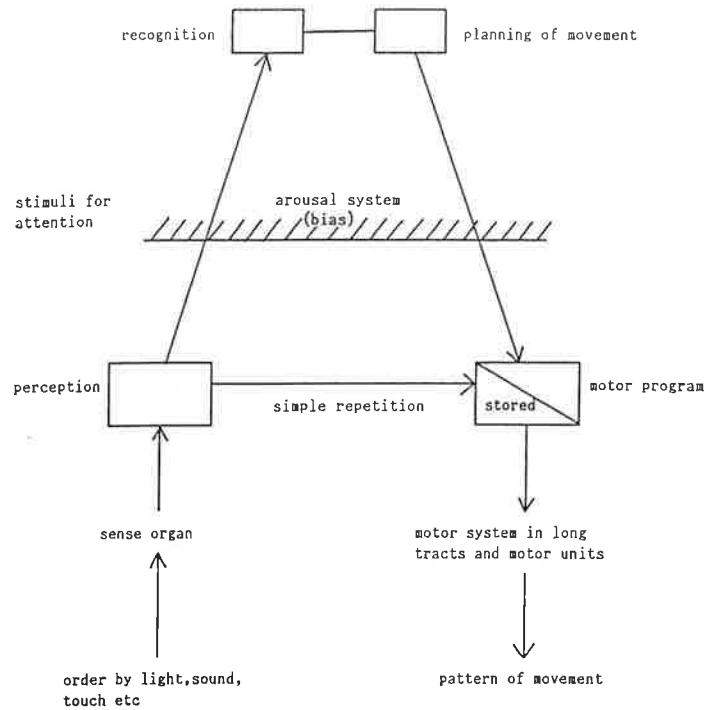


Figure 6 : Schematic illustration for repetitive movement

standing-up movement and the execution of continued muscle contraction, and they might interfere with each other.

In this study, the complex movement of standing-up and its mechanisms was analyzed, but I believe further analysis of these items is necessary to determine the mechanism controlling these movements more precisely in future.

REFERENCES

- 1) Mano Y, Sakakibara T, Takayanagi T (1986) In Annual Report of the Research Committee of Neurological Degenerative Disease. Ministry of Health and Welfare of Japan 221-225.
- 2) Rafal R, Inhoff A, Friedman JH, Bernstein E (1987) J Neurol Neurosurgery Psychiatry 50 : 1267-1273.
- 3) Sheridan MR, Flowers KA, Hurrell J (1987) Brain 110 : 1247-1271.
- 4) Bloxham CA, Dick DJ, Moore M (1987) J Neurol Neurosurgery Psychiatry 50 : 1178-1183.
- 5) Benecke R, Rothwell JC, Dick JPR, Day BL (1987) Brain 109 : 739-757.

DYNAMIC ANALYSIS OF SQUAT POSTURAL SWAYS

HIROMITSU IWAKURA, SHIGERU TANAKA and SATOSHI KASHIWABARA

Department of Rehabilitation Medicine, Teikyo University School of Medicine, 11-1 Kaga 2 Chome, Itabashiku, Tokyo 173 Japan

INTRODUCTION

Human squat posture is unstable. The sway in any direction, however, will always be corrected to hold a dynamic equilibrium of the posture. The squatting movement is utilized involuntarily in the activities of daily living in Japan as well as other Asian countries. We attempted in this paper to find out the characteristics of the movement of squatting down, the holding of the squat posture and the movement of standing up.

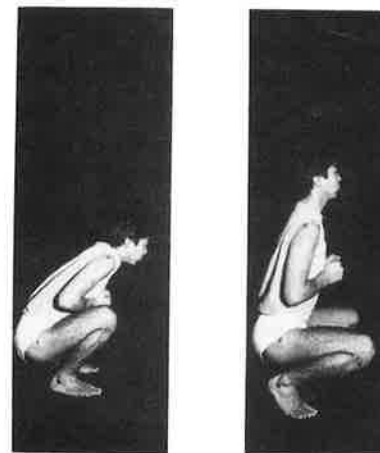
MATERIAL AND METHOD

Ten normal adults and ten hemiparetics due to cerebro vascular accident were selected. All hemiparetics were able to squat down and stand up by themselves. None of the hemiparetics suffered from severe deep sensory disturbances, ataxia, or agnosia.

One force-platform (size 60 cm / 180 cm, Kyowa Dengyo EFP type) and an electrogoniometer with telemeter were used. In the

normal subjects the right knee was measured, but in the hemiparetics only the affected side was measured. The bare feet were placed at interval of 20 cm on the force-platform.

Each subject was instructed to squat with his or her heels on first, and with heels off next. The center of force measurement was recorded on the UV recorder (Fig.1). We defined the force of the antero-posterior component as Y, the lateral component as X and the vertical component of the force as Z. The center of the force was indicated by Xc and Yc.



HEEL ON

HEEL OFF

Fig.1. Squat posture

RESULTS

Vertical force component (Z)

There were special findings in the periods of beginning of squatting and standing up among the normal subjects. A vertical dip followed by a rise curve pattern was demonstrated at the time of beginning of squatting down. On the other hand, an upward movement was characteristic in the vertical component when the subject began to stand up (Fig.2).

In the hemiparetic group, however, the periods of squatting-down as well as standing-up were elongated and fluctuations of vertical force were shown without any other distinctive features during the movement.

Antero-posterior force component (Y)

Increased amplitude of Y wave was shown when the normal subject started to squat. Larger fluctuations were demonstrated in squatting movement with the way of heels off than that of heels on. These findings were seen to correspond to the anterior sway of the center of force during squatting (Yc).

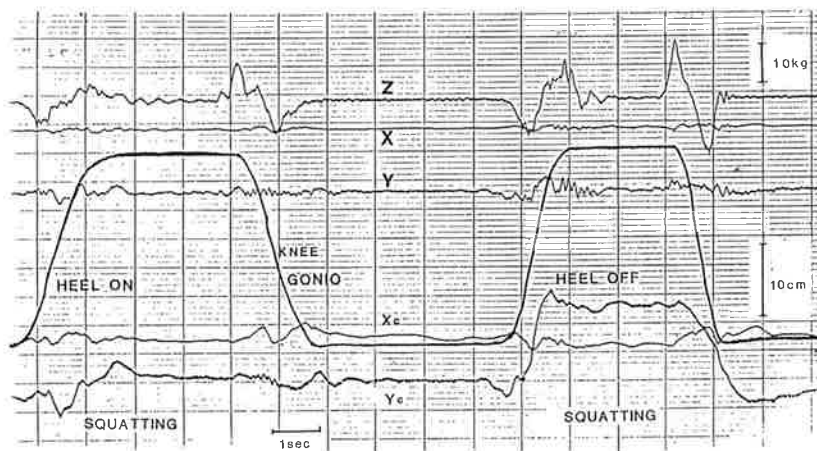


Fig.2. Component of floor reaction force and center of force in squatting movement obtained from a normal subject. On the left, squatting with heels on. On the right, squatting with heels off.
 X, Y, Z : three components of floor reaction force.
 Xc, Yc : center of force
 Knee gonio: knee joint angle from zero (the lowest level) to 145 degree (the highest level).

Lateral force component (X)

In the normal group, there were little fluctuations during the movement. On the other hand, in the hemiparetics right-and-left force component showed wide fluctuations through the squat performance and more with the way of heel-off posture (Fig.3).

Periods of knee movement. The duration time of the motion from extension to the maximum flexed position, and the reversed motion, demonstrated same tendency in the normal subject. The hemiparetics showed slower movements than the normal ($p < 0.01$). Many of them took the characteristic features in which, hemiparetic subject flexed their knee deliberately until they got stable squat postures, but in the phase of standing up their knee extension movements were shown quickly.

Antero-posterior sway (Yc). The center of force movement was traced into two directions, antero-posteriorly and laterally.

In the normal group there were backward movement followed by forward progressions of the center of force during squatting down in the way of heels off. The center of force located on the

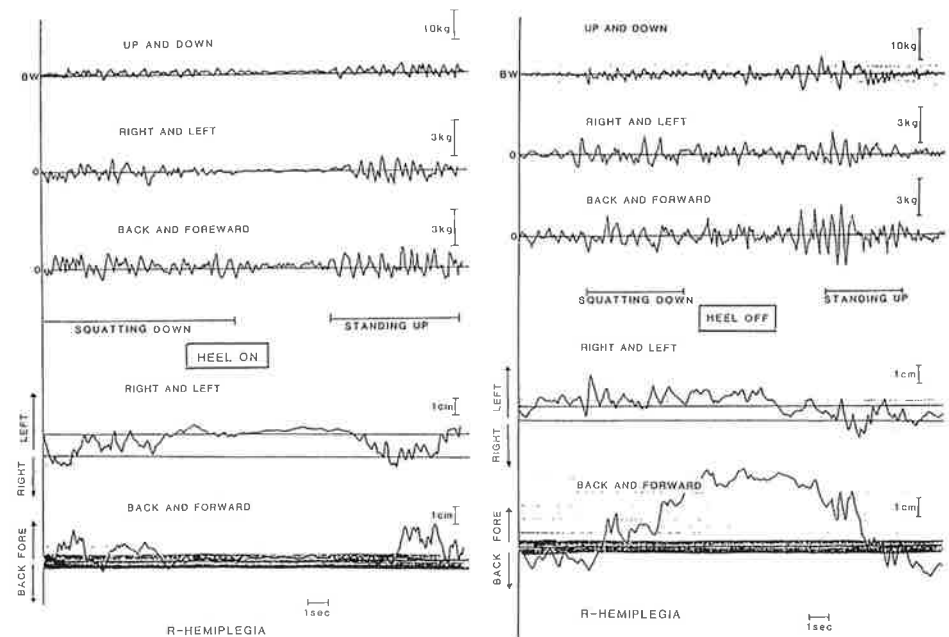


Fig.3. Traces of components of floor reaction force and center of force in squatting movement on a hemiparetic subject. phase

line of fore-foot metatarso-phalangeal joints supporting the of holding a quiet squat posture moved again backward during standing up. These above features were not seen distinctly when the movement was carried out in the way of heels on.

In the hemiparetics a gross movement of the center of force was similar as normal group, however, an obvious fact on antero-posterior instability was seen from the beginning of squatting down until the end of standing up in the way of heels off. Lateral sway (Xc). In the normal group the lateral distance of center of force movement was recognized largest in the periods of squatting down and standing up. Broader sway was demonstrated in the hemiparetics in squatting down ($p < 0.01$), but it was not so large in standing up ($p < 0.05$).

DISCUSSION

The squatting movement is composed of three phases, a motion of squatting, to hold a squat posture and a motion of standing up. In the movement of extremities for instance in the motion of squatting down, a small forward force could be recognized followed by the backward large force which was made by bending of trunk and knees in the case of antero-posterior force component of the force plate.

As regards the time needed to squat, and to be stabilized in a quietly squat posture, it was easy to suppose that the hemiplegics needed a longer time than normal group. In the standing up motion almost the same results were obtained.

To estimate the degree of sway of center of force, the method which we used was to measure the length of maximum fluctuation. The antero-posterior sway was larger than the medio-lateral one in general. The hemiparetics' sway was larger significantly than the normal adults and the sway cycles shown in many hemiparetic subjects were 10 Hz or more which might be connected with the speeds of movement.

REFERENCES

1. Iwakura H, Kashiwabara S, Tanaka S (1986) Jap J Rehab Med 23:138-140
2. Yoshida D, Iwakura H, Inoue F (1983) Scand J Rehab Med 15: 133-140
3. Nashner LM (1985) In: Igarashi M, Black FO (eds) Vestibular and visual control on posture and locomotor equilibrium. Karger, pp 1-8

HIP ABDUCTOR ACTION DURING LEVEL WALKING

KLEISSEN, R.F.M., SCHLECHT, M.C., ZILVOLD, G.

Het Roessingh Rehabilitation Centre
Roessinghsbleekweg 33
7522 AH Enschede, the Netherlands

INTRODUCTION

The clinician frequently examines patients with impaired gait patterns which are attributed to diminished hip abductor function and mechanisms for its compensation.

In order to elucidate this complex of interacting processes methods for assessment and quantification of abductor muscle function are useful. Abductor torque during walking can be calculated from movement and force plate data [1,2], requiring sophisticated instrumentation, which is generally not available in a clinical setting. With clinical application in mind, a method was developed for deriving abductor torque during level walking from surface EMG measurements.

THE MUSCLE MODEL

In order to relate EMG to external abductor torque a muscle equivalent can be defined [3]. There is evidence [4,5,6] that hip abduction during level walking results mainly from action of M. Gluteus medius, M. Gluteus minimus and Tensor Fascia Latae, the M. Gluteus medius being dominant. Under the assumption of isometric action of the abductor group during walking a linear, time invariant second order muscle model can be used to predict muscle force, and hence joint torque, with a fair degree of success [7]. Surface EMG of the M. Gluteus medius is used as input for the model. The model predicts torque, as produced by the abductor muscle equivalent.

Because all data acquisition and processing is performed by computer, a sampled data muscle model is derived from the continuous time prototype. The latter can be described as [8]

$$H(s) = T(s)/E(s) = K / (1 + st_1) (1 + st_2) \quad (1)$$

where $T(t)$ is the abductor torque signal, and $E(t)$ describes the "intensity" of the EMG, expressed in the full-wave rectified and low-pass filtered EMG (3rd order Butterworth filter, -3 dB @ 25 Hz +/- 5%).

Bilinear z-transformation of each first order section leads to the sampled data muscle model:

$$H(z) = T(z)/E(z) \quad \dots\dots(2)$$

$$= K (z+1) (z+1) / [z(1+t_1')+(1-t_1')][z(1+t_2')+(1-t_2')]$$

where $t_i' = 2 t_i/T$ ($i = 1, 2$)(3)

and $1/T$ the sampling frequency.

Each first order section can be realized as a recursive digital filter as

$$y(i) = c[[x(i) + x(i-1)] - y(i-1)(1-t')] / (1+t') \dots\dots(4)$$

where $y(i)$ and $x(i)$ are output- and input data series respectively. Cascading two of such sections realizes the muscle model (2), one of the sections having $c=1$.

PARAMETER ESTIMATION

A calibration recording of EMG data $E(i)$ and torque data $T(i)$ ($i = 1..N$) during dynamic isometric contractions is required to identify the parameters of the model. Evaluation of (2) for $z=1$ yields K . Therefore

$$K = \frac{\sum_{i=1}^N T(i)}{\sum_{i=1}^N E(i)} \quad \dots\dots(5)$$

Optimization of the mean square error between recorded torque and model output gives parameters t_1' and t_2' .

Figure 1 gives an example of the result of such an optimization.

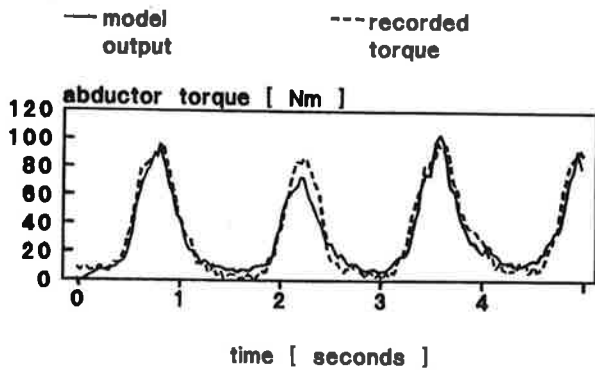


Figure 1: Model output and observed abductor torque after optimization.

Recorded torque and model output after optimization are compared. The abductor torque was recorded with the leg in neutral position using a KIN-COM dynamometer. EMG was recorded using a K_Lab SPA-10 surface EMG electrode/preamplifier, interelectrode distance 23 mm, pick-up area 10 x 10 mm, in a bipolar configuration. The preprocessed EMG signal $E(t)$ and torque signal $T(t)$ were sampled at 200 Hertz.

The parameters found in this way are $K = 0.3 \text{ Nm/microVolt}$, $t_1' = 35$, $t_2' = 5$. This corresponds to continuous time constants $t_1 = 90 \text{ msec}$ and $t_2 = 10 \text{ msec}$.

HIP ABDUCTOR TORQUE DURING WALKING

Applying the muscle model to the EMG of the M. Gluteus medius during walking results in the estimated torque in figure 2. During five seconds four strides were made at a step frequency of 90 steps/minute. The torque signal during the first stride is distorted by the fact that the recursive digital filter has to "run in". Its impulse response lasts approximately 0.3 seconds.

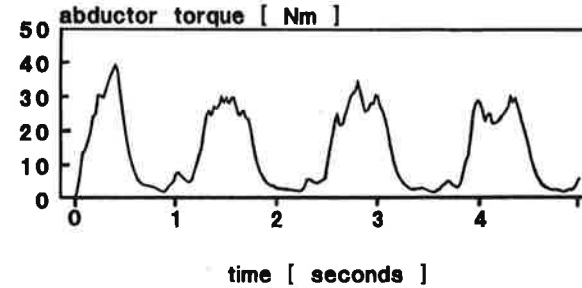


Figure 2: Abductor torque during walking, as predicted by model.

HIP ABDUCTOR ACTIVATION DURING WALKING

Also in other recordings the typical hip abductor torques as determined by Paul and Boccardi are not found. Therefore, in eight normal subjects (age 22-30, one female, seven male) the activation of the M. Gluteus medius was studied at step frequencies 60, 90 and 120 steps/minute, with a constant stride length of 1.2 meters.

Results are summarized in figure 3, where the ensemble averages of the recorded activation patterns are shown. In the graph, 0 en 100% gait cycle correspond to the moment of heel-on, with toe-off around 60 % gait cycle. It is remarkable that the abductor activity is concentrated in the early stance phase, whereas in the late stance phase there is no activity to account for the increase in abducting torque reported by Paul and Boccardi. This discrepancy was already noted by others [1]. Besides, with increasing step frequencies the activation is found to occur progressively early.

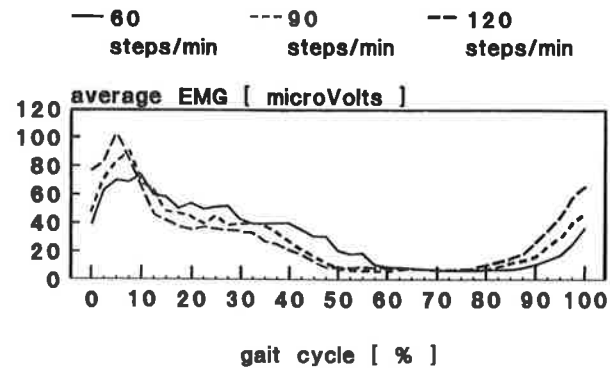


Figure 3: Averaged activation of *M. Gluteus medius* in eight normal subjects.

ACKNOWLEDGEMENTS

This work is supported by a grant from "St. Jorisstichting", Bussum, the Netherlands. For the use of the KIN-COM dynamometer the authors are indebted to the staff of the Rehabilitation Department of the Academic Hospital of the Free University in Amsterdam.

REFERENCES

1. Paul JP (1971) Comparison of EMG signals from leg muscles with corresponding force actions calculated from walkpath measurements
In: Human Locomotor Engineering, Institute of Mechanical Engineering, London
2. Boccardi S et al (1981) *J Biomechanics* 14:35-45
3. Bouisset S (1973) In: Desmedt JE (ed) *New Developments in Electromyography and Clinical Neurophysiology*, vol 1, Karger, Basel, pp 547-583
4. McLeish RD, Charnley J (1970) *J Biomechanics* 3:191-209
5. Merchant AC (1965) *J. Bone Joint Surg* 47A:462-476
6. Inman V (1947) *J. Bone Joint Surg* 29:607-619
7. Hof AL (1984) *Human Movement Science* 3:119-153
8. Cogshall JC, Bekey GA (1970) *Med & Biol Engng* 8:265-270

Activity at muscle level in the leg

DATA REDUCTION BY PREPROCESSING OF EMG DURING DYNAMIC ISOMETRIC CONTRACTION

KLEISSEN, R.F.M., HARLAAR, J., DE KREEK, J.A.

K-Lab Research, P.O. Box 70167,
1007 KD Amsterdam, the Netherlands

INTRODUCTION

Force development as a result of muscle activation is a dynamic phenomenon which's bandwidth is far lower than that of surface EMG. In studies where the relation between surface EMG and muscle force is investigated data reduction by preprocessing of the observed EMG may be desired for reasons of storage efficiency. This preprocessing operation can be described as the extraction of a signal which represents the intensity of muscle activation, and which has a smaller bandwidth than the original EMG. By recording the preprocessed signal instead of the original EMG considerable data reduction may be achieved. However, the EMG information which is relevant for muscle force generation should not be affected significantly. In the following a description of the preprocessing operation is proposed and the practical effects of various preprocessor cut-off frequencies are explored.

INTENSITY OF MUSCLE ACTIVATION AND STANDARD DEVIATION OF SURFACE EMG

Because surface EMG can be described as a temporal and spatial summation of MUAPs it will approximate a random signal with Gaussian distribution when activation levels are not too low. The parameter SD, standard deviation, characterizes the intensity of such a random signal. Changes in the number and firing frequencies of activated motor units contributing to the summation effect in changes in the SD of the resulting signal. Therefore the SD of the surface EMG can be used for describing the intensity of muscle activation.

ESTIMATION OF INTENSITY OF MUSCLE ACTIVATION

When modelling the surface EMG as a zero mean Gaussian random signal [1] with a time dependent standard deviation SD(t)

$$EMG(t) = \underline{N}(0, SD(t))$$

this signal is not stationary and ergodic.

If $SD(t)$ can be considered approximately constant over a time interval T , $SD(t)$ can be estimated as

$$\hat{SD}(t) = 1/T \int_{t-T/2}^{t+T/2} (EMG(\tau))^2 d\tau$$

which describes a convolution of the squared $EMG(t)$ signal and a boxcar window. The choice for T depends on the rate of change in $SD(t)$. T should be as large as possible to maximize the accuracy of the estimate and minimize the bandwidth of the resulting signal. However T should be small enough to track transients in $SD(t)$ accurately.

A practical real-time, on-line preprocessor may employ a full wave rectifier instead of a squaring circuit because for a zero mean Gaussian distributed random variable $r(t)$ with standard deviation SDr [2] the following relation holds:

$$E(|r(t)|) = \sqrt{\frac{2}{\pi}} SDr$$

The window over which the estimate of the expected value of the rectified $N(0, SD(t))$ is determined can be established by choosing a low pass filter with an appropriate impulse response. The length of the impulse response directly determines the length of the estimation window. With increasing window length $\hat{SD}(t)$ becomes progressively smoothed, representing an increasingly distorted muscle activation signal.

A CRITERION FOR DISTORTION IN THE MUSCLE ACTIVATION SIGNAL

A criterion for assessing distortion in the muscle activation signal, obtained from the preprocessor, may be based on the idea that if the preprocessed signal and the original EMG contain the same activation information, the dynamic relation between these signals and muscle force should be identical. This dynamic relation can be described using a muscle model and can be parametrized with the model parameters. The length of the estimation window can be increased up to a point where identification of a muscle model, relating force development as output and original EMG and its preprocessed version as input respectively, results in different values for the model parameters.

EXPERIMENTAL STUDY OF EFFECTS OF ESTIMATION WINDOW LENGTH

In order to find a satisfactory length of the estimation window raw surface EMG of the quadriceps muscles and the resulting knee extension torque were

measured during dynamic isometric contractions at knee angles 70, 110 and 150 degrees, at 1000 hertz sample frequency, with five normal subjects. EMG was recorded using K-Lab SPA-10 bipolar electrode/preamplifiers, interelectrode distance 23 mm, pick-up area 10 mm x 10 mm, employing Medi-Trace pellet electrodes. Knee torque was measured using a KIN-COM dynamometer. Five-second recordings were made, with the quadriceps contracting at 72 contractions per minute. The preprocessor was emulated in software: EMG was rectified and subsequently low pass filtered with a third order digital Butterworth filter.

Using both rectified EMG and its preprocessed version, parameters of a second order, linear, time-invariant, discrete-time muscle model [3] were optimized in such a way that the r.m.s. error between measured force and model output was minimal for preprocessor cut-off frequencies 50, 25, 10, 5, 2.5 hertz. Under the conditions of dynamic isometric contraction the second order muscle model is able to predict muscle force with a fair degree of success [4].

Resulting values for the time constants of the muscle model and the r.m.s. error were normalized to the values found for infinite cut-off frequency, i.e. the filter removed.

RESULTS

It was found that the surface EMG from the M. Vastus medialis gave smallest r.m.s. error between model output and recorded torque in all contractions, so that this muscle was considered a muscle equivalent [5]. The effect of the various cut-off frequencies on the normalized muscle model parameters and the normalized r.m.s. error is presented in figure 1. Muscle model time constants progressively deviated from values found using the unprocessed EMG, indicating increasing distortion in the estimated muscle activation signal with decreasing cut-off frequencies. At 25 hertz this deviation is about 15 %, at an estimation window length of approximately 40 msec. The error between model output using original EMG data as input and recorded knee torque after optimization was 10 - 15 % of the peak torque.

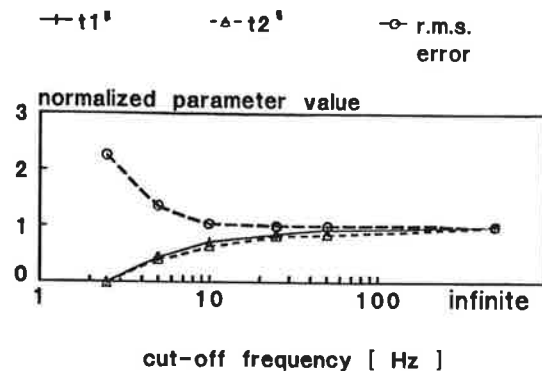


Figure 1: Effect of preprocessing cut-off frequency on muscle model parameters

CONCLUSION

Surface EMG preprocessing can be described as an estimation of the intensity of muscle activation. Bandwidth of the resulting intensity signal is an order of magnitude smaller than bandwidth of the unprocessed EMG, with some distortion of the intensity signal.

REFERENCES

1. Kadefors R (1973) In: Desmedt JE (ed) *New Developments in Electromyography and Clinical Neurophysiology*, vol. 1. Karger, Basel, pp.519-532
2. Papoulis A (1965) *Probability, Random Variables and Stochastic Processes*, McGraw-Hill
3. Kleissen RFM et al. Hip Abductor Action During Level Walking, this proceedings
4. Hof AL (1984) *Human Movement Science* 3:119-153
5. Bouisset J (1973) In: Desmedt JE (ed) *New Developments in Electromyography and Clinical Neurophysiology*, vol.1. Karger, Basel, pp. 547-583

STATISTICAL ELECTROMYOGRAPHY OF CYCLIC MUSCLE ACTION

F. BODEM, K. ALT, A. WACKERHAGEN, H. WAGNER, F. BRUSSATIS, V. WALTHER

Department of Orthopedic Surgery, Biomechanics Laboratory, University of Mainz, Langenbeckstr. 1, D-6500 Mainz (Federal Republic of Germany)

INTRODUCTION

Surface electromyography has been a useful tool for the qualitative evaluation of muscle action in body postures and body movements in many kinesiological investigations. Various attempts have been carried out, too, to find parameters of the EMG - signal that are quantitatively correlated to simultaneous kinematic and dynamic mechanical quantities of muscle contraction. Due to the unknown spatial and temporal distribution of muscle fiber activation over the muscle volume coupled with the limited spatial range of the muscle fiber action potential contribution to the sum potential measured at the electrode location, however, the EMG - signal exhibits very strong fluctuations of its parameters even at perfectly constant mechanical parameters of the simultaneous muscle action. We have carried out in this context measurements of the volume conductor field of the action potential of a muscle fiber with an electrolytic tank model. We were able to estimate from the results of this investigation that the range of muscle fibers that significantly contribute to the surface EMG is less than about 5 mm around the electrodes /1/. This indicates that a single EMG recording can never be representative of the full myoelectrical activation of the complete muscle. Rather characteristic and stable EMG - activation curves of a well defined body movement can be obtained, however, by applying ensemble averaging techniques to the analysis of the raw EMG - signal of a series of identical movements. The EMG - signal of one motion cycle has to be considered in this procedure an element of a statistical ensemble of EMG - time patterns of a suitably great number of mechanically nearly identical cyclic movements. We have applied this method to the kinematic and electromyographic analysis of the human gait .

MATERIAL AND METHODS

The investigation has been carried out with the gait analysis system shown in the schematic diagram of fig. 1. During a continuous gait sequence of 15 meters on a level walkway the following quantities are recorded: 1. The angular motion of the foot, the lower leg, and the thigh in the sagittal plane. The respective angles are measured by an optoelectronic goniometer system, the polarized and modulated light source of which is mounted onto a measuring carriage. This carriage is automatically moved in parallel with the advancing subject by an electric motor drive that is controlled by a signal derived from an optoelectronic measurement of the

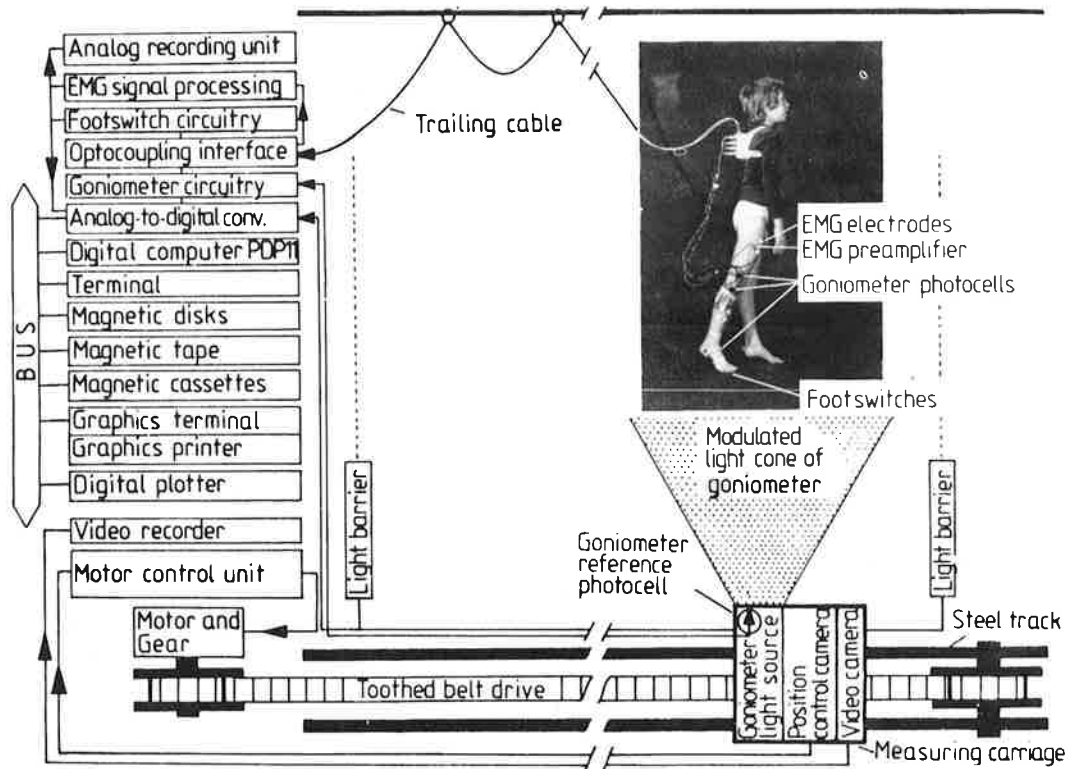


Fig. 1. Schematic diagram of the gait analysis system.

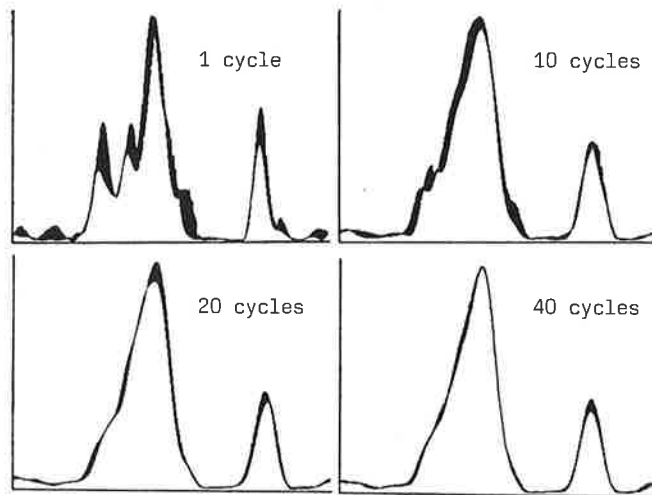


Fig. 2. Residual fluctuation in full wave rectified and digitally filtered EMG - signal averaged over different numbers of gait cycles.

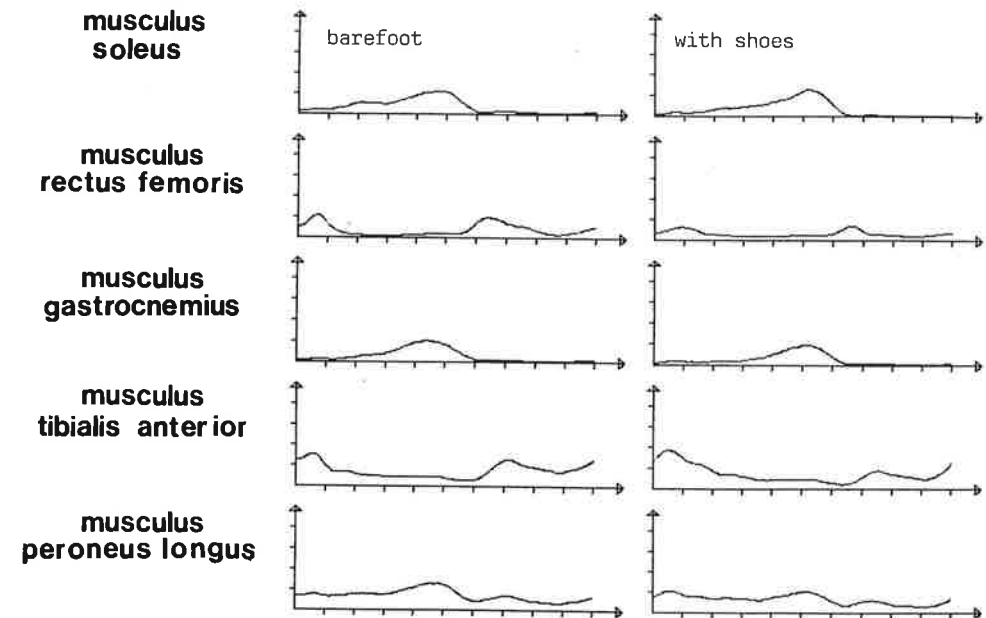


Fig. 3. Processed EMG - signals (full wave rectified, digitally filtered, averaged over 40 cycles) of a healthy subject carrying out a level walk with bare feet (left column) and with shoes (right column).

subject's position /2/. 2. The EMG - signals of selected muscles. The EMG - potentials are picked up by Ag/AgCl - surface electrodes and fed to adjacent pre-amplifiers. 3. The time pattern of the stance phases. This measurement is carried out by foot switches fixed to the subject's heel and toe region.

The signals are conditioned in a box on the subject's back for the transmission to various analog and digital recording and processing units via a trailing cable. The computer processing of the EMG - signals consists of a full wave rectification, a 20th order rectangular digital low pass filter with a cutoff frequency of 10 Hz and a linear averaging of a variable number of gait cycles, the beginning and ending of which is suitably defined and determined by the computer analysis of the recorded angular motion of the leg.

PRELIMINARY RESULTS

Fig.2 shows as a characteristic example the increasing stability of the EMG - signal of the soleus muscle of a walking healthy subject obtained by averaging over an increasing number of gait cycles. The shaded area represents the residual deviation of the corresponding curves computed from ensembles of an equal number of gait cycles taken from different test walks. It has to be noted that some details of the activation pattern that can be identified in the EMG - signal of

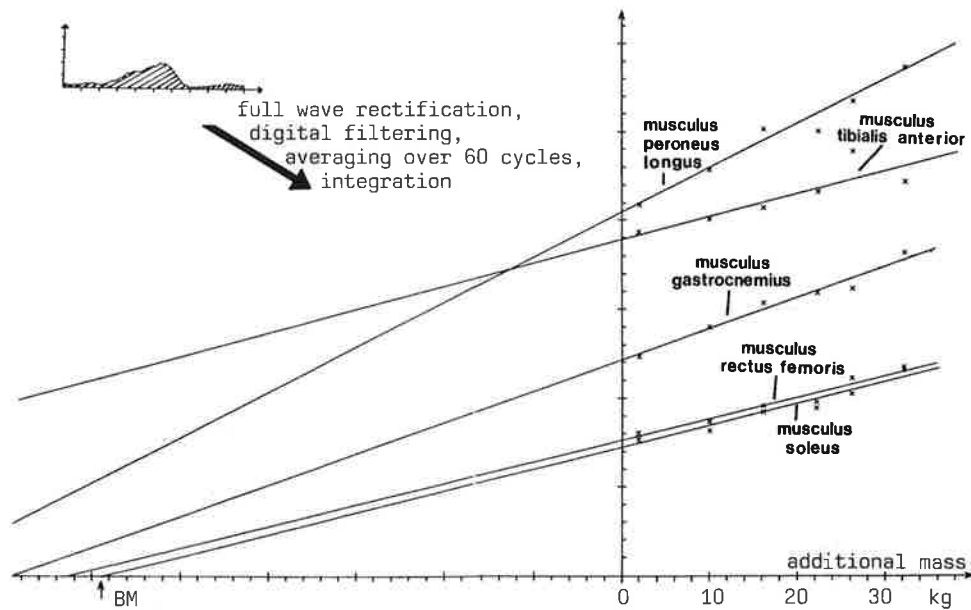


Fig. 4. Correlation between processed EMG - signal (full wave rectification, digital filtering, averaging over 60 cycles, integration) and additional mass carried by healthy subject with body mass (BM) of 59.5 kg in a level walk.

a single cycle despite strong amplitude fluctuations are obviously lost by the averaging. This is probably due to relative temporal shifts of the fine structure of the EMG pattern within the motion cycle caused by irregularities in the subject's walk. Fig. 3 shows the processed EMG signals of some muscles of the leg of another healthy test subject during a level walk with bare feet and wearing shoes. The curves are averages over 100 full strides. The relatively small differences between the corresponding curves are statistically significant, demonstrating a measurable influence of the shoes on the muscle activation pattern during level walk. Fig. 4 shows the results obtained by an additional integration of the averaged EMG curves obtained in level walks carried out by a healthy test subject loaded with different additional masses on her back. A very good linear correlation could be established in some of the investigated muscles as to the relationship between processed and integrated EMG and the carried mass.

Altogether the results obtained so far confirm that suitable averaging of the EMG activity of cyclic motions in gait may be a sensitive method to demonstrate quantitatively the influence of various conditions on muscle activity.

REFERENCES

1. Wackerhagen A (1988) MD dissertation, University of Mainz
2. and 3. Bodem F et al. (1981) Med.Progr.Technol. 8:129-139 and 141-147

INFLUENCE OF CONTRACTION-HISTORY ON EMG AND TORQUE DURING ISOKINETIC KNEE EXTENSION

J. HARLAAR, M. BOBBERT, B.J. HANHART, H. BAKKER

Free University Hospital, Dept. of Rehabilitation Medicine,
De Boelelaan 1117, 1081 HV Amsterdam (The Netherlands)

INTRODUCTION

In studies of human movement, mechanical analysis to predict individual muscle-force meets the indeterminacy problem. This makes modelling necessary; one way to do this, is an EMG-to-force processing method (1). In this model quantified EMG and kinematic data serve as an input to the model. This model should incorporate a force-length and a force-velocity relationship of the Contractile Component (CC). The force-velocity parameter can be estimated from in-situ isokinetic contractions on a dynamometer. The interpretation of these results is complicated by the interaction of the SEC-length and a limited risetime to full active state, before the movement is completed. Especially at higher velocities it is often stated that (2) the measured peak-force originates from a "compromise" between the force-length relationship and the rate at which tension develops. This phenomenon is illustrated in fig. 1 with a model-simulation (Hill model with CC and SEC). The upper curve is associated with a preload to the SEC (the muscle being at maximal active state). The lower curve is to be expected with no preload and a rising active state during the movement.

SIMULATED TORQUE (210 DEG/S)

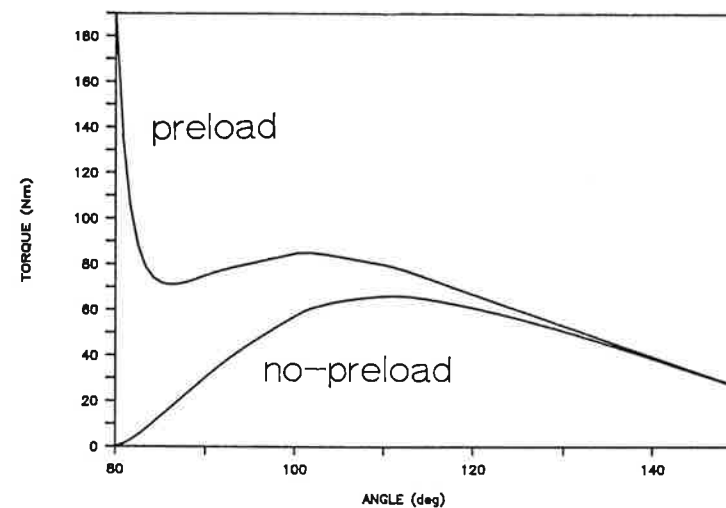


Figure 1

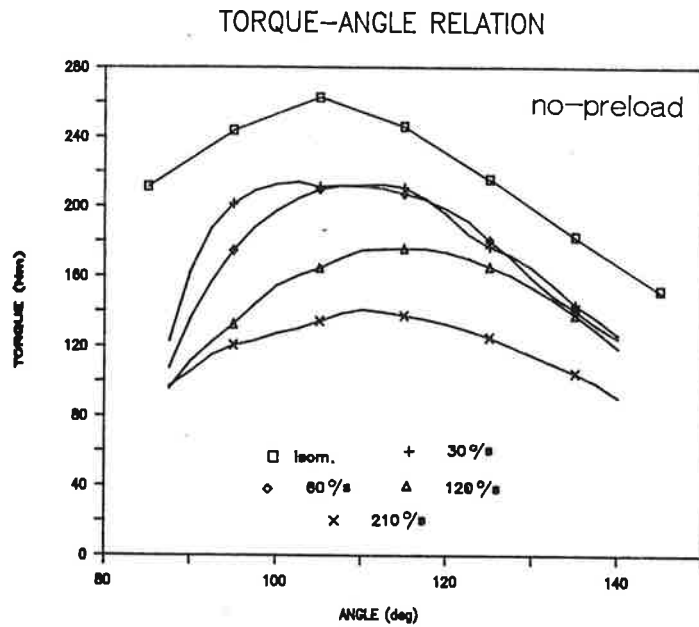


Figure 2

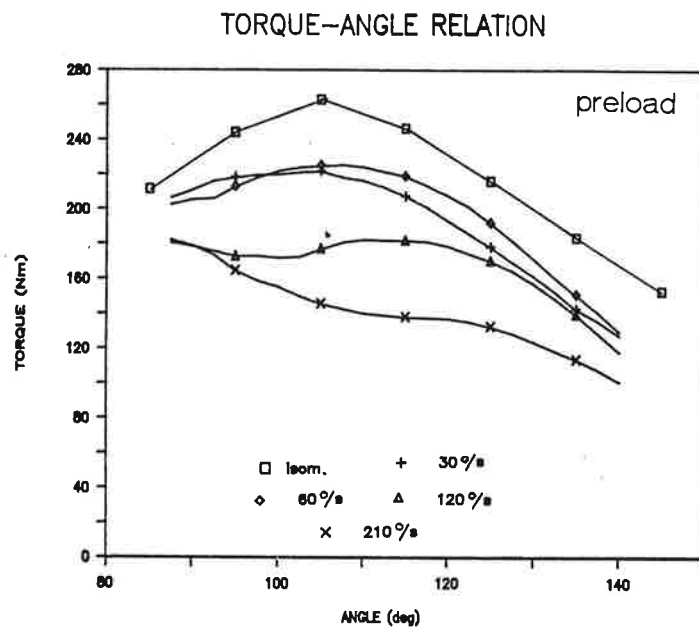


Figure 3

METHOD

We conducted an experiment to study the empirical validity of the model-simulation of figure 1. In "no-preload" contractions movement was started at the onset of contraction. Also "preload" contractions were performed, in which isokinetic movement started after building up tension in the muscle. To do so, knee-extension on a KIN/COM dynamometer (isokinetic mode) was used. In preload-contractions, threshold for starting the movement was set at 90% isometric force. In nopreload-contractions threshold was set at zero. The Range Of Motion was set at 85-145 deg. Both types of contractions were performed at 4 different velocities: 30, 60, 120 and 210 deg/sec. Prior to these contractions isometric contractions were performed at 7 different knee-angles.

MATERIAL

Ten healthy male subjects (ranging 22-35 yr.) participated in this study with their right leg. All contractions were performed at maximal effort, with the hip at 115 deg. All contractions were performed at a random sequence and a rest-pause of 2 minutes was inserted between each of them.

INSTRUMENTATION

Surface-EMG of M. Vastus Med., M. Vastus Lat., M. Rectus Fem. and M. Biceps Fem. was recorded by bipolar electrodes (1 cm², 23 mm. interelectrode-distance) with surfacemounted preamplifiers. Lowfrequent artefacts were removed with a 20 Hz. highpass filter; the total gain was adjusted to the specific output. The Rectified EMG was Smoothed (25 Hz. 3th order lowpass) to obtain the SREMG. Together with force, angle and angularvelocity of the KIN/COM, the SREMG was stored (A/D conversion at 100 Hz.) for off-line processing.

DATA-PROCESSING

For the isometric contractions, all signals were averaged over 1 second, the force being "most constant" (visual inspection), SREMG of isokinetic contractions (both with and without preload) was lowpass filtered at 5 Hz. using a 4th order filter with no phase-lag. This signal was taken relative to the amount of the mean SREMG, taken over the 7 isometric contractions. Force was transformed to torque and corrected for the inertial component due to acceleration of the lower leg during the onset of movement. All signals are expressed as a function of the knee-angle, taken the time-average value over each 2.5 deg. as a point. Finally, ensemble-averaging over the 10 subjects was performed.

RESULTS

The torque-angle curves of both types of contraction-history are shown in figure 2 and 3. Torque at higher angular velocity is clearly lower; the difference between 30 and 60 deg/sec. however is not significant. Preload-contractions show a significant higher output during the first part of the movement: after 105 deg.

FILTERED EMG - ANGLE RELATION

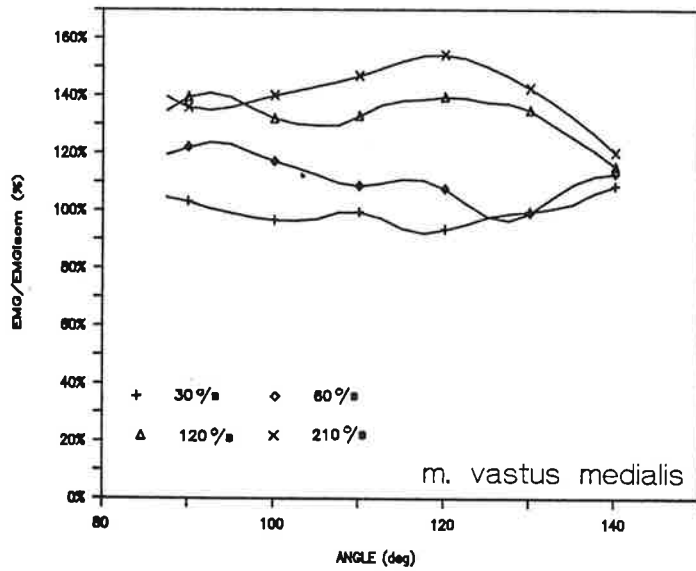


Figure 4

CORRECTED TORQUE-ANGLE RELATION

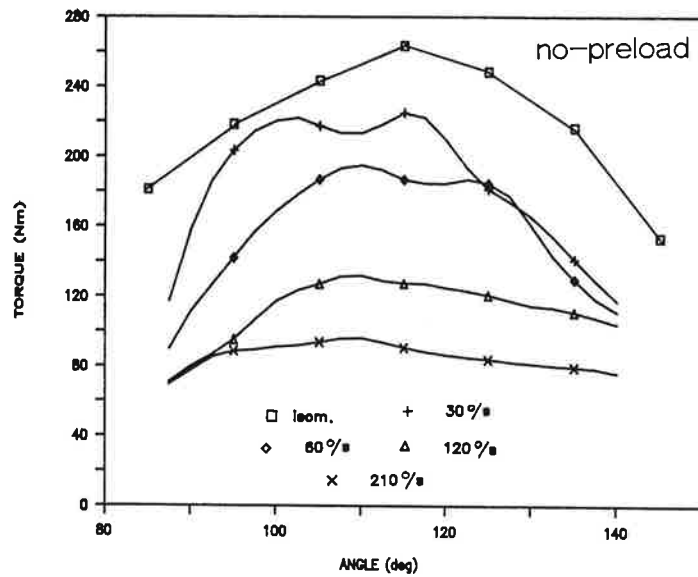


Figure 5

no difference between the two types of contraction-history can be observed. So, as the maximum of the force-length relation occurs at 115 deg., up to 210 deg/sec, peak torque can well be estimated from the nopreload-contractions. For contractions with preload the model (fig. 1) predicts a fast decrease in torque due to release of the SEC; our results show a much slower torque-decrease.

The SREMG curves of all three-extensors show the same dependency of the knee-angle, this is illustrated for the M. Vastus Med. in fig. 4. Taken relative to mean isometric value, SREMG is higher for higher angular velocities, up to 150% for 210 deg/sec. So it seems that muscles are not fully activated by the CNS at low velocity or isometric contraction of the muscle. Anyway, not over the full range of motion (being 60 deg.) or during 3 seconds.

In extracting the velocity-force relationship of the Contractile Component (Hill model) from these figures, one has to take this limited activation into mind. So "Correction" of figure 2 with the relative-activation (as shown in figure 4) gives figure 5. M. Vastus Medialis is taken as representative for the knee-extensors, and the SREMG/muscle-activity relation is assumed to be linear.

To estimate the torque-velocity relation, the torque should be constant over some range, in order to minimize the effects of a change of length in SEC.

TORQUE-VELOCITY FIT

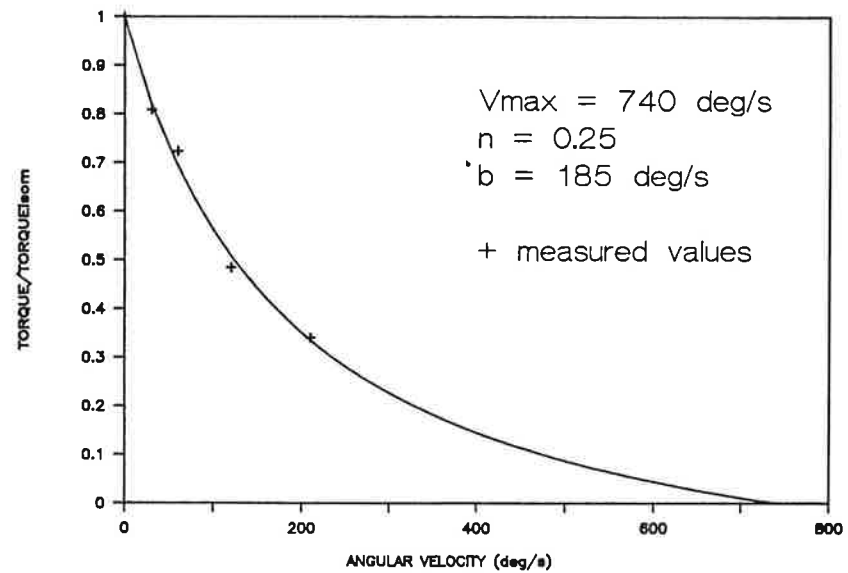


Figure 6

Doing so in figures 2 and 5 (range 105-115 deg.) gives rise to figure 6. Clearly the shape of Hill-equation (derived for maximal artificial stimulation at all velocities) emerges. Curve fitting shows the parameters $n = .25$ and $V_{max} (= b/n) = .32$ m/sec., which agrees very close with literature (3).

CONCLUSION

As the CNS is not able to activate the muscle maximal for all types of contractions, correction has to be made for the activation level, in assessing the force output. This can be done using Smoothed and Rectified Surface EMG.

Tension development in the knee extensors builds up fast enough to estimate the force-velocity relation accurately, from isokinetic knee-extensions up to 210 deg/sec., irrespective to an isometric contraction history.

REFERENCES

1. Hof, A.L. (1984), EMG and muscle force: an introduction. *Human Movement Science* 3, 119-153.
2. Perrine, J.J. and Edgerton, V.R. (1978). Muscle force-velocity and power-velocity relationships under isokinetic loading. *Medicine and Science in Sports*, 10, 159-166.
3. Wickiewicz, T.L., Roy, R.R., Powell, P.L., Perrine, J.J. and Edgerton, V.R. (1984). Muscle architecture and force-velocity relationships in humans. *Journal of applied Physiology: Respiratory, Environmental and Exercise Physiology*, 57, 435-443.

THE CALIES PROJECT

Pierre RABISCHONG — Jean WOLOSZKO

Montpellier (France)

The CALIES Project (Computer-Aided Locomotion by Implanted ElectroStimulation) is a European project that received an official agreement in June 1988, within the EUREKA programs. These gather the efforts undertaken by several European countries to develop an industrial project, the aim of which is the production of a device designed in this contract.

The French Company BERTIN, specialized in advanced engineering, is the industrial coordinator for the project, grouping Italian, Dutch, Irish, English, German and French teams. Each government has accepted to bring a financial contribution during a period of four years. Therefore, the challenge is both industrial and scientific, allowing European teams to work together. Several problems are arisen concerning: the reasons why such a project has been elaborated, the strategy to achieve the objectives, and the developments expected in the future.

I. Why the CALIES Project ?

There are in France about 25 000 paraplegics, 31 years old on average. 74 % of cases are due to traumatic lesions

consecutive to transportation, home or sports injuries. At the European level, the number of paraplegics is estimated to be about 250 000.

Spinal cord injuries can induce either total sections which completely insulate a part of the central nervous system, or incomplete sections allowing partial conduction. Most of time, the patient presents at lesional level a loss of the motor neurons of the anterior horn of the spinal cord, which leads to the loss of the muscles of the corresponding muscular area. Below the lesion, the muscles keep connected to the spinal cord, but they are no longer controlled by the brain. In certain cases, the myotatic reflex due to the hyper excitability of neuromuscular spindles leads to an increase of muscle stiffness during joint activation that is spasticity.

This spasticity can be useful when exerted in extension phase, allowing the patient to start a standing up function. It can be prejudicial, if exerted in the flexion phase, generating muscular and tendinous retractions that seriously compromise the patient's physical comfort. In addition to these motor dysfunctions, there are troubles in sensitivity below the lesion. Sphincteral functions no longer respond to voluntary command and the sexual function is strongly disturbed.

Rehabilitation of paraplegics must tend to prepare the patients to a new way of life, allowing them to use wheelchairs for their transportation, which requires to learn the transfer process on wheelchairs.

We are now aware that such patients must be verticalized every day in order to load the skeleton, which is absolutely necessary for the normal bone mineralization. Spatial programs have shown that astronauts, due to the lack of gravity, are subjected to disturbances in their bone mineralization, recovering a normal rate requiring several months. The bones do not contain nervous structures acting as force transducers. On the other hand, they are composed of hydroxyl-apatite crystals, which appears to be responsible for a piezoelectric effect that can explain the action of mechanical factors upon the bone metabolism. Therefore, the patient can be verticalized with the help of passive devices of "stand-up" type or braces, allowing either pendular or four-point deambulation. However, this kind of deambulation is tiring, not very efficient and cannot be achieved by all the patients.

Consequently the methods allowing the restoration of locomotion are presently of two types : the implantation of embryonic cells in the spinal cord or the functional electrical stimulation in order to actuate by electrical current the muscles having lost their central control.

At the moment, the first method is experimental. It has shown, in rats, that embryonic cells implanted could generate synaptic connections and produce neurotransmitters allowing to improve some functions, such as the bladder function, or to reduce spasticity. Certain surgical procedures have been made on patients with Parkinson's disease by means of surrenal cells implanted within the brain, but clinical results were not convincing. Anyway, this method will not be able to completely restore the multiple and complex connections in the spinal cord that allow the

regulation of motions. Ethical problems raised by the use of embryonic material reinforce the difficulty to promote this technique.

The second method appears to be the only one capable of giving efficient results. The first attempts of this method date back more than twenty-five years. Electrical stimulation can be used transcutaneously, directly applied to the muscle (intramuscular electrodes), around or within the nerves (perineural or intraneural electrodes) or on the anterior root of the spine, or on the spine itself. The stimulation parameters are intensity, frequency and pulse-width of the electrical signal. A large number of investigations allowed, through theoretical and experimental studies, to optimize the parameters, in order to avoid to damage the stimulated structures. In 1961, Liberson applied this technique to hemiplegic patients. Afterwards, numerous medical teams contributed to improve the efficiency to the technique, by increasing the number of stimulation channels and by defining more precisely the stimulation parameters according to our knowledge of the structure of the paralyzed muscle. Muscle reaction to stimulation varies considerably with the fatigue, the detection and characterization of which remains a serious physiological problem. In the case of transcutaneous stimulation, the selectivity and linearity of the muscle response are limited, which excludes achievement of complex close-loop control systems. On the other hand, implantable devices encounter some technical difficulties due to the miniaturization of electronic devices and to the design of electrodes, which is surely the most critical point.

Though a number of medical teams, particularly the Cleveland one, are interested in the implanted electrical stimulation of the upper-limb muscles for tetraplegics, the CALIES Project has been voluntarily limited to the restoration of the lower-limb motor function. This function is achieved both by the voluntary control of different parameters (mostly direction and speed) and by automatic or semi-automatic control of gait sequences (stance and swing phases). These characteristics allow to use artificial substitution devices to actuate automatically and coordinate the activity of the muscles. The patient has to be only responsible for gait starting and stopping, direction and speed control. As the lower limb includes no less than 45 muscles and 42 degrees of freedom, it is not realistic to think of stimulating and coordinating the activity of such a large number of muscles. However, on the same way as for the physiological control of hierarchical type, we can integrate some controls, in order to obtain acceptable functional results. Moreover, the physiological control requires a large number of feedbacks from skin, muscles, tendons and joints, which are unconsciously processed at the subcortical level of brain and cerebellum. In fact, a close-loop control should take care of joint-angle and ground-reaction measurements. Biped locomotion requires two functions : stabilization and propulsion. Stabilization during gait is of dynamic type, by the way of visual, vestibular, cutaneous and proprioceptive afferences. If it seems possible to restore an active controlled propulsion, stabilization is a far more delicate problem and will require, for a long period of time, the use of crutches by patients, which corresponds to a more stable quadruped gait model.

The numerous experimental and fundamental data reported in the literature could allow the Calies Project to be achieved within the next four years.

II. How CALIES can be achieved ?

The necessity of a perfect adequation with the clinical aspects justifies to collect all the scientific and medical data presently available in Europe. Through to the Concerted Action of The COMAC-BME of the European Communities, called "Evaluation of Assistive Devices for Paralyzed Persons", managed by Pr. PEDOTTI from Milan, a subgroup was created on walking restoration. Four workshops held in Oswestry (1985), Montpellier (1986), Enschede (1987) and Montpellier(1988) have made the state of the art of our knowledge regarding the characterization of the paralyzed muscle, the spasticity, the action of the electrical current on tissues, all the clinical aspects (such as the use of ambulatory devices, the hybrid systems and the clinical indications of FES) On the other hand, all the European teams were becoming more familiar to each other and progressively a cooperation project has been established.

To guarantee the industrial success, which is a basic condition of a EUREKA Project, it was decided to create, from the beginning of the project, a European Clinical network. This is divided in three groups, the first for surgical implantation whose objective is to analyze the possibilities and limits of the surgical techniques regarding wire connections and the fixation of the electronic device; the second for rehabilitation problems : before the implantation, for a precise functional assessment of each patient in order to define the indications or contra-

indications, and, after the implantation, to follow up; the third one, for an objective evaluation of the results, allowing to continuously adjust the project and to assure its reliability. These three sub-groups, each of them composed of representatives of every CEE country, will be respectively managed by Pr. SAMII from Hannover, Pr. ZILVOLD from Enschede and Pr. PEDOTTI from Milan. By associating, from the beginning, clinicians, researchers and manufacturers, we can hope to achieve the production of an equipment which can receive the agreement of both producers and users.

This equipment will be composed of an implantable device and an external one. The implantable device will comprise : an electronic implant with eight stimulation channels and eight channels for goniometric and ground-reaction feedbacks, hopefully by the way of implantable microtransducers; wires with hermetic plugs; and biocompatible electrodes which will be put, by microsurgical approach, on the nervous fascicles.

In fact, each nerve comprises bundles corresponding to a precise muscular or cutaneous area. Progress in microsurgery allow to point out the bundle corresponding to the muscle or group of muscles to be stimulated. Electrodes have to be biocompatible and corrosion proof, in order to guarantee long-term use. Current investigations aim at selecting the most reliable biomaterials, among which can be found conductive polymers. Moreover, we have now orthodromic conductive electrodes (wide anode, small cathode) that allow, if required, to avoid stimulating the sensitive fibers, which could cause reflex muscular contra-reactions. The

implanted box has to be as small and light as possible in order to be steadily fastened into a subcutaneous area, easily accessible.

The external part of the system comprises an antenna that transmits the power and the signal, an impulse programmer generating the sequences required by the control and coordination of the different muscles, and a control interface with the patient. Using a walking-machine to generate gait sequences with the help of motors set on an orthosis is necessary for the adjustment of the control system and the patients' gait training before the implantation of the electrodes.

The close-loop system is also necessary to avoid muscular overloading, generating joint damages. On the other hand, this is the only manner to get smooth and smart movements, which is an essential condition for the patients to accept this method.

From the beginning of the project, the indications have been determined. Only injuries between T4 and T11 can benefit of the implantable system. It is necessary to have upper limbs in a functional state for stabilization with crutches, and to have lower limb muscles alive, to be excited by electrical current. The level of spasticity has to be compatible with the mobilization of joints. The motivation of patients has to be strong enough to achieve the complete set of operations

A program of reinforcement of muscles by means of transcutaneous electrical stimulation will be defined, based on the fundamental data we have regarding the histologic repartition of fast and slow muscular fibers changing after a spinal cord

injury and during the electrical stimulation. The contribution of Mortimer and Salmons is, in this regard, particularly important.

The first implantations on patient will only be possible after experiments on animals. We can expect that they should start during the third year of the project

This project is ambitious, as it aims at achieving artificially what others could accomplish beyond the natural principles, with their "Stand up and Walk". However it is not unrealistic to think that deambulation by means of the patients' own muscles, re-actuated by electrical current, will be developed, according to the progress in electronic miniaturization, production of compatible biomaterials and mostly to an efficient co-operation of several medical teams that have accepted to share their competences and enthusiasm. The future will tell us if Europe is able to achieve such a challenge.

REFERENCES

- BAJZEK (T. J.), JAEGER (R.J.) .- "Characterization and control of muscle response to electrical stimulation." .- *Annals of Biomedical Engineering*, Vol. 15, pp. 485-501, 1987.
- CHIZECK (H.J.), MARSOLAIS(E.B.), KOBETIC (R).- "Closed loop controller design of neuroprosthetics for functional walking in paralysed patients." .In *Bridge between Control Science and Technology*. Vol.6 , pp.3013-3019, Oxford Pergamon, 1985.
- CRAGO (P.E.), PECKHAM (P.H.), MORTIMER (J.T.), VAN DER MEULEN (J.P.).-"The choice of pulse duration for chronic electrical stimulation via surface, nerve and intramuscular electrodes." *Ann. Biomed. Eng.*, vol. 2, pp. 252-264, 1974.
- CYBULSKI (G.R.), PENN (R.D.), JAEGER (R.J.).- "Lower extremity functional neuromuscular stimulation in cases of spinal cord injury."- *Neurosurgery* 15, pp. 132-146, 1984.

GRANDJEAN (P.A.), MORTIMER (J.T.).-"Recruitment properties of monopolar and bipolar epymisal electrodes." Ann. Biomed. Eng., Vol.14, pp. 53-66, 1986.

LIBERSON (W.T.), HOLMQUEST (H.J.), SCOTT (D.), DOW (M.).-"Functional electrotherapy : Stimulation of the peroneal nerve synchronized with the swing phase of gait of hemiplegic patients."-Arch. Phys. Med. Rehab., Vol.42, pp. 100-105, 1961.

MARSOLAIS (E.B.), KOBETIC (R.).-"Functional Walking inParalysed Patients by Means of Electrical Stimulation."-Clin. Orth., Vol. 175, pp. 30-36, 1983.

Mc NEAL (D.R.).-" Analysis of a Model for Excitation of Myelinated Nerves." -IEE Trans. Biomed. Eng., Vol. BME-23, pp. 359-357, 1976.

MORTIMER (J.T.), KAUFMAN (D.), ROESMSMAN (U.).-"Intramuscular electrical stimulation : tissue damage." - Ann. Biomed. Eng., vol.8, pp. 235-244, 1980.

PECKHAM (P.H.), MORTIMER (J.T.), VAN DER MEULEN (J.P.).-"Physiologic and metabolic changes in white muscle of cat following induced exercise."- Brain Research, Vol. 50, pp. 424-430, 1973.

PECKHAM (P.H.).-"Functional Electrical Stimulation : Current Status and Future Prospects of Applications to the Neuromuscular System in Spinal Cord Injury." - Paraplegia 25, pp. 279-288, 1987.

RABISCHONG (P.), BONNEL (F.), DOMBRE (E.), PERUCHON (E.), COIFFET (P.), FOURNIER (A.), BREBEC (J-M.) - "Basic studies in elctrical stimulation of limbs" - Part I: Method and approach, Bulletin of Prosthetic Research, Washington D.C. N° 10-22, Fall 1974

SALMONS (S).- The response of skeletal muscle to different patterns of use. Some new developments and concepts In : PETTE (D).- Plasticity of muscle.- New York : de Gruyter, 1980.

STALLARD (J.), MAJOR (R.E.), POINER (R.), FARMER (I.R.), JONES (N.).-"Engineering design considerations of the ORLAU ParaWalker anf FES hybrid system."- Engineering in Medicine, Vol. 15, pp. 123-129, 1986.

VELTINK (P.H.), HERMENS (H.J.), VAN ALSTE (J.A.).-"Multi-electrode intrafascicular and extra-neural stimulation." - Proc. 8th Ann. Conf. of the IEE Eng. in Med. and Biol. Sci., Dallas, pp. 690-693, Nov. 1986.

VODOVNIK (L.), CROCHETIERE (W.J.)and RESWICK (J.B), "Control of Skeletal Joint by Electrical Stimulation of Antagonists" - Med. Biol. Eng., Vol. 5, pp. 97-109, 1967.

WOLOSZKO (J.), GRAILLE (J.),RABISCHONG (E.), RABISCHONG (P.).-"Closed-loop control of knee during standing with FNS." in Proceedings of the Ninth Annual Conference of the IEEE Engineering in Medicine and Biology Society, Boston, Nov. 13-16, 1987, pp: 1222-1223

AUTHOR INDEX

- Acimovic, R., 167
 Ahlin, A., 167
 Akai, F., 79
 Albers, B.A., 221
 Alt, K., 527
 Anderson, P., 467
 Andersson, G.B.J., 437
 Andriacchi, T.P., 437
 Angelotti, M., 417
 Arendt-Nielsen, L., 195, 283
 Ashley, R.K., 371
- Bakker, H., 235, 357, 531
 Balestra, G., 275
 Baratta, R., 19
 Baumgartner, R., 327
 Becher, J., 357
 Belk, D., 467
 Besseling, S., 459
 Bieleman, H.J., 489
 Birjukova, E.V., 481
 Bjerring, P., 195
 Bobbert, M., 531
 Bođem, F., 527
 Bombardi, F., 423
 Bonga, G.J.J., 287
 Boom, H.B.K., 105
 Boon, K.L., 231
 Boucher, J.P., 61
 Bour, L.J., 361
 Bracale, M., 343
 Braahekke, J.P., 431
 Breedveld, P.C., 477
 Brocks, L., 393
 Brundin, L., 309
 Brussatis, F., 527
- Casavant, D.A., 451
 Catani, F., 261
 Colombari, M., 423
 Connors, A., 467
 Crivellini, M., 351
- D'Ambrosia, R., 19
 Daanen, H.A.M., 265
 Dacquino, G., 351
 Davies, S.W., 243
 de Groot, G., 485
 de Jongh, H.J., 473
 de Koning, J.J., 485
- de Kreek, J.A., 235, 523
 De Luca, C.J., 35, 271, 451
 de Pater, L., 287
 de Vos, R.A.I., 135
 della Villa, S., 423
 Denier van der Gon, J.J., 9, 25, 3
 Diemont, B., 291, 295
 Dimitrijevic, M.R., 177
 Dimitrov, G.V., 211, 217
 Dimitrova, N.A., 211, 217
 Divieti, L., 351
 Dubowitz, V., 389
 Dufosse, M., 481
- Eckert, P., 69
 Ekiel, J.S., 55
 Elert, J., 317
 Emley, M.S., 451
 Evenhuis, A.F., 399
 Ewins, D.J., 113, 121
- Fernandez-Bermejo, E., 389
 Fox, B.A., 113
 Frolov, A.A., 481
 Fujii, H., 493
 Fujita, K., 117
 Fujita, M., 493
 Funakawa, I., 191
- Gantchev, G.N., 29
 Gatev, P.G., 29
 Gerdle, B., 255, 317
 Gerner, H., 143
 Gielen, C.C.A.M., 25, 39
 Gilad, I., 445
 Girsch, W., 75, 143
 Gootzen, T.H.J.M., 227
 Granata, C., 423
 Grandori, F., 89
 Gregoric, M., 167, 385
 Grootenboer, H.J., 473
 Gros, N., 367
 Gruber, H., 75, 153
 Guidetti, D., 411
- Hagberg, M., 313
 Hägg, G., 321
 Hammarström, U., 313
 Hanhart, B.J., 531
 Happak, W., 75

Harlaar, J., 235, 357, 523, 531
 Hashimoto, S., 79
 Hayashi, R., 51
 Heckmatt, J.Z., 389
 Henriksson-Larsen, K., 255, 317
 Hermens, H.J., 109, 231, 377, 407
 Hidding, A., 459
 Hof, A.L., 287
 Holle, J., 75, 143
 Holsheimer, J., 85, 95, 99
 Hosokawa, K., 79

 Iguchi, Y., 117
 Ikoma, K., 187, 191
 Iocco, M., 343
 Ioffe, M.E., 481
 Ioku, M., 79
 Itakura, N., 117
 Iwakura, H., 513

 Jäger, M., 301, 441
 Janssen, H., 393
 Jennings, S.J., 171
 Johanson, M.E., 371, 463
 Jonsson, B., 305, 309
 Joosten, E.M.G., 431

 Kashiwabara, S., 513
 Kelih, B., 127, 131
 Kiwerski, J., 157
 Kleissen, R.F.M., 517, 523
 Klemen, A., 385
 Kljajic, M., 127, 131, 167
 Knaflitz, M., 261, 271, 275
 Koller, R., 75
 Koopman, H.F.J.M., 473
 Krajnik, J., 167
 Kralj, B., 161
 Kroon, G.W., 279
 Kubo, K., 117
 Kuipers, W.D., 287

 Lamoreux, L.W., 371
 Landström, U., 309
 Lanfranchi, A., 411
 Lateva, Z.C., 211
 Laurig, W., 301
 Levitan, C., 467
 Levy, M., 65
 Lipczynski, P.T., 113, 121
 Loermans, H.M.Th., 399
 Losert, U., 75
 Lukanovic, A., 161
 Luttmann, A., 301, 441

 Machilda, E., 309
 Maguire, E., 467
 Malezic, M., 167
 Mano, Y., 187, 191, 503
 Maranzana-Figini, M., 291, 295

 Marcello, N., 411
 Massion J., 481
 Matsui, K., 191
 Matsusaka, N., 493
 Matthijsse, P.C., 477
 Mayr, W., 75, 143, 153
 McNamara, K., 467
 Merletti, R., 261, 271, 275
 Merlini, L., 423
 Miklavcic, D., 367
 Minamitani, H., 117
 Misasi, N., 343
 Miscio, G., 43
 Mizrahi, J., 65
 Mouton, L.J., 459
 Mulder, A.J., 109

 Naeije, M., 279
 Nakamuro, T., 187, 191
 Nene, A.V., 171
 Newman, N., 455
 Notermans, S.L.H., 431
 Norimatsu, T., 493

 Ongerboer de Visser, B.W., 361
 Orizio, C., 295
 Ortaggio, F., 411

 Parker, P.A., 243
 Pasniczek, R., 157
 Patrick, J.H., 171
 Paul, J.A., 489
 Paul, J.P., 3
 Pépin, A., 61
 Pepino, A., 343
 Perini, R., 295
 Philips, R., 347
 Pinelli, P., 43
 Pisano, F., 43
 Pizzino, A., 291
 Popovic, D., 337
 Put, J.H.M., 135, 221

 Rabischong, P., 537
 Rau, G., 247, 251
 Ravazzani, P., 89
 Rebersek, S., 367
 Risaliti, R., 417
 Rodillo, E.B., 389
 Rossi, B., 417
 Roy, S.H., 451
 Rozendal, R.H., 489
 Rozman, J., 127, 131
 Rutgers, R., 135
 Rutten, W.L.C., 135, 221, 231

 Sakakibara, T., 503
 Santambrogio, G.C., 351
 Satou, T., 79
 Schaars, A.H., 407

Scheja, H.M., 69
 Schipplein, O.D., 437
 Schlecht, M., 377, 407, 517
 Schneider, J., 247, 251
 Schwirtlich, L., 337
 Shapiro, T., 467
 Shelton, C., 467
 Siciliano, G., 417
 Silny, J., 247, 251
 Sinkjaer, T., 51
 Skinner, S.R., 371
 Soerjanto, R., 347
 Solomonow, M., 19
 Solzi, P., 65
 St. Georges, M., 455
 St. Helen, R., 371
 Ståhlberg, E., 201
 Stanic, U., 127, 131
 Stegeman, D.F., 227, 431
 Stöhr, H., 143
 Streinzer, W., 153
 Struijk, J.J., 95, 99
 Stucchi, M., 351
 Sundelin, G., 313
 Susak, Z., 65
 Suurküla, J., 321
 Suzuki, R., 493
 Swain, I.D., 113, 121

 Takahashi, M., 79
 Takayanagi, T., 187, 191, 503
 Takesako, S., 497
 Tanaka, S., 513
 Tankov, N.T., 29
 Tax, A.A.M., 39
 Taylor, P.N., 113, 121
 Thoma, H., 75, 143, 153
 Trafimow, J.H., 437

 Valencic, V., 385
 van Alsté, J.A., 85, 105, 109

 van Beckum, F.P.H., 99
 van Bruggen, T.A.M., 231
 van der Bij, J., 459
 van der Meulen, J.H.P., 25
 van der Woude, L.H.V., 489
 van Ingen Schenau, G.J., 485
 van Veen, B.K., 99
 van Weerden, T.W., 427
 van Wier, H.J., 135
 Vavken, E., 167
 Veeger, H.E.J., 489
 Veicsteinas, A., 295
 Veltink, P.H., 85, 99
 Vingerhoets, H.M., 227
 Vink, P., 265
 Vogelaar, T.W., 357

 Wackerhagen, A., 527
 Wagner, H., 527
 Wallinga-de Jonge, W., 221, 231, 393, 399
 Walther, V., 527
 Wever, D., 377
 Whitlock, T.L., 113, 121
 Willemsen, A.T.M., 105
 Wilts, G., 231
 Wirtz, P., 221, 393, 399
 Woloszko, J., 537
 Wouda, A.A., 287
 Wretling, M.-L., 255

 Yahia, H., 455
 Yoshida, M.K., 371

 Zieniewicz, M.J., 55
 Zilvold, G., 109, 231, 327, 407, 517
 Zrunek, M., 153
 Zupan, A., 385
 Zwarts, M.J., 283, 427

KEYWORD INDEX

- abductor torque, 517
 absolute measurement, 106
 accelerometers, 105
 accuracy, 25
 activating functions, 99
 activation patterns, 519
 adaptive control, 337
 aiming movements, 25
 all-poles model, 291
 amplitude distribution, 305
 angle measurements, 107
 angle, 445
 angular accelerometer, 371
 angular velocity, 317
 artificial reflex, 109
 assessment, 357
 ataxic patients, 503
 auto-regressive (AR) model, 291
- back pain, 451
 backmuscles, 459
 Balans chair (BC), 467
 biceps muscle, 279
 bilateral recurrent nerve
 paralysis, 153
 bioacceptance, 135
 biomechanical analysis, 485
 biomechanical model, 441, 481
 biomechanical properties of the
 elbow, 369
 biomechanics, 343, 463
 bioresorbable collagen membrane, 79
 bladder automatism, 157
 body movement, 441
 brain stimulation, 89
- calf muscles, 287
 cash registers, 306
 cerebral evoked potentials, 177
 chamber, 489
 childhood, 493
 chronic quadriplegic patients, 61
 clinical evaluation, 407
 closed loop control, 113, 117
 closed loop FES systems, 121
 co-contraction evaluation, 261
 coactivation, 19
 coding of control variables, 11
 common drive, 35
 compliance transfer function, 51
- compression strength, 443
 concentric contractions, 279
 conduction velocity, 271
 contraction-history, 531
 control of movement distance, 11
 conventional EMG, 203
 cortical responses, 195
 cross correlation method, 427
 cross spectrum, 295
 cross-correlation coefficient
 function, 265
 cross-correlation, 283
 crosstalk, 261, 265
 cyclic muscle action, 527
- data reduction, 523
 decentralized control, 117
 delay density estimates, 243
 digital filter, 518
 disorders of neuromuscular
 transmission, 217
 dopamine, 192
 dorsal columns, 95
 dual channel implantable
 stimulator, 127
 Duchenne dystrophy, 407
 Duchenne muscular dystrophy, 389
 dynamic, 317
 dystrophy, 393
- eccentric contractions, 279
 elbow joint, 367
 elderly women, 161
 electrical nerve stimulation, 85
 electrical stimulation, 135, 167,
 171, 217, 271, 351, 271
 electro arch gauge (EAG), 493
 electro-mechanical hammer, 371
 electro-myography, 43
 electrode combinations, 95
 electrode configuration, 99
 electrode-configuration parameters
 235
 electromyographic, 287, 301, 305,
 313, 329, 459, 463, 467, 527
 electrostimulation, 89, 157
 EMG automatic analysis, 411
 EMG interference pattern, 411
 EMG load levels, 313
 EMG preprocessing, 526

- EMG, 19, 121, 279, 317, 322, 401, 421, 451, 489
 EMG-to-force processing, 531
 epimuscular microstimulation method, 399
 epineural electrodes, 75
 equilibrium, 513
 erector spinae, 453
 ergonomics, 305
 evaluation, 327
 extracellular potentials, 211, 217
 extracellular single fibre action potentials, 221
- fast-glycolytic, 401
 fatigue, 65, 283, 287, 295, 318, 321, 421, 427, 451
 femoral nerves, 75
 FES, 5, 65, 113
 fibre type, 255
 field potentials, 95, 99
 field study, 301
 finite lengths, 211
 firing rate influence, 253
 firing rate, 35
 firing, 43
 force, 283, 393
 force-grading mechanisms, 39
 force-platform, 513
 force-velocity relationship, 531
 frequency spectrum, 451
 frozen gait, 187
 FTC-method, 321
 functional electrical stimulation (FES), 65, 113
 functional electrical stimulation, 109, 117, 131, 153, 161
 functional electrostimulation, 105
 functional neuromuscular stimulation, 85
 functional rehabilitation, 143
- gait analysis, 331
 gait efficacy, 337
 gait, 167, 353
 glycogen depletion, 399
 ground reaction, 353
- H/M ratio, 361
 hemiparetic, 167, 513
 hemiplegia, 357
 hemiplegic, 343
 histochemistry, 401
 homecomputer-based instrument, 349
 human gait, 477
 hybrid orthoses, 5
 hybrid, 171
 5-hydroxytryptamine, 192
- IAP duration, 211
- image analysis, 75
 immobilization, 393
 implant, 171
 implantable neurostimulators, 143
 implantable stimulator, 127, 131
 implicit integration routines, 477
 inclinometer, 446
 innervation zone, 243
 innervation, 455
 intermittent claudication, 287
 intervals, 44
 intracranial electric fields, 89
 intraneural stimulation, 135
 intrinsic lumbar back muscles, 266
 invariants, 31
 ischemia, 69
 isokinetic contractions, 531
 isokinetic strength evaluation, 41
 isokinetic, 317
 isometric contraction, 39, 279, 29
- joint, 19
- joint, 19
 jitter, 217
 job rotation, 306
 joint, 19
- kinesiological, 191
 kinesiology, 329, 503
 knee extensions, 255
- laser, 195
 lasers, 3
 lifting, 437, 445
 load manipulation, 441
 logging machines, 305
 long-term electrical muscle stimulation, 385
 lumbar erector spinae, 467
 lumbar spine, 455
 lumbar stress, 441
- macro EMG, 204
 magnetic stimulation, 187, 191
 materials, 3
 mature peripheral nerve, 79
 maximal angular velocity, 371
 mean power frequency, 255
 mechanical stimuli, 55
 mechanisms of bioelectric phenomena, 217
 medial arch of the foot, 493
 medial arch, 497
 median frequency, 287, 451
 MFCV, 427
 mid thoracic paraplegics, 113
 model of electrostimulation, 89
 modelling, 477
 motor central conduction time, 187
 motor control, 9, 25, 55, 329
 motor cortex, 89
 motor performance, 25

- motor points of the gastrocnemius muscle, 377
 motor unit action potentials, 227
 motor unit excitation, 249
 motor unit, 39, 43
 motor units, 35, 247, 399
 movement analysis, 473
 movement control, 39
 movement pattern, 489
 movement, 19
 multi-joint control, 117
 multibond graphs, 477
 multichannel, 143
 multiple system atrophy, 187
 muscle blood flow, 283
 muscle coordination, 9, 485
 muscle fatigue, 109, 275, 303
 muscle fiber conduction velocity, 283, 430
 muscle fiber, 211, 271
 muscle force, 523
 muscle function, 357
 muscle model, 517, 524
 muscle powering, 353
 muscle strain, 302
 muscle tendon reflex, 371
 muscles, 393, 451
 muscular conduction velocity, 251
 muscular dystrophy, 385, 403
 muscular fatigue, 279, 287
 muscular sound, 291, 295
 myalgia, 321
 myelinated nerve fibers, 75
 myofeedback (MFB), 347
 myometry, 412
 myotonia congenita, 427
 myotonic dystrophy, 421
- neck and shoulder muscle activity, 309
 neck, 314
 nerve endings, 455
 neurochemical, 191
 neurologic improvement, 157
 neuropathological, 192
 non numerical control, 337
 noninvasive EMG, 247
 noninvasive multielectrode, 251
- objective quantification of the training results, 349
 occupational health, 301, 441
 orthoses, 389
- pain, 195
 palmarflexors, 51
 paraplegia, 65
 paraplegic locomotion, 171
 paraplegics, 113
 Parkinson's disease, 187, 503
- pathological changes, 77
 patterned electrical stimulation, 61
 pendulum test, 367
 PES, 61
 phenolisation, 377
 phrenic pacemaker, 143
 platform, 343,
 posterior cricoarytenoid muscle (PCM), 153
 power spectrum, 211, 427
 primary myopathies, 208
 programmed movements, 29
 progressive muscular dystrophy (PMD), 411
 propagation velocity, 211
 prosthetic gait, 473
 push-off mechanics, 485
- quadriceps, 65
 quadruped, 481
 quantitative EMG, 414
 quantitative, 195
- reaction time, 505
 receptors, 455
 recruitment of nerve fibres, 95
 recruitment order, 271
 recruitment threshold, 40
 recruitment, 43
 regenerating peripheral nerve, 79
 rehabilitation engineering, 343
 rehabilitation, 3, 61, 327, 389
 reinnervation, 207
 relative measurement, 106
 reperfusion, 69
 repetitive movements, 357
 respiratory paralysis, 143
 restoration of paralyzed extremities, 85
- scanning EMG, 205
 science, 3
 scoliosis, 389
 sedentary work, 313
 selectivity, 135
 self-contained artificial leg, 337
 sheep, 75
 short fibre, 217
 shoulder forward flexion, 317
 shoulder, 314
 signal stationarity, 275
 silicon technology, 135
 silicone tube, 79
 simulation, 473, 477
 single fibre EMG, 201
 sitting position, 463
 sitting, 459
 skeletal muscle, 69
 slope walking, 497

- soleus H-reflex, 361
- spasticity, 371
- spatial and temporal resolution, 247
- spatial filter, 247
- spectral analysis, 121, 291
- spectral parameters, 271
- speed skating, 485
- spinal cord injury, 372
- spinal cord stimulation, 95, 99
- spinal cord, 157
- spinal ligament, 455
- spinal muscular atrophy, 417
- spinal reflex, 55
- spine, 463
- spinocerebellar degeneration, 187
- squat posture, 513
- standing, 109, 113, 459
- state-feedback, 109
- stiffness, 51
- stochastic model, 231
- stochastic process, 291
- strength exercise, 423
- stretch reflexes, 51
- study, 167
- subcutaneous, 167
- superposition of motor commands, 14
- surface electromyogram, 227, 295
- surface EMG patterns, 231
- surface EMG, 235, 254, 265, 407, 427, 517, 523
- surface myoelectric signal, 261, 275
- sway of movement, 503
- synergies, 481
- task conditions, 29
- temperature influence, 253
- test contractions, 321
- tetraplegia, 143
- thigh muscles, 261
- tibial nerve, 377
- time series, 291
- torso, 445
- transcranial stimulation, 89
- transient paresis, 427
- traumatic injuries, 157
- treatment, 161
- trunk control, 463
- upper extremity, 370
- upper limb, 61
- urinary incontinence, 161
- vastus lateralis muscles, 467
- VDT, 313
- VDU, 313
- vibration, 361
- vibratory index, 361
- volume conductor model, 95, 99
- volume conductor modeling, 227
- voluntary contraction, 43
- weak analgesics, 195
- weaving mill, 302
- wheelchairs, 489
- whole body vibration, 309
- zero crossing technique, 321